

AD-A063 740

DOUGLAS AIRCRAFT CO LONG BEACH CALIF
AIRCRAFT WINDSHIELD BIRD IMPACT MATH MODEL. PART 1. THEORY AND --ETC(U)
DEC 77 P H DENKE

F/G 1/3

F33615-75-C-3105

UNCLASSIFIED

MDC-J7174-PT-1

AFFDL-TR-77-99-PT-1

NL

1 OF 6
ADA
063740



AFFDL-TR-77-99

PART 1

② LEVEL III
NW

RT 2 - AD-A062614

**AIRCRAFT WINDSHIELD BIRD IMPACT MATH MODEL,
PART 1 THEORY AND APPLICATION**

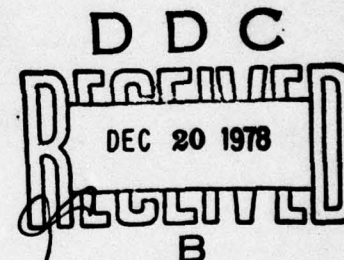
P.H.DENKE

Douglas Aircraft Company
McDonnell Douglas Corporation
3855 Lakewood Boulevard
Long Beach, California 90846

DECEMBER 1977

TECHNICAL REPORT AFFDL-TR-77-99

Final Report For Period July 1975-December 1977



Approved for public release; distribution unlimited

AIR FORCE FLIGHT DYNAMICS LABORATORY
AIR FORCE WRIGHT AERONAUTICAL LABORATORIES
AIR FORCE SYSTEMS COMMAND
WRIGHT-PATTERSON AIR FORCE BASE, OHIO 45433

88 12 11 048

AD A063740

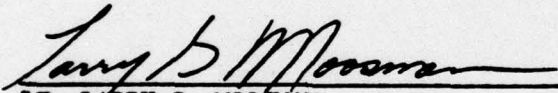
DDC FILE COPY

NOTICE

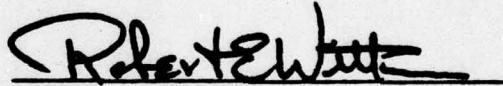
When Government drawings, specifications, or other data are used for any purpose other than in connection with a definitely related Government procurement operation, the United States Government thereby incurs no responsibility, nor any obligation whatsoever; and the fact that the Government may have formulated, furnished, or in any way supplied the said drawings, specifications, or other data, is not to be regarded by implication or otherwise as in any manner licensing the holder or any other person or corporation, or conveying any rights or permission to manufacture, use, or sell any patented invention that may in any way be related thereto.

This report has been reviewed by the Information Office (OI) and is releasable to the National Technical Information Service (NTIS). At NTIS, it will be available to the general public, including foreign nations.

This technical report has been reviewed and is approved for publication.



LT. LARRY G. MOOSMAN
Project Manager
Improved Windshield Protection ADPO
Vehicle Equipment Division



ROBERT E. WITTMAN
Program Manager
Improved Windshield Protection ADPO
Vehicle Equipment Division

FOR THE COMMANDER:



SOLOMON R. METRES
Acting Director
Vehicle Equipment Division

Copies of this report should not be returned unless return is required by security considerations, contractual obligations, or notice on a specific document.

REPORT DOCUMENTATION PAGE		READ INSTRUCTIONS BEFORE COMPLETING FORM	
1. REPORT NUMBER AFFDL-TR-77-99 / Part 1	2. GOVT ACCESSION NO. (19) TR-77-99-PT-2	3. RECIPIENT'S CATALOG NUMBER	
4. TITLE (and Subtitle) AIRCRAFT WINDSHIELD BIRD IMPACT MATH MODEL. PART 1: THEORY AND APPLICATION.		5. TYPE OF REPORT & PERIOD COVERED (9) FINAL REPORT. July 1975 - December 1977	
6. AUTHOR(s) P. H. DENKE		7. PERFORMING ORGANIZATION NUMBER (14) MDG-J7174-PT-4	
8. MONITORING AGENCY NAME & ADDRESS (if different from Controlling Office) (12) 497 P.		9. CONTRACT OR GRANT NUMBER(s) (15) F33615-75-C-3105	
9. PERFORMING ORGANIZATION NAME AND ADDRESS Douglas Aircraft Company McDonnell Douglas Corporation Long Beach, California 90846 426 400 63211F		10. PROGRAM ELEMENT, PROJECT, TASK AREA & WORK UNIT NUMBERS Project: (16) 2202 Task: 02 Work Unit: 01 (17) 02	
11. CONTROLLING OFFICE NAME AND ADDRESS Air Force Flight Dynamics Laboratories (AFFDL/FEW) Air Force Wright Aeronautical Laboratories Air Force Systems Command Wright-Patterson Air Force Base, Ohio 45433		12. REPORT DATE December 1977	
14. MONITORING AGENCY NAME & ADDRESS (if different from Controlling Office)		13. NUMBER OF PAGES (11) 504	
		15. SECURITY CLASS. (of this report) UNCLASSIFIED	
		15a. DECLASSIFICATION/DOWNGRADING SCHEDULE	
16. DISTRIBUTION STATEMENT (of this Report) Approved for public release; distribution unlimited.			
17. DISTRIBUTION STATEMENT (of the abstract entered in Block 20, if different from Report) D D C DEC 20 1978 B			
18. SUPPLEMENTARY NOTES			
19. KEY WORDS (Continue on reverse side if necessary and identify by block number)			
Aircraft	Dynamic	Math Model	Structural Model
Bird Impact	Finite Element	Modal Analysis	Thermal
Canopy	Laminate	Multi-layer	Transient
Computer Program	Large Displacements	Nonlinear	Transparency
Damping	Linear	Plasticity	Windshield
20. ABSTRACT (Continue on reverse side if necessary and identify by block number) This report describes the Bird Impact Math Model (IMPACT), a computer program designed especially for the purpose of calculating transient dynamic responses of aircraft windshield and canopy systems, composed of laminated transparencies and support structures, to bird impact. Part I of the report describes the theoretical basis of the program, and presents applications to classical problems and actual windshield systems.			

20. Abstract (Continued)

The approach is based upon a finite element model of the multilayered transparency and supporting structure, subjected to time-varying loads representing bird impact. The equation of motion for the model is derived, considering geometric and material nonlinearities. The approach to geometric nonlinearities is based upon the method of fictitious forces and deformations. The approach to material nonlinearities is based on the Von Mises yield criterion, and the Pandtl-Reuss equations. The scope of the computing effort is minimized by introducing a modal transformation. The transformed nonlinear differential equation of motion is solved incrementally in time and iteratively within each time step.

Calculated results produced by the program are shown to correlate accurately with exact solutions for simple dynamically loaded structures that exhibit large geometrically nonlinear effects, including snap-through. Linear and geometrically nonlinear analyses of the F-16 canopy subject to bird impact also were attempted. The linear analyses ran successfully, and showed qualitative agreement with test results, but displacements were underestimated, because of geometrically nonlinear effects. The nonlinear analyses of the F-16 canopy were unsuccessful. Reasons for the failure are discussed, and recommendations for further study are presented.

FOREWORD

This report is one of a series of reports that describe work performed by Douglas Aircraft Company, McDonnell Douglas Corporation, 3855 Lakewood Boulevard, Long Beach, California 90846, under the Windshield Technology Demonstrator Program. This work was sponsored by the U. S. Air Force Flight Dynamics Laboratory, Wright-Patterson Air Force Base, under Contract F33615-75-C-3105, Project 2202/0201.

This report is divided into three parts. Part 1 is entitled "Theory and Application", Part 2 is entitled "User's Manual", and Part 3 is entitled "Programming Manual." The principal investigators and authors were P. H. Denke for Part 1, G. R. Eide for Part 2, and R. C. Morris for Part 3.

Mr. D. C. Chapin, Capt., USAF Ret., was the Air Force Project Manager during the conceptual phase of the work reported herein. Lieutenant L. G. Moosman (AFFDL/FEW) succeeded Mr. Chapin during the conduct of the program.

Mr. J. H. Lawrence Jr., was the Program Director for the Douglas Aircraft Company.

This report was submitted to the Air Force on 7 December 1977, and covers the work performed during the period July 1975 through December 1977.

ACCESSION FOR		
NTIS	Write Section	<input checked="" type="checkbox"/>
DDC	Ref Section	<input type="checkbox"/>
UNANNOUNCED		<input type="checkbox"/>
JUSTIFICATION		
BY		
DISTRIBUTION/AVAILABILITY CODES		
Dist.	AVAIL.	and/or SPECIAL
A		

TABLE OF CONTENTS

SECTION	PAGE
I INTRODUCTION	1
II THEORY	9
THE FINITE ELEMENT MODEL	9
Structural Elements	9
Structural Modes	10
Axially Loaded Bars	10
Membrane Elements	12
Cell Elements	14
Element Stiffness Matrices	17
Element Damping Matrices	17
Element Mass Matrices	18
Point Mass Element	18
Material Behavior	18
LOADS	20
THE NONLINEAR EQUATION OF MOTION	22
Force and Displacement Matrices	22
Force and Displacement Transformations	24
Constrained Displacements	30
Constitutive Equations	30
Equation of Motion, Nodal Degrees of Freedom	32
Equation of Motion, Unconstrained Degrees of Freedom	38
APPROACH TO SOLVING THE NONLINEAR EQUATION OF MOTION	41
Fictitious Loads and Material Nonlinearities	42
Fictitious Forces	50
Fictitious Deformations	54
Element Forces	57
Example of Fictitious Forces and Deformations	58
EQUATION OF MOTION, MODAL DEGREES OF FREEDOM	66
Alternate Form of the Load Matrix	67
The Effects of Errors in the Calculated Displacements	70
Corrected Alternate Form of the Load Matrix	75
SOLUTION OF THE LINEARIZED EQUATION OF MOTION	75
Dependence of Load on Time	76
First Order Matrix Differential Equation	81
Solution of the Reduced Equation	83
Particular Solution of the Complete Equation	86
General Solution of the Differential Equation of Motion	91
Initial Conditions	91
Incremental Displacements, Velocities Accelerations	92

TABLE OF CONTENTS (Continued)

SECTION	PAGE
SOLUTION OF THE NONLINEAR EQUATION OF MOTION	94
Iterative Loop	95
III APPLICATIONS	103
STATIC LINEAR CORRELATIONS, CLASSICAL PROBLEMS	103
Cell Element, Elementary Loads	103
Flat Plate, Uniform Pressure	105
Pinched Cylinder	114
Flat Plate, Shear Buckling	114
NONLINEAR DYNAMIC CORRELATIONS, CLASSICAL PROBLEMS	115
Three Bar Truss	115
Flat Truss	121
LINEAR CORRELATIONS WITH TEST RESULTS	
Laminated Beams	125
B-1 Bird Impact Data	132
F-16 Canopy Linear Analysis	132
Bird Impact Loading	134
NONLINEAR ANALYSIS OF THE F-16 CANOPY	139
RUNNING TIMES	143
IV CONCLUSIONS	145
V RECOMMENDATIONS	149
APPENDIX A FORCE AND DISPLACEMENT TRANSFORMATIONS.	153
Forces and Corresponding Displacements	155
Self-Equilibrating Element Forces and Corresponding Deformations	156
Work Done by a Force	158
EQUILIBRIUM TRANSFORMATIONS	159
Variable Equilibrium Transformation	165
MODAL DISPLACEMENT TRANSFORMATIONS	165
APPENDIX B STRESS AND STRAIN TRANSFORMATIONS	169
TRANSFORMATION FOR A RECTANGULAR CARTESIAN REFERENCE FRAME ROTATED ABOUT ONE AXIS	172
Stress Transformation	172
Strain Transformation	176
TRANSFORMATIONS FROM RECTANGULAR TO OBLIQUE COORDINATES	181

TABLE OF CONTENTS (Continued)

SECTION	PAGE
Equilibrium of the Infinitesimal Parallelepiped . . .	182
Stress Transformation.	185
Strain Transformation.	189
Virtual Work Done on a Skewed Finite Element . . .	193
PLANE STRESS TRANSFORMATIONS	199
Rotation of the Rectangular Cartesian Reference Frame	199
Rectangular to Oblique Coordinate Transformation . .	200
Virtual Work on a Skewed Finite Element	201
APPENDIX C ELEMENTS AND NODAL FORCE TRANSFORMATIONS	203
AXIALLY LOADED BARS.	210
Lumped Stiffness and Unassembled Deformation Matrices	210
Stress and Strain	213
Damping Matrix	214
Force Transformation Matrix	215
Mass Matrix	216
LUMPED PARAMETER MEMBRANES	217
Element Geometry	217
Basis of the Lumped Parameter Membrane Element . . .	218
Subelements	221
Lumped Stiffness and Unassembled Deformation Matrices	223
Stresses and Strains	238
Damping Matrix	240
Force Transformation Matrix	240
Mass Matrix	243
LUMPED PARAMETER CELLS	243
Element Geometry	244
Subelements	247
Lumped Stiffness and Unassembled Deformation Matrices	250
Stresses and Strains	268
Damping Matrix	273
Force Transformation Matrix	273
Mass Matrix	285
POINT MASS ELEMENT	287
ADDITIONAL FORCE TRANSFORMATIONS	287
The P_{TF_1} Transformation	288

TABLE OF CONTENTS (Continued)

SECTION	PAGE
The P_{UPT} Transformation	288
APPENDIX D FICTITIOUS FORCES AND DEFORMATIONS	291
AXIALLY LOADED BARS	300
Fictitious Forces, Bars	302
Fictitious Deformations, Bars	303
Evaluation of the Rotation Angles	308
Axially Loaded Bars in Membranes and Cells	317
SHEAR PANELS.	317
Problem	318
Approach	320
Displacement Function	321
Rotated Reference Frames	328
Fictitious Forces and Deformations of the Infinitesimal Element	330
Panel Fictitious Forces	336
Minimum Potential Energy	339
Expansion of the W_{ap} Terms	343
Third Order Approximations	346
Evaluation of $\delta W_{a1}(a_1, 0, 0)$	349
Evaluation of $\Lambda_0(a_1, a_2, a_3)$	351
Evaluation of $\delta \Lambda_4$ and $\delta \Lambda_2$	354
Evaluation of Λ_4 and Λ_2	357
Panel Fictitious Deformations	358
J - Integrals	361
Final Form of the Shear Panel Equations	362
MEMBRANES AND CELLS	368
APPENDIX E MATERIAL NONLINEARITY	369
PRANDTL-REUSS EQUATIONS	373
Triaxial Stress	373
Plane Stress	377
Uniaxial Stress	378
Material Unloading	380
ANALYTIC REPRESENTATION OF STRESS - STRAIN CURVE	380
TEMPERATURE DEPENDENCE OF MATERIAL PROPERTIES	385
ELEMENT COMPLIANCE.	387

TABLE OF CONTENTS (Continued)

SECTION	PAGE
APPENDIX F MODAL TRANSFORMATIONS	391
REQUIREMENTS FOR THE TRANSFORMATION	393
UNDAMPED NATURAL VIBRATION MODES	394
F-16 CANOPY GEOMETRIC NONLINEARITY	395
APPENDIX G BIRD IMPACT LOADS	405
TRAVELING FOOTPRINT JOINT LOADS	409
Joint Load Vectors	415
APPENDIX H EQUATION SUMMARY	419
INITIAL GENERATOR	424
Element Geometry	424
Element Matrices	431
Model Matrices	431
MODAL TRANSFORMATION	434
NONLINEAR INCREMENTAL SOLUTION	434
Transformed Stiffness and Damping Matrices	434
Transformed Thermomechanical Loads	435
Load Variation Constants.	436
Iterative Solution	436
LINEAR INCREMENTAL SOLUTION	473
POSTPROCESSING	474
EXTERNAL LOADS GENERATION	475
REFERENCES	478

LIST OF ILLUSTRATIONS

FIGURE		PAGE
2.1	Axially Loaded Bar Element Forces and Displacements. . .	10
2.2	Axially Loaded Bar with Lumped Element Forces.	11
2.3	Membrane Element Forces.	12
2.4	Membrane Element with Lumped Element Forces	13
2.5	Cell Element Forces.	14
2.6	Cell Element and Lumped Cell Element	15
2.7	Lumped Element Forces for Cell	16
2.8	Simple Structure with Unconstrained and Constrained Degrees of Freedom	25
2.9	Nodal Degrees of Freedom	26
2.10	Element Forces and Displacements	26
2.11	Self-Equilibrating Element Forces.	26
2.12	Components of Unit Value of P_{T6}	28
2.13	Components of Unit Value of \bar{F}_1	28
2.14	Time points and Increments	35
2.15	Components of an Element Force Resulting from Rotation of the Element	51
2.16	Statically Loaded Rectangular Frame	59
2.17	Deformed Rectangular Frame	60
2.18	Fictitious Forces	62
2.19	Nonlinear Displacement of the Rectangular Frame	65
2.20	Original Assumed Variation of Loads with Time	76
2.21	Cosine Variation of the Thermomechanical Load	78
2.22	Sine Variation of the Fictitious Load	79
3.1	Validity of Parallelepiped Cell Element for Simple Loads	104
3.2	Skewed Cell Element	106
3.3	Static Analysis - Simply Supported Square Plate Under Uniform Pressure	107
3.4	Pinched Cylinder Model	108
3.5	Pinched Cylinder Displacements	109
3.6	Stresses and Moments on Section B-C	110
3.7	Stresses and Moments on Section D-C	111

LIST OF ILLUSTRATIONS (Continued)

FIGURE		PAGE
3.8	Shear Stress and Torsional Moment	112
3.9	Buckling Analysis, Simply Supported Square Plate Under Uniform Shear	113
3.10	Three Bar Truss	116
3.11	Displacement of the 3-Bar Truss, High Damping	118
3.12	Displacements of the 3-Bar Truss, Low Damping	119
3.13	Static Response of the Three-Bar Truss	120
3.14	Flat Truss	122
3.15	Response of the Flat Truss	123
3.16	Displacement of the Flat Truss	124
3.17	Statically Loaded Laminated Beam	126
3.18	(a) Static Deflection and (b) Strain Correlations for 36-Inch Beam Model.	127
3.19	Damping Beam Specimen and Finite Element Model. . . .	129
3.20	First Natural Mode of Vibration	130
3.21	Response of the Damping Beam to an Initial Tip Displacement.	131
3.22	Half-Shell Finite Element Model of the F-16 Canopy .	133
3.23	Load-Deflection Curve for Static Test	135
3.24	Vertical Displacement on the Plane of Symmetry, as a Function of Fuselage Station, and Time	137
3.25	Equivalent Stress on the Plane of Symmetry, Inside, as a Function of Fuselage Station, and Time	138
3.26	Envelope of Traveling Wave	140
3.27	Possible Mechanism of F-16 Canopy Response: Traveling Snap-Through Wave.	141
3.28	Nonlinear Canopy Analysis	143
A.1	Displacement Corresponding to a Force	155
A.1.1	Displacement Corresponding to a Force that Varies in Direction	156
A.1.1.1	Self-Equilibrating Element Force	157
A.1.2	Bending Element with Self-Equilibrating Element Forces.	157
A.2	Sets of Forces and Corresponding Displacements	159

LIST OF ILLUSTRATIONS (Continued)

FIGURE		PAGE
A.3	Equilibrium of a Rigid Body	160
A.3.1	Verification of Equation A.7	162
A.4	Example of a Transformation Involving One Set of Self-Equilibrating Forces	162
A.5	Equilibrium of the Nodes	163
A.6	Verification of Equation A.7.2	164
B.1	Rotated Reference Frame	172
B.2	Element for Calculating σ_y and τ_{xy}	173
B.3	Element for Calculating σ_x	174
B.4	Element for Calculating σ_z , τ_{yz} and τ_{zx}	175
B.5	The Components u , v , \bar{u} and \bar{v}	177
B.6	The Coordinates x , y , \bar{x} and \bar{y}	179
B.7	The Oblique Coordinate System	182
B.7.1	Forces Parallel to \bar{x} and \bar{y} on Faces Normal to $\bar{x}\bar{y}$. .	183
B.8	Remaining Forces on Skew Element	184
B.9	Element for Calculating $\bar{\sigma}_x$ and $\bar{\tau}_{xy}$	185
B.10	Element for Calculating $\bar{\sigma}_y$	187
B.11	Element for Calculating $\bar{\sigma}_z$, $\bar{\tau}_{yz}$, and $\bar{\tau}_{zx}$	188
B.12	The Components \bar{u} , \bar{v} , \bar{u} and \bar{v}	189
B.13	Forces and Displacements Parallel to \bar{x} and \bar{y} on Faces Normal to $\bar{x}\bar{y}$	194
B.14	Remaining Forces on the Skewed Finite Element	196
C.1	Bar Nomenclature	210
C.2	Equilibrium of the Lumped Forces and the Element Forces	215
C.3	Membrane Dimensions	217
C.4	Parallelogram Element	218
C.5	Development of the Lumped Parameter Membrane	220
C.6	Subelements of the Approximate Parallelogram	221
C.6.1	Subelement Notation	222
C.7	The j th Subelement	222
C.8	Oblique Coordinates for the p th Subelement	225

LIST OF ILLUSTRATIONS (Continued)

FIGURE		PAGE
C.9	Oblique Element Forces on the pth Subelement	227
C.10	Subelement Forces and Lumped Element Forces	231
C.11	Cell Element Geometry	244
C.12	Definition of the Lumped Cell Element	245
C.13	Lumped Cell Element Surface Geometry	246
C.14	Cell Subelements	248
C.15	jth Subelement	248
C.16	Reference Frames for the jth Subelement	249
C.17	Subelement Forces, jth Subelement	254
C.18	Subelement and Lumped Forces, Upper Surface	258
C.19	Subelement and Lumped Forces, Lower Surface	259
C.20	Subelement and Lumped Forces, Middle Surfaces . . .	260
C.21	Cell Lumped Element Forces	274
C.22	Equivalent Lumped Element Forces in True Geometric Boundaries	275
C.23	Cell Element Forces in Local Degrees of Freedom . .	276
C.24	Unit Edge Vectors	277
C.25	Cell Element Forces in Global Degrees of Freedom . .	278
C.26	Implied Linkage Joining \hat{F} and \bar{F} Forces	280
C.27	Point Mass Element	287
D.1	Symmetric and Antisymmetric Bar Forces	300
D.2	Axially Loaded Bar Forces and Displacements	301
D.3	Displaced Bar.	306
D.4	Substitute Rotation Angles	309
D.5	Dummy Moments and Normal Forces	311
D.6	Notation for Shear Panel Fictitious Forces and Deformations	318
D.6.1	Relationship Between Shear Panel Notations	319
D.8	Coordinates for the Displacement Function	321
D.9	Shear Panel Deformation Mode, $w_e(\bar{x}, \bar{y})$	323
D.10	Oblique Coordinates and Unit Vectors	328
D.11	Differential Fictitious Forces	330

LIST OF ILLUSTRATIONS (Continued)

FIGURE		PAGE
D.12	The \bar{y} Coordinate	348
D.12.1	Fictitious Deformation for $\theta_{\bar{x}1} = \theta_{\bar{y}}$	359
E.1	True Stress, True Strain Curve	381
E.2	Bar Element Load-Deformation Diagram	389
F.1	Cantilever Beam Model, and First Bending Mode	396
F.2	Higher Order Modes	396
F.3	Axial Motion Accompanying Bending	397
F.4	Axial Mode	397
F.5	Displaced Position of Bar AB	399
F.6	Bar Nodal Displacements	401
F.7	Displacements of the Rotated Bar	402
F.8	Forces on the Rotated Bar	403
G.1	Impact Geometry	410
G.2	Impact Force-Time Diagram	412
H.1	Surfaces and Associated Vectors	427
H.2	Replacement Parallelogram	442
H.3	Fictitious Forces, Membrane Element	443
H.4	Fictitious Forces, Cell Element	448

LIST OF TABLES

TABLE		PAGE
1	ITERATIVE LOOP, GEOMETRIC NONLINEARITY, δ TH INCREMENT	97-100
C.1	THE COLUMN MATRICES $\bar{e}_{\alpha T_j}$ FOR MEMBRANES	239
C.2	ELEMENTS OF THE MATRICES $\tilde{F}_{F_{ji}}$	261
C.3	THE MATRIX $\sigma_{F_{ji}}$, FOR THE j TH SUBELEMENT OF THE i TH CELL ELEMENT	264
C.4	THE COLUMN MATRICES $\bar{e}_{\alpha T_j}$ FOR CELL ELEMENTS	266-267
C.5	THE MATRIX \hat{F}_F FOR CELL ELEMENTS	281
C.6	THE MATRIX F'_F FOR CELL ELEMENTS	283
C.7	THE MATRIX F_F FOR CELL ELEMENTS	284
D.1	VALUES OF $\partial \tilde{e}_n / \partial \alpha_p$	341
H.1	ELEMENT MATRICES	432
H.2	APPENDIX D EQUATIONS	461
H.3	FIRST EVALUATION	465
H.4	SECOND EVALUATION	465

LIST OF ABBREVIATIONS, ACRONYMS AND SYMBOLS

A	$-L^{-1}B$
B	Square matrix, the coefficient of y in the first order matrix equation of motion
C	Assembled damping matrix (square) referred to unconstrained degrees of freedom
\bar{C}	Square element damping matrix
$C_{AD\beta}$	$C_{a\beta}$ diagonalized
$C_{A\beta}$	Column matrix. The k th row is $C_{a\beta k}$
$C_{a\beta k}$	Modified constants in the solution of the reduced equation of motion
$\hat{C}_{a\beta k}$	Constants in the solution of the equation of motion
c_f, c_p	Constants
$\bar{C}_{i(\beta)}$	lumped damping matrix (square) for the i th element, applicable during the β th increment
C_T	Assembled damping matrix (square) referred to nodal degrees of freedom
$C_{(\beta)}$	Assembled damping matrix (square) referred to the unconstrained degrees of freedom, applicable during the β th increment
$\bar{C}_{(\beta)}$	Transformed damping matrix, β th increment
d	Preceding a variable, indicates a differential
e	Column matrix of element displacements
\ddot{e}	d^2e/dt^2

LIST OF ABBREVIATIONS, ACRONYMS AND SYMBOLS (Continued)

\bar{e}	Column matrix of element deformations
$\dot{\bar{e}}$	$d\bar{e}/dt$
$\dot{\bar{e}}_f$	Column matrix of fictitious deformation rates
e_{ik}	kth element displacement, ith element, referred to global coordinates
\bar{e}_{ik}	kth element deformation, ith element
$\dot{\bar{e}}_{i\beta}$	Column matrix of rates of displacements of the fictitious forces on the ith element, during the β th increment
$\dot{\bar{e}}_L$	Column matrix of linear element deformation rates
e_z	Base of natural logarithms
\bar{e}_0	Column matrix of unassembled element thermal deformations
$\dot{\bar{e}}_0$	$d\bar{e}_0/dt$
F	Column matrix of element forces
\bar{F}	Column matrix of lumped element forces
F_C	Column matrix of damping element forces
\bar{F}_C	Column matrix of lumped damping element forces
$F_{D\beta}(t-t_{\beta-1})$	$F_{\beta}(t-t_{\beta-1})$ diagonalized
FF&D	Fictitious forces and deformations
$F_{\bar{F}}$	Rectangular matrix of element forces resulting from unit lumped element forces
$\bar{F}_{\bar{F}_{i\beta}}$	Rectangular matrix of the fictitious forces resulting from unit values of the lumped element forces F_{K_i} , for the ith element and the β th increment

LIST OF ABBREVIATIONS, ACRONYMS AND SYMBOLS (Continued)

F_{ik}	kth element force, ith element, referred to global coordinates
\bar{F}_{ik}	kth lumped element force; ith element
F_K	Column matrix of stiffness element forces
\bar{F}_K	Column matrix of lumped stiffness element forces
$\bar{\bar{F}}_{K_{i\beta}}$	Column matrix of fictitious forces on the ith element, during the β th increment
$F_{K0_{i\beta}}$	Column matrix components of the lumped element stiffness forces parallel to the directions of the lumped forces at the beginning of the β th increment
F_M	Column matrix of inertia element forces
$F_{0F_{i\beta}}$	Rectangular matrix of the components $\bar{F}_{K0_{i\beta}}$ resulting from unit values of the lumped element forces \bar{F}_{K_i} , for the ith element, and the β th increment.
$F_\beta(t-t_{\beta-1})$	Column matrix. The time-dependent term in the solution of the reduced equation of motion
$G_{\beta k}$	Column matrix, kth eigenvector of A_β
H_{V_β}	Rectangular matrix. Partition of H_β corresponding to velocities
H_β	Square matrix. The columns are the eigenvectors $G_{\beta k}$
H_{Δ_β}	Rectangular matrix. Partition of H_β corresponding to displacements
I	Unit (identity) matrix
i	Subscript. Indicates the ith structural element

LIST OF ABBREVIATIONS, ACRONYMS AND SYMBOLS (Continued)

Im	Denotes imaginary part of a complex number
IMPACT	Bird Impact Math Model
j	$\sqrt{-1}$
\bar{k}	Square element stiffness matrix
$\bar{k}_{c(\beta)}$	Transformed mechanical impedance matrix (square) for the β th increment
$\bar{k}_{i(\beta)}$	lumped stiffness matrix (square) for the i th element, applicable during the β th increment
$k_{(\beta)}$	Assembled stiffness matrix (square) referred to the unconstrained degrees of freedom, applicable to the β th increment
$\bar{k}_{(\beta)}$	Transformed stiffness matrix, β th increment
L	Square matrix, the coefficient of \dot{y} in the first order matrix equation of motion
M	Assembled mass matrix (square) referred to unconstrained degrees of freedom
\bar{M}	Transformed mass matrix (square)
m	Square element mass matrix
M_T	Assembled mass matrix (square) referred to nodal degrees of freedom
\bar{n}	Number of transformed degrees of freedom
$\left. \begin{matrix} p,q \\ r,s \end{matrix} \right\}$	Element joint numbers
P_{CPT}	Rectangular matrix of components in the constrained degrees of freedom of unit loads in the nodal degrees of freedom
$\bar{P}_{(C)U}$	Column matrix of transformed loads resulting from internal damping forces

LIST OF ABBREVIATIONS, ACRONYMS AND SYMBOLS (Continued)

$P_{(K)TI}$	Column matrix of components in the nodal degrees of freedom of the interior stiffness forces existing at the beginning of an increment
$P_{(K)U}$	Column matrix of components in the unconstrained degrees of freedom of the internal stiffness forces
$\bar{P}_{(K)U}$	Transformed $P_{(K)U}$
$P_{(K)UI}$	Column matrix of components in the unconstrained degrees of freedom of the interior stiffness forces existing at the beginning of an increment
$\bar{P}_{(H)U}$	Column matrix of transformed loads resulting from inertia forces
$P_{(R)T}$	Column matrix of components of the reactions in the nodal degrees of freedom
$P_{(R)U}$	Column matrix of components of the reactions in the unconstrained degrees of freedom
P_T	Column matrix of external loads in the nodal degrees of freedom
P_{TCO}	Column matrix of equivalent external loads in the nodal degrees of freedom resulting from rates of change of unassembled thermal deformation
P_{TF}	Rectangular matrix of components in the nodal degrees of freedom resulting from unit element forces
P_{TF}	Rectangular matrix of components in the nodal degrees of freedom resulting from unit values of the lumped element forces
P_{TR}	Rectangular matrix of components in the nodal degrees of freedom of unit values of the reactions

LIST OF ABBREVIATIONS, ACRONYMS AND SYMBOLS (Continued)

P_{T_3}	$P_{(K)TI} + P_{TCO} + \delta P_{TKO_3} + P_{(\phi)T} + P_{(R)T}$
P_U	Column matrix of external loads in unconstrained degrees of freedom
\bar{P}_U	Column matrix of transformed loads
P_{UCO}	Column matrix of equivalent external loads in the unconstrained degrees of freedom resulting from rates of change of unassembled thermal deformations
P_{UF}	Rectangular matrix of components in the unconstrained degrees of freedom resulting from unit values of the lumped element forces
$P_{UF_{i3}}$	Rectangular matrix of components in the unconstrained degrees of freedom of unit values of the fictitious forces, for the i th element, and the 3 th increment
$P_{UF_{i3}}$	Rectangular matrix of components in the unconstrained degrees of freedom of unit values of the components $F_{KO_{i3}}$ for the i th element, and the 3 th increment
P_{UPT}	Rectangular matrix of components in the unconstrained degrees of freedom of unit loads in the nodal degrees of freedom
P_{U_3}	$P_{UPT} P_{T_3}$
\bar{P}_3	Column matrix of transformed thermomechanical loads for the 3 th increment
$P_{(\phi)T}$	Column matrix of components of the external loads in the nodal degrees of freedom
$P_{(\phi)U}$	Column matrix of components of the external loads in the unconstrained degrees of freedom

LIST OF ABBREVIATIONS, ACRONYMS AND SYMBOLS (Continued)

$\bar{P}_{(\phi)U}$	Transformed $P_{(\phi)U}$
R	Column matrix of reactions
Re	Denotes real part of a complex number
T	Displacement transformation
T	(Superscript) Indicates transposed matrix
t	Time
t_q	Cell element thickness at qth corner
T_β	Period of sinusoidal variations of load for β th increment
$t_{\beta-1}$	Time at the beginning of the β th increment
\bar{v}	$d\bar{\Delta}/dt$
$\dot{\bar{v}}$	$d^2\bar{\Delta}/dt^2$
y	Column matrix of transformed displacements and velocities in the unconstrained degrees of freedom
\dot{y}	dy/dt
y_c	Column matrix. Coefficient of the cosine term in the particular solution of the equation of motion
y_s	Column matrix. Coefficient of the sine term in the particular solution of the equation of motion
$y_{\beta k}$	kth solution of reduced equation of motion
α	Angle
β	Angle
β	(Subscript). Indicates time increment
\bar{y}_{c_β}	$\bar{P}_\beta^c p_\beta$

LIST OF ABBREVIATIONS, ACRONYMS AND SYMBOLS (Continued)

$\gamma_{f\beta}$	$\delta P_{(f)\beta}(t_\beta)c_{f\beta}$
Δ	Column matrix of displacements in the unconstrained degrees of freedom
$\dot{\Delta}$	$d\Delta/dt$
$\ddot{\Delta}$	$d^2\Delta/dt^2$
$\bar{\Delta}$	Column matrix of transformed displacements
$\dot{\bar{\Delta}}$	$d\bar{\Delta}/dt$
$\ddot{\bar{\Delta}}$	$d^2\bar{\Delta}/dt^2$
Δ_c	Column matrix of displacements in the constrained degrees of freedom
$\delta \bar{e}_{f\beta}$	Column matrix of fictitious deformations for the i th element, developed during the β th increment
$\delta \bar{e}_{i\beta}(t)$	$\bar{e}_i(t) - \bar{e}_i(t_{\beta-1})$
$\delta \bar{e}_{L_i\beta}(t)$	$\bar{e}_{L_i}(t) - \bar{e}_{L_i}(t_{\beta-1})$
$\delta \bar{e}_{o_i\beta}(t)$	$\bar{e}_{o_i}(t) - \bar{e}_{o_i}(t_{\beta-1})$
$\delta P_{(\bar{F})\beta}$	Column matrix of loads in the unconstrained degrees of freedom resulting from fictitious forces, developed during the β th increment
$\delta \bar{P}_{(\bar{F})\beta}$	Transformed $\delta P_{(F)\beta}$
$\delta \bar{P}_{(f)\beta}(t_\beta)$	Column matrix of transformed fictitious loads at the end of the β th increment
$\delta P_{Kf\beta}$	Column matrix of loads in the unconstrained degrees of freedom resulting from fictitious deformations, developed during the β th increment

LIST OF ABBREVIATIONS, ACRONYMS AND SYMBOLS (Continued)

$\delta \bar{P}_{kf_B}$	Transformed δP_{kf_B}
δP_{KO_B}	Column matrix of equivalent external loads in the unconstrained degrees of freedom resulting from unassembled deformations developed during the B th increment
$\delta \bar{P}_{KO_B}$	Transformed δP_{KO_B}
δP_{TKO_B}	Column matrix of equivalent external loads in the nodal degrees of freedom resulting from thermal deformations produced in the structure during the B th increment
$\delta P_{UF}(t)$	$P_{UF}(t) - P_{UF}(t_{B-1})$
δP_{UKO_B}	The column matrix of equivalent external loads in the unconstrained degrees of freedom resulting from thermal deformations produced in the structure during the B th increment
$\delta P_{UB}(t_B)$	Column matrix of equilibrium errors in the unconstrained degrees of freedom at t_B
$\delta \bar{P}_U(t_B)$	Column matrix of transformed equilibrium errors at t_B
$\delta \bar{P}_{(\phi)U_B}(t)$	$\bar{P}_{(\phi)U}(t) - \bar{P}_{(\phi)U}(t_{B-1})$
Δ_T	Column matrix of displacements in the nodal degrees of freedom
$\dot{\Delta}_T$	$d\Delta/dt$
$\delta \bar{\Delta}_{CI_B}$	Imaginary part of $\delta \bar{\Delta}_{C_B}$
$\delta \bar{\Delta}_{CR_B}$	Real part of $\delta \Delta_{C_B}$
$\delta \bar{\Delta}_{C_B}$	$\bar{K}_{C(B)}^{-1} \bar{Y}_{C_B}$

LIST OF ABBREVIATIONS, ACRONYMS AND SYMBOLS (Continued)

$\delta \bar{\Delta}_{fI_B}$	Imaginary part of $\delta \bar{\Delta}_{f_B}$
$\delta \bar{\Delta}_{fR_B}$	Real part of $\delta \bar{\Delta}_{f_B}$
$\delta \bar{\Delta}_{f_B}$	$\bar{K}_{C(B)}^{-1} \bar{Y}_{f_B}$
$\delta \Delta_B(t)$	$\Delta(t) - \Delta(t_{B-1})$
$\delta \bar{\Delta}_B(t)$	$\bar{\Delta}(t) - \bar{\Delta}(t_{B-1})$
$\dot{\delta \bar{\Delta}}_B$	$d[\delta \bar{\Delta}_B(t)]/dt = d\bar{\Delta}/dt$
λ_{DB}	λ_B diagonalized
λ_B	Column matrix containing the eigenvalues λ_{Bk}
λ_{Bk}	kth eigenvalue of A_B
π	Circumference/diameter for circle
Σ	Indicates summation
τ_B	Duration of the Bth increment
ψ_C	Column matrix, coefficient of cosine term in first order matrix equation
ψ_f	column matrix, coefficient of sine term in first order matrix equation of motion
ω_{p_B}	Load frequency for Bth increment

SECTION I

INTRODUCTION

In the past, design verification of an aircraft windshield system subjected to bird impact has been accomplished primarily by test. A reliable analytical tool is needed to support the design process, and to reduce the amount of testing required for substantiation. In particular, a mathematical model is needed that can simulate, in some detail, the response of a windshield system to bird impact, including displacements, internal stresses, and strains. The model should be implemented as a computer program.

The present report describes the Bird Impact Math Model (IMPACT), a computer program designed for this purpose. Part 1 of the report describes the theoretical basis of the model, and presents applications and experimental correlations to verify the model, and to show its utility. Part 2 is a user's manual, Part 3 is a programming manual.

The Math Model was developed as part of the Windshield Technology Demonstrator Program, a research effort conducted by the Douglas Aircraft Company, and sponsored by the Air Force Flight Dynamics Laboratory. This program is part of a larger Windshield Protection Program being conducted by the Flight Dynamics Laboratory, to develop improved technologies, that can contribute to increased resistance of aircraft transparent enclosures to birdstrikes.

A basic requirement established for the Math Model is that it should provide computing capability for both parametric studies and design substantiation analyses at reasonable cost.

The design features of a typical aircraft windshield or canopy system and the response mechanism of such a system to impact, impose stringent requirements upon the Math Model. Ideally, the model should be able to account for:

1. The laminated construction of the transparency, its attachment to the supporting structure, and the presence of the supporting structure itself.
2. The loads produced by the impacting bird, and the interaction between bird and windshield.
3. The transient dynamic response of the structure, including displacements, stresses and strains, as functions of time.
4. The thermal environment, and its effects on material properties and response.
5. The existence of significant amounts of damping in interlayer materials.
6. The effects of high strain rates on material properties.
7. Material nonlinearities.
8. Geometric nonlinearities.

The list covers most of the difficult problems in the field of finite element structural analysis. Translated into terms of computer programming and data processing, this statement means that any program able to do the job is likely to run for an unacceptably long time, unless it is designed and optimized specifically for the purpose. A literature search revealed no existing special purpose program meeting the requirements. Therefore the decision was made to develop such a program.

The formulation of the Math Model, presented in Section II of this report, and in the Appendices, covers all of the effects mentioned in the preceding list, except bird-windshield interaction, or target compliance. An attempt to account for this phenomenon was thought to be premature, in view of the shortage of related data available at the beginning of the project. Modification of the program to account for target compliance at a later time may be feasible. Also, the accounting of high strain rate effects was not planned as an automated feature of the program, again because of the shortage of related data, and because the necessary complicated calculations would significantly increase the cost of the analysis. It was determined that user estimation of strain rates and manual input of corresponding material properties would be acceptable.

Not all of the effects covered by the mathematical formulation were converted to computer code, because of time constraints. The effects formulated, but not programmed, include plasticity, thermal loads resulting from damping energy dissipated as heat, and the dependence of material properties on temperature changes occurring after initial impact. Coding in some of these areas is partially completed. The following paragraphs outline the approach, as it is mathematically formulated in Section II, and the Appendices.

The approach is based on the analysis of a finite element model of the windshield system. The model is a set of nodes connected by elements that have mass, damping and stiffness. Some nodes can have constraints, although the formulation provides for completely unconstrained, and otherwise statically unstable, models.

The model is assembled from four kinds of elements: axially loaded bars, membranes, cells, and point masses. The membrane and cell elements are based on the lumped parameter idealization, in the sense that these elements are themselves composed of bars and shear panels.

This approach may seem obsolescent, in the light of recent developments in the field, therefore an explanation of the rationale for the selection of lumped parameter elements is appropriate.

In the past, the lumped parameter model has provided satisfactory results in a wide variety of aerospace applications. One advantage of the model is simplicity. The user not familiar with the theory of finite element analysis can easily grasp the concept, and therefore feel increased confidence in applying the results. A second advantage, important in the present application, is that use of the model facilitates the analysis of geometric nonlinearity resulting from element force rotation, by the method of fictitious loads.

The disadvantages of the conventional bar-panel model have been that "lumping" is required, Poisson coupling is neglected, panels should be rectangular, and plate bending and shell bending are difficult to represent. These disadvantages have been overcome, in the present application, by the newly developed membrane and cell elements, which require no lumping, and automatically account for Poisson coupling and skewness. The cell element can be subjected to out-of-plane bending and torsion. Deformations through the thickness are also represented. Plate and shell structures can be modeled. Thus the advantages have been retained, and the disadvantages have been eliminated.

In the formulation, materials are assumed to be isotropic, and to conform to the Von Mises yield criterion, and the Prandtl-Reuss equations, in the plastic range. Unloading is considered. The dependence of material properties on temperature is taken into account. The equation of motion is solved stepwise in time, and material property effects are taken into account by updating the stiffness and damping matrices at each increment.

Loads are applied at nodes of the model as time dependent vectors. When the angle between the transparency surface and the bird trajectory is small, investigation indicates that the bird slides along the surface,

producing a "traveling footprint". A module in the Math Model preprocessor automatically generates traveling footprint load vectors.

The formulation accounts for thermal loads resulting from initial thermal gradients, and from temperature changes resulting from heat generated due to damping, without heat transfer.

Two kinds of geometric nonlinearities are considered: nonlinearities resulting from changes in shapes of elements, as when a bar becomes shorter and thicker, and therefore stiffer; and nonlinearities resulting from rotations of element forces. Nonlinearities of the first kind are taken into account by updating element stiffness and damping matrices for each increment. Nonlinearities of the second kind are accounted for by coordinate updating; and within each increment, by the method of fictitious forces and deformations (FF & D).

The formulation of the FF & D method is a feature of this report. A rational basis for the method is established. Changes in element stiffness resulting from element force rotations, appearing in the equation of motion as coefficients of the unknown displacements, are shown to be precisely replaceable by terms on the right of the equation, representing loads resulting from fictitious element forces and deformations. These forces and deformations exist; they are fictitious only in the sense that they are not considered in linear theory.

A modal transformation is introduced. Such a transformation appears essential to keep computing costs within reasonable limits for large models.

Corrections for equilibrium errors resulting from coordinate updating are also provided.

The transformed nonlinear differential equation of motion is solved incrementally in time, and iteratively within each increment. The pur-

pose of the iterative loop within the increment is to satisfy the equation of motion, considering the presence of the fictitious load terms.

During any one iteration, the differential equation is linearized. The linearized equation is solved exactly. Approximate numerical integration algorithms are not employed. This approach seems to be quite reliable. No difficulties with loss of accuracy, or singularity of the initial condition equations, were experienced in solving the linearized equations, during any of numerous applications of the final version of the computer program.

Applications of the Math Model to classical problems and simple structures, linear and nonlinear, are presented in Section III. The linear applications verify the cell element as a satisfactory building block for finite element modeling. The nonlinear applications show that the Math Model gives accurate results for simple structures exhibiting very large geometric nonlinearities, including snap-through effects.

Applications to statically loaded and vibrating laminated beams show satisfactory correlations with test data for displacements, and for stresses within the layers.

Correlations of calculated linear results with test data for the F-16 canopy subjected to bird impact loads show that calculated responses tend to be proportional to measured values, but stresses and displacements are underestimated.

An application of the Math Model nonlinear option to the F-16 canopy produced erroneous results. In Appendix F, the difficulty is studied, and attributed to the use of an unsuitable modal transformation. The problem is that modes suitable to describe the motion immediately after impact can become unsuitable after coordinates have been updated several times. The difficulty can be anticipated whenever the analysis

is extensive enough to require a modal transformation. The analysis in Appendix F shows why the difficulty occurs, and leads to recommendations for corrective action.

The modal approach to nonlinear analysis undoubtedly can provide satisfactory results, if enough suitable modes are employed. The question remaining to be answered is whether a set of such modes can be found small enough so that the feasible model size will not be unduly limited.

The Math Model, in its present form is considered satisfactory for linear analysis of windshield systems subjected to bird impact. The geometrically nonlinear version is operational, but the code needs further optimization. It gives accurate results for simple structures exhibiting pronounced nonlinearities. The applicability to structures having more than a few elements remains to be evaluated, pending development of a better understanding of suitable modal transformations.

The linear code is suitable for parametric studies, and for more detailed design evaluations, depending on the complexity of the finite element models employed. The linear option also can provide useful information for substantiation, if nonlinear effects are small, or if test data permitting the evaluation of such effects are available.

Part 2 of this report, the User's Manual, provides instruction in the use of the Math Model computer program. This part also contains data on typical running times for various modules and options. The times for the linear option are considered acceptable. The times for the nonlinear option indicate the feasibility of the approach, although the code requires further optimization, and the successful use of modes in nonlinear analysis of large models has yet to be demonstrated.

Part 3, the Programming Manual, described the approach to optimizing the code, and the details of the program. Appendix H of Part 1 summarizes

the basic equations in approximately the order of solution reflected in the program. The strategy of code optimization includes keeping the matrices as small as possible, by employing individual element mass, damping and stiffness matrices in place of assembled structural matrices, and by taking full advantage of the modal transformation.

The linear option of the Math Model computer code is considered to meet the basic intent of the project: to provide a tool for parametric studies and for design substantiation analysis, at reasonable cost. Development of a better understanding of modal transformations applicable to large displacement analysis, plus refinements of the nonlinear code, are expected to provide an economically feasible nonlinear capability. Use of this capability can lead to significant reductions in the costs of bird impact testing required for design verification.

SECTION II

THEORY

This section presents the theoretical basis of the Math Model. The primary purpose of this discussion is to provide an understanding of the approach. Consequently many subjects are treated briefly, because detailed treatments would diminish the clarity of the presentation. Detailed discussions are contained in the Appendices. Appendix H also provides a summary of the mathematics and logic that form the basis of the associated computer program.

The subjects considered in this section are the finite element model, the nonlinear equation of motion, and the method of solving this equation.

THE FINITE ELEMENT MODEL

This subsection contains descriptions of the structural elements, the assembly of these elements into the structural model, and element material properties.

Structural Elements

The model is composed of four kinds of elements: (1) axially loaded bars, (2) membranes, (3) cells, and (4) point masses. The membrane and cell elements are themselves composed of axially loaded bars and shear panels, or lumped parameter elements. Forces acting upon the bars, membranes and cells are resolved into two different sets of components, called "element forces" and "lumped element forces". These components are defined in the following paragraphs.

Structural Nodes

Nodes for the structural model are classified as "joints" and "shear" nodes. Joints are nodes that are contiguous to the ends of bars, and the corners of membrane and cell elements. Shear nodes are contiguous to the centers of bar, membrane, and cell element edges.

Axially Loaded Bars

In this subsection, a subscript i , indicating element number, is omitted from the symbols denoting individual element forces and deformations, for simplicity. For example, F_1 and e_1 are written in place of F_{i_1} and e_{i_1} .

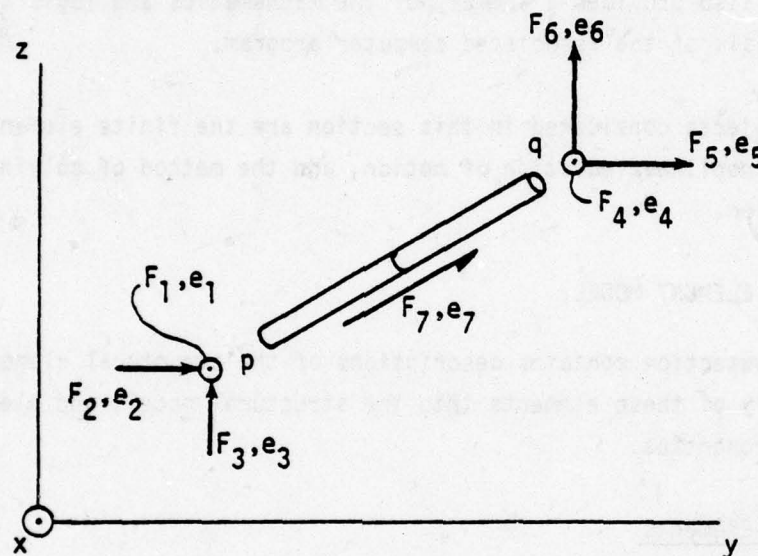


Figure 2.1. Axially Loaded Bar Element Forces and Displacements

Figure 2.1 shows the bar element, with its element forces and displacements. The sets of forces on each end are parallel to the global coordinate axes. The force at the middle is parallel to the bar. The resultants of the end forces are parallel to the bar, since the bar is axially loaded. The symbols p and q denote node numbers, defined by the user, when he specifies, on the input sheet, that the bar connects nodes p and q . When $p < q$, F_7 is positive in the sense shown.

This element can be connected to other elements at each end, and at its center.

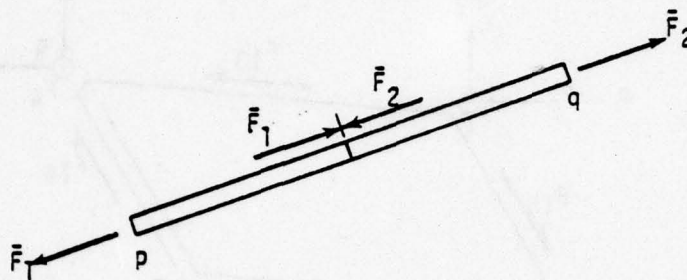


Figure 2.2. Axially Loaded Bar with Lumped Element Forces

Figure 2.2 shows the axially loaded bar with its "lumped" element forces. Two lumped axial element forces act on the bar, numbered as shown. The corresponding element deformations, designated \bar{e}_1 and \bar{e}_2 , are equal to the works done by unit values of \bar{F}_1 and \bar{F}_2 , during a virtual displacement, as explained in Appendix A. In this simple case, the deformations are equal to the elongations of the two halves of the bar.

The F components and the \bar{F} components are statically equivalent, consequently the relationships among these components can be derived from equilibrium, as explained in Appendix C.

The reason for introducing lumped element forces is that they are useful in formulating the effects of geometric nonlinearity, by the method of fictitious forces and deformations.

Membrane Elements

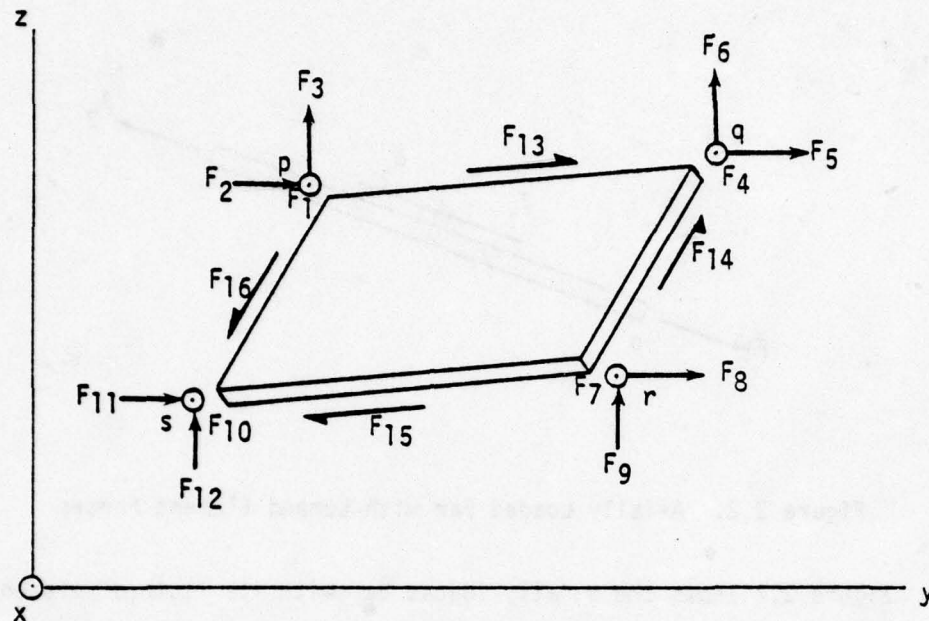


Figure 2.3. Membrane Element Forces

The membrane element, with its element forces, is shown in Figure 2.3. The shape of the element is approximately that of a flat parallelogram. The forces at the corners are parallel to the global coordinate axes. The other forces are parallel to the edges, and act at the centers of the edges. The symbols p , q , r and s identify joints connected by the panel, as established by the user. The positive senses for the edge shear forces are defined in Appendix C, and are not necessarily as shown. The element displacement vectors, denoted e_1, e_2, \dots, e_{16} , coincide with the force vectors.

This element has corner and edge connectivity.

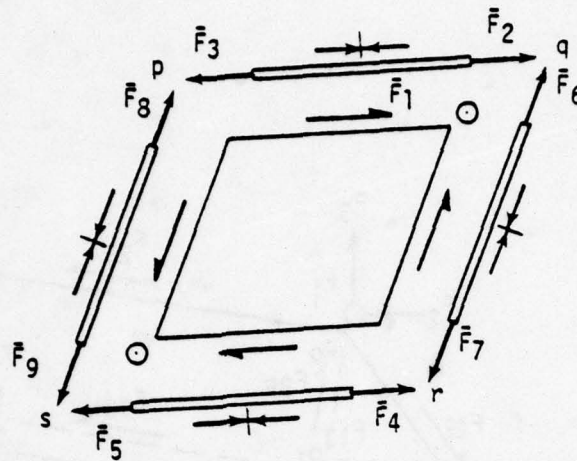


Figure 2.4. Membrane Element with Lumped Element Forces

The membrane element with lumped element forces is shown in Figure 2.4. The membrane is considered to be composed of a shear panel and four bars, according to the usual lumped parameter approach. Each bar has two self-equilibrating element forces, designated as shown. The shear panel has six self-equilibrating components. The two components at corners q and s are normal to the approximate plane of the panel. When the panel is warped, these components are required for equilibrium. The other components act at midpoints of panel edges. The complete set of six shear panel forces is designated \bar{F}_1 . The element force \bar{F}_1 has a unit value, by definition, when the vector on edge pq is equal to unity.

The corresponding deformations are designated $\bar{e}_1, \bar{e}_2, \dots, \bar{e}_9$. The deformations are equal to the works done by unit values of the element forces, during a virtual displacement.

Equations relating the F and \bar{F} forces can be written on the basis of equilibrium.

Cell Elements

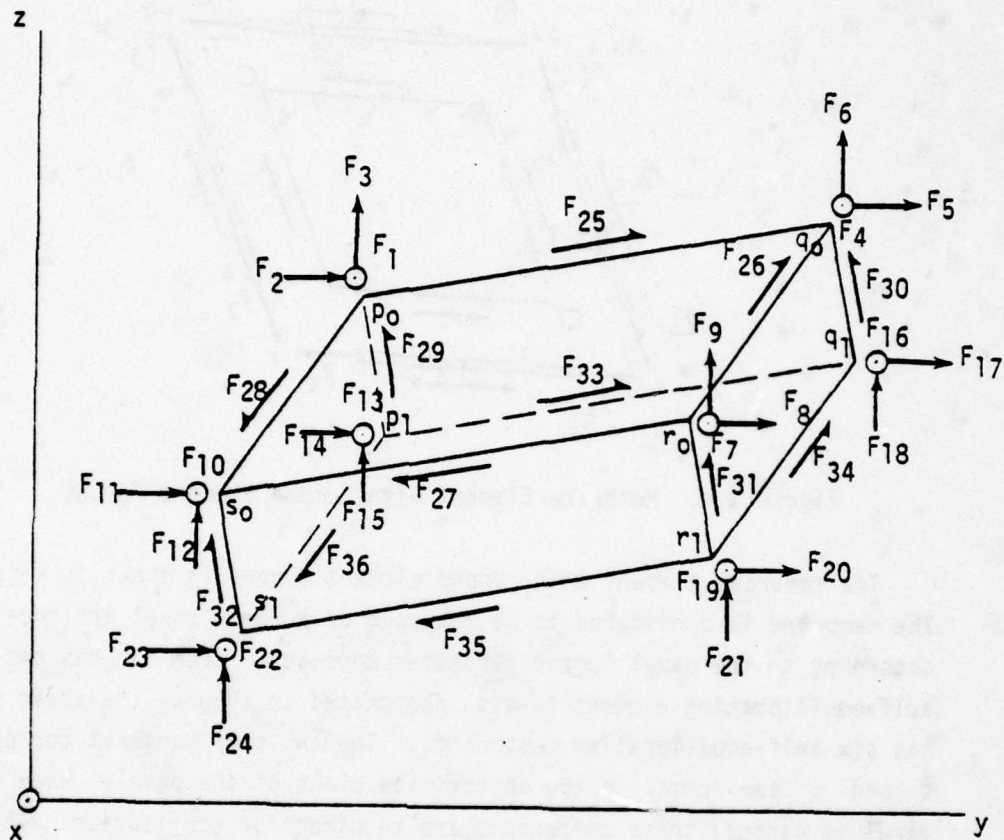


Figure 2.5. Cell Element Forces

The cell element, with its element forces, is shown in Figure 2.5. The symbols p_0 , q_0 , r_0 , s_0 , p_1 , q_1 , r_1 , s_1 identify joints connected by the cell, as established by the user. The surfaces $p_0q_0r_0s_0$ and $p_1q_1r_1s_1$ are approximate parallelograms, and are approximately flat and parallel. The edges p_0p_1 , q_0q_1 , r_0r_1 and s_0s_1 are approximately normal to the upper and lower surfaces. The forces at the corners are parallel to the global coordinate axes. The other forces are parallel to the edges of the cell, and act at the centers of the edges. The positive senses for the edge shear forces are defined

in Appendix C, and are not necessarily as shown. The element displacement vectors e_1, e_2, \dots, e_{36} , coincide with the force vectors.

This element has corner and edge connectivity.

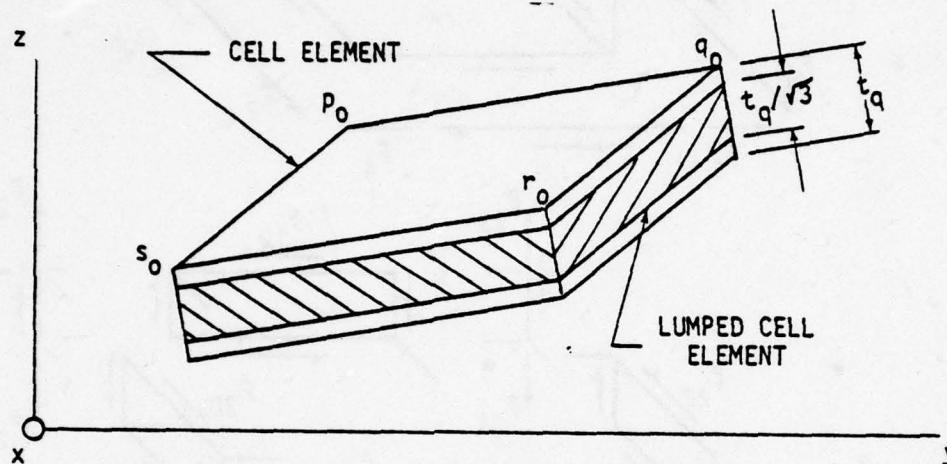


Figure 2.6. Cell Element and Lumped Cell Element

Figure 2.6 shows the method of lumping the cell element. The thickness of the lumped element is reduced by a factor of $1/\sqrt{3}$, so that the lumped element can have the same bending, torsional, normal and shearing stiffnesses in the elastic range as the actual plate element being represented, as explained in Appendix C.

The lumped elements for the cell, and their element forces, are shown in Figure 2.7. The lumped structure is essentially a torque box. Cross-sectional areas of bars and thicknesses of shear panels are selected so that the element will have the proper stiffness. The lumped element of reduced thickness is joined to the upper and lower surfaces of the cell by means of a statically determinate linkage, as described in Appendix C.

Each bar of the lumped element has two self-equilibrating element force components and each shear panel has six components, as in the case of the

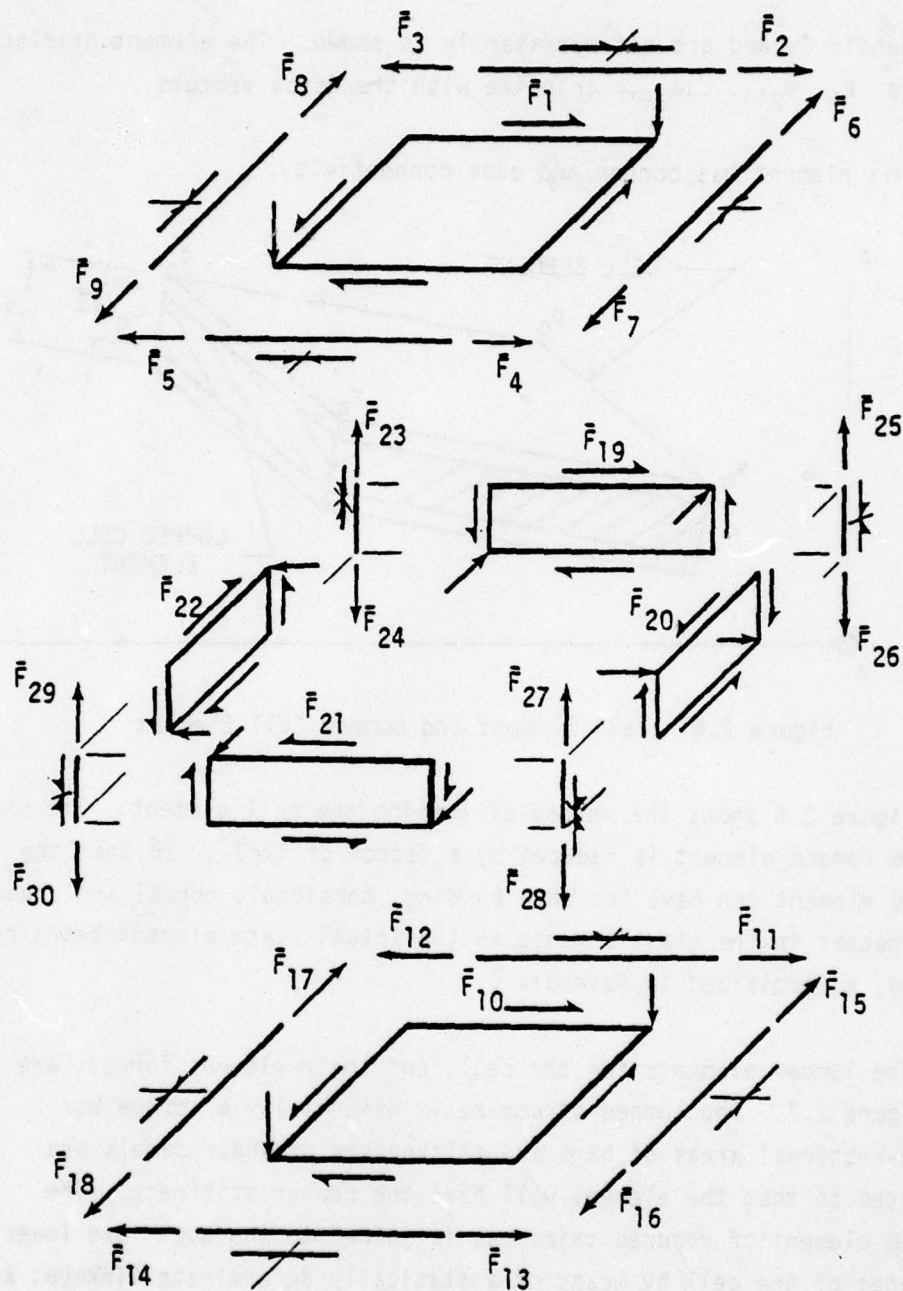


Figure 2.7. Lumped Element Forces for Cell

membrane, designated as shown. The corresponding element deformations are designated $\bar{e}_1, \bar{e}_2, \dots, \bar{e}_{30}$. The deformations are equal to the works done by unit values of the element forces, during a virtual deformation.

Equations relating the F and \bar{F} forces can be derived on the basis of equilibrium.

Element Stiffness Matrices

Stiffness matrices for the bar, membrane and cell elements are derived in Appendix C. Matrices of unassembled deformations resulting from temperature changes are also presented.

The derivations for the bar element are conventional.

The matrices for the membrane element are derived on the assumption that the element is approximately a flat parallelogram, although equilibrium is satisfied for any shape. In the applications, the shape of the element should not be allowed to depart too much from the flat parallelogram. The matrices automatically account for the effects of Poisson's ratio, and membrane skewness. The lumping procedure is also accomplished automatically.

The matrices for the cell are derived on the assumption that the element is approximately a parallelepiped having two parallelogram faces and four rectangular faces. In the applications, the element should not be allowed to depart too much from this shape, although equilibrium is satisfied for any shape. The matrices account for the effects of Poisson's ratio and skewness. Lumping is automatic.

Element Damping Matrices

Damping matrices for bar, membrane and cell elements are derived from the corresponding stiffness matrices by multiplying by suitable scale

factors. This procedure does not imply that the assembled damping matrix for the structure is a scale factor times the assembled stiffness matrix, since each element can have a different scale factor. Damping force vectors for the elements coincide with stiffness force vectors.

Element Mass Matrices

Inertia force vectors for the elements coincide with stiffness force vectors, except that no inertia force vectors are provided at the mid-points of bars, or at the centers of membrane and cell edges. Also, no lumped inertia forces are defined. Mass matrices for the elements are taken from the literature. (See Appendix C and Reference 1.)

Point Mass Element

This element represents a finite mass concentrated at a point. Three components of inertia force and displacement are defined for the element parallel to the global coordinate axes. Point mass elements can be affixed to joints but not to shear nodes.

Material Behavior

The following paragraphs describe material properties considered in the theoretical formulation of the Math Model. The formulation accounts for several phenomena not implemented in the computer program, because of time constraints. The phenomena not implemented include the effects of plasticity; thermal loads resulting from damping energy dissipated as heat; and the dependence of material properties on temperature changes occurring after initial impact. The effects of damping, and the dependence of material properties on initial temperatures, are included in the program.

The materials comprising the model are assumed to be isotropic. The Math Model can be modified to accommodate anisotropic elastic materials with relatively few changes.

Plasticity is considered in the formulation in deriving element stresses and strains. Load is applied to the structure incrementally in time. The components of strain occurring during an increment are assumed to be related to the corresponding incremental stress components according to the Prandtl-Reuss equations which satisfy the Von Mises yield criterion. Plastic strains are assumed to occur in any element only as long as the equivalent stress increases. As soon as the equivalent stress starts to decrease (i.e., the element starts to "unload") the element is assumed to become elastic, and to remain elastic thereafter. The term "equivalent stress" is defined in Appendix D, on Plasticity.

In windshields and canopies subjected to bird impact, damping effects are not very significant, except in the interlayers of laminated transparencies, and even there they are small, because only the brief period during and immediately after impact is of interest. Consequently linear viscous damping is assumed, to simplify the analysis. Section III presents a test-analysis correlation for a laminated cantilever beam, that confirms the validity of this assumption.

In the formulation, temperatures at initial impact are considered to be input, and these temperatures are updated incrementally, assuming that damping energy dissipated during an increment is converted to heat. No heat transfer is considered because of the brief duration of impact. Thermal stresses are taken into account.

Material stiffness, damping and thermal properties are temperature dependent, and these properties are considered to be updated during the solution.

Many material properties are strain rate dependent. The user accounts for this dependence by estimating strain rates expected at various points in the transparency, and inputting material properties reflecting these estimated rates. Strain rate dependence is not automatically taken into account during the calculation, because such a procedure would greatly increase the cost of the calculation. Furthermore the roughness of available data concerning the effects of strain rate does not justify a more elaborate approach at this time.

LOADS

The loads that the impacting bird produces on the windshield or canopy, are functions of the bird mass, bird shape, angle of incidence, and relative velocity of bird and transparency before and after initial impact. The loaded region apparently is not confined to the initial area of impact. Data obtained from F-16 canopy tests indicate that, after initial impact, the bird slides along the surface, applying loads along the path of contact, for an appreciable distance. The problem is complicated by the fact that the transparency displaces during contact, so that the relative velocity may be less or more than it was before contact, depending on whether the surface is retreating from the bird, or rebounding into it. This effect is referred to subsequently as bird-windshield interaction, or target compliance.

The effects of target compliance were considered to be beyond the scope of the present investigation. The effects of an area of contact that moves along the surface are considered. Such a moving contact area is subsequently called a traveling footprint.

When the complications resulting from target compliance are eliminated, the loads produced by the bird on the transparency can be calculated separately from, and prior to, the transparency response. Accordingly, Appendix G presents the method of calculating the bird impact loads, considering a traveling footprint.

The subsequent analysis contains provisions for thermal loads. These provisions have not been implemented in the Math Model computer program, consequently the method of computing thermal loads is not discussed in detail.

THE NONLINEAR EQUATION OF MOTION

The equation of motion is derived, considering geometric and material nonlinearities.

Force and Displacement Matrices

Matrices of forces and displacements are defined, to provide a basis for deriving the equation of motion.

The element forces and displacements, and the self-equilibrating ("lumped") element forces and deformations were defined and numbered as described in preceding paragraphs. Now number the structural elements themselves, consecutively, beginning with 1. Axially loaded bars, membranes, cells and point masses are included in this numbering scheme. Bars and panels that are components of cells and membranes are not individually numbered. Let

$\bar{F}_i(t)$, $\bar{e}_i(t)$ = column matrices of self-equilibrating element forces and deformations of the i th element at time t . If the i th element is a cell, $\bar{F}_i(t)$ has 30 rows, since a cell has 30 self-equilibrating element forces, as shown in Figure 2.7.

$F_i(t)$, $e_i(t)$ = column matrices of element forces and displacements of the i th element at time t . Again, if the i th element is a cell, $F_i(t)$ has 36 rows, since a cell had 36 element forces, as shown in Figure 2.5.

Structural nodes are of two kinds: joints and shear nodes, as previously defined. Each joint has three degrees of freedom, parallel to the global axes, and each shear node has one, parallel to a bar, or to the edge of a membrane or cell.

Let

$P_T(t)$, $\Delta_T(t)$ = column matrices of external loads and displacements in the nodal degrees of freedom, at time t .

The subscript "T" stands for "total" and indicates that all nodal degrees of freedom, whether constrained or unconstrained, are included in these matrices.

Some nodes are unconstrained, others are constrained by reactions. All shear nodes are unconstrained, as reactions are allowed only at joints.

A set of unconstrained degrees of freedom is defined. Unconstrained joint degrees of freedom are parallel to the global axes. Shear node degrees of freedom, all unconstrained, are parallel to the bars and to the edges of membranes and cells.

A set of constrained degrees of freedom is also defined for joints. The constrained degrees of freedom are parallel to joint reactions which can be inclined to the global axes. Choosing the constrained degrees of freedom in this manner means that reactions have no components in unconstrained degrees of freedom. As will be shown, the effect of this choice is to eliminate reactions from the equation of motion, even when they are inclined. Let

$P_U(t)$, $\Delta(t)$ = column matrices of nodal loads and displacements in the unconstrained degrees of freedom at time t .

$R(t)$, $\Delta_C(t)$ = column matrices of reactions and displacements in the constrained degrees of freedom at time t .

A modal displacement transformation of the kind described in Appendix A is applied, as a means of reducing the order of the matrices

involved in the equation of motion. Let

$\bar{P}_U(t), \bar{\Delta}(t)$ = column matrices of transformed loads and displacements at time t .

Other sets of forces and displacements, or deformations, are defined in the process of deriving the element stiffness matrices in Appendix C, but these quantities are not required in deriving the equation of motion.

Force and Displacement Transformations

Let

$\bar{F}_i(t)$ = a rectangular matrix of element forces resulting from unit values of the lumped element forces for the i th element at time t .

P_{TF_i} = a rectangular matrix of components in the nodal degrees of freedom resulting from unit values of the element forces of the i th element.

P_{UPT}, P_{CPT} = rectangular matrices of components in the unconstrained and constrained degrees of freedom of unit loads in the nodal degrees of freedom.

From these definitions, and the definitions of the force matrices previously given, it follows that

$$F_i(t) = F_{\bar{F}_i}(t) \bar{F}_i(t) \quad (1)$$

$$P_T(t) = P_{TF_i} F_i(t) \quad (2)$$

$$\begin{Bmatrix} P_U(t) \\ R(t) \end{Bmatrix} = \begin{bmatrix} P_{UPT} \\ P_{CPT} \end{bmatrix} P_T(t) \quad (3)$$

The matrices $F_{\bar{F}}(t)$, P_{TF} , P_{UPT} and P_{CPT} can be derived from equilibrium. For example, consider the simple structure shown in Figure 2.8, consisting of an axially loaded bar parallel to the YZ plane, and five constraints, at time t . The figure shows unconstrained and constrained degrees of freedom.

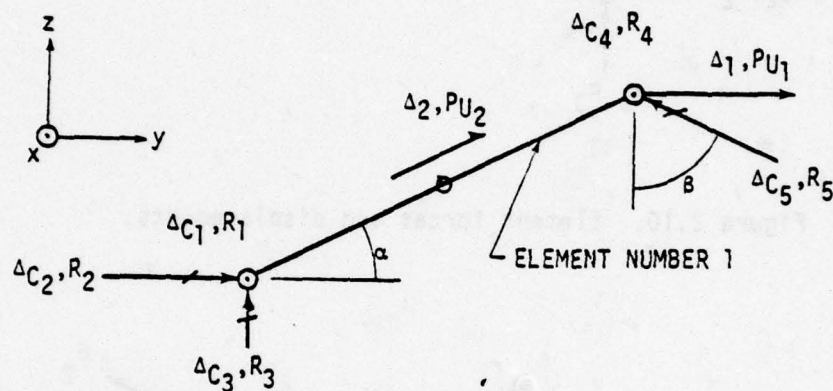


Figure 2.8. Simple structure with unconstrained and constrained degrees of freedom.

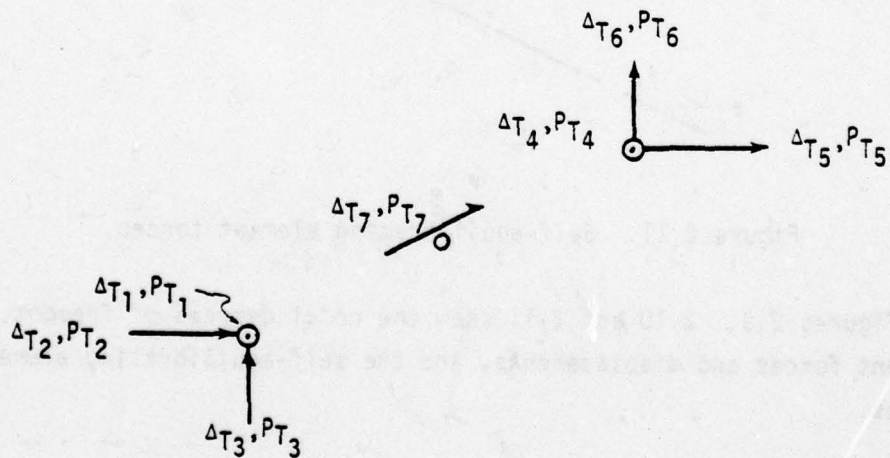


Figure 2.9. Nodal degrees of freedom.

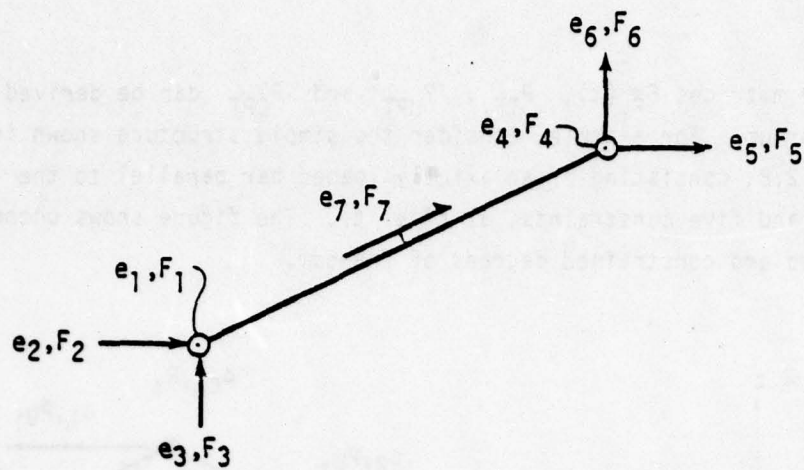


Figure 2.10. Element forces and displacements.

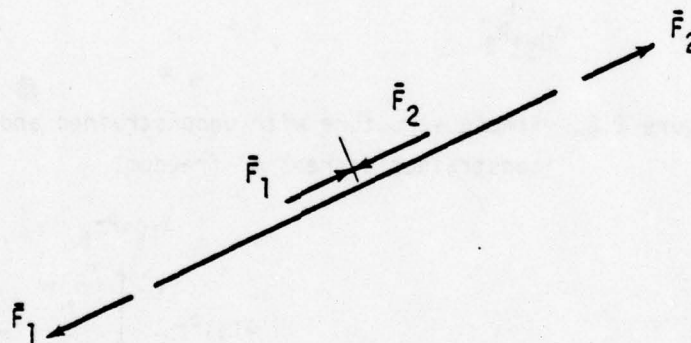


Figure 2.11. Self-equilibrating element forces.

Figures 2.9, 2.10 and 2.11 show the nodal degrees of freedom, the element forces and displacements, and the self-equilibrating element forces.

The following force transformation matrices are derived from the figures:

$$P_{UPT} = \begin{bmatrix} 0 & 0 & 0 & 0 & 1 & \tan \beta & 0 \\ 0 & 0 & 0 & 0 & 0 & 0 & 1 \end{bmatrix} \quad (4)$$

$$P_{CPT} = \begin{bmatrix} 1 & & & & & & \\ & 1 & & & & & \\ & & 1 & & & & \\ & & & 1 & & & \\ & & & & 0 & \frac{1}{\cos \beta} & 0 \end{bmatrix} \quad (5)$$

$$P_{TF_1} = -I \quad (\text{negative unit matrix}) \quad (6)$$

$$F_{F_1} = \begin{bmatrix} 0 & 0 \\ -\cos \alpha & 0 \\ -\sin \alpha & 0 \\ 0 & 0 \\ 0 & \cos \alpha \\ 0 & \sin \alpha \\ 1 & -1 \end{bmatrix} \quad (7)$$

These matrices can be derived through equilibrium considerations. For example, the definition of P_{UPT} shows that the element in the 1st row and 6th column of this matrix must be the component in the 1st unconstrained degree of freedom, shown in Figure 2.8, of a unit force in the 6th nodal degree of freedom, shown in Figure 2.9. These components are shown in Figure 2.12. The vertical vector represents a unit force in the 6th nodal degree of freedom. The horizontal vector is the component of this vector in the 1st unconstrained degree of freedom, and represents the element in the 1st row and 6th column of P_{UPT} .

The diagonal component, from Figures 2.8 and 2.9, represents the element in the 5th row and 6th column of P_{CPT} .

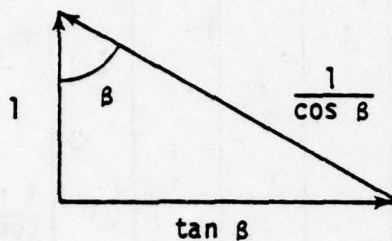


Figure 2.12. Components of a unit value of P_{T6} .

The matrix P_{TF1} would be the unit matrix since, from Figures 2.9 and 2.10, the P_T and F components are all parallel, except that the P_T components act on the nodes, while the F components act on the elements, and components equal and opposite to the F components act on the nodes. Hence the minus sign. If a structure has more than one element, the matrix P_{TFi} , for the i th element, becomes a Boolean matrix, composed of -1's and 0's.

Figure 2.13(a) shows a unit value of self-equilibrating element force number 1, shown in Figure 2.11. Figure 2.13(b) shows this vector broken into components parallel to the element forces of Figure 2.10. The first column of the matrix \bar{F}_{F1} can be derived by comparing Figures 2.13(a) and 2.13(b).

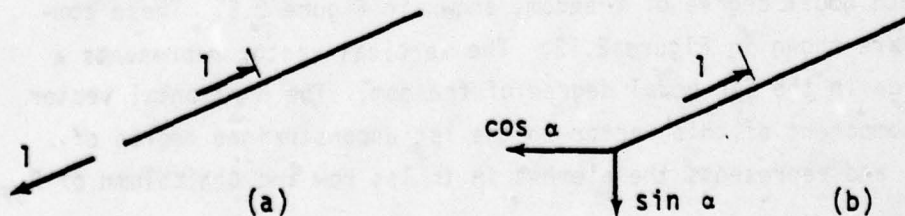


Figure 2.13. Components of a unit value of \bar{F}_1 .

Note that the elements of the matrix $F_{\bar{F}}(t)$ are functions of time, as the notation indicates, because the \bar{F} components rotate with respect to the global reference frame, as the structure deforms. The other force transformation matrices, P_{TF_i} , P_{UPT} and P_{CPT} , are constant.

The displacement transformations can now be derived from the force transformations according to the principle of virtual work, as described in Appendix A. From Equations 1, 2 and 3, the displacement transformations are

$$d\bar{e}_i = F_{\bar{F}_i}^T(t) de_i \quad (8)$$

$$e_i'(t) = -P_{TF_i}^T \Delta_T(t) \quad (9)$$

$$\Delta_T(t) = \begin{bmatrix} P_{UPT}^T & P_{CPT}^T \end{bmatrix} \begin{Bmatrix} \Delta(t) \\ \Delta_C(t) \end{Bmatrix} \quad (10)$$

Equation 8 must be written in differential form because the transformation $F_{\bar{F}}$ is a function of time. Equation 9 is based upon a consideration of the work done on the structural nodes by the external loads, and by forces that are equal and opposite to the element forces. The minus is the result of the fact that forces opposite to the element forces act on the nodes.

In addition to these transformations, a modal transformation of the kind described in Appendix A is employed. This transformation is

$$\Delta(t) = T\bar{\Delta}(t) \quad (11)$$

where

T = a rectangular modal transformation matrix

$\bar{\Delta}(t)$ = a column matrix of modal amplitudes

Each column of the matrix T represents a natural vibration mode of the undamped structure. If T is a square non-singular matrix, the number of modal amplitudes, or transformed displacements, is equal to the number of untransformed displacements, and no approximation is introduced. If T is rectangular, with more rows than columns, the number of transformed displacements is significantly reduced, although approximations are thus introduced. If T is an appropriate transformation, the approximations are small. The method of computing T is described in Appendix F.

The force transformation corresponding to Equation 11 is

$$\bar{P}_U(t) = T^T P_U(t) \quad (12)$$

This equation is derived on the basis of virtual work, as described in Appendix A.

Constrained Displacements

The assumption is now made that reactions are not displaced. Therefore

$$\Delta_C(t) = 0 \quad (13)$$

Constitutive Equations

The element forces contained in the matrix $F_i(t)$ represent sums of inertia, damping, and stiffness forces. Let

$F_{M_i}(t)$, $F_{C_i}(t)$, $F_{K_i}(t)$ = column matrices of inertia, damping, and stiffness forces acting upon the i th element.

The matrix of resultant forces on the i th element is therefore

$$F_i(t) = F_{M_i}(t) + F_{C_i}(t) + F_{K_i}(t) \quad (14)$$

Let

$\bar{F}_{C_i}(t)$, $\bar{F}_{K_i}(t)$ = column matrices of self-equilibrating damping and stiffness forces acting upon the i th element.

Self-equilibrating inertia force matrices are not defined, because the element mass matrices referred to global coordinates are independent of element orientation, and because no inertia force components are defined for shear nodes (See Appendix C).

The self-equilibrating stiffness forces are related to the corresponding deformations according to the equation

$$d\bar{F}_{K_i} = \bar{k}_i(t) (d\bar{e}_i - d\bar{e}_{0_i}) \quad (15)$$

where

\bar{e}_{0_i} = a column matrix of unassembled thermal deformations for the i th element.

$\bar{k}_i(t)$ = a square stiffness matrix for the i th element.

Equation 15 must be written in differential form, because the stiffness matrix \bar{k}_i is a function of time, as a result of geometric nonlinearity and plasticity. The matrix $d\bar{e}_i$ represents the total element deformations resulting from both mechanical and thermal loads. Therefore the difference $d\bar{e}_i - d\bar{e}_{0_i}$ represents deformations resulting from mechanical loads only. Consequently the differential element force matrix is proportional to this difference, as the equation indicates. Refer to Appendices C and E for the derivation of \bar{k}_i .

Similarly, the self-equilibrating damping forces are related to the rates of change of the element deformations according to the equation

$$\bar{F}_{C_i}(t) = \bar{c}_i(t) [\dot{\bar{e}}_i(t) - \dot{\bar{e}}_{0_i}(t)] \quad (16)$$

where $\dot{\bar{e}}_i(t) = d\bar{e}_i/dt$, $\dot{\bar{e}}_{o_i}(t) = d\bar{e}_{o_i}/dt$ (17)

and

$\bar{c}_i(t)$ = a square damping matrix for the i th element.

Equation 17 is based on the assumption of linear viscous damping. See Appendix C for the derivation of $\bar{c}_i(t)$.

Inertia forces are related to element accelerations according to the equation

$$F_{M_i}(t) = m_i \ddot{e}_i(t) \quad (18)$$

where $\ddot{e}_i(t) = d^2 e_i / dt^2$ (19)

and

m_i = a square mass matrix for the i th element.

The mass matrix can be considered constant. See Appendix C.

Equation of Motion, Nodal Degrees of Freedom

The nodes of the structure must be in equilibrium under the action of the inertia forces, the damping forces, the stiffness forces, the external loads, and the reactions. Therefore

$$\sum_i P_{TF_i} F_{M_i}(t) + \sum_i P_{TF_i} F_{C_i}(t) + \sum_i P_{TF_i} F_{K_i}(t) + P_{(\phi)T}(t) + P_{(R)T}(t) = 0 \quad (20)$$

where

$P_{(\phi)T}(t)$, $P_{(R)T}(t)$ = column matrices of components of the external loads and the reactions in the nodal degrees of freedom at time t .

Equation 20 is the equilibrium equation for components of forces in the nodal degrees of freedom. The first term represents components

of inertia forces in these degrees of freedom, since P_{TF_i} is a matrix of components resulting from unit values of the element forces, and $F_{M_i}(t)$ is a matrix of inertia element forces for the i th element. The product $P_{TF_i} F_{M_i}(t)$ is summed on i , so that the contributions of inertia forces acting on all elements adjacent to each node will be taken into account. Similarly, the second and third terms represent the components of damping and stiffness forces. The last two terms are the contributions of external loads and reactions.

Equation 1 expresses the relation between the element forces, and the self-equilibrating element forces. In particular, for damping and stiffness element forces,

$$F_{C_i}(t) = F_{\bar{F}_i}(t) \bar{F}_{C_i}(t) \quad (21)$$

$$F_{K_i}(t) = F_{\bar{F}_i}(t) \bar{F}_{K_i}(t) \quad (22)$$

Substituting these expressions into Equation 20 gives

$$\sum_i P_{TF_i} [F_{M_i}(t) + F_{\bar{F}_i}(t) \bar{F}_{C_i}(t) + F_{\bar{F}_i}(t) \bar{F}_{K_i}(t)] + P_{(\phi)T}(t) + P_{(R)T}(t) = 0 \quad (23)$$

The element forces are now eliminated from the equilibrium equation by invoking the constitutive relations and the displacement transformations. From Equations 8 and 9,

$$de_i = - F_{\bar{F}_i}^T(t) P_{TF_i}^T d\Delta_T(t) \quad (24)$$

$$\therefore d\bar{e}_i = - P_{T\bar{F}_i}^T(t) d\Delta_T(t) \quad (25)$$

$$\text{where } P_{T\bar{F}_i}(t) = P_{TF_i} F_{\bar{F}_i}(t) \quad (26)$$

Dividing Equation 25 by the differential dt , and employing Equation 17 gives

$$\dot{\bar{e}}_i(t) = -P_{TF_i}^T(t)\dot{\Delta}_T(t) \quad (27)$$

where

$$\dot{\Delta}_T(t) = d\Delta_T/dt \quad (28)$$

Differentiating Equation 9 twice with respect to time, gives

$$\ddot{e}_i(t) = -P_{TF_i}^T\ddot{\Delta}_T(t) \quad (29)$$

where $\ddot{e}_i(t) = d^2e_i/dt^2$ $\ddot{\Delta}_T(t) = d^2\Delta_T/dt^2$ (30)

From Equations 15 and 17,

$$d\bar{F}_{K_i} = \bar{k}_i(t) \left[\dot{\bar{e}}_i(t) - \dot{\bar{e}}_{o_i}(t) \right] dt \quad (31)$$

Substituting $\ddot{e}_i(t)$ from Equation 29 into Equation 18 gives

$$F_{M_i}(t) = -m_i P_{TF_i}^T \ddot{\Delta}_T(t) \quad (33)$$

Substituting $\dot{\bar{e}}_i(t)$ from Equation 27 into Equations 16 and 31 gives

$$\bar{F}_{C_i}(t) = \bar{c}_i(t) \left[-P_{TF_i}^T(t)\dot{\Delta}_T(t) - \dot{\bar{e}}_{o_i}(t) \right] \quad (34)$$

$$d\bar{F}_{K_i} = \bar{k}_i(t) \left[-P_{TF_i}^T(t)\dot{\Delta}_T(t) - \dot{\bar{e}}_{o_i}(t) \right] dt \quad (35)$$

Figure 2.14 shows the division of time into increments. The time at the beginning of the β th increment is $t_{\beta-1}$.

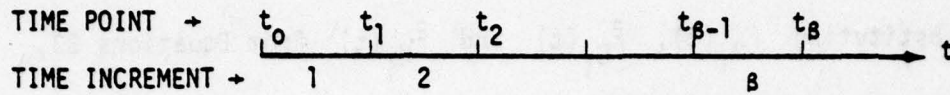


Figure 2.14. Time points and increments.

Integrate Equation 35 with respect to time, from $t = t_{\beta-1}$ to $t = t$. The upper limit of integration is any time in the β th increment.

$$\therefore \int_{t_{\beta-1}}^t d\bar{F}_{K_i} = - \int_{t_{\beta-1}}^t \bar{k}_i(t) \left[P_{TF_i}^T(t) \dot{\Delta}_T(t) + \dot{\bar{e}}_{o_i}(t) \right] dt \quad (36)$$

$$\therefore \bar{F}_{K_i}(t) = \bar{F}_{K_i}(t_{\beta-1}) - \int_{t_{\beta-1}}^t \bar{k}_i(t) \left[P_{TF_i}^T(t) \dot{\Delta}_T(t) + \dot{\bar{e}}_{o_i}(t) \right] dt \quad (37)$$

From Equations 23 and 26,

$$\begin{aligned} \sum_i P_{TF_i} \bar{F}_{M_i}(t) + \sum_i P_{TF_i}(t) \bar{F}_{C_i}(t) + \sum_i P_{TF_i}(t) \bar{F}_{K_i}(t) \\ + P_{(\phi)T}(t) + P_{(R)T}(t) = 0 \end{aligned} \quad (38)$$

Substituting $F_{M_i}(t)$, $\bar{F}_{C_i}(t)$ and $\bar{F}_{K_i}(t)$ from Equations 33, 34, and 37 into Equation 38 gives

$$\begin{aligned}
 & - \sum_i P_{TF_i} m_i P_{TF_i}^T \ddot{a}_T(t) + \sum_i P_{TF_i}(t) \bar{c}_i(t) \left[-P_{TF_i}^T(t) \dot{a}_T(t) - \dot{\bar{e}}_{O_i}(t) \right] \\
 & + \sum_i P_{TF_i}(t) \left\{ \bar{F}_{K_i}(t_{B-1}) - \int_{t_{B-1}}^t \bar{k}_i(t) \left[P_{TF_i}^T(t) \dot{a}_T(t) + \dot{\bar{e}}_{O_i}(t) \right] dt \right\} \\
 & + P_{(\phi)T}(t) + P_{(R)T}(t) = 0
 \end{aligned} \tag{39}$$

Let

$$M_T = \sum_i P_{TF_i} m_i P_{TF_i}^T \tag{40}$$

$$C_T(t) = \sum_i P_{TF_i}(t) \bar{c}_i(t) P_{TF_i}^T(t) \tag{41}$$

$$P_{(K)TI}(t) = \sum_i P_{TF_i}(t) \bar{F}_{K_i}(t_{B-1}) \tag{42}$$

$$P_{TCO}(t) = - \sum_i P_{TF_i}(t) \bar{c}_i(t) \dot{\bar{e}}_{O_i}(t) \tag{43}$$

$$\delta P_{TKO_B}(t) = - \sum_i P_{TF_i}(t) \int_{t_{B-1}}^t \bar{k}_i(t) \dot{\bar{e}}_{O_i}(t) dt \tag{44}$$

Combining Equations 39, 40, 41, 42, 43 and 44 gives

$$M_T \ddot{\Delta}_T(t) + C_T(t) \dot{\Delta}_T(t) + \sum_i P_{TF_i}(t) \int_{t_{B-1}}^t \bar{k}_i(t) P_{TF_i}^T(t) \dot{\Delta}_T(t) dt$$

$$= P_{(K)TI}(t) + P_{TCO}(t) + \delta P_{TKO_B}(t) + P_{(\phi)T}(t) + P_{(R)T}(t) \quad (45)$$

where $t_{B-1} < t < t_B$ (46)

Equation 45 is the nonlinear equation of motion, expressed in terms of the unknown nodal displacements, $\Delta_T(t)$, for the B th time increment. The new symbols in the equation have the following significance:

$M_T, C_T(t)$ = assembled mass and damping matrices (square)
referred to the nodal degrees of freedom.

$P_{(K)TI}(t)$ = a column matrix of components in the nodal degrees of freedom at time t of the interior stiffness forces existing at the beginning of the increment.

$P_{TCO}(t)$ = a column matrix of equivalent external loads in the nodal degrees of freedom resulting from rates of change of unassembled thermal deformations at time t .

$\delta P_{TKO_B}(t)$ = a column matrix of equivalent external loads in the nodal degrees of freedom resulting from thermal deformations produced in the structure between the beginning of the B th increment and the time t

Let

$$P_{T_B}(t) = P_{(K)TI}(t) + P_{TCO}(t) + \delta P_{TKO_B}(t) + P_{(\phi)T}(t) + P_{(R)T}(t) \quad (47)$$

Combining Equations 45 and 47 gives

$$M_T \ddot{\Delta}_T(t) + C_T(t) \dot{\Delta}_T(t) + \sum_i P_{TF_i}(t) \int_{t_{B-1}}^t \bar{k}_i(t) P_{TF_i}(t) \dot{\Delta}_T(t) dt = P_{TB}(t) \quad (48)$$

where

$P_{TB}(t)$ = a column matrix of thermomechanical loads in the nodal degrees of freedom.

Equation of Motion, Unconstrained Degrees of Freedom

The equation of motion is written in terms of components of displacement in the unconstrained degrees of freedom.

From Equations 10 and 13,

$$\Delta_T(t) = P_{UPT}^T \Delta(t) \quad (49)$$

Substituting $\Delta_T(t)$ from Equation 49 into Equation 48, and multiplying the resulting expression on the left by P_{UPT} gives

$$M \ddot{\Delta}(t) + C(t) \dot{\Delta}(t) + \sum_i P_{UF_i}(t) \int_{t_{B-1}}^t \bar{k}_i(t) P_{UF_i}^T(t) \dot{\Delta}(t) dt = P_{UB}(t) \quad (50)$$

where

$$M = P_{UPT} M_T P_{UPT}^T \quad (51)$$

$$C(t) = P_{UPT} C_T(t) P_{UPT}^T \quad (52)$$

$$P_{UF_i}(t) = P_{UPT} P_{TF_i}(t) \quad (53)$$

$$P_{U_B}(t) = P_{UPT} P_{T_B}(t) \quad (54)$$

$$\text{and } \dot{\Delta}(t) = d\Delta/dt, \quad \ddot{\Delta}(t) = d^2\Delta/dt^2 \quad (55)$$

Equation 50 is the equation of motion written in terms of components of displacement in the unconstrained degrees of freedom. From Equations 47 and 54,

$$P_{U_B}(t) = P_{(K)UI}(t) + P_{UCO}(t) + \delta P_{UKO_B}(t) + P_{(\phi)U}(t) + P_{(R)U}(t) \quad (56)$$

where

$$P_{(K)UI}(t) = P_{UPT} P_{(K)TI}(t) \quad (57)$$

$$P_{UCO}(t) = P_{UPT} P_{TCO}(t) \quad (58)$$

$$\delta P_{UKO_B}(t) = P_{UPT} \delta P_{TKO_B}(t) \quad (59)$$

$$P_{(\phi)U}(t) = P_{UPT} P_{(\phi)T}(t) \quad (60)$$

$$P_{(R)U}(t) = P_{UPT} P_{(R)T}(t) \quad (61)$$

Eliminating $P_{(K)TI}(t)$, $P_{TCO}(t)$ and $\delta P_{TKO_B}(t)$ from Equations 42, 43, 44, 57, 58 and 59, and employing Equation 53 gives

$$P_{(K)UI}(t) = \sum_i P_{UF_i}(t) \bar{F}_{K_i}(t_{B-1}) \quad (62)$$

$$P_{UCO}(t) = - \sum_i P_{UF_i}(t) \bar{c}_i(t) \dot{\bar{e}}_{O_i}(t) \quad (63)$$

$$\delta P_{UKO_B}(t) = - \sum_i P_{UF_i}(t) \int_{t_{B-1}}^t \bar{k}_i(t) \dot{e}_{o_i}(t) dt \quad (64)$$

Also, from Equations 60 and 61, it follows that

$P_{(\phi)U}(t)$, $P_{(R)U}(t)$ = column matrices of components in the unconstrained degrees of freedom of unit values of the external loads and reactions.

Now the reactions have no components in the unconstrained degrees of freedom, because of the way that constrained and unconstrained degrees of freedom are defined (see the paragraph on "Force and Displacement Matrices").

$$\therefore P_{(R)U}(t) = 0 \quad (65)$$

$$\text{and } P_{U_B}(t) = P_{(K)UI}(t) + P_{UCO}(t) + \delta P_{UKO_B}(t) + P_{(\phi)U}(t) \quad (66)$$

Thus the reactions have been eliminated from the equation of motion. The fact that $P_{(R)U}(t) = 0$ can be verified from the example given in the paragraph on "Force and Displacement Transformations". Equation 4 gives P_{UPT} for the structure of Figure 2.8. The symbol $P_{(R)T}(t)$ denotes a matrix of components in the nodal degrees of freedom of the reactions. This matrix can be written

$$P_{(R)T}(t) = P_{TR}R(t) \quad (67)$$

where

P_{TR} = a rectangular matrix of components in the nodal degrees of freedom of unit values of the reactions.

$R(t)$ = a column matrix of reactions at time t .

The directions of the reactions are assumed to remain constant during the motion. From Figure 2.8 and 2.9

$$P_{TR} = \begin{bmatrix} 1 & & & & \\ & 1 & & & \\ & & 1 & & \\ & & & 1 & \\ & & & & -\sin\theta \\ & & & & \cos\theta \\ 0 & 0 & 0 & 0 & 0 \end{bmatrix} \quad (68)$$

From Equations 61 and 67,

$$P_{(R)U}(t) = P_{UPT} P_{TR} R(t) \quad (69)$$

But, from Equations 4 and 68,

$$P_{UPT} P_{TR} = 0 \quad (70)$$

$$\therefore P_{(R)U}(t) = 0 \quad (71)$$

APPROACH TO SOLVING THE NONLINEAR EQUATION OF MOTION

The untransformed differential equation of motion, Equation 50, is nonlinear, because the matrices $P_{UF_1}(t)$, $C(t)$ and $\bar{K}_1(t)$, which are coefficients of the matrix of dependent variables $\Delta(t)$, are influenced by large displacements and plasticity. The force transformation matrices $P_{UF_1}(t)$ are functions of displacements, because the lumped element forces rotate as the structure deforms, and thus introduce geometric nonlinearities. The assembled damping matrix $C(t)$ represents a nonlinearity, because it

involves $P_{UF_i}(t)$, and the element damping matrices $\bar{c}_i(t)$. The element damping matrices introduce nonlinearities because of plasticity and because the shapes of the elements can change if strains are very large. Similarly, the element stiffness matrices $\bar{k}_i(t)$ involve material and geometric nonlinearities. On the right hand side of the equation nonlinearities are introduced because the matrix $P_U(t)$ also depends on $P_{UF_i}(t)$, $\bar{c}_i(t)$ and $\bar{k}_i(t)$.

The approach to the solution of the equation of motion, considering the nonlinearities, includes the following features:

1. Time-wise incremental solution of the equation, with material property and nodal coordinate updating at the end of each time step.
2. Iterative solution of the geometrically nonlinear equation within each time step, based upon the method of Fictitious Forces and Deformations (FF&D).

Thus, two approaches to the geometrically nonlinear problem are provided: the incremental solution with coordinate updating, and the FF&D method. It is hoped that this dual approach will provide a more efficient and reliable solution to the problem, especially in intractable cases. In at least one case, the FF&D method provides a solution where coordinate updating fails: the buckling of a plane structure subjected to in-plane loads.

Fictitious Loads and Material Nonlinearities

Consider, first, the geometric nonlinearities resulting from the dependence of $P_{UF_i}(t)$ on time. From Equations 50 and 66, the equation of motion can be put in the form

$$\begin{aligned}
& \ddot{M}\Delta(t) + C(t)\dot{\Delta}(t) + \sum_i P_{U\bar{F}_i}(t) \int_{t_{B-1}}^t \bar{k}_i(t) P_{U\bar{F}_i}^T(t) \dot{\Delta}(t) dt \\
& = P_{(K)UI}(t) + P_{UCO}(t) + \delta P_{UKO_B}(t) + P_{(\phi)U}(t)
\end{aligned} \tag{72}$$

From Equations 62, 64 and 72,

$$\begin{aligned}
& \ddot{M}\Delta(t) + C(t)\dot{\Delta}(t) + \sum_i P_{U\bar{F}_i}(t) \int_{t_{B-1}}^t \bar{k}_i(t) P_{U\bar{F}_i}^T(t) \dot{\Delta}(t) dt \\
& = \sum_i P_{U\bar{F}_i}(t) \bar{F}_{K_i}(t_{B-1}) + P_{UCO}(t) - \sum_i P_{U\bar{F}_i}(t) \int_{t_{B-1}}^t \bar{k}_i(t) \dot{e}_{O_i}(t) dt \\
& \quad + P_{(\phi)U}(t)
\end{aligned} \tag{73}$$

The damping matrix $C(t)$ has not been written explicitly in terms of $P_{U\bar{F}_i}(t)$ for two reasons: (1) The effect of damping on the response of a windshield system to bird impact is small because of the short duration of impact, (2) Most of the damping in laminated transparencies occurs in the interlayers. This material acts primarily in shear in planes normal to the transparency surface. Consequently, the damping forces are not expected to contribute significantly to geometric nonlinearity, and such effects are therefore not considered.

In addition, $P_{UCO}(t)$ is a matrix of equivalent loads resulting from time rates of change of the unassembled thermal deformations. Since $P_{UCO}(t)$ represents a damping effect, its influence on the response is small. Therefore take

$$P_{UCO}(t) = 0 \tag{74}$$

The force transformation matrix $P_{UF_i}(t)$ can be written in the form

$$P_{UF_i}(t) = P_{UF_i}(t_{B-1}) + \delta P_{UF_i}(t), \quad (75)$$

where $P_{UF_i}(t_{B-1})$ = the value of $P_{UF_i}(t)$ at the beginning of the B th increment, and $\delta P_{UF_i}(t)$ is the change in P_{UF_i} occurring between times t_{B-1} and t , resulting from rotations of the lumped element forces during the time increment.

Substitute $P_{UCO}(t)$ and $P_{UF_i}(t)$ from Equations 74 and 75 into Equation 73 :

$$\begin{aligned} & M\ddot{\Delta}(t) + C(t)\dot{\Delta}(t) \\ & + \sum_i \left[P_{UF_i}(t_{B-1}) + \delta P_{UF_i}(t) \right] \int_{t_{B-1}}^t \bar{k}_i(t) P_{UF_i}^T(t) \dot{\Delta}(t) dt \\ & = \sum_i \left[P_{UF_i}(t_{B-1}) + \delta P_{UF_i}(t) \right] F_{K_i}(t_{B-1}) \\ & - \sum_i \left[P_{UF_i}(t_{B-1}) + \delta P_{UF_i}(t) \right] \int_{t_{B-1}}^t \bar{k}_i(t) \dot{e}_{O_i}(t) dt + P_{(\phi)U}(t) \end{aligned} \quad (76)$$

Therefore

$$\begin{aligned} & M\ddot{\Delta}(t) + C(t)\dot{\Delta}(t) + \sum_i P_{UF_i}(t_{B-1}) \int_{t_{B-1}}^t \bar{k}_i(t) P_{UF_i}^T(t) \dot{\Delta}(t) dt \\ & = \sum_i P_{UF_i}(t_{B-1}) \bar{F}_{K_i}(t_{B-1}) - \sum_i P_{UF_i}(t_{B-1}) \int_{t_{B-1}}^t \bar{k}_i(t) \dot{e}_{O_i}(t) dt \\ & \quad + P_{(\phi)U}(t) + \delta P_{(\bar{F})_B}(t) \end{aligned} \quad (77)$$

where

$$\begin{aligned} \delta P_{(\bar{F})_B}(t) &= \sum_i \delta P_{U\bar{F}_i}(t) \int_{t_{B-1}}^t \bar{k}_i(t) \left[-P_{U\bar{F}_i}^T(t) \dot{\Delta}(t) - \dot{\bar{e}}_{o_i}(t) \right] dt \\ &+ \sum_i \delta P_{U\bar{F}_i}(t) \bar{F}_{K_i}(t_{B-1}). \end{aligned} \quad (78)$$

But, from Equations 35 and 49,

$$d\bar{F}_{K_i} = \bar{k}_i(t) \left[-P_{T\bar{F}_i}^T(t) P_{UP}^T \dot{\Delta}(t) - \dot{\bar{e}}_{o_i}(t) \right] dt \quad (79)$$

Combining Equations 53 and 74 gives

$$d\bar{F}_{K_i} = \bar{k}_i(t) \left[-P_{U\bar{F}_i}^T(t) \dot{\Delta}(t) - \dot{\bar{e}}_{o_i}(t) \right] dt \quad (80)$$

Therefore from Equations 78 and 80,

$$\delta P_{(\bar{F})_B}(t) = \sum_i \delta P_{U\bar{F}_i}(t) \int_{t_{B-1}}^t d\bar{F}_{K_i} + \sum_i \delta P_{U\bar{F}_i}(t) \bar{F}_{K_i}(t_{B-1}). \quad (81)$$

$$\therefore \delta P_{(\bar{F})_B}(t) = \sum_i \delta P_{U\bar{F}_i}(t) \bar{F}_{K_i}(t) \quad (82)$$

Now eliminate $P_{U\bar{F}_i}^T(t)$ from Equation 77, employing Equation 75:

$$M\ddot{\Delta}(t) + C(t)\dot{\Delta}(t) + \sum_i P_{U\bar{F}_i}(t_{B-1}) \int_{t_{B-1}}^t \bar{k}_i(t) P_{U\bar{F}_i}^T(t_{B-1}) \dot{\Delta}(t) dt - \delta P_{K_f_B}(t)$$

$$\begin{aligned}
&= \sum_i P_{UF_i}(t_{B-1}) \bar{F}_{K_i}(t_{B-1}) - \sum_i P_{UF_i}(t_{B-1}) \int_{t_{B-1}}^t \bar{k}_i(t) \dot{\bar{e}}_{o_i}(t) dt \\
&\quad + P_{(\phi)U}(t) + \delta P_{(F)_B}(t)
\end{aligned} \tag{83}$$

$$\text{where } \delta P_{Kf_B}(t) = - \sum_i P_{UF_i}(t_{B-1}) \int_{t_{B-1}}^t \bar{k}_i(t) \delta P_{UF_i}^T(t) \dot{\Delta}(t) dt \tag{84}$$

The physical significances of the matrices $\delta P_{(F)_B}(t)$ and $\delta P_{Kf_B}(t)$ are explained in subsequent paragraphs.

In Equation 83, the element stiffness matrix $\bar{k}_i(t)$ is a function of time. As a simplification, consider $\bar{k}_i(t)$ constant during the B th increment. If the increment is not too long, this assumption should be satisfactory. Therefore replace $\bar{k}_i(t)$ by $\bar{k}_{i(B)}$, where

$\bar{k}_{i(B)}$ = the constant lumped stiffness matrix for the i th element applicable during the B th increment.

The term on the left of Equation 83 involving $\bar{k}_i(t)$ can now be simplified, thus:

$$\begin{aligned}
&\sum_i P_{UF_i}(t_{B-1}) \int_{t_{B-1}}^t \bar{k}_i(t) P_{UF_i}^T(t_{B-1}) \dot{\Delta}(t) dt \\
&= \sum_i P_{UF_i}(t_{B-1}) \bar{k}_{i(B)} P_{UF_i}^T(t_{B-1}) \int_{t_{B-1}}^t \dot{\Delta}(t) dt
\end{aligned} \tag{85}$$

$$= K_{(B)} \delta \Delta_B(t) \tag{86}$$

where
$$K_{(B)} = \sum_i P_{UF_i}(t_{B-1}) \bar{k}_{i(B)} P_{UF_i}^T(t_{B-1}) \quad (87)$$

and
$$\delta \Delta_B(t) = \Delta(t) - \Delta(t_{B-1}) \quad (88)$$

Similarly the terms on the right of Equation 83 involving $\bar{k}_i(t)$ can be simplified:

$$-\sum_i P_{UF_i}(t_{B-1}) \int_{t_{B-1}}^t \bar{k}_i(t) \ddot{e}_{o_i}(t) dt = -\sum_i P_{UF_i}(t_{B-1}) \bar{k}_{i(B)} \int_{t_{B-1}}^t \ddot{e}_{o_i}(t) dt \quad (89)$$

$$= \delta P_{K_{O_B}}(t) \quad (90)$$

where
$$\delta P_{K_{O_B}}(t) = -\sum_i P_{UF_i}(t_{B-1}) \bar{k}_{i(B)} \delta \ddot{e}_{o_i B}(t), \quad (91)$$

and
$$\delta \ddot{e}_{o_i B}(t) = \ddot{e}_{o_i}(t) - \ddot{e}_{o_i}(t_{B-1}) \quad (92)$$

Simplify the expression for $\delta P_{K_f B}(t)$ by replacing $\bar{k}_i(t)$ by $\bar{k}_{i(B)}$ in Equation 84:

$$\therefore \delta P_{K_f B}(t) = -\sum_i P_{UF_i}(t_{B-1}) \bar{k}_{i(B)} \int_{t_{B-1}}^t \delta P_{UF_i}^T(t) \dot{\Delta}(t) dt \quad (93)$$

Also let
$$P_{(K)U}(t_{B-1}) = \sum_i P_{UF_i}(t_{B-1}) \bar{F}_{K_i}(t_{B-1}) \quad (94)$$

Combining Equations 83, 86, 90 and 94 gives

$$\begin{aligned} M\ddot{\Delta}(t) + C(t)\dot{\Delta}(t) + K_{(B)}\delta\Delta_B(t) &= P_{(K)U}(t_{B-1}) + \delta P_{K_{O_B}}(t) \\ &+ P_{(\phi)U}(t) + \delta P_{(F)_B}(t) + \delta P_{K_f B}(t) \end{aligned} \quad (95)$$

From Equations 91 and 92, it follows that

$P_{K_0\beta}(t)$ = a column matrix of equivalent external loads in the unconstrained degrees of freedom resulting from unassembled deformations developed during the β th increment.

From Equation 94 :

$P_{(K)U}(t_{\beta-1})$ = a column matrix of components in the unconstrained degrees of freedom of the internal stiffness forces at time $t_{\beta-1}$.

The lumped element forces are given, from Equations 27 and 37, by

$$\bar{F}_{K_i}(t) = \bar{F}_{K_i}(t_{\beta-1}) + \int_{t_{\beta-1}}^t \bar{k}_i(t) [\ddot{e}_i(t) - \ddot{e}_{o_i}(t)] dt \quad (96)$$

Replacing $\bar{k}_i(t)$ by $\bar{k}_{i(\beta)}$ in Equation 96 gives

$$\bar{F}_{K_i}(t) = \bar{F}_{K_i}(t_{\beta-1}) + \bar{k}_{i(\beta)} \int_{t_{\beta-1}}^t [\ddot{e}_i(t) - \ddot{e}_{o_i}(t)] dt \quad (97)$$

Therefore, from Equation 92,

$$\bar{F}_{K_i}(t) = \bar{F}_{K_i}(t_{\beta-1}) + \bar{k}_{i(\beta)} [\delta \bar{e}_{i\beta}(t) - \delta \bar{e}_{o_i\beta}(t)] \quad (98)$$

where

$$\delta \bar{e}_{i\beta}(t) = \bar{e}_i(t) - \bar{e}_i(t_{\beta-1}) \quad (99)$$

Equation 98 gives the lumped element forces in terms of the incremental element deformations.

Now, from Equations 41, 52 and 53,

$$C(t) = \sum_i P_{UF_i}(t) \bar{c}_i(t) P_{UF_i}^T(t) \quad (100)$$

As previously explained, the geometric nonlinearity of the damping matrix $C(t)$, resulting from the variation of $P_{UF_i}(t)$ during the time increment, is not considered. Therefore replace $P_{UF_i}(t)$ by its value at the beginning of the increment, $P_{UF_i}(t_{\beta-1})$, in Equation 100. Also assume that $\bar{c}_i(t)$ can be replaced by $\bar{c}_{i(\beta)}$, where

$\bar{c}_{i(\beta)}$ = the constant lumped damping matrix for the i th element applicable during the β th increment.

This assumption also should be satisfactory if the increment is not too long. The matrix $C(t)$ is thus replaced by the matrix $C_{(\beta)}$, where

$$C_{(\beta)} = \sum_i P_{UF_i}(t_{\beta-1}) \bar{c}_{i(\beta)} P_{UF_i}^T(t_{\beta-1}) \quad (101)$$

Replacing $C(t)$ in Equation 95 by $C_{(\beta)}$ given by Equation 101 gives

$$\begin{aligned} M\ddot{\Delta}(t) + C_{(\beta)}\dot{\Delta}(t) + K_{(\beta)}\Delta_{\beta}(t) &= P_{(K)}U(t_{\beta-1}) + \delta P_{K0_{\beta}}(t) \\ &+ P_{(\phi)}U(t) + \delta P_{(\bar{F})_{\beta}}(t) + \delta P_{Kf_{\beta}}(t) \end{aligned} \quad (102)$$

where

$$t_{\beta-1} < t < t_{\beta} \quad (103)$$

Thus the material nonlinearities have been eliminated in Equation 102, by assuming that the element stiffness and damping matrices can be considered constant during each time increment. These nonlinearities will be taken into account by updating the element stiffness and damping matrices for each increment. This updating also will account for large strains that result from significant changes of shape of the elements during loading.

The geometric nonlinearities resulting from rotations of element forces have been eliminated from the left side of Equation 102, and appear only on the right side, where they are more tractable. These nonlinearities appear in $\delta P_{(\bar{F})_B}(t)$ and $\delta P_{Kf_B}(t)$ which are called matrices of fictitious loads. The justification for this nomenclature and the methods for evaluating these matrices are presented in subsequent paragraphs.

Fictitious Forces

Let

$P_{(K)U}(t)$ = a column matrix of components in the unconstrained degrees of freedom of the interior stiffness forces existing at time t .

Therefore,
$$P_{(K)U}(t) = \sum_i P_{U\bar{F}_i}(t) \bar{F}_{K_i}(t), \quad (104)$$

since $P_{U\bar{F}_i}(t)$ is a matrix of components in the unconstrained degrees of freedom of unit values of the self equilibrating or lumped element forces, and $\bar{F}_{K_i}(t)$ is a matrix of lumped forces. Note the distinction between $P_{(K)U}(t)$ and the matrix $P_{(K)UI}(t)$ given in Equation 62. Now let

$\bar{F}_{K_{0iB}}(t), \bar{F}_{K_{1iB}}(t)$ = column matrices of components of the lumped element stiffness forces, $\bar{F}_{K_i}(t)$, parallel and normal to the directions of the lumped forces at the beginning of the β th increments, for the i th element.

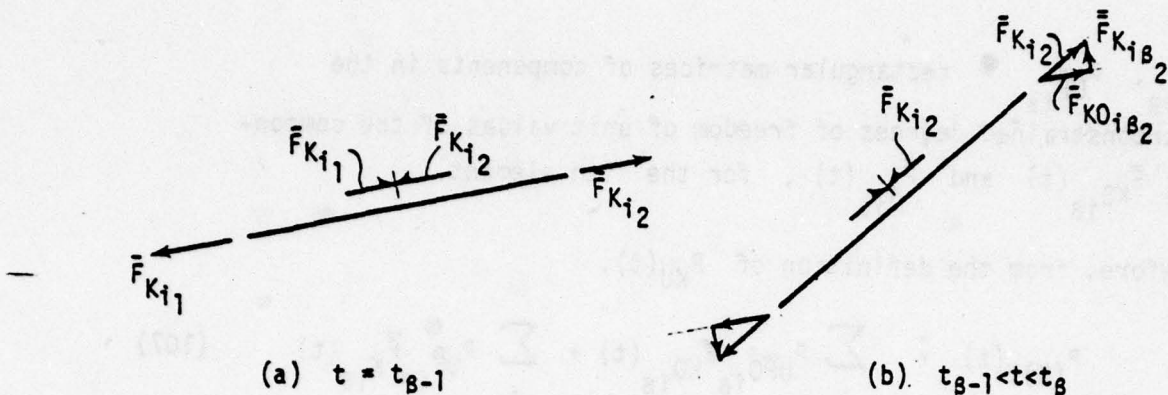


Figure 2.15. Components of an element force resulting from rotation of the element.

Figure 2.15(a) shows an axially loaded bar at the beginning of the β th increment. Figure 2.15(b) shows the element force components at a later time, after the bar has rotated. Note that the components of the self-equilibrating forces acting upon the shear node at the center of the bar need not be broken into components $\bar{F}_{K_{0i}}$ and \bar{F}_{K_i} , because the shear node degree of freedom is assumed to rotate with the bar. Let

$F_{OF_{i\beta}}(t)$, $\bar{F}_{F_{i\beta}}(t)$ = rectangular matrices of the components $F_{K_{0i\beta}}(t)$ and $\bar{F}_{K_{i\beta}}(t)$ resulting from unit values of the element forces $F_{K_i}(t)$ at time t during the β th increment. (The matrix $F_{OF_{i\beta}}(t)$ is actually square.)

Therefore, from the preceding definitions,

$$F_{K_{0i\beta}}(t) = F_{OF_{i\beta}}(t)F_{K_i}(t) \quad (105)$$

$$\bar{F}_{K_{i\beta}}(t) = \bar{F}_{F_{i\beta}}(t)F_{K_i}(t) \quad (106)$$

Let

$P_{UFO_{i\beta}}$, $P_{UF_{i\beta}}$ = rectangular matrices of components in the unconstrained degrees of freedom of unit values of the components $\bar{F}_{KO_{i\beta}}(t)$ and $\bar{F}_{K_{i\beta}}(t)$, for the i th element.

— Therefore, from the definition of $P_{KU}(t)$,

$$P_{(K)U}(t) = \sum_i P_{UFO_{i\beta}} \bar{F}_{KO_{i\beta}}(t) + \sum_i P_{UF_{i\beta}} \bar{F}_{K_{i\beta}}(t) \quad (107)$$

The matrices $P_{UFO_{i\beta}}$ and $P_{UF_{i\beta}}$ are constant during the β th increment, since the components $\bar{F}_{KO_{i\beta}}(t)$ and $\bar{F}_{K_{i\beta}}(t)$ are always parallel and normal to the directions of the lumped forces at the beginning of the increment. Note that

$$P_{UFO_{i\beta}} = P_{UF_i}(t_{\beta-1}) \quad (108)$$

$$\therefore P_{(K)U}(t) = \sum_i P_{UF_i}(t_{\beta-1}) \bar{F}_{KO_{i\beta}}(t) + \sum_i P_{UF_{i\beta}} \bar{F}_{K_{i\beta}}(t) \quad (109)$$

Substituting $\bar{F}_{KO_{i\beta}}(t)$ and $\bar{F}_{K_{i\beta}}(t)$ from Equations 105 and 106 into Equation 109 gives

$$P_{(K)U}(t) = \sum_i \left[P_{UF_i}(t_{\beta-1}) \bar{F}_{OF_{i\beta}}(t) + P_{UF_{i\beta}} \bar{F}_{F_{i\beta}}(t) \right] \bar{F}_{K_i}(t) \quad (110)$$

Comparing Equations 104 and 110 shows that

$$P_{UF_i}(t) = P_{UF_i}(t_{\beta-1}) \bar{F}_{OF_{i\beta}}(t) + P_{UF_{i\beta}} \bar{F}_{F_{i\beta}}(t) \quad (111)$$

Eliminating $P_{UF_i}(t)$ from Equations 75 and 111 gives

$$\delta P_{UF_i}(t) = P_{UF_i}(t_{B-1}) \left[\bar{F}_{OF_{iB}}(t) - I \right] + P_{UF_{iB}} \bar{F}_{F_{iB}}(t) \quad (112)$$

where I = the unit matrix.

Now, in Equation 105 when $t = t_{B-1}$,

$$\bar{F}_{KO_{iB}}(t_{B-1}) = \bar{F}_{OF_{iB}}(t_{B-1}) \bar{F}_{K_i}(t_{B-1}) \quad (113)$$

But, from Figure 2.15,

$$\bar{F}_{KO_{iB}}(t_{B-1}) = \bar{F}_{K_i}(t_{B-1}), \quad (114)$$

since $\bar{F}_{KO_{iB}}$ is the component of \bar{F}_{K_i} parallel to its direction at the beginning of the increment. Therefore, from Equations 113 and 114.

$$\bar{F}_{OF_{iB}}(t_{B-1}) = I \quad (115)$$

Thus, at the beginning of the increment, the first term on the right of Equation 112 is zero. Also, the term $\bar{F}_{OF}(t) - I$ represents force components parallel, rather than normal, to the initial directions of the lumped forces at t_{B-1} . These components should have little effect upon structural responses in the presence of buckling and other large displacement effects. Therefore, delete the first term to simplify the analysis. The method of fictitious forces and deformations can be developed without this approximation, but in the present incremental approach, it is worthwhile.

Setting the first term on the right of Equation 112 equal to zero gives

$$\delta P_{UF_i}(t) = P_{UF_{iB}} \bar{F}_{F_{iB}}(t) \quad (116)$$

Substituting $\delta P_{UF_i}(t)$ from Equation 116 into Equation 82 gives

$$\delta P(\bar{F})_B(t) = \sum_i P_{UF_{iB}} \bar{F}_{F_{iB}}(t) \bar{F}_{K_i}(t) \quad (117)$$

Therefore, from Equations 106 and 117,

$$\delta P(\bar{F})_B(t) = \sum_i P_{UF_{iB}} \bar{F}_{K_{iB}}(t) \quad (118)$$

Now, the forces contained in the column matrix $\bar{F}_{K_{iB}}(t)$ are components of the lumped element forces resulting from rotations of the elements, as shown in Figure 2.15. These forces are called fictitious forces. Actually they exist; but from the point of view of linear small displacement theory they are fictitious, because, in linear theory, displacements are supposed to be too small to affect the directions of the element forces. Therefore

$\bar{F}_{K_{iB}}(t)$ = a column matrix of fictitious forces acting on the i th element at time t during the B th increment.

From Equation 118, the matrix $\delta P(\bar{F})_B(t)$ can be defined as follows:

$\delta P(\bar{F})_B(t)$ = a column matrix of loads in the unconstrained degrees of freedom, resulting from fictitious forces at time t developed during the B th increment.

Fictitious Deformations

Eliminate $\dot{\Delta}_T(t)$ from Equations 27 and 49:

$$\therefore \dot{\bar{e}}_i(t) = -P_{TF_i}^T(t) P_{UPT}^T \dot{\Delta}(t) \quad (119)$$

From Equations 53 and 119:

$$\dot{\bar{e}}_i(t) = -P_{UF_i}^T(t)\dot{\Delta}(t) \quad (120)$$

From Equations 75 and 120,

$$\dot{\bar{e}}_i(t) = - \left[P_{UF_i}^T(t_{\beta-1}) + \delta P_{UF_i}^T(t) \right] \dot{\Delta}(t) \quad (121)$$

$$\therefore \dot{\bar{e}}_i(t) = \dot{\bar{e}}_{L_i}(t) - \dot{\bar{e}}_{f_i}(t) \quad (122)$$

where

$$\dot{\bar{e}}_{L_i}(t) = -P_{UF_i}^T(t_{\beta-1})\dot{\Delta}(t) \quad (123)$$

$$\dot{\bar{e}}_{f_i}(t) = \delta P_{UF_i}^T(t)\dot{\Delta}(t) \quad (124)$$

Now the force transformation matrix, $P_{UF_i}(t)$, depends solely on structural geometry. The matrix $P_{UF_i}(t_{\beta-1})$ therefore reflects the geometry existing at the beginning of the β th increment. In the theory of small displacements, the geometry of the structure is considered to be unaffected by displacements. The matrix $\dot{\bar{e}}_{L_i}(t)$, given by Equation 123, therefore represents deformation rates that would be computed by linear theory, since it is expressed in terms of the geometry existing at the beginning of the increment, and the displacements existing at a later time. Since $\dot{\bar{e}}_{L_i}(t)$ represents linear deformation rates, and $\dot{\bar{e}}_i(t)$ represents total deformation rates, $\dot{\bar{e}}_{f_i}(t)$ must, from Equation 122, represent the effects of geometric nonlinearity. The matrix $\dot{\bar{e}}_{f_i}(t)$ is called the fictitious deformation rate matrix, because it is not taken into account in linear theory.

From Equations 93 and 124,

$$\delta P_{Kf_\beta}(t) = - \sum_i P_{UF_i}^T(t_{\beta-1}) \bar{k}_{i(\beta)} \delta \bar{e}_{f_i\beta}(t) \quad (125)$$

where

$$\delta \bar{e}_{f_{i\beta}}(t) = \int_{t_{\beta-1}}^t \dot{\bar{e}}_{f_i}(t) dt \quad (126)$$

The symbol $\dot{\bar{e}}_{f_i}(t)$ denotes a matrix of fictitious deformation rates. Therefore, from Equation 126,

$\delta \bar{e}_{f_{i\beta}}(t)$ = a column matrix of incremental fictitious deformations developed between times $t_{\beta-1}$ and t .

From Equation 125, the matrix $\delta P_{Kf_{\beta}}(t)$ can be defined as follows:

$\delta P_{Kf_{\beta}}(t)$ = a column matrix of loads in the unconstrained degrees of freedom, resulting from fictitious deformations, at time t developed during the β th increment.

Eliminate $\dot{\bar{e}}_{f_i}$ from Equations 124 and 126:

$$\therefore \delta \bar{e}_{f_{i\beta}}(t) = \int_{t_{\beta-1}}^t \delta P_{UF_i}^T(t) \dot{\Delta}(t) dt \quad (127)$$

Eliminate $\delta P_{UF_i}^T(t)$ from Equations 116 and 127:

$$\therefore \delta \bar{e}_{f_{i\beta}}(t) = \int_{t_{\beta-1}}^t \bar{F}_{i\beta}^T(t) P_{UF_{i\beta}}^T \dot{\Delta}(t) dt \quad (128)$$

Let

$$\dot{\bar{e}}_{i\beta}(t) = - P_{UF_{i\beta}}^T \dot{\Delta}(t) \quad (129)$$

where

$\dot{\bar{e}}_{i\beta}(t)$ = a column matrix of rates of displacements of the fictitious forces acting on the i th element during the β th increment.

This definition follows from Equation 129, considering the fact that $P_{UF_{i\beta}}^{\bar{e}}$ is a matrix of components in the unconstrained degrees of freedom of the fictitious forces acting on the i th element, and $\dot{\bar{a}}(t)$ is a column matrix of displacements in the unconstrained degrees of freedom, according to the method of virtual work as described in Appendix A. From Equations 128 and 129;

$$\delta \bar{e}_{f_{i\beta}}(t) = - \int_{t_{\beta-1}}^t \bar{F}_{F_{i\beta}}^T(t) \dot{\bar{e}}_{i\beta}(t) dt \quad (130)$$

Integrate Equation 122:

$$\int_{t_{\beta-1}}^t \dot{\bar{e}}_i(t) dt = \int_{t_{\beta-1}}^t [\dot{\bar{e}}_{L_i}(t) - \dot{\bar{e}}_{f_i}(t)] dt \quad (131)$$

Therefore, from Equations 99, 126 and 131,

$$\delta \bar{e}_{i\beta}(t) = \delta \bar{e}_{L_{i\beta}}(t) - \delta \bar{e}_{f_{i\beta}}(t) \quad (132)$$

where

$$\delta \bar{e}_{L_{i\beta}}(t) = \bar{e}_{L_i}(t) - \bar{e}_{L_i}(t_{\beta-1}) \quad (133)$$

Element Forces

The element stiffness forces are expressed in terms of the linear incremental deformations, the fictitious incremental deformations, and the unassembled incremental thermal deformations, from Equations 98 and 132 by

$$\bar{F}_{K_i}(t) = \bar{F}_{K_i}(t_{\beta-1}) + \bar{k}_{i(\beta)} [\delta \bar{e}_{L_{i\beta}}(t) - \delta \bar{e}_{f_{i\beta}}(t) - \delta \bar{e}_{o_{i\beta}}(t)] \quad (134)$$

Integrate Equation 123:

$$\int_{t_{B-1}}^t \ddot{e}_{L_i}(t) dt = - P_{UF_i}^T(t_{B-1}) \int_{t_{B-1}}^t \dot{\Delta}(t) dt \quad (135)$$

Therefore, from Equations 88, 133 and 135,

$$\delta \ddot{e}_{L_i}(t) = - P_{UF_i}^T(t_{B-1}) \delta \Delta_B(t) \quad (136)$$

The element damping forces are obtained from Equation 16 by replacing $\bar{c}_i(t)$ by $\bar{c}_{i(B)}$, and setting $\dot{e}_{o_i}(t)$ equal to zero, according to previous assumptions, giving

$$\bar{F}_{C_i}(t) = \bar{c}_{i(B)} \dot{e}_i(t) \quad (137)$$

The nonlinear effects of damping forces are not considered, also according to a previous assumption. Therefore, setting $\dot{e}_{f_i}(t) = 0$ in Equation 122 gives

$$\dot{e}_i(t) = \dot{e}_{L_i}(t) \quad (138)$$

Therefore

$$\bar{F}_{C_i}(t) = \bar{c}_{i(B)} \dot{e}_{L_i}(t) \quad (139)$$

Example of Fictitious Forces and Deformations

Figure 2.16(a) shows a simple two-dimensional structure, constrained in two directions at A and C, and constrained horizontally at B. The figure shows the notation for vertical load and displacement at B. Figure 2.16(b) shows the notation for lumped element forces, and fictitious forces. To simplify the presentation, the bars are assumed to

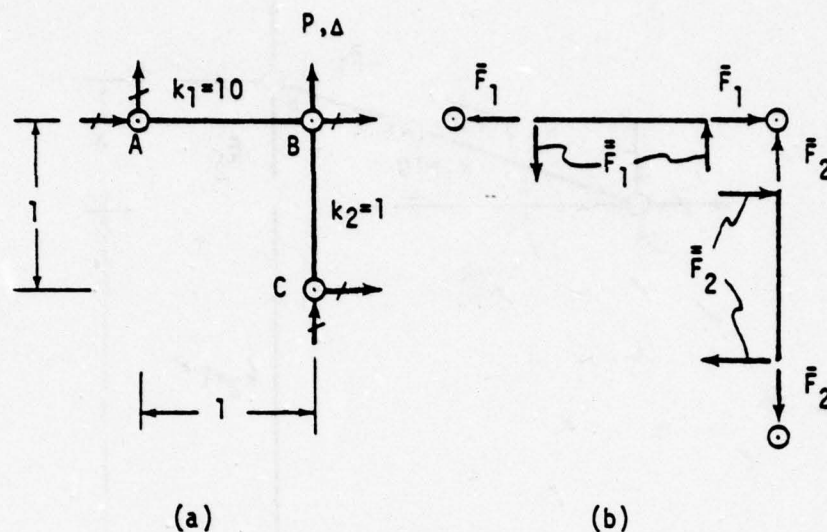


Figure 2.16. Statically loaded rectangular frame.

have no shear nodes, and each bar has only one self-equilibrating element force. The bar stiffnesses, k_1 and k_2 , are assumed to remain constant, no matter how much the bars stretch. Thus the bars behave somewhat like coil springs. The problem is to calculate Δ , the vertical displacement of joint B, resulting from P, a static vertical load at B, considering large displacements.

The exact solution to this problem is first presented. Figure 2.17 shows the deformed structure.

From the equilibrium of joint B,

$$P - \bar{F}_1 \sin \alpha - \bar{F}_2 = 0 \quad (140)$$

where α is defined as shown in the figure. But

$$\bar{F}_1 = k_1(\sqrt{1+\Delta^2} - 1) \quad (141)$$

$$\bar{F}_2 = k_2 \Delta \quad (142)$$

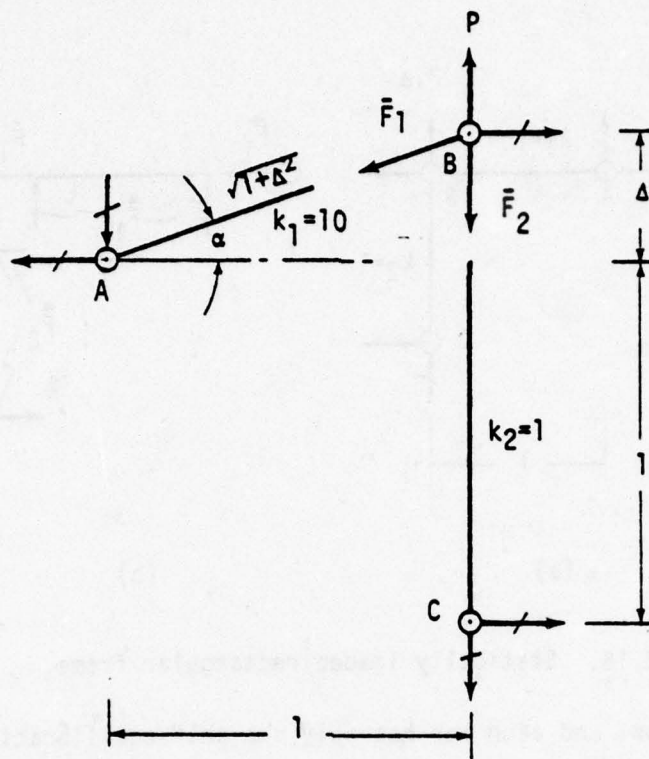


Figure 2.17. Deformed rectangular frame.

$$\sin \alpha = \frac{\Delta}{\sqrt{1+\Delta^2}} \quad (143)$$

Eliminating \bar{F}_1 , \bar{F}_2 and $\sin \alpha$ from Equations 140, 141, 142 and 143, setting $k_1 = 10$, $k_2 = 1$, and rearranging terms gives

$$11\Delta - \frac{10\Delta}{\sqrt{1+\Delta^2}} = P \quad (144)$$

The problem is now solved by the method given in preceding paragraphs. Assume that the structure has no mass, no damping, and no unassembled thermal deformations. Consider only one time increment, and assume that the load at the beginning of this increment is zero. Therefore, in Equation 102,

$$M = C_{(B)} = P_{(K)U}(t_{B-1}) = \delta P_{K0_B}(t) = 0 \quad (145)$$

Also, from Figure 2.16 (a),

$$P_{(\phi)U}(t) = P(t) \quad (146)$$

In Equation 146, the load is assumed to be applied gradually as a function of time. Since mass and damping are zero, a change in the load will be felt instantaneously by all parts of the structure. The way in which P depends on t is consequently of no importance. Therefore assume that the load is applied in such a way that the angle α , shown in Figure 2.17, is equal to the time.

$$\therefore \alpha(t) = t \quad (147)$$

This assumption simplifies the analysis.

From Equations 102, 145 and 146,

$$K_{(B)} \delta \Delta_B(t) = P(t) + \delta P_{(F)}(t) + \delta P_{Kf_B}(t) \quad (148)$$

From Figure 2.16, the element force transformations are

$$P_{UF_1}(t_{B-1}) = 0 \quad P_{UF_2}(t_{B-1}) = -1 \quad (149)$$

The element stiffnesses are

$$k_{1(B)} = 10 \quad k_{2(B)} = 1 \quad (150)$$

Also,

$$\delta \bar{e}_{f_{2B}} = 0, \quad (151)$$

since the vertical bar will not rotate under the load.

Therefore, from Equations 125, 149 and 151

$$\delta P_{Kf_B}(t) = 0 \quad (152)$$

From Equations 87, 149 and 150,

$$K_{(B)} = 1 \quad (153)$$

Substituting $\delta P_{Kf_B}(t)$ and $K_{(B)}$ from Equations 152 and 153 into Equation 148 gives

$$\delta \Delta_B(t) = P(t) + \delta P_{(\bar{F})_B}(t) \quad (154)$$

From Figure 2.16(b), the fictitious force transformations are,

$$P_{U\bar{F}_{1B}} = -1 \quad P_{U\bar{F}_{2B}} = 0 \quad (155)$$

Figure 2.18 shows the fictitious force components of the element forces. From the figure,

$$\bar{\bar{F}}_1(t) = \bar{F}_1(t) \sin \alpha(t) \quad \bar{\bar{F}}_2(t) = 0 \quad (156)$$

Therefore the fictitious forces resulting from unit values of the element forces are

$$\bar{\bar{F}}_{\bar{F}_{1B}}(t) = \sin \alpha(t) \quad \bar{\bar{F}}_{\bar{F}_{2B}}(t) = 0 \quad (157)$$

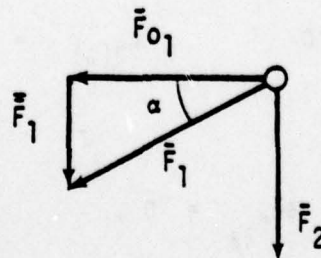


Figure 2.18. Fictitious forces.

Substituting $P_{UF_{1\beta}}$ and $\bar{F}_{1\beta}(t)$ from Equations 155 and 157 into Equation 117 gives

$$\delta P(\bar{F})_{\beta}(t) = -\bar{F}_{K_1}(t) \sin \alpha(t) \quad (158)$$

From Equations 136 and 149, the linear deformation in bar 1 is

$$\delta \bar{e}_{L_{1\beta}}(t) = 0 \quad (159)$$

Therefore, from Equations 134, 150 and 159,

$$F_{K_1}(t) = -10 \delta e_{f_{1\beta}}(t) \quad (160)$$

since $\bar{F}_{K_1}(t_{\beta-1})$ and $\delta \bar{e}_{O_{1,\beta}}(t)$ are zero. From Equations 128, 155 and 157, the fictitious deformation in bar 1 is

$$\delta \bar{e}_{f_{1\beta}}(t) = - \int_{t_{\beta-1}}^t \sin \alpha(t) \dot{\Delta}(t) dt \quad (161)$$

From Figure 2.17,

$$\Delta(t) = \tan \alpha(t) \quad (162)$$

$$\therefore \dot{\Delta}(t) = \sec^2 \alpha(t) \dot{\alpha}(t) \quad (163)$$

Substituting $\dot{\Delta}(t)$ from Equation 163 into Equation 161, employing Equation 147 and taking $t_{\beta-1}=0$ gives

$$\delta \bar{e}_{f_{1\beta}}(t) = - \int_0^t \sin t \sec^2 t dt \quad (164)$$

$$\therefore \delta e_{f_{1\beta}}(t) = 1 - \frac{1}{\cos t} \quad (165)$$

Eliminating $\bar{F}_{K_1}(t)$ and $\delta \bar{e}_{f_{1\beta}}(t)$ from Equations 158, 160 and 165, and employing Equation 147 gives,

$$\delta P(\bar{F})_{\beta}(t) = 10(\sin t - \tan t) \quad (166)$$

From Equations 147 and 162

$$\tan t = \Delta(t) \quad (167)$$

$$\therefore \sin t = \frac{\Delta(t)}{\sqrt{1+\Delta^2(t)}} \quad (168)$$

Combine Equations 166, 167 and 168:

$$\delta P(\bar{F})_{\beta}(t) = 10 \left[\frac{\Delta(t)}{\sqrt{1+\Delta^2(t)}} - \Delta(t) \right] \quad (169)$$

From Equation 88

$$\delta \Delta_{\beta}(t) = \Delta(t), \quad (170)$$

since $\Delta(t_{\beta-1}) = 0$. Substituting $\delta P(\bar{F})_{\beta}(t)$ and $\delta \Delta_{\beta}(t)$ from Equations 169. and 170 into Equation 154, and rearranging terms, gives

$$11\Delta(t) - \frac{10\Delta(t)}{\sqrt{1+\Delta^2(t)}} = P(t), \quad (171)$$

which, according to Equation 144, is the exact answer to the problem.

Figure 2.19 is a graph of displacement vs. load. The result is highly nonlinear.

This problem has been worked in detail to show the significance of various quantities involved in the formulation of the nonlinear equation of motion. Note that the assumption implied in deleting the term $\bar{F}_{OF_{1\beta}}(t) - I$ in Equation 112 produced no approximation. The

reason is that the component \bar{F}_{01} , shown in Figure 2.18, has no effect, because it is carried by the horizontal reaction at B, shown in Figure 2.16 (a).

A solution of the problem, with point B unconstrained, would provide a measure of the approximation introduced by deleting $\bar{F}_{0\bar{F}_{iB}}(t)-I$. The case of B constrained is considered, however, to represent the situation existing in stiffened or unstiffened plate or shell structures, which tend to be stiff in two directions, and flexible in a third.

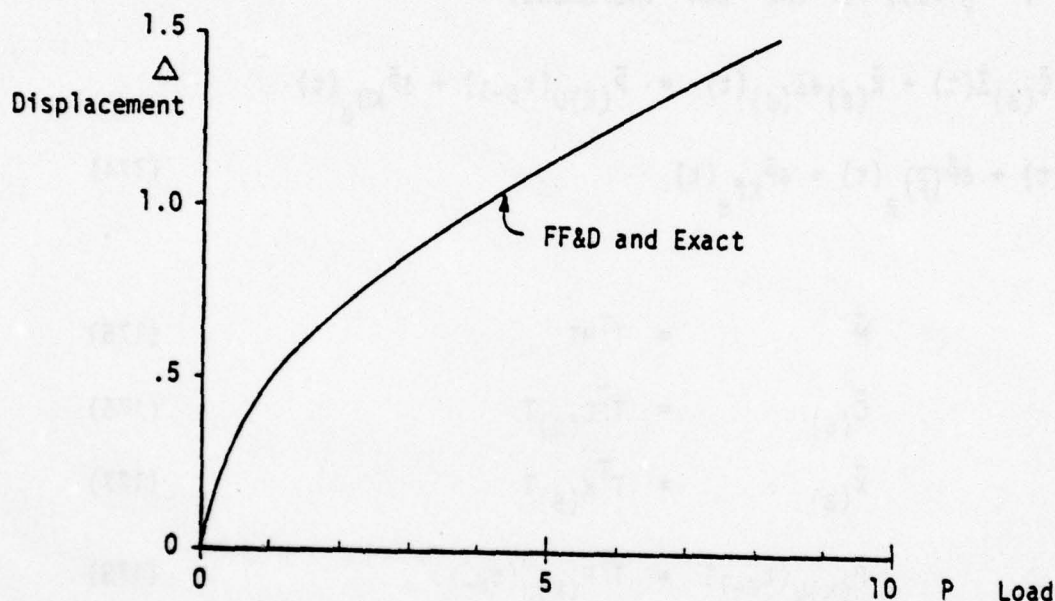


Figure 2.19. Nonlinear displacement of the rectangular frame.

This example illustrates only bar fictitious forces and deformations. Shear panels also have fictitious forces and deformations as described in Appendix D.

EQUATION OF MOTION, MODAL DEGREES OF FREEDOM

Substituting $\Delta(t)$ from Equation 11 into Equation 88 gives

$$\delta\Delta_B(t) = T\delta\bar{\Delta}_B(t) \quad (172)$$

where

$$\delta\bar{\Delta}_B(t) = \bar{\Delta}(t) - \bar{\Delta}(t_{B-1}) \quad (173)$$

Substituting $\Delta(t)$ from Equation 11 and $\delta\Delta_B(t)$ from Equation 172 into Equation 102, and multiplying the resulting equation on the left by T^T gives, for the g th increment,

$$\begin{aligned} \bar{M}\ddot{\bar{\Delta}}(t) + \bar{C}_{(B)}\dot{\bar{\Delta}}(t) + \bar{K}_{(B)}\delta\bar{\Delta}_{(B)}(t) &= \bar{P}_{(K)U}(t_{B-1}) + \delta\bar{P}_{KO_B}(t) \\ + \bar{P}_{(\phi)U}(t) + \delta\bar{P}_{(F)_B}(t) + \delta\bar{P}_{Kf_B}(t) \end{aligned} \quad (174)$$

where

$$\bar{M} = T^TMT \quad (175)$$

$$\bar{C}_{(B)} = T^TC_{(B)}T \quad (176)$$

$$\bar{K}_{(B)} = T^TK_{(B)}T \quad (177)$$

$$\bar{P}_{(K)U}(t_{B-1}) = T^TP_{(K)U}(t_{B-1}) \quad (178)$$

$$\delta\bar{P}_{KO_B}(t) = T^T\delta P_{KO_B}(t) \quad (179)$$

$$\bar{P}_{(\phi)U}(t) = T^TP_{(\phi)U}(t) \quad (180)$$

$$\delta\bar{P}_{(F)_B}(t) = T^T\delta P_{(F)_B}(t) \quad (181)$$

$$\delta\bar{P}_{Kf_B}(t) = T^T\delta P_{Kf_B}(t) \quad (182)$$

Let

$$\bar{P}_{N_B}(t) = \bar{P}_{(K)U}(t_{B-1}) + \delta\bar{P}_{KO_B}(t) + \bar{P}_{(\phi)U}(t) + \delta\bar{P}_{(F)_B}(t) + \delta\bar{P}_{Kf_B}(t) \quad (183)$$

Combining Equations 174 and 183 gives

$$\ddot{\bar{M}}\Delta(t) + \bar{C}_{(\beta)}\dot{\Delta}(t) + \bar{K}_{(\beta)}\delta\bar{\Delta}_{(\beta)}(t) = \bar{P}_{N_{\beta}}(t) \quad (184)$$

Equation 184 is the equation of motion, written in terms of the modal displacements, and the nonlinear thermomechanical loads, which are given by equation 183. The subscript N attached to $\bar{P}_{N_{\beta}}(t)$ indicates that this matrix includes the nonlinearities resulting from fictitious loads.

Alternate Form of the Load Matrix

At $t = t_{\beta-1}$, Equation 174 becomes

$$\ddot{\bar{M}}\Delta(t_{\beta-1}) + \bar{C}_{(\beta)}\dot{\Delta}(t_{\beta-1}) = \bar{P}_{(K)U}(t_{\beta-1}) + \bar{P}_{(\phi)U}(t_{\beta-1}), \quad (185)$$

since, from Equations 75, 82, 84, 91, 92, 173, 179, 181 and 182,

$$\delta\bar{\Delta}_{(\beta)}(t_{\beta-1}) = \delta\bar{P}_{K0_{\beta}}(t_{\beta-1}) = \delta\bar{P}_{(\bar{F})_{\beta}}(t_{\beta-1}) = \delta\bar{P}_{Kf_{\beta}}(t_{\beta-1}) = 0 \quad (186)$$

Subtracting Equation 185 from Equation 183, and rearranging terms gives

$$\begin{aligned} \bar{P}_{N_{\beta}}(t) = & \delta\bar{P}_{K0_{\beta}}(t) + \delta\bar{P}_{(\phi)U}(t) + \delta\bar{P}_{(\bar{F})_{\beta}}(t) + \delta\bar{P}_{Kf_{\beta}}(t) \\ & + \ddot{\bar{M}}\Delta(t_{\beta-1}) + \bar{C}_{(\beta)}\dot{\Delta}(t_{\beta-1}) \end{aligned} \quad (187)$$

$$\text{where} \quad \delta\bar{P}_{(\phi)U_{\beta}}(t) = \bar{P}_{(\phi)U}(t) - \bar{P}_{(\phi)U}(t_{\beta-1}) \quad (188)$$

$$\text{Let} \quad \bar{P}_{(M)U}(t_{\beta-1}) = -\ddot{\bar{M}}\Delta(t_{\beta-1}) \quad (189)$$

$$\bar{P}_{(C)U}(t_{\beta-1}) = -\bar{C}_{(\beta)}\dot{\Delta}(t_{\beta-1}) \quad (190)$$

Therefore, from Equations 187, 189 and 190,

$$\begin{aligned}\bar{P}_{N_B}(t) = & \delta\bar{P}_{KO_B}(t) + \delta\bar{P}_{(\phi)U_B}(t) + \delta\bar{P}_{(\bar{F})_B}(t) + \delta\bar{P}_{Kf_B}(t) \\ & - \bar{P}_{(M)U}(t_{B-1}) - \bar{P}_{(C)U}(t_{B-1})\end{aligned}\quad (191)$$

Equation 191 is an alternate form of the load matrix. In this form, as compared to Equation 183, the external load matrix $\bar{P}_{(\phi)U}(t)$ is replaced by the incremental load matrix $\delta\bar{P}_{(\phi)U_B}(t)$, and the matrix $\bar{P}_{(K)U}(t_{B-1})$ of components of the internal stiffness forces in the unconstrained degrees of freedom is replaced by the matrices $-\bar{P}_{(M)U}(t_{B-1})$ and $-\bar{P}_{(C)U}(t_{B-1})$. These last two matrices are now identified, and the notation is justified.

From Equations 176 and 190

$$\bar{P}_{(C)U}(t_{B-1}) = -T^T C_{(B)} T \dot{\Delta}(t_{B-1}) \quad (192)$$

Therefore, from Equation 11,

$$\bar{P}_{(C)U}(t_{B-1}) = -T^T C_{(B)} \dot{\Delta}(t_{B-1}) \quad (193)$$

Substituting $C_{(B)}$ from Equation 101 yields

$$\bar{P}_{(C)U}(t_{B-1}) = -T^T \sum_i P_{UF_i}(t_{B-1}) \bar{C}_{i(B)} P_{UF_i}^T(t_{B-1}) \dot{\Delta}(t_{B-1}) \quad (194)$$

Combining Equations 27 and 49 gives

$$\dot{\bar{e}}_i(t_{B-1}) = -P_{TF_i}^T(t_{B-1}) P_{UPT}^T \dot{\Delta}(t_{B-1}) \quad (195)$$

Therefore, from Equation 53,

$$\dot{\bar{e}}_i(t_{B-1}) = -P_{UF_i}^T(t_{B-1}) \dot{\Delta}(t_{B-1}) \quad (196)$$

Thus, Equation 194 becomes

$$\bar{P}_{(C)U}(t_{\beta-1}) = T^T \sum_i P_{UF_i}(t_{\beta-1}) \bar{C}_{i(\beta)} \dot{e}_i(t_{\beta-1}) \quad (197)$$

Substituting $\bar{F}_{C_i}(t)$ from Equation 137 gives

$$\bar{P}_{(C)U}(t_{\beta-1}) = T^T \sum_i P_{UF_i}(t_{\beta-1}) \bar{F}_{C_i}(t_{\beta-1}) \quad (198)$$

$$\therefore \bar{P}_{(C)U}(t_{\beta-1}) = T^T P_{(C)U}(t_{\beta-1}) \quad (199)$$

$$\text{where } P_{(C)U}(t_{\beta-1}) = \sum_i P_{UF_i}(t_{\beta-1}) \bar{F}_{C_i}(t_{\beta-1}) \quad (200.1)$$

Equation 200.1 shows that

$P_{(C)U}(t_{\beta-1})$ = a column matrix of components in the unconstrained degrees of freedom of the internal damping forces at $t_{\beta-1}$.

Equation 199 shows that

$\bar{P}_{(C)U}(t_{\beta-1})$ = a column matrix of transformed loads resulting from internal damping forces at $t_{\beta-1}$.

In a similar manner, it can be shown that

$$\bar{P}_{(M)U}(t_{\beta-1}) = T^T \sum_i P_{UF_i} F_{M_i}(t_{\beta-1}) \quad (200.2)$$

where $F_{M_i}(t_{\beta-1})$ is a matrix of element inertia forces. Equation 200.2 shows that

$\bar{P}_{(M)U}(t_{\beta-1})$ = a column matrix of transformed loads resulting from inertia forces at $t_{\beta-1}$.

The Effects of Errors in the Calculated Displacements

The transformed equation of motion, Equation 184 is solved for the incremental displacements, $\delta \bar{\Delta}_B(t)$, as explained in a subsequent section of the report. From the transformed displacements, all other structural responses, including nodal velocities, nodal accelerations, element forces, stresses and strains, are computed.

After the nodal displacements are calculated, the nodal coordinates are updated, to reflect the effects of displacements on geometry. At this point, nodal equilibrium is checked, by summing the components of internal and external forces acting on the nodes. The fictitious loads are not considered in this check, because the coordinate updating procedure accounts for element force rotation.

The transformed equilibrium equation for structural nodes subjected to external and internal force at the end of the β th increment is

$$\bar{P}_{(M)U}(t_B) + \bar{P}_{(C)U}(t_B) + \bar{P}_{(K)U}(t_B) + \bar{P}_{(\phi)U}(t_B) = 0 \quad (201)$$

where

$$\bar{P}_{(M)U}(t_B) = T^T \sum_i P_{UF_i}(t_B) \bar{F}_{M_i}(t_B) \quad (202)$$

$$\bar{P}_{(C)U}(t_B) = T^T \sum_i P_{UF_i}(t_B) \bar{F}_{C_i}(t_B) \quad (203)$$

$$\bar{P}_{(K)U}(t_B) = T^T \sum_i P_{UF_i}(t_B) \bar{F}_{K_i}(t_B) \quad (204)$$

Equation 201 states that the sums of the components of the inertia forces, the damping forces, the stiffness forces, and the external loads in the transformed degrees of freedom are zero, at $t = t_B$. The notation $P_{UF_i}(t_B)$ in Equations 202, 203 and 204, reflects the

AD-A063 740

DOUGLAS AIRCRAFT CO LONG BEACH CALIF
AIRCRAFT WINDSHIELD BIRD IMPACT MATH MODEL. PART 1. THEORY AND --ETC(U)

F/G 1/3

DEC 77 P H DENKE

F33615-75-C-3105

UNCLASSIFIED

MDC-J7174-PT-1

AFFDL-TR-77-99-PT-1

NL

2 OF 6
ADA
063740



fact that the damping and stiffness force components are based on updated coordinates.

If equilibrium is not satisfied exactly, the sum of the matrices in Equation 201 will not be zero. In this case let

$$\delta \bar{P}_{U_B}(t_B) = \bar{P}_{(M)U}(t_B) + \bar{P}_{(C)U}(t_B) + \bar{P}_{(K)U}(t_B) + \bar{P}_{(\phi)U}(t_B) \quad (205)$$

where

$\delta P_{U_B}(t_B)$ = a column matrix of transformed equilibrium errors.

This matrix generally will not be null, because of approximations in the analysis.

The effects of equilibrium errors can be minimized by a corrective procedure. To simplify the presentation of this procedure, consider a structure having zero mass and damping. Also consider small deflections, zero thermal deformation, and no modal transformation. In this case the governing equation for structural response is the familiar displacement method equation:

$$K\Delta(t) = P_{(\phi)U}(t) . \quad (206)$$

The displacements and loads are still shown as functions of time, so that the effects of applying the loads in increments can be considered. The effect of a load variation is instantaneously felt in all parts of the structure, since mass and damping are zero.

Now, express the displacements in incremental form. From Equation 88,

$$\Delta(t) = \Delta(t_{B-1}) + \delta \Delta_B(t) \quad (207)$$

From Equations 206 and 207

$$K\delta\Delta_B(t) = P_{(\phi)}U(t) - K\Delta(t_{B-1}) \quad (208)$$

For the simple case under consideration, Equation 208 is equivalent to the equation of motion, Equation 184. The terms on the right of Equation 208 are equivalent to the load matrix, Equation 183. The second term on the right of Equation 208 represents the components in the unconstrained degrees of freedom of the internal stiffness forces existing at the beginning of the β th increment. This term can be shown to be equivalent to the term $\bar{P}_{KU}(t_{B-1})$ in Equation 183.

Now suppose, because of approximations in the analysis, that displacements calculated at the beginning of the β th increment are incorrect, so that

$$\Delta(t) = \Delta_e(t_{B-1}) + \delta\Delta_{e_B}(t) \quad (209)$$

where $\Delta(t)$ continues to represent a column matrix of correct displacements at time t during the β th increment, but

$\Delta_e(t_{B-1})$ = a column matrix of incorrect displacements at t_{B-1} , and

$\delta\Delta_{e_B}(t)$ = a column matrix of incremental displacements which, when added to $\Delta_e(t_{B-1})$, give the correct displacements.

From Equations 207 and 209,

$$\delta\Delta_B(t) = \delta\Delta_{e_B}(t) + \Delta_e(t_{B-1}) - \Delta(t_{B-1}) \quad (210)$$

Substituting $\delta\Delta_B(t)$ from Equation 210 into Equation 208 gives

$$K\delta\Delta_{e_B}(t) = P_{(\phi)}U(t) - K\Delta_e(t_{B-1}) \quad (211)$$

The second term on the right of Equation 211 again represents the components in the unconstrained degrees of freedom of the internal stiffness forces. Equation 211 states that if this term is calculated on the basis of erroneous displacements computed at the beginning of the β th increment, then the corresponding incremental displacements, $\delta\Delta_e(t)$, when added to the erroneous displacements $\Delta_e(t_{\beta-1})$, as in Equation 209, will produce the correct total displacements $\Delta(t)$, at time t .

Equation 208 therefore has the property of producing incremental displacements that tend to correct errors existing in displacements calculated at the beginning of the increment. When the solution of the equation of motion, Equation 184, is based on the load matrix of Equation 183, the result is also expected to tend to be self-correcting.

Now the displacement equation, Equation 206, expresses the equilibrium of internal stiffness forces and external loads. From Equation 206,

$$P_{(\phi)U}(t_{\beta-1}) - K\Delta(t_{\beta-1}) = 0 \quad (212)$$

This equation states that the sums of components of external loads and stiffness forces are zero at $t_{\beta-1}$. If $\Delta(t_{\beta-1})$ in Equation 212 is replaced by the erroneous $\Delta_e(t_{\beta-1})$, then these sums are no longer zero. Let

$$\delta P_{U\beta}(t_{\beta-1}) = P_{(\phi)U}(t_{\beta-1}) - K\Delta_e(t_{\beta-1}) \quad (213)$$

where

$\delta P_{U\beta}(t_{\beta-1})$ = a column matrix of equilibrium errors in the unconstrained degrees of freedom.

Substituting $P_{(\phi)U}(t_{\beta-1})$ from Equation 206 into Equation 213 gives

$$\delta P_{U_{\beta}}(t_{\beta-1}) = K[\Delta(t_{\beta-1}) - \Delta_e(t_{\beta-1})] \quad (214)$$

An alternate form of Equation 208 is now derived. Setting $t = t_{\beta-1}$ in Equation 208 gives

$$0 = P_{(\phi)U}(t_{\beta-1}) - K\Delta(t_{\beta-1}), \quad (215)$$

since $\delta\Delta_{\beta}(t_{\beta-1}) = 0$. Subtracting Equation 215 from Equation 208 gives

$$K\delta\Delta_{\beta}(t) = \delta P_{(\phi)U_{\beta}}(t) \quad (216)$$

where
$$\delta P_{(\phi)U_{\beta}}(t) = P_{(\phi)U}(t) - P_{(\phi)U}(t_{\beta-1}) \quad (217)$$

Equation 216 simply states that the incremental displacements are the displacements that result from incremental loads. The term on the right of this equation corresponds to the alternate form of the load matrix, Equation 191. Substituting $\delta\Delta_{\beta}(t)$ from Equation 210 into Equation 216, and rearranging terms gives

$$K\delta\Delta_{e_{\beta}}(t) = \delta P_{(\phi)U_{\beta}}(t) + K[\Delta(t_{\beta-1}) - \Delta_e(t_{\beta-1})] \quad (218)$$

Combining Equations 214 and 218 gives

$$K\delta\Delta_{e_{\beta}}(t) = \delta P_{(\phi)U_{\beta}}(t) + \delta P_{U_{\beta}}(t_{\beta-1}) \quad (219)$$

In Equation 219, $\delta\Delta_{e_{\beta}}(t)$ is a matrix of incremental displacements which correct the erroneous displacements calculated at $t_{\beta-1}$, as shown by Equation 209. Now the term $\delta P_{(\phi)U}(t)$, in Equation 219, corresponds to the alternate form of the load matrix, Equation 191, as mentioned in the preceding paragraph. Therefore Equation 219 states

that the correcting incremental displacements, $\delta \Delta_e(t)$, can be calculated from the alternate form of the load matrix, if the equilibrium errors, $\delta P_{U_B}(t_{B-1})$, are added to the right side of the equation.

Corrected Alternate Form of the Load Matrix

Adding the transformed equilibrium errors given by Equation 205 to the right side of Equation 191 gives

$$\begin{aligned} \bar{P}_{N_B}(t) = & \delta \bar{P}_{K_{O_B}}(t) + \delta \bar{P}_{(\phi)U_B}(t) + \delta \bar{P}_{(F)_B}(t) + \delta \bar{P}_{K_{f_B}}(t) \\ & - \bar{P}_{(M)U}(t_{B-1}) - \bar{P}_{(C)U}(t_{B-1}) + \delta \bar{P}_{U_{B-1}}(t_{B-1}) \end{aligned} \quad (220)$$

Equation 220 applies to the β th increment. The subscript on the equilibrium error term is therefore t_{B-1} to reflect the fact that these errors are computed from Equation 205 at the end of the preceding increment. Note that eliminating the equilibrium error matrix, $\delta \bar{P}_{U_B}(t_B)$, from Equations 205 and 220, yields the other form of the load matrix, Equation 183.

SOLUTION OF THE LINEARIZED EQUATION OF MOTION

The nonlinear differential equation of motion, Equation 184, is solved incrementally in time, and iteratively within each increment. The use of modes reduces the calculation to feasible dimensions.

Nonlinearities enter the equation in several ways. The damping and stiffness matrices, $\bar{C}_{(B)}$ and $\bar{K}_{(B)}$, are functions of material properties and displacements, which are functions of time. The load matrix, $\bar{P}_{N_B}(t)$, is a function of displacement and time, through the fictitious load matrices $\delta \bar{P}_{(F)_B}(t)$ and $\delta \bar{P}_{K_{f_B}}(t)$, as shown in Equations 183 or 191.

During an iteration within a time increment, material properties and geometry are considered constant, so that \bar{M} , $\bar{C}_{(B)}$ and $\bar{K}_{(B)}$ are

constant, and $\bar{P}_{N_B}(t)$ is a function of time only. Thus the differential equation is linearized, and linear methods can be employed in its solution.

The linearized differential equation is solved exactly. No approximate integrating algorithms are employed.

Dependence of Load on Time

In solving the linearized equation, an assumption about the dependence of load on time is necessary. The assumption is that thermo-mechanical loads are approximately constant within the increment, while fictitious loads vary approximately linearly from zero at the beginning of the increment. The reason for including the word "approximately" in the preceding statement will be clarified.

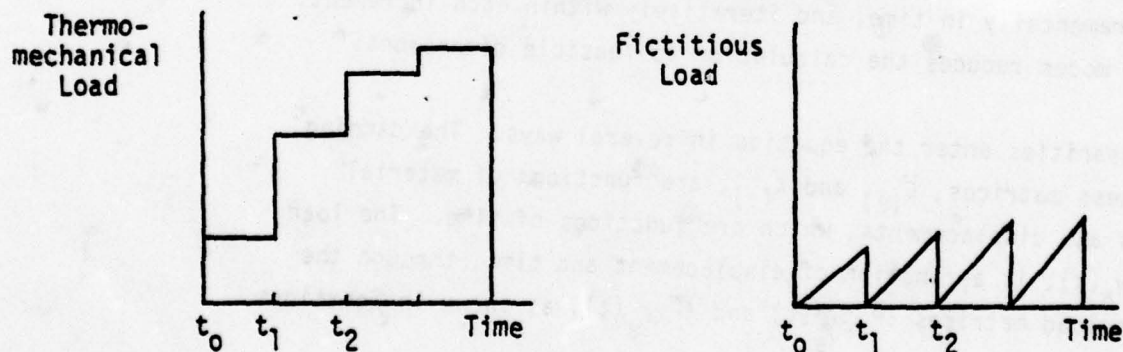


Figure 2.20. Original assumed variation of loads with time.

Initially in the development of the Math Model, loads were assumed to vary as shown in Figure 2.20. Thermomechanical loads were considered constant within the increment, while fictitious loads varied linearly in each time step, starting from zero. Fictitious loads are zero at the beginning of each increment, because the coordinate updating procedure eliminates the need for carrying forward fictitious loads calculated in the preceding step.

The difficulty with assuming constant or linearly varying loads is that the resulting solution contains the inverse of the stiffness matrix, $\bar{K}_{(\beta)}$. If $\bar{K}_{(\beta)}$ is singular or poorly conditioned, the solution fails. Now $\bar{K}_{(\beta)}$ can be singular in practical problems. For example, if the structure is unsupported, $\bar{K}_{(\beta)}$ is singular. Again, $\bar{K}_{(\beta)}$ may be initially well conditioned, but when it is updated during the incremental solution, it can become poorly conditioned, or singular. Such a circumstance can occur in a snap-through problem, since stiffness tends to vanish at snap-through. $\bar{K}_{(\beta)}$ also can become singular as a result of yielding or failure of some of the structural elements. These considerations are significant in the analysis of windshield systems, and other impact problems.

In order to avoid this difficulty, loads are assumed to vary sinusoidally with time within the increment, in such a way that the load variations shown in Figure 2.20 are approximated. When the variation is sinusoidal, rather than constant or linear, the inverse of the stiffness matrix is replaced by the inverse of the impedance matrix, $\bar{K}_{C(\beta)}$, where

$$\bar{K}_{C(\beta)} = \bar{K}_{(\beta)} - \omega_{p\beta}^2 \bar{M} + j \omega_{p\beta} \bar{C}_{(\beta)} \quad (221)$$

and

$$j = \sqrt{-1} \quad (222)$$

The symbol $\omega_{p\beta}$ denoting frequency of the load, is discussed in the next paragraph.

The advantage of this approach is that the impedance matrix is never singular in practical problems.

The assumed load expression is

$$\bar{P}_{N_B}(t) = \bar{P}_B c_{p_B} \cos \omega_{p_B}(t-t_{B-1}) + \delta \bar{P}_{(f)_B}(t_B) c_{f_B} \sin \omega_{p_B}(t-t_{B-1}) \quad (223)$$

where

\bar{P}_B = a column matrix of transformed thermomechanical loads for the B th increment (constant during the increment),

$\delta \bar{P}_{(f)_B}(t_B)$ = a column matrix of transformed fictitious loads at the end of the B th increment,

ω_{p_B} = load frequency for the B th increment,

c_{p_B}, c_{f_B} = scalar constants to be determined.

The frequency ω_{p_B} is chosen small enough so that the first term on the right of Equation 223, representing thermomechanical loads, is nearly constant, and the second term, representing fictitious loads, varies in an approximately linear manner.

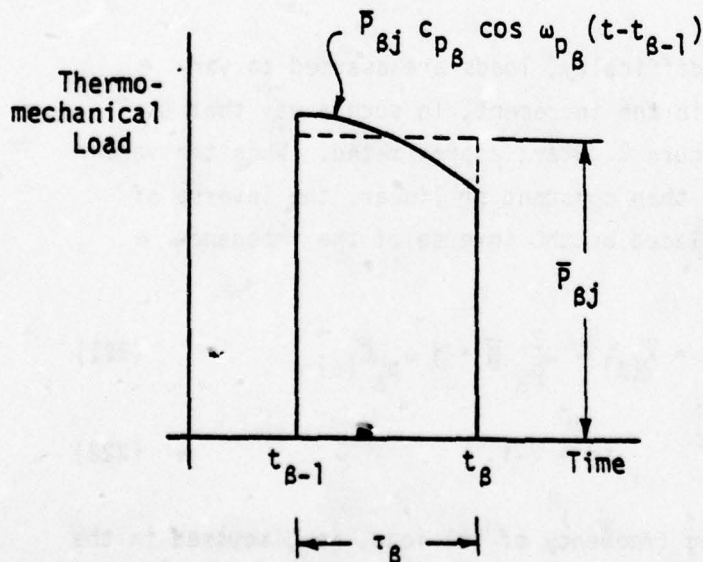


Figure 2.21. Cosine variation of the thermomechanical load.

Figure 2.21 shows the cosine variation of the j th thermo-mechanical load (solid line), compared to the variation if it were assumed constant (dotted). The constant c_{p_B} is chosen to make the average value of the cosine variations in the increment equal to the value \bar{P}_{Bj} . Therefore,

$$\frac{1}{\tau_B} \int_{t_{B-1}}^{t_B} \bar{P}_{Bj} c_{p_B} \cos \omega_{p_B} (t - t_{B-1}) dt = \bar{P}_{Bj}, \quad (224)$$

or

$$c_{p_B} \int_{t_{B-1}}^{t_B} \cos \omega_{p_B} (t - t_{B-1}) dt = \tau_B. \quad (225)$$

Therefore,

$$c_{p_B} = \frac{\omega_{p_B} \tau_B}{\sin \omega_{p_B} \tau_B} \quad (226)$$

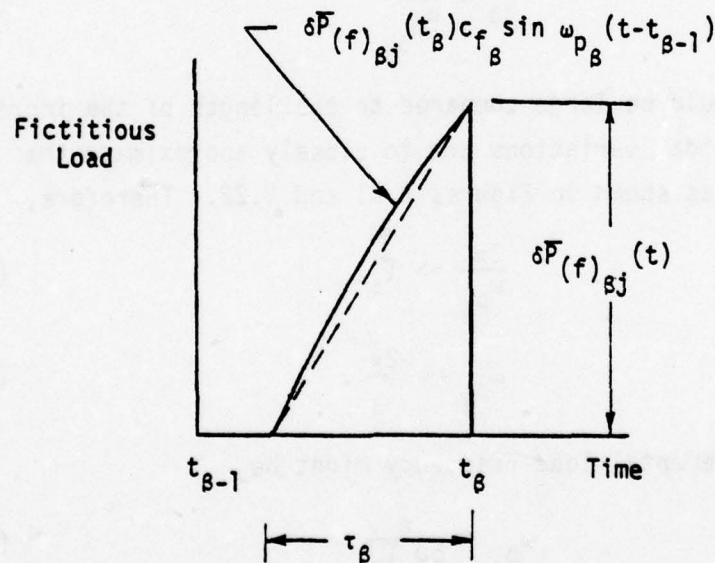


Figure 2.22. Sine variation of the fictitious load.

Figure 2.22 shows the sine variation of the fictitious load, compared to the linear variation (dotted line). The constant c_{f_B} is chosen to make the sinusoidally varying load equal to $\delta \bar{P}_{(f)_{Bj}}(t_B)$ the end of the increment. Therefore,

$$\delta \bar{P}_{(f)_{Bj}}(t_B) c_{f_B} \sin \omega_{p_B} (t_B - t_{B-1}) = \delta \bar{P}_{f_{Bj}}(t_B), \quad (227)$$

and

$$c_{f_B} = \frac{1}{\sin \omega_{p_B} \tau_B} \quad (228)$$

It appears to be important to make the fictitious loads equal to their correct values at the end of the increment.

Now the period of the sinusoidal variation of load in Equation 223 is

$$\tau_B = \frac{2\pi}{\omega_{p_B}} \quad (229)$$

This period should be large compared to the length of the increment if the sinusoidal variations are to closely approximate the linear variations, as shown in Figures 2.21 and 2.22. Therefore,

$$\frac{2\pi}{\omega_{p_B}} \gg \tau_B, \quad (230)$$

or

$$\omega_{p_B} \ll \frac{2\pi}{\tau_B}. \quad (231)$$

A suitable incremental load frequency might be

$$\omega_{p_B} = \frac{\pi}{50 \tau_B} \quad (232)$$

With such a choice of frequency, the loads will vary approximately as shown in Figure 2.20.

The solution of the differential equation can be based on the form of the load matrix given by either Equation 183 or Equation 191. In

the development of the computer program the alternate form, given by Equation 220, was chosen. Comparing Equations 223 and 220 shows that the thermomechanical load matrix is given by

$$\begin{aligned} \bar{P}_B = & \delta \bar{P}_{K O_B}(t_B) + \delta \bar{P}_{(\phi) U_B}(t_B) - \bar{P}_{(M) U}(t_{B-1}) \\ & - \bar{P}_{(C) U}(t_{B-1}) + \delta \bar{P}_{U_{B-1}}(t_{B-1}) . \end{aligned} \quad (233)$$

In Equation 233, the first two matrices on the right hand side have the following significance:

$\delta \bar{P}_{K O_B}(t_B)$ = a column matrix of equivalent transformed loads resulting from unassembled thermal deformations developed during the B th increment.

$\delta \bar{P}_{(\phi) U_B}(t_B)$ = a column matrix of transformed external loads added during the B th increment.

Since these matrices are considered constant during the increment, the implied assumption is that all of the load is added instantaneously at the beginning of the increment.

Again, comparing Equations 223 and 220 shows that the fictitious load matrix is given by

$$\delta \bar{P}_{(f)_B}(t_B) = \delta \bar{P}_{(\bar{F})_B}(t_B) + \delta \bar{P}_{K f_B}(t_B) \quad (234)$$

First Order Matrix Differential Equation

Substituting $P_{N_B}(t)$ from Equation 223 into Equation 184 gives

$$\begin{aligned} \bar{M} \ddot{\Delta}(t) + \bar{C}_{(B)} \dot{\Delta}(t) + \bar{K}_{(B)} \Delta(t) = & \bar{P}_B c_{p_B} \cos \omega_{p_B}(t - t_{B-1}) \\ & + \delta \bar{P}_{(f)_B}(t_B) c_{f_B} \sin \omega_{p_B}(t - t_{B-1}). \end{aligned} \quad (235)$$

The equation of motion, Equation 235, is a second order matrix

differential equation. It represents a set of \bar{n} second order scalar differential equations, where \bar{n} = the number of transformed degrees of freedom.

The second order equation is now transformed into a first order matrix equation, representing a set of $2\bar{n}$ first order scalar differential equations.

$$\text{Let} \quad \bar{v}(t) = \dot{\bar{\Delta}}(t), \quad (236)$$

$$\text{Therefore,} \quad \dot{\bar{v}}(t) = \ddot{\bar{\Delta}}(t), \quad (237)$$

$$\text{where} \quad \dot{\bar{v}}(t) = d\bar{v}(t)/dt. \quad (238)$$

Differentiating Equation 173 with respect to time gives

$$\delta \dot{\bar{\Delta}}_B(t) = \dot{\bar{\Delta}}(t) \quad (239)$$

$$\text{where} \quad \delta \dot{\bar{\Delta}}_B(t) = d[\delta \bar{\Delta}_B(t)]/dt \quad (240)$$

Eliminating $\dot{\bar{\Delta}}(t)$ from Equations 236 and 239 gives

$$\delta \dot{\bar{\Delta}}_B(t) - \bar{v}(t) = 0. \quad (241)$$

Eliminating $\dot{\bar{\Delta}}(t)$ and $\ddot{\bar{\Delta}}(t)$ from Equations 235, 236 and 237 gives

$$\begin{aligned} \bar{M}\dot{\bar{v}}(t) + \bar{C}_{(B)}\bar{v}(t) + \bar{K}_{(B)}\delta \bar{\Delta}_{(B)}(t) &= \bar{P}_B c_{p_B} \cos \omega_{p_B}(t-t_{B-1}) \\ &+ \delta \bar{P}_{(f)_B}(t_B) c_{f_B} \sin \omega_{p_B}(t-t_{B-1}). \end{aligned} \quad (242)$$

Equations 241 and 242 can be written:

$$\begin{aligned} \begin{bmatrix} 0 & \bar{M} \\ I & 0 \end{bmatrix} \begin{Bmatrix} \delta \dot{\bar{\Delta}}_B(t) \\ \dot{\bar{v}}(t) \end{Bmatrix} + \begin{bmatrix} \bar{K}_{(B)} & \bar{C}_{(B)} \\ 0 & -I \end{bmatrix} \begin{Bmatrix} \delta \bar{\Delta}_B(t) \\ \bar{v}(t) \end{Bmatrix} \\ = \begin{Bmatrix} \bar{P}_B c_{p_B} \\ 0 \end{Bmatrix} \cos \omega_{p_B}(t-t_{B-1}) + \begin{Bmatrix} \delta \bar{P}_{(f)_B}(t_B) c_{f_B} \\ 0 \end{Bmatrix} \sin \omega_{p_B}(t-t_{B-1}) \end{aligned} \quad (243)$$

Let

$$y_{\beta}(t) = \begin{Bmatrix} \delta \bar{\Delta}_{\beta}(t) \\ \bar{v}(t) \end{Bmatrix} \quad (244)$$

Therefore

$$\dot{y}_{\beta}(t) = \begin{Bmatrix} \delta \dot{\bar{\Delta}}_{\beta}(t) \\ \dot{\bar{v}}(t) \end{Bmatrix} \quad (245)$$

Also, let

$$L_{\beta} = \begin{bmatrix} 0 & \bar{M} \\ I & 0 \end{bmatrix} \quad B_{\beta} = \begin{bmatrix} \bar{K}_{(\beta)} & \bar{C}_{(\beta)} \\ 0 & -I \end{bmatrix} \quad (246)$$

$$\psi_{c_{\beta}} = \begin{Bmatrix} \bar{P}_{\beta} c_{p_{\beta}} \\ 0 \end{Bmatrix} \quad \psi_{f_{\beta}} = \begin{Bmatrix} \delta \bar{P}_{(f)_{\beta}}(t_{\beta}) c_{f_{\beta}} \\ 0 \end{Bmatrix} \quad (247)$$

Combining Equations 243, 244, 245, 246, and 247 gives

$$L_{\beta} \dot{y}_{\beta}(t) + B_{\beta} y_{\beta}(t) = \psi_{c_{\beta}} \cos \omega_{p_{\beta}}(t-t_{\beta-1}) + \psi_{f_{\beta}} \sin \omega_{p_{\beta}}(t-t_{\beta-1}) \quad (248)$$

Equation 248 is a matrix differential equation that represents a set of $2\bar{n}$ linear, ordinary, first order differential equations with constant coefficients. The solution of such an equation is a standard procedure.

Solution of the Reduced Equation

Setting the right hand side of Equation 248 equal to zero gives the reduced equation:

$$L_{\beta} \dot{y}_{\beta}(t) + B_{\beta} y_{\beta}(t) = 0 \quad (249)$$

Multiplying Equation 249 on the left by L_{β}^{-1} gives

$$\dot{y}_{\beta}(t) - A_{\beta} y_{\beta}(t) = 0 \quad (250)$$

where

$$A_{\beta} = -L_{\beta}^{-1} B_{\beta} \quad (251)$$

From Equations 246 and 251,

$$A_{\beta} = \left[\begin{array}{c|c} 0 & I \\ \hline -M^{-1}K_{(\beta)} & -M^{-1}C_{(\beta)} \end{array} \right] \quad (252)$$

Consider

$$y_{\beta k}(t) = G_{\beta k} e^{\lambda_{\beta k} t} \quad (253)$$

where $G_{\beta k}$ is an unknown column matrix, $\lambda_{\beta k}$ is an unknown scalar, and e_2 is the base of natural logarithms. Substituting $\bar{y}_{\beta k}$ from Equation 253 into Equation 250 gives

$$\lambda_{\beta k} G_{\beta k} e^{\lambda_{\beta k} t} - A_{\beta} G_{\beta k} e^{\lambda_{\beta k} t} = 0 \quad (254)$$

Factoring $G_{\beta k} e^{\lambda_{\beta k} t}$ and multiplying by -1 gives

$$(A_{\beta} - \lambda_{\beta k} I) G_{\beta k} e^{\lambda_{\beta k} t} = 0 \quad (255)$$

This equation is satisfied if

$$(A_{\beta} - \lambda_{\beta k} I) G_{\beta k} = 0 \quad (256)$$

Therefore $y_{\beta k}$ given by Equation 253 is a solution of Equation 250 if $\lambda_{\beta k}$ and $G_{\beta k}$ are an eigenvalue and an eigenvector of the characteristic equation, Equation 256.

Now, Equation 252 shows that A_{β} is a real, square, unsymmetric matrix of order $2\bar{n}$. Therefore Equation 256 has $2\bar{n}$ sets of eigenvalues and eigenvectors that are either real or occur in complex conjugate pairs. Therefore the solution of Equation 250 given by Equation 253, can be written more generally in the form

$$y_{\beta}(t) = \sum_{k=1}^{2\bar{n}} \hat{C}_{a_{\beta k}} G_{\beta k} e^{\lambda_{\beta k} t} \quad (257)$$

where $\lambda_{\beta k}$ and $G_{\beta k}$ are the k th eigenvalue and eigenvector of Equation 256, and the $\hat{C}_{a_{\beta k}}$'s are constants needed to satisfy the initial conditions.

Equation 257 can be written in the form

$$y_{\beta}(t) = \sum_{k=1}^{2\bar{n}} \hat{C}_{a_{\beta k}} G_{\beta k} e_2^{\lambda_{\beta k} t_{\beta-1}} e_2^{\lambda_{\beta k} (t-t_{\beta-1})} \quad (258)$$

where it is understood that Equation 258 applies to the β th increment.
Therefore

$$y_{\beta}(t) = \sum_{k=1}^{2\bar{n}} C_{a_{\beta k}} G_{\beta k} e_2^{\lambda_{\beta k} (t-t_{\beta-1})} \quad (259)$$

where the term $e_2^{\lambda_{\beta k} t_{\beta-1}}$ has been absorbed into the unknown constant $C_{a_{\beta k}}$. The eigenvector $G_{\beta k}$ is a column matrix with $2\bar{n}$ rows.

Equation 259 can be written in simpler form thus:

$$y_{\beta}(t) = H_{\beta} F_{\beta}(t-t_{\beta-1}) C_{a_{\beta}} \quad (260)$$

where

$$H_{\beta} = \left[G_{\beta 1} \mid G_{\beta 2} \mid \dots \right] \quad (261)$$

$$F_{\beta}(t-t_{\beta-1}) = \begin{Bmatrix} e_2^{\lambda_{\beta 1} (t-t_{\beta-1})} \\ e_2^{\lambda_{\beta 2} (t-t_{\beta-1})} \\ \vdots \end{Bmatrix} \quad (262)$$

$$C_{a\beta} = \begin{Bmatrix} C_{a\beta 1} \\ C_{a\beta 2} \\ \vdots \\ \vdots \end{Bmatrix} \quad (263)$$

and $F_D(t-t_{\beta-1}) = F_{\beta}(t-t_{\beta-1})$ diagonalized.

Particular Solution of the Complete Equation

A particular solution of Equation 248 is needed. It now becomes convenient to return to the second order matrix differential equation. Let

$$\bar{Y}_{C\beta} = \bar{P}_{\beta} C_{P\beta} \quad (264)$$

and

$$\bar{Y}_{f\beta} = \delta \bar{P}_{(f)\beta}(t_{\beta}) C_{f\beta} \quad (265)$$

Substituting $\bar{Y}_{C\beta}$ and $\bar{Y}_{f\beta}$ from Equations 264 and 265 into Equation 235 gives

$$\begin{aligned} \bar{M}\ddot{\bar{\Delta}}(t) + \bar{C}_{(\beta)}\dot{\bar{\Delta}}(t) + \bar{K}_{(\beta)}\bar{\Delta}_{(\beta)}(t) &= \bar{Y}_{C\beta} \cos \omega_{p\beta}(t-t_{\beta-1}) \\ &+ \bar{Y}_{f\beta} \sin \omega_{p\beta}(t-t_{\beta-1}) \end{aligned} \quad (266)$$

A particular solution of Equation 266 is also a particular solution of Equation 248, since the equations are equivalent.

Consider the equation

$$\bar{M}\ddot{\bar{\Delta}}(t) + \bar{C}_{(\beta)}\dot{\bar{\Delta}}(t) + \bar{K}_{(\beta)}\bar{\Delta}_{(\beta)}(t) = \bar{Y}_{\beta} e^{j\omega_{p\beta}(t-t_{\beta-1})} \quad (267)$$

$$\text{Now } \bar{\gamma}_\beta e_\beta^{j\omega_{p\beta}(t-t_{\beta-1})} = \bar{\gamma}_\beta \left[\cos \omega_{p\beta}(t-t_{\beta-1}) + j \sin \omega_{p\beta}(t-t_{\beta-1}) \right] \quad (263)$$

Thus the right hand side of Equation 267 is complex, and

$$\text{Re} \left[\bar{\gamma}_\beta e_\beta^{j\omega_{p\beta}(t-t_{\beta-1})} \right] = \bar{\gamma}_\beta \cos \omega_{p\beta}(t-t_{\beta-1}) \quad (269)$$

$$\text{Im} \left[\bar{\gamma}_\beta e_\beta^{j\omega_{p\beta}(t-t_{\beta-1})} \right] = \bar{\gamma}_\beta \sin \omega_{p\beta}(t-t_{\beta-1}) \quad (270)$$

where Re and Im indicate the real and imaginary parts.

The solution, $y_\beta(t)$, of Equation 267, must also be complex, since the forcing function is complex. The real part of the solution is the solution corresponding to the real part of the forcing function, and the imaginary part of the solution is the solution corresponding to the imaginary part of the forcing function.

Therefore it follows from Equations 269 and 270 that the real part of the solution of Equation 267, with $\bar{\gamma}_\beta$ set equal to $\bar{\gamma}_{C_\beta}$, plus the imaginary part of the solution of Equation 267, with $\bar{\gamma}_\beta$ set equal to $\bar{\gamma}_{f_\beta}$, is the solution of Equation 266.

In Equation 267, take

$$\delta \bar{\Delta}_{(\beta)}(t) = \delta \bar{\Delta}_{C(\beta)} e_\beta^{j\omega_{p\beta}(t-t_{\beta-1})} \quad (271)$$

where $\delta \bar{\Delta}_{C(\beta)}$ is an unknown column matrix.

From Equations 239 and 271

$$\dot{\bar{\Delta}}_{(\beta)}(t) = j\omega_{p\beta} \delta \bar{\Delta}_{C(\beta)} e_\beta^{j\omega_{p\beta}(t-t_{\beta-1})} \quad (272)$$

$$\text{Therefore, } \ddot{\bar{\Delta}}_{(\beta)}(t) = -\omega_{p\beta}^2 \delta \bar{\Delta}_{C(\beta)} e_\beta^{j\omega_{p\beta}(t-t_{\beta-1})} \quad (273)$$

Combining Equations 267, 271, 272 and 273 gives

$$\begin{aligned} & \left[-\omega_p^2 \bar{M} + j\omega_p \bar{C}_{(B)} + \bar{K}_{(B)} \right] \delta \bar{\Delta}_{C(B)} e^{j\omega_p (t-t_B-1)} \\ & = \bar{\gamma}_B e^{j\omega_p (t-t_B-1)} \end{aligned} \quad (274)$$

Equation 274 is satisfied if

$$\bar{K}_{C(B)} \delta \bar{\Delta}_{C(B)} = \bar{\gamma}_B \quad (275)$$

where $\bar{K}_{C(B)} = \bar{K}_{(B)} - \omega_p^2 \bar{M} + j\omega_p \bar{C}_{(B)}$. (276)

$\bar{K}_{C(B)}$ is the mechanical impedance matrix.

Solving Equation 275 for $\delta \bar{\Delta}_{C(B)}$, and substituting the result into Equation 271 gives

$$\delta \bar{\Delta}_{(B)}(t) = \bar{K}_{C(B)}^{-1} \bar{\gamma}_B e^{j\omega_p (t-t_B-1)} \quad (277)$$

Taking the real part of this expression with $\bar{\gamma}_B = \bar{\gamma}_{C_B}$, and the imaginary part with $\bar{\gamma}_B = \bar{\gamma}_{f_B}$ gives

$$\delta \bar{\Delta}_{(B)}(t) = \text{Re} \left[\bar{K}_{C(B)}^{-1} \bar{\gamma}_{C_B} e^{j\omega_p (t-t_B-1)} \right] + \text{Im} \left[\bar{K}_{C(B)}^{-1} \bar{\gamma}_{f_B} e^{j\omega_p (t-t_B-1)} \right] \quad (278)$$

Let $\delta \bar{\Delta}_{C_B} = \bar{K}_{C(B)}^{-1} \bar{\gamma}_{C_B}$ (279)

$$\delta \bar{\Delta}_{f_B} = \bar{K}_{C(B)}^{-1} \bar{\gamma}_{f_B} \quad (280)$$

Combining Equations 278, 279 and 280 gives

$$\delta\bar{\Delta}_{(B)}(t) = \text{Re} \left[\delta\bar{\Delta}_{C_B} e^{j\omega_{p_B}(t-t_{B-1})} \right] + \text{Im} \left[\delta\bar{\Delta}_{f_B} e^{j\omega_{f_B}(t-t_{B-1})} \right] \quad (281)$$

where, from Equations 264, 265, 279 and 280,

$$\delta\bar{\Delta}_{C_B} = \bar{K}_{C(B)}^{-1} \bar{P}_B c_{p_B} \quad (282)$$

$$\delta\bar{\Delta}_{f_B} = \bar{K}_{C(B)}^{-1} \delta\bar{P}_{(f)_B}(t_B) c_{f_B} \quad (283)$$

Now $\delta\bar{\Delta}_{C_B}$ and $\delta\bar{\Delta}_{f_B}$ can be written

$$\delta\bar{\Delta}_{C_B} = \delta\bar{\Delta}_{CR_B} + j\delta\bar{\Delta}_{CI_B} \quad (284)$$

$$\delta\bar{\Delta}_{f_B} = \delta\bar{\Delta}_{fR_B} + j\delta\bar{\Delta}_{fI_B} \quad (285)$$

where

$\delta\bar{\Delta}_{CR_B}, \delta\bar{\Delta}_{CI_B}$ = real and imaginary parts of $\delta\bar{\Delta}_{C_B}$

$\delta\bar{\Delta}_{fR_B}, \delta\bar{\Delta}_{fI_B}$ = real and imaginary parts of $\delta\bar{\Delta}_{f_B}$

Eliminating $\delta\bar{\Delta}_{C_B}$ and $\delta\bar{\Delta}_{f_B}$ from Equations 281, 284, and 285, and expanding the exponential terms gives

$$\begin{aligned} \delta\Delta_{(B)}(t) = & \text{Re} \left\{ (\delta\Delta_{CR_B} + j\delta\Delta_{CI_B}) \left[\cos \omega_{p_B}(t-t_{B-1}) + j \sin \omega_{p_B}(t-t_{B-1}) \right] \right\} \\ & + \text{Im} \left\{ (\delta\Delta_{fR_B} + j\delta\Delta_{fI_B}) \left[\cos \omega_{p_B}(t-t_{B-1}) + j \sin \omega_{p_B}(t-t_{B-1}) \right] \right\} \quad (286) \end{aligned}$$

Expanding the terms in brackets on the right hand side of Equation 286, and taking the real and imaginary parts gives

$$\begin{aligned}\delta\bar{\Delta}_{(\beta)}(t) &= (\delta\bar{\Delta}_{CR_{\beta}} + \delta\bar{\Delta}_{fI_{\beta}})\cos \omega_{p_{\beta}}(t-t_{\beta-1}) \\ &+ (\delta\bar{\Delta}_{fR_{\beta}} - \delta\bar{\Delta}_{CI_{\beta}})\sin \omega_{p_{\beta}}(t-t_{\beta-1})\end{aligned}\quad (287)$$

From Equations 241 and 287,

$$\begin{aligned}\bar{v}(t) &= -\omega_{p_{\beta}}(\delta\bar{\Delta}_{CR_{\beta}} + \delta\bar{\Delta}_{fI_{\beta}})\sin \omega_{p_{\beta}}(t-t_{\beta-1}) \\ &+ \omega_{p_{\beta}}(\delta\bar{\Delta}_{fR_{\beta}} - \delta\bar{\Delta}_{CI_{\beta}})\cos \omega_{p_{\beta}}(t-t_{\beta-1})\end{aligned}\quad (288)$$

Employing Equation 244, Equations 287 and 288 can be written in the form

$$y_{\beta}(t) = y_{C_{\beta}} \cos \omega_{p_{\beta}}(t-t_{\beta-1}) + y_{S_{\beta}} \sin \omega_{p_{\beta}}(t-t_{\beta-1})$$

where

$$y_{C_{\beta}} = \begin{Bmatrix} \delta\bar{\Delta}_{CR_{\beta}} + \delta\bar{\Delta}_{fI_{\beta}} \\ \omega_{p_{\beta}}(\delta\bar{\Delta}_{fR_{\beta}} - \delta\bar{\Delta}_{CI_{\beta}}) \end{Bmatrix} \quad (289)$$

$$y_{S_{\beta}} = \begin{Bmatrix} \delta\bar{\Delta}_{fR_{\beta}} - \delta\bar{\Delta}_{CI_{\beta}} \\ -\omega_{p_{\beta}}(\delta\bar{\Delta}_{CR_{\beta}} + \delta\bar{\Delta}_{fI_{\beta}}) \end{Bmatrix} \quad (290)$$

Equation 289 is a particular solution of the differential equation of motion, Equation 248.

General Solution of the Differential Equation of Motion

Combining the solution of the reduced equation, known as the complementary function, from Equation 260, with the particular solution of the complete equation, from Equation 289, gives the general solution of the equation of motion:

$$y_B(t) = H_B F_{D_B}(t-t_{B-1})C_{a_B} + y_{C_B} \cos \omega_{p_B}(t-t_{B-1}) + y_{S_B} \sin \omega_{p_B}(t-t_{B-1}) \quad (292)$$

Initial Conditions

The column matrix of unknown constants, C_{a_B} , is evaluated by substituting the conditions at the beginning of the B th increment into Equation 292. From Equation 244,

$$y_B(t_{B-1}) = \begin{Bmatrix} 0 \\ \bar{v}(t_{B-1}) \end{Bmatrix} \quad (293)$$

since, from Equation 173, $\delta \bar{\Delta}_B(t_{B-1}) = 0$.

From Equation 262, $F_{D_B}(t-t_{B-1}) = I$ at $t = t_{B-1}$, since F_{D_B} is F_B diagonalized. Setting $t = t_{B-1}$ in Equation 292 gives

$$y_B(t_{B-1}) = H_B C_{a_B} + y_{C_B} \quad (294)$$

Therefore

$$C_{a_B} = H_B^{-1} [y_B(t_{B-1}) - y_{C_B}] \quad (295)$$

Thus the unknown constants are evaluated.

Incremental Displacements, Velocities, Accelerations

Let $C_{aD_B} = C_{a_B}$ diagonalized (296)

Therefore, from Equations 262, 263 and 296, -

$$F_{D_B}(t-t_{B-1})C_{a_B} = C_{aD_B}F_B(t-t_{B-1}), \quad (297)$$

since $F_{D_B}(t-t_{B-1})$ is $F_B(t-t_{B-1})$ diagonalized. Also partition H_B with respect to velocity and displacement components:

$$H_B = \begin{bmatrix} H_{\Delta_B} \\ H_{V_B} \end{bmatrix} \quad (298)$$

where each partition of H_B has \bar{n} rows.

Substituting $y_B(t)$, y_{C_B} , y_{S_B} and H_B from Equations 244, 290, 291 and 298 into Equation 292 and employing Equation 297 gives

$$\begin{aligned} \begin{Bmatrix} \delta \bar{\Delta}_B(t) \\ \bar{v}(t) \end{Bmatrix} &= \begin{bmatrix} H_{\Delta_B} \\ H_{V_B} \end{bmatrix} C_{aD_B} F_B(t-t_{B-1}) + \begin{Bmatrix} \delta \bar{\Delta}_{CR_B} + \delta \bar{\Delta}_{fI_B} \\ \omega_{p_B} (\delta \bar{\Delta}_{fR_B} - \delta \bar{\Delta}_{CI_B}) \end{Bmatrix} \cos \omega_{p_B} (t-t_{B-1}) \\ &+ \begin{Bmatrix} \delta \bar{\Delta}_{fR_B} - \delta \bar{\Delta}_{CI_B} \\ -\omega_{p_B} (\delta \bar{\Delta}_{CR_B} + \delta \bar{\Delta}_{fI_B}) \end{Bmatrix} \sin \omega_{p_B} (t-t_{B-1}) \end{aligned} \quad (299)$$

From Equation 299 incremental displacements and velocities are given by

$$\begin{aligned} \delta \bar{\Delta}_B(t) &= H_{\Delta_B} C_{aD_B} F_B(t-t_{B-1}) + (\delta \bar{\Delta}_{CR_B} + \delta \bar{\Delta}_{fI_B}) \cos \omega_{p_B} (t-t_{B-1}) \\ &+ (\delta \bar{\Delta}_{fR_B} - \delta \bar{\Delta}_{CI_B}) \sin \omega_{p_B} (t-t_{B-1}) \end{aligned} \quad (300)$$

and

$$\begin{aligned} \dot{V}(t) = & H_{V_B} C_{aD_B} F_B(t-t_{B-1}) + \omega_{p_B} (\delta \bar{\Delta}_{fR_B} - \delta \bar{\Delta}_{CI_B}) \cos \omega_{p_B} (t-t_{B-1}) \\ & - \omega_{p_B} (\delta \bar{\Delta}_{CR_B} + \delta \bar{\Delta}_{fI_B}) \sin \omega_{p_B} (t-t_{B-1}) \end{aligned} \quad (301)$$

From Equation 262,

$$\frac{d}{dt} F_B(t-t_{B-1}) = \begin{Bmatrix} \lambda_{B1} e^{\lambda_{B1}(t-t_{B-1})} \\ \lambda_{B2} e^{\lambda_{B2}(t-t_{B-1})} \\ \vdots \\ \vdots \end{Bmatrix} \quad (302)$$

$$\text{Therefore } \frac{d}{dt} F_B(t-t_{B-1}) = \lambda_{D_B} F_B(t-t_{B-1}) \quad (303)$$

$$\text{where } \lambda_B = \begin{Bmatrix} \lambda_{B1} \\ \lambda_{B2} \\ \vdots \\ \vdots \end{Bmatrix} \quad (304)$$

$$\text{and } \lambda_{D_B} = \lambda_B \text{ diagonalized.} \quad (305)$$

Differentiating Equation 301 with respect to time, and employing Equation 303 gives

$$\begin{aligned} \ddot{V}(t) = & H_{V_B} C_{aD_B} \lambda_{D_B} F_B(t-t_{B-1}) - \omega_{p_B}^2 (\delta \bar{\Delta}_{CR_B} + \delta \bar{\Delta}_{fI_B}) \cos \omega_{p_B} (t-t_{B-1}) \\ & - \omega_{p_B}^2 (\delta \bar{\Delta}_{fR_B} - \delta \bar{\Delta}_{CI_B}) \sin \omega_{p_B} (t-t_{B-1}) \end{aligned} \quad (306)$$

Transformed incremental displacements, velocities and accelerations are given by Equations 300, 301 and 306.

Untransformed incremental displacements are given by Equation 172.
Untransformed velocities and accelerations are given by

$$\dot{\Delta}(t) = v(t) = T\bar{v}(t) \quad (307)$$

$$\ddot{\Delta}(t) = \dot{v}(t) = T\dot{\bar{v}}(t) \quad (308)$$

SOLUTION OF THE NONLINEAR EQUATION OF MOTION

The nonlinear equation of motion is solved incrementally in time, and iteratively within each increment, employing the solution of the linearized equation.

All of the basic equations needed for the nonlinear solution are presented in preceding subsections. These equations involve numerous matrices that are defined, and presumed known in the derivation, relating to geometric, inertia, damping and stiffness properties of the structure, as well as to bird impact loads, and the modal transformation. These matrices are derived in terms of basic data in Appendix C on Elements, Appendix D on Fictitious Forces and Deformations, Appendix E on Material Nonlinearity, Appendix F on Bird Impact Loads, and Appendix G on the Modal Transformation.

This section, on the theoretical basis of the Math Model, is now concluded with a description of the iterative loop employed within each time increment to solve the nonlinear equation. This loop was originally planned to account for three kinds of nonlinearities: (1) material nonlinearities, (2) geometric nonlinearities resulting from changes in element geometry, and (3) geometric nonlinearities resulting from element rotations. A fourth nonlinearity resulting from bird-windshield interaction is significant, and warrants further study.

In the preceding paragraph, nonlinearities of the first kind refer to the effects of yielding, as described by the Von Mises yield

criterion, and the Prantl-Reuss equations. Nonlinearities in the second category refer, for example, to the increased stiffness that a bar element would experience, if it were subjected to compression loads large enough to appreciably decrease the length of the bar, and to significantly increase its cross section. Nonlinearities of the third kind result from rotations of element forces, and are taken into account by the method of fictitious forces and deformations.

Results of bird impact tests conducted on the F-16 canopy indicated that nonlinearities of the third kind were of greatest interest, and therefore these nonlinearities were emphasized. Some programming in connection with categories 1 and 2 was accomplished, but not completed.

The following paragraphs describe the iterative loop developed to solve the equation of motion, considering geometric nonlinearities resulting from element rotations.

Iterative Loop

The equation of motion being solved is:

$$\begin{aligned} \bar{M}\ddot{\bar{\Delta}}(t) + \bar{C}_{(B)}\dot{\bar{\Delta}}(t) + \bar{K}_{(B)}\bar{\Delta}_{(B)}(t) &= \bar{P}_B c_{p_B} \cos \omega_{p_B}(t-t_{B-1}) \\ &+ \delta\bar{P}_{(f)_B}(t_B) c_{f_B} \sin \omega_{p_B}(t-t_{B-1}) \end{aligned} \quad (\text{Ref. Eq. 235})$$

In this equation, \bar{M} is a constant matrix. The scalars c_{p_B} , c_{f_B} , ω_{p_B} and t_{B-1} are known for each increment. The matrices $\bar{C}_{(B)}$, $\bar{K}_{(B)}$ and \bar{P}_B are available from the preceding increment. The unknowns are the incremental displacements $\bar{\Delta}_{(B)}(t)$, and the fictitious loads $\delta\bar{P}_{(f)_B}(t_B)$. At the beginning of the β th increment, the fictitious loads $\delta\bar{P}_{(f)_B}(t_B)$ are set equal to zero, and the equation is solved for $\bar{\Delta}_{(B)}(t)$, and its derivatives. The first approximation to

$\delta \bar{P}_{(f)}(t_{\beta})$ is then calculated from the incremental displacements.

The new $\delta P_{(f)}(t_{\beta})$ is substituted into the equation, and the process is repeated for a specified number of iterations. The final displacements, velocities and accelerations are presumed to be correct, and the stiffness, damping and thermomechanical load matrices, $\bar{C}_{(\beta+1)}$, $\bar{K}_{(\beta+1)}$ and $\bar{P}_{(\beta+1)}$ are calculated for use in the next increment. After completion of the incremental solution, the output is examined to determine if the convergence of the iterative process in each increment is satisfactory. If not, the solution can be repeated with an increased number of iterations per increment.

The reason why the iterative process is stopped after a specified number of iterations, instead of being allowed to proceed to convergence, is that the nonlinear solution is experimental. A suitable criterion for convergence would have taken time to develop, and many of the experimental runs would have been needlessly lengthened at a time when rapid turn-around was important. The nonlinear solutions for simple structures exhibiting large geometric nonlinearities presented in Section III converged very satisfactorily in five iterations or less.

Table 1 presents the iterative loop, considering geometric nonlinearities resulting from element rotations, for the β th time increment. Input to the loop includes the transformed mass matrix \bar{M} and the modal transformation matrix T , which are constant for the entire incremental solution. The element transformed stiffness and damping matrices, $\bar{k}_{i(\beta)}$ and $\bar{c}_{i(\beta)}$, are also considered constant for the incremental solution. Unassembled thermal deformations are not considered, therefore the matrices $\delta \bar{e}_{0i\beta}(t_{\beta})$ and $\delta \bar{P}_{K0\beta}(t_{\beta})$ are taken equal to zero. The mechanical load matrix, $\delta \bar{P}_{(\phi)U\beta}(t_{\beta})$, and the scalars τ_{β} and $\omega_{p\beta}$ are known for each increment. All other variables are known either from a prior iteration, or a prior

TABLE 1. ITERATIVE LOOP, GEOMETRIC NONLINEARITY, β TH INCREMENT

STEP	INPUT MATRICES	OPERATION	OUTPUT MATRICES	EQUATION, APPENDIX REFERENCES
1		Set fictitious loads and deformations equal to zero.		
2	$\bar{M}, \bar{C}(\beta), \bar{K}(\beta),$ $\bar{v}(t_{\beta-1}), \bar{P}_\beta,$ $\delta \bar{P}(\tau)_\beta: c_{p_\beta}, c_{f_\beta},$ ω_{p_β}	Compute transformed incremental displacements, and transformed velocities and accelerations at $t=t_\beta$.	$A_\beta, \lambda_{\beta k}, G_{\beta k}, H_\beta$ $F_\beta(t-t_{\beta-1}), \bar{K}_C(\beta), \delta \bar{\Delta}_C \beta$ $\delta \bar{\Delta}_f \beta, y_{C_\beta}, y_\beta(t_{\beta-1}), c_{a_\beta}$ $H_{\Delta_\beta}, H_{v_\beta}, \delta \bar{\Delta}_\beta(t_\beta)$ $\bar{v}(t_\beta), \dot{\bar{v}}(t_\beta)$	252, 256, 261, 262 276, 282, 283 289, 293, 295, 298, 300, 301, 306
3	$\delta \bar{\Delta}_\beta(t_\beta), \bar{v}(t_\beta)$ $\dot{\bar{v}}(t_\beta), T$	Compute untransformed incremental displacements. Also velocities and accelerations.	$\delta \Delta_\beta(t_\beta), v(t_\beta)$ $\dot{v}(t_\beta)$	172, 307 308
4	$P_{ij} \bar{F}_i(t_{\beta-1}), \delta \Delta_\beta(t_\beta)$ $\bar{F}_{K_1}(t_{\beta-1}), \bar{K}_i(\beta),$ $\delta \bar{e}_{f_{i\beta}}(t_\beta),$ $\delta \bar{e}_{o_{i\beta}}(t_\beta)=0$	Compute lumped element deformations, and lumped stiffness forces.	$\delta \bar{e}_{L_{i\beta}}(t_\beta), \bar{F}_{K_1}(t_\beta)$	136, 134
5		Update coordinates at $t=t_\beta$ by adding incremental displacements to old coordinates.		

TABLE 1. ITERATIVE LOOP, GEOMETRIC NONLINEARITY, β TH INCREMENT
(CONTINUED)

STEP	INPUT MATRICES	OPERATION	OUTPUT MATRICES	EQUATION, APPENDIX REFERENCES
6		Compute bar lengths, panel edge lengths and skew angles, and fictitious force transformation at $t=t_\beta$.	$P_{UF\ i\beta}$	Appendices C and D.
7		Compute average bar lengths, panel edge lengths and skew angles, and average fictitious force transformation for β th increment.	$P_{UF\ i(\beta)}$	
8	$P_{UF\ i(\beta)}, \delta\Delta_\beta(t_\beta)$	Compute fictitious forces and deformations.	$\delta\bar{e}_{i\beta}(t_\beta),$ $\bar{F}_{K_{i\beta}}(t_\beta), \delta\bar{e}_{f_{i\beta}}(t_\beta)$	Appendix D D.44, D53, D.55, D.304, D.312
9	$P_{UF\ i\beta}, \bar{F}_{K_{i\beta}}(t_\beta),$ $P_{UF\ i}(t_{\beta-1}), \bar{k}_i(\beta)$ $\delta\bar{e}_{f_{i\beta}}(t_\beta), T$	Compute fictitious transformed external loads.	$\delta P_{(\bar{F})_\beta}(t_\beta), \delta P_{Kf_\beta}(t_\beta)$ $\delta\bar{P}_{(\bar{F})_\beta}(t_\beta), \delta\bar{P}_{Kf_\beta}(t_\beta)$ $\delta\bar{P}_{(f)_\beta}(t_\beta)$	125, 118, 181 182, 234
10		Repeat steps 2 through 9 for a specified number of iterations.		

TABLE 1. ITERATIVE LOOP, GEOMETRIC NONLINEARITY, BTH INCREMENT
(CONTINUED)

STEP	INPUT MATRICES	OPERATION	OUTPUT MATRICES	EQUATION, APPENDIX REFERENCES
11	$v(t_B), P_{UF_i}(t_{B-1})$ $\bar{c}_i(B)$	Compute lumped element velocities and damping forces.	$\dot{\Delta}(t_B), \dot{\bar{e}}_{L_i}(t_B)$ $\bar{F}_{C_i}(t_B)$	307, 123, 139
12		Compute updated element force transformation based on updated coordinates.	$P_{UF_i}(t_B)$	Appendix C
13	$\bar{v}(t_B), \bar{M}, T,$ $P_{UF_i}(t_B), \bar{F}_{C_i}(t_B)$ $\bar{F}_{K_i}(t_B), \bar{P}_{(\phi)U}(t_{B-1})$ $\delta P_{(\phi)U_B}(t_B)$	Compute unbalanced loads.	$\ddot{\Delta}(t_B), \bar{P}_{MU}(t_B)$ $\bar{P}_{CU}(t_B), \bar{P}_{KU}(t_B)$ $\bar{P}_{(\phi)U}(t_B), \delta \bar{P}_{U_B}(t_B)$	237, 189, 203, 204, 188, 205
14	$\delta \bar{P}_{K0_{B+1}}(t_{B+1})=0$ $\delta \bar{P}_{(\phi)U_{B+1}}(t_{B+1})$ $\bar{P}_{(M)U}(t_B), \bar{P}_{(C)U}(t_B)$ $\delta \bar{P}_{U_B}(t_B)$	Compute corrected load matrix for the next increment.	\bar{P}_{B+1}	233

TABLE 1. ITERATIVE LOOP, GEOMETRIC NONLINEARITY, β TH INCREMENT
(CONTINUED)

STEP	INPUT MATRICES	OPERATION	OUTPUT MATRICES	EQUATION, APPENDIX REFERENCES
15	$P_{UF_i}(t_\beta), \bar{k}_i(\beta+1)$ $\bar{c}_i(\beta+1), T$	Compute updated assembled damping and stiffness matrices at $t=t_\beta$.	$K_{(\beta+1)}, C_{(\beta+1)}$ $\bar{K}_{(\beta+1)}, \bar{C}_{(\beta+1)}$	87, 101, 176, 177

increment. The table shows the input matrices required for each step, the operation being performed, the matrices output for each step, and equation and appendix references.

Table 1 is intended only to give a general idea of the operations performed in the iterative loop. For this reason, non-matrix input and output data are not described. Also the iterative solution is not accomplished by the Math Model in exactly the order indicated by the table, because this order is not optimum for computation. The optimized order of calculations is summarized in Appendix H. The basic strategy in optimizing the calculations, as described in Appendix H, is to keep the matrices as small as possible, by taking full advantage of the modal transformation.

In addition to outputting velocities, accelerations, incremental displacements and element forces, as indicated in Table I, the Math Model also outputs total displacements, element stresses, element strains and other data.

A linear version of the Math Model is also available. In this version, called the linear incremental option, the iterative loop is executed once per increment, no fictitious loads are calculated, and all calculations that become unnecessary as a result of these simplifications are deleted.

SECTION III APPLICATIONS

The objectives of this section are to show the utility of the Math Model as a general purpose tool for analyzing transient dynamic responses of windshield systems to impact; and to verify the validity of the model through correlations of calculated results with known solutions of classical problems, and with test data.

STATIC LINEAR CORRELATIONS, CLASSICAL PROBLEMS

The results of these studies are offered to provide verification of the cell element as a building block for finite element modelling. In addition, the flat plate buckling study tends to verify the first order fictitious force terms for shear panels. These results were obtained by solving the familiar static displacement method equation. No modal transformations were employed.

The theoretical basis of the cell element, including the method of calculating stresses, is given in Appendix C.

Cell Element, Elementary Loads

Figure 3.1 shows that the rectangular parallelepiped cell element produces correct displacements for nine elementary loads. The length and width of the element are a and b , and the thickness is h . Young's modulus is E , and Poisson's ratio is ν .

The nine loads are shown on the left of the figure. The first three loads represent pure shear on the element, the next three, pure tension. Loads 7 and 8 represent pure bending, while load 9 represents pure torsion.

The flexibility matrix on the right of the figure represents element deformations resulting from unit value of the loads. The rows of the matrix correspond to deformations, the columns to loads. The deformation corresponding to any particular load is defined as the work done by a

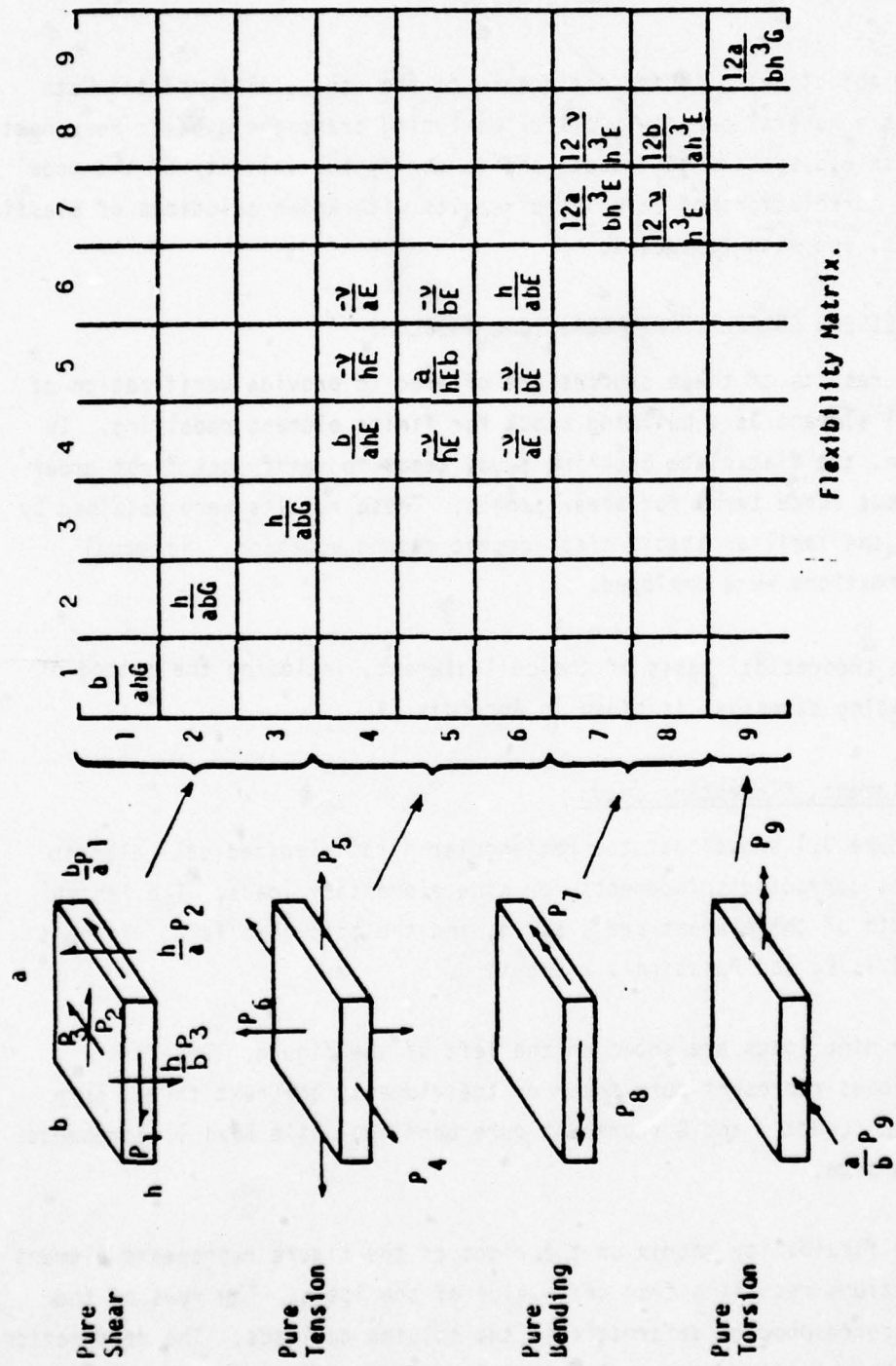


Figure 3.1. Validity of parallelepiped cell element for simple loads.

unit value of the load during a virtual displacement, in accordance with Appendix A. For example, the term in Row 4 and Column 4 of the matrix represents the elongation of the element in the direction of P_4 , resulting from a unit value of P_4 . This term is equal to $b/(ahE)$, which is correct. Similarly, the term in Row 4, Column 5, represents the elongation in the direction of P_4 , resulting from a unit value of P_5 . This value is $-v/(hE)$, which is also correct.

All of the terms in the flexibility matrix are correct, and none are missing, which shows that the element gives correct deformations for all nine elementary loads, with correct Poisson's coupling, in the linearly elastic case.

The same kind of check was made for the skewed cell element shown in Figure 3.2. The figure shows the planform dimensions. The thickness of the element was unity. The skewed element was subjected to nine loading conditions corresponding to the loads applied to the parallelepiped. Joint B was constrained from moving in all three directions, Joint A was constrained from moving in the y and z directions, the joint directly under B, on the lower surface, was constrained from moving in the y direction. Displacements were calculated, according to the element algorithms, in all corner joint unconstrained degrees of freedom, and in all edge shear node degrees of freedom for the nine loading conditions. The results were compared with values calculated from classical plate theory, and were found to check to within at least six significant figures, showing that the element correctly accounts for the effects of skewness, as well as Poisson coupling.

Flat Plate, Uniform Pressure

Figure 3.3 shows a simply supported square plate subjected to uniform lateral load. The plate was modelled as shown, with cell elements. The figure shows good agreement between theoretical results (Reference 3), and the results of the finite element analysis.

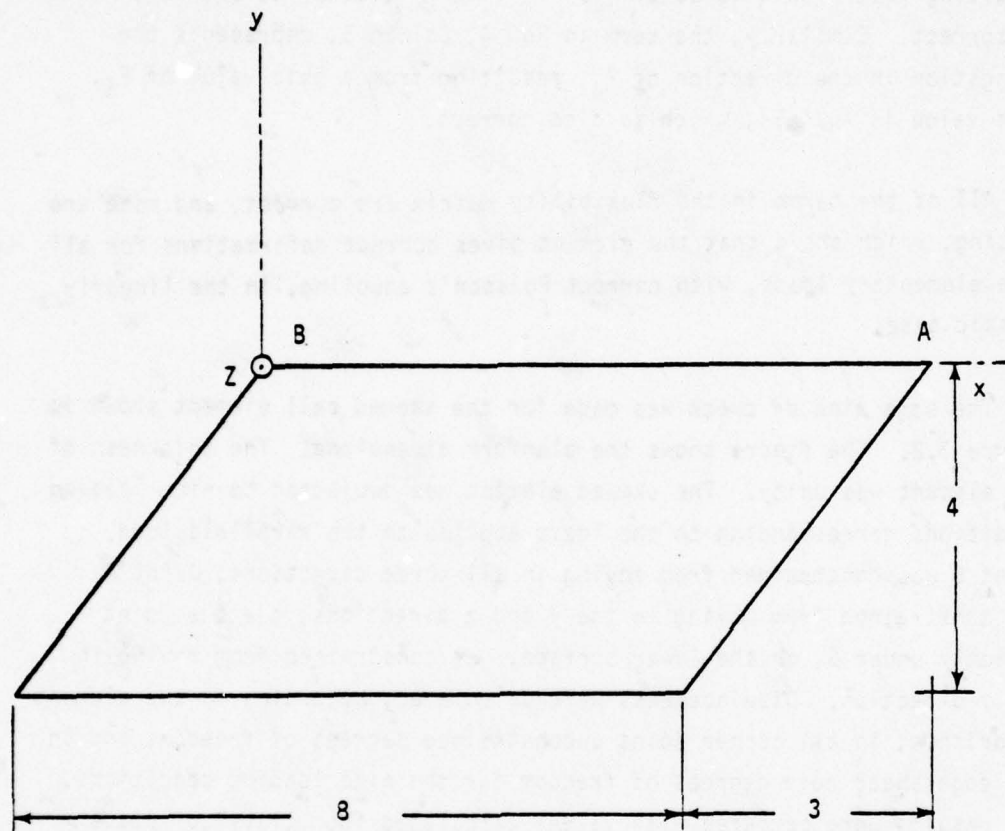


Figure 3.2. Skewed cell element.

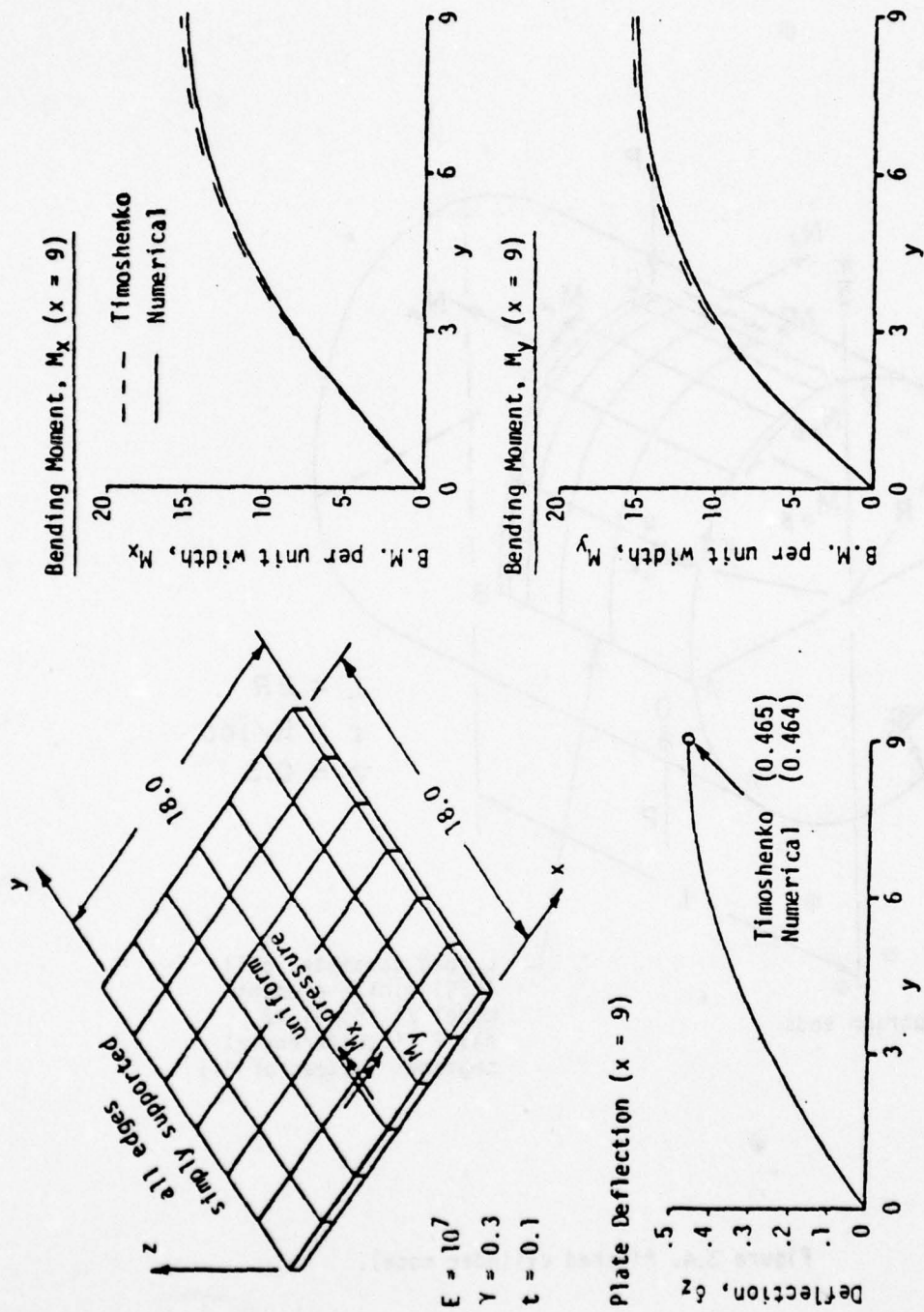


Figure 3.3. Static analysis - simply supported square plate under uniform pressure.

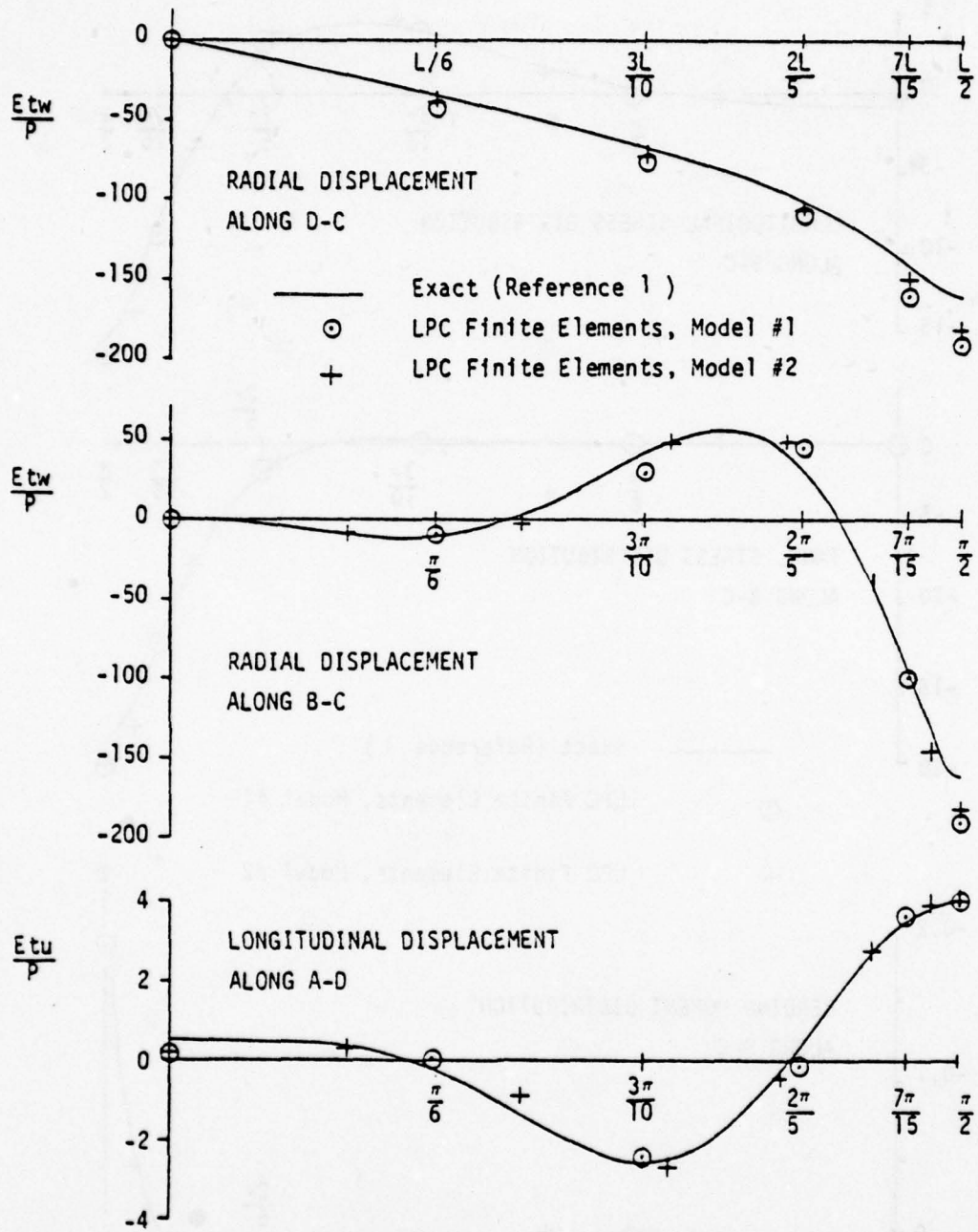


Figure 3.5. Pinched cylinder displacements.

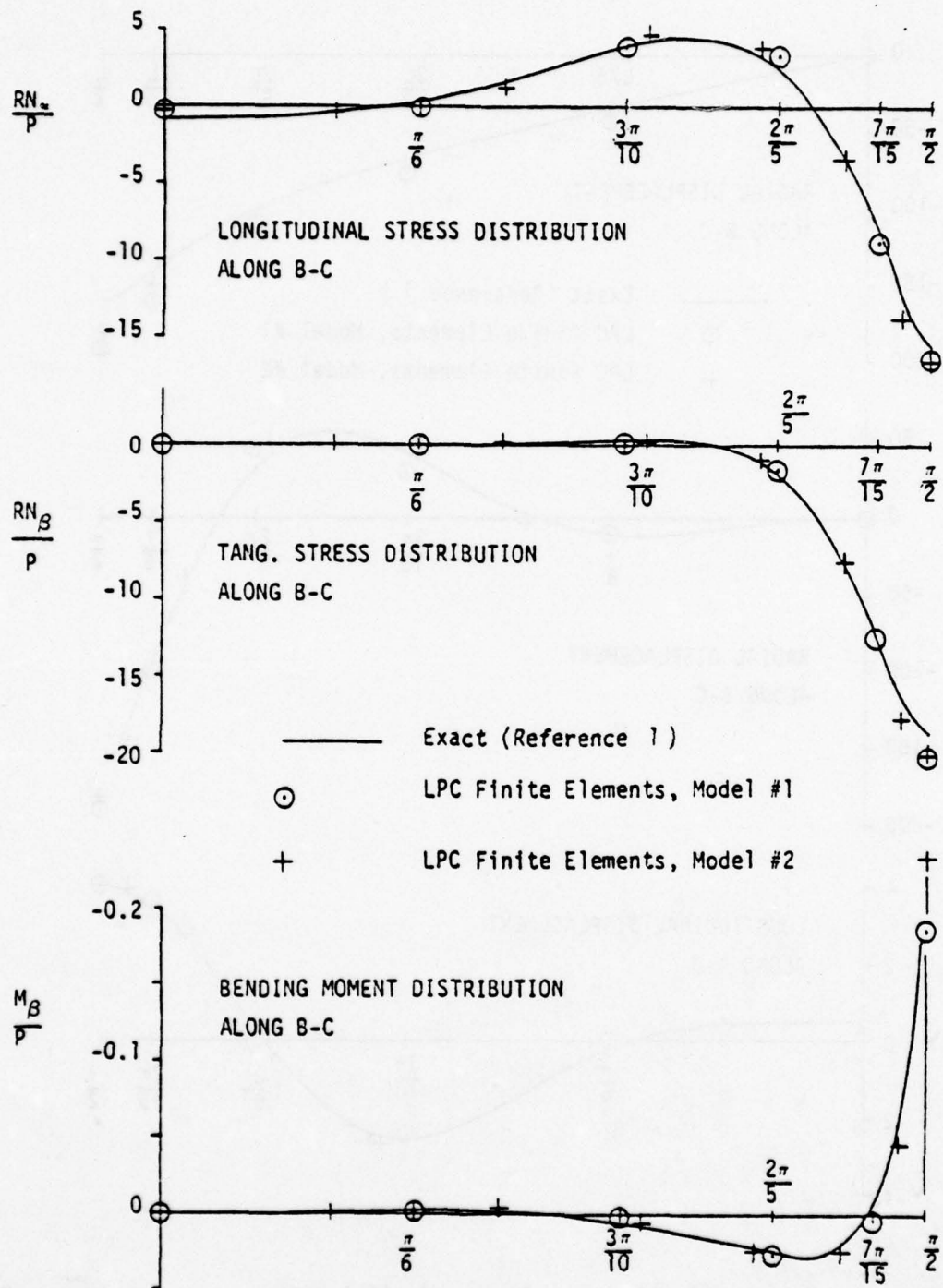


Figure 3.6. Stresses and moments on Section B-C.

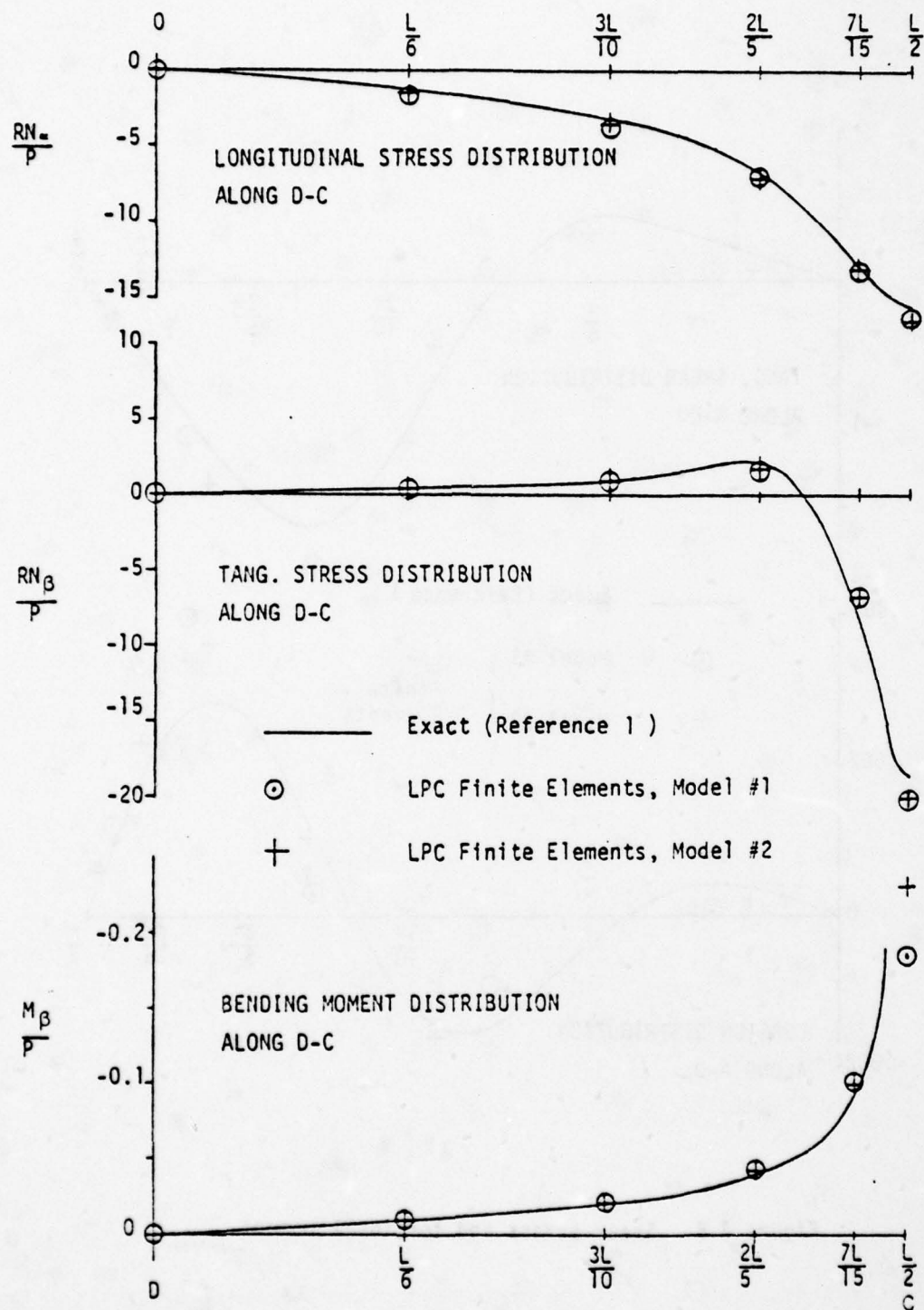


Figure 3.7. Stresses and moments on Section D-C.

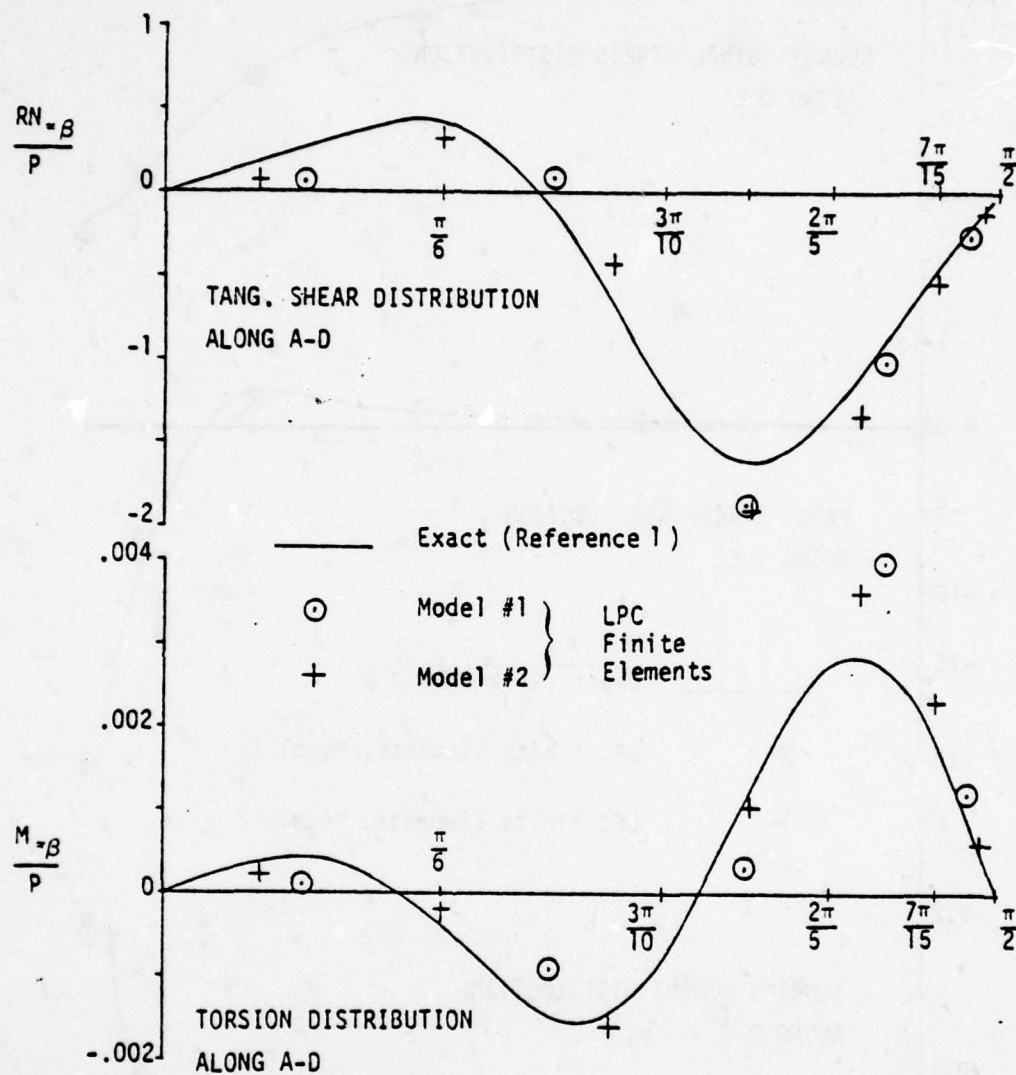
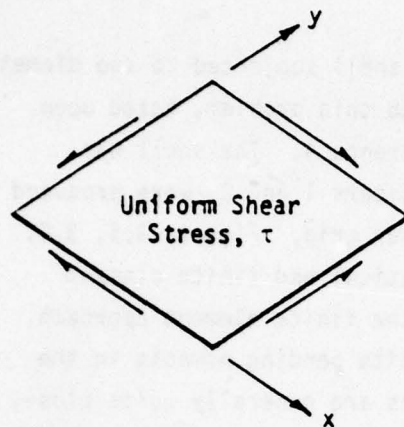


Figure 3.8. Shear stress and torsional moment.



Buckling Stress (psi)

Theoretical $\tau_B = 2606$

Numerical $\tau_B = 2455$ (5.8%)

Buckling Mode

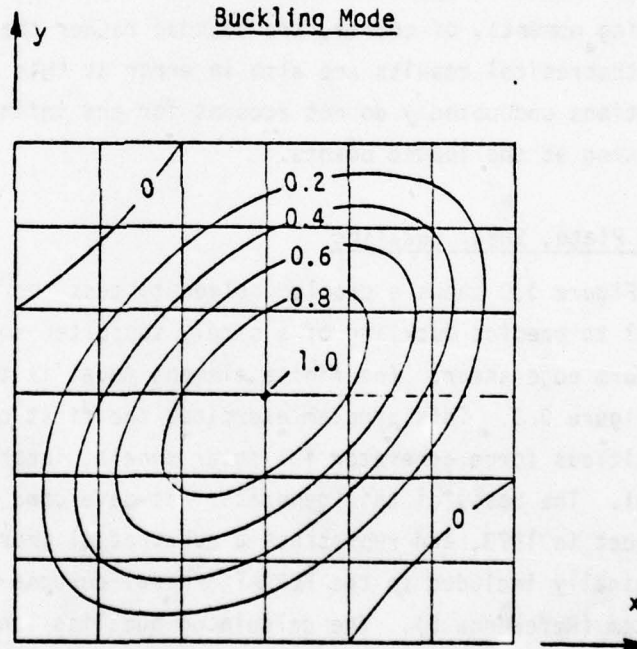


Figure 3.9. Buckling analysis, simply supported square plate under uniform shear.

Pinched Cylinder

Figure 3.4 shows a circular cylindrical shell subjected to two diametrically opposed loads. A precise solution to this problem, based upon the Flügge shell equations, is given in Reference 4. The shell was modelled with cell elements. Two models, Numbers 1 and 2, were produced as shown. Model Number 2 had a slightly finer grid. Figures 3.5, 3.6, 3.7 and 3.8 show correlations between theoretical and finite element results. This problem is a severe test of the finite element approach, because the concentrated loads produce infinite bending moments in the shell at the loaded points. The correlations are generally quite close, except at the points where loads are applied. At these points, the finite element radial displacements are about 12 percent too high, while the bending moments, of course, are bounded rather than infinite. However, the theoretical results are also in error at this point, since the Flügge equations undoubtedly do not account for the infinitely large strains existing at the loaded points.

Flat Plate, Shear Buckling

Figure 3.9 shows a problem solved to test the ability of the Math Model to predict buckling of a simply supported square plate loaded in uniform edge shear. The finite element model is the same as the one shown in Figure 3.3. This problem exercises the first order capability of the fictitious force generator for shear panels, incorporated in the Math Model. The basis of this generator was developed as part of an IRAD project in 1973, and represents a substantial improvement over the method originally included in the FORMAT general purpose structural analysis system (Reference 5). The calculated buckling load is 5.8 percent lower than the classical value (Reference 2). This result is considered satisfactory in view of the difficulty of the shear buckling problem, the coarseness of the model, and the fact that the predicted buckling load is conservative.

NONLINEAR DYNAMIC CORRELATIONS, CLASSICAL PROBLEMS

These studies demonstrate the capability of the Math Model to predict the dynamic response of simple structures exhibiting large geometric nonlinearities resulting from rotations of element forces.

Three Bar Truss

Figure 3.10 shows a structure consisting of three axially loaded members, and a concentrated mass. The nodes at A, B and C are constrained in two directions. The node at D is constrained horizontally. The figure shows the notation for vertical displacement and load at D.

Members AD and BD have significant stiffness, but negligible damping and mass. Member CD has significant damping, but negligible mass and stiffness. The stiffness of members AD and BD, given by $k = 1$, are assumed to remain constant, even for very large displacements. Thus, these members behave somewhat like coil springs. The mass at D is $m = 1$.

Beginning at $t = 0$, a vertical load, equal to unity, is applied in the downward direction, for an indefinite period of time. This load is sufficient to cause the structure to "snap through" at some point in time. Snap-through occurs when node D coincides with a point on the line joining nodes A and B. When the structure finally reaches equilibrium, node D is below Line AB.

The problem is solved for two values of damping, of member CD. In the high damping case, the damping parameter is $c = 2$. In the low damping case, $c = 0.05$. All dimensions, loads, and other parameters are understood to be in consistent units.

The problem was solved exactly, to provide a basis of comparison for results given by the Math Model. The exact result for the vertical motion of point D is given by the solution of the differential equation

Dimensions are
shown at $t = 0$

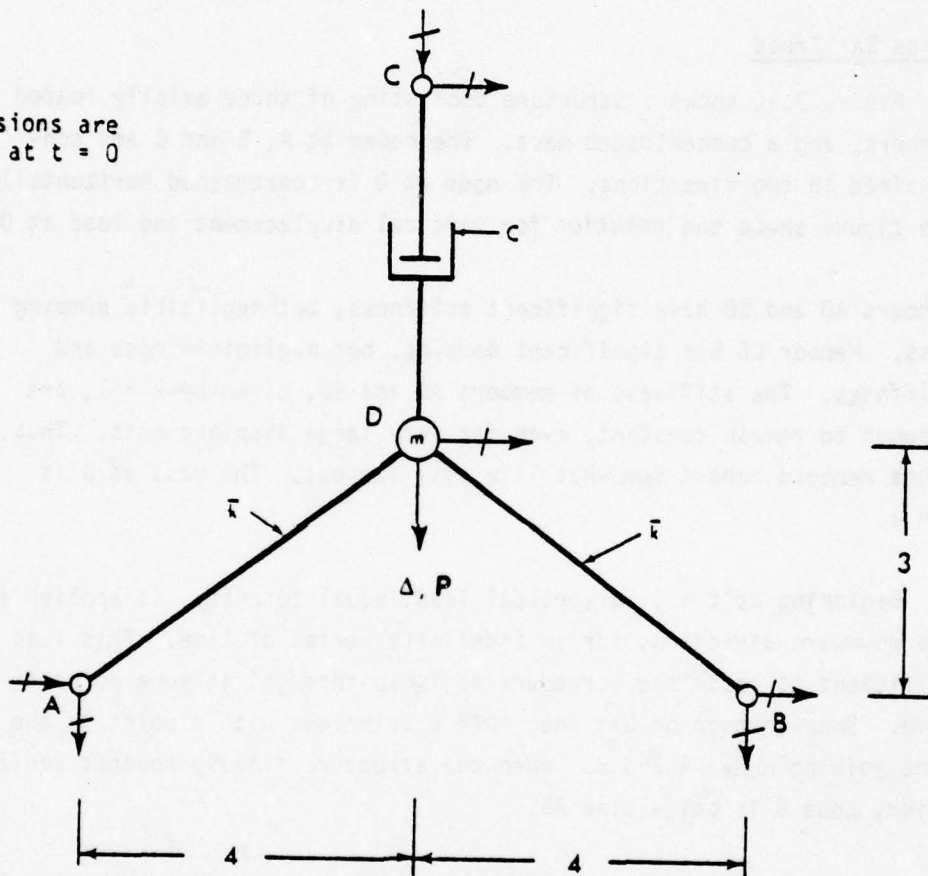


Figure 3.10. Three bar truss.

$$m\ddot{\Delta} + c\dot{\Delta} + K(\Delta)\Delta = P, \quad (309)$$

where $m = 1$,
 $c = 2$ (high damping) ,
 $c = 0.05$ (low damping),

$$K(\Delta) = \frac{2(3-\Delta)(6-\Delta)}{[16 + (3-\Delta)^2]^{1/2} \{5 + [16 + (3-\Delta)^2]^{1/2}\}}. \quad (310)$$

and $P = 0$ for $t < 0$
 $P = 1$ for $t > 0$.

The stiffness $K(\Delta)$ can be found by writing the equation for the force produced by bars AD and BD on node D, in terms of the displacement Δ . The differential equation was solved numerically by a computer code called Continuous System Modeling Program (CSMP) (Reference 6).

Figure 3.11 shows the results for the high damping case. The solid line is the exact result from CSMP. The points, indicated by plus marks, show the results given by the Math Model, for time increments of $\tau = 1.5$, with five iterations per increment. The agreement is good. The linear solution, shown by the dotted lines, is grossly in error as expected.

Figure 3.12 shows results for low damping. In this case, the truss oscillates for a long period of time, after snapping through. The solid line again shows the CSMP result. The plus marks and circles show the Math Model results for time increments of $\tau = 0.75$ and $\tau = 0.25$, with five iterations per increment. The results for $\tau = 0.25$ are good. The results for $\tau = 0.75$ are satisfactory for most engineering purposes.

The static response of the three bar truss can be obtained from Equation 309 by setting m and c equal to zero. The load P can then be calculated as a function of the displacement Δ . Figure 3.13 is a graph of the static response. As the load is increased from zero at point O, to about 0.5, the displacement follows the curve to point A. After this point, the load theoretically decreases as displacement is increased.

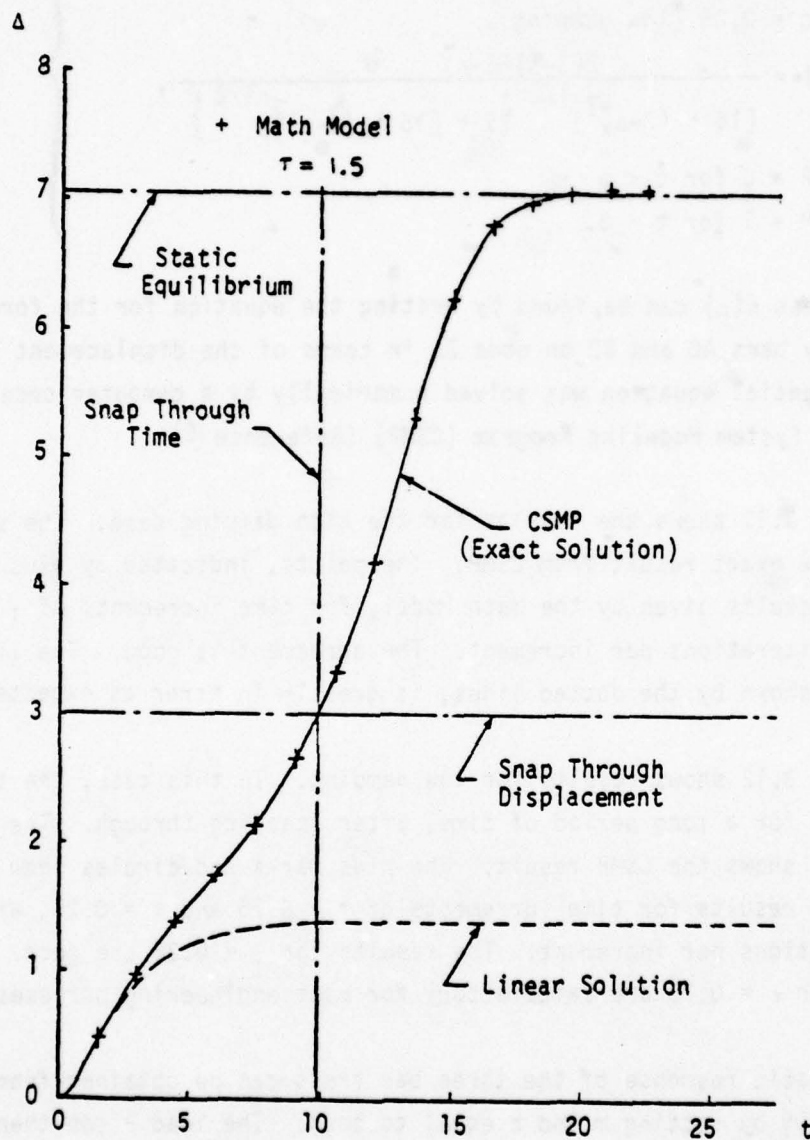


Figure 3.11. Displacement of the 3-bar truss, high damping.

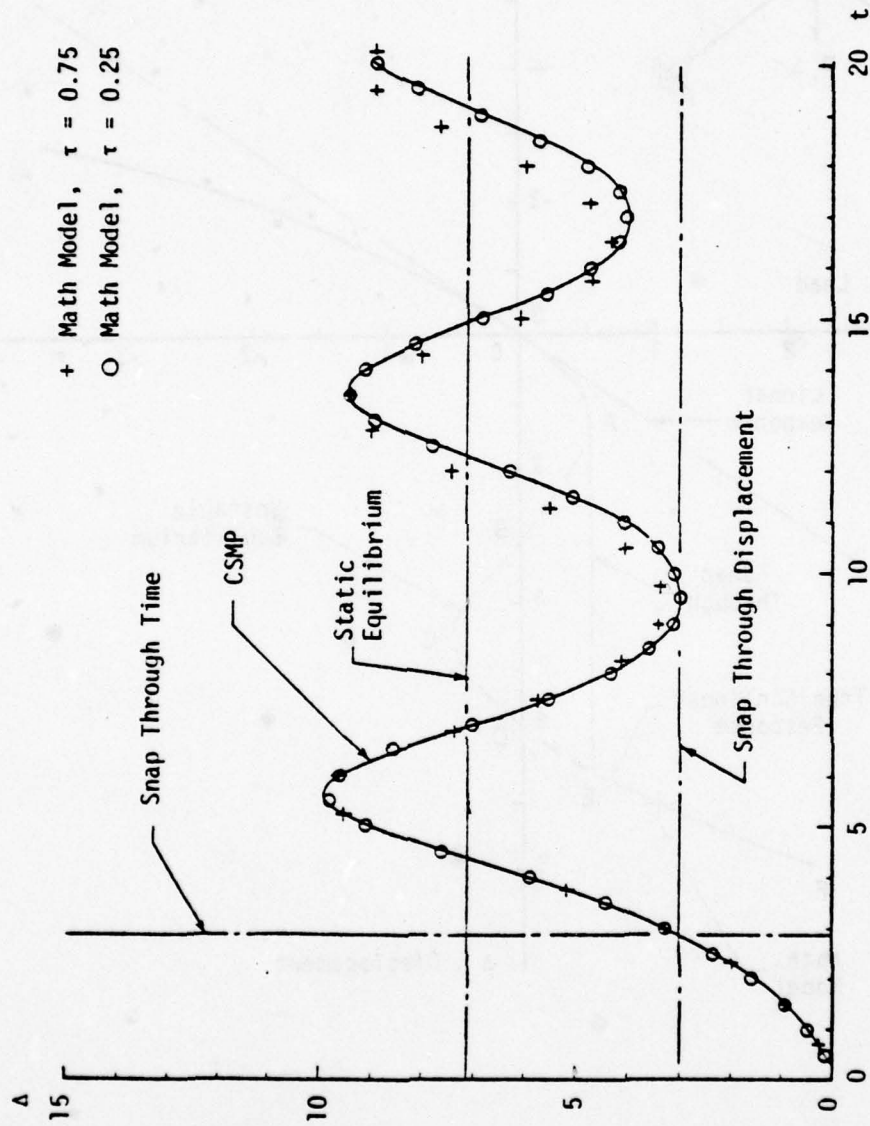


Figure 3.12. Displacement of the 3-bar truss, low damping.

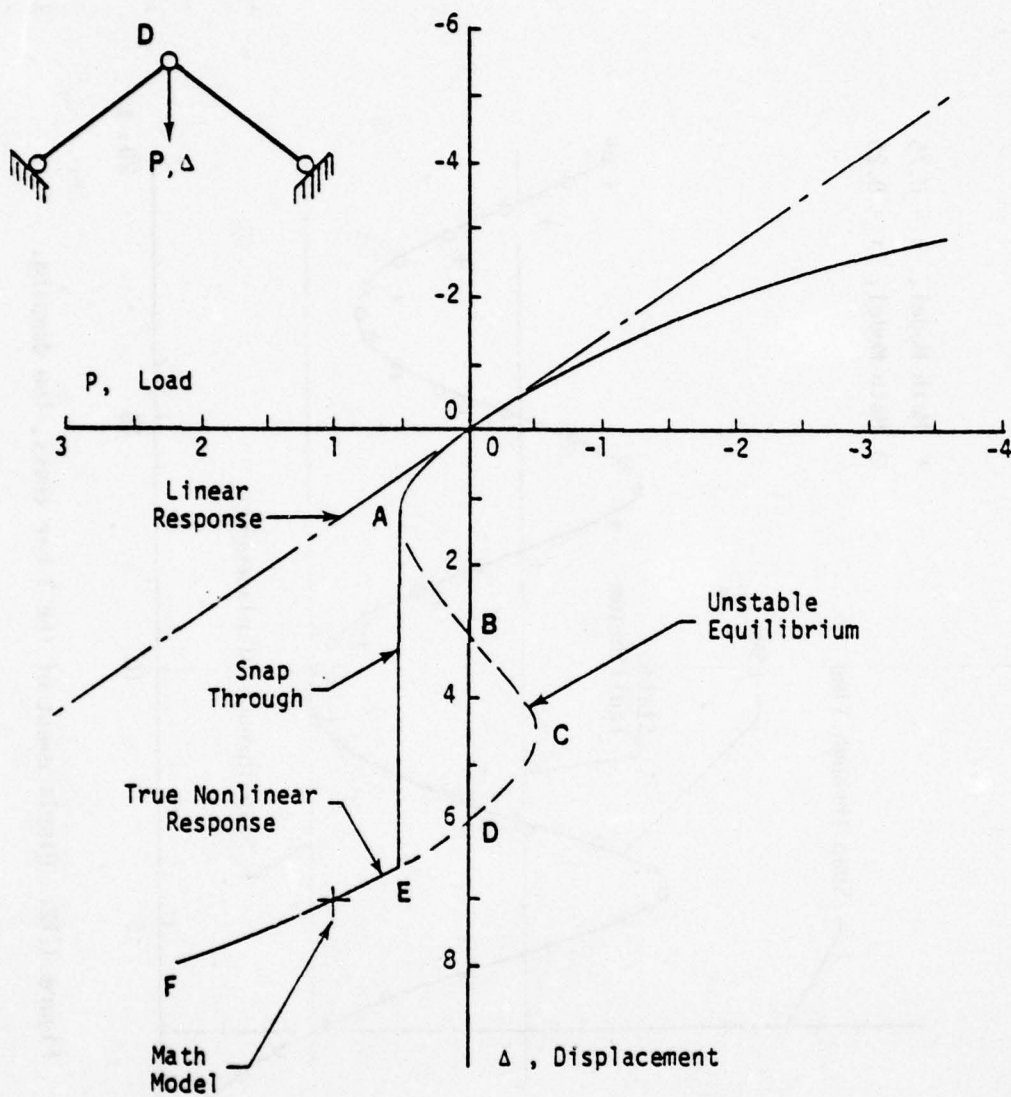


Figure 3.13. Static response of the three bar truss.

At point B, where $\Delta = 3$, the load is again zero. Further increases of displacement cause the load to become negative. At C, the load reaches a minimum value, after which it increases to zero, at a displacement of 6. Further increases of displacement cause the load to increase.

The dashed segment, ABCDE, represents unstable equilibrium. If load were applied by hanging a weight at node D of the truss, the displacement would actually follow the curve OAEF, as the weight is increased from zero, because of the instability. The straight line segment AE represents snap-through. Linear response is shown by the dash-dot line.

The static response curve illustrates the pronounced nonlinear character of the problem. The point labeled "Math Model", for $P = 1$, was taken from Figure 3.11, which gives a value of about 7.07 as the displacement corresponding to static equilibrium.

Flat Truss

Figure 3.14 shows a structure, called the flat truss. Basically, the structure consists of two very stiff bars, AC and CE, hinged at point C, and a mass at C. The bars are supported vertically at A and E, but are free to move horizontally without friction at these points. Bars AC and CE have very small masses and small damping constants. The dotted line CG represents a bar with very small stiffness, mass and damping. The reason for introducing the weak bar CG, and the small amount of mass and damping in AC and CE, is to prevent singularities in the solution.

The exact solution to this problem can be found easily by calculating the response of the mass M to the load P, since no other forces of any significance are acting, and the acceleration is constant and equal to unity.

Figure 3.15 shows the positions assumed by the structure at three different times. At $t = \sqrt{10}$, the truss has completely folded. At all times, the length of each bar is precisely 5 inches, and the bar forces

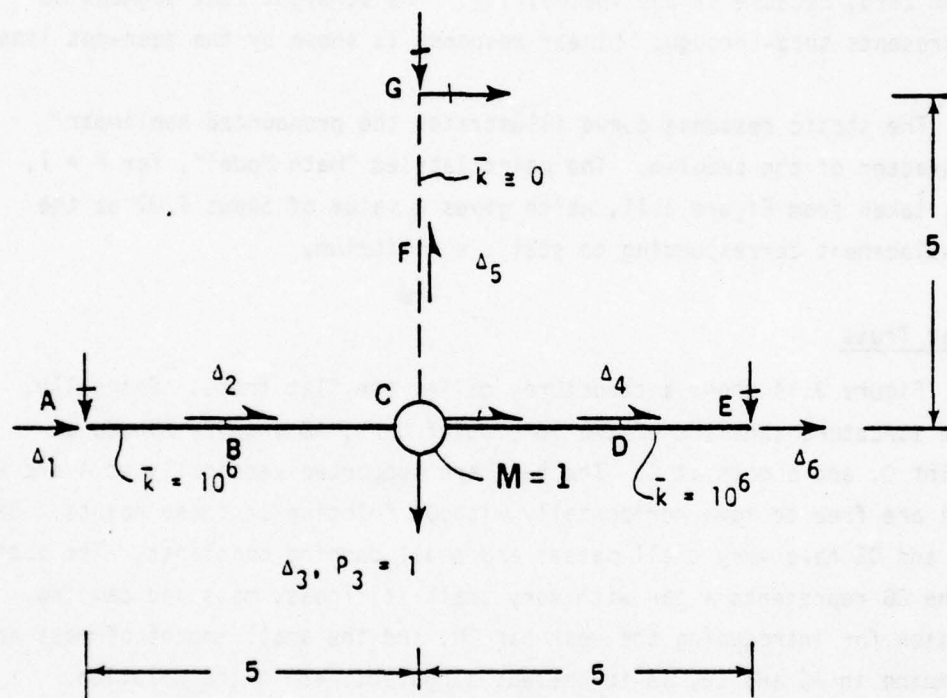


Figure 3.14. Flat truss.

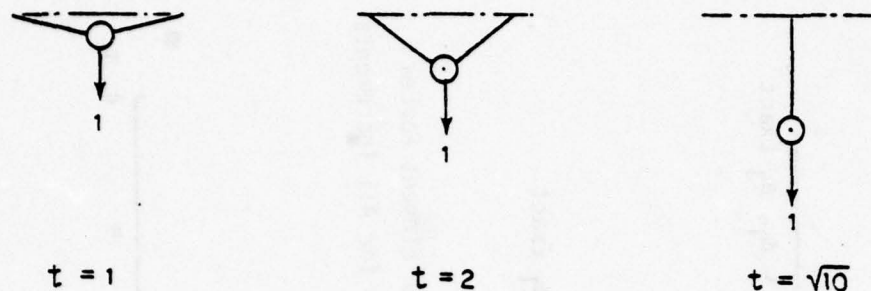


Figure 3.15. Response of the flat truss.

are essentially zero, except immediately after $t = \sqrt{10}$, when the bars suddenly begin to support the full external load, after a brief period of oscillation.

This structure and the 3-bar truss, represent two extremes, in that the ends of the flat truss are free to move horizontally, while the ends of the 3-bar truss are prevented from such motion.

Figure 3.16 shows the displacement response of the flat truss. The solid lines represent exact results. The curves labeled Δ_1 and Δ_3 give the horizontal displacement of point A and the vertical displacement of point C, of Figure 3.14, as functions of time. The circles show results calculated by the Math Model for time increments of 0.25 with five iterations per increment. For all time increments, the Math Model gave essentially zero forces in the bars.

This problem is a challenge for a general purpose structural analysis program, even though the exact solution is easily obtained, because the structural elements rotate through large angles.

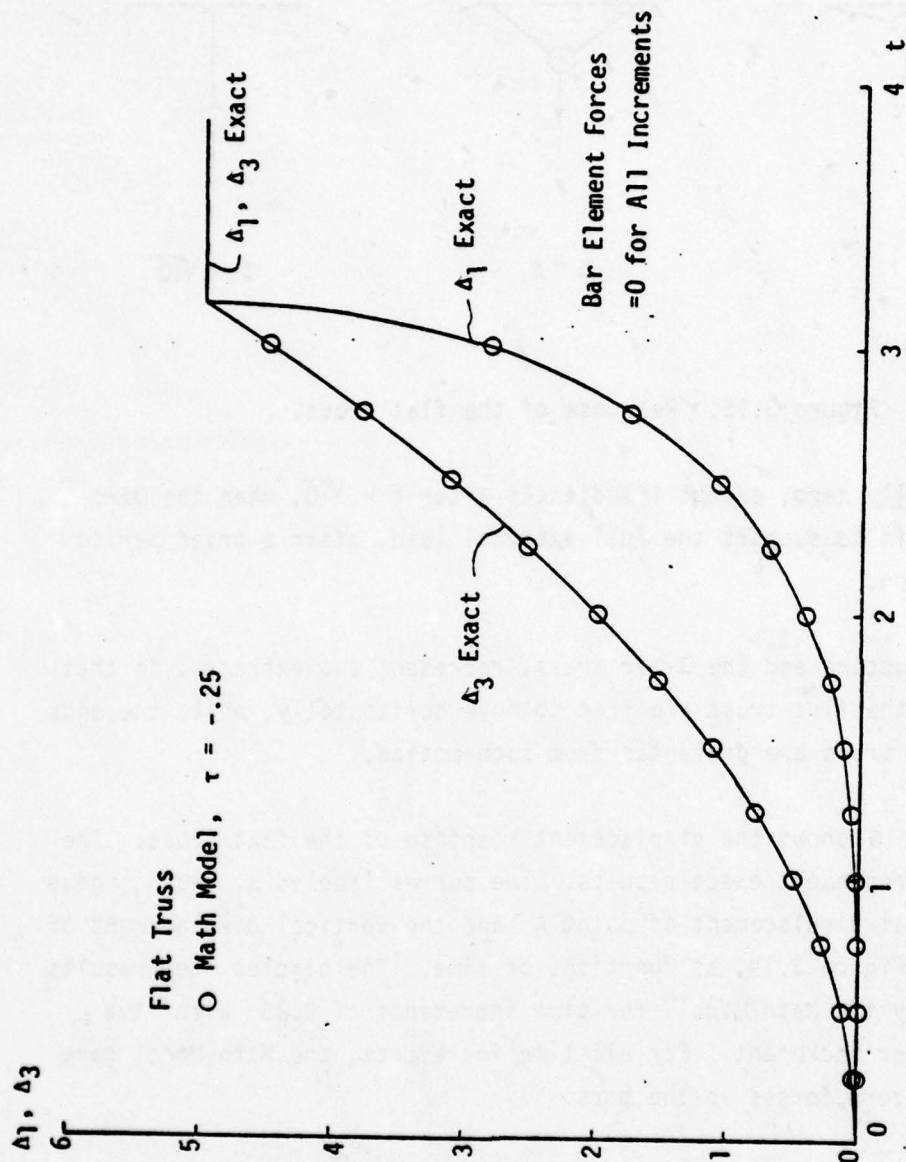


Figure 3.16. Displacement of the flat truss

LINEAR CORRELATIONS WITH TEST RESULTS

These studies are presented to show applications of the Math Model linear analysis capability to typical aircraft windshield and canopy construction.

Laminated Beams

A number of laminated beams were tested under static and dynamic conditions, as described in Reference 7.

Instrumented Beam

Figure 3.17 shows a laminated beam, 36 inches long by 8 inches wide, composed of three structural plies and two interlayers. Ply materials and thicknesses are shown in Figure 3.13 (b). The beam was simply supported at the ends, and loaded at the third points.

One-fourth of the beam, bounded by longitudinal and transverse planes of symmetry, was modelled, as shown in Figure 3.17. The structural plies and interlayers were separately represented by cell elements. The stiffness properties of the lower interlayer at the end were modified to represent stiffness supplied by a row of bolts. These bolts are shown in Figure 3.18(a). The bolt stiffnesses were represented by increasing the shear stiffnesses of the appropriate cell elements.

A static analysis was performed, employing a transformation based on modes corresponding to the five lowest natural frequencies of the specimen. Figure 3.18 (a) shows the comparison of measured and calculated displacements at the beam centerline. Figure 3.18 (b) shows the comparison of strains calculated through the thickness of the laminate, with test data. These comparisons are considered satisfactory. They demonstrate the capability of the Math Model to produce reliable results for a laminated transparency. The comparisons also support the feasibility of the modal approach to strain and displacement analysis, and show the inapplicability of engineering beam theory.

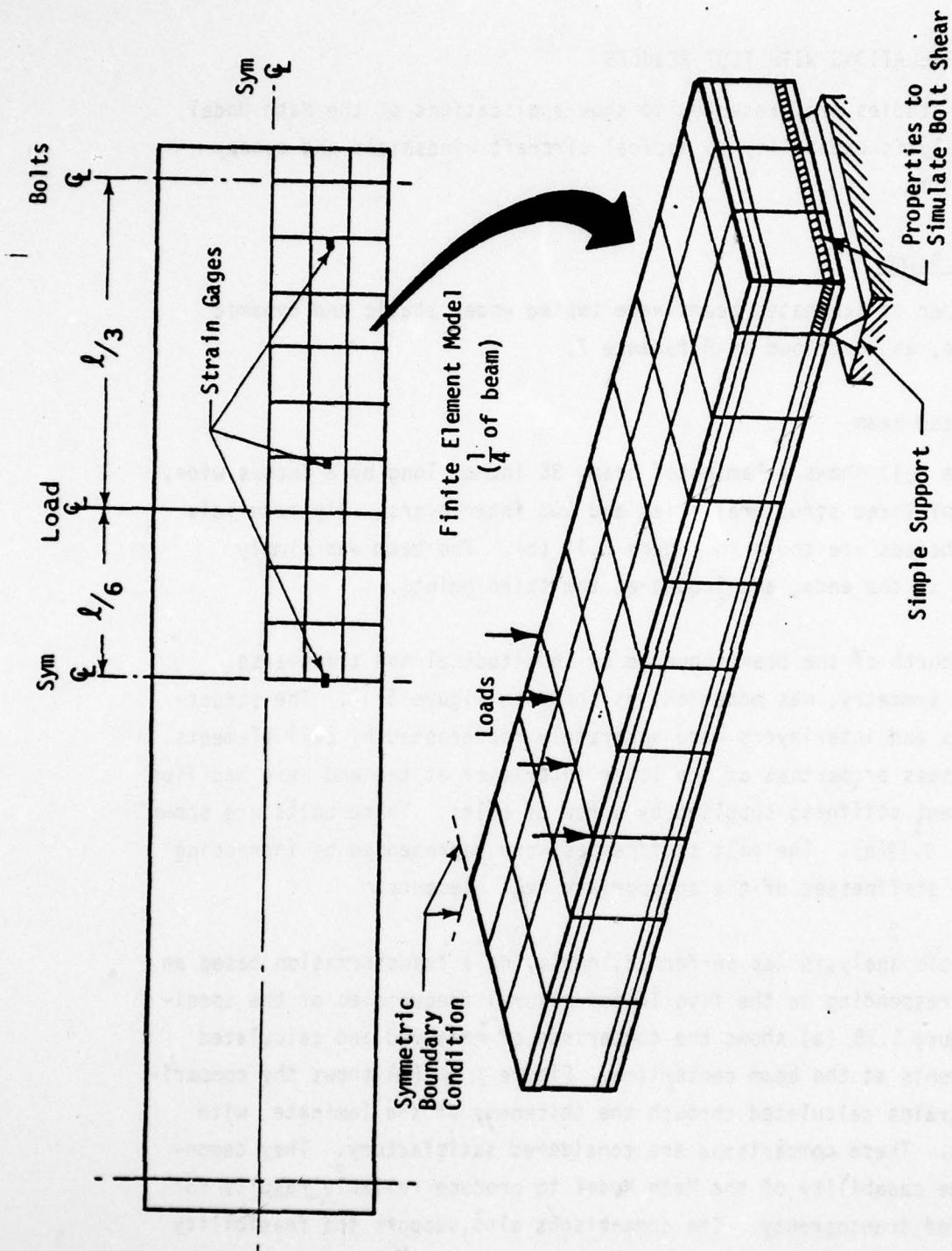
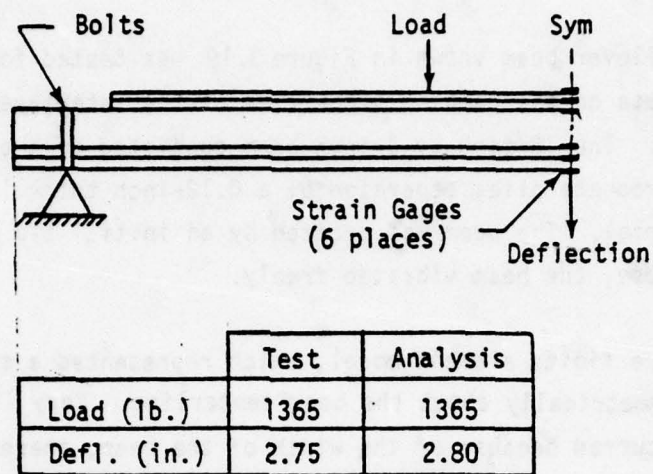
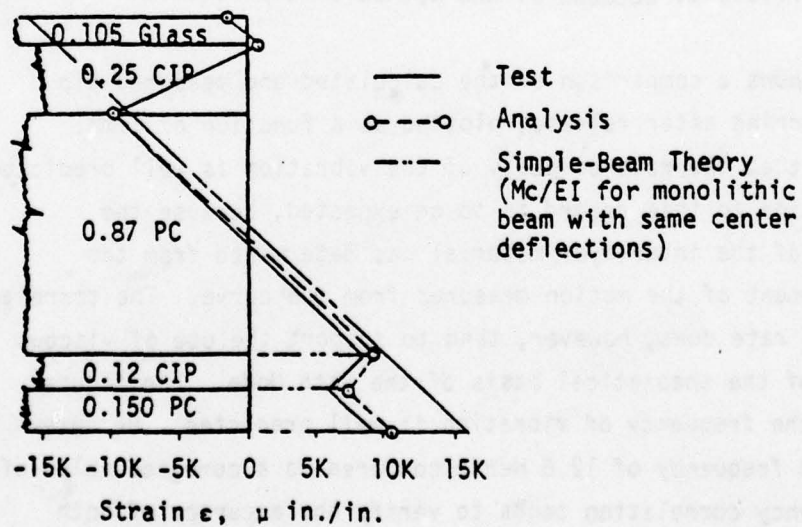


Figure 3.17. Statically loaded laminated beam.



(a) Static Deflection



(b) Strain Correlations

Figure 3.18. (a) Static deflection and (b) Strain correlations for 36-inch beam model.

Damping Beam

The laminated cantilever beam shown in Figure 3.19 was tested for the purpose of providing data on the damping properties of the interlayer material (Reference 7). The 18-inch by 8-inch beam consisted of two 0.25-inch thick polycarbonate plies separated by a 0.12-inch thick layer of CIP interlayer material. The beam was excited by an initial tip displacement. After release, the beam vibrated freely.

The figure shows the finite element model, which represented a strip 1 inch wide located symmetrically about the beam centerline. Very little anticlastic bending occurred because of the width of the beam, therefore anticlastic constraints were applied to the model, as shown. Structural plies and interlayers were represented separately by cell elements.

A linear modal analysis of the vibration was performed, employing only the first bending mode, which is shown in Figure 3.20. The figure shows the large shear strains occurring in the interlayer. One mode was considered sufficient, because of the method of tip release.

Figure 3.21 shows a comparison of the calculated and measured tip displacement occurring after release, plotted as a function of time. The figure shows that the rate of decay of the vibration is well predicted, but good correlation in this regard is to be expected, because the damping property of the interlayer material was determined from the logarithmic decrement of the motion measured from the curve. The correlation of the decay rate does, however, tend to support the use of viscous damping as part of the theoretical basis of the Math Mode. The figure also shows that the frequency of vibration is well predicted. Measurements show a test frequency of 12.6 Hertz compared to a computed value of 12.8. The frequency correlation tends to verify the accuracy of both the stiffness and mass matrices employed in the analysis for cell elements.

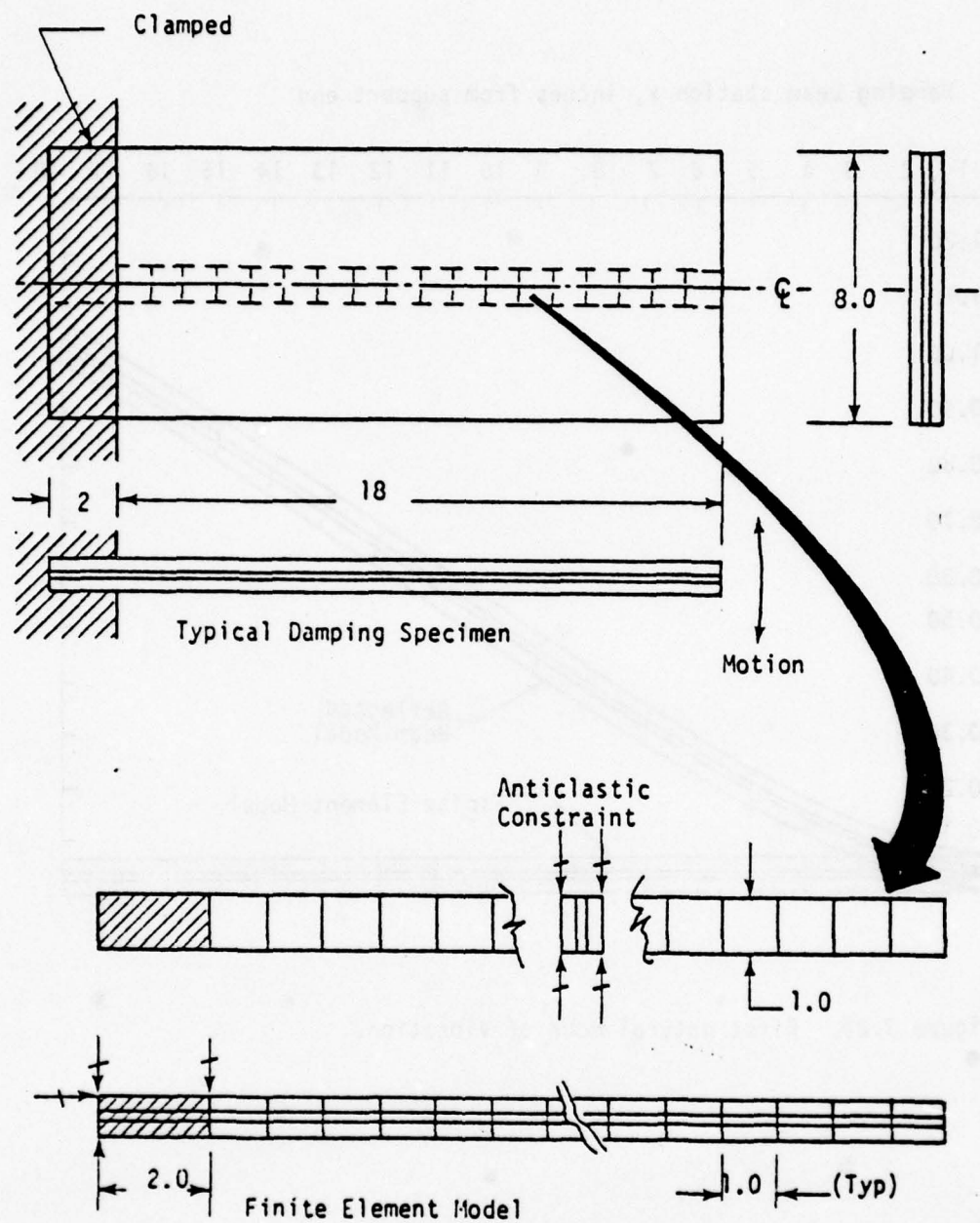


Figure 3.19. Damping beam specimen and finite element model.

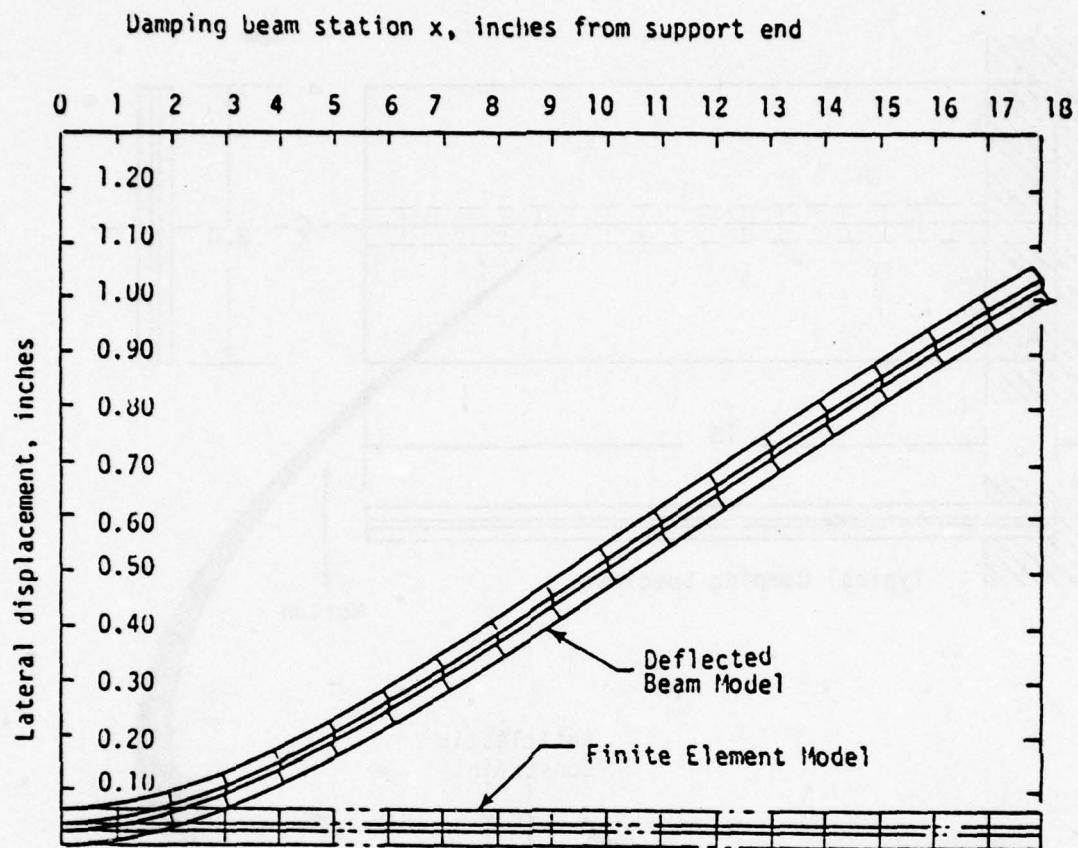


Figure 3.20. First natural mode of vibration.

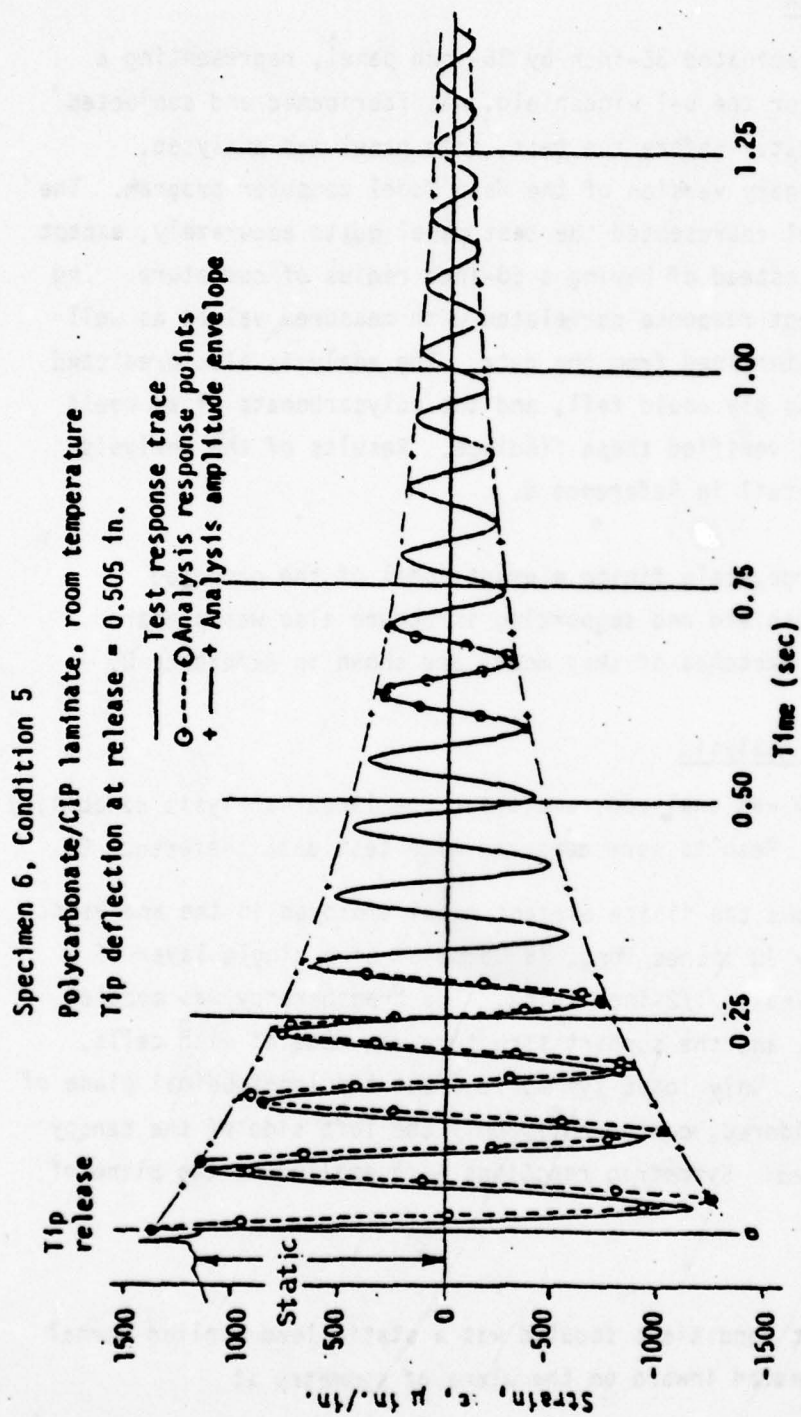


Figure 3.21. Response of the damping beam to an initial tip displacement.

B-1 Bird Impact Data

A seven layer laminated 36-inch by 36-inch panel, representing a proposed redesign for the B-1 windshield, was fabricated and subjected to a bird impact test. Before the test, this panel was analyzed, employing a preliminary version of the Math Model computer program. The finite element model represented the test panel quite accurately, except that it was flat, instead of having a 60-inch radius of curvature. The computed displacement response correlated with measured values as well as they could be determined from the data. The analysis also predicted that the outer glass ply would fail, and the polycarbonate plies would not fail. The test verified these findings. Results of the analysis are presented in detail in Reference 8.

A realistic large scale finite element model of the proposed redesigned B-1 windshield and supporting structure also was prepared, but not analyzed. Sketches of this model are shown in Reference 8.

F-16 Canopy Linear Analysis

The F-16 canopy was analyzed, employing the linear analysis capability of the Math Model. Results were compared with test data (Reference 9).

Figure 3.22 shows the finite element model employed in the analysis. The canopy, roughly 90 inches long, is composed of a single layer of polycarbonate, nominally 1/2-inch thick. The transparency was modeled with cell elements, and the support structure was modeled with cells, membranes and bars. Only loads symmetric about the longitudinal plane of symmetry were considered, consequently only the left side of the canopy needed to be modeled. Symmetric reactions were applied on the plane of symmetry.

Static Loading

One of the test conditions studied was a static load applied normal to the surface directed inward on the plane of symmetry at

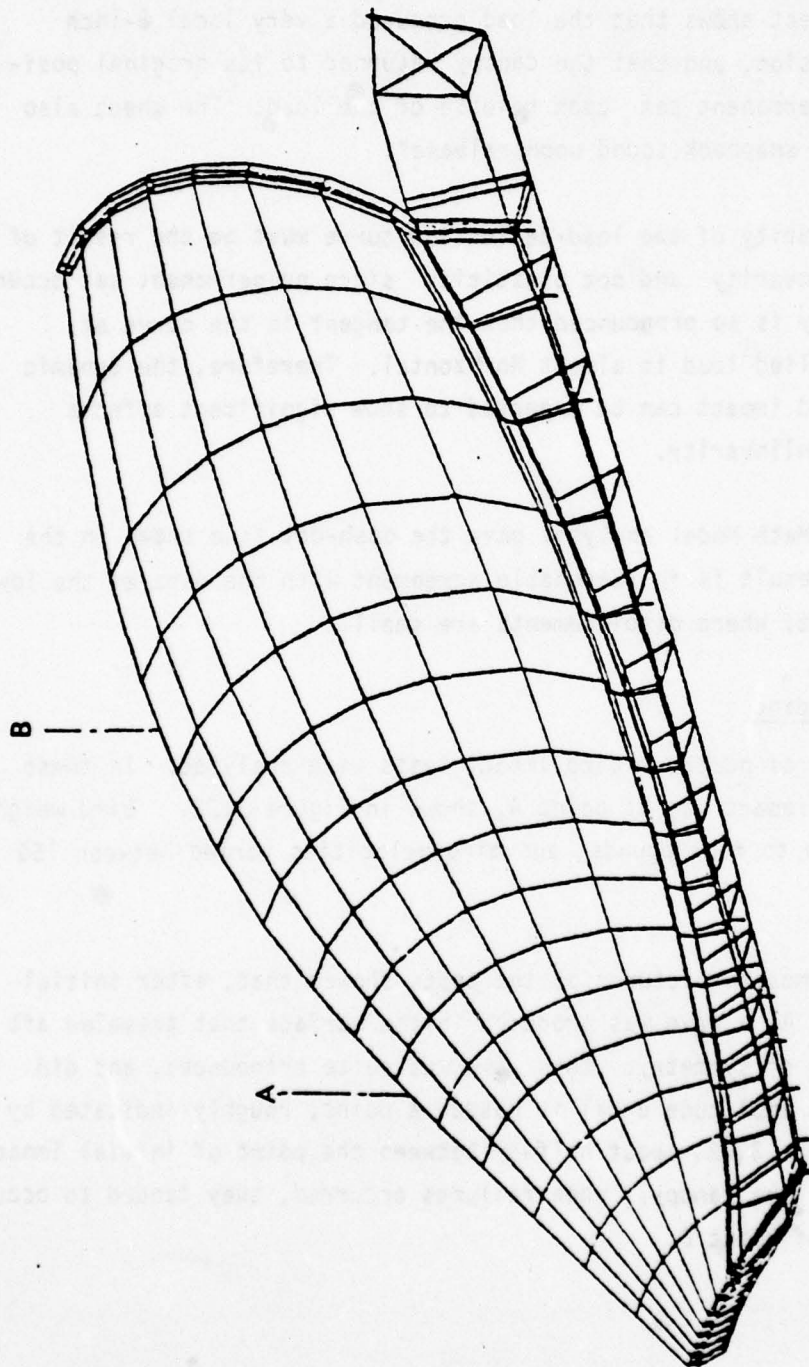


Figure 3.22. Half-shell finite element model of the F-16 canopy.

point A as shown in Figure 3.22. The solid line in Figure 3.23 shows the resulting load-deflection curve, which is nonlinear. The original data sheet for the test shows that the load produced a very local 8-inch diameter depression, and that the canopy returned to its original position without permanent set upon release of the load. The sheet also records "a loud snapback sound upon release".

The nonlinearity of the load-deflection curve must be the result of geometric nonlinearity and not plasticity since no permanent set occurred. The nonlinearity is so pronounced that the tangent to the curve at the maximum applied load is almost horizontal. Therefore, the dynamic response to bird impact can be expected to show significant effects of geometric nonlinearity.

The linear Math Model analysis gave the dash-dot line shown in the figure. This result is in reasonable agreement with the data at the lower end of the curve, where displacements are small.

Bird Impact Loading

The results of numerous bird impact tests were analyzed. In these tests, initial impact was at point A, shown in Figure 3.22. Bird weights ranged from two to four pounds, and bird velocities varied between 150 and 350 knots.

High speed motion pictures of the tests showed that, after initial impact at point A, a wave was produced in the surface that traveled aft along the plane of symmetry. This wave was quite pronounced, and did not diminish in amplitude until it passed a point, roughly indicated by point B in Figure 3.22, about halfway between the point of initial impact, and the back of the canopy. When failures occurred, they tended to occur in the region of point B.

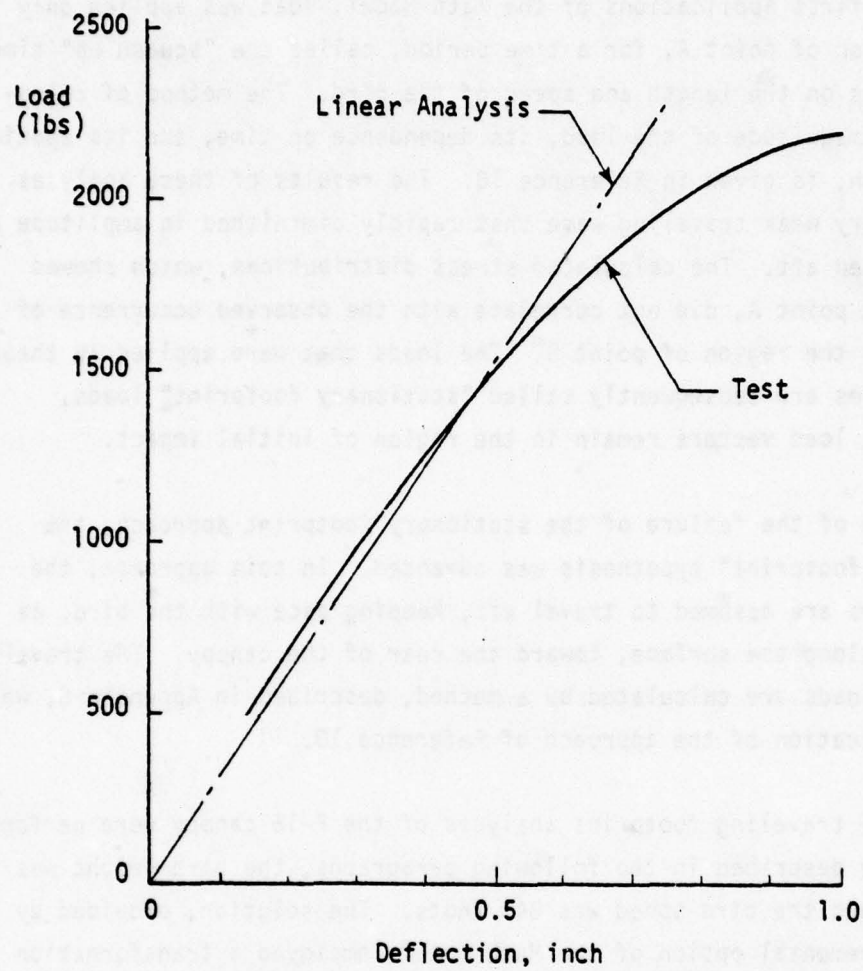


Figure 3.23. Load-deflection curve for static test.

In the first applications of the Math Model, load was applied only in the region of point A, for a time period, called the "squash up" time, that depends on the length and speed of the bird. The method of calculating the magnitude of the load, its dependence on time, and its spatial distribution, is given in Reference 10. The results of these analyses showed a very weak traveling wave that rapidly diminished in amplitude as it progressed aft. The calculated stress distributions, which showed maximums at point A, did not correlate with the observed occurrence of failures in the region of point B. The loads that were applied in these early studies are subsequently called "stationary footprint" loads, because the load vectors remain in the region of initial impact.

In view of the failure of the stationary footprint approach, the "traveling footprint" hypothesis was advanced. In this approach, the load vectors are assumed to travel aft, keeping pace with the bird, as it slides along the surface, toward the rear of the canopy. The traveling footprint loads are calculated by a method, described in Appendix G, which is a modification of the approach of Reference 10.

Several traveling footprint analyses of the F-16 canopy were performed. In the case described in the following paragraphs, the bird weight was 4 pounds, and the bird speed was 340 knots. The solution, provided by the linear incremental option of the Math Model, employed a transformation based on the lowest 30 natural vibration modes of the finite element model shown in Figure 3.22. Figure 3.24 shows the results. Vertical displacements are plotted at points along the canopy centerline, for different times, which are shown in seconds. The figure shows a strong traveling wave, peaking at the crown of the canopy.

Figure 3.25 shows equivalent stresses on the canopy inner surface centerline for the same test. When the equivalent stress, equal to twice the octahedral shear stress, reaches the ultimate tensile stress determined in a uniaxial tensile test, failure occurs, according to an

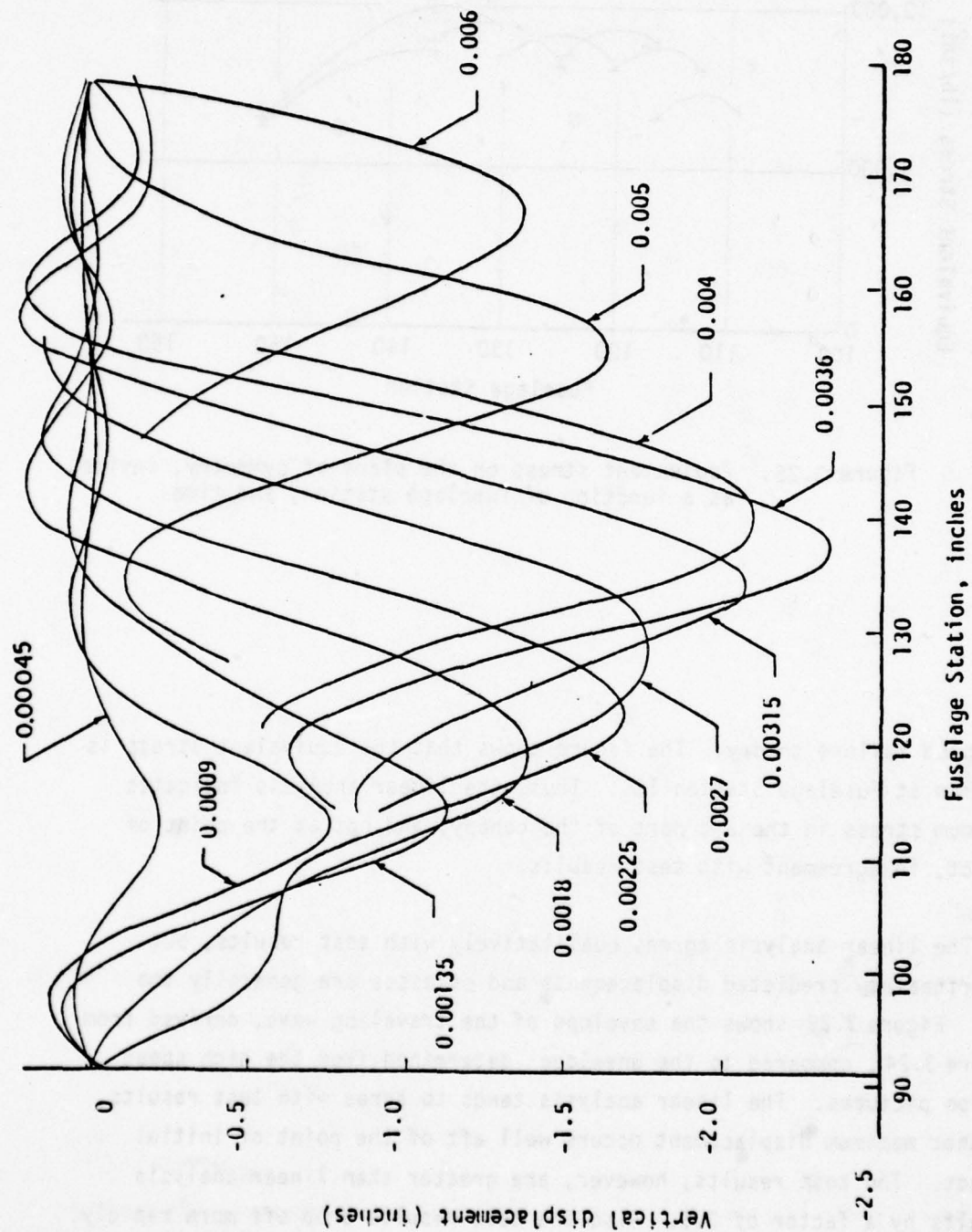


Figure 3.24. Vertical displacement on the plane of symmetry, as a function of fuselage station, and time.

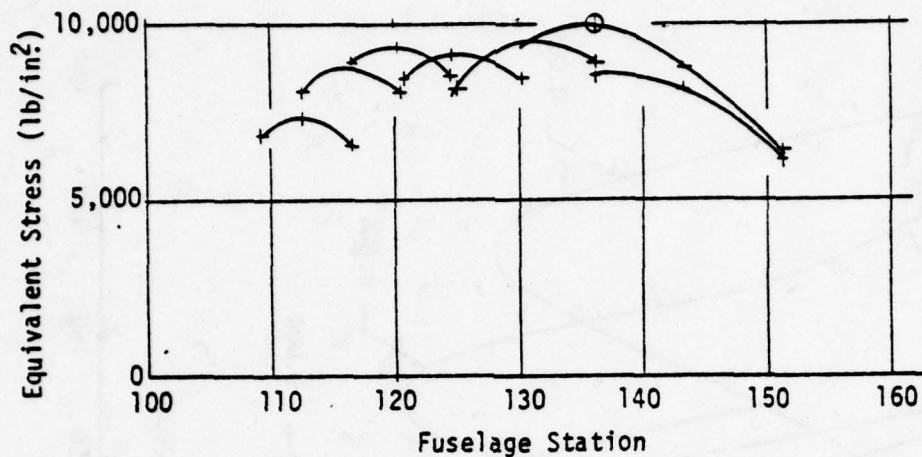


Figure 3.25. Equivalent stress on the plane of symmetry, inside, as a function of fuselage station, and time.

accepted failure theory. The figure shows that the equivalent stress is maximum at Fuselage Station 136. Thus, the linear analysis indicates maximum stress in the aft part of the canopy, and not at the point of impact, in agreement with test results.

The linear analysis agrees qualitatively with test results, but unfortunately predicted displacements and stresses are generally too low. Figure 3.26 shows the envelope of the traveling wave, derived from Figure 3.24, compared to the envelope determined from the high speed motion pictures. The linear analysis tends to agree with test results, in that maximum displacement occurs well aft of the point of initial impact. The test results, however, are greater than linear analysis results by a factor of 3.6. Also the test results drop off more rapidly, after reaching the peak, than the analysis shows.

Subsequent testing of specimens taken from the canopy indicated that the value of Young's modulus, E , used in the analysis, was too high. Re-analysis with a lower value of E gave the dash-dot curve shown in Figure 3.26, but the maximum test displacement is still 2.8 times greater than the analytical maximum.

The large discrepancy between linear results and observed displacements is believed to be a geometrically nonlinear effect, in view of the fact that the static test results, shown in Figure 3.23, show a pronounced geometric nonlinearity. Figure 3.27 shows a possible mechanism of nonlinear wave propagation. Shortly after impact, according to this hypothesis, snap-through occurs, producing a wave of greater amplitude than linear theory predicts. This wave travels aft to some point near the rear of the canopy, where it snaps out, and becomes a linear wave. Such a mechanism would explain the observed discrepancy, since snap-through behavior is well known to have the capability of producing much larger displacements than linear theory predicts. For example, see Figure 3.11, showing displacements of the three bar truss.

NONLINEAR ANALYSIS OF THE F-16 CANOPY

The traveling snap-through wave hypothesis can be tested by applying the Math Model nonlinear incremental option to the problem. Such an analysis was attempted, but the attempt was unsuccessful. A difficulty was encountered, which could not be overcome in the available time.

The nonlinear option was applied to the same test condition discussed previously in connection with the linear analysis, in which the bird weight was 4 pounds, and the bird speed was 340 knots. The model employed for this study was similar to the one shown in Figure 3.22, except that more transverse stations were added aft of point B, giving more detail in the rear part of the canopy. Also, the entire structure was modeled only with cell elements.

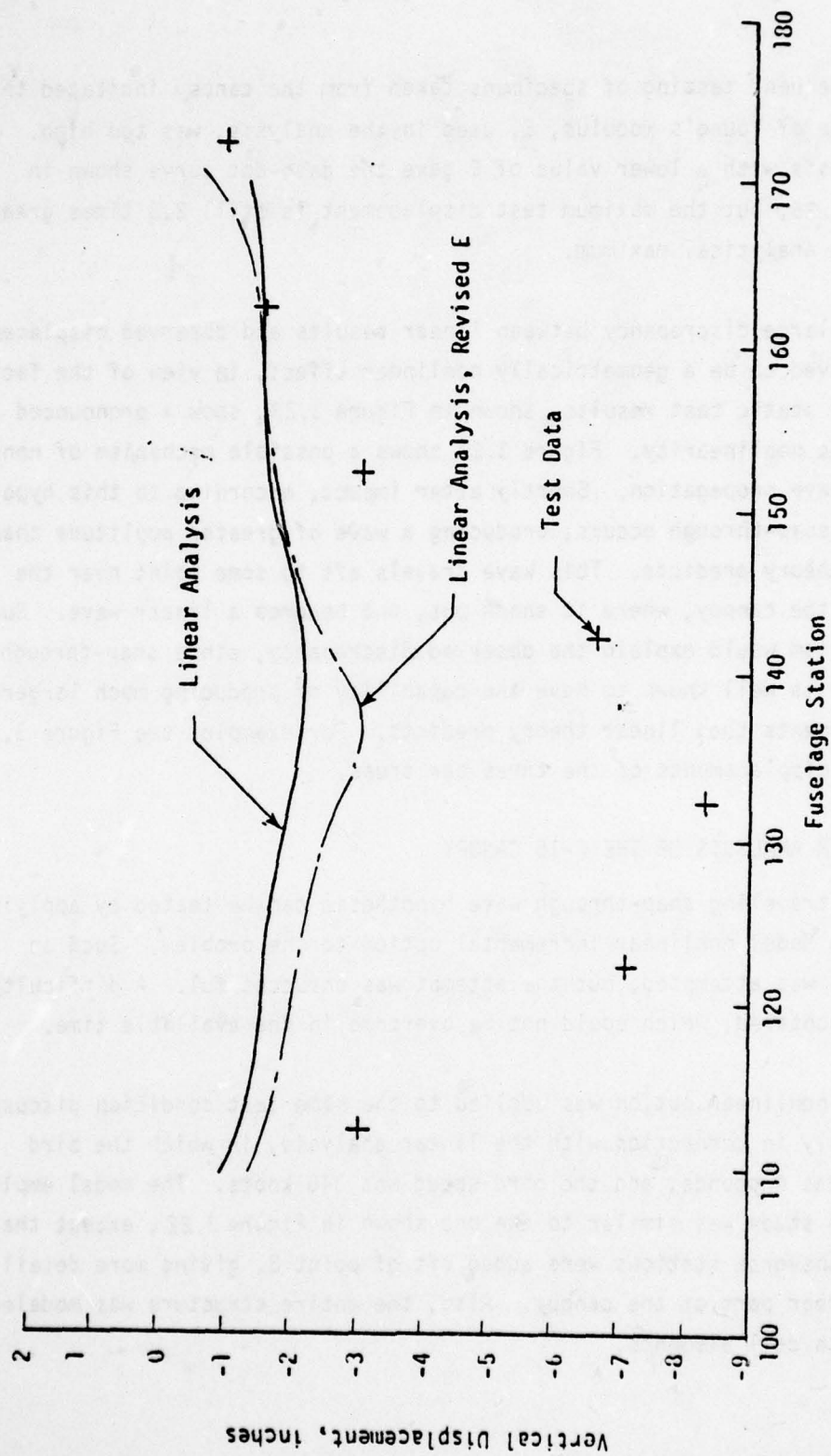


Figure 3.26. Envelope of traveling wave.

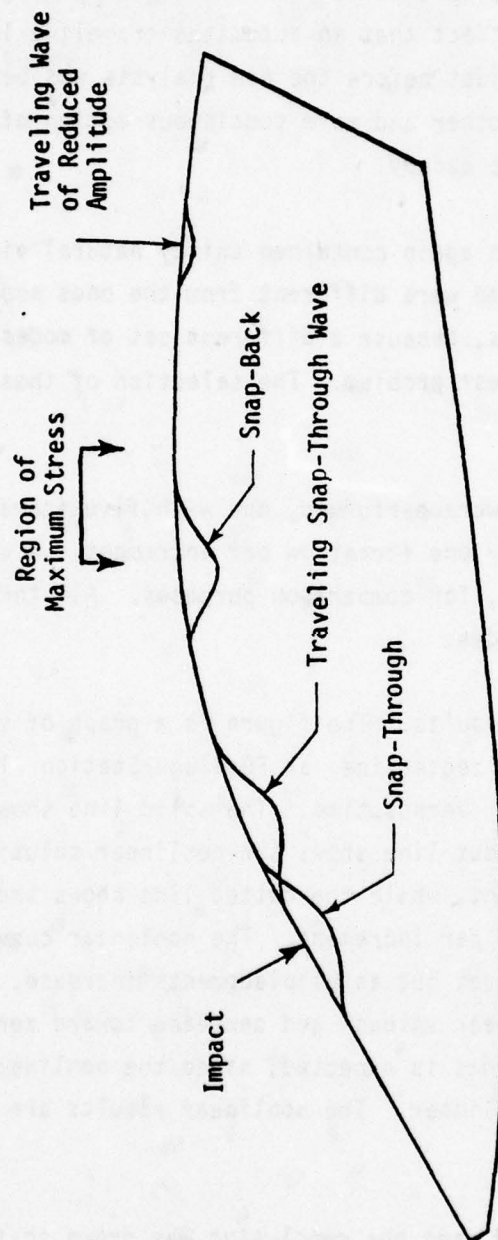


Figure 3.27. Possible mechanism of F-16 canopy response: traveling snap-through wave.

The loads applied in the new analysis differed somewhat from the loads of the previous study, in that the new loads were more gradually applied, as a result of the fact that an automated traveling loads generator became available just before the new analysis was begun. The new generator allowed a smoother and more continuous motion of the load vectors along the top of the canopy.

The modal transformation again contained thirty natural vibration modes, but the modes selected were different from the ones employed in the previous linear analysis, because a different set of modes was thought to be needed for the nonlinear problem. The selection of these modes is discussed in Appendix F.

Two nonlinear analyses were performed, one with five iterations per increment, and one with only one iteration per increment. A new linear analysis also was performed, for comparison purposes. All three analyses employed the same set of modes.

Figure 3.28 shows the results. The figure is a graph of vertical displacements at the canopy centerline at Fuselage Station 113.9 near the point of initial impact versus time. The solid line shows the linear solution. The dash-dot line shows the nonlinear solution with five iterations per increment, while the dotted line shows the nonlinear solution with one iteration per increment. The nonlinear curves at first follow the linear curve, but as displacements increase, the nonlinear results depart from the linear values and decrease toward zero. This result is the opposite of what is expected, since the nonlinear results should be greater than the linear. The nonlinear results are undoubtedly incorrect.

This matter was studied and the conclusion was drawn that the difficulty probably lies in the selection of modes and not in the theoretical basis of the Math Model or in the computer program. The subject is discussed in Appendix F on Modes where a possible explanation of the difficulty is presented. Section V provides recommendations for corrective action.

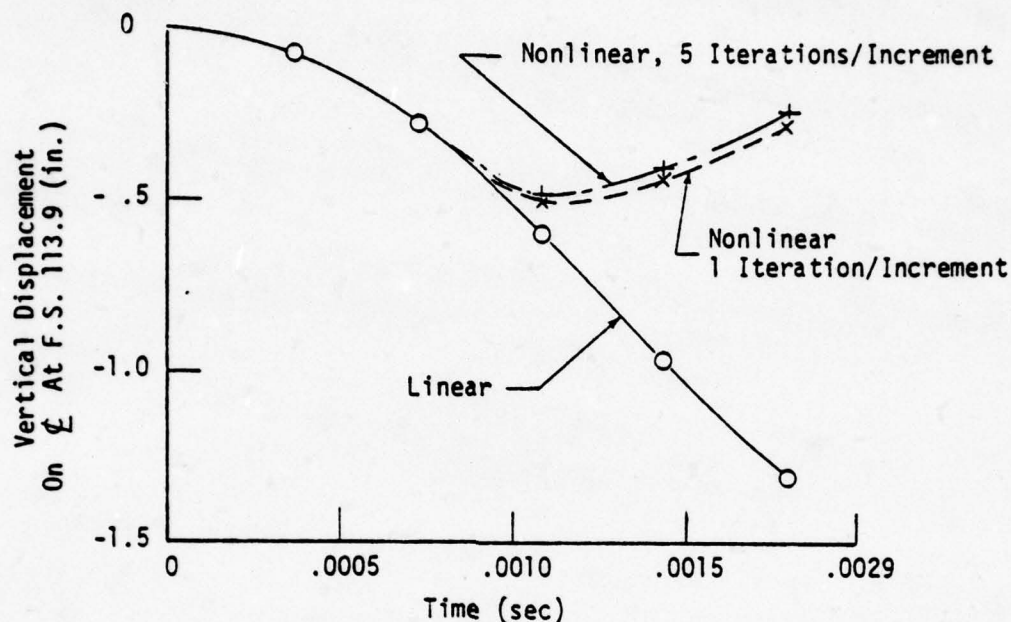


Figure 3.28. Nonlinear canopy analysis.

RUNNING TIMES

The Math Model computer program includes a preprocessor; the incremental solution with linear and nonlinear options, and a postprocessor. These modules, and the associated running times, are discussed in detail in Parts 2 and 3 of this report. For the analysis of the F-16 canopy described in the preceding paragraphs the nonlinear module with five iterations per increment required about 430 CPU seconds/increment and 310 IO seconds/increment on the CDC Cyber 74 computer employing 160,000 decimal words of core. These times are quoted as an indication of the feasibility of the nonlinear code. The efficiency of this code can be improved by further optimization.

SECTION IV

CONCLUSIONS

A mathematical model capable of simulating the response of an aircraft windshield to bird impact has been developed. The model is based upon a finite element representation of the windshield system.

Part I, Section II, of the report describes the theoretical basis of the model. The mathematical formulation accounts for:

1. The laminated transparency, its edge attachments, and its supporting structure.
2. Traveling footprint bird impact loads.
3. The transient dynamic response of the structure, including displacements, stresses and strains, as functions of time.
4. The effects of the thermal environment on material properties and response.
5. Structural damping, especially in interlayers.
6. Material nonlinearities.
7. Geometric nonlinearities.

The effects of bird-windshield interaction, or target compliance, has not been formulated. Also, the user accounts for high strain rate effects by estimating strain rates prior to the calculation and inputting appropriate material properties.

The formulation of material nonlinearities is based on the Von Mises yield criterion and the Prandtl-Reuss equations. Geometric nonlinearities are taken into account by coordinate updating and by the method of fictitious loads.

Responses are calculated by solving the nonlinear equation of motion for the finite element model. The equation is solved incrementally in time and iteratively within each increment. The equation is linearized for each increment, and the linearized differential equation is solved exactly.

Part 3 of the report, the Programming Manual, describes the computer program, and the approach to optimizing the code. Effects formulated in Part 1, but not converted to computer code include plasticity, thermal loads resulting from damping energy dissipated as heat, and the dependence of material properties on temperature changes occurring after initial impact.

The program includes a preprocessor, the incremental solution, and a postprocessor. The preprocessor includes a laminate generator for computing interior nodal coordinates of a laminated transparency from surface coordinates and layer thicknesses, and a traveling footprint load generator. The incremental solution includes a linear option, and a geometrically nonlinear option. The postprocessor printed output provides nodal displacements, velocities, accelerations, displaced nodal coordinates, strain components, stress components and equivalent stresses.

The incremental solution linear option is optimized to minimize computing cost. The geometrically nonlinear option will need further optimization, consistent with the final formulation. The nonlinear formulation of Part 1 Section II is thought to be in final form, except for details, in view of the derivation, which is believed sound, and the correlations shown in Part 1 Section III for simple structures with large geometric nonlinearities.

Part 2 of the report, the User's Manual, contains instructions

for applying the computer program. This part provides a user oriented description of the finite element model, the input, the program modules, and the output. Examples of the use of the program are provided, with representative samples of finite element model diagrams, filled-out input formats, and printed output. Part 2 also presents data on running times.

Section III of Part 1 presents applications of the Math Model. Applications to static analyses of classical problems verify the validity of the cell element. Applications to dynamic analyses of simple nonlinear structures demonstrate the capability of the program to account accurately for large geometric nonlinearities including snap-through. Analytical results for statically and dynamically loaded laminated beams show good correlations with test data. A linear analysis of the F-16 canopy subjected to bird impact shows qualitative agreement with test results, but displacements and stresses are underestimated. The underestimation is attributed to geometric nonlinearity. An attempt to apply the Math Model nonlinear incremental solution to the canopy failed. The lack of success is attributed to the use of an unsuitable modal transformation.

The linear incremental option of the Math Model is considered suitable for parametric studies of windshield systems and for detailed design evaluations, depending on the complexity of the finite element model employed. The linear option can also provide useful information for final design substantiation if nonlinear effects are small or if test data permitting the evaluation of nonlinear effects are available.

The geometrically nonlinear option gives accurate results for simple structures exhibiting large geometric nonlinearities. The applicability to large structures remains to be evaluated, pending

development of a better understanding of suitable modal transformations.

SECTION V

RECOMMENDATIONS

The Math Model is recommended as a tool for use in designing bird impact resistant aircraft windshields and canopies.

Current procedures for designing and substantiating windshield systems include extensive testing programs in which birds are shot at transparency systems under controlled temperature conditions. If a transparency fails, little information useful for analysis is provided, as the typical test is basically "go/no-go". Also the test specimen, which is costly, must be discarded if extensively damaged.

The Math Model offers the possibility of reducing the scope and expense of this testing effort, especially after experience leads to improvements in the model and confidence develops in the information it provides.

Applications of the model to existing aircraft are recommended as a means of gaining experience. A finite element model of the B-1 windshield and supporting structure was produced, as described in Section II of this report. Application of the Math Model linear analysis option to the B-1 finite element model is suggested. Applications to other aircraft, such as the B-52, should be considered.

The failure of the geometrically nonlinear analysis of the F-16 canopy, mentioned in Section II, is attributed in Appendix F to the use of an unsuitable modal transformation. Further study of this matter, including the development and application of a new modal transformation, is recommended. Analysis of a structure of lesser difficulty than the canopy such as a nonlinear beam is considered advisable before repeating the canopy study.

In connection with the modal study, the possibility of eliminating shear node degrees of freedom from the equations of motion should be considered, as a means of simplifying the mode selection problem.

The field of bird impact loads, including the effect of target compliance, needs further study. A suggested approach is to incorporate compliant target effects, based on the relative velocity of the bird and the moving windshield, into the Math Model as a means of studying effects on impact loads. Improved data on the distribution of pressure within the footprint and further verification of the traveling footprint hypothesis are necessary.

The effects on dynamic response of material nonlinearities, thermal loads resulting from damping energy dissipated as heat, and the dependence of material properties on temperature changes occurring after initial impact were mathematically formulated, and some coding was completed in these areas. This work should be completed.

The Math Model nonlinear option is applicable to statically stable or unstable structures, but the linear option applies only to stable structures. A program change to remove this restriction for the linear option is recommended.

In the nonlinear analysis, fictitious loads are assumed to vary approximately linearly with time during an increment, but thermomechanical loads are assumed to be constant. A better assumption would be that all loads vary approximately linearly. A programming change to implement this assumption for both linear and nonlinear cases is recommended.

A feature called "Multiconnect" was planned for the Math Model, to allow two or more small cells to be contiguous to a single face of a larger cell. This automated feature would be useful as a means of decreasing total problem size, while allowing increased mesh

fineness in the region of interest. Implementation of Multiconnect is recommended.

Implementation of an interactive or batch mode plot capability in the Math Model postprocessor can be considered, together with other user convenience features.

APPENDIX A

FORCE AND DISPLACEMENT TRANSFORMATIONS

LIST OF SYMBOLS FOR APPENDIX A

These symbols are defined in the list at the front of this report.

This appendix describes the force and displacement transformations that are employed in deriving the equations of motion for the finite element model.

Forces and Corresponding Displacements

The displacement corresponding to a force is defined as the work done by a unit value of the force during a virtual displacement.

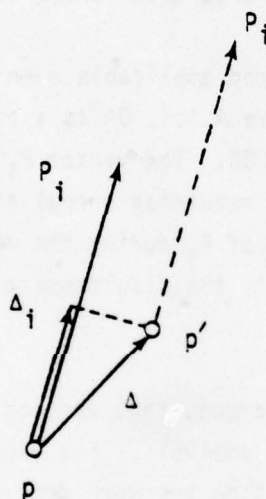


Figure A.1. Displacement corresponding to a force.

Figure A.1 illustrates the definition. The particle p , acted upon by the force P_i , is displaced the amount Δ to the position p' . The projection of Δ upon the direction of the force is Δ_i . The work done by a unit value of P_i is Δ_i , consequently Δ_i is the displacement corresponding to P_i , according to the definition.

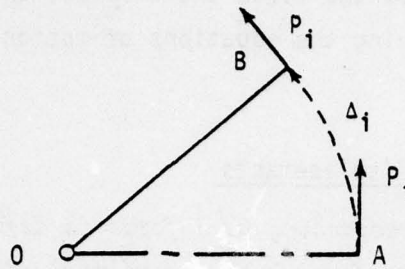


Figure A.1.1. Displacement corresponding to a force that varies in direction

The definition is considered applicable even if the direction of the force changes. Thus, in Figure A.1.1, OA is a rigid bar that rotates about point O to the position OB. The vector P_i represents a force acting at the end of the bar, remaining normal to the bar as it rotates. The work done by a unit value of P_i during the motion is equal to the arc length Δ_i . Therefore Δ_i is the displacement corresponding to P_i , according to the definition.

The corresponding displacement, thus defined, is usually what is meant by displacement in structural analysis. For example, the displacement of a node is found by calculating the work done by a unit dummy load acting on the node in the direction of the desired deflection. The concept of corresponding displacement is needed in the present approach, because forces and displacements referred to nonorthogonal axes are considered.

Self-Equilibrating Element Forces and Corresponding Deformations

The concept of the self-equilibrating element force, and its corresponding deformation, is useful in developing stiffness and unassembled deformation matrices for the cell and membrane elements employed in the Math Model. The self-equilibrating element force is a more generalized concept than the force concept of the preceding paragraph. Figure A.1.1.1(a) shows an axially loaded bar element acted upon by the self-equilibrating element forces F_1 . The symbol F_1 denotes a pair of forces. Figure A.1.1.1(b) shows the element when $F_1 = 2$.

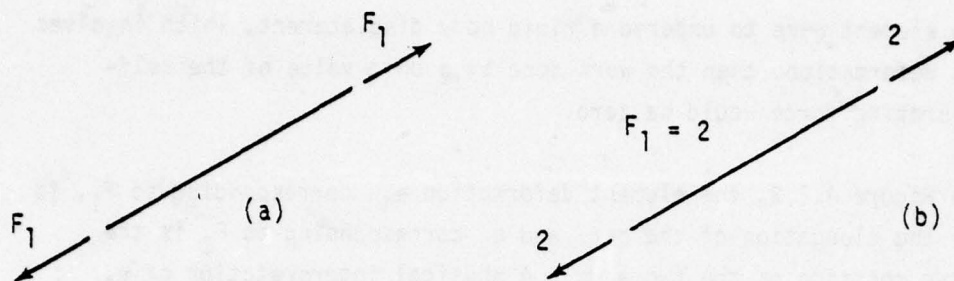


Figure A.1.1.1 Self-equilibrating element force.

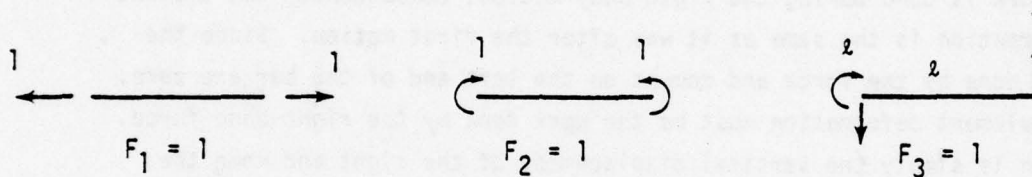


Figure A.1.2. Bending element with self-equilibrating element forces.

Figure A.1.2 shows a bending element with three self-equilibrating element forces defined as indicated. Any self-equilibrating combination of forces on the element can be derived by a linear combination of the three unit forces shown.

The element deformation corresponding to a self-equilibrating element force is defined as the work done by a unit value of the element force during a virtual deformation. This definition of element deformation applies even when the directions of the vectors comprising the element force change, provided that the relative directions of the vectors remain constant. Extension of the definition to the case of variable relative directions of the vectors is not required in the present study. The quantity so defined is clearly a deformation, because

if the element were to undergo a rigid body displacement, which involves a zero deformation, then the work done by a unit value of the self-equilibrating force would be zero.

In Figure A.1.2, the element deformation e_1 , corresponding to F_1 , is simply the elongation of the bar, and e_2 corresponding to F_2 is the relative rotation of the two ends. A physical interpretation of e_3 corresponding to F_3 can be obtained in the following manner: Let the bar be subjected to a virtual displacement which deforms the bar. Following this displacement, produce a rigid body motion, such that the displacement and slope of the left end of the bar are restored to zero. No work is done during the rigid body motion, consequently the element deformation is the same as it was after the first motion. Since the work done by the force and moment on the left end of the bar are zero, the element deformation must be the work done by the right hand force, which is simply the vertical displacement of the right end when the displacement and rotation of the left end are zero. However, other equally valid interpretations are possible. Suppose that the rigid body motion were such as to restore the vertical displacement of both ends of the bar to zero. In this case the deformation would be the work done by the moment, equal to the rotation of the left end times the length of the bar. The numerical value of the element deformation interpreted either way is the same.

Work Done by a Force

The work done by a force of constant magnitude is equal to the force times its corresponding displacement. This result follows from the definition of corresponding displacement. The statement is true even if the direction of the force changes, as long as the magnitude of the force remains constant. If the magnitude of the force varies with time, the definition still applies, as long as the time period considered is infinitesimal.

The definition also applies to self-equilibrating forces and corresponding deformations.

EQUILIBRIUM TRANSFORMATIONS

Often a set of forces and corresponding displacements are defined for a set of rigid bodies, such as the nodes of a finite element model, and a need arises to transform to a second set of statically equivalent forces and corresponding displacements. For example, a set of forces and displacements oriented in a random manner may act on the nodes of a structure, and an equivalent set of forces and displacements may be required oriented parallel to global axes. In the equilibrium transformation approach, the two sets of forces are considered to be statically equivalent. One set of forces is derived from the other, on the basis of equilibrium, assuming that this is possible. The displacement transformation follows from virtual work. Consider a set of rigid bodies, such as the nodes of a finite element model. Consider two sets of forces, \bar{P}_i and P_j acting upon these bodies, and the corresponding displacements $\bar{\Delta}_i$ and Δ_j . Assume that the \bar{P}_i forces are able to equilibrate the P_j 's no matter what choice of P_j 's is made.

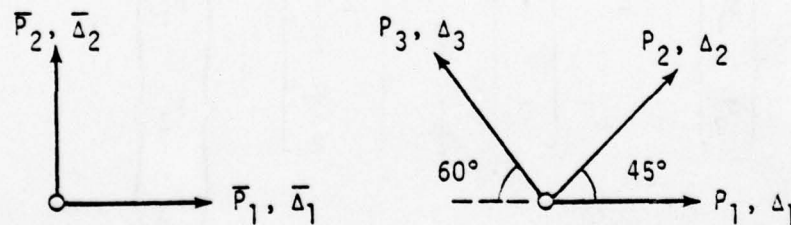


Figure A.2. Sets of forces and corresponding displacements.

Figure A.2 shows such a set of force vectors and corresponding displacement vectors acting upon a single node. Let \bar{P} and P be column matrices containing the sets of forces \bar{P}_i and P_j . A transformation \bar{P}_p is calculated from equilibrium, such that

$$\bar{P} = \bar{P}_p P \quad (A.1)$$

The two sets of forces shown in Figure A.2 are considered to be statically equivalent. In Figure A.3, both sets of forces are shown acting on the node, with the signs of the P forces reversed, so that the node is in equilibrium. Therefore, from static equilibrium, ...

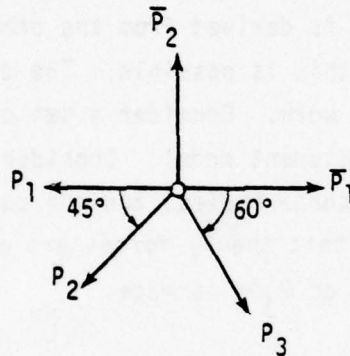


Figure A.3. Equilibrium of a rigid body.

$$\begin{Bmatrix} \bar{P}_1 \\ \bar{P}_2 \end{Bmatrix} = \begin{bmatrix} 1 & \frac{1}{\sqrt{2}} & -\frac{1}{2} \\ 0 & \frac{1}{\sqrt{2}} & \frac{\sqrt{3}}{2} \end{bmatrix} \begin{Bmatrix} P_1 \\ P_2 \\ P_3 \end{Bmatrix} \quad (A.2)$$

\bar{P}
 \bar{P}_p
 P

The matrices are denoted according to the symbols written under the equation.

The transformation \bar{P}_p can be calculated in this manner when the number of independent equilibrium equations is sufficient.

The displacement transformation can now be derived from the principle of virtual work. Consider the rigid bodies in equilibrium under the actions of the \bar{P} forces and the P forces reversed. Produce virtual displacements of the rigid bodies, keeping the forces constant. Let $\bar{\Delta}$ and Δ be column matrices containing the displacements $\bar{\Delta}_i$ and Δ_i . Since the bodies are rigid and in equilibrium, the virtual work, V , is zero. Therefore,

$$V = \sum_i \bar{P}_i \bar{\Delta}_i - \sum_j P_j \Delta_j = 0 \quad (A.3)$$

Therefore,

$$P^T \Delta = \bar{P}^T \bar{\Delta} \quad (A.4)$$

Eliminating \bar{P} from equations A.1 and A.4 gives

$$P^T \Delta = P^T \bar{P}_P^T \bar{\Delta} \quad (A.5)$$

This equation holds for any choice of P . Therefore,

$$\Delta = \bar{P}_P^T \bar{\Delta} \quad (A.6)$$

This is the displacement transformation.

Note that this derivation applies even if some of the forces and displacements are self-equilibrating element forces and corresponding deformations, because a deformation is defined as the work done by a unit value of the corresponding element force during a virtual displacement. Equation A.3 therefore holds.

For the example of Figure A.2, substituting \bar{P}_P from equation A.2 into equation A.6, and expanding the Δ and $\bar{\Delta}$ matrices, gives

$$\begin{Bmatrix} \Delta_1 \\ \Delta_2 \\ \Delta_3 \end{Bmatrix} = \begin{bmatrix} 1 & 0 \\ \frac{1}{\sqrt{2}} & \frac{1}{\sqrt{2}} \\ -\frac{1}{2} & \frac{\sqrt{3}}{2} \end{bmatrix} \begin{Bmatrix} \bar{\Delta}_1 \\ \bar{\Delta}_2 \end{Bmatrix} \quad (A.7)$$

Reference to Figure A.2 shows that equation A.7 is correct. For example, if $\bar{\Delta}_1 = 0$ and $\bar{\Delta}_2 = 1$, then equation A.7 gives $\Delta_3 = \sqrt{3}/2$. Figure A.3.1, which shows the motion of the node for $\bar{\Delta}_1 = 0$, $\bar{\Delta}_2 = 1$, gives $\Delta_3 = \cos 30^\circ = \sqrt{3}/2$.

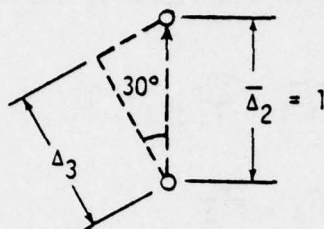


Figure A.3.1. Verification of equation A.7.

Figure A.4 shows an application of the force transformation when self-equilibrating element forces are involved.

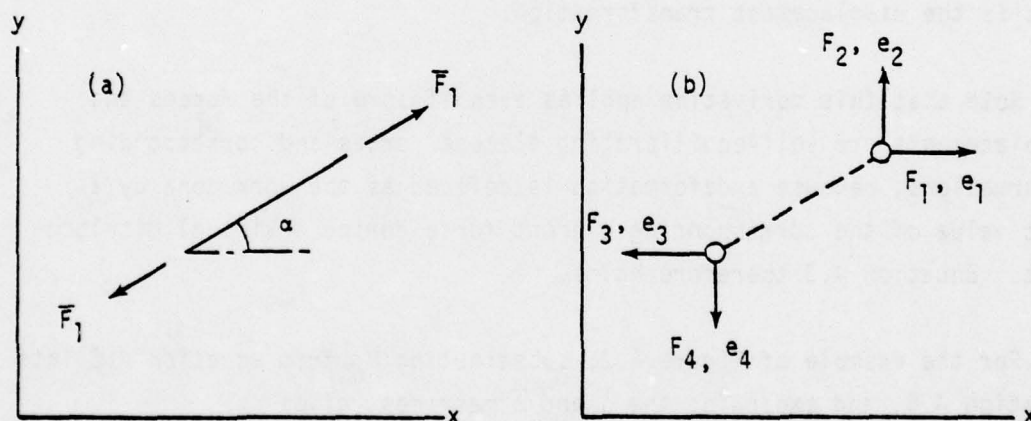


Figure A.4. Example of a transformation involving one set of self-equilibrating forces.

Figure A.4(a) shows the self-equilibrating force \bar{F}_1 acting upon an axially loaded bar. The corresponding deformation is \bar{e}_1 . Figure A.4(b) shows the forces F_i acting on the nodes adjacent to the bar, resolved into components parallel to the global coordinate axes. The displacements corresponding to the F_i forces are denoted e_i . Only the equilibrium of the nodes needs to be considered in deriving the transformation. Consider the bar to be removed, and apply the F forces and the \bar{F} forces reversed to the nodes, as in Figure A.5.

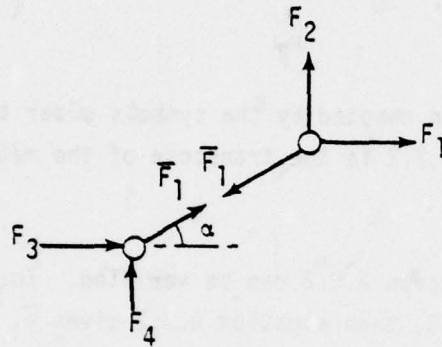


Figure A.5. Equilibrium of the nodes.

From equilibrium:

$$\begin{pmatrix} F_1 \\ F_2 \\ F_3 \\ F_4 \end{pmatrix} = \begin{pmatrix} \cos \alpha \\ \sin \alpha \\ -\cos \alpha \\ -\sin \alpha \end{pmatrix} \bar{F}_1 \quad (A.7.1)$$

$\begin{matrix} F & F_{\bar{F}} & \bar{F} \end{matrix}$

The matrices are denoted according to the symbols written under the equation.

Equation A.7.1 is analogous to equation A.1. Therefore, by analogy with equation A.6,

$$\bar{e}_1 = \begin{bmatrix} \cos \alpha & \sin \alpha & -\cos \alpha & -\sin \alpha \end{bmatrix} \begin{Bmatrix} e_1 \\ e_2 \\ e_3 \\ e_4 \end{Bmatrix} \quad (\text{A.7.2})$$

\bar{e}_1

F_F^T

e

where the matrices are again denoted by the symbols under the equation. The matrix F_F^T in equation A.7.2 is the transpose of the matrix F_F in equation A.7.1.

The correctness of equation A.7.2 can be verified. For example, if $e_1 = 1$, and $e_2 = e_3 = e_4 = 0$, then equation A.7.2 gives $\bar{e}_1 = \cos \alpha$. Figure A.6 shows this result to be correct. Note that the displacement e_1 is implicitly assumed to be small, so that the rotation of the bar is negligible.

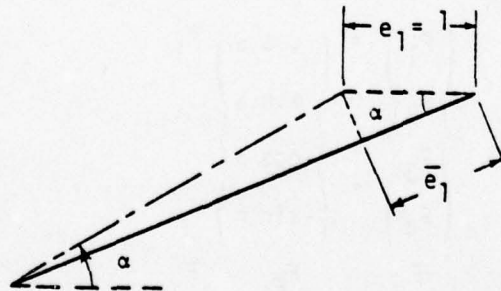


Figure A.6. Verification of Equation A.7.2.

Variable Equilibrium Transformation

The displacement transformation given by equation A.6 applies as long as the force transformation matrix, \bar{P}_p , remains constant during the motion, as assumed in the derivation. If \bar{P}_p varies with time, the transformation still applies, provided it is written in differential form, as

$$d\Delta = \bar{P}_p^T(t) d\bar{\Delta} , \quad (A.7.3)$$

where the notation $\bar{P}_p(t)$ indicates that \bar{P}_p is a function of time. Such a variation would occur, in the case of the bar of Figure A.4(a), if the bar and its axial loads should rotate significantly during the motion that produces the displacements e_1 , e_2 , e_3 and e_4 .

MODAL DISPLACEMENT TRANSFORMATIONS

Consider a finite element model for which Δ and P are column matrices of nodal displacements and loads. If the structure has a large number of degrees of freedom, the number of unknown displacements is often reduced in dynamic problems by employing a transformation of the form.

$$\Delta = T\bar{\Delta} , \quad (A.8)$$

where T is a rectangular matrix having more rows than columns. The columns of T are linearly independent.

Here a set of rigid bodies is not under consideration, and no simple interpretation of the physical significance of the transformation is available. The elements of $\bar{\Delta}$ can be called generalized displacements.

When the columns of T are taken equal to natural modes of the structure, usually corresponding to the lower natural frequencies, T is called a modal transformation. The elements of $\bar{\Delta}$ can be called modal displacements or modal coordinates. Specifying the modal displacements

$\bar{\Delta}$ specifies the nodal displacements Δ .

If the modal transformation includes all of the natural modes, then T is square and nonsingular, and Equation A.8 gives

$$\bar{\Delta} = T^{-1} \Delta \quad (A.9)$$

In this case, a value of $\bar{\Delta}$ can be found corresponding to any value of Δ .

If T has more rows than columns, because some natural modes have been omitted, then Equation A.8 cannot be solved for $\bar{\Delta}$. Therefore, introducing the transformation given by Equation A.8 means that only displacements of the structure corresponding to possible choices of $\bar{\Delta}$ are allowed. This fact implies that artificial constraints are introduced, and equilibrium is not exactly satisfied.

Postulate the existence of generalized loads corresponding to the generalized displacements. Let \bar{P} be a column matrix of generalized loads. Apply the nodal loads P and the generalized loads \bar{P} , reversed, to the structure.

Define \bar{P} in such a way that when a virtual displacement of the structure is produced, corresponding to any choice of $\bar{\Delta}$, the virtual work, V , is zero. Therefore, during such a displacement,

$$V = P^T \Delta - \bar{P}^T \bar{\Delta} = 0 \quad (A.10)$$

Therefore $\bar{P}^T \bar{\Delta} = P^T \Delta$, (A.11)

and $\bar{\Delta}^T \bar{P} = \Delta^T P$ (A.12)

Substituting Δ from Equation A.8 into Equation A.12 gives

$$\bar{\Delta}^T \bar{P} = \bar{\Delta}^T T^T P \quad (A.13)$$

This equation holds for any choice of $\bar{\Delta}$. Therefore

$$\bar{P} = T^T P \quad (A.14)$$

Equation A.14 is the transformation for the generalized loads.

When T has more rows than columns, because some modes have been omitted, equilibrium is not exactly satisfied, but if the omitted modes are only slightly excited during the dynamic loading of the structure, the resulting approximations are small.

APPENDIX B
STRESS AND STRAIN TRANSFORMATIONS

LIST OF SYMBOLS FOR APPENDIX B

Symbols appearing in Appendix B are defined in this list.

a, b	Length and width of plate element
B	Square matrix. Relates $\bar{\epsilon}_{\bar{e}}$ to $\bar{\sigma}_{\bar{g}}^T$
dA	Surface area of infinitesimal element
h	Thickness of plate element
P	A point
P	(Subscript). Indicates plane stress
T	(Superscript). Denotes transposed matrix
u, v, w	Displacement components referred to xyz
$\bar{u}, \bar{v}, \bar{w}$	Displacements components referred to $\bar{x}\bar{y}\bar{z}$
$\bar{u}, \bar{v}, \bar{w}$	Displacement components referred to $\bar{x}\bar{y}\bar{z}$
V	Volume of plate element
W_1, W_2, W_3	Virtual works done on plate element
x, y, z	Rectangular Cartesian coordinates
$\bar{x}, \bar{y}, \bar{z}$	Coordinates referred to the xyz frame rotated about the z axis
$\bar{x}, \bar{y}, \bar{z}$	Oblique coordinates
Δ	Displacement
∂	Denotes partial differentiation
ϵ	Column matrix of strain components referred to xyz
$\bar{\epsilon}$	Column matrix of strain components referred to $\bar{x}\bar{y}\bar{z}$
$\bar{\epsilon}$	Column matrix of strain components referred to $\bar{x}\bar{y}\bar{z}$

AD-A063 740

DOUGLAS AIRCRAFT CO LONG BEACH CALIF
AIRCRAFT WINDSHIELD BIRD IMPACT MATH MODEL. PART 1. THEORY AND --ETC(U)

F/G 1/3

DEC 77 P H DENKE

F33615-75-C-3105

UNCLASSIFIED

MDC-J7174-PT-1

AFFDL-TR-77-99-PT-1

NL

3 OF 6
ADA
063740



LIST OF SYMBOLS FOR APPENDIX B (Continued)

$\epsilon_x, \epsilon_y, \epsilon_z$ $\gamma_{xy}, \gamma_{yz}, \gamma_{zx}$	Strain components referred to xyz
$\bar{\epsilon}_x, \bar{\epsilon}_y, \bar{\epsilon}_z$ $\bar{\gamma}_{xy}, \bar{\gamma}_{yz}, \bar{\gamma}_{zx}$	Strain components referred to $\bar{x}\bar{y}\bar{z}$
$\tilde{\epsilon}_x, \tilde{\epsilon}_y, \tilde{\epsilon}_z$ $\tilde{\gamma}_{xy}, \tilde{\gamma}_{yz}, \tilde{\gamma}_{zx}$	Strain components referred to $\tilde{x}\tilde{y}\tilde{z}$
$\bar{\epsilon}_\epsilon$	Square matrix. Transforms ϵ strains to $\bar{\epsilon}$ strains
$\bar{\epsilon}_{\bar{\epsilon}}$	Square matrix. Transforms $\bar{\epsilon}$ strains to $\tilde{\epsilon}$ strains
ζ	Rotation angle of the xyz reference frame
θ	Angle between the \bar{x} and \tilde{y} axes
σ	Column matrix of stress components referred to xyz
$\bar{\sigma}$	Column matrix of stress components referred to $\bar{x}\bar{y}\bar{z}$
$\tilde{\sigma}$	Column matrix of stress components referred to $\tilde{x}\tilde{y}\tilde{z}$
$\sigma_x, \sigma_y, \sigma_z$ $\tau_{xy}, \tau_{yz}, \tau_{zx}$	Stress components referred to xyz
$\bar{\sigma}_x, \bar{\sigma}_y, \bar{\sigma}_z$ $\bar{\tau}_{xy}, \bar{\tau}_{yz}, \bar{\tau}_{zx}$	Stress components referred to $\bar{x}\bar{y}\bar{z}$
$\tilde{\sigma}_x, \tilde{\sigma}_y, \tilde{\sigma}_z$ $\tilde{\tau}_{xy}, \tilde{\tau}_{yz}, \tilde{\tau}_{zx}$	Stress components referred to $\tilde{x}\tilde{y}\tilde{z}$
$\sigma_{\bar{\sigma}}$	Square matrix. Transforms $\bar{\sigma}$ stresses to σ stresses
$\tilde{\sigma}_{\bar{\sigma}}$	Square matrix. Transforms $\tilde{\sigma}$ stresses to σ stresses

This Appendix presents stress and strain transformations required in deriving membrane and cell element stiffness and unassembled deformation matrices.

TRANSFORMATIONS FOR A RECTANGULAR CARTESIAN REFERENCE FRAME ROTATED ABOUT ONE AXIS.

Consider a solid body subjected to a condition of triaxial stress. Let x, y, z be rectangular cartesian coordinates in the body. Rotate the xyz reference frame about the z axis through an angle ζ , as shown in Figure B.1. Denote the new coordinates $\bar{x}, \bar{y}, \bar{z}$.

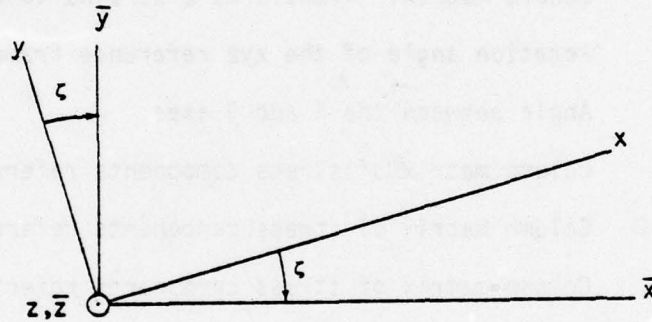


Figure B.1 Rotated Reference Frame

Stress Transformation

Let

$\sigma_x, \sigma_y, \sigma_z, \tau_{xy}, \tau_{yz}, \tau_{zx}$ = the components of the stress tensor referred to the xyz reference frame.

$\bar{\sigma}_x, \bar{\sigma}_y, \bar{\sigma}_z, \bar{\tau}_{xy}, \bar{\tau}_{yz}, \bar{\tau}_{zx}$ = the components of the stress tensor referred to the $\bar{x}\bar{y}\bar{z}$ reference frame.

Figure B.2(a) shows an infinitesimal prismatic element having five

faces. Three of the faces are normal to the $\bar{x}\bar{y}$ plane. These faces are parallel to the $\bar{x}\bar{z}$, $\bar{y}\bar{z}$, and $x\bar{z}$ planes, as shown. The other two faces are parallel to the $\bar{x}\bar{y}$ plane. The figure shows the dimensions of the element.

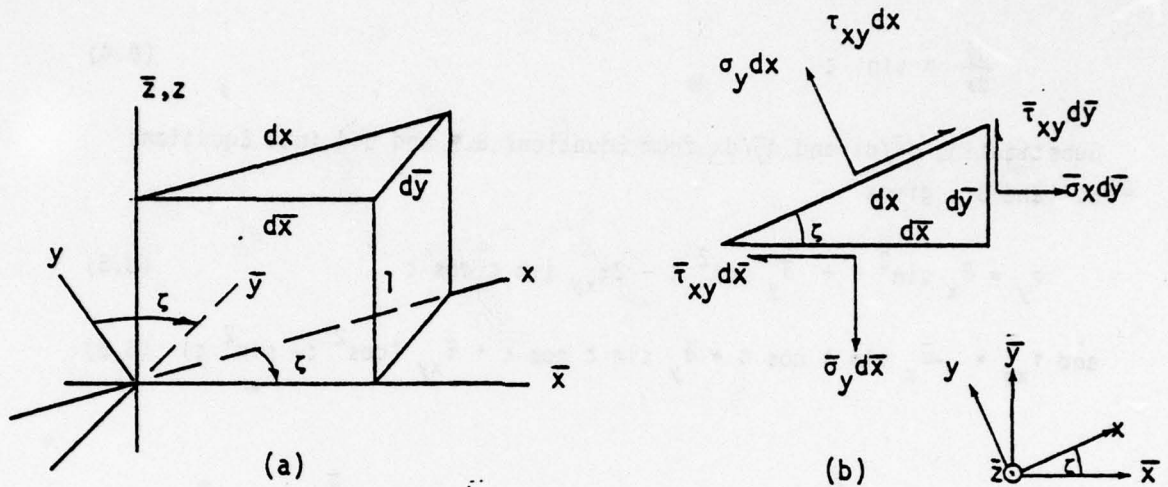


Figure B.2. Element for Calculating σ_y and τ_{xy} .

Figure B.2 (b) shows forces acting on the element. Forces parallel to z are not shown, because the equilibrium equations to be written are for force components parallel to $\bar{x}\bar{y}$. Forces parallel to the $\bar{x}\bar{y}$ plane act upon the top and bottom surfaces of the element. Let these forces be expressed in terms of stress components referred to the $\bar{x}\bar{y}\bar{z}$ system. In this case, the forces on the top of the prism are equal and opposite to the forces on the bottom. These forces cancel out in the equilibrium equations, therefore, they are not shown.

Summing force components parallel to the x and y axes gives

$$\sigma_y dx = \bar{\sigma}_x d\bar{y} \sin \zeta - \bar{\tau}_{xy} d\bar{y} \cos \zeta + \bar{\sigma}_y d\bar{x} \cos \zeta - \bar{\tau}_{xy} d\bar{x} \sin \zeta \quad (B.1)$$

$$\tau_{xy} dx = -\bar{\sigma}_x d\bar{y} \cos \zeta - \bar{\tau}_{xy} d\bar{y} \sin \zeta + \bar{\sigma}_y d\bar{x} \sin \zeta + \bar{\tau}_{xy} d\bar{x} \cos \zeta \quad (B.2)$$

But, from Figure B.2 (b),

$$\frac{d\bar{x}}{dx} = \cos \zeta \quad (B.3)$$

$$\frac{d\bar{y}}{dy} = \sin \zeta \quad (B.4)$$

Substituting $d\bar{x}/dx$ and $d\bar{y}/dy$ from Equations B.3 and B.4 into Equations B.1 and B.2 gives

$$\sigma_y = \bar{\sigma}_x \sin^2 \zeta + \bar{\sigma}_y \cos^2 \zeta - 2\tau_{xy} \sin \zeta \cos \zeta \quad (B.5)$$

$$\text{and } \tau_{xy} = -\bar{\sigma}_x \sin \zeta \cos \zeta + \bar{\sigma}_y \sin \zeta \cos \zeta + \bar{\tau}_{xy} (\cos^2 \zeta - \sin^2 \zeta) \quad (B.6)$$

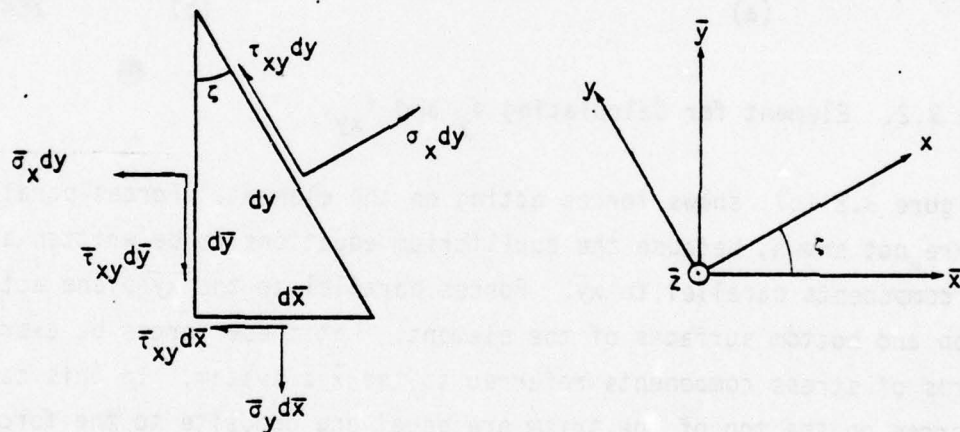


Figure B.3 Element for Calculating σ_x .

Figure B.3 shows a prismatic element similar to the element of Figure B.2 oriented to permit calculation of σ_x . Summing components parallel to the x axis gives

$$\sigma_x dy = \bar{\sigma}_x d\bar{y} \cos \zeta + \bar{\tau}_{xy} d\bar{y} \sin \zeta + \bar{\sigma}_y d\bar{x} \sin \zeta + \bar{\tau}_{xy} d\bar{x} \cos \zeta \quad (B.7)$$

$$\text{But } \frac{d\bar{x}}{dy} = \sin \zeta \quad (B.8)$$

$$\frac{d\bar{y}}{d\bar{y}} = \cos \zeta \quad (\text{B.9})$$

Substituting $d\bar{x}/d\bar{y}$ and $d\bar{y}/d\bar{y}$ from Equations B.8 and B.9 into Equation B.7 gives

$$\sigma_x = \bar{\sigma}_x \cos^2 \zeta + \bar{\sigma}_y \sin^2 \zeta + 2\bar{\tau}_{xy} \sin \zeta \cos \zeta \quad (\text{B.10})$$

Figure B.4 shows an element formed from the element of Figure B.2(a), by reducing the thickness, so that the ratio of the thickness to any one of the other dimensions approaches zero. In this case, the forces acting on the sides are negligible. Figure B.4(a) shows the forces acting on the top surface of the element, Figure B.4(b) shows the forces acting on the bottom. The areas of the top and bottom surfaces are each dA .

Writing the equations of equilibrium for components of forces parallel to the x , y and z axes, and dividing out the area dA , gives

$$\sigma_z = \bar{\sigma}_z \quad (\text{B.11})$$

$$\tau_{yz} = \bar{\tau}_{yz} \cos \zeta - \bar{\tau}_{zx} \sin \zeta \quad (\text{B.14})$$

$$\tau_{zx} = \bar{\tau}_{yz} \sin \zeta + \bar{\tau}_{zx} \cos \zeta \quad (\text{B.15})$$

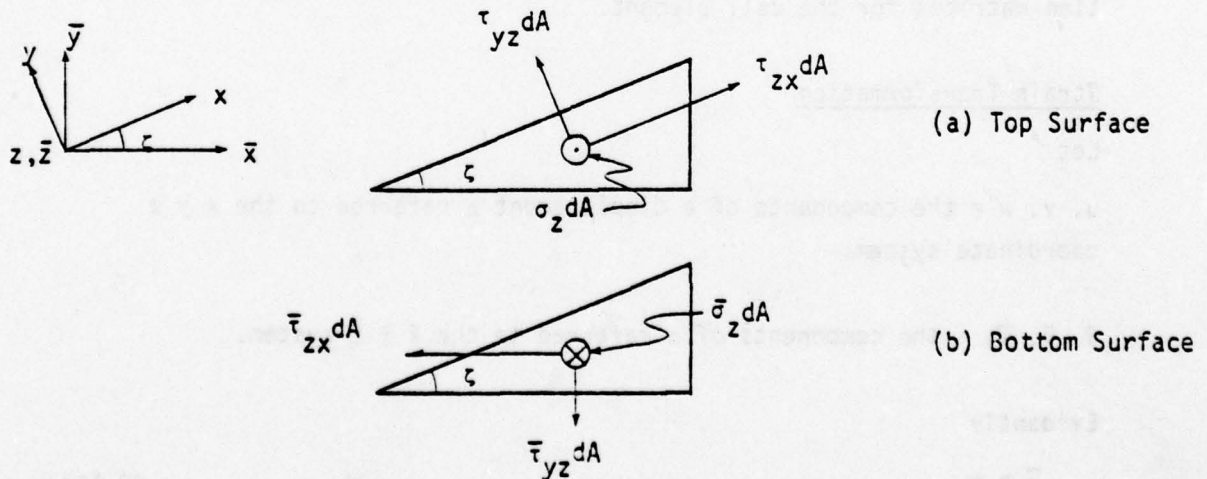


Figure B.4 Element for Calculating σ_z , τ_{yz} and τ_{zx} .

From Equations B.5, B.6, B.10, B.11, B.14 and B.15:

$$\left\{ \begin{array}{c} \sigma_x \\ \sigma_y \\ \sigma_z \\ \tau_{xy} \\ \tau_{yz} \\ \tau_{zx} \end{array} \right\} = \left[\begin{array}{ccc|ccc|ccc} 2\sin \zeta \cos \zeta & \sin^2 \zeta & \cos^2 \zeta & 0 & 0 & 0 & \bar{\tau}_{xy} \\ -2\sin \zeta \cos \zeta & \cos^2 \zeta & \sin^2 \zeta & 0 & 0 & 0 & \bar{\sigma}_y \\ 0 & 0 & 0 & 0 & 0 & 1 & \bar{\sigma}_x \\ \cos^2 \zeta - \sin^2 \zeta & \sin \zeta \cos \zeta & -\sin \zeta \cos \zeta & 0 & 0 & 0 & \bar{\tau}_{zx} \\ 0 & 0 & 0 & -\sin \zeta & \cos \zeta & 0 & \bar{\tau}_{yz} \\ 0 & 0 & 0 & \cos \zeta & \sin \zeta & 0 & \bar{\sigma}_z \end{array} \right] \quad (B.16)$$

σ
 $\sigma_{\bar{\sigma}}$
 $\bar{\sigma}$

The matrices in Equation B.16 are denoted according to the symbols written under the equation.

$$\therefore \sigma = \sigma_{\bar{\sigma}} \bar{\sigma} \quad (B.17)$$

This is the stress transformation. The elements of $\bar{\sigma}$ are arranged in an order which is useful in deriving the stiffness and unassembled deformation matrices for the cell element.

Strain Transformation

Let

u, v, w = the components of a displacement Δ referred to the $x y z$ coordinate system.

$\bar{u}, \bar{v}, \bar{w}$, = the components of Δ referred to the $\bar{x} \bar{y} \bar{z}$ system.

Evidently

$$\bar{w} = w, \quad (B.18)$$

since the \bar{z} and z axes are parallel.

Figure B.5 shows the relationships among the components u , v , \bar{u} and \bar{v} .

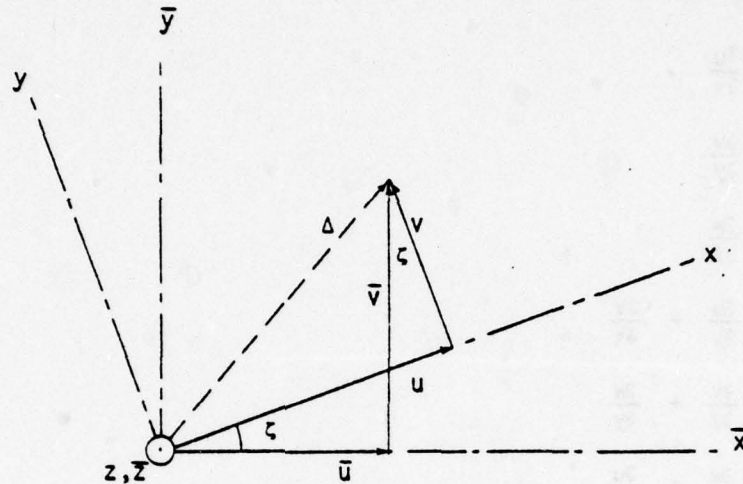


Figure B.5. The Components u , v , \bar{u} and \bar{v} .

From Figure B.5,

$$\bar{u} = u \cos \zeta - v \sin \zeta \quad (\text{B.19})$$

$$\bar{v} = u \sin \zeta + v \cos \zeta \quad (\text{B.20})$$

Let

$\epsilon_x, \epsilon_y, \epsilon_z, \gamma_{xy}, \gamma_{yz}, \gamma_{zx}$ = the components of the strain tensor referred to the xyz system.

$\bar{\epsilon}_x, \bar{\epsilon}_y, \bar{\epsilon}_z, \bar{\gamma}_{xy}, \bar{\gamma}_{yz}, \bar{\gamma}_{zx}$ = the components of the strain tensor referred to the $\bar{x}\bar{y}\bar{z}$ system.

The strain components are related to the displacement components in the xyz system by

$$\epsilon_x = \frac{\partial u}{\partial x} \quad (B.21)$$

$$\epsilon_y = \frac{\partial v}{\partial y} \quad (B.22)$$

$$\epsilon_z = \frac{\partial w}{\partial z} \quad (B.23)$$

$$\gamma_{xy} = \frac{\partial u}{\partial y} + \frac{\partial v}{\partial x} \quad (B.24)$$

$$\gamma_{yz} = \frac{\partial v}{\partial z} + \frac{\partial w}{\partial y} \quad (B.25)$$

$$\gamma_{zx} = \frac{\partial w}{\partial x} + \frac{\partial u}{\partial z} \quad (B.26)$$

Similarly, in the $\bar{x}\bar{y}\bar{z}$ system,

$$\bar{\epsilon}_x = \frac{\partial \bar{u}}{\partial \bar{x}} \quad (B.27)$$

$$\bar{\epsilon}_y = \frac{\partial \bar{v}}{\partial \bar{y}} \quad (B.28)$$

$$\bar{\epsilon}_z = \frac{\partial \bar{w}}{\partial \bar{z}} \quad (B.29)$$

$$\bar{\gamma}_{xy} = \frac{\partial \bar{u}}{\partial \bar{y}} + \frac{\partial \bar{v}}{\partial \bar{x}} \quad (B.30)$$

$$\bar{\gamma}_{yz} = \frac{\partial \bar{v}}{\partial \bar{z}} + \frac{\partial \bar{w}}{\partial \bar{y}} \quad (B.31)$$

$$\bar{\gamma}_{zx} = \frac{\partial \bar{w}}{\partial \bar{x}} + \frac{\partial \bar{u}}{\partial \bar{z}} \quad (B.32)$$

If x, y, z and $\bar{x}, \bar{y}, \bar{z}$ are the coordinates of the same point P, then, evidently

$$z = \bar{z} \quad (B.33)$$

Figure B.6 shows the relationships among the coordinates x , y , \bar{x} and \bar{y} .

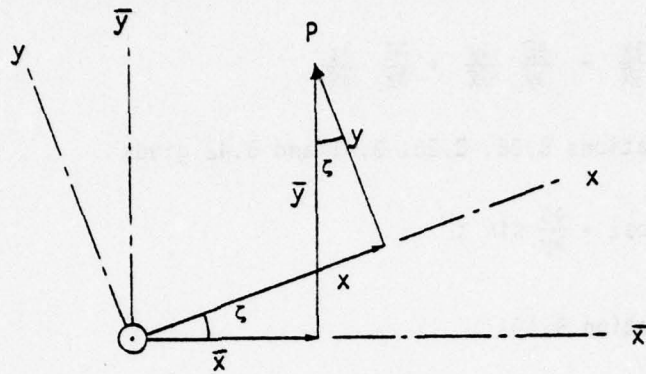


Figure B.6 The coordinates x , y , \bar{x} and \bar{y} .

From Figure B.6,

$$x = \bar{x} \cos \zeta + \bar{y} \sin \zeta \quad (\text{B.34})$$

$$y = -\bar{x} \sin \zeta + \bar{y} \cos \zeta \quad (\text{B.35})$$

From Equations B.33, B.34 and B.35,

$$\frac{\partial x}{\partial \bar{x}} = \cos \zeta \quad (\text{B.36})$$

$$\frac{\partial x}{\partial \bar{y}} = \sin \zeta \quad (\text{B.37})$$

$$\frac{\partial y}{\partial \bar{x}} = -\sin \zeta \quad (\text{B.38})$$

$$\frac{\partial y}{\partial \bar{y}} = \cos \zeta \quad (\text{B.39})$$

$$\frac{\partial z}{\partial \bar{z}} = 1 \quad (\text{B.40})$$

$$\frac{\partial x}{\partial \bar{z}} = \frac{\partial y}{\partial \bar{z}} = \frac{\partial z}{\partial \bar{x}} = \frac{\partial z}{\partial \bar{y}} = 0 \quad (\text{B.41})$$

From Equation B.27, according to the rules for partial differentiation,

$$\bar{\epsilon}_x = \frac{\partial \bar{u}}{\partial x} \frac{\partial x}{\partial \bar{x}} + \frac{\partial \bar{u}}{\partial y} \frac{\partial y}{\partial \bar{x}} + \frac{\partial \bar{u}}{\partial z} \frac{\partial z}{\partial \bar{x}} \quad (\text{B.42})$$

Combining Equations B.36, B.38, B.41 and B.42 gives

$$\bar{\epsilon}_x = \frac{\partial \bar{u}}{\partial x} \cos \zeta - \frac{\partial \bar{u}}{\partial y} \sin \zeta \quad (\text{B.43})$$

But, from Equation B.19,

$$\frac{\partial \bar{u}}{\partial x} = \frac{\partial u}{\partial x} \cos \zeta - \frac{\partial v}{\partial x} \sin \zeta \quad (\text{B.44})$$

$$\frac{\partial \bar{u}}{\partial y} = \frac{\partial u}{\partial y} \cos \zeta - \frac{\partial v}{\partial y} \sin \zeta \quad (\text{B.45})$$

Combining Equations B.43, B.44 and B.45,

$$\bar{\epsilon}_x = \frac{\partial u}{\partial x} \cos^2 \zeta + \frac{\partial v}{\partial y} \sin^2 \zeta - \left(\frac{\partial u}{\partial y} + \frac{\partial v}{\partial x} \right) \sin \zeta \cos \zeta \quad (\text{B.46})$$

Combining Equations B.21, B.22, B.24 and B.46 gives

$$\bar{\epsilon}_x = \epsilon_x \cos^2 \zeta + \epsilon_y \sin^2 \zeta - \gamma_{xy} \sin \zeta \cos \zeta \quad (\text{B.47})$$

Similarly, it can be shown that:

$$\bar{\epsilon}_y = \epsilon_x \sin^2 \zeta + \epsilon_y \cos^2 \zeta + \gamma_{xy} \sin \zeta \cos \zeta \quad (\text{B.48})$$

$$\bar{\epsilon}_z = \epsilon_z \quad (\text{B.49})$$

$$\bar{\gamma}_{xy} = 2\epsilon_x \sin \zeta \cos \zeta - 2\epsilon_y \sin \zeta \cos \zeta + \gamma_{xy} (\cos^2 \zeta - \sin^2 \zeta) \quad (\text{B.50})$$

$$\bar{\gamma}_{yz} = \gamma_{yz} \cos \zeta + \gamma_{zx} \sin \zeta \quad (\text{B.51})$$

$$\bar{\gamma}_{zx} = -\gamma_{yz} \sin \zeta + \gamma_{zx} \cos \zeta \quad (\text{B.52})$$

From Equations B.47, B.48, B.49, B.50, B.51 and B.52:

$$\begin{matrix} \bar{\epsilon}_{xy} \\ \bar{\epsilon}_y \\ \bar{\epsilon}_x \\ \bar{\epsilon}_{zx} \\ \bar{\epsilon}_{yz} \\ \bar{\epsilon}_z \end{matrix} = \begin{bmatrix} 2\sin\zeta\cos\zeta & -2\sin\zeta\cos\zeta & 0 & \cos^2\zeta - \sin^2\zeta & 0 & 0 \\ \sin^2\zeta & \cos^2\zeta & 0 & \sin\zeta\cos\zeta & 0 & 0 \\ \cos^2\zeta & \sin^2\zeta & 0 & -\sin\zeta\cos\zeta & 0 & 0 \\ 0 & 0 & 0 & 0 & -\sin\zeta & \cos\zeta \\ 0 & 0 & 0 & 0 & \cos\zeta & \sin\zeta \\ 0 & 0 & 1 & 0 & 0 & 0 \end{bmatrix} \begin{matrix} \epsilon_x \\ \epsilon_y \\ \epsilon_z \\ \gamma_{xy} \\ \gamma_{yz} \\ \gamma_{zx} \end{matrix}$$

$\bar{\epsilon}$
 $\bar{\epsilon}_\epsilon$
 ϵ

. . . (B.53)

The matrices in Equation B.53 are denoted according to the symbols written under the equation.

$$\bar{\epsilon} = \bar{\epsilon}_\epsilon \epsilon \quad (B.54)$$

This is the strain transformation. The elements of $\bar{\epsilon}$ and ϵ are arranged in the same order as the elements of $\bar{\sigma}$ and σ in Equation B.16. Comparing Equations B.16 and B.54, shows that

$$\bar{\epsilon}_\epsilon = \sigma_{\bar{\sigma}}^T \quad (B.55)$$

Thus the strain transformation is the transpose of the stress transformation.

TRANSFORMATIONS FROM RECTANGULAR TO OBLIQUE COORDINATES.

These transformations are given by Morley for the case of plane stress (Reference 11). They are generalized here to include the case of triaxial stress, considering the coordinate system shown in Figure B.7. The figure shows the oblique system, $\bar{x} \bar{y} \bar{z}$, and its orientation relative to the

rectangular $\bar{x} \bar{y} \bar{z}$ system. The \bar{x} and \bar{z} axes coincide with \bar{x} and \bar{z} . The \bar{y} axis lies in the $\bar{x} \bar{y}$ plane, and makes an angle θ with the \bar{x} axis. If \bar{x} , \bar{y} , \bar{z} and \bar{x} , \bar{y} , \bar{z} are the coordinates of the same point P, then from the figure,

$$\bar{x} = \bar{x} + \bar{y} \cos \theta \quad (8.56)$$

$$\bar{y} = \bar{y} \sin \theta \quad (8.57)$$

$$\bar{z} = \bar{z} \quad (8.58)$$

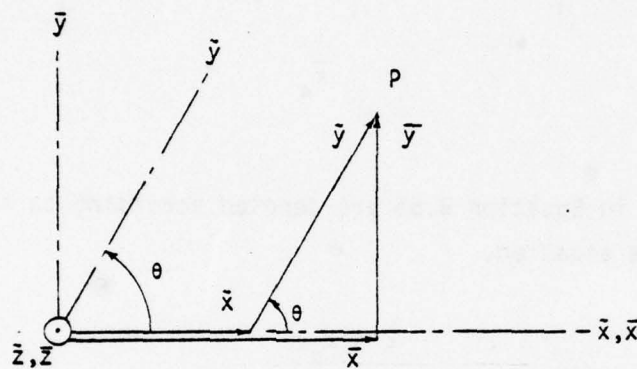


Figure 8.7 The Oblique Coordinate System.

Equilibrium of the Infinitesimal Parallelepiped

Let

$\bar{\sigma}_x, \bar{\sigma}_y, \bar{\sigma}_z, \bar{\tau}_{xy}, \bar{\tau}_{yz}, \bar{\tau}_{zx}$ = the components of the stress tensor referred to the $\bar{x} \bar{y} \bar{z}$ reference frame.

Figure 8.7.1 shows an infinitesimal skewed element, with faces parallel to the coordinate planes. The stresses on this element must be defined so that equilibrium is satisfied, when the stresses in the region of the element are constant.

Figure B.8 shows the remaining forces acting on the element. Figure B.8 (a) shows forces acting on the top surface of the element, Figure B.8 (b) shows forces acting on sides, and Figure B.8 (c) shows forces acting on the bottom. The forces on any face are again found by multiplying the appropriate stresses by the area of the face. Note that the shear stresses on the top and bottom surfaces, by definition, are τ_{yz} and τ_{zx} ; but

the shear stresses on the sides are $\tau_{yz} \sin \theta$ and $\tau_{zx} \sin \theta$. Thus the shear stresses on the sides are not the same as the corresponding stresses on the top and bottom, unless $\theta = \pi/2$. This relationship is necessary for equilibrium.

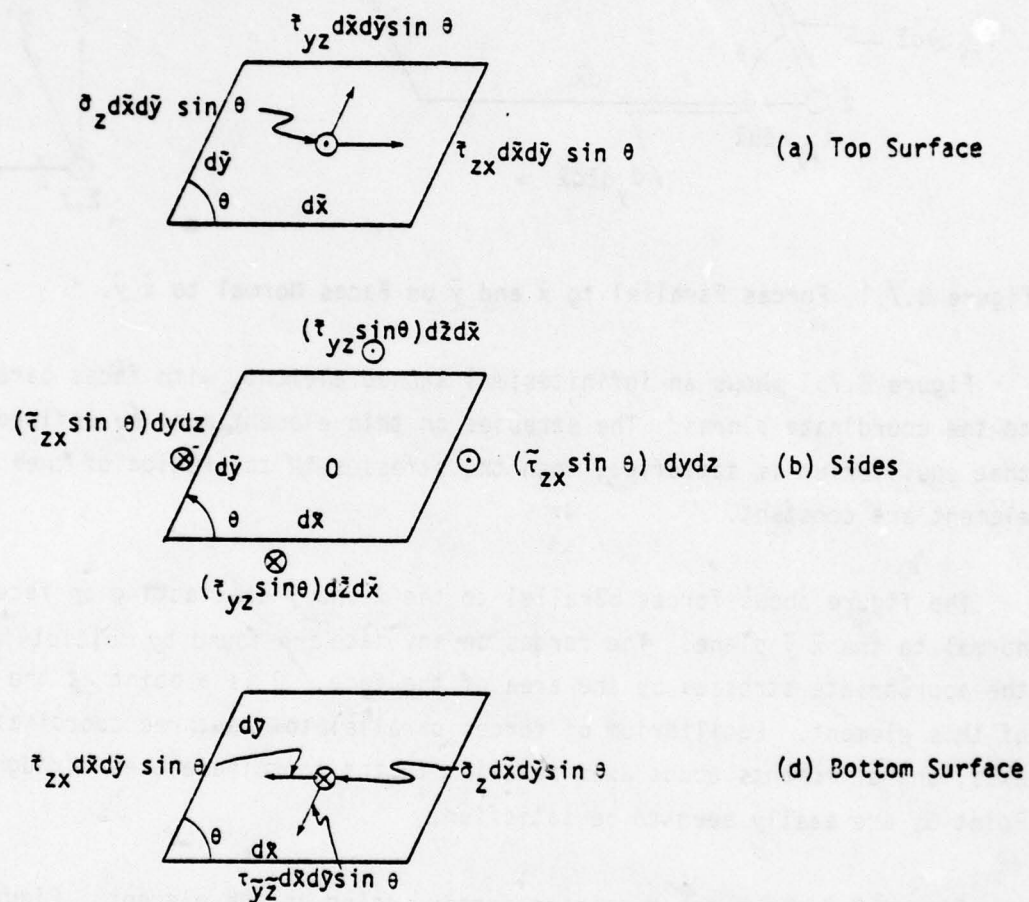


Figure 8.8 Remaining Forces on Skew Element.

If all forces shown in Figure B.8 are considered, equilibrium is easily seen to be satisfied for sums of forces parallel to the coordinate axes, and for the sum of moments about a vertical axis through O. The sum of moments about an axis parallel to \bar{x} through O is given by

$$(\tau_{yz} d\bar{x} d\bar{y} \sin \theta \sin \theta) d\bar{z} - (\tau_{yz} \sin \theta) d\bar{z} d\bar{x} \cdot d\bar{y} \sin \theta = 0 \quad (B.59)$$

The first term on the left of Equation B.59 represents the moment of forces on the top and bottom surfaces, the second term represents the moment of forces on the sides. The sum of moments about an axis parallel to \bar{y} through O are given by

$$(\tau_{zx} d\bar{x} d\bar{y} \sin \theta \sin \theta) d\bar{z} - (\tau_{zx} \sin \theta) d\bar{y} d\bar{z} \cdot d\bar{x} \sin \theta = 0 \quad (B.60)$$

Thus the element is in equilibrium.

Stress Transformation

Figure B.9 shows an element formed from the element of Figure B.7.1 by passing a plane through point A parallel to the $\bar{y}\bar{z}$ plane, and reducing the thickness to unity. The figure shows forces parallel to the $\bar{x}\bar{y}$ plane acting on the faces of the element normal to $\bar{x}\bar{y}$. Forces parallel to \bar{z} are

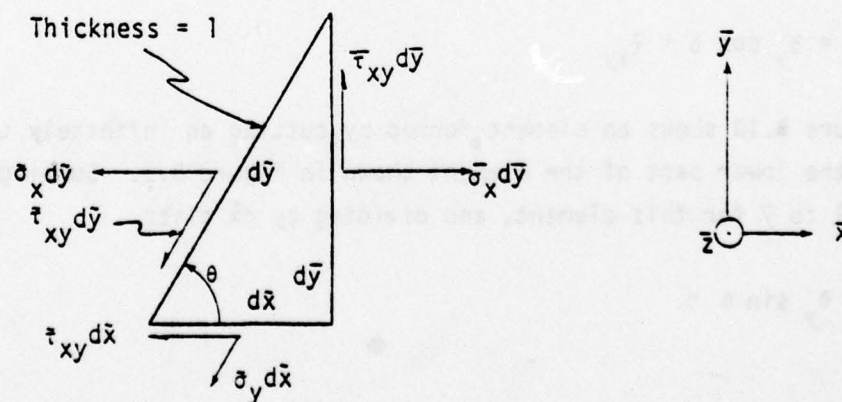


Figure B.9 Element for Calculating $\bar{\sigma}_x$ and $\bar{\tau}_{xy}$.

not considered. Assume that the forces acting on the upper and lower faces of the element are all expressed in terms of stress components referred to the $\bar{x} \bar{y} \bar{z}$ system. In this case the forces on the top and bottom surfaces are equal and opposite, and therefore need not be considered in the equilibrium equations for force components parallel to $\bar{x}\bar{y}$. These forces are consequently not shown.

Summing forces parallel to \bar{x} and \bar{y} gives

$$\bar{\sigma}_x d\bar{y} = \bar{\sigma}_x d\bar{y} + \bar{\tau}_{xy} d\bar{y} \cos \theta + \bar{\sigma}_y d\bar{x} \cos \theta + \bar{\tau}_{xy} d\bar{x} \quad (\text{B.61})$$

$$\bar{\tau}_{xy} d\bar{y} = \bar{\tau}_{xy} d\bar{y} \sin \theta + \bar{\sigma}_y d\bar{x} \sin \theta \quad (\text{B.62})$$

now $\frac{d\bar{x}}{d\bar{y}} = \cot \theta \quad (\text{B.63})$

$$\frac{d\bar{y}}{d\bar{y}} = \csc \theta \quad (\text{B.64})$$

Dividing Equations B.61 and B.62 by $d\bar{y}$, employing Equations B.63 and B.64 to eliminate $d\bar{x}/d\bar{y}$ and $d\bar{y}/d\bar{y}$ and rearranging terms gives

$$\bar{\sigma}_x = \bar{\sigma}_x \frac{1}{\sin \theta} + \bar{\sigma}_y \frac{\cos^2 \theta}{\sin \theta} + \bar{\tau}_{xy} \cdot 2 \frac{\cos \theta}{\sin \theta} \quad (\text{B.65})$$

$$\bar{\tau}_{xy} = \bar{\sigma}_y \cos \theta + \bar{\tau}_{xy} \quad (\text{B.66})$$

Figure B.10 shows an element formed by cutting an infinitely thin slice off of the lower part of the element shown in Figure B.9. Summing forces parallel to \bar{y} for this element, and dividing by $d\bar{x}$ gives

$$\bar{\sigma}_y = \bar{\sigma}_y \sin \theta \quad (\text{B.67})$$

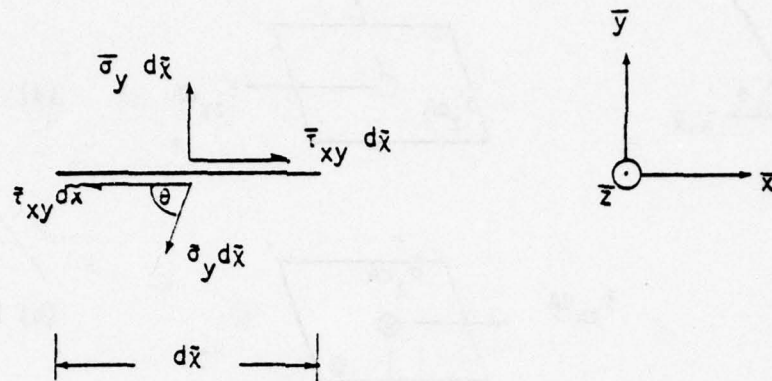


Figure B.10. Element for Calculating $\bar{\sigma}_y$.

Figure B.11 shows an element formed from the element of Figure B.7.1, by reducing the thickness, so that the ratio of the thickness to any one of the other dimensions approaches zero. The forces acting on the sides are therefore negligible. Figure B.11 (a) shows the forces acting on the top surface of the element, Figure B.11 (b) shows the forces acting on the bottom. The areas of the top and bottom surfaces are each dA .

Writing the equations of equilibrium for forces parallel to the \bar{x} , \bar{y} and \bar{z} axes, and dividing out the area dA , gives

$$\bar{\sigma}_z = \sigma_z \quad (B.68)$$

$$\bar{\tau}_{yz} = \tau_{yz} \sin \theta \quad (B.69)$$

$$\bar{\tau}_{zx} = \tau_{yz} \cos \theta + \tau_{zx} \quad (B.70)$$

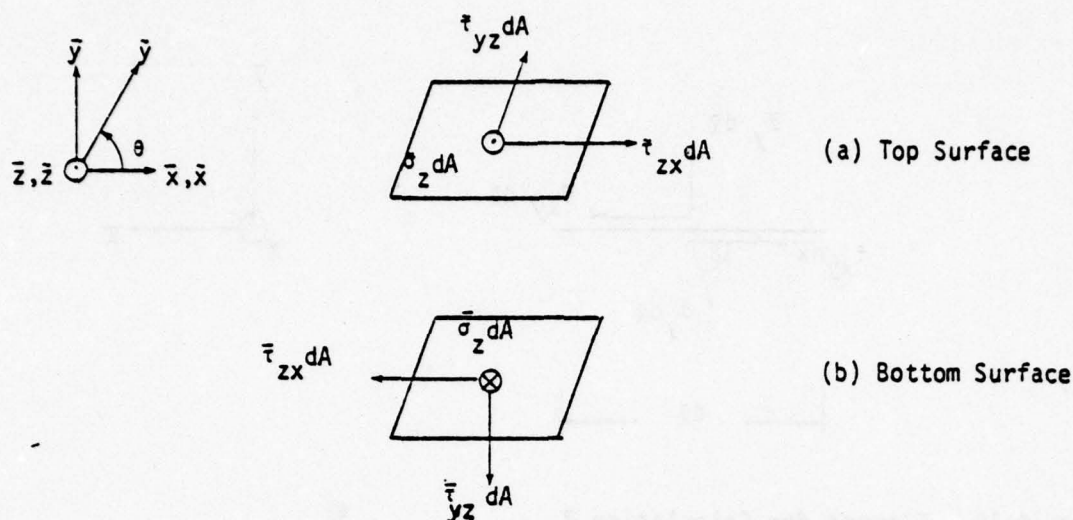


Figure B.11. Element for Calculating $\bar{\sigma}_z$, $\bar{\tau}_{yz}$, and $\bar{\tau}_{zx}$.

From Equations B.65, B.66, B.67, B.68, B.69 and B.70,

$$\begin{Bmatrix} \bar{\tau}_{xy} \\ \bar{\sigma}_y \\ \bar{\sigma}_x \\ \bar{\tau}_{zx} \\ \bar{\tau}_{yz} \\ \bar{\sigma}_z \end{Bmatrix} = \begin{bmatrix} 1 & \cos \theta & 0 \\ 0 & \sin \theta & 0 \\ 2 \frac{\cos \theta}{\sin \theta} & \frac{\cos^2 \theta}{\sin \theta} & \frac{1}{\sin \theta} \\ 1 & \cos \theta & 0 \\ 0 & \sin \theta & 0 \\ 0 & 0 & 1 \end{bmatrix} \begin{Bmatrix} \tau_{xy} \\ \sigma_y \\ \sigma_x \\ \tau_{zx} \\ \tau_{yz} \\ \sigma_z \end{Bmatrix} \quad (B.70.1)$$

$\bar{\sigma} \qquad \qquad \qquad \bar{\sigma}_\theta \qquad \qquad \qquad \sigma$

The matrices in Equation B.70.1 are denoted according to the symbols written under the equation.

$$\therefore \quad \bar{\sigma} = \bar{\sigma}_\theta \sigma \quad (B.70.2)$$

This is the stress transformation.

Strain Transformation

Let

\bar{u} , \bar{v} , \bar{w} = the components of a displacement Δ referred to the \bar{x} , \bar{y} , \bar{z} coordinate system.

Following Morley (Reference 11), the displacement components in the oblique system are defined as the projections of the displacement vector upon the coordinate axes.

Therefore $\bar{w} = \bar{w}$ (B.71)
since the \bar{z} and \bar{z} axes are parallel.

Figure B.12 shows the relationships among the components \bar{u} , \bar{v} , \bar{u} and \bar{v} .

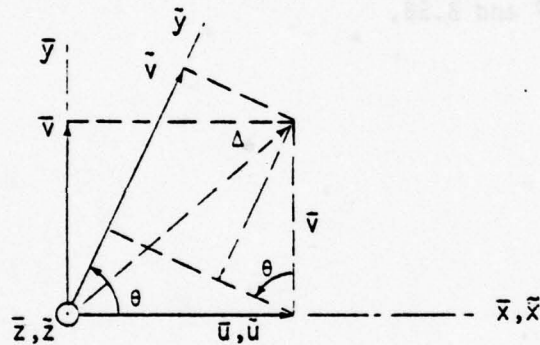


Figure B.12. The Components \bar{u} , \bar{v} , \tilde{u} and \tilde{v} .

From Figure B.12,

$$\tilde{u} = \bar{u} \quad (B.72)$$

$$\tilde{v} = \bar{u} \cos \theta + \bar{v} \sin \theta \quad (B.73)$$

Again following Morley, the strain components in the oblique systems are defined by

$$\epsilon_x = \frac{\partial \bar{u}}{\partial \bar{x}} \quad (\text{B.74})$$

$$\epsilon_y = \frac{\partial \bar{v}}{\partial \bar{y}} \quad (\text{B.75})$$

$$\epsilon_z = \frac{\partial \bar{w}}{\partial \bar{z}} \quad (\text{B.76})$$

$$\bar{\gamma}_{xy} = \frac{\partial \bar{v}}{\partial \bar{y}} + \frac{\partial \bar{v}}{\partial \bar{x}} \quad (\text{B.77})$$

$$\bar{\gamma}_{yz} = \frac{\partial \bar{v}}{\partial \bar{z}} + \frac{\partial \bar{w}}{\partial \bar{y}} \quad (\text{B.78})$$

$$\bar{\gamma}_{zx} = \frac{\partial \bar{w}}{\partial \bar{x}} + \frac{\partial \bar{u}}{\partial \bar{z}} \quad (\text{B.79})$$

From Equations B.56, B.57 and B.58,

$$\frac{\partial \bar{x}}{\partial \bar{x}} = 1 \quad (\text{B.80})$$

$$\frac{\partial \bar{x}}{\partial \bar{y}} = \cos \theta \quad (\text{B.81})$$

$$\frac{\partial \bar{y}}{\partial \bar{y}} = \sin \theta \quad (\text{B.82})$$

$$\frac{\partial \bar{z}}{\partial \bar{z}} = 1 \quad (\text{B.83})$$

$$\frac{\partial \bar{x}}{\partial \bar{z}} = \frac{\partial \bar{y}}{\partial \bar{x}} = \frac{\partial \bar{y}}{\partial \bar{z}} = \frac{\partial \bar{z}}{\partial \bar{x}} = \frac{\partial \bar{z}}{\partial \bar{y}} = 0 \quad (\text{B.84})$$

From Equation B.74, according to the rules for partial differentiation,

$$\epsilon_x = \frac{\partial \bar{u}}{\partial \bar{x}} \frac{\partial \bar{x}}{\partial \bar{x}} + \frac{\partial \bar{u}}{\partial \bar{y}} \frac{\partial \bar{y}}{\partial \bar{x}} + \frac{\partial \bar{u}}{\partial \bar{z}} \frac{\partial \bar{z}}{\partial \bar{x}} \quad (\text{B.85})$$

Combining Equations B.80, B.84 and B.85 gives

$$\bar{\epsilon}_x = \frac{\partial \bar{u}}{\partial \bar{x}} \quad (B.86)$$

Therefore, from Equations B.72 and B.86

$$\bar{\epsilon}_x = \frac{\partial \bar{u}}{\partial \bar{x}} \quad (B.87)$$

and therefore, from Equations B.27 and B.87,

$$\bar{\epsilon}_x = \bar{\epsilon}_x \quad (B.88)$$

From Equations B.75, according to the rules of partial differentiation,

$$\bar{\epsilon}_y = \frac{\partial \bar{v}}{\partial \bar{x}} \frac{\partial \bar{x}}{\partial \bar{y}} + \frac{\partial \bar{v}}{\partial \bar{y}} \frac{\partial \bar{y}}{\partial \bar{y}} + \frac{\partial \bar{v}}{\partial \bar{z}} \frac{\partial \bar{z}}{\partial \bar{y}} \quad (B.89)$$

Combining Equations B.81, B.82, B.84 and B.89 gives

$$\bar{\epsilon}_y = \frac{\partial \bar{v}}{\partial \bar{x}} \cos \theta + \frac{\partial \bar{v}}{\partial \bar{y}} \sin \theta \quad (B.90)$$

But, from Equations B.73 and B.90,

$$\bar{\epsilon}_y = \left(\frac{\partial \bar{u}}{\partial \bar{x}} \cos \theta + \frac{\partial \bar{v}}{\partial \bar{x}} \sin \theta \right) \cos \theta + \left(\frac{\partial \bar{u}}{\partial \bar{y}} \cos \theta + \frac{\partial \bar{v}}{\partial \bar{y}} \sin \theta \right) \sin \theta \quad (B.91)$$

$$\therefore \bar{\epsilon}_y = \frac{\partial \bar{u}}{\partial \bar{x}} \cos^2 \theta + \frac{\partial \bar{v}}{\partial \bar{y}} \sin^2 \theta + \left(\frac{\partial \bar{u}}{\partial \bar{y}} + \frac{\partial \bar{v}}{\partial \bar{x}} \right) \sin \theta \cos \theta \quad (B.92)$$

Combining Equations B.27, B.28, B.30 and B.92 gives

$$\bar{\epsilon}_y = \bar{\epsilon}_x \cos^2 \theta + \bar{\epsilon}_y \sin^2 \theta + \bar{\gamma}_{xy} \sin \theta \cos \theta \quad (B.93)$$

Similarly, it can be shown that:

$$\bar{\epsilon}_z = \bar{\epsilon}_z \quad (B.94)$$

$$\bar{\gamma}_{xy} = 2\bar{\epsilon}_x \cos \theta + \bar{\gamma}_{xy} \sin \theta \quad (B.95)$$

$$\bar{\gamma}_{yz} = \bar{\gamma}_{yz} \sin \theta + \bar{\gamma}_{zx} \cos \theta \quad (B.96)$$

$$\bar{\gamma}_{zx} = \bar{\gamma}_{zx} \quad (B.97)$$

From Equations B.88, B.93, B.94, B.95, B.96 and B.97,

$$\begin{Bmatrix} \bar{\gamma}_{xy} \\ \bar{\epsilon}_y \\ \bar{\epsilon}_x \\ \bar{\gamma}_{zx} \\ \bar{\gamma}_{yz} \\ \bar{\epsilon}_z \end{Bmatrix} = \begin{bmatrix} \sin \theta & 0 & 2 \cos \theta \\ \sin \theta \cos \theta & \sin^2 \theta & \cos^2 \theta \\ 0 & 0 & 1 \\ & & & 1 & 0 & 0 \\ & & & \cos \theta & \sin \theta & 0 \\ & & & 0 & 0 & 1 \end{bmatrix} \begin{Bmatrix} \bar{\gamma}_{xy} \\ \bar{\epsilon}_y \\ \bar{\epsilon}_x \\ \bar{\gamma}_{zx} \\ \bar{\gamma}_{yz} \\ \bar{\epsilon}_z \end{Bmatrix} \quad (B.98)$$

$\bar{\epsilon} \qquad \qquad \qquad \bar{\epsilon}_e \qquad \qquad \qquad \bar{\epsilon}$

The matrices in Equation B.98 are denoted according to the symbols written under the equation. The column matrix $\bar{\epsilon}$ is defined as in Equation B.53.

$$\bar{\epsilon} = \bar{\epsilon}_e \bar{\epsilon} \quad (B.99)$$

This is the strain transformation. Note that

$$\bar{\epsilon}_e = B \sigma_\theta^T \quad (B.100)$$

$$\text{where } B = \begin{bmatrix} I_{3 \times 3} \sin \theta \\ I_{3 \times 3} \end{bmatrix}, \quad (B.101)$$

$I_{3 \times 3}$ = a third order unit matrix,

and where, from Equation B.70.1,

$$\bar{\sigma}_\theta^T = \begin{bmatrix} 1 & 0 & 2 \frac{\cos \theta}{\sin \theta} & 1 & 0 & 0 \\ \cos \theta & \sin \theta & \frac{\cos^2 \theta}{\sin \theta} & \cos \theta & \sin \theta & 0 \\ 0 & 0 & \frac{1}{\sin \theta} & 0 & 0 & 1 \end{bmatrix} \quad (B.102)$$

In this case, the strain transformation is not equal to the transpose of the stress transformation.

Virtual Work Done on a Skewed Finite Element

The virtual work done on a skewed finite element with faces parallel to the oblique coordinate planes, subjected to constant stresses and to linear virtual displacements, is needed in deriving cell element stiffness and unassembled deformation matrices.

Figure B.13 shows such an element, oriented, without loss of generality, as shown, with respect to the coordinate axes. The $\bar{x} \bar{y}$ plane coincides with the bottom parallelogram face of the element. The dimensions of the element are as shown.

The element is subjected to a constant stress field. The Figure shows the forces parallel to the x and y axes acting on faces normal to the $\bar{x} \bar{y}$ plane, resulting from this field. The forces are expressed in terms of stress components, according to established notation.

At the time that the element is supporting the constant stress field, it is subjected to a set of virtual displacements that are linear functions of the coordinates. These linear displacements can result from constant

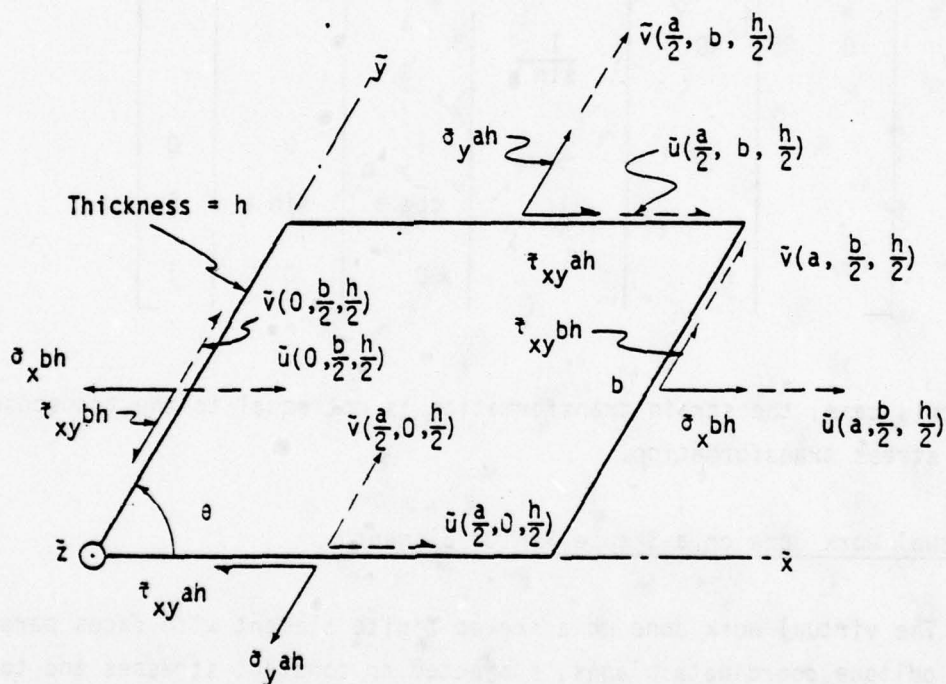


Figure B.13. Forces and Displacements Parallel to \bar{x} and \bar{y} on Faces Normal to $\bar{x} \bar{y}$.

thermal strains applied to the element, or they can result from a constant stress field, not necessarily the same as the one the element is supporting. Figure B.13 shows the displacements at the midpoints of the faces normal to the $\bar{x} \bar{y}$ plane, resulting from the linear displacement field. Functional notation is employed. Thus $\bar{v}(a, \frac{b}{2}, \frac{h}{2})$ means the displacement component parallel to \bar{y} at $\bar{x} = a, \bar{y} = \frac{b}{2}, \bar{z} = \frac{h}{2}$.

The displacement vectors represent the actual displacements of the corresponding forces, by virtue of the way that displacement components are defined. In fact, the force and displacement vectors represent corresponding forces and displacements, in the sense of Appendix A. Therefore, the virtual work done on the element by the forces shown in Figure B.13 is

$$\begin{aligned} W_1 = & \bar{\sigma}_x b n \left[\bar{u}(a, \frac{b}{2}, \frac{h}{2}) - \bar{u}(0, \frac{b}{2}, \frac{h}{2}) \right] + \bar{\sigma}_y a n \left[\bar{v}(\frac{a}{2}, b, \frac{h}{2}) - \bar{v}(\frac{a}{2}, 0, \frac{h}{2}) \right] \\ & + \bar{\tau}_{xy} b n \left[\bar{v}(a, \frac{b}{2}, \frac{h}{2}) - \bar{v}(0, \frac{b}{2}, \frac{h}{2}) \right] + \bar{\tau}_{xy} a n \left[\bar{u}(\frac{a}{2}, b, \frac{h}{2}) - \bar{u}(\frac{a}{2}, 0, \frac{h}{2}) \right] \end{aligned} \quad (B.103)$$

Now, since the displacement field under consideration is linear:

$$\frac{\partial \bar{u}}{\partial \bar{x}} = \frac{1}{a} \left[\bar{u}(a, \frac{b}{2}, \frac{h}{2}) - \bar{u}(0, \frac{b}{2}, \frac{h}{2}) \right] \quad (B.104)$$

$$\frac{\partial \bar{u}}{\partial \bar{y}} = \frac{1}{b} \left[\bar{u}(\frac{a}{2}, b, \frac{h}{2}) - \bar{u}(\frac{a}{2}, 0, \frac{h}{2}) \right] \quad (B.105)$$

$$\frac{\partial \bar{v}}{\partial \bar{x}} = \frac{1}{a} \left[\bar{v}(a, \frac{b}{2}, \frac{h}{2}) - \bar{v}(0, \frac{b}{2}, \frac{h}{2}) \right] \quad (B.106)$$

$$\frac{\partial \bar{v}}{\partial \bar{y}} = \frac{1}{b} \left[\bar{v}(\frac{a}{2}, b, \frac{h}{2}) - \bar{v}(\frac{a}{2}, 0, \frac{h}{2}) \right] \quad (B.107)$$

Combining Equations B.103, B.104, B.105, B.106 and B.107 gives

$$W_1 = abn \left[\bar{\sigma}_x \frac{\partial \bar{u}}{\partial \bar{x}} + \bar{\sigma}_y \frac{\partial \bar{v}}{\partial \bar{y}} + \bar{\tau}_{xy} \left(\frac{\partial \bar{u}}{\partial \bar{y}} + \frac{\partial \bar{v}}{\partial \bar{x}} \right) \right] \quad (B.108)$$

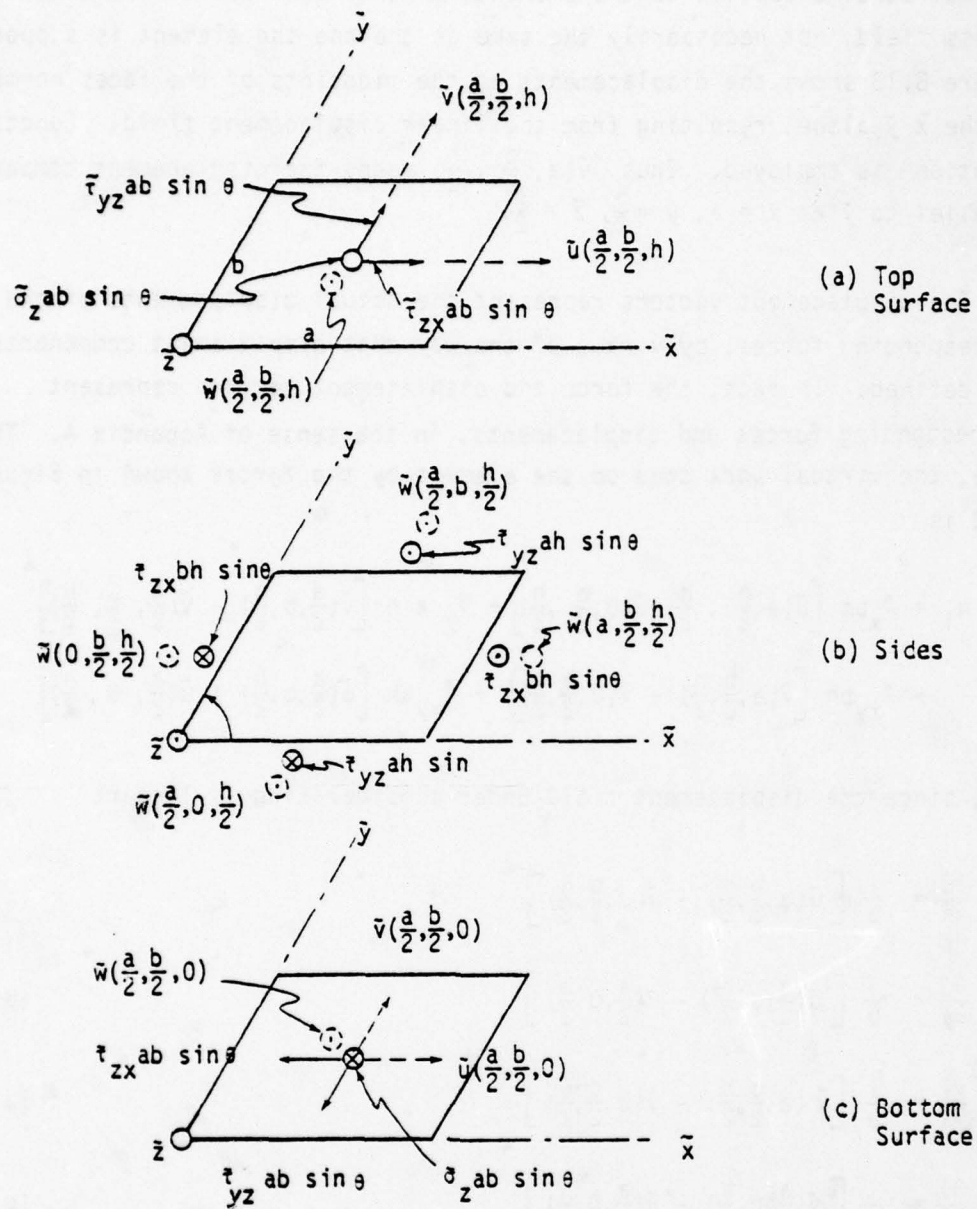


Figure B.14. Remaining Forces on the Skewed Finite Element.

The volume of the element is

$$V = a b h \sin \theta \quad (B.109)$$

Combining Equations B.74, B.75, B.77 and B.109 gives

$$W_1 = \frac{V}{\sin \theta} (\sigma_x \epsilon_x + \sigma_y \epsilon_y + \tau_{xy} \gamma_{xy}) \quad (B.110)$$

Figure B.14 shows the remaining forces on the element, and their corresponding displacements. The work done by these forces during the virtual displacement is

$$\begin{aligned} W_2 = & \tau_{zx} a b \sin \theta \left[u\left(\frac{a}{2}, \frac{b}{2}, h\right) - u\left(\frac{a}{2}, \frac{b}{2}, 0\right) \right] \\ & + \tau_{zx} b h \sin \theta \left[\bar{w}\left(a, \frac{b}{2}, \frac{h}{2}\right) - \bar{w}\left(0, \frac{b}{2}, \frac{h}{2}\right) \right] \\ & + \tau_{yz} a b \sin \theta \left[v\left(\frac{a}{2}, \frac{b}{2}, h\right) - v\left(\frac{a}{2}, \frac{b}{2}, 0\right) \right] \\ & + \tau_{yz} a h \sin \theta \left[\bar{w}\left(\frac{a}{2}, b, \frac{h}{2}\right) - \bar{w}\left(\frac{a}{2}, 0, \frac{h}{2}\right) \right] \\ & + \sigma_z a b \sin \theta \left[\bar{w}\left(\frac{a}{2}, \frac{b}{2}, h\right) - \bar{w}\left(\frac{a}{2}, \frac{b}{2}, 0\right) \right] \end{aligned} \quad (B.111)$$

$$\text{Now, } \frac{\partial \bar{u}}{\partial z} = \frac{1}{h} \left[u\left(\frac{a}{2}, \frac{b}{2}, h\right) - u\left(\frac{a}{2}, \frac{b}{2}, 0\right) \right] \quad (B.112)$$

$$\frac{\partial \bar{v}}{\partial z} = \frac{1}{h} \left[v\left(\frac{a}{2}, \frac{b}{2}, h\right) - v\left(\frac{a}{2}, \frac{b}{2}, 0\right) \right] \quad (B.113)$$

$$\frac{\partial \bar{w}}{\partial x} = \frac{1}{a} \left[\bar{w}\left(a, \frac{b}{2}, \frac{h}{2}\right) - \bar{w}\left(0, \frac{b}{2}, \frac{h}{2}\right) \right] \quad (B.114)$$

$$\frac{\partial \bar{w}}{\partial y} = \frac{1}{b} \left[\bar{w}\left(\frac{a}{2}, b, \frac{h}{2}\right) - \bar{w}\left(\frac{a}{2}, 0, \frac{h}{2}\right) \right] \quad (B.115)$$

$$\frac{\partial \bar{w}}{\partial z} = \frac{1}{h} \left[\bar{w}\left(\frac{a}{2}, \frac{b}{2}, h\right) - \bar{w}\left(\frac{a}{2}, \frac{b}{2}, 0\right) \right] \quad (B.116)$$

Combining Equations B.111, B.112, B.113, B.114, B.115 and B.116 gives:

$$W_2 = abh \sin \theta \left[\bar{\tau}_{yz} \left(\frac{\partial v}{\partial z} + \frac{\partial \bar{w}}{\partial y} \right) + \bar{\tau}_{zx} \left(\frac{\partial \bar{w}}{\partial x} + \frac{\partial \bar{u}}{\partial z} \right) + \bar{\sigma}_z \frac{\partial \bar{w}}{\partial z} \right] \quad (B.117)$$

Combining Equations B.76, B.78, B.79, B.109, and B.117 gives

$$W_2 = V(\bar{\tau}_{yz} \bar{\gamma}_{yz} + \bar{\tau}_{zx} \bar{\gamma}_{zx} + \bar{\sigma}_z \bar{\epsilon}_z) \quad (B.118)$$

The total virtual work done on the element is

$$W = W_1 + W_2 \quad (B.119)$$

Substituting W_1 and W_2 from Equations B.110 and B.118 into Equation B.119 gives

$$W = V \left[\frac{1}{\sin \theta} (\bar{\sigma}_x \bar{\epsilon}_x + \bar{\sigma}_y \bar{\epsilon}_y + \bar{\tau}_{xy} \bar{\gamma}_{xy}) + \bar{\tau}_{yz} \bar{\gamma}_{yz} + \bar{\tau}_{zx} \bar{\gamma}_{zx} + \bar{\sigma}_z \bar{\epsilon}_z \right] \quad (B.120)$$

This equation can be put in the form

$$W = V \begin{bmatrix} \bar{\tau}_{xy} \\ \bar{\sigma}_y \\ \bar{\sigma}_x \\ \bar{\tau}_{zx} \\ \bar{\tau}_{yz} \\ \bar{\sigma}_z \end{bmatrix}^T \begin{bmatrix} \frac{1}{\sin \theta} & & & & & \\ & \frac{1}{\sin \theta} & & & & \\ & & \frac{1}{\sin \theta} & & & \\ & & & 1 & & \\ & & & & 1 & \\ & & & & & 1 \end{bmatrix} \begin{bmatrix} \bar{\gamma}_{xy} \\ \bar{\epsilon}_y \\ \bar{\epsilon}_x \\ \bar{\gamma}_{zx} \\ \bar{\gamma}_{yz} \\ \bar{\epsilon}_z \end{bmatrix} \quad (B.121)$$

The matrices in this equation can be identified from Equations B.70.1, B.98 and B.101. Therefore

$$W = \bar{v} \bar{\sigma}^T B^{-1} \bar{z} \quad (B.122)$$

Equation B.122 gives the virtual work done on a skewed finite parallelepiped with sides parallel to the oblique coordinate planes, subjected to a constant stress field, and virtual displacements that are linear functions of the coordinates.

PLANE STRESS TRANSFORMATIONS

These transformations are needed in deriving membrane element stiffness and unassembled deformation matrices.

Rotation of the Rectangular Cartesian Reference Frame

In plane stress,

$$\tau_{zx} = \tau_{yz} = \sigma_z = \bar{\tau}_{zx} = \bar{\tau}_{yz} = \bar{\sigma}_z = \bar{\tau}_{zx} = \bar{\tau}_{yz} = \bar{\sigma}_z = 0 \quad (B.123)$$

Therefore, from Equation B.16,

$$\left. \begin{aligned} \sigma_x &= \bar{\sigma}_x \cos^2 \zeta + \bar{\sigma}_y \sin^2 \zeta + \bar{\tau}_{xy} \cdot 2 \sin \zeta \cos \zeta \\ \sigma_y &= \bar{\sigma}_x \sin^2 \zeta + \bar{\sigma}_y \cos^2 \zeta - \bar{\tau}_{xy} \cdot 2 \sin \zeta \cos \zeta \\ \tau_{xy} &= -\bar{\sigma}_x \sin \zeta \cos \zeta + \bar{\sigma}_y \sin \zeta \cos \zeta + \bar{\tau}_{xy} (\cos^2 \zeta - \sin^2 \zeta) \end{aligned} \right\} \quad (B.124)$$

Equations B.124 can be written

$$\underbrace{\begin{Bmatrix} \sigma_x \\ \sigma_y \\ \tau_{xy} \end{Bmatrix}}_{\sigma_p} = \underbrace{\begin{bmatrix} \cos^2 \zeta & \sin^2 \zeta & 2 \sin \zeta \cos \zeta \\ \sin^2 \zeta & \cos^2 \zeta & -2 \sin \zeta \cos \zeta \\ -\sin \zeta \cos \zeta & \sin \zeta \cos \zeta & \cos^2 \zeta - \sin^2 \zeta \end{bmatrix}}_{\sigma_{\bar{p}p}} \underbrace{\begin{Bmatrix} \bar{\sigma}_x \\ \bar{\sigma}_y \\ \bar{\tau}_{xy} \end{Bmatrix}}_{\bar{\sigma}_p} \quad (B.125)$$

The matrices in Equation B.125 are denoted according to the symbols written under the equation.

$$\sigma_p = \sigma_{\bar{\sigma}p} \bar{\sigma}_p \quad (B.126)$$

Equation B.126 is the stress transformation.

Similarly, from Equation B.53,

$$\begin{Bmatrix} \bar{\epsilon}_x \\ \bar{\epsilon}_y \\ \bar{\gamma}_{xy} \end{Bmatrix}_{\bar{\epsilon}_p} = \begin{bmatrix} \cos^2 \zeta & \sin^2 \zeta & -\sin \zeta \cos \zeta \\ \sin^2 \zeta & \cos^2 \zeta & \sin \zeta \cos \zeta \\ 2\sin \zeta \cos \zeta & -2\sin \zeta \cos \zeta & \cos^2 \zeta - \sin^2 \zeta \end{bmatrix} \begin{Bmatrix} \epsilon_x \\ \epsilon_y \\ \epsilon_{xy} \end{Bmatrix}_{\epsilon_p} \quad (B.127)$$

The matrices in Equation B.127 are denoted according to the symbols written under the equation.

$$\bar{\epsilon}_p = \bar{\epsilon}_{\epsilon p} \epsilon_p \quad (B.128)$$

Comparing Equations B.125 and B.127 shows that

$$\bar{\epsilon}_{\epsilon p} = \sigma_{\bar{\sigma}p}^T \quad (B.129)$$

Therefore, from Equations B.128 and B.129,

$$\bar{\epsilon}_p = \sigma_{\bar{\sigma}p}^T \epsilon_p \quad (B.130)$$

Equation B.130 is the strain transformation.

Rectangular to Oblique Coordinate Transformation

From Equation B.70.1,

$$\begin{Bmatrix} \bar{\sigma}_x \\ \bar{\sigma}_y \\ \bar{\tau}_{xy} \end{Bmatrix}_{\bar{\sigma}_p} = \begin{bmatrix} \frac{1}{\sin \theta} & \frac{\cos^2 \theta}{\sin \theta} & \frac{2\cos \theta}{\sin \theta} \\ 0 & \sin \theta & 0 \\ 0 & \cos \theta & 1 \end{bmatrix} \begin{Bmatrix} \sigma_x \\ \sigma_y \\ \tau_{xy} \end{Bmatrix}_{\sigma_p} \quad (B.131)$$

The matrices in Equation B.131 are denoted according to the symbols written under the equation.

$$\therefore \quad \bar{\sigma}_p = \bar{\sigma}_{\theta p} \bar{\sigma}_p \quad (B.132)$$

Equation B.132 is the stress transformation.

From Equation B.98,

$$\begin{Bmatrix} \bar{\epsilon}_x \\ \bar{\epsilon}_y \\ \bar{\gamma}_{xy} \end{Bmatrix}_{\bar{\epsilon}_p} = \begin{bmatrix} 1 & 0 & 0 \\ \cos^2 \theta & \sin^2 \theta & \sin \theta \cos \theta \\ 2 \cos \theta & 0 & \sin \theta \end{bmatrix} \begin{Bmatrix} \bar{\epsilon}_x \\ \bar{\epsilon}_y \\ \bar{\gamma}_{xy} \end{Bmatrix}_{\bar{\epsilon}_p} \quad (B.133)$$

The matrices in Equation B.133 are denoted according to the symbols written under the equation.

$$\therefore \quad \bar{\epsilon}_p = \bar{\epsilon}_{\theta p} \bar{\epsilon}_p \quad (B.134)$$

From Equations B.131 and B.133,

$$\bar{\epsilon}_{\theta p} = \bar{\sigma}_{\theta p}^T \sin \theta \quad (B.135)$$

Therefore, from Equations B.134 and B.135

$$\bar{\epsilon}_p = \bar{\sigma}_{\theta p}^T \bar{\epsilon}_p \sin \theta \quad (B.136)$$

Equation B.136 is the strain transformation.

Virtual Work on a Skewed Finite Element

From Equations B.120 and B.123,

$$W_p = \frac{V}{\sin \theta} (\bar{\sigma}_x \bar{\epsilon}_x + \bar{\sigma}_y \bar{\epsilon}_y + \bar{\tau}_{xy} \bar{\gamma}_{xy}) \quad (B.137)$$

Therefore, from Equation B.137 and the definitions of σ_p and ϵ_p given in Equations B.131 and B.133,

$$W_p = \frac{V}{\sin \theta} \sigma_p^T \epsilon_p \quad (B.138)$$

Equation B.138 gives the virtual work done on a skewed finite parallelepiped with sides parallel to the oblique coordinate planes, subjected to a constant plane stress field, and virtual displacements that are linear functions of the coordinates.

APPENDIX C
ELEMENTS AND NODAL FORCE TRANSFORMATIONS

LIST OF SYMBOLS FOR APPENDIX C

Symbols appearing in Appendix C not defined in this list are defined in the lists at the front of this report or at the beginning of Appendix B.

A	Membrane or cell subelement surface area
A_b	Bar cross-sectional area
a, b, c, d	Half-lengths of membrane edges, or of a surface of a cell
$\bar{a}, \bar{b}, \bar{c}, \bar{d}$	Unit vectors pointing from p to q, r to q, r to s and p to s. For bars and membranes
\bar{b}_3	A unit vector pointing from r_1 to r_0
C_C	Square matrix or scalar. Material damping compliance
c, d	Subscripts denoting average stresses and strains in upper and lower surfaces (true geometric boundaries) of cell
C_K	Square matrix or scalar. Material compliance
C_{Kc}, C_{Kd}	Square compliance matrices for upper and lower cell boundaries
d	Preceding a variable, indicates a differential
\bar{D}	Element flexibility matrix (square)
\bar{D}	Subelement flexibility matrix (square)
\bar{d}_2	A unit vector pointing from p_0 to p_1
\bar{e}	Column matrix of subelement deformations
\bar{e}	A vector normal to ps and pq
\bar{e}_0	A unit vector pointing from q_0 to q_1
$e_{T\Delta}^i$	Column matrix of unassembled thermal deformations resulting from a unit temperature change, for a bar

LIST OF SYMBOLS FOR APPENDIX C (Continued)

$\bar{e}_{\alpha T}$	Column matrix of unassembled lumped element thermal deformations, resulting from a unit temperature change in a subelement, and a unit coefficient of thermal expansion
$\tilde{e}_{\alpha T}$	Column matrix of unassembled subelement thermal deformations, resulting from a unit temperature change, and a unit coefficient of thermal expansion
\bar{F}	Column matrix of subelement force components
\hat{F}	Column matrix of equivalent lumped cell element forces in true geometric boundaries
F'	Column matrix of cell element forces in local degrees of freedom
$F_{F'}$	Square matrix. Transforms cell element forces in local degrees of freedom to element forces in global degrees of freedom
$F_{\bar{F}}$	Rectangular matrix. Transforms cell lumped element forces to element forces in global degrees of freedom
$\bar{F}_{\bar{F}}$	Rectangular matrix. Transforms \bar{F} to \bar{F} for a cell
$\hat{F}_{\bar{F}}$	Square matrix. Transforms cell lumped element forces to equivalent lumped element forces
$F' \hat{F}_{\bar{F}}$	Rectangular matrix. Transforms cell equivalent lumped element forces to element forces in local degrees of freedom
\bar{f}_0	A unit vector pointing from s_0 to s_1
f_1	1 if $p < q$, otherwise -1
f_2	1 if $r < q$, otherwise -1

LIST OF SYMBOLS FOR APPENDIX C (Continued)

f_3	1 if $r < s$, otherwise -1
f_4	1 if $p < s$, otherwise -1
i	(Subscript). Element number
J	Column matrix of plane unassembled strains resulting from a unit change of temperature and a unit coefficient of thermal expansion
j	(Subscript). Subelement number
K	Shear panel factor
l	Bar length
m_p	Mass of the point mass element
P	(Subscript). Denotes plane stress
\bar{ps}, \bar{pq}	Vectors equal in magnitude to edges ps and pq , pointing from p to s and p to q , for a membrane
p, q, r, s	Joint numbers
p, q, r, s	(Subscripts). Refer to joint numbers
S	Square matrix. Divided by t_m , it transforms \tilde{F} to $\tilde{\sigma}_p$ for membrane
T	Temperature
T	(Superscript). Denotes transposed matrix
\tilde{T}	Rectangular matrices that transform membrane element forces into subelement forces
t_m	Thickness of membrane element
$\bar{t}_p, \bar{t}_q, \bar{t}_r, \bar{t}_s$	Vectors from points p_0 to p_1 , q_0 to q_1 , r_0 to r_1 , s_0 to s_1 .

LIST OF SYMBOLS FOR APPENDIX C (Continued)

T_{Δ}	Difference between temperature and reference temperature
U	(Subscript). Denotes uniaxial stress
V	Element volume
W	Virtual work done on a cell subelement
W_p	Virtual work done on a membrane subelement
x, y, z	Reference coordinates for membrane or cell subelement
x, y, z	(Subscripts). Denote the components of a vector
$\bar{x}, \bar{y}, \bar{z}$	Rotated reference coordinates for membrane or cell subelement. The \bar{x} axis is parallel to one edge
$\bar{x}, \bar{y}, \bar{z}$	Oblique coordinates for membrane or cell subelement
x_a, y_a, z_a	Reference coordinates, upper surface of lumped cell
x_b, y_b, z_b	Reference coordinates, lower surface of lumped cell
Z	$\sigma_{\bar{\sigma}p} \bar{\sigma}_{\bar{\sigma}p}$
α	$(3 + \sqrt{3})/6$
α_T	Coefficient of thermal expansion
β	$(3 - \sqrt{3})/6$
β	(Subscript). Increment number
γ	$1/\sqrt{3}$
δT	Change in temperature developed during an increment
$\delta \epsilon_B$	Change in strain at center of a bar developed during an increment
$\delta \epsilon_{p,AV}$	Column matrix of changes in membrane average strains developed during an increment

LIST OF SYMBOLS FOR APPENDIX C (Continued)

$\delta\sigma_B$	Change in σ_B developed during an increment
$\delta\sigma_{p,AV}$	Change in $\delta\sigma_{p,AV}$ developed during an increment
$\delta\sigma_S$	Change in σ_S developed during an increment
ϵ_c, ϵ_d	Column matrices of average strains in upper and lower boundaries of cell
ϵ_0	Column matrix of unassembled thermal strains
ϵ_S	Column matrix of average strains in upper and lower boundaries of cell, combined
$\epsilon_{\sigma S}$	Square matrix. Combined compliance matrix for upper and lower cell boundaries
ζ	Angle between the \bar{x} and x axes for a membrane or cell element
θ	Angle between adjacent sides of a membrane, or a surface of a cell
ρ	Mass per unit volume
σ_a, σ_b	Column matrices of average stress components in the upper and lower surfaces of a lumped cell element, weighted according to subelement volumes
σ_B	Stress at center of bar element
σ_c, σ_d	Column matrices of average stresses in upper and lower boundaries of cell
$\sigma_{\bar{F}}$	Rectangular matrix. Transforms \bar{F} to σ for a cell
$\sigma_{\bar{F}}$	Square matrix. Transforms \bar{F} to σ for a cell
$\bar{\sigma}_{\bar{F}}$	Square matrix. Transforms \bar{F} to $\bar{\sigma}$ for a cell
$\sigma_{\bar{F}a}, \sigma_{\bar{F}b}$	Rectangular matrices that transform lumped cell element stiffness forces to average stress components in the upper and lower surfaces of the lumped cell.

LIST OF SYMBOLS FOR APPENDIX C (Continued)

$\sigma_{\bar{F}B}$	Row matrix of bar stresses resulting from unit element forces
$\sigma_{\bar{F},LPM}$	Rectangular matrix of average membrane stresses resulting from unit lumped element forces
σ_L	Column matrix of average stress components in the upper and lower surfaces of the lumped cell element, combined
$\sigma_{L\bar{F}}$	Rectangular matrix. Transforms lumped cell element forces into average stresses in the upper and lower surfaces of the lumped cell.
$\sigma_{p,AV}$	Column matrix of membrane average stresses
σ_S	Column matrix of average stresses in upper and lower boundaries of cell, combined
$\sigma_{S\sigma}$	Square matrix. Transforms stresses in lumped cell element boundaries to true geometric boundaries
0	(Subscript). Denotes upper surface of a cell
1	(Subscript). Denotes lower surface of a cell
6	(Subscript). Denotes upper surface of a lumped cell
7	(Subscript). Denotes upper surface of a lumped cell

This appendix presents stiffness matrices, unassembled deformation matrices, damping matrices, force transformation matrices, and mass matrices; for bar, membrane, cell and point mass elements. The nodal force transformation matrices P_{TF_i} and P_{UP_T} are also derived.

The time period considered in the analysis is the g th increment, although the subscript g is often omitted, to simplify notation. During this increment, element geometry and material properties are considered constant, in accordance with the approach of Section II.

AXIALLY LOADED BARS

Matrices for axially loaded bars are derived.

Lumped Stiffness and Unassembled Deformation Matrices

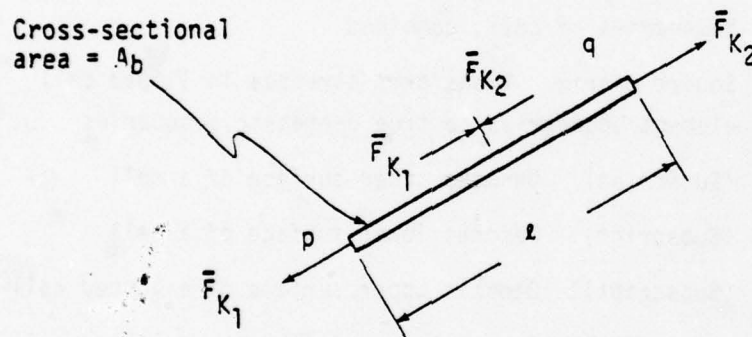


Figure C.1 Bar Nomenclature.

Figure C.1 shows the bar dimensions and notation for the lumped element stiffness forces.

Consider an infinitesimal period of time, dt , in the g th increment. During this time, the relation between bar deformations, bar forces, and bar unassembled deformations is

$$\begin{Bmatrix} d\bar{e}_1 \\ d\bar{e}_2 \end{Bmatrix} = \frac{2C_{KU}}{2A_b} \begin{Bmatrix} d\bar{F}_{K1} \\ d\bar{F}_{K2} \end{Bmatrix} + \begin{Bmatrix} d\bar{e}_{o1} \\ d\bar{e}_{o2} \end{Bmatrix} \quad (C.1)$$

where C_{KU} is the uniaxial material compliance for the bar. When the bar is elastic, C_{KU} is the reciprocal of Young's modulus. Otherwise, C_{KU} is given by the Prandtl-Reuss equations. See Appendix E.

The solution of Equation C.1 for the differential element forces can be put in the form

$$\begin{Bmatrix} d\bar{F}_{K1} \\ d\bar{F}_{K2} \end{Bmatrix} = \frac{2A_b}{2C_{KU}} \begin{bmatrix} 1 & 0 \\ 0 & 1 \end{bmatrix} \left(\begin{Bmatrix} d\bar{e}_1 \\ d\bar{e}_2 \end{Bmatrix} - \begin{Bmatrix} d\bar{e}_{o1} \\ d\bar{e}_{o2} \end{Bmatrix} \right) \quad (C.2)$$

Comparing Equation C.2 with Equation 15 shows that

$$K_{i(\beta)} = 2 \left(\frac{A_b}{2C_{KU}} \right)_{i\beta} \begin{bmatrix} 1 & 0 \\ 0 & 1 \end{bmatrix}, \quad (C.3)$$

where the subscript i indicates the i th element, and the subscript β indicates quantities that are applicable during the β th increment. Equation C.3 is applicable when the i th element is a bar.

During impact, temperature changes resulting from dissipated damping energy are calculated for each element, and for each increment. The incremental temperature change for an element is an average, considered constant over the volume of the element. The resulting incremental unassembled deformations for the i th element and the β th increment are given by

$$\begin{Bmatrix} \delta \bar{e}_{o_1} \\ \delta \bar{e}_{o_2} \end{Bmatrix}_{i\beta} = \delta T_{i,\beta-1} \begin{Bmatrix} \alpha_{T\frac{l}{2}} \\ \alpha_{T\frac{l}{2}} \end{Bmatrix}_{i\beta} \quad (C.4)$$

where

$\delta T_{i,\beta-1}$ = the change in temperature of the i th element developed during the β -1st increment.

$\alpha_{T_{i\beta}}$ = the coefficient of thermal expansion for the i th element, and the β th increment. The temperature change, $\delta T_{i,\beta-1}$, is employed in Equation C.4 because it is the latest temperature change available for use in the β th increment. Equation C.4 can be written

$$\delta \bar{e}_{o_{i\beta}}(t_\beta) = \delta T_{i,\beta-1} \bar{e}'_{T\Delta_i} \quad \beta=2,3 \dots \quad (C.5)$$

where $\delta \bar{e}_{o_{i\beta}}(t_\beta)$ is defined as in Equation 92,

$$\text{and } \bar{e}'_{T\Delta_i} = \begin{Bmatrix} \alpha_{T\frac{l}{2}} \\ \alpha_{T\frac{l}{2}} \end{Bmatrix}_i, \quad (C.6)$$

Equation C.6 is applicable when the i th element is a bar, for all increments subsequent to the first.

At time $t=0$, thermal gradients can exist in the structure. Unassembled deformations resulting from these gradients are computed in a slightly different manner. Joint temperatures, instead of average element temperatures are defined, and temperatures are assumed to vary linearly between joints. Therefore the incremental unassembled deformations applicable to the i th element, and the first increment, based on temperatures at the bar quarter points, are given by

$$\begin{Bmatrix} \delta \bar{\epsilon}_{o_1} \\ \delta \bar{\epsilon}_{o_2} \end{Bmatrix}_{i,1} = \alpha_{T_i} \frac{z_i}{2} \begin{Bmatrix} \frac{3}{4} T_{\Delta p} + \frac{1}{4} T_{\Delta q} \\ \frac{1}{4} T_{\Delta p} + \frac{3}{4} T_{\Delta q} \end{Bmatrix}_i \quad (C.7)$$

where

$T_{\Delta p_i}, T_{\Delta q_i}$ = the differences between the temperatures at the p and q joints of the ith bar, and the reference temperature, at time $t=0$.

Equation C.7 applies when the ith element is a bar.

The method of calculating the bar unassembled thermal deformations for the first increment is unfortunately not consistent with the methods of computing these deformations for the membrane and the cell. To make the bar consistent with the cell and membrane, the temperatures should be assumed uniform in each half of the bar, and equal to the temperatures at the adjacent joints.

Stress and Strain

These quantities are computed at the centers of bars.

Stresses for bar-panel models of the type being considered are usually calculated according to two rules, which have been established on the basis of experience gained by comparing calculated results with test data. The rules are:

1. Axial stresses at the ends of bars are considered correct.
2. Shear stresses at the centers of panels are considered correct.

The stresses for the pinched cylinder described in Section III were calculated according to these rules. Reference 12 contains other comparisons with test data where the rules served as the basis for computing stresses.

The stresses at the ends of the bar are calculated according to the rule for axial stress. The stress at the center is then computed, assuming that the stress variation along the length of the bar is linear. Therefore the stress at the center of the bar is given by

$$\sigma_B = \frac{1}{2} \left[\frac{1}{A_b} \mid \frac{1}{A_b} \right] \begin{Bmatrix} \bar{F}_{K_1} \\ \bar{F}_{K_2} \end{Bmatrix} \quad (C.8)$$

For the i th element, at the end of the s th time increment, this equation can be written in the form

$$\sigma_{B_i}(t_s) = \sigma_{FB_{iB}} \bar{F}_{K_i}(t_s) \quad (C.9)$$

where

$$\sigma_{FB_{iB}} = \left[\frac{1}{2A_b} \mid \frac{1}{2A_b} \right]_{iB} \quad (C.10)$$

Equation C.10 applies when the i th element is a bar.

Equation C.9 gives stresses resulting from stiffness forces. Stresses resulting from damping forces are not calculated.

The incremental axial strain at the center of the bar is given by

$$\delta \epsilon_{B_{iB}}(t_s) = C_{KU_{iB}} \delta \sigma_{B_{iB}}(t_s) \quad (C.11)$$

$$\text{where } \delta \sigma_{B_{iB}}(t_s) = \sigma_{B_i}(t_s) - \sigma_{B_i}(t_{s-1}) \quad (C.11.1)$$

Equation C.11 gives strains resulting from stresses. Thermal strains are not included

Damping Matrix

This matrix is obtained by replacing the stiffness compliance, C_{KU} , by the damping compliance, C_{CU} , in Equation C.3:

$$\bar{c}_{i(s)} = 2 \left(\frac{A_b}{i C_{CU}} \right)_{is} \begin{bmatrix} 1 & 0 \\ 0 & 1 \end{bmatrix} \quad (C.12)$$

The damping compliance is found by multiplying the elastic stiffness compliance, equal to the reciprocal of Young's modulus, by an experimentally determined constant.

Equation C.12 applies when the i th element is a bar.

Force Transformation Matrix

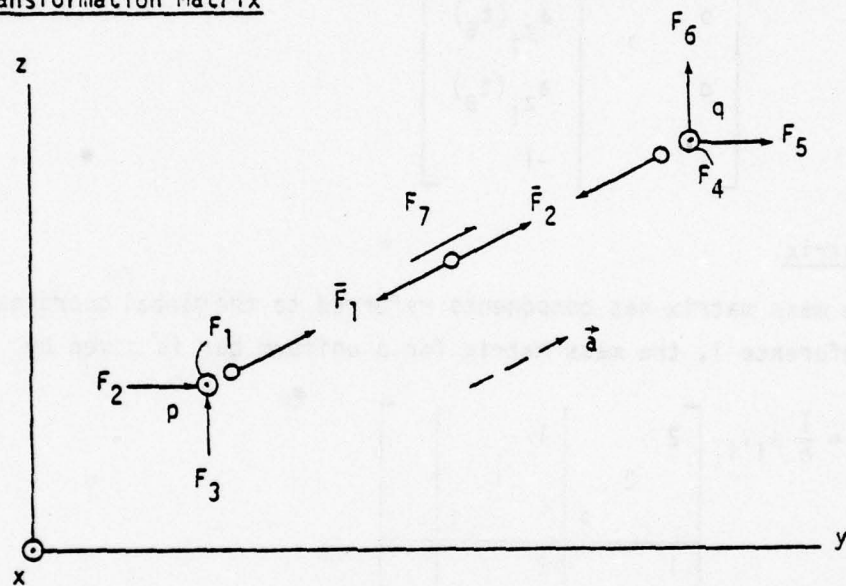


Figure C.2 Equilibrium of the Lumped Forces and the Element Forces

Figure C.2 shows the lumped element forces reversed, and the element forces, acting upon the bar nodes. Let \vec{a} = a unit vector parallel to the bar, pointing from p to q.

a_x, a_y, a_z = the components of \vec{a} .
The figure shows \vec{a} .

The force transformation matrix, F_{F_i} is a matrix of F forces resulting

from unit values of the \bar{F}_i forces. From the figure, this matrix is given, for the i th element and the s th increment, by

$$F_{\bar{F}_i}(t_s) = \begin{bmatrix} -a_{x_i}(t_s) & 0 \\ -a_{y_i}(t_s) & 0 \\ -a_{z_i}(t_s) & 0 \\ 0 & a_{x_i}(t_s) \\ 0 & a_{y_i}(t_s) \\ 0 & a_{z_i}(t_s) \\ 1 & -1 \end{bmatrix} \quad (C.13)$$

Mass Matrix

The mass matrix has components referred to the global coordinates. From Reference 1, the mass matrix for a uniform bar is given by

$$M_i = \frac{1}{6} \rho_i V_i \begin{bmatrix} 2 & 1 & \\ & 2 & 1 \\ & & 2 \\ 1 & 2 & \\ & 1 & 2 \\ & & 2 \end{bmatrix} \quad (C.14)$$

where

ρ_i = the density (mass per unit volume) of the i th element

V_i = the volume of the i th element

Components of inertia force in the shear node degrees of freedom are not considered.

Equation C.14 applies when the i th element is a bar.

LUMPED PARAMETER MEMBRANES

Stiffness, unassembled deformation, damping and mass matrices are presented for the membrane. A transformation matrix relating lumped element forces to element forces is derived.

Element Geometry

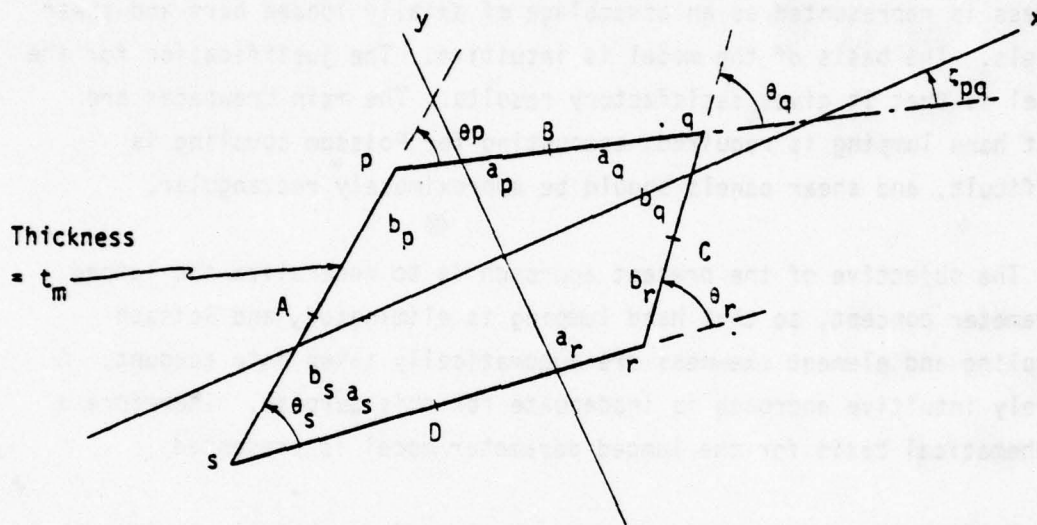


Figure C.3 Membrane Dimensions.

Figure C.3 shows dimensions of the element. The element is approximately flat, and has approximately the shape of a parallelogram. Points A , B , C and D are mid points of the membrane edges. The dimensions and angles shown are calculated from the coordinates of the corners.

A local rectangular Cartesian reference frame is established as indicated. The position of the origin is not defined, because the only

purpose of the frame is to provide reference directions for components of stress and strain.

All symbols in Figure C.3 should have subscript "i"s, to indicate element number, but these subscripts are deleted, to simplify the notation.

Basis of the Lumped Parameter Membrane Element

In the original lumped parameter model, a plate subjected to plane stress is represented as an assemblage of axially loaded bars and shear panels. The basis of the model is intuitive. The justification for the model is that it gives satisfactory results. The main drawbacks are that hand lumping is required, accounting for Poisson coupling is difficult, and shear panels should be approximately rectangular.

The objective of the present approach is to generalize the lumped parameter concept, so that hand lumping is eliminated, and Poisson coupling and element skewness are automatically taken into account. A purely intuitive approach is inadequate for this purpose. Therefore a mathematical basis for the lumped parameter model is presented.

The approach is based on an assumed piecewise constant stress distribution in the element, and the principle of virtual work.



Figure C.4 Parallelogram Element.

Figure C.4 shows a parallelogram element subjected to plane stress. The element is divided into four equal subelements. Each subelement is assumed to be subjected to a constant stress field. Each subelement stress field has three parameters, therefore the number of element stress parameters is 12. A subsequent assumption specifies that all of the shear stresses, referred to oblique coordinates parallel to the sides of the elements, are equal. This assumption reduces the number of independent element stress parameters to nine, which is equal to the number of self-equilibrating element forces. Equilibrium and compatibility are satisfied within subelements, but not on subelement boundaries, except on the average.

Strain components in each subelement are calculated in terms of the stress components, the material compliance matrix, and unassembled strains.

Figure C.5(a) illustrates the next step in the development of the element. Transformations are calculated relating the stress components in each subelement to self-equilibrating force components acting on subelement boundaries. These force components are transformed into the self-equilibrating forces shown in Figure C.5(b), on the basis of virtual work. The latter components are the lumped element forces defined in Figure 2.4

The final step is to consider the subelements replaced by the shear panel and bars shown in Figure C.5(c). This step involves no mathematical manipulation; it simply provides a different way of visualizing the element, that will be familiar to many users, and that seems to be well adapted to geometrically nonlinear analysis.

When the element is subjected to element forces equivalent to a constant stress field, the resulting displacements are exact, showing that the formulation correctly accounts for Poisson coupling, and skewness.

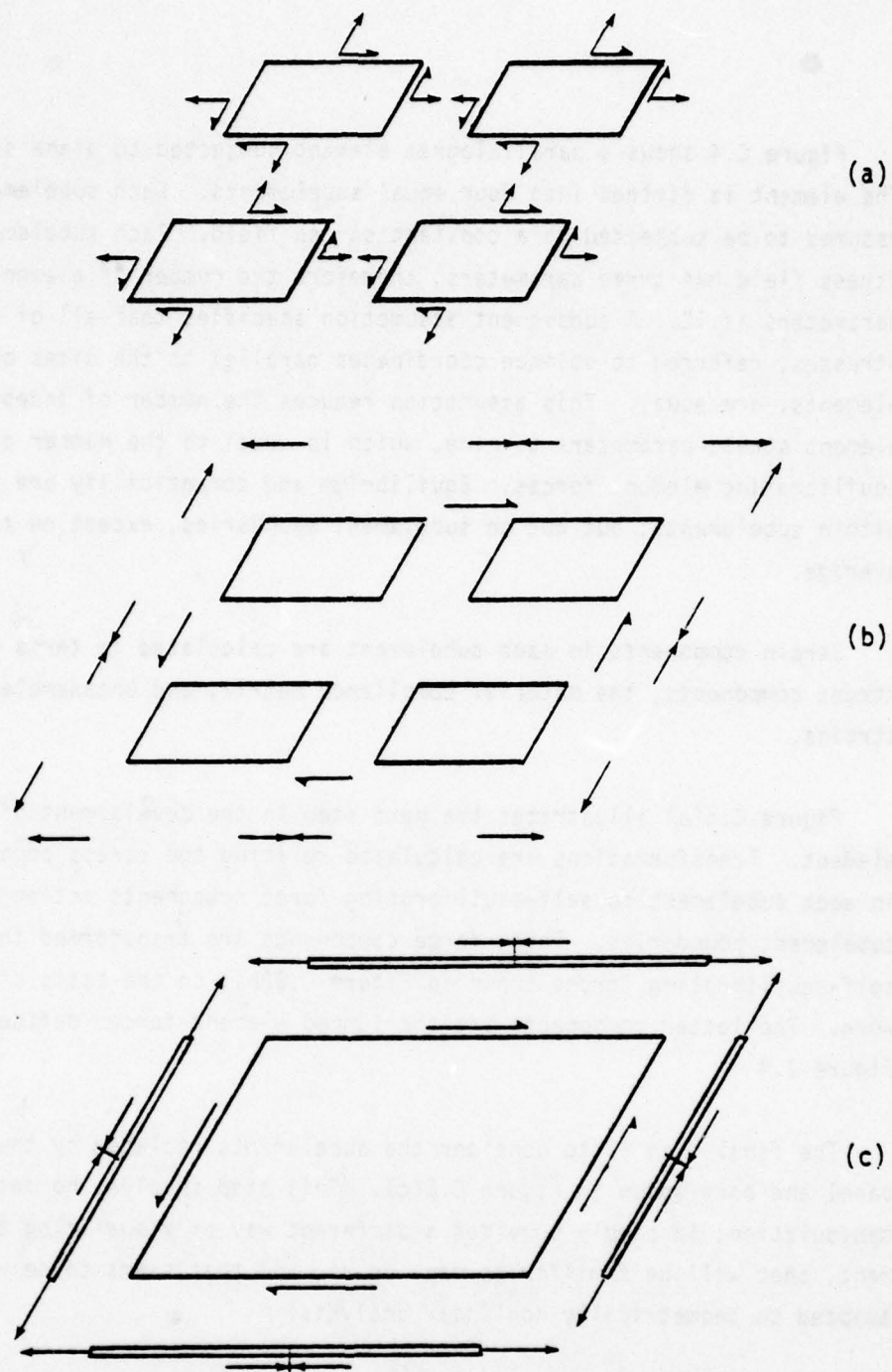


Figure C.5 Development of the Lumped Parameter Membrane.

When a rectangular element is considered, and Poisson's ratio is set equal to zero, the element has the same properties as the equivalent conventional bar-panel model.

Subelements

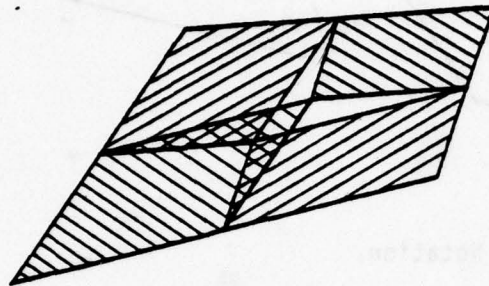


Figure C.6 Subelements of the Approximate Parallelogram.

The approximate parallelogram element, or quadrilateral, is broken into parallelogram subelements, as shown in Figure C.6. These subelements do not quite fit, as the figure shows, although areas where subelements overlap are equal to areas where gaps exist, so that the total area is accounted for. This lack of fit is the reason for recommending that membrane elements should not be allowed to depart too far from parallelograms, in the applications.

Figure C.6.1 shows subelement notation. The subelements are numbered p, q, r, s , to correspond with element corners.

Figure C.7 shows the j th subelement, where the index j can have the values p, q, r and s . In other words, the figure shows any one of the subelements. The figure also shows two reference frames. The $x_j y_j$ reference frame is parallel to the xy reference frame of Figure C.3.

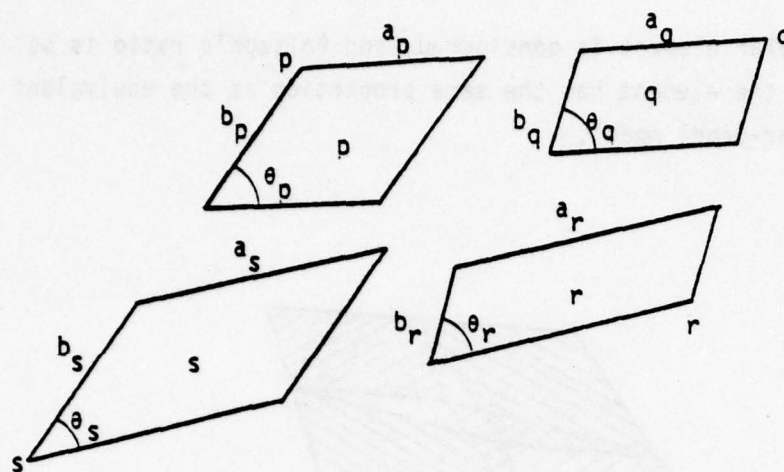


Figure C.6.1 Subelement Notation.

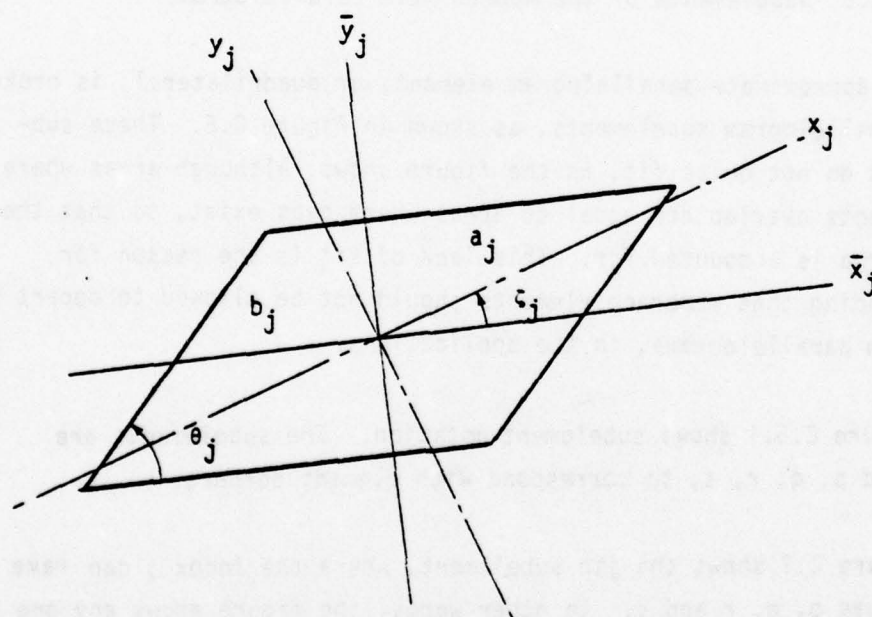


Figure C.7 The j th Subelement.

The $\bar{x}_j\bar{y}_j$ frame is also a rectangular cartesian frame. The \bar{x}_j axis is parallel to edge pq when $j = p$ or q . (See Figure C.3.) When $j = r$ or s , the \bar{x}_j axis is parallel to rs. It can be shown that

$$\zeta_j = \zeta_{pq} \quad \text{if } j = p \text{ or } q \quad (\text{C.14.1})$$

$$\zeta_j = \zeta_{pq} - \theta_p + \theta_s \quad \text{if } j = r \text{ or } s \quad (\text{C.14.2})$$

Lumped Stiffness and Unassembled Deformation Matrices

Let

$\epsilon_{x_j}, \epsilon_{y_j}, \gamma_{xy_j}$ = strain components referred to the x_jy_j axes

$\sigma_{x_j}, \sigma_{y_j}, \tau_{xy_j}$ = stress components referred to the x_jy_j axes.

$$\text{Let } \epsilon_{p_j} = \left\{ \epsilon_{x_j} \mid \epsilon_{y_j} \mid \gamma_{xy_j} \right\} \quad (\text{column}) \quad (\text{C.15})$$

$$\sigma_{p_j} = \left\{ \sigma_{x_j} \mid \sigma_{y_j} \mid \tau_{xy_j} \right\} \quad (\text{column}) \quad (\text{C.16})$$

Small increments of the stiffness stress components are proportional to incremental strains. Damping stress components proportional to rates of change of strain also exist, but are not computed. No notation is established for damping stresses.

Consider an infinitesimal period of time dt , in the s th increment. During this time, the relation between strains, stresses, and unassembled thermal strains in the j th subelement is given, in differential form, by

$$d\epsilon_{p_j} = C_{kp} d\sigma_{p_j} + d\epsilon_{0p_j}, \quad (\text{C.17})$$

where

C_{kp} = a square plane stress compliance matrix for the membrane material.

ϵ_{0p_j} = a column matrix of unassembled thermal strains in the j th subelement.

See Appendix E for C_{kp} . This matrix is the same for all four subelements.

The temperature distribution in each subelement is assumed to be uniform over the volume of the subelement. When such a distribution changes slightly with time, while remaining uniform, it produces equal unassembled tensile strains and no shear strain. Therefore the matrix of unassembled thermal strains is given, in differential form, by

$$d\epsilon_{0p_j} = \alpha_T dT_j \begin{Bmatrix} 1 \\ 1 \\ 0 \end{Bmatrix}, \quad (C.18)$$

where

dT_j = the differential temperature change in the j th subelement.

The stresses and strains are now referred to the \bar{x}_j, \bar{y}_j reference frame shown in Figure C.7. The required transformations are given, in Appendix B, by Equations B.126 and B.130. In differential form, these equations are

$$d\sigma_{p_j} = \sigma_{\bar{\sigma}p_j} d\bar{\sigma}_{p_j} \quad (C.19)$$

$$d\bar{\epsilon}_{p_j} = \sigma_{\bar{\sigma}p_j}^T d\epsilon_{p_j} \quad (C.20)$$

where

$$\bar{\sigma}_{p_j} = \left\{ \bar{\sigma}_x \mid \bar{\sigma}_y \mid \bar{\tau}_{xy} \right\}_j \quad (\text{Column}) \quad (C.20.1)$$

$$\epsilon_{p_j} = \left\{ \bar{\epsilon}_x \mid \bar{\epsilon}_y \mid \bar{\epsilon}_{xy} \right\}_j \quad (\text{Column}) \quad (C.20.2)$$

The transformation matrix $\sigma_{\bar{\sigma}p_j}$ is defined in Equation B.125, with the

understanding that subscript j 's are attached to the ϵ symbols. In differentiating Equation B.126, the matrix $\sigma_{\bar{\alpha}p_j}$ need not be differentiated, since geometry is considered constant in the p th increment.

Substituting $d\sigma_{p_j}$ from Equation C.19 into Equation C.17, multiplying on the left by $\sigma_{\bar{\alpha}p_j}^T$, and employing Equation C.20, gives

$$d\bar{\epsilon}_{p_j} = \sigma_{\bar{\alpha}p_j}^T C_{Kp} \sigma_{\bar{\alpha}p_j} d\bar{\sigma}_{p_j} + \sigma_{\bar{\alpha}p_j}^T d\epsilon_{op_j} \quad (C.21)$$

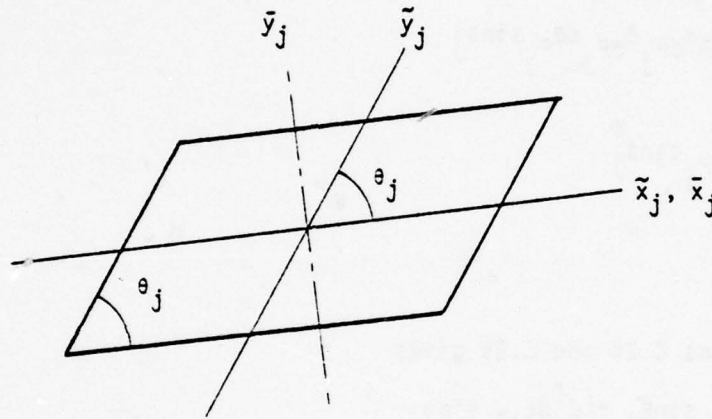


Figure C.8 Oblique Coordinates for the p th Subelement.

The stresses and strains are now referred to the \tilde{x}_j, \tilde{y}_j reference frame shown in Figure C.8. From Equations B.132 and B.136, the required differential stress and strain transformations are

$$d\bar{\sigma}_{p_j} = \bar{\sigma}_{\bar{\alpha}p_j} d\bar{\sigma}_{p_j} \quad (C.22)$$

$$\text{and } d\bar{\epsilon}_{p_j} = \bar{\sigma}_{\bar{\alpha}p_j}^T d\bar{\epsilon}_{p_j} \sin \theta_j \quad (C.23)$$

where

$$\bar{a}_{p_j} = \left\{ \bar{a}_x \mid \bar{a}_y \mid \bar{a}_{xy} \right\}_j \quad (\text{Column}) \quad (C.23.1)$$

$$\bar{e}_{p_j} = \left\{ \bar{e}_x \mid \bar{e}_y \mid \bar{e}_{xy} \right\}_j \quad (\text{Column}) \quad (C.23.2)$$

The transformation matrix $\bar{\sigma}_{ap_j}$ is defined in Equation B.13.1.

Substituting $d\bar{a}_{p_j}$ from Equation C.22 into Equation C.21, multiplying on the left by $\bar{\sigma}_{ap_j}^T \sin \theta_j$, and employing Equation C.23, gives

$$\begin{aligned} d\bar{e}_{p_j} &= \bar{\sigma}_{ap_j}^T \sigma_{ap_j}^T C_{KP} \sigma_{ap_j} \bar{\sigma}_{ap_j} d\bar{a}_{p_j} \sin \theta_j \\ &+ \bar{\sigma}_{ap_j}^T \sigma_{ap_j}^T d\epsilon_{op_j} \sin \theta_j \end{aligned} \quad (C.24)$$

$$\text{Let } Z_j = \sigma_{ap_j} \bar{\sigma}_{ap_j} \quad (C.25)$$

Combining Equations C.24 and C.25 gives

$$d\bar{e}_{p_j} = Z_j^T C_{KP} Z_j d\bar{a}_{p_j} \sin \theta_j + Z_j^T d\epsilon_{op_j} \sin \theta_j \quad (C.26)$$

From Equation C.25, and the values of σ_{ap} and $\bar{\sigma}_{ap}$ given in Equations B.125 and B.131, the matrix Z_j is evaluated as:

$$Z_j = \frac{1}{\sin \theta_j} \begin{bmatrix} \cos^2 \zeta & \cos^2(\theta - \zeta) & 2\cos(\theta - \zeta)\cos \zeta \\ \sin^2 \zeta & \sin^2(\theta - \zeta) & -2\sin(\theta - \zeta)\sin \zeta \\ -\sin \zeta \cos \zeta & \sin(\theta - \zeta)\cos(\theta - \zeta) & \sin(\theta - \zeta)\cos \zeta - \cos(\theta - \zeta)\sin \zeta \end{bmatrix}_j \quad \dots (C.27)$$

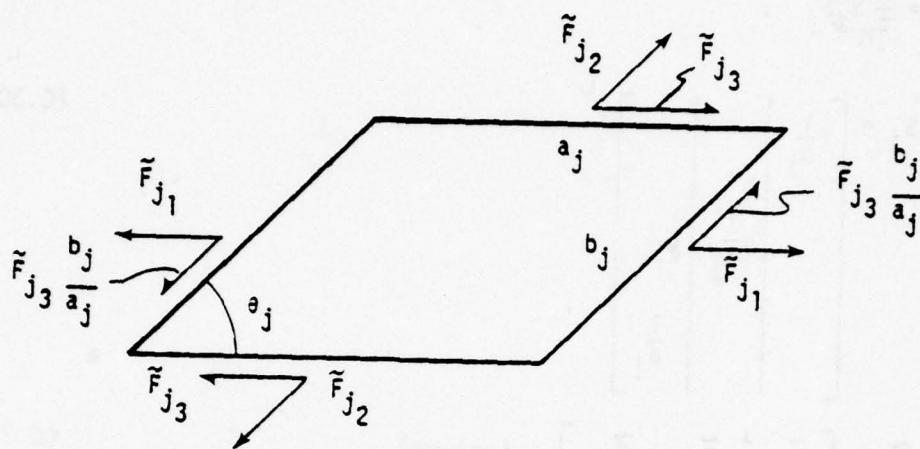


Figure C.9 Oblique Element Forces on the pth Subelement.

The oblique stress components are transformed into the self-equilibrating element stiffness forces shown in Figure C.9. Three self-equilibrating forces are defined. Element deformations corresponding to these forces in the sense of Appendix A are also defined, and designated \tilde{e}_{j1} , \tilde{e}_{j2} and \tilde{e}_{j3} .

The oblique stress components are uniform over the volume of the element. Therefore these components are related to the \tilde{F} forces according to the equation

$$\begin{Bmatrix} \sigma_{xj} \\ \sigma_{yj} \\ \tau_{xyj} \end{Bmatrix} = \frac{1}{t_M} \begin{bmatrix} \frac{1}{b_j} \\ \frac{1}{a_j} \\ \frac{1}{a_j} \end{bmatrix} \begin{Bmatrix} \tilde{F}_{j1} \\ \tilde{F}_{j2} \\ \tilde{F}_{j3} \end{Bmatrix} \quad (C.23)$$

Equation C.28 can be written

$$\delta p_j = \frac{1}{t_M} S_j \tilde{F}_j, \quad (C.29)$$

$$\text{where } S_j = \begin{bmatrix} \frac{1}{b_j} & & \\ & \frac{1}{a_j} & \\ & & \frac{1}{a_j} \end{bmatrix}, \quad (C.30)$$

$$\tilde{F}_j = \left\{ \tilde{F}_{j1} \mid \tilde{F}_{j2} \mid \tilde{F}_{j3} \right\} \text{ (column)}. \quad (C.31)$$

Equation C.29 is the force transformation. The displacement transformation is found by virtual work. Consider the j th subelement subjected to the uniform oblique stress field. Produce virtual displacements that are linear functions of the coordinates. The virtual work done by the stresses acting on the edges is given, according to Equation 8.138, by

$$w_{p_j} = \frac{A_j \tau_M}{\sin \theta_j} \delta p_j^T z_{p_j}, \quad (C.32)$$

where A_j is the surface area of the j th subelement.

Now consider the subelement acted upon by \tilde{F} forces that are statically equivalent to the oblique stresses, and produce the same virtual displacements considered in the preceding paragraph. The virtual work must be the same as before, since the displacements are the same, and the forces are statically equivalent. Therefore, from Appendix A,

$$w_{p_j} = \tilde{F}_j^T \tilde{e}_j, \quad (C.33)$$

$$\text{where } \tilde{e}_j = \left\{ \tilde{e}_{j_1} \mid \tilde{e}_{j_2} \mid \tilde{e}_{j_3} \right\} \quad (\text{column}). \quad (C.34)$$

From Equations C.32 and C.33,

$$\tilde{F}_j^T \tilde{e}_j = \frac{A_j t_M}{\sin \theta_j} \partial_{p_j}^T \tilde{e}_{p_j} \quad (C.35)$$

Substituting ∂_{p_j} from Equation C.29 into Equation C.35 gives

$$\tilde{F}_j^T \tilde{e}_j = \frac{A_j}{\sin \theta_j} \tilde{F}_j^T S_j^T \tilde{e}_{p_j} \quad (C.36)$$

Equation C.36 holds for any value of \tilde{F}_j .

$$\therefore \tilde{e}_j = \frac{A_j}{\sin \theta_j} S_j^T \tilde{e}_{p_j} \quad (C.37)$$

Equation C.37 is the displacement transformation. Equations C.29 and C.37 can be written in differential form, corresponding to the differential time dt , as

$$d\partial_{p_j} = \frac{1}{t_M} S_j d\tilde{F}_j \quad (C.38)$$

$$d\tilde{e}_j = \frac{A_j}{\sin \theta_j} S_j^T d\tilde{e}_{p_j} \quad (C.39)$$

Substituting $d\partial_{p_j}$ from Equation C.38 into Equation C.26, multiplying

on the left by $\frac{A_j}{\sin \theta_j} S_j^T$, and employing Equation C.39 gives

$$d\tilde{e}_j = \frac{A_j}{t_M} S_j^T Z_j^T C_{KP} Z_j S_j d\tilde{F}_j + A_j S_j^T Z_j^T d\epsilon_{op_j} \quad (C.40)$$

$$\text{Let } \tilde{D}_j = \frac{A_j}{t_M} S_j^T Z_j^T C_{KP} Z_j S_j \quad (C.41)$$

$$d\tilde{e}_{o_j} = A_j S_j^T Z_j^T d\epsilon_{op_j} \quad (C.42)$$

$$\therefore d\tilde{e}_j = \tilde{D}_j d\tilde{F}_j + d\tilde{e}_{o_j} \quad (C.42.1)$$

Equation C.42.1 gives the deformations of the j th subelement in terms of the subelement forces and the subelement unassembled deformations.

The subelement forces are now transformed into lumped element forces. The subelement stiffness forces are shown in Figure C.10(a). Figure C.10(b) shows the lumped element stiffness forces, as originally defined in Figure 2.4. Both sets of forces are self-equilibrating. The subelements are parallelograms, but they are not necessarily all the same shape. The shear panel in Figure C.10(b) is not necessarily a parallelogram. The figure shows the six self-equilibrating components of the shear panel force \bar{F}_{K_1} .

The factors K_1, K_2, \dots, K_5 are calculated from equilibrium and panel geometry.

Assume that the subelement forces can be expressed in terms of the lumped element forces as follows:

$$\tilde{F}_{p_1} = \bar{F}_{K_3} \quad (C.43)$$

$$\tilde{F}_{p_2} = \bar{F}_{K_8} \quad (C.44)$$

$$\tilde{F}_{p_3} = \bar{F}_{K_1}/2 \quad (C.45)$$

$$\tilde{F}_{q_1} = \bar{F}_{K_2} \quad (C.46)$$

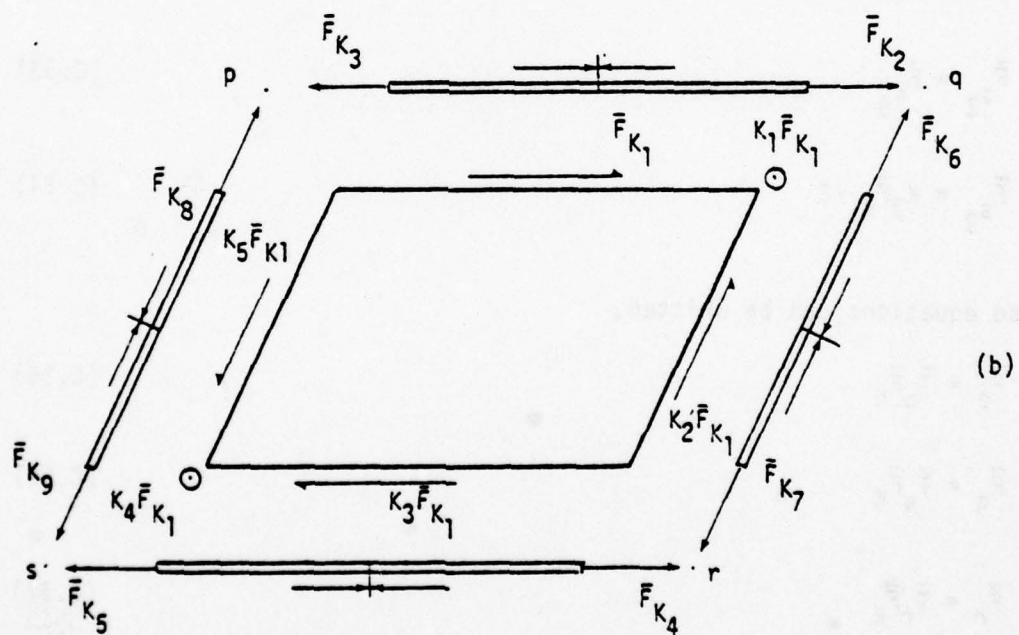
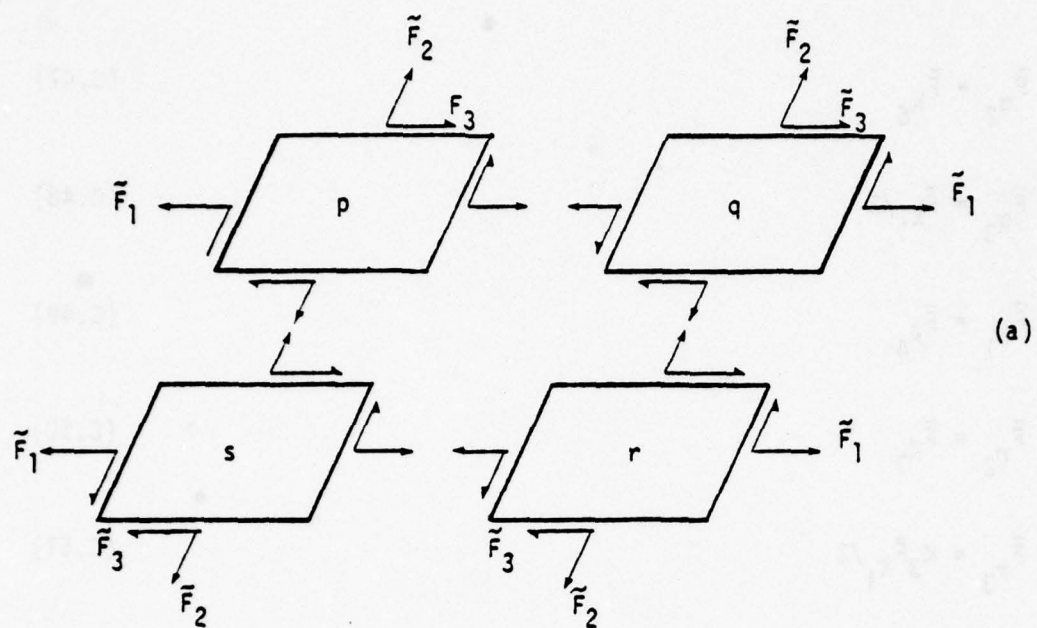


Figure C.10 Subelement Forces and Lumped Element Forces.

$$\bar{F}_{q_2} = \bar{F}_{K_6} \quad (C.47)$$

$$\bar{F}_{q_3} = \bar{F}_{K_1}/2 \quad (C.48)$$

$$\bar{F}_{r_1} = \bar{F}_{K_4} \quad (C.49)$$

$$\bar{F}_{r_2} = \bar{F}_{K_7} \quad (C.50)$$

$$\bar{F}_{r_3} = K_3 \bar{F}_{K_1}/2 \quad (C.51)$$

$$\bar{F}_{s_1} = \bar{F}_{K_5} \quad (C.52)$$

$$\bar{F}_{s_2} = \bar{F}_{K_9} \quad (C.53)$$

$$\bar{F}_{s_3} = K_3 \bar{F}_{K_1}/2 \quad (C.54)$$

These equations can be written,

$$\bar{F}_p = \bar{T}_p \bar{F}_K \quad (C.55)$$

$$\bar{F}_q = \bar{T}_q \bar{F}_K \quad (C.56)$$

$$\bar{F}_r = \bar{T}_r \bar{F}_K \quad (C.57)$$

$$\bar{F}_s = \bar{T}_s \bar{F}_K \quad (C.58)$$

where

$$\tilde{F}_j = \left\{ \tilde{F}_{j_1} \mid \tilde{F}_{j_2} \mid \tilde{F}_{j_3} \right\} \quad (\text{Column}) \quad j = p, q, r, s. \quad (C.59)$$

$$\tilde{F}_K = \left\{ \tilde{F}_{K_1} \mid \tilde{F}_{K_2} \mid \dots \mid \tilde{F}_{K_9} \right\} \quad (\text{Column}) \quad (C.60)$$

$$\text{and } \tilde{T}_p = \begin{bmatrix} & & 1 & & & & & & \\ & & & & & & & 1 & \\ & & & & & & & & \\ \frac{1}{2} & & & & & & & & \end{bmatrix} \quad (C.61)$$

$$\tilde{T}_q = \begin{bmatrix} & 1 & & & & & & & \\ & & & & & & & 1 & \\ & & & & & & & & \\ \frac{1}{2} & & & & & & & & \end{bmatrix} \quad (C.62)$$

$$\tilde{T}_r = \begin{bmatrix} & & 1 & & & & & & \\ & & & & & & & 1 & \\ & & & & & & & & \\ \frac{K_3}{2} & & & & & & & & \end{bmatrix} \quad (C.63)$$

$$\tilde{T}_s = \begin{bmatrix} & & & 1 & & & & & \\ & & & & & & & 1 & \\ & & & & & & & & \\ \frac{K_3}{2} & & & & & & & & \end{bmatrix} \quad (C.64)$$

Equations C.55, C.56, C.57 and C.58 can be written

$$\tilde{F}_{ji} = \tilde{T}_{ji} \bar{F}_{K_i} \quad j = p, q, r, s, \quad (C.65)$$

where the subscript i , indicating element number, has been restored.

Equation C.65 is the force transformation. The justification for this transformation is that it is consistent with the conventional bar-panel model.

The transformation implies the existence of a linkage joining the \tilde{F} and the \bar{F}_K forces. Consider this linkage acted upon by the \bar{F}_K forces, and the \tilde{F} forces reversed. Produce a virtual displacement. Assume that the linkage is such that when the virtual displacement is produced, no work is done. Therefore

$$\bar{F}_{K_i}^T \tilde{e}_i - \sum_j \tilde{F}_{ji}^T \tilde{e}_{ji} = 0 \quad j = p, q, r, s. \quad (C.66)$$

Combining Equations C.65 and C.66, and rearranging terms gives

$$\bar{F}_{K_i}^T \tilde{e}_i = \bar{F}_{K_i}^T \sum_j \tilde{T}_{ji}^T \tilde{e}_{ji} \quad (C.67)$$

This equation holds for any choice of \bar{F}_{K_i} . Therefore

$$\tilde{e}_i = \sum_j \tilde{T}_{ji}^T \tilde{e}_{ji} \quad j = p, q, r, s. \quad (C.68)$$

Equation C.68 is the displacement transformation.

Equations C.65 and C.68 can be written in differential form as

$$d\tilde{F}_{ji} = \tilde{T}_{ji} d\bar{F}_{K_i} \quad j = p, q, r, s. \quad (C.68.1)$$

$$d\bar{e}_i = \sum_j \tilde{T}_{ji}^T d\tilde{e}_{ji} \quad (C.68.2)$$

Restoring the subscript i , for element number, in Equation C.42.1 gives, for the deformations of the j th subelement,

$$d\tilde{e}_{ji} = \tilde{D}_{ji} d\tilde{F}_{ji} + d\tilde{e}_{o_{ji}} \quad (C.69)$$

Substituting $d\tilde{F}_{ji}$ from Equation C.68.1 into Equation C.69, multiplying on the left by \tilde{T}_{ji}^T , summing on j , and employing Equation C.68.2, gives

$$d\bar{e}_i = \sum_j \tilde{T}_{ji}^T \tilde{D}_{ji} \tilde{T}_{ji} d\bar{F}_{K_i} + \sum_j \tilde{T}_{ji}^T d\tilde{e}_{o_{ji}} \quad (C.70)$$

$$\text{Let } \bar{D}_i = \sum_j \tilde{T}_{ji}^T \tilde{D}_{ji} \tilde{T}_{ji} \quad (C.71)$$

$$d\bar{e}_{o_i} = \sum_j \tilde{T}_{ji}^T d\tilde{e}_{o_{ji}} \quad (C.72)$$

combining Equations C.70, C.71 and C.72 gives

$$d\bar{e}_i = \bar{D}_i d\bar{F}_{K_i} + d\bar{e}_{o_i} \quad (C.73)$$

Solving Equation C.73 for $d\bar{F}_{K_i}$ gives

$$d\bar{F}_{K_i} = \bar{D}_i^{-1} (d\bar{e}_i - d\bar{e}_{o_i}) \quad (C.74)$$

Comparing Equations C.15 and C.74 shows that

$$\bar{k}_i = \bar{D}_i^{-1} \quad (C.75)$$

Restoring the subscript i in Equation C.41, and combining Equations C.41, C.71 and C.75 gives

$$\bar{k}_i = \left(\sum_j \tilde{T}_{ji}^T \frac{A_j}{t_M} S_j^T Z_j^T C_{KP} Z_j S_j \tilde{T}_{ji} \right)^{-1} \quad (C.76)$$

$$\therefore \bar{k}_{i(\beta)} = \left[\frac{1}{t_M} \sum_j A_j (Z_j S_j \tilde{T}_{ji})^T C_{KP} (Z_j S_j \tilde{T}_{ji}) \right]_{i\beta}^{-1} \quad (C.77)$$

Equation C.77 gives the membrane element lumped stiffness matrix, applicable during the β th increment.

Restoring the subscript i in Equation C.42, and combining Equations C.42 and C.72 gives

$$d\bar{e}_{oi} = \sum_j \tilde{T}_{ji}^T A_{ji} S_{ji}^T Z_{ji}^T d\epsilon_{opji} \quad (C.78)$$

Equation C.18 can be written

$$d\epsilon_{opji} = \alpha_{Ti} dT_{ji} J_P \quad (C.80)$$

for the i th element, where

$$J_P = \left\{ 1 \mid 1 \mid 0 \right\} . \quad (\text{Column}) \quad (C.81)$$

Eliminating $d\epsilon_{opji}$ from Equations C.78 and C.80 gives

$$d\bar{e}_{oi} = \alpha_{Ti} \sum_j dT_{ji} \bar{e}_{\alpha Tji} \quad (C.82)$$

$$\text{where } \bar{e}_{\alpha Tji} = \tilde{T}_{ji}^T A_{ji} S_{ji}^T Z_{ji}^T J_P \quad (C.83)$$

Therefore, the unassembled deformations developed during the β th increment are given by

$$\delta \bar{e}_{0i\beta}(t_\beta) = \alpha_{T_{i\beta}} \sum_j \delta T_{ji,\beta-1} \bar{e}_{\alpha_{T_{ji\beta}}} \quad (C.83.1)$$

where

$\delta T_{ji,\beta-1}$ = the change in temperature of the j th subelement of the i th element developed during the β -1st increment.

The temperature changes are assumed to be uniform over the volume of the element. For the first increment,

$$\delta T_{ji,\beta-1} = T_{\Delta ji} \quad \beta = 1 \quad (C.83.2)$$

where

$T_{\Delta ji}$ = the difference between the temperature at the defining point of the j th subelement of the i th element and the reference temperature at $t = 0$.

The subelement defining point is the corner which the subelement has in common with the element. For subsequent increments,

$$\delta T_{ji,\beta-1} = \delta T_{i,\beta-1} \quad \beta > 1 \quad (C.83.3)$$

where

$\delta T_{i,\beta-1}$ = the change in temperature of the i th element, considered uniform over the element, developed during the β -1st increment.

The column matrix $\bar{e}_{\alpha T_{ji}}$ can be explicitly evaluated. Deleting the subscript i in Equation C.83 gives

$$\bar{e}_{\alpha T_j} = \tilde{T}_j^T \bar{e}_{\alpha T_j} \quad , \quad (C.83.4)$$

$$\text{where } \bar{e}_{\alpha T_j} = A_j S_j^T Z_j^T J_p \quad (C.83.5)$$

The surface area of the j th subelement is

$$A_j = a_j b_j \sin \theta_j \quad (C.83.6)$$

Substituting A_j , S_j , Z_j and J_p from Equations C.27, C.30, C.81 and C.83.6 into Equation C.83.5 gives

$$\bar{e}_{\alpha T_j} = \left\{ a_j \mid b_j \mid 2b_j \cos \theta_j \right\} \quad (\text{Column}) \quad (C.83.7)$$

Substituting the \tilde{T}_j matrices from Equations C.61, C.62, C.63 and C.64, and the column matrix $\bar{e}_{\alpha T_j}$ from Equation C.83.7, into Equation C.83.4 gives the matrix $\bar{e}_{\alpha T_j}$. There are four of these matrices, one for each subelement. Table C.1 gives the elements of the column matrix $\bar{e}_{\alpha T_j}$ for each subelement.

Equations C.77 and C.83.1 apply when the i th element is a membrane.

Stresses and Strains

Combining the force transformations, Equations C.19, C.22, C.38 and C.68.1, and restoring the subscript i , gives

$$d\sigma_{p_{ji}} = \sigma_{\bar{p}_{ji}} \bar{\sigma}_{\bar{p}_{ji}} \frac{1}{t_{M_i}} S_{ji} \tilde{T}_{ji} d\bar{F}_{K_i} \quad (C.86)$$

TABLE C.1. THE COLUMN MATRICES \bar{e}_{aT_j} FOR MEMBRANES

Row	Subelement Number (j)			
	p	q	r	s
1	$b_p \cos \theta_p$	$b_q \cos \theta_q$	$K_3 b_r \cos \theta_r$	$K_3 b_s \cos \theta_s$
2	o	a_q	o	o
3	a_p	o	o	o
4	o	o	a_r	o
5	o	o	o	a_s
6	o	b_q	o	o
7	o	o	b_r	o
8	b_p	o	o	o
9	o	o	o	b_s

From Equations C.25 and C.86,

$$d\sigma_{p_{ji}} = \frac{1}{t_{M_i}} Z_{ji} S_{ji} \tilde{T}_{ji} d\bar{F}_{K_i} \quad (C.87)$$

Integrating Equation C.87 gives

$$\sigma_{p_{ji}} = \frac{1}{t_{M_i}} Z_{ji} S_{ji} \tilde{T}_{ji} \bar{F}_{K_i} \quad (C.88)$$

No integration constant is needed, since the stresses are zero when the element forces are zero.

From Equation C.88, the average stress in the element is given by

$$\sigma_{p,AV_i}(t_B) = \sigma_{\bar{F},LPM_{iB}} \bar{F}_{K_i}(t_B) \quad (C.89)$$

$$\text{where } \sigma_{\bar{F},LPM_{iB}} = \frac{1}{4t_{M_{iB}}} \sum_j Z_{jiB} S_{jiB} \tilde{T}_{jiB} \quad (C.90)$$

From Equation C.17, the average incremental strain in the element, resulting from stress, is given by

$$\delta \epsilon_{p,AV_{iB}}(t_B) = C_{KP_{iB}} \delta \sigma_{p,AV_{iB}}(t_B) \quad (C.91)$$

$$\text{where } \delta \sigma_{p,AV_{iB}}(t_B) = \sigma_{p,AV_i}(t_B) - \sigma_{p,AV_i}(t_{B-1}) \quad (C.91.1)$$

Equation C.91 does not account for thermal strain.

Equations C.89 and C.91 apply when the i th element is a membrane.

Damping Matrix

The damping matrix is found by replacing the stiffness compliance matrix, C_{KP_i} , by the damping compliance matrix, C_{CP_i} , in Equation C.77:

$$\bar{c}_{i(B)} = \left[\frac{1}{t_M} \sum_j A_j (Z_j S_j \bar{T}_j)^T C_{CP} (Z_j S_j \bar{T}_j) \right]_{i,B}^{-1} \quad (C.92)$$

The damping compliance matrix is found by multiplying the elastic stiffness compliance matrix by an experimentally determined constant. See Appendix E.

Equation C.92 applies when the i th element is a membrane.

Force Transformation Matrix

This matrix can be found by comparing Figures 2.3 and C.10(b). Note that the positive senses for element forces F_{13} , F_{14} , F_{15} and F_{16} in Figure 2.3 depend on the numbering of joints p , q , r and s , as established by the user. The forces are defined as positive when they point from a lower numbered to a higher numbered joint. Let

\vec{a} , \vec{b} , \vec{c} , \vec{d} = unit vectors pointing from p to q , r to q , r to s , and p to s .

In vector notation let

$$\vec{e} = \vec{ps} \times \vec{pq} / |\vec{ps} \times \vec{pq}| \quad (C.93)$$

where

\vec{ps} , \vec{pq} = vectors equal in magnitude to edges ps and pq , pointing from p to s and p to q .

The vector \vec{e} is thus perpendicular to \vec{ps} and \vec{pq} .

Also let

a_x, a_y, a_z = the components of \vec{a} in the global system.

Similarly denote the components of \vec{b} , \vec{c} , \vec{d} and \vec{e} .

Equation C.94 gives the matrix $F_{\bar{f}}$. The first twelve rows of this matrix can be found by considering the equilibrium of the four joints at the corners of the membrane, acted upon by the \vec{F} and F forces. Similarly, the last four rows are found by considering the equilibrium of the four axially loaded bars of Figure C.10, acted upon by the \vec{F} and F forces. The f factors in these rows are required because of the method of defining the positive senses of F_{13} , F_{14} , F_{15} and F_{16} .

$$F_{\bar{F}_i}(t) = \begin{bmatrix} & & -a_x & & & & & -d_x & \\ & & -a_y & & & & & -d_y & \\ & & -a_z & & & & & -d_z & \\ e_x K_1 & a_x & & & & b_x & & & \\ e_y K_1 & a_y & & & & b_y & & & \\ e_z K_1 & a_z & & & & b_z & & & \\ & & & -c_x & & & -b_x & & \\ & & & -c_y & & & -b_y & & \\ & & & -c_z & & & -b_z & & \\ e_x K_4 & & & & c_x & & & & d_x \\ e_y K_4 & & & & c_y & & & & d_y \\ e_z K_4 & & & & c_z & & & & d_z \\ f_1 & -f_1 & f_1 & 0 & 0 & 0 & 0 & 0 & 0 \\ f_2 K_2 & 0 & 0 & 0 & 0 & -f_2 & f_2 & 0 & 0 \\ f_3 K_3 & 0 & 0 & f_3 & -f_3 & 0 & 0 & 0 & 0 \\ f_4 K_5 & 0 & 0 & 0 & 0 & 0 & 0 & f_4 & -f_4 \end{bmatrix}_i \quad (C.94)$$

where $f_1 = 1$ if $p < q$, otherwise $f_1 = -1$ (C.95)

$f_2 = 1$ if $r < q$, otherwise $f_2 = -1$ (C.96)

$f_3 = 1$ if $r < s$, otherwise $f_3 = -1$ (C.97)

$f_4 = 1$ if $p < s$, otherwise $f_4 = -1$ (C.98)

Equation C.94 applies when the i th element is a membrane.

Mass Matrix

The mass matrix has components parallel to the global coordinates. From Reference 1, the mass matrix is given by

$$m_i = \frac{\rho_i V_i}{36} \begin{bmatrix} 4 & 2 & 1 & 2 & \\ & 4 & 2 & 1 & 2 \\ & & 4 & 2 & 1 \\ 2 & 4 & 2 & 1 & \\ 2 & & 4 & 2 & 1 \\ 1 & 2 & 4 & 2 & \\ 1 & & 2 & 4 & 2 \\ 2 & 1 & 2 & 4 & \\ 2 & & 1 & 2 & 4 \\ 2 & 1 & 2 & 4 & \\ & & & & \end{bmatrix} \quad (C.99)$$

where

ρ_i, V_i = mass density and volume of the i th element.

Equation C.99 applies when the i th element is a membrane.

LUMPED PARAMETER CELLS

Cell element matrices are derived. The approach is similar to the approach employed for membrane elements.

Element Geometry

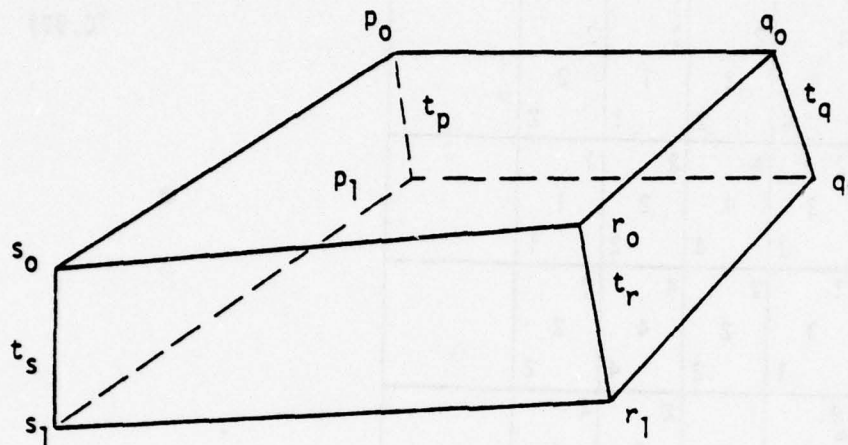


Figure C.11 Cell Element Geometry.

Figure C.11 shows the cell element. Surfaces $p_0q_0r_0s_0$ and $p_1q_1r_1s_1$ are approximate parallelograms. The other four surfaces are approximate rectangles. The global coordinates of the eight corners, input by the user, or by a program module called the laminate generator, define the geometry of the element. The figure shows the notation for corner thicknesses. All symbols in Figure C.11 should have subscript "i"s to indicate element number, but these subscripts are omitted, to simplify the notation.

Figure C.12 defines the lumped cell element, bounded by the surfaces $p_6q_6r_6s_6$ and $p_7q_7r_7s_7$. The ratio β is given by

$$\beta = \frac{3-\sqrt{3}}{6} \quad (C.100)$$

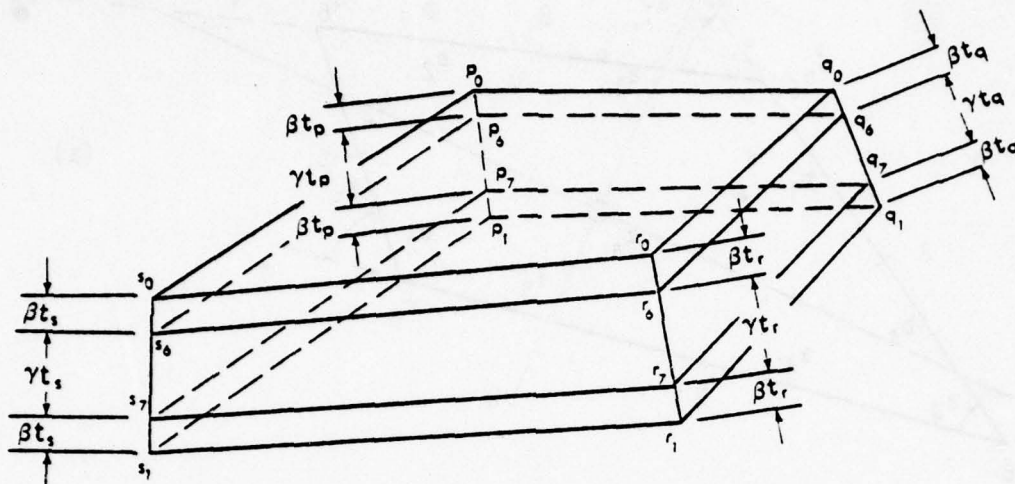


Figure C.12 Definition of the Lumped Cell Element.

The ratio of lumped cell element thickness to element thickness is

$$\gamma = 1/\sqrt{3} \quad (C.101)$$

The physical reasoning underlying the reduced thickness of the lumped element is that the ability of the cell to resist normal forces should be lumped at a distance from the middle plane of the cell equal to the radius of gyration of the cross-section, so that the cell can simultaneously have correct axial and bending stiffnesses.

Figure C.13 shows the geometry of the two surfaces of the lumped cell element that are approximate parallelograms. Points A, B, C, D, E, F, G and H denote midpoints of edges. The figure defines the a's, the b's, and the θ 's. Thus a_1 is half the length of edge p_6q_6 . The figure also defines rectangular Cartesian reference frames. The $x_a y_a$ plane coincides with the approximate plane of the quadrilateral $p_6q_6r_6s_6$.

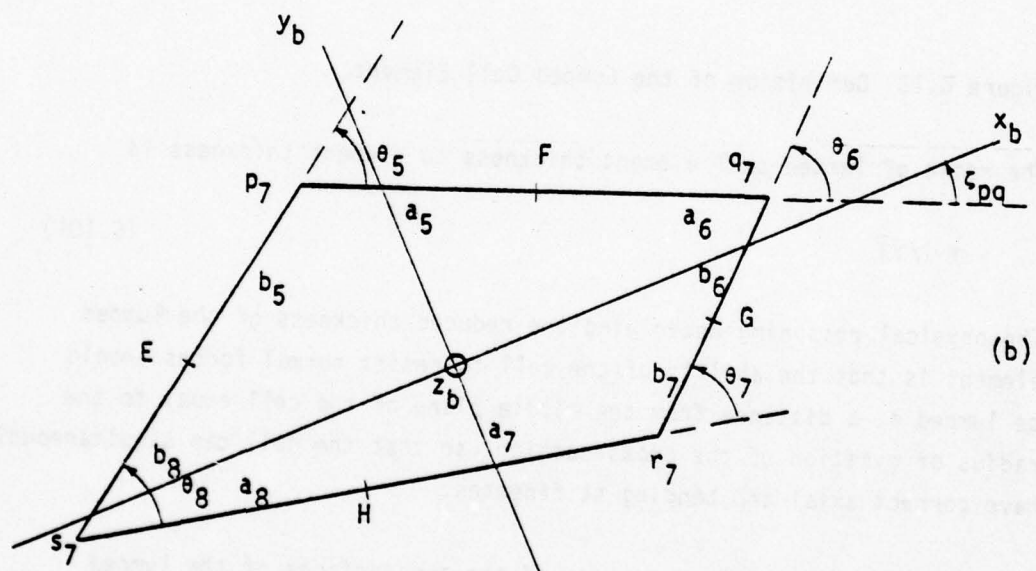
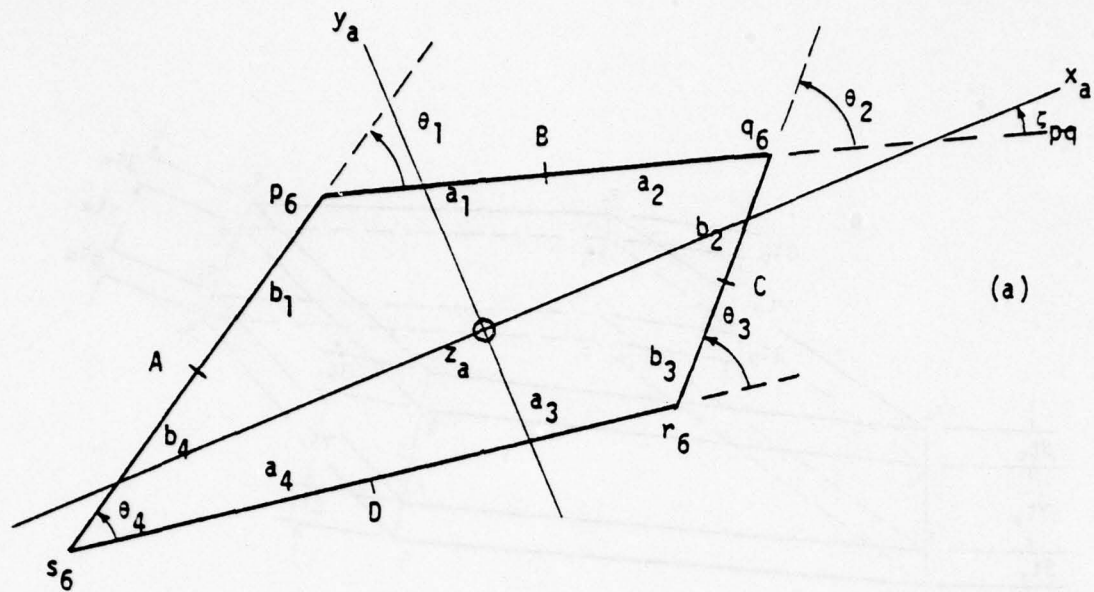


Figure C.13 Lumped Cell Element Surface Geometry.

Similarly the $x_b y_b$ plane coincides with the approximate plane $p_7 q_7 r_7 s_7$. The angles ϵ_{pq} shown in Figures C.13 (a) and (b) are equal. The origins of the reference frames are not defined, since the only purpose of these frames is to provide reference directions for components of stress and strain.

Subelements

The original element is divided into eight subelements. These subelements are parallelepipeds. As with the membrane, the cell subelements do not quite fit together, since the element is only approximately a parallelepiped. Figure C.14 shows the subelements for a parallelepiped element. For clarity, the element is separated at the midplane. The subelements are numbered as indicated.

Figure C.15 shows the j th subelement, with dimensions. The quantities a_j , b_j and θ_j are as defined in Figure C.13. The thicknesses t_j are average values for each subelement, computed according to the following formulas, employing vector notation:

$$t_1 = t_5 = \frac{1}{32} \left| 9\vec{t}_p + 3\vec{t}_q + \vec{t}_r + 3\vec{t}_s \right| \quad (C.102)$$

$$t_2 = t_6 = \frac{1}{32} \left| 3\vec{t}_p + 9\vec{t}_q + 3\vec{t}_r + \vec{t}_s \right| \quad (C.103)$$

$$t_3 = t_7 = \frac{1}{32} \left| \vec{t}_p + 3\vec{t}_q + 9\vec{t}_r + 3\vec{t}_s \right| \quad (C.104)$$

$$t_4 = t_8 = \frac{1}{32} \left| 3\vec{t}_p + \vec{t}_q + 3\vec{t}_r + 9\vec{t}_s \right| \quad (C.105)$$

Figure C.16 shows reference frames for the j th subelement. The $x_j y_j z_j$ frame is parallel to the $x_a y_a z_a$ frame of Figure C.13, when $j = 1, 2, 3, 4$. Otherwise it is parallel to $x_b y_b z_b$.

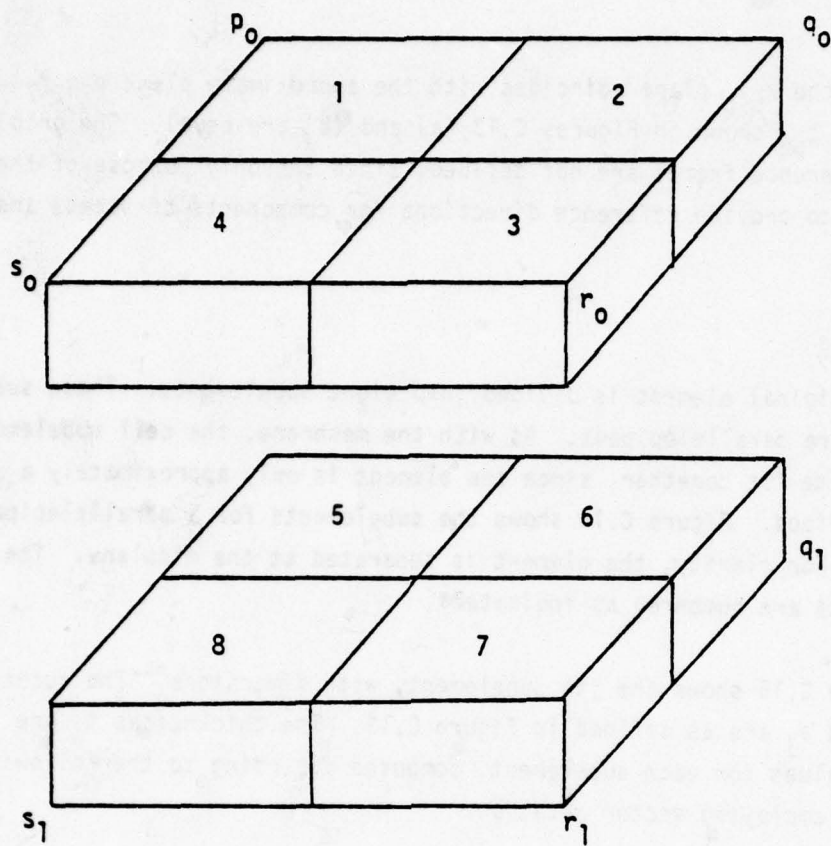


Figure C.14 Cell Subelements.

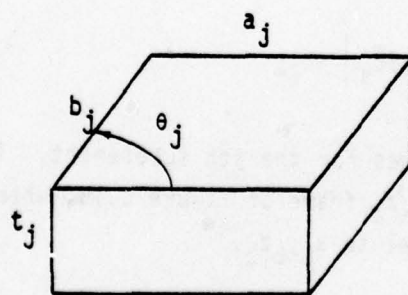


Figure C.15 j th Subelement.

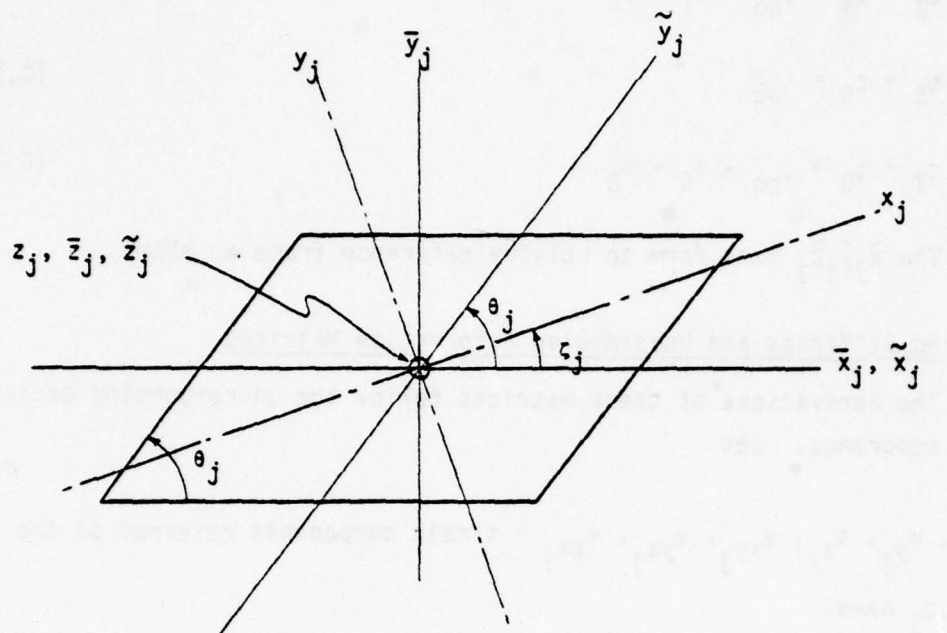


Figure C.16 Reference Frames for the j th Subelement.

The $\bar{x}_j \bar{y}_j \bar{z}_j$ axes also form a rectangular Cartesian reference frame. The direction of \bar{x}_j is defined as follows (refer to Figure C.13):

\bar{x}_j is parallel to $p_6 q_6$ if $j = 1, 2$

\bar{x}_j is parallel to $r_6 s_6$ if $j = 3, 4$

\bar{x}_j is parallel to $p_7 q_7$ if $j = 5, 6$

\bar{x}_j is parallel to $r_7 s_7$ if $j = 7, 8$

It can be shown that

$$\zeta_1 = \zeta_2 = \zeta_{pq} \quad (C.106)$$

$$\zeta_3 = \zeta_4 = \zeta_{pq} - \theta_1 + \theta_4 \quad (C.107)$$

$$\zeta_5 = \zeta_6 = \zeta_{pq} \quad (C.108)$$

$$\zeta_7 = \zeta_8 = \zeta_{pq} - \theta_5 + \theta_8 \quad (C.109)$$

The $\tilde{x}_j, \tilde{y}_j, \tilde{z}_j$ axes form an oblique reference frame as shown.

Lumped Stiffness and Unassembled Deformation Matrices

The derivations of these matrices follow the corresponding derivations for membranes. Let

$\epsilon_{x_j}, \epsilon_{y_j}, \epsilon_{z_j}, \gamma_{xy_j}, \gamma_{yz_j}, \gamma_{zx_j}$ = strain components referred to the $x_j y_j z_j$ axes.

$\sigma_{x_j}, \sigma_{y_j}, \sigma_{z_j}, \tau_{xy_j}, \tau_{yz_j}, \tau_{zx_j}$ = stiffness stress components referred to the $x_j y_j z_j$ axes.

These stresses and strains are assumed to be uniform over the volume of the subelement.

$$\text{Let } \epsilon_j = \left\{ \epsilon_x \mid \epsilon_y \mid \epsilon_z \mid \gamma_{xy} \mid \gamma_{yz} \mid \gamma_{zx} \right\}_j \quad (\text{Column}) \quad (C.110)$$

$$\sigma_j = \left\{ \sigma_x \mid \sigma_y \mid \sigma_z \mid \tau_{xy} \mid \tau_{yz} \mid \tau_{zx} \right\}_j \quad (\text{Column}) \quad (C.111)$$

During an infinitesimal period of time, dt , in the s th increment, the relation between strains, stresses and unassembled thermal strains in the j th subelement is given, in differential form, by

$$d\epsilon_j = C_{K_j} d\sigma_j + d\epsilon_{0j}, \quad (C.112)$$

where

C_{K_j} = a square stress compliance matrix for the cell material

ϵ_{0j} = a column matrix of unassembled thermal strains in the j th subelement.

See Appendix E for C_{K_j} . Assume that

$$C_{K_1} = C_{K_2} = C_{K_3} = C_{K_4} = C_{K_a} \quad (C.112.1)$$

$$C_{K_5} = C_{K_6} = C_{K_7} = C_{K_8} = C_{K_b} \quad (C.112.2)$$

where C_{K_a} and C_{K_b} are compliance matrices for the upper and lower tiers of subelements shown in Figure C.14.

The temperature distribution in each subelement is assumed to be uniform over the volume of the subelement. When such a distribution changes slightly with time, while remaining uniform, it produces equal unassembled tensile strains, and no shear strains. Therefore, the matrix of unassembled thermal strains is given, in differential form, by

$$d\epsilon_{0j} = \alpha_T dT_j \{ 1 \mid 1 \mid 1 \mid 0 \mid 0 \mid 0 \} \quad (\text{Column}) \quad (C.113)$$

Equation C.112 is now transformed according to the membrane approach. The transformations employed to pass from stress and strain components referred to $x_j y_j z_j$ coordinates to components referred to $\bar{x}_j \bar{y}_j \bar{z}_j$ are given by Equations B.17, B.54, and B.55. In differential form, these equations are:

$$d\sigma_j = \sigma_{\bar{\sigma}_j} d\bar{\sigma}_j \quad (C.114)$$

$$d\bar{\epsilon}_j = \sigma_{\bar{\sigma}_j}^T d\epsilon_j \quad (C.115)$$

where

$$\bar{\sigma}_j = \left\{ \bar{\tau}_{xy} \mid \bar{\sigma}_y \mid \bar{\sigma}_x \mid \bar{\tau}_{zx} \mid \bar{\tau}_{yz} \mid \bar{\sigma}_z \right\}_j \quad (\text{Column}) \quad (\text{C.116})$$

$$\bar{\epsilon}_j = \left\{ \bar{\gamma}_{xy} \mid \bar{\epsilon}_y \mid \bar{\epsilon}_x \mid \bar{\gamma}_{zx} \mid \bar{\gamma}_{yz} \mid \bar{\epsilon}_z \right\}_j \quad (\text{Column}) \quad (\text{C.117})$$

The transformation matrix $\sigma_{\bar{\sigma}_j}$ is defined in Equation B.16.

Eliminating $d\epsilon_j$ and $d\sigma_j$ from Equations C.112, C.114 and C.115 gives

$$d\bar{\epsilon}_j = \sigma_{\bar{\sigma}_j}^T C_{K_j} \sigma_{\bar{\sigma}_j} d\bar{\sigma}_j + \sigma_{\bar{\sigma}_j}^T d\epsilon_{0j} \quad (\text{C.118})$$

Similarly, Equation C.118 is transformed to skew coordinates. The transformations, from Equations B.70, B.99, and B.110, are, in differential form:

$$d\bar{\sigma}_j = \bar{\sigma}_{\bar{\sigma}_j} d\bar{\sigma}_j \quad (\text{C.119})$$

$$d\bar{\epsilon}_j = B_j \bar{\sigma}_{\bar{\sigma}_j}^T d\bar{\epsilon}_j \quad (\text{C.120})$$

where

$$\bar{\sigma}_j = \left\{ \bar{\tau}_{xy} \mid \bar{\sigma}_y \mid \bar{\sigma}_x \mid \bar{\tau}_{zx} \mid \bar{\tau}_{yz} \mid \bar{\sigma}_z \right\}_j \quad (\text{Column}) \quad (\text{C.121})$$

$$\bar{\epsilon}_j = \left\{ \bar{\gamma}_{xy} \mid \bar{\epsilon}_y \mid \bar{\epsilon}_x \mid \bar{\gamma}_{zx} \mid \bar{\gamma}_{yz} \mid \bar{\epsilon}_z \right\}_j \quad (\text{Column}) \quad (\text{C.122})$$

The transformation matrix $\bar{\sigma}_{\bar{\sigma}_j}$ is defined in Equation B.70.1. The matrix

B_j is given by Equation B.101.

Eliminating $d\bar{\epsilon}_j$ and $d\bar{\sigma}_j$ from Equations C.118, C.119 and C.120 gives

$$d\tilde{\epsilon}_j = B_j \bar{\sigma}_{\tilde{\sigma}_j}^T \sigma_{\tilde{\sigma}_j}^T C_{K_j} \sigma_{\tilde{\sigma}_j} \bar{\sigma}_{\tilde{\sigma}_j} d\tilde{\sigma}_j + B_j \bar{\sigma}_{\tilde{\sigma}_j}^T \sigma_{\tilde{\sigma}_j}^T d\epsilon_{0j} \quad (C.123)$$

The oblique components of stress and strain are transformed into subelement forces and deformations.

Six subelement forces are defined as shown in Figure C.17. These forces are self-equilibrating. Note that the shear stresses on the upper and lower faces resulting from \tilde{F}_4 are equal to $\tilde{F}_4/(ab \sin\theta)$, whereas the shear stresses on the two side faces resulting from \tilde{F}_4 are equal to $\tilde{F}_4 / (ab)$. This distribution of stresses is consistent with the discussion on "Equilibrium of the Infinitesimal Element" given in Appendix B, and also with the forces acting on a skewed finite element shown in Figure B.14. Subscript j 's, indicating the subelement number, have been omitted from the figure for clarity:

Subelement deformations corresponding to the self-equilibrating element forces are designated $\tilde{\epsilon}_{j1}, \tilde{\epsilon}_{j2} \dots \tilde{\epsilon}_{j6}$.

Let

$$\tilde{F}_j = \left\{ \tilde{F}_1 \mid \tilde{F}_2 \mid \tilde{F}_3 \mid \tilde{F}_4 \mid \tilde{F}_5 \mid \tilde{F}_6 \right\}_j \quad (\text{Column}) \quad (C.124)$$

$$\tilde{\epsilon}_j = \left\{ \tilde{\epsilon}_1 \mid \tilde{\epsilon}_2 \mid \tilde{\epsilon}_3 \mid \tilde{\epsilon}_4 \mid \tilde{\epsilon}_5 \mid \tilde{\epsilon}_6 \right\}_j \quad (\text{Column}) \quad (C.125)$$

Since the stress distribution is assumed uniform in the subelement, the relationship between the oblique stress components and the subelement forces is given by

$$\bar{\sigma}_j = \bar{\sigma}_{\tilde{F}_j} \tilde{F}_j \quad , \quad (C.126)$$

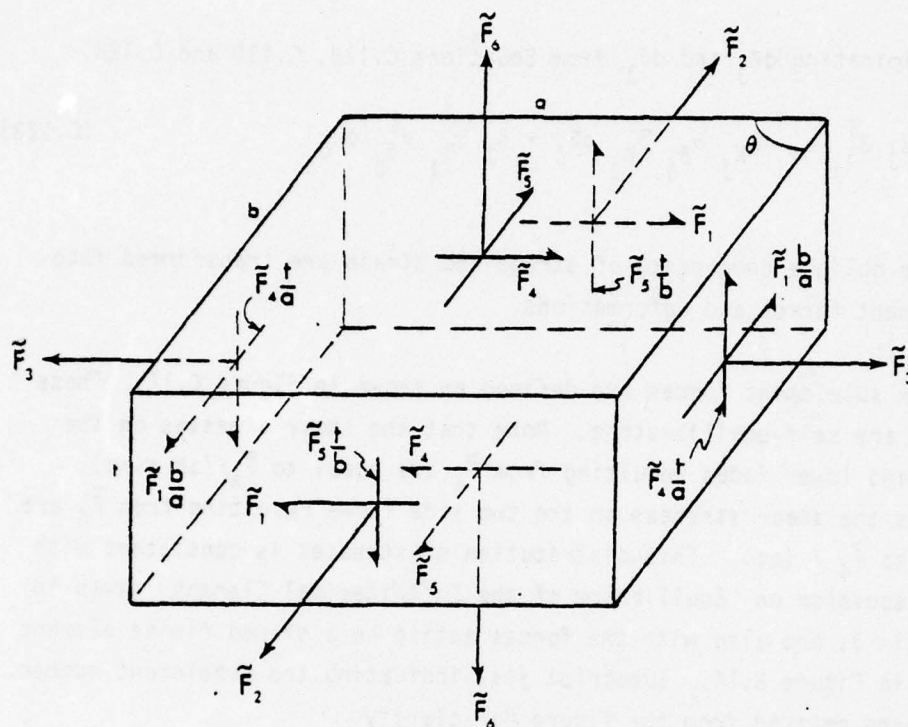


Figure C.17 Subelement Forces, j th Subelement.

where

$$\tilde{\sigma}_{F_j} = \begin{bmatrix} \frac{1}{at} & & & & & \\ & \frac{1}{at} & & & & \\ & & \frac{1}{bt} & & & \\ & & & \frac{1}{A} & & \\ & & & & \frac{1}{A} & \\ & & & & & \frac{1}{A} \end{bmatrix}_j \quad (C.127)$$

$$\text{and } A_j = a_j b_j \sin \theta_j \quad (\text{scalar}) \quad (\text{C.128})$$

Equation C.126 is the force transformation. Now consider the j th subelement subjected to the uniform oblique stress field, and produce virtual displacements that are linear functions of the coordinates. The virtual work done on the subelement boundaries is given by Equation B.122 as

$$W_j = V_j \tilde{\sigma}_j^T B_j^{-1} \tilde{\epsilon}_j \quad (\text{C.129})$$

$$\text{where } V_j = A_j t_j \quad (\text{scalar}) \quad (\text{C.130})$$

Now consider the subelement acted upon by \tilde{F} forces that are statically equivalent to the oblique stresses, and produce the same virtual displacements. The resulting virtual work is, from Appendix A,

$$W_j = \tilde{F}_j^T \tilde{e}_j \quad (\text{C.131})$$

The virtual works in Equations C.130 and C.131 are the same, therefore,

$$\tilde{F}_j^T \tilde{e}_j = V_j \tilde{\sigma}_j^T B_j^{-1} \tilde{\epsilon}_j \quad (\text{C.132})$$

From Equations C.126 and C.132,

$$\tilde{F}_j^T \tilde{e}_j = V_j \tilde{F}_j^T \tilde{\sigma}_{F_j}^T B_j^{-1} \tilde{\epsilon}_j \quad (\text{C.133})$$

This equation holds for any choice of \tilde{F}_j . Therefore

$$\tilde{e}_j = V_j \tilde{\sigma}_{F_j}^T B_j^{-1} \tilde{\epsilon}_j \quad (\text{C.134})$$

Equation C.134 is the displacement transformation. Equations C.126 and C.134 can be written in differential form as

$$d\tilde{\sigma}_j = \tilde{\sigma}_{\tilde{F}_j} d\tilde{F}_j \quad (C.135)$$

$$d\tilde{e}_j = V_j \tilde{\sigma}_{\tilde{F}_j}^T B_j^{-1} d\tilde{e}_j \quad (C.136)$$

Eliminating $d\tilde{e}_j$ and $d\tilde{\sigma}_j$ from Equations C.123, C.135 and C.136 gives

$$d\tilde{e}_j = V_j (\sigma_{\tilde{F}_j}^T C_{K_j} \sigma_{\tilde{F}_j} d\tilde{F}_j + \sigma_{\tilde{F}_j}^T d\epsilon_{0_j}) \quad (C.137)$$

$$\text{where } \sigma_{\tilde{F}_j} = \sigma_{\tilde{\sigma}_j} \tilde{\sigma}_{\tilde{\sigma}_j} \tilde{\sigma}_{\tilde{F}_j} \quad (C.138)$$

The subelement forces are transformed into lumped element forces. The matrices of lumped element stiffness forces and element deformations, defined in Section II, are given by

$$\bar{F}_K = \left\{ \bar{F}_{K_1} \mid \bar{F}_{K_2} \mid \dots \mid \bar{F}_{K_{30}} \right\} \quad (\text{Column}) \quad (C.139)$$

$$\bar{e} = \left\{ \bar{e}_1 \mid \bar{e}_2 \mid \dots \mid \bar{e}_{30} \right\} \quad (\text{Column}) \quad (C.140)$$

The force transformation is

$$\tilde{F}_{ji} = \tilde{F}_{\tilde{F}_{ji}} \bar{F}_{K_i} \quad j = 1, 2 \dots 8 \quad (C.141)$$

In Equation C.141, the subscript j indicates subelement number. The subscript i , indicating element number, has been restored.

The procedure for establishing the transformation matrices, $\tilde{F}_{\tilde{F}_{ji}}$, is essentially the same as for the membrane. Figures C.18, C.19 and C.20 show the correspondence between subelement and lumped element forces, for the upper, lower, and middle surfaces, of the lumped element. Note the similarity between Figures C.10, C.18 and C.19.

In Figures C.18, C.19 and C.20, the lumped shear panel forces each have six self-equilibrating components. The only lumped shear components that are labelled are the ones required in forming the transformation. The factors $K_{3,2}$, $K_{3,3}$, $K_{3,4}$, $K_{3,5}$, $K_{3,6}$, and $K_{3,7}$ are calculated from panel geometry. An approximation has, however, been introduced. These factors are based on the true geometry of the unlumped element, rather than of the lumped element. When the upper and lower faces of the cell are parallelograms, and the other faces are rectangles, the factors are correct.

The elements of the matrices \tilde{F}_{ji} are listed in Table C.2. The factors of $1/\sqrt{3}$ appearing in the table are found to be necessary to give the cell element the correct stiffness for through-the-thickness shear.

The justification for the subelement to lumped element force transformation is that it leads to correct displacements for the nine elementary loadings described in Section III.

The displacement transformation corresponding to Equation C.141 is derived by the method of virtual work. The derivation is the same as for the membrane. Therefore, from Equation C.68, considering the analogy between Equations C.65 and C.141,

$$\bar{e}_i = \sum_j \tilde{F}_{ji}^T \tilde{e}_{ji} \quad j = 1, 2 \dots 8. \quad (C.142)$$

Writing Equations C.141 and C.142 in differential form gives

$$d\tilde{F}_{ji} = \tilde{F}_{ji} d\bar{F}_{K_i} \quad (C.143)$$

$$d\bar{e}_i = \sum_j \tilde{F}_{ji}^T d\tilde{e}_{ji} \quad (C.144)$$

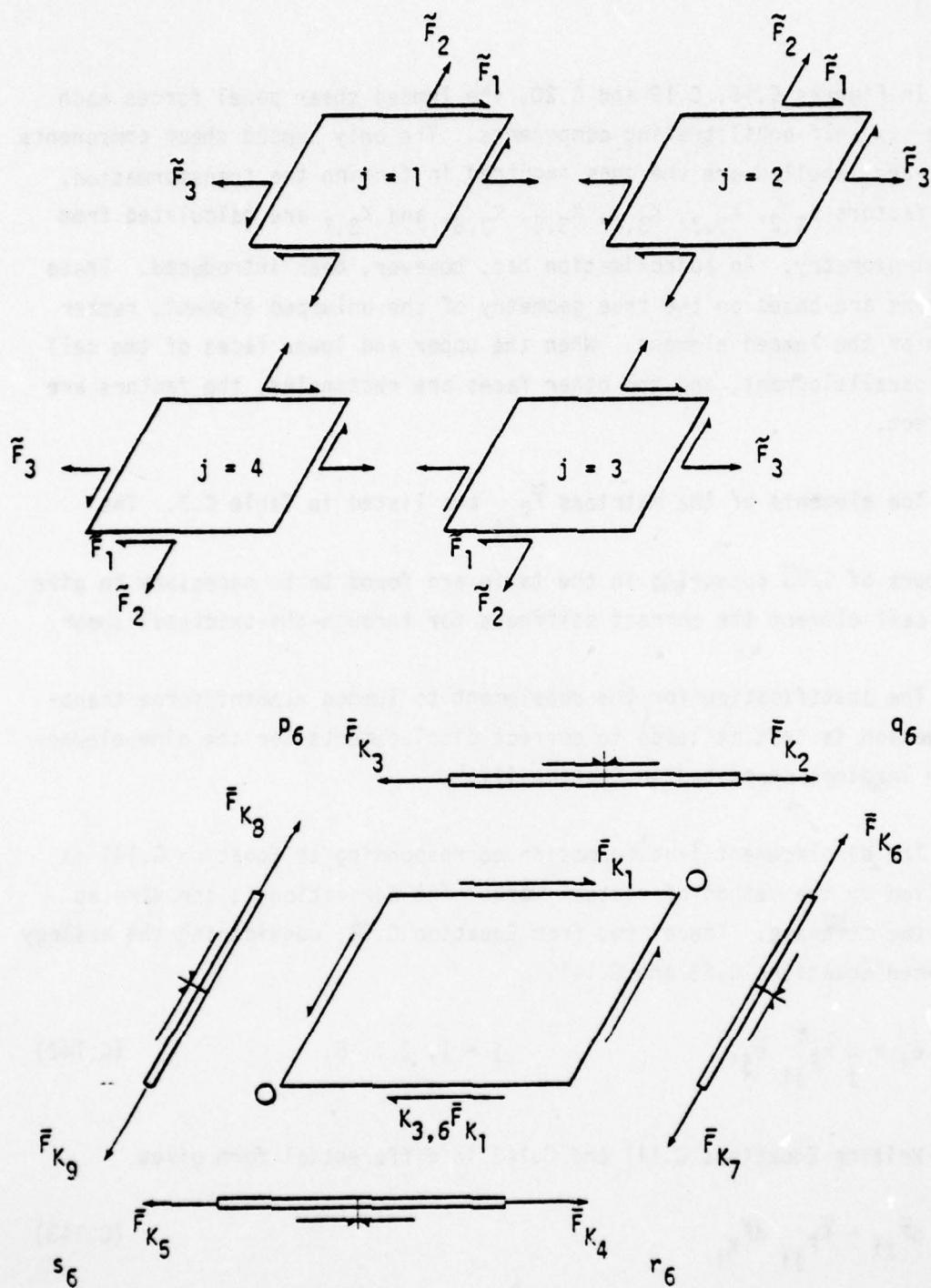


Figure C.18 Subelement and Lumped Forces, Upper Surface.

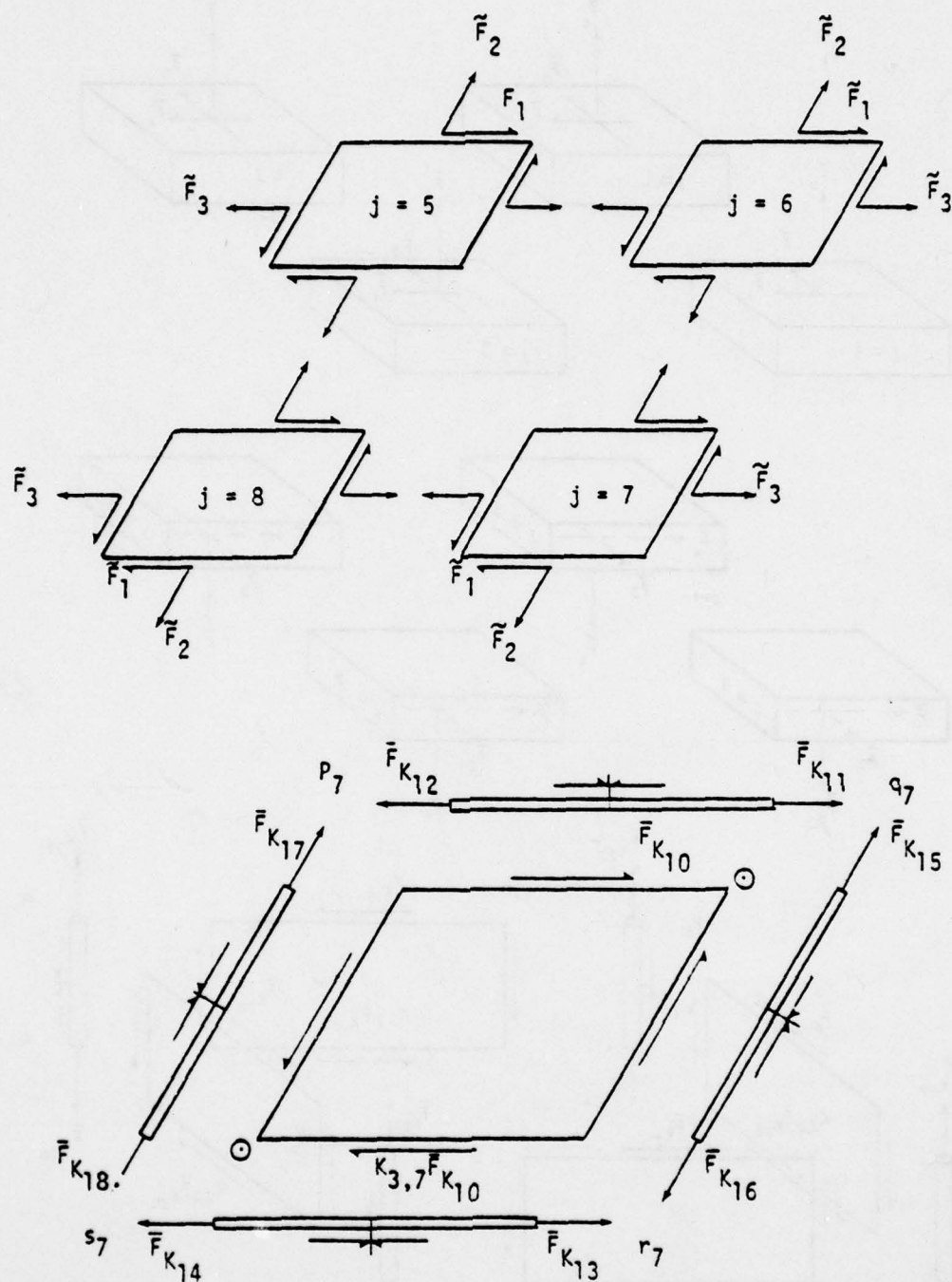


Figure C.19 Subelement and Lumped Forces, Lower Surface.

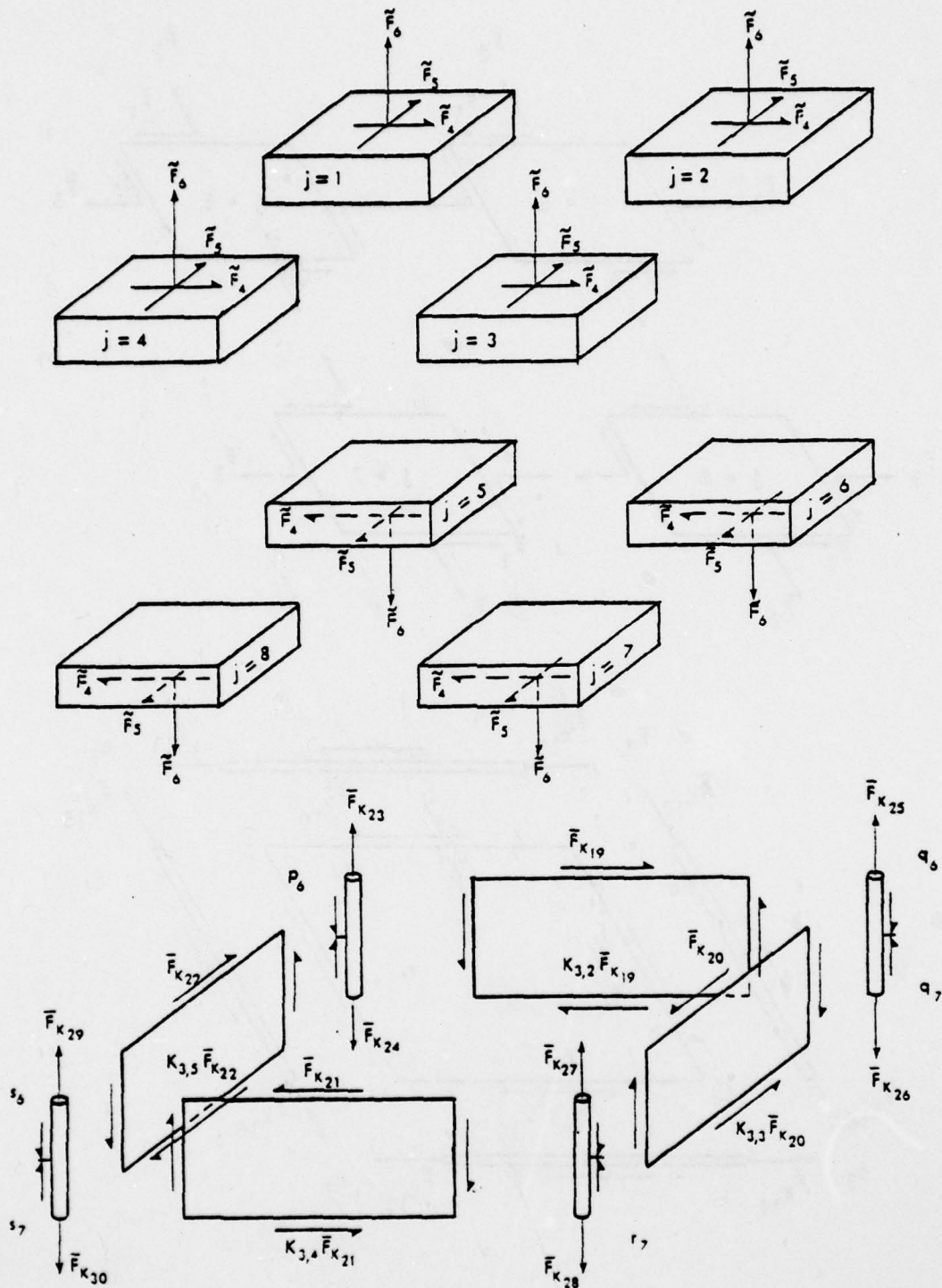


Figure C.20 Subelement and Lumped Forces, Middle Surfaces.

TABLE C.2. ELEMENTS OF THE MATRICES \tilde{F}_{ji}

Row	Subelement 1		Subelement 2		Subelement 3		Subelement 4	
	Col.	Value	Col.	Value	Col.	Value	Col.	Value
1	1	$\frac{1}{2}$	1	$\frac{1}{2}$	1	$\frac{1}{2} K_{3,6}$	1	$\frac{1}{2} K_{3,6}$
2	8	1	6	1	7	1	9	1
3	3	1	2	1	4	1	5	1
4	19	$\frac{1}{2\sqrt{3}}$	19	$\frac{1}{2\sqrt{3}}$	21	$-\frac{1}{2\sqrt{3}}$	21	$-\frac{1}{2\sqrt{3}}$
5	22	$\frac{1}{2\sqrt{3}}$	20	$-\frac{1}{2\sqrt{3}}$	20	$-\frac{1}{2\sqrt{3}}$	22	$\frac{1}{2\sqrt{3}}$
6	23	1	25	1	27	1	29	1

Row	Subelement 5		Subelement 6		Subelement 7		Subelement 8	
	Col.	Value	Col.	Value	Col.	Value	Col.	Value
1	10	$\frac{1}{2}$	10	$\frac{1}{2}$	10	$\frac{1}{2} K_{3,7}$	10	$\frac{1}{2} K_{3,7}$
2	17	1	15	1	16	1	18	1
3	12	1	11	1	13	1	14	1
4	19	$\frac{1}{2\sqrt{3}} K_{3,2}$	19	$\frac{1}{2\sqrt{3}} K_{3,2}$	21	$-\frac{1}{2\sqrt{3}} K_{3,4}$	21	$-\frac{1}{2\sqrt{3}} K_{3,4}$
5	22	$\frac{1}{2\sqrt{3}} K_{3,5}$	20	$-\frac{1}{2\sqrt{3}} K_{3,3}$	20	$-\frac{1}{2\sqrt{3}} K_{3,3}$	22	$\frac{1}{2\sqrt{3}} K_{3,5}$
6	24	1	26	1	28	1	30	1

Restoring the subscript i , for element number, in Equation C.137, and eliminating $d\tilde{\epsilon}_{ji}$ and $d\tilde{F}_{ji}$ from Equations C.137, C.143 and C.144 gives

$$d\bar{\epsilon}_i = \bar{D}_i d\bar{F}_{K_i} + d\bar{\epsilon}_{o_i} \quad (C.145)$$

$$\text{where } \bar{D}_i = \sum_j V_{ji} \sigma_{F_{ji}}^T C_{K_{ji}} \sigma_{F_{ji}} \quad (C.146)$$

$$d\bar{\epsilon}_{o_i} = \sum_j V_{ji} \sigma_{F_{ji}}^T d\epsilon_{o_{ji}} \quad (C.147)$$

$$\text{and } \sigma_{F_{ji}} = \sigma_{F_{ji}}^* \tilde{F}_{F_{ji}} \quad (C.148)$$

Solving Equation C.145 for $d\bar{F}_{K_i}$ gives

$$d\bar{F}_{K_i} = \bar{D}_i^{-1} (d\bar{\epsilon}_i - d\bar{\epsilon}_{o_i}) \quad (C.149)$$

Comparing Equations C.15 and C.149 shows that

$$\bar{k}_i = \bar{D}_i^{-1} \quad (C.150)$$

Eliminating \bar{D}_i from Equations C.146 and C.150, gives

$$\bar{k}_{i(\beta)} = \left(\sum_j V_j \sigma_{F_j}^T C_{K_j} \sigma_{F_j} \right)^{-1}_{i\beta} \quad (C.151)$$

for the β th increment. This is the lumped stiffness matrix for the cell element.

The matrix $\sigma_{F_{ji}}^*$, which is involved in Equation C.151 through Equation C.148, can be explicitly evaluated, by substituting $\sigma_{\bar{\sigma}_j}$, $\bar{\sigma}_{\bar{\sigma}_j}$, and $\tilde{\epsilon}_{F_j}^*$ from

Equations B.16, B.70.1 and C.127 into Equation C.138. Table C.3 gives the elements of σ_{Fji}^T

Equation C.113 can be written

$$d\epsilon_{0ji} = \alpha_{T_i} dT_{ji} J \quad (C.152)$$

for the i th element, where

$$J = \{1 \mid 1 \mid 1 \mid 0 \mid 0 \mid 0\} \quad (\text{Column}) \quad (C.153)$$

Eliminating $d\epsilon_{0ji}$ from Equations C.147 and C.152 gives

$$d\bar{\epsilon}_{0i} = \alpha_{T_i} \sum_j dT_{ji} \bar{e}_{\alpha Tji} \quad (C.154)$$

$$\text{where } \bar{e}_{\alpha Tji} = V_{ji} \sigma_{Fji}^T J \quad (C.155)$$

Therefore, from Equation C.154, the unassembled deformations developed during the s th increment are given by

$$\delta \bar{\epsilon}_{0iB}(t_B) = \alpha_{T_{iB}} \sum_j \delta T_{ji,B-1} \bar{e}_{\alpha TjiB} \quad (C.156)$$

where the temperature change in the j th subelement, $\delta T_{ji,B-1}$, is defined the same as for the membrane. See Equations C.83.2 and C.83.3.

The column matrix $\bar{e}_{\alpha Tji}$ can be explicitly evaluated. Eliminating σ_{Fji}^T from Equations C.148 and C.155, and deleting the subscript i gives

TABLE C.3. THE MATRIX $\sigma_{F_{ji}}$, FOR THE jTH SUBELEMENT OF THE iTH CELL ELEMENT

$\frac{2 \cos(\theta-\zeta) \cos \zeta}{a t \sin \theta}$	$\frac{\cos^2(\theta-\zeta)}{a t \sin \theta}$	$\frac{\cos^2 \zeta}{b t \sin \theta}$	0	0	0
$-\frac{2 \sin(\theta-\zeta) \sin \zeta}{a t \sin \theta}$	$\frac{\sin^2(\theta-\zeta)}{a t \sin \theta}$	$\frac{\sin^2 \zeta}{b t \sin \theta}$	0	0	0
0	0	0	0	0	$\frac{1}{a b \sin \theta}$
$\frac{\sin(\theta-\zeta) \cos \zeta}{a t \sin \theta}$ $-\frac{\cos(\theta-\zeta) \sin \zeta}{a t \sin \theta}$	$\frac{\sin(\theta-\zeta) \cos(\theta-\zeta)}{a t \sin \theta}$	$-\frac{\sin \zeta \cos \zeta}{b t \sin \theta}$	0	0	0
0	0	0	$\frac{-\sin \zeta}{a b \sin \theta}$	$\frac{\sin(\theta-\zeta)}{a b \sin \theta}$	0
0	0	0	$\frac{\cos \zeta}{a b \sin \theta}$	$\frac{\cos(\theta-\zeta)}{a b \sin \theta}$	0

ij

$$\bar{e}_{\alpha T_j} = \tilde{F}_{F_j}^T \tilde{e}_{\alpha T_j} \quad (C.157)$$

$$\text{where } \tilde{e}_{\alpha T_j} = V_j \sigma_{F_j}^T J, \quad (C.157.1)$$

since V_j is a scalar. From Equations C.138 and C.157.1,

$$\tilde{e}_{\alpha T_j} = V_j \tilde{\sigma}_{F_j}^T \tilde{\sigma}_{\bar{\sigma}_j}^T \sigma_{\bar{\sigma}_j}^T J \quad (C.158)$$

combining Equations C.138 and C.158 gives

$$\tilde{e}_{\alpha T_j} = V_j \sigma_{F_j}^T J \quad (C.158.1)$$

Substituting V_j from Equation C.130, σ_{F_j} from Table C.3, and J from Equation C.153, into Equation C.158.1, and employing Equation C.128 gives

$$\tilde{e}_{\alpha T_j} = \left\{ 2b \cos \theta \mid b \mid a \mid o \mid o \mid t \right\}_j \quad (\text{Column}) \quad (C.159)$$

Substituting $\tilde{e}_{\alpha T_j}$ from Equation C.159, and the elements of the matrix \tilde{F}_{F_j} from Table C.2, into Equation C.157, gives the matrix $\bar{e}_{\alpha T_j}$. There are eight of these column matrices, since the subelement number, j , ranges from 1 to 8. Table C.4 gives the elements of the column matrix $\bar{e}_{\alpha T_j}$, for each subelement.

Equations C.151 for the stiffness matrix, and C.156, for unassembled deformations, apply when the i th element is a cell.

TABLE C.4. THE COLUMN MATRICES \bar{e}_{aT_j} FOR CELL ELEMENTS

Row	Subelement Number (j)							
	1	2	3	4	5	6	7	8
1	$b_1 \cos \theta_1$	$b_2 \cos \theta_2$	$K_{3,6} b_3 \cos \theta_3$	$K_{3,6} b_4 \cos \theta_4$				
2	0	a_2	0	0				
3	a_1	0	0	0				
4	0	0	a_3	0				
5	0	0	0	a_4				
6	0	b_2	0	0				
7	0	0	b_3	0				
8	b_1	0	0	0				
9	0	0	0	b_4				
10					$b_5 \cos \theta_5$	$b_6 \cos \theta_6$	$K_{3,7} b_7 \cos \theta_7$	$K_{3,7} b_8 \cos \theta_8$
11					0	a_6	0	0
12					a_5	0	0	0
13					0	0	a_7	0
14					0	0	0	a_8
15					0	b_6	0	0

AD-A063 740

DOUGLAS AIRCRAFT CO LONG BEACH CALIF
AIRCRAFT WINDSHIELD BIRD IMPACT MATH MODEL. PART 1. THEORY AND --ETC(U)

F/G 1/3

DEC 77 P H DENKE

F33615-75-C-3105

UNCLASSIFIED

MDC-J7174-PT-1

AFFDL-TR-77-99-PT-1

NL

4 OF 6
ADA
063740



TABLE C.4. THE COLUMN MATRICES \bar{e}_{aj} FOR CELL ELEMENTS (CONTINUED)

Row	Subelement Number (j)							
	1	2	3	4	5	6	7	8
16					0	0	b_7	0
17					b_5	0	0	0
18					0	0	0	b_8
19								
20								
21								
22								
23	t_1	0	0	0	0	0	0	0
24	0	0	0	0	t_5	0	0	0
25	0	t_2	0	0	0	0	0	0
26	0	0	0	0	0	t_6	0	0
27	0	0	t_3	0	0	0	0	0
28	0	0	0	0	0	0	t_7	0
29	0	0	0	t_4	0	0	0	0
30	0	0	0	0	0	0	0	t_8

Stresses and Strains

Combining the force transformations, Equations C.114, C.119, C.135 and C.143, and restoring the subscript i , for element number, gives

$$d\sigma_{ji} = \sigma_{\bar{\sigma}_{ji}} \bar{\sigma}_{\bar{\sigma}_{ji}} \bar{\sigma}_{\bar{F}_{ji}} \bar{F}_{\bar{F}_{ji}} d\bar{F}_{K_i} \quad (C.160)$$

From Equations C.138 and C.160,

$$d\sigma_{ji} = \sigma_{\bar{F}_{ji}} \bar{F}_{\bar{F}_{ji}} d\bar{F}_{K_i}, \quad (C.161)$$

and from Equations C.148 and C.161,

$$d\sigma_{ji} = \sigma_{\bar{F}_{ji}} d\bar{F}_{K_i} \quad (C.162)$$

Integrating Equation C.162 gives

$$\sigma_{ji} = \sigma_{\bar{F}_{ji}} \bar{F}_{K_i} \quad (C.163)$$

No integration constant is needed, since the stresses are zero when the element forces are zero.

Because of the way the transformation $\bar{F}_{\bar{F}_{ji}}$ is constructed, the stresses

σ_{ji} represent average stresses in the subelements in the surfaces $p_6q_6r_6s_6$ and $p_7q_7r_7s_7$ (Figure C.12), which are the upper and lower surfaces of the lumped element. Let

$$\sigma_{a_i} = \left(\sum_{j=1}^4 v_{ji} \right)^{-1} \sum_{j=1}^4 v_{ji} \sigma_{ji} \quad (C.164)$$

$$\sigma_{b_i} = \left(\sum_{j=5}^8 v_{ji} \right)^{-1} \sum_{j=5}^8 v_{ji} \sigma_{ji} \quad (C.165)$$

The matrices σ_{a_i} and σ_{b_i} therefore are column matrices of average stress components in the surfaces $p_6 q_6 r_6 s_6$ and $p_7 q_7 r_7 s_7$, weighted according to subelement volumes. Substituting σ_{ji} from Equation C.163 into Equations C.164 and C.165 gives

$$\sigma_{a_i} = \sigma_{Fa_i} \bar{F}_{K_i} \quad (C.166)$$

$$\text{and } \sigma_{b_i} = \sigma_{Fb_i} \bar{F}_{K_i} \quad (C.167)$$

$$\text{where } \sigma_{Fa_i} = \left(\sum_{j=1}^4 v_{ji} \right)^{-1} \sum_{j=1}^4 v_{ji} \sigma_{Fji} \quad (C.168)$$

$$\text{and } \sigma_{Fb_i} = \left(\sum_{j=5}^8 v_{ji} \right)^{-1} \sum_{j=5}^8 v_{ji} \sigma_{Fji} \quad (C.169)$$

$$\text{Let } \sigma_{L_i} = \begin{bmatrix} \sigma_{a_i} \\ \sigma_{b_i} \end{bmatrix} \quad (C.170)$$

where

σ_{L_i} = a column matrix of average stress components in the upper and lower surfaces of the lumped element.

Substituting σ_{a_i} and σ_{b_i} from Equations C.166 and C.167 into Equation C.170 gives

$$\sigma_{L_i} = \sigma_{L\bar{F}_i} \bar{F}_{K_i} \quad (C.171)$$

$$\text{where } \sigma_{L\bar{F}_i} = \begin{bmatrix} \sigma_{\bar{F}a_i} \\ \sigma_{\bar{F}b_i} \end{bmatrix} \quad (C.172)$$

Let

$\sigma_{xc_i}, \sigma_{yc_i}, \sigma_{zc_i}, \tau_{xyc_i}, \tau_{yzc_i}, \tau_{zxc_i}$ = average stress components in surface $p_0 q_0 r_0 s_0$ (see Figure C.12).

$\sigma_{xd_i}, \sigma_{yd_i}, \sigma_{zd_i}, \tau_{xyd_i}, \tau_{yzd_i}, \tau_{zxd_i}$ = average stress components in surface $p_1 q_1 r_1 s_1$.

These stresses are in the true geometric boundaries of the element. Let

$$\sigma_{c_i} = \left\{ \sigma_{xc_i} \mid \sigma_{yc_i} \mid \sigma_{zc_i} \mid \tau_{xyc_i} \mid \tau_{yzc_i} \mid \tau_{zxc_i} \right\}, \quad (C.173)$$

$$\sigma_{d_i} = \left\{ \sigma_{xd_i} \mid \sigma_{yd_i} \mid \sigma_{zd_i} \mid \tau_{xyd_i} \mid \tau_{yzd_i} \mid \tau_{zxd_i} \right\}, \quad (C.174)$$

$$\text{and } \sigma_{S_i} = \begin{bmatrix} \sigma_{c_i} \\ \sigma_{d_i} \end{bmatrix} \quad (C.175)$$

The average stresses in the true geometric boundaries are related to the average stresses in the lumped element boundaries according to the equation

$$\sigma_{S_i} = \sigma_{S_0} \sigma_{L_i}, \quad (C.176)$$

where $\sigma_{s\sigma}$ is a square transformation matrix that is based on the assumption that the stress components σ_x , σ_y and τ_{xy} vary linearly through the thickness of the element, while σ_z , τ_{yz} and τ_{zx} are constant. The matrix $\sigma_{s\sigma}$ is given in Appendix H.

Substituting σ_{L_i} from Equation C.171 into Equation C.176 gives

$$\sigma_{s_i}(t_\beta) = \sigma_{s\sigma} \sigma_{L\bar{F}_{i\beta}} \bar{F}_{K_i}(t_\beta) \quad (C.177)$$

Equation C.177 gives the average stresses in the true geometric boundaries of the cell, in terms of the lumped element forces, at time t_β .

Let

$\epsilon_{xc_i}, \epsilon_{yc_i}, \epsilon_{zc_i}, \gamma_{xyc_i}, \gamma_{yzc_i}, \gamma_{zxc_i}$ = average strain components in surface $p_0 q_0 r_0 s_0$.

$\epsilon_{xd_i}, \epsilon_{yd_i}, \epsilon_{zd_i}, \gamma_{xyd_i}, \gamma_{yzd_i}, \gamma_{zxd_i}$ = average strain components in surface $p_1 q_1 r_1 s_1$.

Let

$$\epsilon_{c_i} = \left\{ \epsilon_{xc_i} \mid \epsilon_{yc_i} \mid \epsilon_{zc_i} \mid \gamma_{xyc_i} \mid \gamma_{yzc_i} \mid \gamma_{zxc_i} \right\} \quad (C.178)$$

$$\epsilon_{d_i} = \left\{ \epsilon_{xd_i} \mid \epsilon_{yd_i} \mid \epsilon_{zd_i} \mid \gamma_{xyd_i} \mid \gamma_{yzd_i} \mid \gamma_{zxd_i} \right\} \quad (C.179)$$

$$\text{and } \epsilon_{s_i} = \left\{ \begin{matrix} \epsilon_{c_i} \\ \epsilon_{d_i} \end{matrix} \right\} \quad (C.180)$$

The symbol ϵ_{s_i} denotes a column matrix of average strains in the true geometric boundaries of the cell. Assume that increments of average strain can be computed from increments of average stress according to the equation.

$$\delta \epsilon_{s_{i\beta}}(t_\beta) = \epsilon_{\sigma s_{i\beta}} \delta \sigma_{s_{i\beta}}(t_\beta) \quad , \quad (C.181)$$

$$\text{where } \delta \sigma_{s_{i\beta}}(t_\beta) = \sigma_{s_i}(t_\beta) - \sigma_{s_i}(t_{\beta-1}) \quad , \quad (C.182)$$

$$\epsilon_{\sigma s_{i\beta}} = \left[\begin{array}{c|c} C_{Kc} & \\ \hline & C_{Kd} \end{array} \right]_{i\beta} \quad (C.183)$$

and

C_{Kc}, C_{Kd} = square compliance matrices for the surfaces $p_0 q_0 r_0 s_0$ and

$p_1 q_1 r_1 s_1$.

From Equation C.177, the incremental average stresses developed during the β th increment are given in terms of the incremental element forces by

$$\delta \sigma_{s_{i\beta}}(t_\beta) = \sigma_{s\sigma} \sigma_{L\bar{F}_{i\beta}} \delta \bar{F}_{K_{i\beta}}(t_\beta) \quad (C.184)$$

Combining Equations C.181 and C.184 gives

$$\delta \epsilon_{s_{i\beta}}(t_\beta) = \epsilon_{\sigma s_{i\beta}} \sigma_{s\sigma} \sigma_{L\bar{F}_{i\beta}} \delta \bar{F}_{K_{i\beta}}(t_\beta) \quad (C.185)$$

Equation C.185 gives the increments of average strain developed during the β th time increment in the geometric boundaries of the cell resulting from stress. The Equation does not include the contribution of thermal strain.

Equation C.177 and C.185 apply when the i th element is a cell.

Damping Matrix

The damping matrix is found by replacing the stiffness compliance matrix, C_{K_j} , by the damping compliance matrix C_{C_j} , in Equation C.151:

$$\bar{c}_{i(\beta)} = \left(\sum_j V_j \sigma_{F_j}^T C_{C_j} \sigma_{F_j} \right)^{-1}_{i\beta} \quad (C.186)$$

The damping compliance matrix is found by multiplying the elastic stiffness compliance matrix by an experimentally determined constant. See Appendix E.

Equation C.186 applies when the i th element is a cell.

Force Transformation Matrix

The derivation of the force transformation matrix, $F_{\bar{F}}$, involves four sets of force vectors, all statically equivalent. Figure C.21 shows the lumped element forces, previously defined in Section II, and designated \bar{F} . The figure is a copy of Figure 2.7, with some additional information. The corners of the lumped cell are identified as $p_6 r_6 s_6 t_6 p_7 r_7 s_7 t_7$, in accordance with Figure C.12. Also, the thicknesses of the lumped cell at the corners are equal to the cell thicknesses shown in Figure C.11 divided by $\sqrt{3}$, as indicated.

The self-equilibrating lumped element forces are first transformed into equivalent lumped forces at the true element boundaries. These forces, also self-equilibrating are defined as shown in Figure C.22. The figure also shows notation. The shear panel K factors are computed from panel geometry, and static equilibrium.

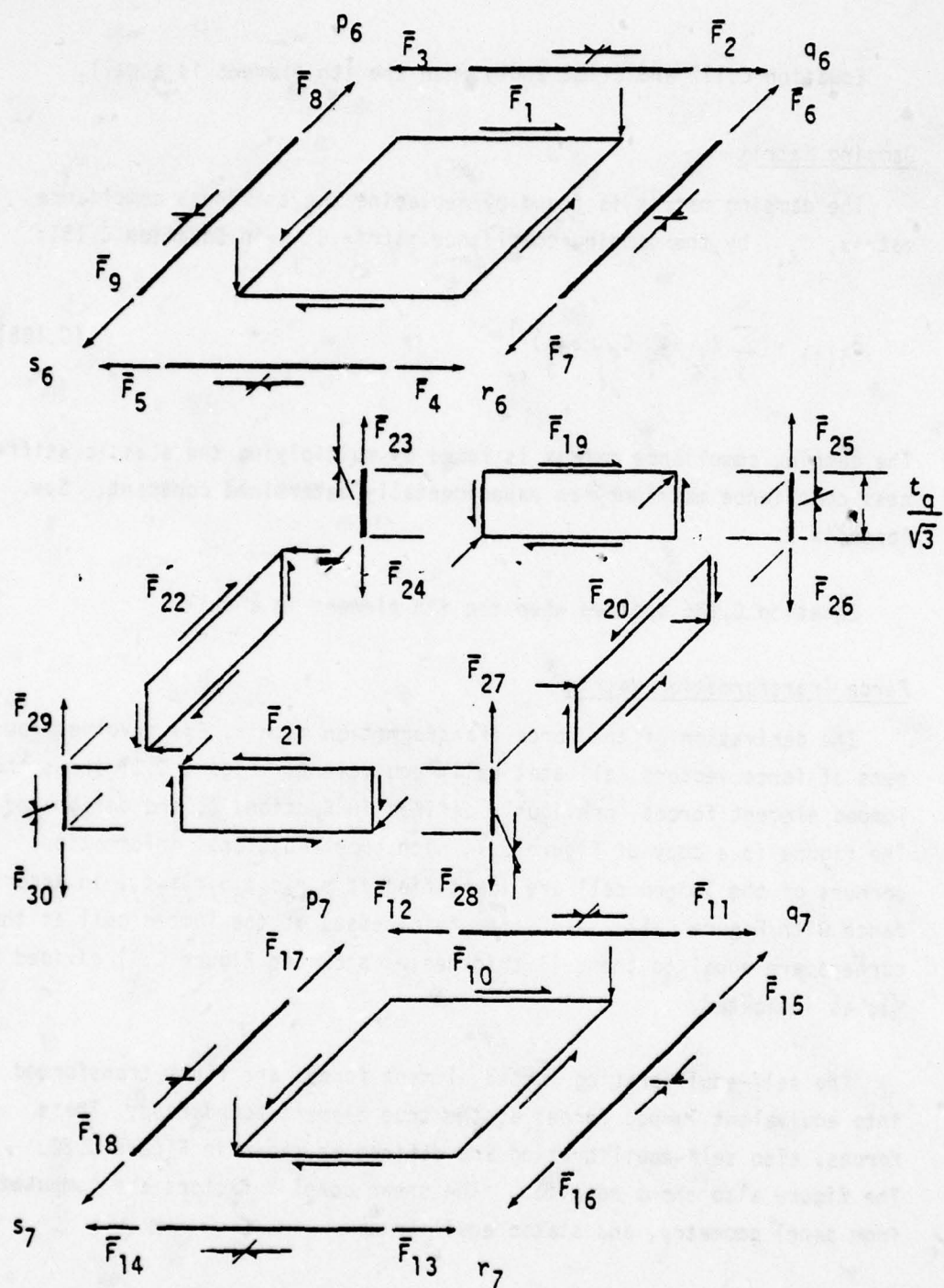


Figure C.21 Cell Lumped Element Forces.

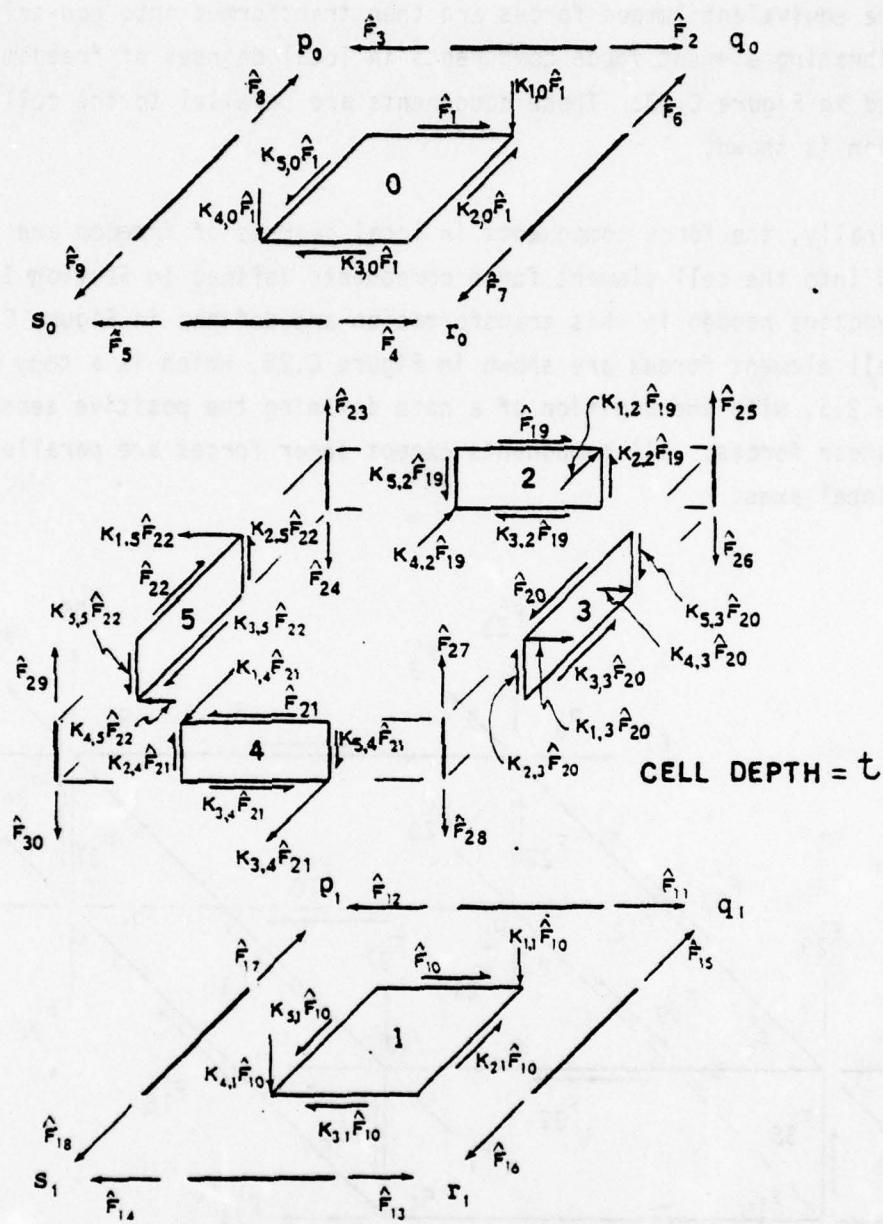


Figure C.22 Equivalent Lumped Element Forces in True Geometric Boundaries.

The equivalent lumped forces are then transformed into non-self-equilibrating element force components in local degrees of freedom, as defined in Figure C.23. These components are parallel to the cell edges. Notation is shown.

Finally, the force components in local degrees of freedom are transformed into the cell element force components defined in Section II. Unit vectors needed in this transformation are defined in Figure C.24. The cell element forces are shown in Figure C.25, which is a copy of Figure 2.5, with the addition of a note defining the positive sense of edge shear forces. All components except shear forces are parallel to the global axes.

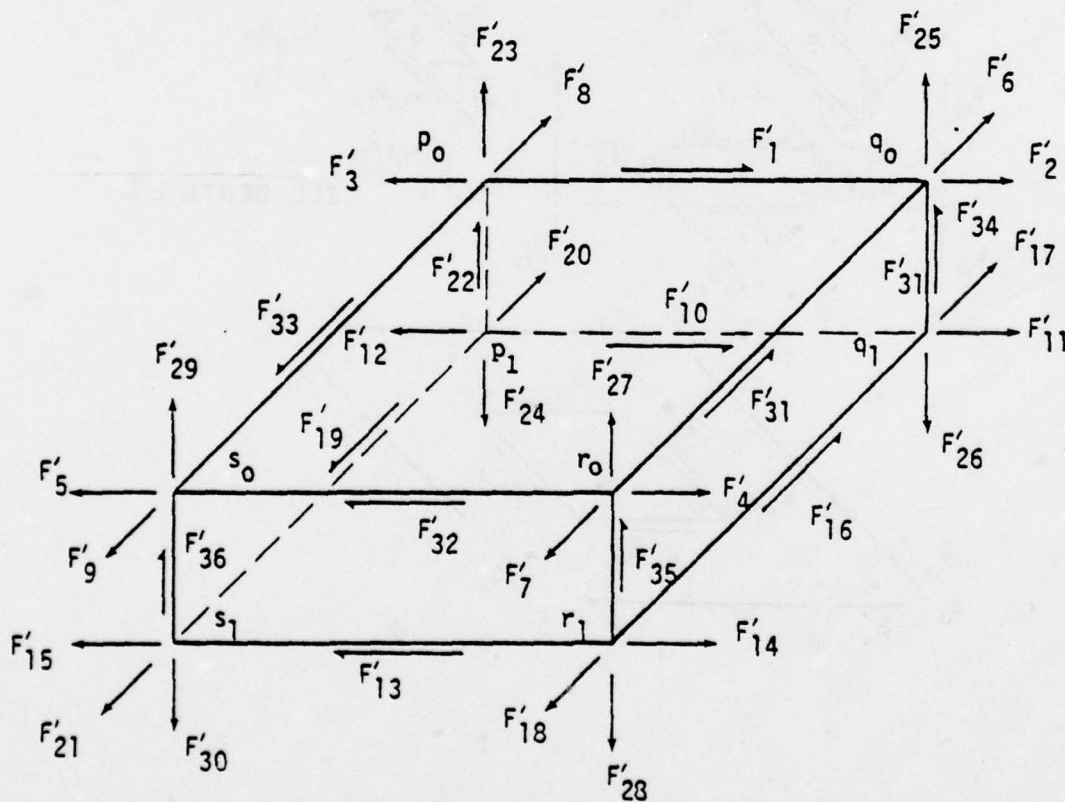


Figure C.23 Cell Element Forces in Local Degrees of Freedom.

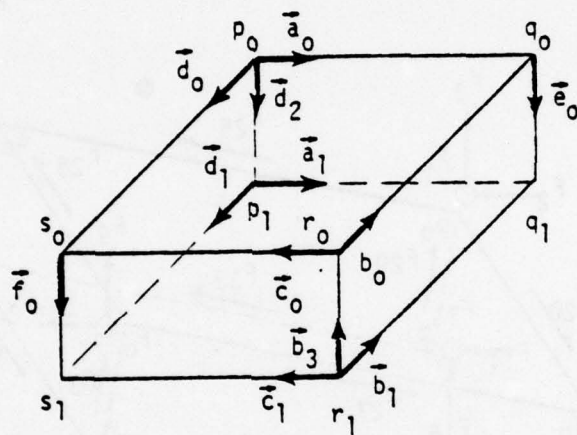


Figure C.24 Unit Edge Vectors.

Note: The positive sense for shear node forces is from the lower to the higher numbered joint, not necessarily as shown.

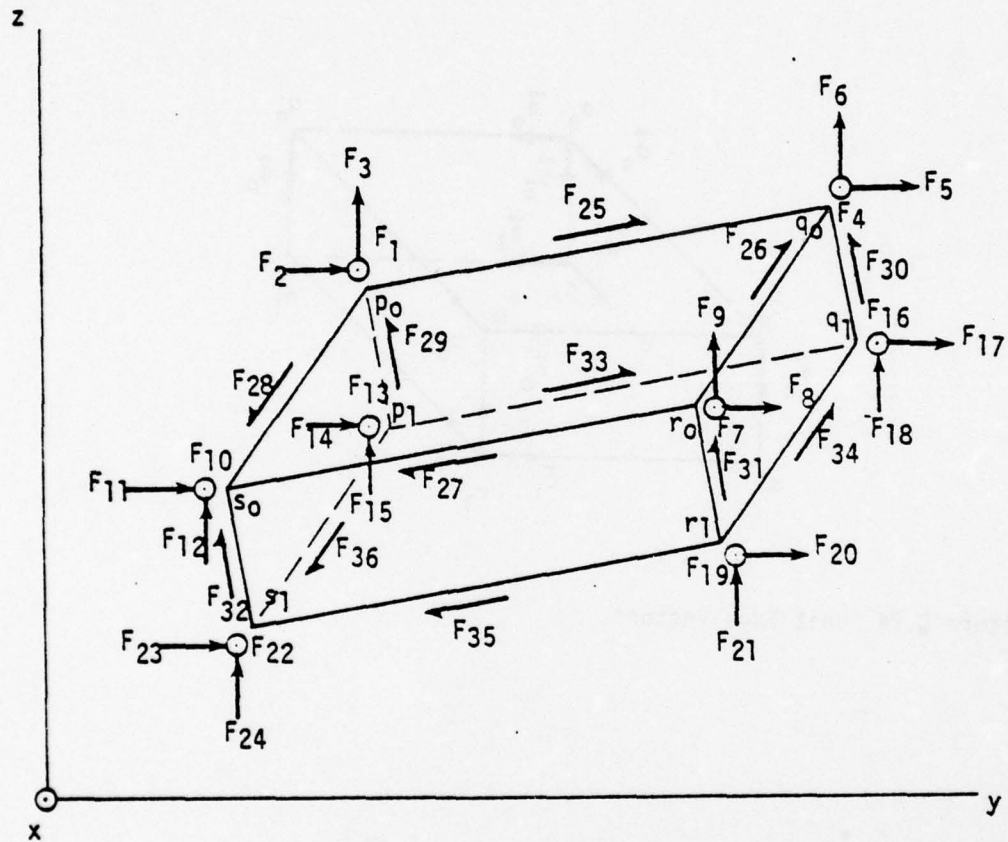


Figure C.25 Cell Element Forces in Global Degrees of Freedom.

The three transformations among the four sets of components described in preceding paragraphs are, for the i th element:

$$\hat{F}_i(t) = \hat{F}_{\bar{F}_i} \bar{F}_i(t) \quad (C.187)$$

$$F'_i(t) = F'_{\hat{F}_i}(t) \hat{F}_i(t) \quad (C.188)$$

$$F_i(t) = F_{F'_i}(t) F'_i(t) \quad (C.189)$$

where the matrices $\bar{F}_i(t)$ and $F_i(t)$ are as defined in Section II, and

$\hat{F}_i(t)$ = a column matrix of equivalent self-equilibrating lumped element forces in the true geometric boundary of the i th element at time t ,

$F'(t)$ = a column matrix of non-self-equilibrating element forces in the local degrees of freedom of the i th element at time t .

also

$\hat{F}_{\bar{F}_i}(t)$ = a square matrix of \hat{F} components resulting from unit values of the \bar{F} components for the i th element at time t ,

$F'_{\hat{F}_i}(t)$ = a rectangular matrix of F' components resulting from unit values of the \hat{F} components for the i th element at time t ,

$F_{F'_i}(t)$ = a square matrix of F components resulting from unit values of the F' components for the i th element at time t .

Combining Equations C.187, C.188 and C.189 gives

$$F_i(t) = F_{\bar{F}_i}(t) \bar{F}_i(t) \quad (C.189.1)$$

$$\text{where } F_{\bar{F}_i}(t) = F_{F_i}'(t) \hat{F}_{\bar{F}_i}(t) \hat{F}_{\bar{F}_i} \quad (C.189.2)$$

The elements of the $\hat{F}_{\bar{F}}$ matrix are given in Table C.5. The symbols β and γ are defined in Equations C.100 and C.101. The symbol α is defined as

$$\alpha = \beta + \gamma = \frac{3 + \sqrt{3}}{6} \quad (C.190)$$

The transformation of Equation C.187 implies the existence of a simple linkage joining the \bar{F} and \hat{F} forces, consisting of bars approximately normal to surfaces 0 and 1 of Figure C.22, at the element corners, and at the shear nodes. For example, Equation C.187 is equivalent to a set of 30 scalar equations. The first equation of the set is, from Equation C.187, and Table C.5,

$$\hat{F}_1 = \alpha \bar{F}_1 + \beta \bar{F}_{10} \quad (C.191)$$

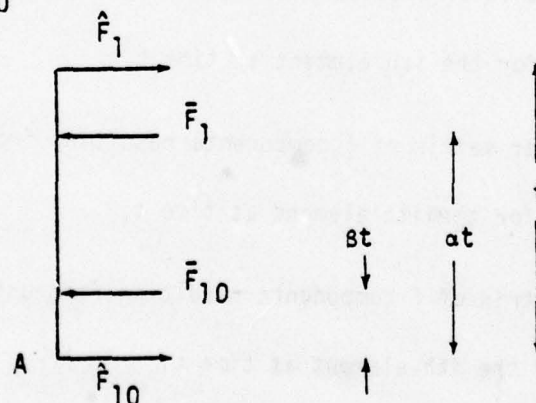


Figure C.26 Implied Linkage Joining \hat{F} and \bar{F} Forces.

TABLE C.5. THE MATRIX \hat{F}_F FOR CELL ELEMENTS

α α α α α α α α	β β β β β β β β		
β β β β β β β β	α α α α α α α α		
		γ γ γ γ	
			1 1 1 1 1 1 1

Figure C.26 shows a bar joining the forces \hat{F}_1 and \hat{F}_{10} , and \bar{F}_1 and \bar{F}_{10} reversed (see Figures C.21 and C.22). Taking moments about point A gives Equation C.191.

The same physical interpretation applies to the first 18 rows of $\hat{F}_{\bar{F}}$. This interpretation also applied to rows 19, 20, 21 and 22, which contain the factor γ , when the surfaces 2, 3, 4 and 5 of Figure C.22 are rectangles or parallelograms, so that $K_{3,2} = 1$. When this is not the case, some other more complicated linkage, involving other forces, must be implied. Note, however, that $\hat{F}_{\bar{F}}$ relates two self-equilibrating sets of forces, so that the bars and shear panels are always in equilibrium.

The last eight rows of $\hat{F}_{\bar{F}}$ equate \hat{F}_{23} and \bar{F}_{23} , \hat{F}_{24} and \bar{F}_{24} , and so on, for all forces approximately normal to surfaces 0 and 1.

The justification of the $\hat{F}_{\bar{F}}$ transformation is that it leads to correct displacements for the nine elementary loadings described in Section III.

The elements of the $F_{\bar{F}}$ matrix are given in Table C.6. This matrix is easily derived by inspection of Figures C.22 and C.23. Rows corresponding to F' vectors that are shear forces (row numbers 1, 10, 13, 16, 19, 22, 31, 32, 33, 34, 35 and 36) can be derived by considering the equilibrium of the twelve axially loaded bars shown in Figure C.22, subjected to the \hat{F} and F' forces. The remaining rows are similarly derived by considering the equilibrium of joints.

The elements of matrix $F_{F'}$ are given in Table C.7. The purpose of this transformation matrix is to resolve the F' components acting at the corners of the cell into components parallel to the global axes. The matrix can be derived by inspection of Figures C.23, C.24 and C.25.

In the matrix $F_{F'}$, a_{0_x} , a_{0_y} , a_{0_z} = the components of the unit vector \bar{a}_0 , referred to the global coordinates. The components of the other

TABLE C.6 THE MATRIX F'_F FOR CELL ELEMENTS

[illegible]

[illegible]

unit vectors in Figure C.24 are similarly represented. The g factors in F_F are introduced to account for the method of defining the positive sense of the F shear forces, as noted in Figure C.25. These factors are defined as follows:

$$\begin{array}{lll}
 g_1 = 1 & \text{if} & p_0 < q_0 \\
 g_2 = 1 & \text{if} & r_0 < q_0 \\
 g_3 = 1 & \text{if} & r_0 < s_0 \\
 g_4 = 1 & \text{if} & p_0 < s_0 \\
 g_5 = 1 & \text{if} & p_1 < p_0 \\
 g_6 = 1 & \text{if} & q_1 < q_0 \\
 g_7 = 1 & \text{if} & r_1 < r_0 \\
 g_8 = 1 & \text{if} & s_1 < s_0 \\
 g_9 = 1 & \text{if} & p_1 < q_1 \\
 g_{10} = 1 & \text{if} & r_1 < q_1 \\
 g_{11} = 1 & \text{if} & r_1 < s_1 \\
 g_{12} = 1 & \text{if} & p_1 < s_1
 \end{array} \quad (C.192)$$

Otherwise, the g factors are equal to -1.

Mass Matrix

Reference 1 gives a mass matrix for a parallelepiped. Employing this matrix for the i th element gives

[illegible]

... (C.193)

where ρ_i , V_i = mass density and volume of the i th element.

Equation C.193 applies when the i th element is a cell.

POINT MASS ELEMENT

This element is a particle having three components of force and displacement parallel to the global axes, as shown in Figure C.26.

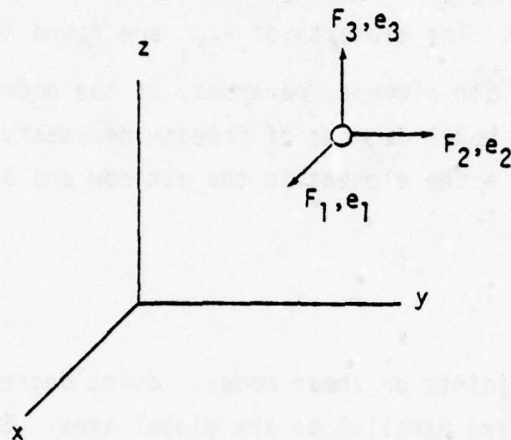


Figure C.26 Point Mass Element.

The point mass has zero stiffness and damping, therefore the stiffness, unassembled deformation and damping matrices for the element are null. The mass matrix is

$$m_i = m_p \begin{bmatrix} 1 & 0 & 0 \\ 0 & 1 & 0 \\ 0 & 0 & 1 \end{bmatrix}, \quad (C.194)$$

where m_p is the mass of the element.

Equation C.194 applies when the i th element is a point mass.

ADDITIONAL FORCE TRANSFORMATIONS

The transformations P_{TF_i} and P_{UPT} , defined in Section II, are derived.

The P_{TF_i} Transformation

As defined in Section II, P_{TF_i} is a rectangular matrix of components in the nodal degrees of freedom resulting from unit values of the element forces of the i th element. The elements of P_{TF_i} are found by applying the element forces of the i th element, reversed, to the nodes, and then finding components in the nodal degrees of freedom necessary to balance these forces. Let $P_{TF_i \alpha\beta}$ = the element in the α th row and β th column of

P_{TF_i} .

The nodes are either joints or shear nodes. Joint degrees of freedom and joint element forces are parallel to the global axes. Shear node degrees of freedom and shear element forces are parallel to bars and to the edges of membranes and cells. Therefore

$P_{TF_i \alpha\beta}$ is equal to -1 when the α th nodal displacement vector coincides with the β th element force vector of the i th element. Otherwise $P_{TF_i \alpha\beta}$ is zero.

The P_{UPT} Transformation

The column matrices $P_T(t)$, $P_U(t)$ and $R(t)$ are defined in Section II. The components in the nodal degrees of freedom, $P_T(t)$, can be expressed in terms of the components in the unconstrained degrees of freedom, $P_U(t)$, and the reactions, $R(t)$, by the equation

$$P_T(t) = \left[P_{TPU} \mid P_{TR} \right] \begin{Bmatrix} P_U(t) \\ R(t) \end{Bmatrix} \quad (C.195)$$

where

P_{TPU} , P_{TR} = rectangular matrices of components in the nodal degrees of freedom of unit values of the components in the unconstrained degrees of freedom, and of the reaction.

The matrix P_{TPU} is Boolean (consisting of 1's and 0's), since the unconstrained degrees of freedom are all parallel to nodal degrees of freedom. The matrix P_{TR} contains direction cosines of the reactions. The matrix $\begin{bmatrix} P_{TPU} & P_{TR} \end{bmatrix}$ is square and nonsingular. Therefore, from Equation C.195,

$$\begin{Bmatrix} P_U(t) \\ R(t) \end{Bmatrix} = \begin{bmatrix} P_{TPU} & P_{TR} \end{bmatrix}^{-1} P_T(t) \quad (C.196)$$

Comparing equation C.196 with Equation 3 shows that the matrix P_{UPT} is equal to a matrix formed from the first n_U rows of $\begin{bmatrix} P_{TPU} & P_{TR} \end{bmatrix}^{-1}$, where n_U is the number of unconstrained degrees of freedom.

Thus, P_{UPT} can be calculated from the direction cosines of the reactions. The matrix $\begin{bmatrix} P_{TPU} & P_{TR} \end{bmatrix}$ is a large matrix, but it very sparse. The inverse can be found by inverting partitions no larger than 3×3 , and this need be done only for joints that have inclined reactions.

APPENDIX D
FICTITIOUS FORCES AND DEFORMATIONS

LIST OF SYMBOLS FOR APPENDIX D

Symbols appearing in Appendix D not defined in this list are defined in the list at the front of the report

\bar{A}	Panel area
a'	a when $\bar{F} > 0$, b when $\bar{F} < 0$
a, b	Shear panel dimensions
A, B, C, D	Corners of shear panel
A, B, C, D	(Subscripts). Denote coordinates of shear panel corners
b_1	$4ab$
b_2	$b+a$
b_3	$b-a$
$b_4(u)$	b_3+4u
c_2, c_4	a, b
d	Preceding a variable, indicates a differential
$d\bar{e}$	Column matrix of differential displacements of dummy normal bar forces
$\dot{\bar{e}}$	Column matrix of rates of displacement of fictitious forces
$\dot{\bar{e}}_k$	Rate of displacement of k th fictitious force
\bar{e}_u	Column matrix of displacements of fictitious moments per unit shear panel area
\bar{e}_{03}	Normal distance from point A to the xy plane at beginning of increment
\bar{F}	Column matrix of dummy normal bar force

LIST OF SYMBOLS FOR APPENDIX D (Continued)

$\bar{\bar{F}}$	Column matrix of fictitious forces resulting from a unit value of the lumped element force
$\bar{\bar{F}}_U$	Column matrix of fictitious moments per unit shear panel area resulting from a unit shear flow
\bar{F}_K	Lumped element force
$\bar{\bar{F}}_K$	Column matrix of fictitious forces
\bar{F}_{KU}	Q, shear flow
$\bar{\bar{F}}_{KU}$	Column matrix of fictitious moments per unit shear panel area
$\bar{\bar{F}}_M$	Rectangular matrix of dummy normal bar forces resulting from unit dummy moments
$\bar{\bar{F}}_n$	nth fictitious force
\bar{f}_n	Value of the nth shear panel force at the end of the increment, that would exist if the panel were flat and coincident with the xy plane at the beginning of the increment
\bar{f}_{no}	Value of \bar{f}_n resulting from displacing the flat panel into its deformed position at the beginning of the increment
\bar{F}_S, \bar{F}_A	Symmetric and antisymmetric lumped bar forces
$f(u)$	Any function of the variable u, and any other independent variables
\bar{F}_1, \bar{F}_2	Dummy forces applied normal to bar at O end
\bar{F}_3, \bar{F}_4	Dummy forces applied normal to bar at B end
$\bar{g}, \bar{h}, \bar{k}$	Unit vectors parallel to the \bar{x}, \bar{y} and z axes

LIST OF SYMBOLS FOR APPENDIX D (Continued)

$\bar{g}_2, \bar{h}_2, \bar{k}_2$	The unit vectors \bar{g} , \bar{h} and \bar{k} after the rotations $\theta_{\bar{y}}$ and $\theta_{\bar{x}1}$
i	(Subscript). Indicates element number
J_k	$\int_0^b \int_0^a b_4^k(u) d\eta d\zeta \quad k = 0, 1, 2, 3, 4$
\bar{k}_1	The unit vector \bar{k} after the rotation $\theta_{\bar{y}}$
l	Bar length
l_0	Projection of bar length upon position at beginning of increment
$l(\bar{s})$	Average bar length during s th increment
M	Column matrix of dummy bar moments
m_r	Functions of panel dimensions and skew angle, $r = 1, 2 \dots .22$
M_η, M_ζ	Moments about the η and ζ axes
m_η, m_ζ	Fictitious moments about η and ζ per unit shear panel area
M_1, M_2	Dummy moments applied to bar corresponding to e_1 and e_2
\bar{m}_5, \bar{m}_7	Functions of panel dimensions and skew angle
$n_{k,1}, n_{k,2}, n_{k,3}$	} First, second and third order contributions to the k th fictitious force
n_γ	The γ th fictitious panel force. $\gamma = 1, 2, 3, 4$
$n_{\gamma k}$	First, second and third order contributions to n_γ . $k = 1, 2, 3$

LIST OF SYMBOLS FOR APPENDIX D (Continued)

\bar{n}_3	$\delta W_{a1}(\bar{a}_1, 0, 0)$
\bar{n}_3	$\Lambda_Q(\bar{a}_1, \bar{a}_2, \bar{a}_3)$
$\bar{n}_{3k}, \bar{n}_{3k}$	First, second and third order contributions to \bar{n}_3 , $\bar{n}_3 \cdot k = 1, 2, 3$
p, q, r, s	Joint numbers at corners of shear panel
P_{UF}	Rectangular matrix of components in the unconstrained degrees of freedom of unit values of the dummy normal bar forces
$P_{UF}(\bar{s})$	Average value of P_{UF} during the s th increment
$P_{UF}(\bar{s})$	Average fictitious force transformation, s th increment
Q	Panel shear flow
\bar{r}	$a' \delta \bar{e}_f$
\bar{r}_1, \bar{r}_2	First and second order contributions to \bar{r}
r_2	Second order contribution to the fictitious deformation
t	Time
t_{s-1}	Time at beginning of s th increment
u	$\eta - \zeta$
u_2	$\bar{u}_2 + \bar{u}_2$
\bar{u}_2	$\delta \bar{\Lambda}_2(\bar{a}_1, \bar{a}_2, \bar{a}_3)$
\bar{u}_2	$\Lambda_2(\bar{a}_1, \bar{a}_2, \bar{a}_3)$
u_4	$\bar{u}_4 + \bar{u}_4$

LIST OF SYMBOLS FOR APPENDIX D (Continued)

\bar{u}_4	$\delta \bar{\Lambda}_4(\bar{a}_1, \bar{a}_2, \bar{a}_3)$
\bar{u}_4	$\Lambda_4(\bar{a}_1, \bar{a}_2, \bar{a}_3)$
$\bar{u}_{4k}, \bar{u}_{2k}$ $\bar{u}_{4k}, \bar{u}_{2k}$ u_{4k}, u_{2k}	$\left. \begin{array}{l} \\ \\ \end{array} \right\}$ First, second and third order contributions to $\bar{u}_4, \bar{u}_2, \bar{u}_4, \bar{u}_2, u_4, u_2$. $k = 1, 2, 3$
W	Shear panel potential energy
w	Virtual displacement of panel parallel to z
\bar{w}	Panel displacement parallel to z
$w_e, w_{\bar{y}R}$ $w_{\bar{x}R}, w_r$	$\left. \begin{array}{l} \\ \\ \end{array} \right\}$ Panel displacement modes
$w_{e\bar{x}}, w_{e\bar{y}}$	$\partial w_e / \partial \bar{x}, \partial w_e / \partial \bar{y}$
$w_{\bar{x}}, w_{\bar{y}}$	$\partial w / \partial \bar{x}, \partial w / \partial \bar{y}$
W_{ap}	Work done in fictitious distributed rotational springs, resulting from a unit value of the displacement parameter a_p
x, y, z	Local element coordinates
\bar{x}, \bar{y} \bar{x}, \bar{y}	$\left. \begin{array}{l} \\ \\ \end{array} \right\}$ Cartesian coordinate axes for shear panel. \bar{x} bisects θ . (Subscripts). Indicate components of a vector parallel to \bar{x} and \bar{y} axes
\bar{x}_1	Rotated position of \bar{x} axis
a_1, a_2 a_3, a_4	$\left. \begin{array}{l} \\ \\ \end{array} \right\}$ Virtual values of the panel displacement parameters

LIST OF SYMBOLS FOR APPENDIX D (Continued)

\bar{a}_1, \bar{a}_2 \bar{a}_3, \bar{a}_4	} }	Panel displacement parameters
$a_{1,0}$	\bar{e}_{03}	
β		(Subscript). Indicates increment number
Δ		Column matrix of displacements in the unconstrained degrees of freedom
$\dot{\Delta}$		Rate of change of Δ
$\delta \bar{e}$		Column matrix of displacements of dummy normal bar force developed during a time increment
$\delta \bar{e}_f$		Fictitious deformation corresponding to lumped element force
$\delta \bar{e}_k$		Displacement of kth dummy normal bar force developed during a time increment
$\delta \bar{e}_n$		Displacement of nth fictitious force developed during time increment
δl		Difference between bar length and its projection on initial bar position
δW_{a1}		$W_{a1}(\bar{a}_1, 0, 0) - W_{a1}(\bar{a}_{1,0}, 0, 0)$
$\delta \bar{a}_1$		$\bar{a}_1 - \bar{a}_{1,0}$
$\delta \Delta$		Change of Δ developed during an increment
$\delta \zeta_{\bar{y}}$		$\zeta_{\bar{y}} - \zeta_{\bar{y}0}$
$\delta \eta_{\bar{y}}$		$\eta_{\bar{y}} - \eta_{\bar{y}0}$
$\delta \bar{\Lambda}_2$		$\bar{\Lambda}_2(\bar{a}_1, \bar{a}_2, \bar{a}_3) - \bar{\Lambda}_2(\bar{a}_{1,0}, 0, 0)$

LIST OF SYMBOLS FOR APPENDIX D (Continued)

$\delta \bar{A}_4$	$\bar{A}_4(\bar{a}_1, \bar{a}_2, \bar{a}_3) - \bar{A}_4(\bar{a}_1, 0, 0)$
$\zeta_{\bar{y}}$	$\eta_{\bar{y}} + \bar{a}_2$
η, ζ	Oblique coordinates for shear panel
$\eta_{\bar{x}}$	$\theta_{\bar{x}1}(\bar{a}_1, 0, 0)$
$\eta_{\bar{y}}$	$\theta_{\bar{y}}(\bar{a}_1, 0, 0)$
$\eta_{\bar{y}0}, \zeta_{\bar{y}0}$	Values of $\eta_{\bar{y}}$ and $\zeta_{\bar{y}}$ corresponding to $\bar{a}_1 = \bar{a}_1, 0$, $\bar{a}_2 = \bar{a}_3 = \bar{a}_4 = 0$
θ	Shear panel skew angle
$\bar{\theta}$	Column matrix of bar rotations θ_1 and θ_2
θ_x, θ_z	Angles which a bar makes with the x and z axes
$\dot{\theta}_x, \dot{\theta}_z$	Rates of change of θ_x and θ_z
$\theta_{\bar{x}1}$	Rotation angle of panel about \bar{x}_1 axis
$\theta_{\bar{y}}$	Angle of rotation of panel about \bar{y} axis
$\theta_{\eta}, \theta_{\zeta}$	Rotations corresponding to M_{η}, M_{ζ}
θ_1	$(\pi/2) - \theta_z$
θ_2	$(\pi/2) - \theta_x$
Λ_Q	$\int_0^{\bar{a}_2} \frac{\partial}{\partial \bar{a}_1} W_{a2}(\bar{a}_1, a_2, 0) da_2 + \int_0^{\bar{a}_3} \frac{\partial}{\partial \bar{a}_1} W_{a3}(\bar{a}_1, \bar{a}_2, a_3) da_3$
Λ_R	$\int_0^{\bar{a}_3} \frac{\partial}{\partial \bar{a}_2} W_{a3}(\bar{a}_1, \bar{a}_2, a_3) da_3$
Λ_2	$-\frac{\bar{y}_3}{\bar{A}} \Lambda_R(\bar{a}_1, \bar{a}_2, \bar{a}_3)$

LIST OF SYMBOLS FOR APPENDIX D (Continued)

$\bar{\Lambda}_2$	$-\frac{\bar{y}_B}{\bar{A}} W_{\alpha 2}(\bar{\alpha}_1, \bar{\alpha}_2, 0) - \frac{\bar{x}_B}{\bar{A}} W_{\alpha 3}(\bar{\alpha}_1, \bar{\alpha}_2, \bar{\alpha}_3)$
$\bar{\Lambda}_4$	$\frac{\bar{y}_D}{\bar{A}} \Lambda_R(\bar{\alpha}_1, \bar{\alpha}_2, \bar{\alpha}_3)$
$\bar{\Lambda}_4$	$\frac{\bar{y}_D}{\bar{A}} W_{\alpha 2}(\bar{\alpha}_1, \bar{\alpha}_2, 0) + \frac{\bar{x}_D}{\bar{A}} W_3(\bar{\alpha}_1, \bar{\alpha}_2, \bar{\alpha}_3)$
\bar{u}, \bar{v}	Unit vectors parallel to the η and ζ axes
\bar{u}_2, \bar{v}_2	The unit vectors \bar{u} and \bar{v} after the rotations $\theta_{\bar{y}}$ and $\theta_{\bar{x}1}$
ξ	Half skew angle
τ	Length of time increment
$\phi_2(\alpha_1, \alpha_2, 0)$	$\sin \theta_{\bar{y}}$
$\phi_3(\alpha_1, \alpha_2, \alpha_3)$	$\cos \theta_{\bar{y}} \sin \theta_{\bar{x}1}$
ψ_f	$(\theta_{\bar{x}1}^2 \sin^2 \xi - \theta_{\bar{y}}^2 \cos^2 \xi)/a'$
$\psi(\bar{\alpha}_1, 0, 0)$	$-2Q [w_{e,\bar{x}} \phi_2(\bar{\alpha}_1, 0, 0) \cos^2 \xi + w_{e,\bar{y}} \phi_3(\bar{\alpha}_1, 0, 0) \sin^2 \xi]$
ψ_2	$\frac{Q}{a} [-\phi_2(\bar{\alpha}_1, \bar{\alpha}_2, 0) \cos \xi + \phi_3(\bar{\alpha}_1, \bar{\alpha}_2, \bar{\alpha}_3) \sin \xi]$
ψ_4	$\frac{Q}{b} [-\phi_2(\bar{\alpha}_1, \bar{\alpha}_2, 0) \cos \xi - \phi_3(\bar{\alpha}_1, \bar{\alpha}_2, \bar{\alpha}_3) \sin \xi]$

This Appendix presents fictitious forces and deformations for axially loaded bars and shear panels.

AXIALLY LOADED BARS

$$\begin{array}{c}
 \bar{F}_1 \quad \xleftarrow{\quad \xrightarrow{\bar{F}_2 - \bar{F}_1} \quad} \quad \bar{F}_2 \\
 \\
 = \frac{1}{2} (\bar{F}_1 + \bar{F}_2) \quad \xleftarrow{\quad \xrightarrow{\bar{F}_2 - \bar{F}_1} \quad} \quad \frac{1}{2} (\bar{F}_1 + \bar{F}_2) = \bar{F}_S \\
 + \frac{1}{2} (\bar{F}_1 - \bar{F}_2) \quad \xleftarrow{\quad \xrightarrow{\bar{F}_2 - \bar{F}_1} \quad} \quad \frac{1}{2} (\bar{F}_1 - \bar{F}_2) = \bar{F}_A
 \end{array}$$

Figure D.1. Symmetric and antisymmetric bar forces.

Figure D.1 shows the lumped element forces on an axially loaded bar, defined as in Figure 2.2, broken into symmetric and antisymmetric components, \bar{F}_S and \bar{F}_A . The antisymmetric component \bar{F}_A is not expected to contribute significantly to the large displacement problem. For example, consider a beam-column. If such a member is in compression along its entire length, lateral displacements are magnified. If the member is in tension along its entire length, lateral displacements are reduced. But, if the member is partly in compression and partly in tension, the nonlinear effect tends to be nullified. Therefore, assume that the nonlinear effect of \bar{F}_A is negligible, and base the calculation of fictitious forces on \bar{F}_S .

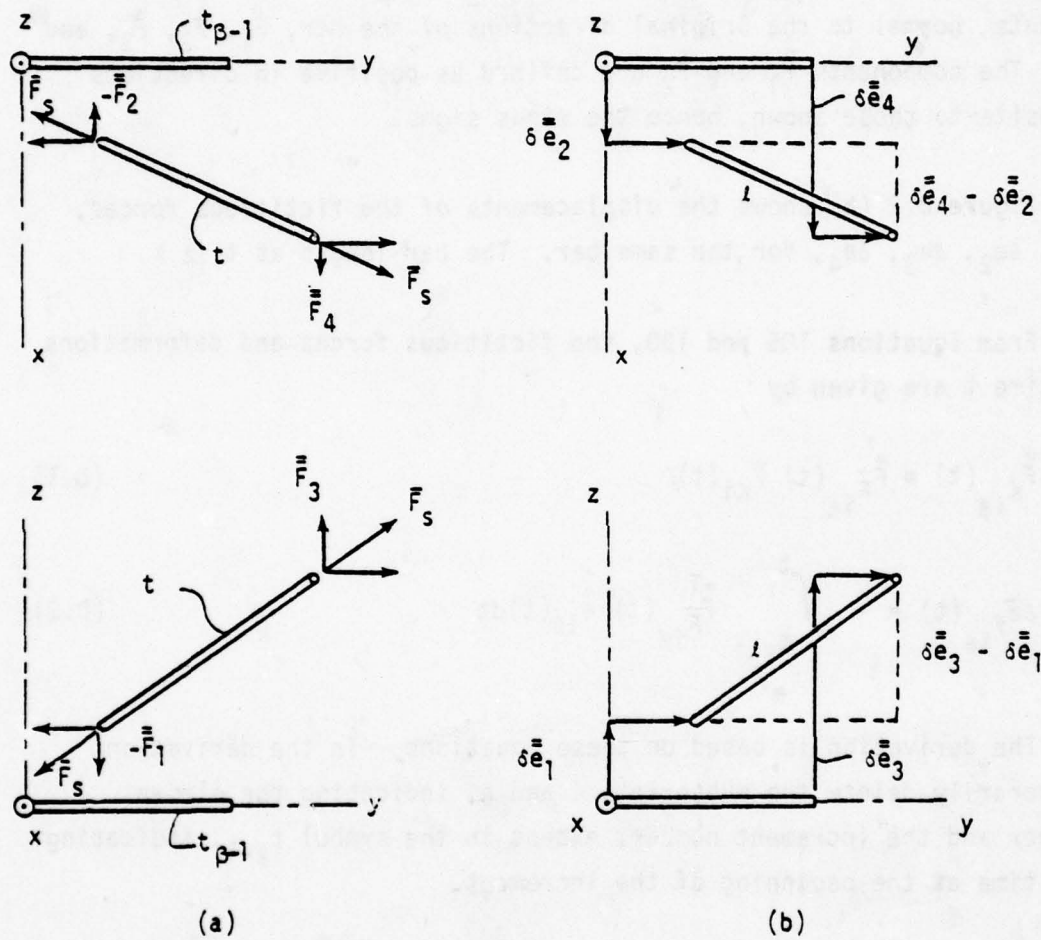


Figure D.2 Axially loaded bar forces and displacements.

Figure D.2 (a) shows two views of an axially loaded bar at time $t_{\beta-1}$, at the beginning of the β^{th} increment; and at time t , any time in the increment. A local reference frame is shown, with the y -axis coinciding with the bar at $t_{\beta-1}$. The x and z axes can be any two orthogonal axes also orthogonal to y . The figure shows the symmetric component of the lumped element forces, \bar{F}_S , and the fictitious components, normal to the original directions of the bar, \bar{F}_1 , \bar{F}_2 , \bar{F}_3 , and \bar{F}_4 . The components \bar{F}_1 and \bar{F}_2 are defined as positive in directions opposite to those shown, hence the minus signs.

Figure D.2 (b) shows the displacements of the fictitious forces, δe_1 , δe_2 , δe_3 , δe_4 , for the same bar. The bar length at t is l .

From Equations 106 and 130, the fictitious forces and deformations at time t are given by

$$\bar{F}_{K_{i\beta}}(t) = \bar{F}_{F_{i\beta}}(t) \bar{F}_{K_i}(t) \quad (D.1)$$

$$\delta \bar{e}_{f_{i\beta}}(t) = - \int_{t_{\beta-1}}^t \bar{F}_{F_{i\beta}}^T(t) \dot{\bar{e}}_{i\beta}(t) dt \quad (D.2)$$

The derivation is based on these equations. In the derivation, temporarily delete the subscripts i and β , indicating the element number and the increment number, except in the symbol $t_{\beta-1}$, indicating the time at the beginning of the increment.

Fictitious Forces, Bars

Let

$\theta_x(t)$, $\theta_z(t)$ = the angles which the bar makes with the x and z axes at time t .

From Figure D.2 (a)

$$\left. \begin{aligned} -\bar{F}_1(t) &= \bar{F}_S(t) \cos \theta_z(t) \\ -\bar{F}_2(t) &= \bar{F}_S(t) \cos \theta_x(t) \\ \bar{F}_3(t) &= \bar{F}_S(t) \cos \theta_z(t) \\ \bar{F}_4(t) &= \bar{F}_S(t) \cos \theta_x(t) \end{aligned} \right\} \quad (D.3)$$

Axially loaded bars are considered to have two lumped element forces, \bar{F}_1 and \bar{F}_2 , as shown in Figure D.1. Discarding the antisymmetric component \bar{F}_A , however, means that the bar can be considered to have only the one lumped force, \bar{F}_S . Therefore, temporarily consider one lumped element force, \bar{F}_S , per bar, to simplify the derivation. From Equations D.3,

$$\begin{Bmatrix} \bar{F}_1(t) \\ \bar{F}_2(t) \\ \bar{F}_3(t) \\ \bar{F}_4(t) \end{Bmatrix} = \begin{Bmatrix} -\cos \theta_z(t) \\ -\cos \theta_x(t) \\ \cos \theta_z(t) \\ \cos \theta_x(t) \end{Bmatrix} \bar{F}_S(t) \quad (D.4)$$

Comparing Equations D.1 and D.4 shows that,

$$\bar{F}_F(t) = \begin{Bmatrix} -\cos \theta_z(t) \\ -\cos \theta_x(t) \\ \cos \theta_z(t) \\ \cos \theta_x(t) \end{Bmatrix} \quad (D.5)$$

Fictitious Deformations, Bars

The matrix of rates of displacement of the fictitious forces can be written,

$$\dot{\bar{\mathbf{e}}}(t) = \begin{Bmatrix} \dot{\bar{e}}_1(t) \\ \dot{\bar{e}}_2(t) \\ \dot{\bar{e}}_3(t) \\ \dot{\bar{e}}_4(t) \end{Bmatrix} \quad (\text{D.6})$$

where the symbols $\dot{\bar{e}}_1$, etc., indicate time derivatives of the displacements shown in Figure D.2 (b).

Substituting $\bar{\mathbf{F}}(t)$ and $\dot{\bar{\mathbf{e}}}(t)$ from Equations D.5 and D.6 into Equation D.2 gives,

$$\delta \bar{e}_f(t) = - \int_{t_{B-1}}^t \left\{ \left[\dot{\bar{e}}_3(t) - \dot{\bar{e}}_1(t) \right] \cos \theta_z(t) + \left[\dot{\bar{e}}_4(t) - \dot{\bar{e}}_2(t) \right] \cos \theta_x(t) \right\} dt \quad (\text{D.7})$$

Now, from Figure D.2 (b),

$$\delta \bar{e}_3(t) - \delta \bar{e}_1(t) = \lambda(t) \cos \theta_z(t) \quad (\text{D.8})$$

$$\delta \bar{e}_4(t) - \delta \bar{e}_2(t) = \lambda(t) \cos \theta_x(t) \quad (\text{D.9})$$

Differentiating Equation D.8 with respect to time gives,

$$\dot{\bar{e}}_3(t) - \dot{\bar{e}}_1(t) = \dot{\lambda}(t) \cos \theta_z(t) - \lambda(t) \sin \theta_z(t) \dot{\theta}_z(t) \quad (\text{D.10})$$

where the dots indicate time derivatives. The first term on the right of Equation D.10 is expected to be very small compared to the second term. Therefore, neglecting this term,

$$\dot{\bar{e}}_3(t) - \dot{\bar{e}}_1(t) = - \lambda(t) \sin \theta_z(t) \dot{\theta}_z(t) \quad (\text{D.11})$$

Similarly, from Equation D.9,

$$\dot{\bar{e}}_4(t) - \dot{\bar{e}}_2(t) = -\lambda(t) \sin \theta_x(t) \dot{\theta}_x(t) \quad (D.12)$$

Combining Equations D.7, D.11 and D.12 gives

$$\begin{aligned} \delta \bar{e}_f(t) = \int_{t_{B-1}}^t \lambda(t) & \left[\sin \theta_z(t) \cos \theta_z(t) \dot{\theta}_z(t) \right. \\ & \left. + \sin \theta_x(t) \cos \theta_x(t) \dot{\theta}_x(t) \right] dt \end{aligned} \quad (D.13)$$

In evaluating the integral of Equation D.13, assume that $\lambda(t)$ can be replaced by its average value during the increment, denoted by $\lambda(\bar{B})$. Also,

$$\left. \begin{aligned} \dot{\theta}_z(t) dt &= d\theta_z \\ \dot{\theta}_x(t) dt &= d\theta_x \end{aligned} \right\} \quad (D.14)$$

Combining Equations D.13 and D.14, and replacing $\lambda(t)$ by $\lambda(\bar{B})$ gives

$$\delta \bar{e}_f(t) = +\lambda(\bar{B}) \int_{\frac{\pi}{2}}^{\theta_z} \sin \theta_z \cos \theta_z d\theta_z + \lambda(\bar{B}) \int_{\frac{\pi}{2}}^{\theta_x} \sin \theta_x \cos \theta_x d\theta_x \quad (D.15)$$

Since $\theta_z = \theta_x = \frac{\pi}{2}$ at $t = t_{B-1}$. Integrating Equation D.15 gives

$$\delta \bar{e}_f(t) = -\frac{1}{2} \lambda(\bar{B}) \left(\cos^2 \theta_z + \cos^2 \theta_x \right) \quad (D.16)$$

A physical interpretation of the fictitious deformation, $\delta \bar{e}_f(t)$, is now given

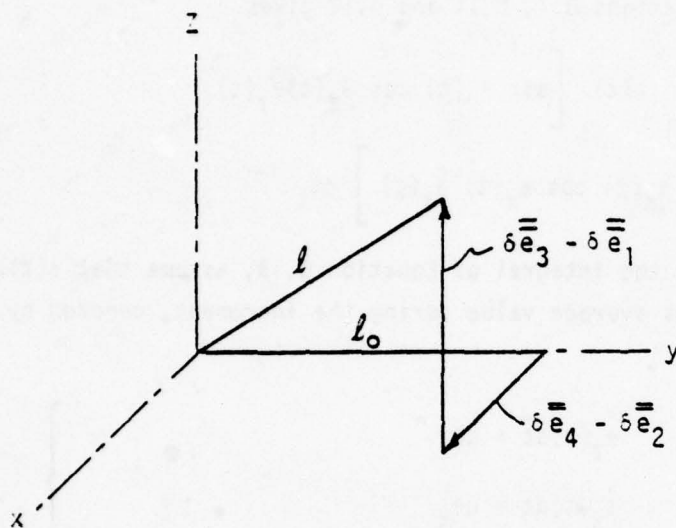


Figure D.3. Displaced bar.

Figure D.3 shows the bar of Figure D.2, translated parallel to itself, so that the lower end of the bar is restored to its initial position at the origin. Let

l_0 = the projection of the bar length onto its initial position
(the y axis)

From Figure D.3

$$l_0^2 + (\delta \bar{e}_3 - \delta \bar{e}_1)^2 + (\delta \bar{e}_4 - \delta \bar{e}_2)^2 = l^2 \quad (D.17)$$

Assume that the length of the bar remains constant and equal to $l_{(\beta)}$ during the motion. Let

δl = the difference between the length of the bar, and the length of the bar projected upon its original position.

Therefore
$$\delta l = l_{(\beta)} - l_0 \quad (D.18)$$

Combining Equations D.8, D.9, D.17, and D.18, and taking $l(t) = l_{(\beta)}$, gives

$$\left[l_{(\beta)} - \delta l \right]^2 + l_{(\beta)}^2 \cos^2 \theta_z + l_{(\beta)}^2 \cos^2 \theta_x = l_{(\beta)}^2 \quad (D.19)$$

Therefore

$$-2l_{(\beta)} \delta l + \delta l^2 + l_{(\beta)}^2 \cos^2 \theta_z + l_{(\beta)}^2 \cos^2 \theta_x = 0 \quad (D.20)$$

The objective in this appendix is to develop a third order approximation for fictitious forces, and a second order approximation for fictitious deformations. This degree of approximation implies that the rotation of the bar is small, and δl is small compared to $l_{(\beta)}$. Therefore the term δl^2 in Equation D.20 can be neglected. Deleting δl^2 from Equation D.20 and solving for δl gives

$$\delta l \approx \frac{1}{2} l_{(\beta)} (\cos^2 \theta_z + \cos^2 \theta_x) \quad (D.21)$$

Comparing Equations D.16 and D.21 shows that the fictitious deformations represents the difference between the length of the bar, and the length of the bar projected upon its initial position.

Evaluation of the Rotation Angles

So far, the simplifying assumptions that have been made concerning geometric nonlinearities are:

1. The term $\bar{F}_{0F_{iB}}(t) - I$ was deleted from Equation 112.
2. The effect of the antisymmetric bar force component, \bar{F}_A , was neglected.
3. The time derivative of the bar length was considered negligible in Equation D.10.
4. The length of the bar was replaced by its average value in the integration of Equation D.13.

From this point, numerous options are open for further development of the theory. A requirement for the selected approach is that it must be feasible for application to shear panels, as well as bars. The approach chosen is to express the fictitious forces and deformations as power series in the angles of rotation of the bar, discarding powers higher than the third. Powers up to the third are thought to be necessary to provide the capability of dealing with post-buckling problems, such as the *Elastica* (Reference 2). Unfortunately, the angles θ_z and θ_x are not suitable for this purpose, since they are equal to $\pi/2$ at the beginning of the increment.

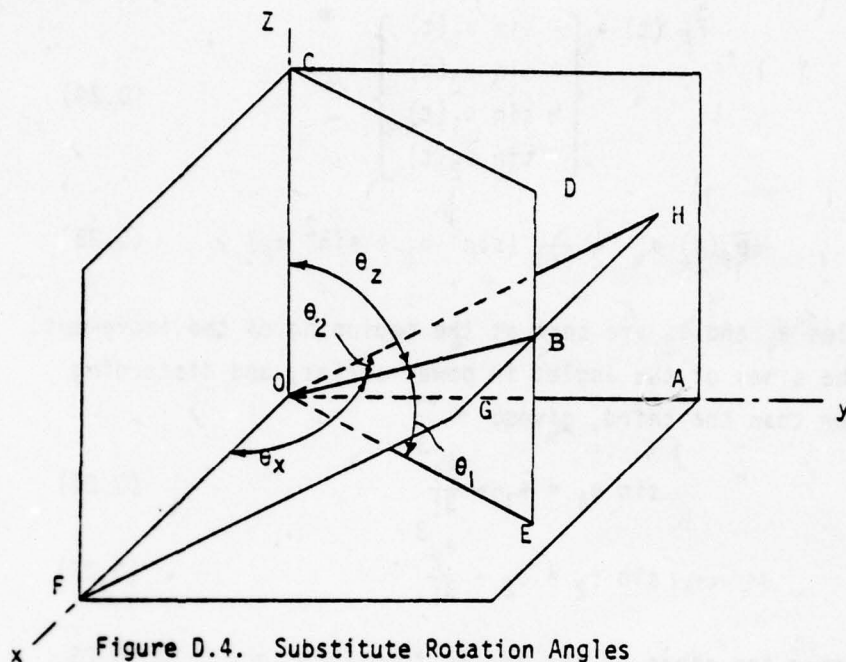


Figure D.4. Substitute Rotation Angles

Figure D.4 shows the reference frame, with the bar in its initial position at OA. Line OB represents the bar in its rotated position, translated so that its lower end is at the origin. CDEO is a plane containing the z axis and the bar. FGHO contains the x axis, and the bar. The figures shows the angles θ_z and θ_x . The angles θ_1 and θ_2 are defined as shown. The plane CDEO is normal to the xy plane, since it contains the z axis.

Therefore,
$$\theta_z = \frac{\pi}{2} - \theta_1 \quad (D.22)$$

Similarly,
$$\theta_x = \frac{\pi}{2} - \theta_2 \quad (D.23)$$

Eliminating θ_z and θ_x from Equation D.5, D.16, D.22 and D.23 gives,

$$\bar{F}_F(t) = \begin{Bmatrix} -\sin \theta_1(t) \\ -\sin \theta_2(t) \\ \sin \theta_1(t) \\ \sin \theta_2(t) \end{Bmatrix} \quad (D.24)$$

and

$$\delta \bar{e}_f(t) = -\frac{1}{2} \lambda(\beta) (\sin^2 \theta_1 + \sin^2 \theta_2) \quad (D.25)$$

The angles θ_1 and θ_2 are zero at the beginning of the increment. Expanding the sines of the angles in power series, and discarding powers higher than the third, gives:

$$\sin \theta_1 = \theta_1 - \frac{\theta_1^3}{3!} \quad (D.26)$$

$$\sin \theta_2 = \theta_2 - \frac{\theta_2^3}{3!} \quad (D.27)$$

Eliminating the sines of the angles from Equations D.24, D.25, D.26, and D.27, and deleting powers higher than the third, gives

$$\bar{F}_F(t) = \begin{Bmatrix} -\theta_1(t) + \frac{1}{6} \theta_1^3(t) \\ -\theta_2(t) + \frac{1}{6} \theta_2^3(t) \\ \theta_1(t) - \frac{1}{6} \theta_1^3(t) \\ \theta_2(t) - \frac{1}{6} \theta_2^3(t) \end{Bmatrix} \quad (D.28)$$

and

$$\delta e_f(t) = -\frac{1}{2} \lambda(\beta) (\theta_1^2 + \theta_2^2). \quad (D.29)$$

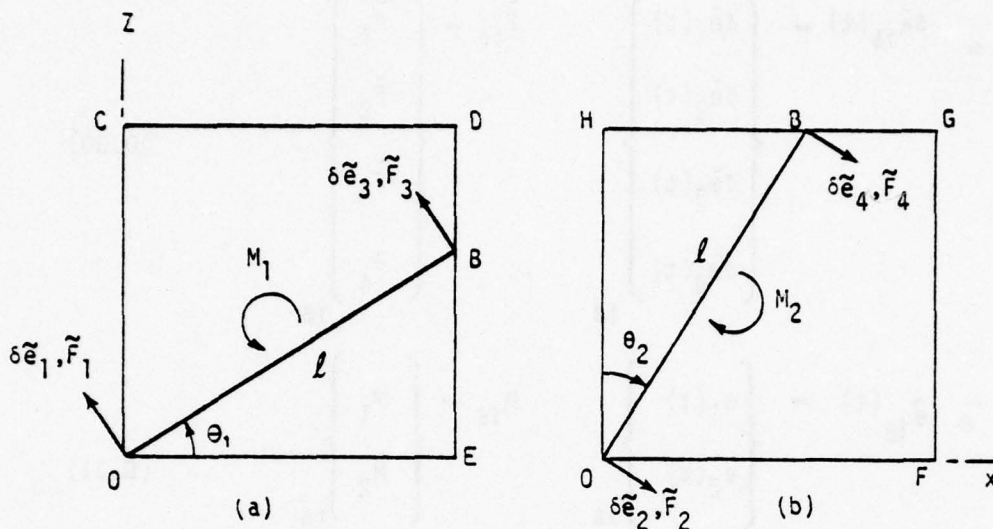


Figure D.5. Dummy moments and normal forces.

Figures D.5 (a) and (b) show views looking directly down on the planes CDEO and FGHO shown in Figure D.4. In Figure D.5 (a), \tilde{F}_1 and \tilde{F}_3 are dummy forces applied normal to the bar at O and B, in the plane CDEO. The forces remain normal to the bar, and in the plane CDEO, as the bar rotates. The corresponding displacements $\delta \tilde{e}_1$ and $\delta \tilde{e}_3$ represent the works done by unit values of \tilde{F}_1 and \tilde{F}_3 when the bar is displaced. The moment M_1 is a dummy moment applied in the plane. The angle θ_1 is the displacement corresponding to this moment, since θ_1 is equal to the work done by a unit value of M_1 during a displacement. The forces \tilde{F}_2 , \tilde{F}_4 and M_2 and the displacements $\delta \tilde{e}_2$, $\delta \tilde{e}_4$ and θ_2 shown in Figure D.5 (b) are similarly defined.

The displacements $\delta \tilde{e}_1$, $\delta \tilde{e}_2$, $\delta \tilde{e}_3$, and $\delta \tilde{e}_4$ are first calculated, and the rotations θ_1 and θ_2 are calculated from these displacements.

Define the following matrices applicable to the i^{th} bar element, and the β^{th} increment:

$$\delta \tilde{e}_{i\beta}(t) = \begin{Bmatrix} \delta \tilde{e}_1(t) \\ \delta \tilde{e}_2(t) \\ \delta \tilde{e}_3(t) \\ \delta \tilde{e}_4(t) \end{Bmatrix}_{i\beta} \quad \tilde{F}_{i\beta} = \begin{Bmatrix} \tilde{F}_1 \\ \tilde{F}_2 \\ \tilde{F}_3 \\ \tilde{F}_4 \end{Bmatrix}_{i\beta} \quad (D.30)$$

$$\bar{\theta}_{i\beta}(t) = \begin{Bmatrix} \theta_1(t) \\ \theta_2(t) \end{Bmatrix}_{i\beta} \quad M_{i\beta} = \begin{Bmatrix} M_1 \\ M_2 \end{Bmatrix}_{i\beta} \quad (D.31)$$

Now, according to the rule for displacement transformations given in appendix A,

$$d\tilde{e}_{i\beta} = - P_{U\tilde{F}}^T \tilde{F}_{i\beta}(t) d\Delta \quad (D.32)$$

$$\bar{\theta}_{i\beta}(t) = \tilde{F}_{M_{i\beta}}^T \delta \tilde{e}_{i\beta} \quad (D.33)$$

where

$P_{U\tilde{F}}^T$ = a rectangular matrix of components in the unconstrained degrees of freedom of unit values of the dummy normal forces applied to the i^{th} bar element during the β^{th} increment.

$\tilde{F}_{M_{i\beta}}^T$ = a rectangular matrix of values of the dummy normal forces applied to the i^{th} element during the β^{th} increment resulting from unit values of the dummy moments.

The minus in Equation D.32 is the result of the fact that forces opposite to the \tilde{F} forces act on the nodes.

These force transformations can be obtained from equilibrium. The transformation $\bar{F}_{m_{i\beta}}$ can be written explicitly. From Figures D.5 (a) and (b),

$$\begin{Bmatrix} \bar{F}_1 \\ \bar{F}_2 \\ \bar{F}_3 \\ \bar{F}_4 \end{Bmatrix}_{i\beta} = \begin{bmatrix} -1/l_i(\bar{\beta}) & 0 \\ 0 & -1/l_i(\bar{\beta}) \\ 1/l_i(\bar{\beta}) & 0 \\ 0 & 1/l_i(\bar{\beta}) \end{bmatrix} \begin{Bmatrix} M_1 \\ M_2 \end{Bmatrix}_{i\beta} \quad (D.34)$$

Therefore,

$$\bar{F}_{M_{i\beta}} = \begin{bmatrix} -1/l_i(\bar{\beta}) & 0 \\ 0 & -1/l_i(\bar{\beta}) \\ 1/l_i(\bar{\beta}) & 0 \\ 0 & 1/l_i(\bar{\beta}) \end{bmatrix} \quad (D.35)$$

Equation D.32 can be written

$$d\bar{e}_{i\beta} = -P_{uF_{i\beta}}^T(t) \dot{\Delta}(t) dt \quad (D.35.1)$$

Integrating Equation D.35.1 with respect to time gives

$$\delta\bar{e}_{i\beta}(t_\beta) = - \int_{t_{\beta-1}}^{t_\beta} P_{uF_{i\beta}}^T(t) \dot{\Delta}(t) dt, \quad (D.35.2)$$

for the matrix $\delta\bar{e}_{i\beta}$ at the end of the increment. Now, assume that the displacements contained in $\delta\bar{e}_{i\beta}(t_\beta)$ depend only on the nodal displacements existing at the beginning and end of the increment, and not on the way in which the nodal velocities depend on time. Therefore, assume that

$$\dot{\Delta}(t) = \frac{\delta\Delta_B(t_B)}{\tau_B} \quad (D.36)$$

Substituting $\dot{\Delta}(t)$ from Equation D.36 into Equation D.35.2 gives

$$\delta\tilde{e}_{iB}(t_B) = -P_{UF_{i(B)}}^T \delta\Delta_B(t_B), \quad (D.37)$$

where

$$P_{UF_{i(B)}} = \frac{1}{\tau_B} \int_{t_{B-1}}^{t_B} P_{UF_{iB}}(t) dt \quad (D.38)$$

Equation D.38 states that

$P_{UF_{i(B)}}$ = the average value of the matrix $P_{UF_{iB}}(t)$ during the B th time increment.

If the increment is not too long, the matrix $P_{UF_{iB}}(t)$ can be assumed to vary linearly with time during the increment. In this case, the average value is given simply by

$$P_{UF_{i(B)}} = \frac{1}{2} \left[P_{UF_{iB}}(t_{B-1}) + P_{UF_{iB}}(t_B) \right]. \quad (D.39)$$

At t_{B-1} , the vectors contained in the matrix \tilde{F}_{iB} coincide with the fictitious force vectors contained in the matrix \bar{F}_{iB} .

Therefore

$$P_{UF_{iB}}(t_{B-1}) = P_{UF_{iB}} \quad (D.40)$$

Similarly,

$$P_{UF_{iB}}(t_B) = P_{UF_{i, B+1}} \quad (D.41)$$

Substituting $P_{UF_{i\beta}}(t_{\beta-1})$ and $P_{UF_{i\beta}}(t_{\beta})$ from Equations D.40 and D.41 into Equation D.39 gives

$$P_{UF_i(\bar{\beta})} = P_{UF_i(\bar{\beta})}^{\bar{}} \quad (D.42)$$

where the average fictitious force transformation matrix for the β th increment is defined as

$$P_{UF_i(\bar{\beta})}^{\bar{}} = \frac{1}{2} \left(P_{UF_{i\beta}}^{\bar{}} + P_{UF_{i, \beta+1}}^{\bar{}} \right) \quad (D.43)$$

Substituting $P_{UF_i(\bar{\beta})}$ from Equation D.42 into Equation D.37

gives
$$\delta \tilde{e}_{i\beta}(t_{\beta}) = - P_{UF_i(\bar{\beta})}^T \delta \Delta_{\beta}(t_{\beta}) \quad (D.44)$$

Substituting $\theta_{i\beta}$, $\tilde{F}_{M_{i\beta}}$ and $\delta \tilde{e}_{i\beta}$ from Equations D.30, D.31 and D.35 into Equation D.33 gives, at the end of the β th increment:

$$\theta_{1_{i\beta}}(t_{\beta}) = \frac{1}{2_{i(\bar{\beta})}} \left[\delta \tilde{e}_{3_{i\beta}}(t_{\beta}) - \delta \tilde{e}_{1_{i\beta}}(t_{\beta}) \right] \quad (D.45)$$

$$\theta_{2_{i\beta}}(t_{\beta}) = \frac{1}{2_{i(\bar{\beta})}} \left[\delta \tilde{e}_{4_{i\beta}}(t_{\beta}) - \delta \tilde{e}_{2_{i\beta}}(t_{\beta}) \right] \quad (D.46)$$

Substituting $\tilde{F}_{F_{i\beta}}(t)$ from Equation D.28 into Equation D.1, and replacing $\tilde{F}_{K_i}(t)$ by $\tilde{F}_{S_i}(t)$ gives, at the end of the β th increment,

$$\bar{F}_{K_{iB}}(t_B) = \begin{bmatrix} -\theta_{1_{iB}}(t_B) + \frac{1}{6} \theta_{1_{iB}}^3(t_B) \\ -\theta_{2_{iB}}(t_B) + \frac{1}{6} \theta_{2_{iB}}^3(t_B) \\ \theta_{1_{iB}}(t_B) - \frac{1}{6} \theta_{1_{iB}}^3(t_B) \\ \theta_{2_{iB}}(t_B) - \frac{1}{6} \theta_{2_{iB}}^3(t_B) \end{bmatrix} \bar{F}_{S_i}(t_B) \quad (D.47)$$

Equation D.47 can be written.

$$\bar{F}_{K_{iB}}(t_B) = \begin{bmatrix} n_{1,1} + n_{1,3} \\ n_{2,1} + n_{2,3} \\ -n_{1,1} - n_{1,3} \\ -n_{2,1} - n_{2,3} \end{bmatrix}_{iB} \quad (D.48)$$

where

$$n_{1,1_{iB}} = -\theta_{1_{iB}}(t_B) \bar{F}_{S_i}(t_B) \quad (D.49)$$

$$n_{1,3_{iB}} = \frac{1}{6} \theta_{1_{iB}}^3(t_B) \bar{F}_{S_i}(t_B) \quad (D.50)$$

$$n_{2,1_{iB}} = -\theta_{2_{iB}}(t_B) \bar{F}_{S_i}(t_B) \quad (D.51)$$

$$n_{2,3_{iB}} = \frac{1}{6} \theta_{2_{iB}}^3(t_B) \bar{F}_{S_i}(t_B) \quad (D.52)$$

Equations D.48 through D.52 give the fictitious bar forces for the B th increment in terms of the rotation angles and the symmetric components of the lumped bar forces. The rotation angles are given by Equations D.45 and D.46 in terms of the $\delta\tilde{\alpha}$'s, which can be found from Equations D.44 and D.30. The fictitious force matrix, as implied in Equation D.4, is defined by

$$\bar{F}_{K_{iB}}(t) = \left\{ \bar{F}_1(t) \mid \bar{F}_2(t) \mid \bar{F}_3(t) \mid \bar{F}_4(t) \right\}_{iB} \quad (\text{column}) \quad (D.53)$$

Equation D.29 gives the fictitious deformation for the complete bar. The fictitious deformations for the two halves of the bar, for the i th element, at the end of the β th increment, are given from Equation D.29 by

$$\begin{bmatrix} \delta e_{f1_{i\beta}}(t_\beta) \\ \delta e_{f2_{i\beta}}(t_\beta) \end{bmatrix} = -\frac{1}{4} l_{i(\beta)} \begin{bmatrix} \theta_{1_{i(\beta)}}^2(t_\beta) + \theta_{2_{i\beta}}^2(t_\beta) \end{bmatrix} \begin{Bmatrix} 1 \\ 1 \end{Bmatrix} \quad (D.54)$$

The two fictitious deformations correspond to the two lumped element deformations defined for each bar. Equation D.54 can be written

$$\delta e_{f_{i\beta}}(t_\beta) = r_{2_{i\beta}} \quad (D.55)$$

where

$$\delta e_{f_{i\beta}}(t_\beta) = \left\{ \delta e_{f1_{i\beta}}(t_\beta) \mid \delta e_{f2_{i\beta}}(t_\beta) \right\} \quad (\text{Column}) \quad (D.56)$$

$$r_{2_{i\beta}} = -\frac{1}{4} l_{i(\beta)} \begin{bmatrix} \theta_{1_{i\beta}}^2(t_\beta) + \theta_{2_{i\beta}}^2(t_\beta) \end{bmatrix} \begin{Bmatrix} 1 \\ 1 \end{Bmatrix} \quad (D.57)$$

Equations D.55 and D.57 give the fictitious bar deformations for the β th increment in terms of the rotation angles.

Axially Loaded Bars in Membranes and Cells

The method and notation established in the preceding discussion apply when the i th element is an axially loaded bar. When the bar is a component of a membrane or cell, instead of a separate element, the method of calculating fictitious forces and deformations is essentially the same. The differences in procedure and notation are described in a later subsection of this Appendix, entitled "Membranes and Cells".

SHEAR PANELS

This subsection presents fictitious forces and deformations for parallelogram shear panels. Individual panels are considered. The method of integrating these results into the calculations for membranes and cells is discussed in a following subsection.

Problem

Figure D.6 shows the notation for the shear panel, including the panel dimensions a and b , the skew angle θ , and the shear flow Q . Four fictitious forces are defined, one at each corner of the panel. The fictitious forces and their corresponding deformations are designated \bar{F}_j and $\delta\bar{e}_j$, where $j = 1, 2, 3, 4$. The time is understood to be some time during the β th increment, at the beginning of which \bar{F}_j and $\delta\bar{e}_j$ are zero. Time is not specified, because it is not required. The panel can be considered to form part of the i th element, when the i th element is a cell or membrane. Subscript β 's and i 's, to indicate increment and element numbers, are omitted to simplify the notation.

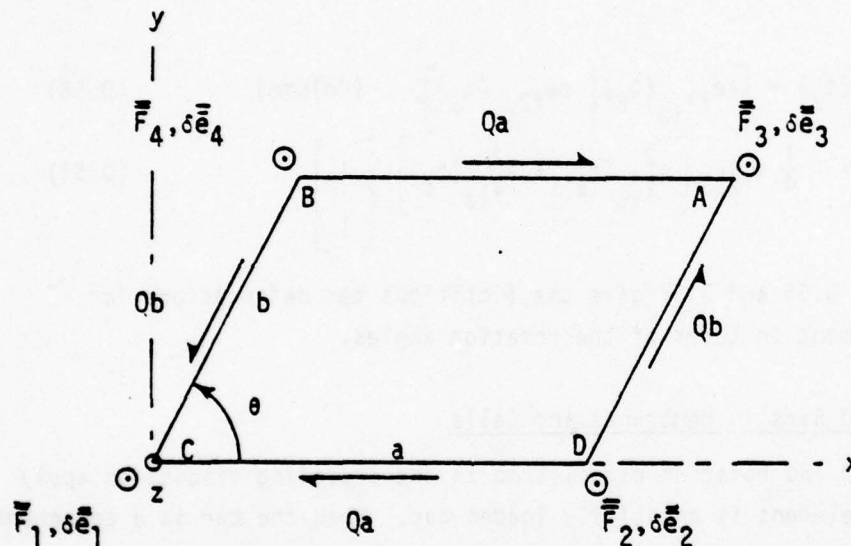


Figure D.6. Notation for shear panel fictitious forces and deformations.

If a given panel is only approximately a parallelogram, it is replaced by an equivalent parallelogram panel, according to the method described in Appendix H.

The rectangular cartesian xyz reference frame, and the symbols A, B C and D assigned to the panel corners, are established as follows: At the end of the β th increment, select one of the two corners that the shear

forces on adjacent edges point toward, and label that corner "A". Label the other corners B, C and D, counterclockwise, as shown. Select the xyz reference frame so that the origin is at C, the x axis passes through D, and the xy plane passes through B. The xy plane generally does not pass through A, since, in general, the panel is warped.

A different notation for panel corners and the shear forces acting on the element is established in Figure 2.4, Section II.

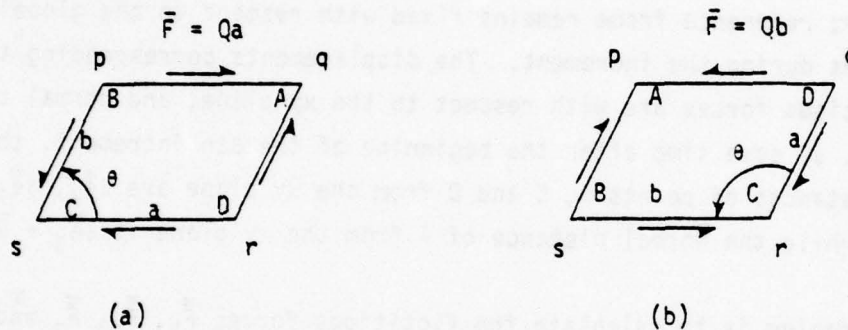


Figure D.6.1. Relationship between shear panel notations.

In Figure 2.4, the corners are labeled p, q, r and s in the clockwise direction. The element force \bar{F} acts on edge pq, positive when it points from p to q, negative when it points from q to p. Figure D.6.1 shows the relationship between two notations, for the case when the panel is a true parallelogram. Figure D.6.1(a) shows the case when \bar{F} is positive. In this case, corner q can be selected as Corner A, since the adjacent shear forces point toward q. The length of pq is a, and the element force is equal to Qa . Figure D.6.1(b) shows the case when \bar{F} is negative. In this case, corner p can be selected as A, the lengths of pq is b, and the element force is Qb .

The fictitious panel deformation, $d\bar{e}_f$, is defined as the fictitious deformation corresponding to the element force \bar{F} .

The new shear panel notation is necessary because of the nature of the assumed normal displacement function, subsequently described.

Let

\bar{e}_{03} = the normal distance from Point A to the xy plane at the beginning of the β th increment.

The xyz reference frame remains fixed with respect to the global coordinates during the increment. The displacements corresponding to the fictitious forces are with respect to the xy plane, and normal to it. Thus, at some time after the beginning of the β th increment, the normal distances of points B, C and D from the xy plane are $\delta\bar{e}_4$, $\delta\bar{e}_1$, and $\delta\bar{e}_2$, while the normal distance of A from the xy plane is $\delta\bar{e}_3 + \bar{e}_{03}$.

The problem is to calculate the fictitious forces \bar{F}_1 , \bar{F}_2 , \bar{F}_3 and \bar{F}_4 , and the fictitious deformation $\delta\bar{e}_f$, as functions of the lumped element force, \bar{F} , the displacements $\delta\bar{e}_1$, $\delta\bar{e}_2$, $\delta\bar{e}_3$, and $\delta\bar{e}_4$, and the initial displacement \bar{e}_{03} .

Approach

The fictitious forces and deformation of an infinitesimal element of the panel are integrated to yield the fictitious forces and deformation of the panel.

As was the case for the bar, the fictitious forces acting on an element of the panel, resulting from rotations of the edge shear forces, are functions of the rotation angles. When these angles increase, the fictitious forces increase. The relationship between rotation angles and forces is nonlinear. These effects can be represented by fictitious springs attached to the element. The springs are such that they produce

forces equal to the fictitious forces on the element, when the element is displaced.

The mathematical model of the shear panel established for the purpose of fictitious force analysis, therefore, consists of a plate having negligible stiffness. Attached to this plate are distributed nonlinear springs. The forces produced by the springs on the plate are functions of the lateral displacements. The functional relationship is single-valued. When the displacements return to zero, so do the forces. The mathematical model is consequently a nonlinear elastic structure.

The approach to the problem is based upon the method of minimum potential energy, which is applicable to nonlinear elastic structures (Reference 1). The shape of the displaced structure is represented by a mathematical function of the coordinates, containing undetermined parameters. The potential energy of the structure is calculated, and the parameters are selected to minimize the energy. The fictitious forces and deformations are then evaluated.

Displacement Function

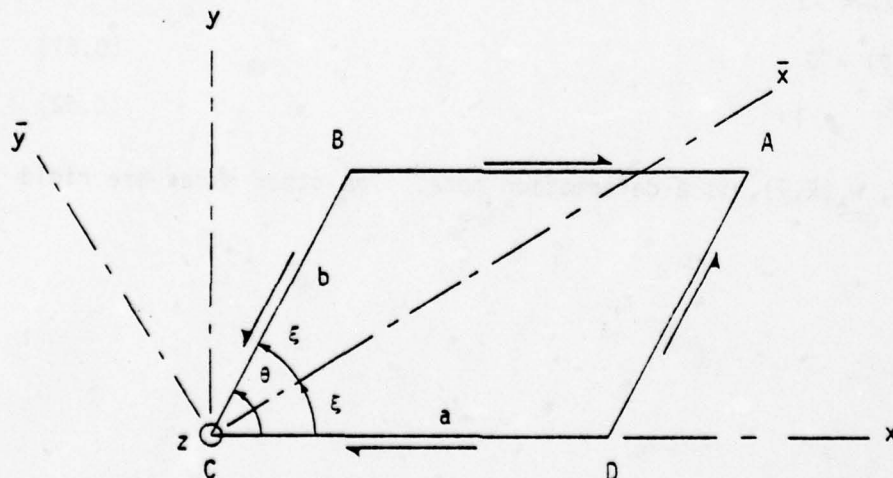


Figure D.8. Coordinates for the displacement function.

The displacement function is written in terms of the $\bar{x}\bar{y}$ coordinates established as shown in Figure D.8. The $\bar{x}\bar{y}$ plane coincides with the xy plane of the xyz reference frame. The \bar{x} axis bisects the angle BCD.

The assumed displacement function is expressed in modal form as

$$\bar{w}(\bar{x}, \bar{y}) = w_e(\bar{x}, \bar{y}) \bar{a}_1 + w_{\bar{y}R}(\bar{x}) \bar{a}_2 + w_{\bar{x}R}(\bar{y}) \bar{a}_3 + w_R \bar{a}_4 \quad (D.58)$$

where

$\bar{w}(\bar{x}, \bar{y})$ = the distance from point (\bar{x}, \bar{y}) in the $\bar{x}\bar{y}$ plane to the displaced surface, measured parallel to z .

$w_e(\bar{x}, \bar{y})$, $w_{\bar{y}R}(\bar{x})$, $w_{\bar{x}R}(\bar{y})$, w_R = displacement modes

\bar{a}_1 , \bar{a}_2 , \bar{a}_3 , \bar{a}_4 = displacement parameters

The displacement modes are given by

$$w_e(\bar{x}, \bar{y}) = \frac{b+a}{4abc \cos \xi} \bar{x} + \frac{b-a}{4abs \sin \xi} \bar{y} - \frac{1}{2abs \sin^2 \xi} \bar{y}^2 \quad (D.59)$$

$$w_{\bar{y}R}(\bar{x}) = -\bar{x} \quad (D.60)$$

$$w_{\bar{x}R}(\bar{y}) = \bar{y} \quad (D.61)$$

$$w_R = 1 \quad (D.62)$$

The function, $w_e(\bar{x}, \bar{y})$, is a deformation mode. The other modes are rigid body modes.

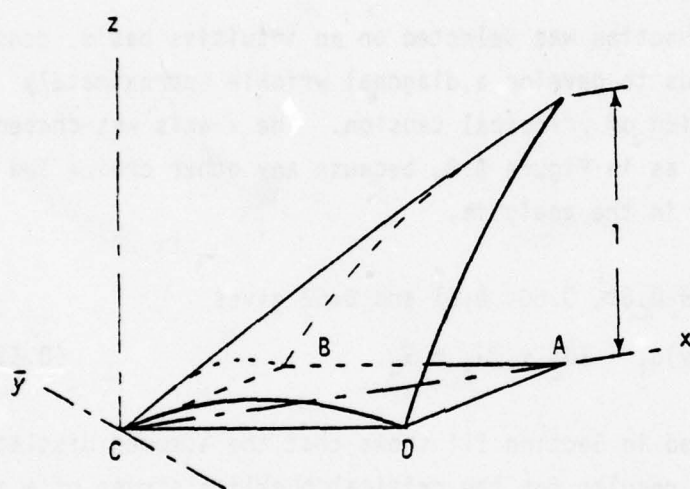


Figure D.9. Shear panel deformation mode, $w_e(\bar{x}, \bar{y})$.

Figure D.9 shows the deformation mode, $w_e(\bar{x}, \bar{y})$, for a rhombic panel. The lateral displacement given by this mode is later shown to be unity at Point A, and zero at B, C and D, as the figure indicates. The deformed surface is singly curved.

The modes $w_{\bar{y}R}(\bar{x})$ and $w_{\bar{x}R}(\bar{y})$ represent unit rigid body rotations about the \bar{y} and \bar{x} axes. The mode w_R represents a unit rigid body translation parallel to z .

The displacement function was selected on an intuitive basis, considering that a shear panel tends to develop a diagonal wrinkle approximately parallel to the direction of principal tension. The x axis was chosen to bisect the angle θ , as in Figure D.8, because any other choice led to a singularity later in the analysis.

Combining Equations D.58, D.60, D.61 and D.62 gives

$$\bar{w}(\bar{x}, \bar{y}) = w_e(\bar{x}, \bar{y})\bar{a}_1 - \bar{x}\bar{a}_2 + \bar{y}\bar{a}_3 + \bar{a}_4 \quad (D.63)$$

An example presented in Section III shows that the assumed displacement function leads to good results for the critical buckling stress of a square simply supported plate subjected to edge shearing stresses.

From Figure D.8, the coordinates of the panel corners in the $\bar{x}\bar{y}$ system are

$$\bar{x}_A = (b + a) \cos \xi \quad (D.64)$$

$$\bar{y}_A = (b - a) \sin \xi \quad (D.65)$$

$$\bar{x}_B = b \cos \xi \quad (D.66)$$

$$\bar{y}_B = b \sin \xi \quad (D.67)$$

$$\bar{x}_C = \bar{y}_C = 0 \quad (D.68)$$

$$\bar{x}_D = a \cos \xi \quad (D.69)$$

$$\bar{y}_D = -a \sin \xi \quad (D.70)$$

Substituting the coordinates of Points A, B, C and D into Equation D.59 gives

$$w_e(\bar{x}_A, \bar{y}_A) = 1 \quad (D.71)$$

$$w_e(\bar{x}_B, \bar{y}_B) = w_e(\bar{x}_C, \bar{y}_C) = w_e(\bar{x}_D, \bar{y}_D) = 0 \quad (D.72)$$

Writing Equation D.63 for each of the four points, A, B, C and D, and employing Equations D.71 and D.72 gives

$$\bar{w}(\bar{x}_A, \bar{y}_A) = \bar{\alpha}_1 - \bar{x}_A \bar{\alpha}_2 + \bar{y}_A \bar{\alpha}_3 + \bar{\alpha}_4 \quad (D.73)$$

$$\bar{w}(\bar{x}_B, \bar{y}_B) = -\bar{x}_B \bar{\alpha}_2 + \bar{y}_B \bar{\alpha}_3 + \bar{\alpha}_4 \quad (D.74)$$

$$\bar{w}(\bar{x}_C, \bar{y}_C) = \bar{\alpha}_4 \quad (D.75)$$

$$\bar{w}(\bar{x}_D, \bar{y}_D) = -\bar{x}_D \bar{\alpha}_2 + \bar{y}_D \bar{\alpha}_3 + \bar{\alpha}_4 \quad (D.76)$$

The displacements at corners A, B, C and D are given by $\delta \bar{e}_3 + \bar{e}_{03}$, $\delta \bar{e}_4$, $\delta \bar{e}_1$, and $\delta \bar{e}_2$. Therefore

$$\bar{w}(\bar{x}_A, \bar{y}_A) = \delta \bar{e}_3 + \bar{e}_{03} \quad (D.77)$$

$$\bar{w}(\bar{x}_B, \bar{y}_B) = \delta \bar{e}_4 \quad (D.78)$$

$$\bar{w}(\bar{x}_C, \bar{y}_C) = \delta \bar{e}_1 \quad (D.79)$$

$$\bar{w}(\bar{x}_D, \bar{y}_D) = \delta \bar{e}_2 \quad (D.80)$$

Eliminating $\bar{w}(\bar{x}_A, \bar{y}_A)$, $\bar{w}(\bar{x}_B, \bar{y}_B)$, $\bar{w}(\bar{x}_C, \bar{y}_C)$ and $\bar{w}(\bar{x}_D, \bar{y}_D)$ from Equations D.73 to D.80 gives

$$\delta \bar{e}_1 = \bar{\alpha}_4 \quad (D.80.1)$$

$$\delta \bar{e}_2 = -\bar{x}_D \bar{a}_2 + \bar{y}_D \bar{a}_3 + \bar{a}_4 \quad (D.80.2)$$

$$\delta \bar{e}_3 = \bar{a}_1 - \bar{x}_A \bar{a}_2 + \bar{y}_A \bar{a}_3 + \bar{a}_4 - \bar{e}_{03} \quad (D.80.3)$$

$$\delta \bar{e}_4 = -\bar{x}_B \bar{a}_2 + \bar{y}_B \bar{a}_3 + \bar{a}_4 \quad (D.80.4)$$

Solving Equations D.80.1 to D.80.4 for the displacement parameters gives

$$\bar{a}_1 = \delta \bar{e}_1 - \delta \bar{e}_2 + \delta \bar{e}_3 - \delta \bar{e}_4 + \bar{e}_{03} \quad (D.81)$$

$$\bar{a}_2 = \frac{1}{\bar{A}} \left[\bar{y}_D (\delta \bar{e}_4 - \delta \bar{e}_1) - \bar{y}_B (\delta \bar{e}_2 - \delta \bar{e}_1) \right] \quad (D.82)$$

$$\bar{a}_3 = \frac{1}{\bar{A}} \left[\bar{x}_D (\delta \bar{e}_4 - \delta \bar{e}_1) - \bar{x}_B (\delta \bar{e}_2 - \delta \bar{e}_1) \right] \quad (D.83)$$

$$\bar{a}_4 = \delta \bar{e}_1 \quad (D.84)$$

$$\text{where } \bar{A} = \bar{x}_D \bar{y}_B - \bar{x}_B \bar{y}_D \quad (D.85)$$

Substituting \bar{x}_B , \bar{y}_B , \bar{x}_D and \bar{y}_D from Equations D.66, D.67, D.69 and D.70 into Equation D.85 gives

$$\bar{A} = ab \sin 2 \xi \quad (D.86)$$

Therefore, \bar{A} is the panel area. Equation D.81 can be written

$$\bar{a}_1 = \delta \bar{a}_1 + \bar{a}_{1,0} \quad (D.86.1)$$

$$\text{where } \delta \bar{a}_1 = \delta \bar{e}_1 - \delta \bar{e}_2 + \delta \bar{e}_3 - \delta \bar{e}_4 \quad (D.87)$$

$$\text{and } \bar{a}_{1,0} = \bar{e}_{03} \quad (D.88)$$

At the beginning of the increment, $\delta \bar{e}_1$, $\delta \bar{e}_2$, $\delta \bar{e}_3$ and $\delta \bar{e}_4$ are zero. Therefore, from Equations D.81 to D.84 and Equation D.88, the panel is in its initial position when $\bar{a}_1 = \bar{a}_{1,0}$, and \bar{a}_2 , \bar{a}_3 and \bar{a}_4 are zero.

The displacements $\delta \bar{e}_j$ ($j = 1, 2, 3, 4$) are displacements corresponding to fictitious forces, as shown in Figure D.6. The $\delta \bar{e}$'s are, therefore, normal to the approximate plane of the panel at the beginning of the j th increment. The $\delta \bar{e}$'s are analogous to the $\delta \bar{e}$'s for the bar element, which are normal to the position of the bar at the beginning of the increment.

In the case of the bar, it was shown that the $\delta \bar{e}$'s should be replaced by the $\delta \tilde{e}$'s, where these quantities are displacements of unit vectors that remain normal to the bar as the bar rotates. The symbol $\delta \tilde{e}$ therefore represents an arc length instead of a normal distance. This substitution was made when the sines of the rotation angles were replaced by power series expansions, discarding powers higher than the third.

In the subsequent derivation for the shear panel, similar power series expansions are introduced. In view of the similarity of the two approaches, it is considered appropriate to introduce the $\delta \tilde{e}$'s in the place of the $\delta \bar{e}$'s, although no mathematical argument can be given for this substitution.

Equations D.82, D.83, D.84 and D.87 are, therefore, written in the form

$$\bar{\alpha}_2 = \frac{1}{A} \left[\bar{y}_D (\delta \tilde{e}_4 - \delta \tilde{e}_1) - \bar{y}_B (\delta \tilde{e}_2 - \delta \tilde{e}_1) \right] \quad (D.89)$$

$$\bar{\alpha}_3 = \frac{1}{A} \left[\bar{x}_D (\delta \tilde{e}_4 - \delta \tilde{e}_1) - \bar{x}_B (\delta \tilde{e}_2 - \delta \tilde{e}_1) \right] \quad (D.90)$$

$$\bar{\alpha}_4 = \delta \tilde{e}_1 \quad (D.91)$$

$$\delta \bar{\alpha}_1 = \delta \tilde{e}_1 - \delta \tilde{e}_2 + \delta \tilde{e}_3 - \delta \tilde{e}_4 \quad (D.92)$$

Rotated Reference Frames

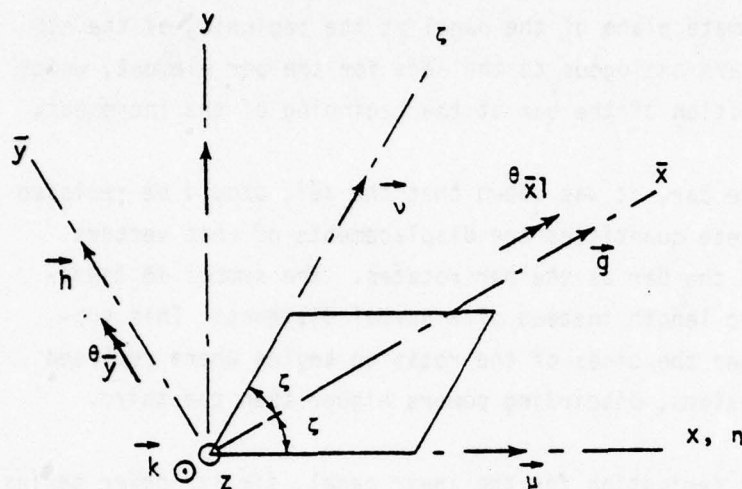


Figure D.10. Oblique coordinates and unit vectors.

In Figure D.10, the oblique coordinate axes n and ζ are established parallel to the edges of the shear panel.

Let

\vec{g} , \vec{h} , \vec{k} = unit vectors parallel to the \bar{x} , \bar{y} and z axes.

\vec{u} , \vec{v} = unit vectors parallel to the n and ζ axes.

The figure shows the positive senses of these vectors.

The components of the unit vector \vec{u} in the $\bar{x}\bar{y}z$ system are $u_{\bar{x}} = \cos \xi$ and $u_{\bar{y}} = \sin \xi$. Therefore,

$$\vec{u} = \vec{g} \cos \xi - \vec{h} \sin \xi \quad (D.93)$$

Similarly,
$$\vec{v} = \vec{g} \cos \xi + \vec{h} \sin \xi \quad (D.94)$$

Rotate the plane containing the panel about the \bar{y} axis through an angle $\theta_{\bar{y}}$. Designate as \bar{x}_1 , the rotated position of the \bar{x} axis. Now rotate the

plane about \bar{x}_1 , through an angle $\theta_{\bar{x}1}$. Figure D.10 shows the positive senses of the vectors representing $\theta_{\bar{y}}$ and $\theta_{\bar{x}1}$.

When the plane containing the panel is subjected to these rotations, all of the axes and unit vectors shown in the figure rotate with it. The directions of the unit vectors change, but their relative directions remain constant. Let

$\vec{g}_2, \vec{h}_2, \vec{k}_2$ = the unit vectors \vec{g}, \vec{h} and \vec{k} after the rotations $\theta_{\bar{y}}$ and $\theta_{\bar{x}1}$.

\vec{u}_2, \vec{v}_2 = the unit vectors \vec{u} and \vec{v} after the rotations $\theta_{\bar{y}}$ and $\theta_{\bar{x}1}$.

Therefore, from Equations D.93 and D.94,

$$\vec{u}_2 = \vec{g}_2 \cos \xi - \vec{h}_2 \sin \xi \quad (D.95)$$

$$\text{and} \quad \vec{v}_2 = \vec{g}_2 \cos \xi + \vec{h}_2 \sin \xi \quad (D.96)$$

since the relative directions of the vectors remain constant.

Let

\vec{k}_1 = the unit vector \vec{k} after the rotation $\theta_{\bar{y}}$.

The rotation $\theta_{\bar{y}}$ causes \vec{k} to tilt toward the \bar{x} axis.

$$\therefore \quad \vec{k}_1 = \vec{g} \sin \theta_{\bar{y}} + \vec{k} \cos \theta_{\bar{y}} \quad (D.97)$$

The rotation $\theta_{\bar{x}1}$ causes \vec{k}_1 to tilt away from the \bar{y} axis.

$$\text{Therefore} \quad \vec{k}_2 = -\vec{h} \sin \theta_{\bar{x}1} + \vec{k}_1 \cos \theta_{\bar{x}1} \quad (D.98)$$

$$\text{Similarly} \quad \vec{h}_2 = \vec{h} \cos \theta_{\bar{x}1} + \vec{k}_1 \sin \theta_{\bar{x}1} \quad (D.99)$$

The rotation $\theta_{\bar{x}1}$ does not affect \bar{g} . Therefore,

$$\bar{g}_2 = \bar{g} \cos \theta_{\bar{y}} - \bar{k} \sin \theta_{\bar{y}} \quad (D.100)$$

Eliminating \bar{k}_1 from Equations D.97, D.98 and D.99 gives

$$\bar{h}_2 = \bar{g} \sin \theta_{\bar{y}} \sin \theta_{\bar{x}1} + \bar{h} \cos \theta_{\bar{x}1} + \bar{k} \cos \theta_{\bar{y}} \sin \theta_{\bar{x}1} \quad (D.101)$$

$$\bar{k}_2 = \bar{g} \sin \theta_{\bar{y}} \cos \theta_{\bar{x}1} - \bar{h} \sin \theta_{\bar{x}1} + \bar{k} \cos \theta_{\bar{y}} \cos \theta_{\bar{x}1} \quad (D.102)$$

These results are needed in calculating the fictitious forces on the rotated element.

Fictitious Forces and Deformations of the Infinitesimal Element

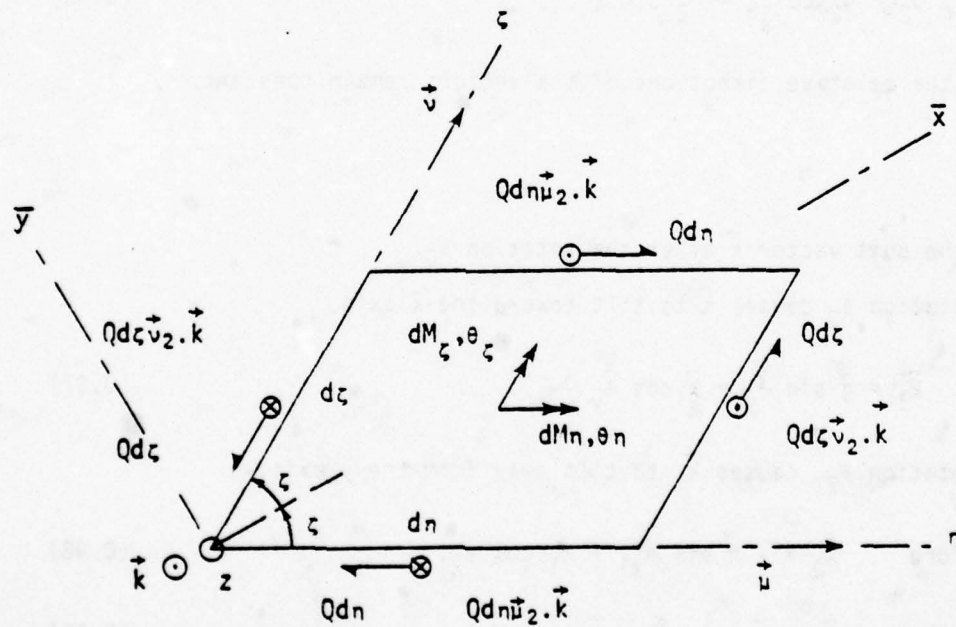


Figure D.11. Differential fictitious forces.

Figure D.11 shows an infinitesimal plate element with sides parallel to the oblique axes η and ζ . The element is subjected to the shear flow Q . The figure shows a shear force on each edge resulting from this shear flow.

When the element rotates about the \bar{y} axis, and then about the displaced position of the \bar{x} axis, the shear forces become tilted, and develop components normal to the original plane of the element. These components are also shown. For example, consider the shear force $Qd\zeta$ acting on the right hand edge of the element. This vector initially points in the direction of the unit vector \bar{v} . After the rotations $\theta_{\bar{y}}$ and $\theta_{\bar{x}_1}$, it points in the direction of the unit vector \bar{v}_2 . Therefore, the tilted shear force is represented in magnitude and direction by the vector $Qd\zeta\bar{v}_2$. The vertical component of this vector is found by forming the dot product of the vector with the unit vector \bar{k} , as shown. The other normal components are found in a similar manner. These normal components are the fictitious forces acting on the element.

Inspection of the figure shows that the only resultants of the fictitious forces are moments, since the sum of the normal components parallel to z is zero. Let

dM_{η} and dM_{ζ} = moments about the η and ζ axes that are the resultants of the fictitious forces acting on the infinitesimal element.

The figure shows dM_{η} and dM_{ζ} . Also let

θ_{η} and θ_{ζ} = the virtual works done by unit values of dM_{η} and dM_{ζ} during a virtual displacement of the infinitesimal element.

Thus θ_{η} and θ_{ζ} represent the rotations of dM_{η} and dM_{ζ} . The figure shows θ_{η} and θ_{ζ} .

Considering the equilibrium of moments acting on the element about the η and ζ axes gives

$$dM_{\eta} + dM_{\zeta} \cos 2\xi = Q d\eta \vec{u}_2 \cdot \vec{k} d\zeta \sin 2\xi. \quad (D.103)$$

$$dM_{\eta} \cos 2\xi + dM_{\zeta} = -Q d\zeta \vec{v}_2 \cdot \vec{k} d\eta \sin 2\xi \quad (D.104)$$

Solving Equations D.103 and D.104 for dM_{η} and dM_{ζ} gives

$$dM_{\eta} \sin^2 2\xi = Q d\eta d\zeta \sin 2\xi (\vec{u}_2 \cdot \vec{k} + \vec{v}_2 \cdot \vec{k} \cos 2\xi) \quad (D.105)$$

$$dM_{\zeta} \sin^2 2\xi = -Q d\eta d\zeta \sin 2\xi (\vec{v}_2 \cdot \vec{k} + \vec{u}_2 \cdot \vec{k} \cos 2\xi) \quad (D.106)$$

Define the moments per unit area,

$$m_{\eta} = \frac{dM_{\eta}}{d\eta d\zeta \sin 2\xi} \quad (D.107)$$

$$m_{\zeta} = \frac{dM_{\zeta}}{d\eta d\zeta \sin 2\xi} \quad (D.108)$$

Eliminating dM_{η} and dM_{ζ} from Equations D.105, D.106, D.107 and D.108 gives

$$m_{\eta} \sin^2 2\xi = Q (\vec{u}_2 \cdot \vec{k} + \vec{v}_2 \cdot \vec{k} \cos 2\xi) \quad (D.109)$$

$$m_{\zeta} \sin^2 2\xi = -Q (\vec{v}_2 \cdot \vec{k} + \vec{u}_2 \cdot \vec{k} \cos 2\xi) \quad (D.110)$$

From Equations D.100 and D.101.

$$\vec{g}_2 \cdot \vec{k} = -\sin \theta_y \quad (D.111)$$

$$\vec{h}_2 \cdot \vec{k} = \cos \theta_{\bar{y}} \sin \theta_{\bar{x}1} \quad (D.112)$$

Combining Equations D.95, D.96, D.111 and D.112 gives

$$\bar{u}_2 \cdot \bar{k} = -\sin \theta_{\bar{y}} \cos \xi - \cos \theta_{\bar{y}} \sin \theta_{\bar{x}1} \sin \xi \quad (D.113)$$

$$\bar{v}_2 \cdot \bar{k} = -\sin \theta_{\bar{y}} \cos \xi + \cos \theta_{\bar{y}} \sin \theta_{\bar{x}1} \sin \xi \quad (D.114)$$

Substituting $\bar{u}_2 \cdot \bar{k}$ and $\bar{v}_2 \cdot \bar{k}$ from Equations D.113 and D.114 into Equations D.109 and D.110 gives

$$m_n \sin^2 2\xi = -2Q(\sin \theta_{\bar{y}} \cos^3 \xi + \cos \theta_{\bar{y}} \sin \theta_{\bar{x}1} \sin^3 \xi) \quad (D.115)$$

$$m_\xi \sin^2 2\xi = 2Q(\sin \theta_{\bar{y}} \cos^3 \xi - \cos \theta_{\bar{y}} \sin \theta_{\bar{x}1} \sin^3 \xi) \quad (D.116)$$

Equations D.115 and D.116 gives the fictitious moments per unit area parallel to the oblique coordinate axes acting on the infinitesimal element resulting from the shear flow Q , and the rotations $\theta_{\bar{y}}$ and $\theta_{\bar{x}1}$.

The fictitious deformation of the infinitesimal element is calculated from Equation D.2. Differentiating this equation with respect to time, and dropping the subscripts i and β , gives

$$d\bar{e}_f = -\bar{F}_f^T(t) d\bar{e} \quad , \quad (D.117)$$

where $d\bar{e}_f$ is the differential fictitious deformation, $\bar{F}_f(t)$ is a matrix of fictitious forces resulting from a unit value of the element force, and $d\bar{e}$ is a column matrix of differential displacements of the fictitious forces.

Consider a plate element similar to the infinitesimal element shown in Figure D.11, except that it has unit area. This element remains flat during the rotations $\theta_{\bar{y}}$ and $\theta_{\bar{x}1}$, as does the infinitesimal element.

Define the shear flow Q acting on the unit element as the element force, \bar{F}_{KU} . The moments m_n and m_z can be considered to be the fictitious forces on the element, since they are statically equivalent to the normal components of the shear forces. The rotations θ_n and θ_z are, therefore, the displacements of the fictitious forces.

Equations D.115 and D.116 can be written in the form

$$\bar{F}_{KU}(t) = \bar{F}_{FU}(t) \bar{F}_{KU}(t) \quad (D.118)$$

where $\bar{F}_{KU}(t) = \left\{ m_n \mid m_z \right\}$ (column) (D.119)

$$\bar{F}_{FU}(t) = \frac{2}{\sin^2 2\xi} \begin{bmatrix} -\sin \theta_{\bar{y}} \cos^3 \xi - \cos \theta_{\bar{y}} \sin \theta_{\bar{x}1} \sin^3 \xi \\ \sin \theta_{\bar{y}} \cos^3 \xi - \cos \theta_{\bar{y}} \sin \theta_{\bar{x}1} \sin^3 \xi \end{bmatrix} \quad (D.120)$$

and $\bar{F}_{KU}(t) = Q$. (D.121)

The matrix of diaplacements of fictitious forces is

$$\bar{e}_u(t) = \left\{ \theta_n \mid \theta_z \right\} \quad (\text{column}) \quad (D.122)$$

Substituting $\bar{F}_{FU}(t)$ and $\bar{e}_u(t)$ from Equations D.120 and D.122 into Equation D.117 gives the fictitious deformation of the unit element:

$$d\bar{e}_{fu} = \frac{2}{\sin^2 2\xi} \left[\sin \theta_{\bar{y}} \cos^3 \xi (d\theta_n - d\theta_z) + \cos \theta_{\bar{y}} \sin \theta_{\bar{x}1} \sin^3 \xi (d\theta_n + d\theta_z) \right] \quad (D.123)$$

The rotation angles θ_n and θ_z must now be evaluated in terms of $\theta_{\bar{y}}$ and $\theta_{\bar{x}1}$. To evaluate θ_n , apply to the infinitesimal element a unit moment about the n axis. This moment can be represented by a unit vector pointing in the direction of the n axis. Therefore, the vector \bar{u} represents the unit moment, and the components of the moment referred to \bar{x} and \bar{y} are $u_{\bar{x}}$

and $u_{\bar{y}}$. Apply the unit moment to the element, and equilibrate it with the components $u_{\bar{x}}$ and $u_{\bar{y}}$ reversed. Produce the rotations $\theta_{\bar{y}}$ and $\theta_{\bar{x}1}$. During this motion the unit moment and its components $u_{\bar{x}}$ and $u_{\bar{y}}$, reversed, maintain the same relative positives. The virtual work is zero, since the moments are in equilibrium. Therefore,

$$\theta_n - u_{\bar{y}}\theta_{\bar{y}} - u_{\bar{x}}\theta_{\bar{x}1} = 0 \quad (D.124)$$

In Equation D.124, the work done by the unit moment about n is θ_n , by definition of θ_n . The component $u_{\bar{y}}$ does the work $u_{\bar{y}}\theta_{\bar{y}}$ during the rotation $\theta_{\bar{y}}$, and no work during the rotation $\theta_{\bar{x}1}$. The component $u_{\bar{x}}$ does no work during the rotation $\theta_{\bar{y}}$, and it does the work $u_{\bar{x}}\theta_{\bar{x}1}$ during the rotation $\theta_{\bar{x}1}$.

From Figure D.11

$$u_{\bar{x}} = \cos \xi \quad (D.125)$$

$$u_{\bar{y}} = -\sin \xi \quad (D.126)$$

Eliminating $u_{\bar{x}}$ and $u_{\bar{y}}$ from Equations D.124, D.125 and D.126 gives

$$\theta_n = -\theta_{\bar{y}} \sin \xi + \theta_{\bar{x}1} \cos \xi \quad (D.127)$$

Similarly, it can be shown that

$$\theta_c = \theta_{\bar{y}} \sin \xi + \theta_{\bar{x}1} \cos \xi \quad (D.128)$$

Eliminating θ_n and θ_c from Equations D.123, D.127 and D.128 gives

$$d\bar{e}_{fu} = \frac{2}{\sin 2\xi} (-\cos^2 \xi \sin \theta_{\bar{y}} d\theta_{\bar{y}} + \sin^2 \xi \cos \theta_{\bar{y}} \sin \theta_{\bar{x}1} d\theta_{\bar{x}1}) \quad (D.129)$$

Equation D.129 gives the change in the fictitious deformation resulting from very small changes in $\theta_{\bar{y}}$ and $\theta_{\bar{x}1}$. To integrate the equation, keep $\theta_{\bar{x}1}$ equal to zero and allow $\theta_{\bar{y}}$ to increase from zero to $\theta_{\bar{y}}$. Then keep $\theta_{\bar{y}}$ constant and allow $\theta_{\bar{x}1}$ to increase from zero to $\theta_{\bar{x}1}$. Therefore,

$$\begin{aligned} \bar{e}_{fu} = \frac{2}{\sin 2\xi} & \left(-\cos^2 \xi \int_0^{\theta_{\bar{y}}} \sin \theta_{\bar{y}} d\theta_{\bar{y}} \right. \\ & \left. + \sin^2 \xi \cos \theta_{\bar{y}} \int_0^{\theta_{\bar{x}1}} \sin \theta_{\bar{x}1} d\theta_{\bar{x}1} \right) \end{aligned} \quad (D.130)$$

Therefore,

$$\bar{e}_{fu} = \frac{2}{\sin 2\xi} \left[-\cos^2 \xi (1 - \cos \theta_{\bar{y}}) + \sin^2 \xi \cos \theta_{\bar{y}} (1 - \cos \theta_{\bar{x}1}) \right] \quad (D.131)$$

Equation D.131 gives the fictitious deformation of an element of unit area subjected to the rotations $\theta_{\bar{x}}$ and $\theta_{\bar{y}}$, corresponding to the shear flow Q . The fictitious deformation of an infinitesimal element of dimensions dn and $d\zeta$ and skew angle 2ξ , corresponding to the shear flow Q , is, therefore,

$$d\bar{e}_{fQ} = \bar{e}_{fu} dn d\zeta \sin 2\xi \quad (D.131.1)$$

Panel Fictitious Forces

Consider the potential energy resulting from a displacement of the panel normal to the xy plane. This displacement, $\bar{w}(\bar{x}, \bar{y})$, is given in terms of the parameters, $\bar{\alpha}_1$, $\bar{\alpha}_2$, $\bar{\alpha}_3$ and $\bar{\alpha}_4$, by Equation D.63. The total energy is equal to the energy stored in the distributed rotational springs attached to the infinitesimal elements, minus the work done by the fictitious forces acting at the panel corners (see Figure D.6).

The need exists to distinguish between the equilibrium value of the displacement, \bar{w} , and a virtual displacement different from the equilibrium value.

Let

$w(\bar{x}, \bar{y})$ = the virtual displacement of the panel normal to the xy plane,
not necessarily equal to the equilibrium displacement.

Therefore,

$$w(\bar{x}, \bar{y}) = w_e(\bar{x}, \bar{y}) \alpha_1 - \bar{x}\alpha_2 + \bar{y}\alpha_3 + \alpha_4 \quad (D.132)$$

where

$\alpha_1, \alpha_2, \alpha_3, \alpha_4$ = virtual values of the displacement parameters, not
necessarily equal to their equilibrium values.

At the beginning of the sth time increment, the panel is warped, but the fictitious forces are considered zero, since the effects of fictitious forces from the preceding increment are eliminated by coordinate updating. The fictitious forces at the end of the sth increment are calculated by assuming that the panel is flat at the beginning of the increment. These forces are corrected by subtracting the fictitious forces that result from displacing the panel from the flat position to its deformed position at the beginning of the increment.

Let

\bar{f}_n = the value of the nth fictitious force at the end of the increment ($n = 1, 2, 3, 4$), that would exist if the panel were flat and coincident with the xy plane (defined as in Figure D.6) at the beginning of the increment.

\bar{f}_{no} = the value of \bar{f}_n resulting from deforming the flat panel into its position at the beginning of the increment.

Therefore,
$$\bar{F}_n = \bar{f}_n - \bar{f}_{no} \quad (D.133)$$

Consider an infinitesimal virtual displacement of the panel. This displacement produces the rotations $d\theta_n$ and $d\theta_\zeta$ of the infinitesimal element, which is subjected to the moments $m_n dA$ and $m_\zeta dA$, where dA is the element area. The virtual displacement also produces the displacements $d\tilde{e}_1, d\tilde{e}_2, d\tilde{e}_3$ and $d\tilde{e}_4$, of the fictitious forces $\bar{f}_1, \bar{f}_2, \bar{f}_3$ and \bar{f}_4 . Therefore, the differential potential energy of the panel is

$$dW = \int_A (m_n d\theta_n + m_\zeta d\theta_\zeta) dA - \sum_{n=1}^4 \bar{f}_n d\tilde{e}_n \quad (D.134)$$

The rotation angles and corner displacements are functions of the displacement parameters. Therefore,

$$d\theta_n = \sum_{p=1}^3 \frac{\partial \theta_n}{\partial \alpha_p} d\alpha_p \quad (D.135)$$

$$d\theta_\zeta = \sum_{p=1}^3 \frac{\partial \theta_\zeta}{\partial \alpha_p} d\alpha_p \quad (D.136)$$

$$d\tilde{e}_n = \sum_{p=1}^4 \frac{\partial \tilde{e}_n}{\partial \alpha_p} d\alpha_p \quad (D.137)$$

The rotation angles θ_n and θ_ζ are not functions of α_4 , which represents a rigid body translation.

Substituting $d\theta_n, d\theta_\zeta$ and $d\tilde{e}_n$ from Equations D.135, D.136 and D.137 into Equation D.134 gives

$$dW = \sum_{p=1}^3 W_{\alpha p}(\alpha_1, \alpha_2, \alpha_3) d\alpha_p - \sum_{n=1}^4 \bar{f}_n \sum_{p=1}^4 \frac{\partial \tilde{e}_n}{\partial \alpha_p} d\alpha_p \quad (D.138)$$

$$\text{where } W_{\alpha p} = \int_A (m_n \frac{\partial \theta_n}{\partial \alpha_p} + m_\zeta \frac{\partial \theta_\zeta}{\partial \alpha_p}) dA \quad (D.139)$$

The finite displacement represented by the parameters $\bar{\alpha}_1, \bar{\alpha}_2, \bar{\alpha}_3$ and $\bar{\alpha}_4$ is imposed. This displacement is produced in steps:

Step 1. Produce $\alpha_1 = \bar{\alpha}_1$, keeping $\alpha_2 = \alpha_3 = \alpha_4 = 0$.

Step 2. Produce $\alpha_2 = \bar{\alpha}_2$, keeping $\bar{\alpha}_1$, constant, $\alpha_3 = \alpha_4 = 0$.

Step 3. Produce $\alpha_3 = \bar{\alpha}_3$, keeping $\bar{\alpha}_1, \bar{\alpha}_2$ constant, $\alpha_4 = 0$.

Step 4. Produce $\alpha_4 = \bar{\alpha}_4$, keeping $\bar{\alpha}_1, \bar{\alpha}_2, \bar{\alpha}_3$ constant.

The displacements are applied this way to simplify solving the resulting simultaneous equations for the fictitious forces, including evaluating various terms that appear in these equations. The stepwise application of displacements is allowable, since the distributed moments are single valued functions of the displacements.

The fictitious forces are considered constant during the virtual displacement in accordance with the minimum potential energy method. From Equations D.80.1 to D.80.4, the displacements $\delta \tilde{e}_n$ are seen to be linear functions of the α 's, since the $\delta \tilde{e}$ displacements were replaced by the $\delta \tilde{e}$ displacements, according to a previous assumption. Therefore, the derivatives, $\partial \tilde{e}_n / \partial \alpha_p$, are independent of the displacement parameters.

Integrating Equation D.139, considering the stepwise displacement application, gives

$$\begin{aligned}
 W = & \int_0^{\bar{\alpha}_1} W_{\alpha_1}(\alpha_1, 0, 0) d\alpha_1 - \sum_{n=1}^4 \bar{f}_n \frac{\partial \tilde{e}_n}{\partial \alpha_1} \bar{\alpha}_1 \\
 & + \int_0^{\bar{\alpha}_2} W_{\alpha_2}(\bar{\alpha}_1, \alpha_2, 0) d\alpha_2 - \sum_{n=1}^4 \bar{f}_n \frac{\partial \tilde{e}_n}{\partial \alpha_2} \bar{\alpha}_2 \\
 & + \int_0^{\bar{\alpha}_3} W_{\alpha_3}(\bar{\alpha}_1, \bar{\alpha}_2, \alpha_3) d\alpha_3 - \sum_{n=1}^4 \bar{f}_n \frac{\partial \tilde{e}_n}{\partial \alpha_3} \bar{\alpha}_3 \\
 & - \sum_{n=1}^4 \bar{f}_n \frac{\partial \tilde{e}_n}{\partial \alpha_4} \bar{\alpha}_4
 \end{aligned} \tag{D.140}$$

Minimum Potential Energy

The total potential energy, considered as a function of the displacement parameters, is minimum when the panel is in equilibrium, therefore,

$$\frac{\partial W}{\partial \bar{\alpha}_p} = 0 \quad p = 1, 2, 3, 4 \quad (D.141)$$

It can be easily shown that

$$\frac{\partial}{\partial \bar{u}} \int_0^{\bar{u}} f(u) du = f(\bar{u}) \quad (D.142)$$

where $f(u)$ is any function of any variable u , and any other independent variables. Applying Equation D.141 to Equation D.140, considering Equation D.142, gives

$$\begin{aligned} \sum_{n=1}^4 \bar{f}_n \frac{\partial \bar{e}_n}{\partial \bar{\alpha}_1} = & W_{\alpha_1}(\bar{\alpha}_1, 0, 0) + \int_0^{\bar{\alpha}_2} \frac{\partial}{\partial \bar{\alpha}_1} W_{\alpha_2}(\bar{\alpha}_1, \alpha_2, 0) d\alpha_2 \\ & + \int_0^{\bar{\alpha}_3} \frac{\partial}{\partial \bar{\alpha}_1} W_{\alpha_3}(\bar{\alpha}_1, \bar{\alpha}_2, \alpha_3) d\alpha_3 \end{aligned} \quad (D.143)$$

$$\sum_{n=1}^4 \bar{f}_n \frac{\partial \bar{e}_n}{\partial \bar{\alpha}_2} = W_{\alpha_2}(\bar{\alpha}_2, \bar{\alpha}_2, 0) + \int_0^{\bar{\alpha}_3} \frac{\partial}{\partial \bar{\alpha}_2} W_{\alpha_3}(\bar{\alpha}_1, \bar{\alpha}_2, \alpha_3) d\alpha_3 \quad (D.144)$$

$$\sum_{n=1}^4 \bar{f}_n \frac{\partial \bar{e}_n}{\partial \bar{\alpha}_3} = W_{\alpha_3}(\bar{\alpha}_1, \bar{\alpha}_2, \bar{\alpha}_3) \quad (D.145)$$

$$\sum_{n=1}^4 \bar{f}_n \frac{\partial \bar{e}_n}{\partial \bar{\alpha}_4} = 0 \quad (D.146)$$

Equations D.143, D.144, D.145 and D.146 are a set of four simultaneous linear equations in the unknown fictitious forces, \bar{f}_1 , \bar{f}_2 , \bar{f}_3 and \bar{f}_4 .

The derivatives $\partial \bar{e}_n / \partial \alpha_p$ are found by partially differentiating Equations D.80.1 to D.80.4, and substituting $\delta \bar{e}_n$ for $\delta \bar{e}_n$, in accordance with a previous assumption. These derivatives are given in Table D.1.

Substituting the derivatives from Table D.1 into Equations D.143 to D.146 gives

TABLE D.1. VALUES OF $\partial \tilde{e}_n / \partial \alpha_p$

n	$\frac{\partial \tilde{e}_n}{\partial \alpha_1}$	$\frac{\partial \tilde{e}_n}{\partial \alpha_2}$	$\frac{\partial \tilde{e}_n}{\partial \alpha_3}$	$\frac{\partial \tilde{e}_n}{\partial \alpha_4}$
1	0	0	0	1
2	0	$-\bar{x}_D$	\bar{y}_D	1
3	1	$-\bar{x}_A$	\bar{y}_A	1
4	0	$-\bar{x}_B$	\bar{y}_B	1

$$\bar{f}_3 = W_{\alpha 1}(\bar{\alpha}_1, 0, 0) + \Lambda_Q(\bar{\alpha}_1, \bar{\alpha}_2, \bar{\alpha}_3) \quad (D.147)$$

$$-\bar{x}_D \bar{f}_2 - \bar{x}_A \bar{f}_3 - \bar{x}_B \bar{f}_4 = W_{\alpha 2}(\bar{\alpha}_1, \bar{\alpha}_2, 0) + \Lambda_R(\bar{\alpha}_1, \bar{\alpha}_2, \bar{\alpha}_3) \quad (D.148)$$

$$\bar{y}_D \bar{f}_2 + \bar{y}_A \bar{f}_3 + \bar{y}_B \bar{f}_4 = W_{\alpha 3}(\bar{\alpha}_1, \bar{\alpha}_2, \bar{\alpha}_3) \quad (D.149)$$

$$\bar{f}_1 + \bar{f}_2 + \bar{f}_3 + \bar{f}_4 = 0 \quad (D.150)$$

where

$$\Lambda_Q = \int_0^{\bar{\alpha}_2} \frac{\partial}{\partial \bar{\alpha}_1} W_{\alpha 2}(\bar{\alpha}_1, \alpha_2, 0) d\alpha_2 + \int_0^{\bar{\alpha}_3} \frac{\partial}{\partial \bar{\alpha}_1} W_{\alpha 3}(\bar{\alpha}_1, \bar{\alpha}_2, \alpha_3) d\alpha_3 \quad (D.151)$$

$$\Lambda_R = \int_0^{\bar{\alpha}_3} \frac{\partial}{\partial \bar{\alpha}_2} W_{\alpha 3}(\bar{\alpha}_1, \bar{\alpha}_2, \alpha_3) d\alpha_3 \quad (D.152)$$

Eliminating \bar{f}_2 from Equations D.148 and D.149, and employing the coordinates of the corners from Equations D.64 through D.70, and the panel area, \bar{A} , from Equation D.85, gives

$$\bar{f}_4 + \bar{f}_3 = \bar{\Lambda}_4(\bar{\alpha}_1, \bar{\alpha}_2, \bar{\alpha}_3) + \Lambda_4(\bar{\alpha}_1, \bar{\alpha}_2, \bar{\alpha}_3) \quad (D.153)$$

where

$$\bar{\Lambda}_4 = \frac{\bar{y}_D}{\bar{A}} W_{\alpha 2}(\bar{\alpha}_1, \bar{\alpha}_2, 0) + \frac{\bar{x}_D}{\bar{A}} W_{\alpha 3}(\bar{\alpha}_1, \bar{\alpha}_2, \bar{\alpha}_3) \quad (D.154)$$

$$\Lambda_4 = \frac{\bar{y}_D}{\bar{A}} \Lambda_R (\bar{\alpha}_1, \bar{\alpha}_2, \bar{\alpha}_3) \quad (D.155)$$

Similarly, eliminating \bar{f}_4 from Equations D.148 and D.149 gives

$$\bar{f}_2 + \bar{f}_3 = \bar{\Lambda}_2 (\bar{\alpha}_1, \bar{\alpha}_2, \bar{\alpha}_2) + \Lambda_2 (\bar{\alpha}_1, \bar{\alpha}_2, \bar{\alpha}_3) \quad (D.156)$$

where

$$\bar{\Lambda}_2 = -\frac{\bar{y}_B}{\bar{A}} W_{\alpha 2} (\bar{\alpha}_1, \bar{\alpha}_2, 0) - \frac{\bar{x}_B}{\bar{A}} W_{\alpha 3} (\bar{\alpha}_1, \bar{\alpha}_2, \bar{\alpha}_3) \quad (D.157)$$

$$\Lambda_2 = -\frac{\bar{y}_B}{\bar{A}} \Lambda_R (\bar{\alpha}_1, \bar{\alpha}_2, \bar{\alpha}_3) \quad (D.158)$$

Setting $\bar{\alpha}_1$ equal to $\bar{\alpha}_{1,0}$, and $\bar{\alpha}_2$, $\bar{\alpha}_3$ and $\bar{\alpha}_4$ equal to zero in Equations D.151, D.152, D.155 and D.158 gives

$$\Lambda_Q = \Lambda_R = \Lambda_4 = \Lambda_2 = 0 \quad , \quad (D.158.1)$$

corresponding to the initial position of the panel. Setting $\bar{\alpha}_1 = \bar{\alpha}_{1,0}$, and $\bar{\alpha}_2 = \bar{\alpha}_3 = \bar{\alpha}_4 = 0$ in Equations D.147, D.150, D.153 and D.156, and employing Equation D.158.1, gives

$$\bar{f}_{3,0} = W_{\alpha 1} (\bar{\alpha}_{1,0}, 0, 0) \quad , \quad (D.158.2)$$

$$\bar{f}_{1,0} + \bar{f}_{2,0} + \bar{f}_{3,0} + \bar{f}_{4,0} = 0 \quad , \quad (D.158.3)$$

$$\bar{f}_{4,0} + \bar{f}_{3,0} = \bar{\Lambda}_4 (\bar{\alpha}_{1,0}, 0, 0) \quad , \quad (D.158.4)$$

$$\bar{f}_{2,0} + \bar{f}_{3,0} = \bar{\Lambda}_2 (\bar{\alpha}_{1,0}, 0, 0) \quad , \quad (D.158.5)$$

since $\bar{f}_{1,0}$, $\bar{f}_{2,0}$, $\bar{f}_{3,0}$ and $\bar{f}_{4,0}$ are the values of \bar{f}_n corresponding to the initial position of the panel. Subtracting Equations D.158.2, D.158.3, D.158.4 and D.158.5 from Equations D.147, D.150, D.153 and D.156, and employing Equation D.133, gives

$$\bar{F}_3 = \delta W_{a1}(\bar{a}_1, 0, 0) + \Lambda_Q(\bar{a}_1, \bar{a}_2, \bar{a}_3) \quad (D.158.6)$$

$$\bar{F}_1 + \bar{F}_2 + \bar{F}_3 + \bar{F}_4 = 0 \quad (D.158.7)$$

$$\bar{F}_4 + \bar{F}_3 = \delta \bar{\Lambda}_4(\bar{a}_1, \bar{a}_2, \bar{a}_3) + \Lambda_4(\bar{a}_1, \bar{a}_2, \bar{a}_3) \quad (D.158.8)$$

$$\bar{F}_2 + \bar{F}_3 = \delta \bar{\Lambda}_2(\bar{a}_1, \bar{a}_2, \bar{a}_3) + \Lambda_2(\bar{a}_1, \bar{a}_2, \bar{a}_3) \quad (D.158.9)$$

where

$$\delta W_{a1}(\bar{a}_1, 0, 0) = W_{a1}(\bar{a}_1, 0, 0) - W_{a1}(\bar{a}_{1,0}, 0, 0) \quad (D.158.10)$$

$$\delta \bar{\Lambda}_4(\bar{a}_1, \bar{a}_2, \bar{a}_3) = \bar{\Lambda}_4(\bar{a}_1, \bar{a}_2, \bar{a}_3) - \bar{\Lambda}_4(\bar{a}_{1,0}, 0, 0) \quad (D.158.11)$$

$$\delta \bar{\Lambda}_2(\bar{a}_1, \bar{a}_2, \bar{a}_3) = \bar{\Lambda}_2(\bar{a}_1, \bar{a}_2, \bar{a}_3) - \bar{\Lambda}_2(\bar{a}_{1,0}, 0, 0) \quad (D.158.12)$$

Equations D.158.6, D.158.8, D.158.9 and D.158.7 can be solved in that order, for \bar{F}_3 , \bar{F}_4 , \bar{F}_2 and \bar{F}_1 . The terms on the right hand side of these equations are functions of the moments m_n and m_c , and the rotation angles θ_n and θ_c . The moments are given in terms of the rotation angles by Equations D.115 and D.116. The rotation angles can be found from the displacement function, Equation D.132.

Expansion of The W_{ap} Terms

Reference to Figure D.10 shows that the rotation angles are given approximately by

$$\theta_{\bar{y}} = -w_{\bar{x}} \quad (D.159)$$

$$\theta_{\bar{x}1} = w_{\bar{y}} \quad (D.160)$$

$$\text{where } w_{\bar{x}} = \partial w / \partial \bar{x} \quad (D.161)$$

$$w_{\bar{y}} = \partial w / \partial \bar{y} \quad (D.162)$$

The use of the approximations represented by Equations D.159 and D.160 is discussed subsequently under the heading "Third Order Approximation". From Equations D.132, D.159 and D.160,

$$\theta_{\bar{y}}(\alpha_1, \alpha_2, 0) = -w_{e,\bar{x}} \alpha_1 + \alpha_2 \quad (D.163)$$

$$\theta_{\bar{x}1}(\alpha_1, 0, \alpha_3) = w_{e,\bar{y}} \alpha_1 + \alpha_3 \quad (D.164)$$

$$\text{where } w_{e,\bar{x}} = \partial w_e / \partial \bar{x} \quad (D.165)$$

$$w_{e,\bar{y}} = \partial w_e / \partial \bar{y} \quad (D.166)$$

Substituting $\theta_{\bar{y}}$ and $\theta_{\bar{x}1}$ from Equations D.163 and D.164 into Equations D.127 and D.128 gives

$$\theta_n = (w_{e,\bar{x}} \sin \xi + w_{e,\bar{y}} \cos \xi) \alpha_1 - \alpha_2 \sin \xi + \alpha_3 \cos \xi \quad (D.167)$$

$$\theta_z = (-w_{e,\bar{x}} \sin \xi + w_{e,\bar{y}} \cos \xi) \alpha_1 + \alpha_2 \sin \xi + \alpha_3 \cos \xi \quad (D.168)$$

Substituting θ_n and θ_z from Equations D.167 and D.168 into Equation D.139, for $p = 1, 2$ and 3 , gives

$$w_{\alpha 1} = \int_A [w_{e,\bar{x}}(m_n - m_z) \sin \xi + w_{e,\bar{y}}(m_n + m_z) \cos \xi] dA \quad (D.169)$$

$$w_{\alpha 2} = -\sin \xi \int_A (m_n - m_z) dA \quad (D.170)$$

$$w_{\alpha 3} = \cos \xi \int_A (m_n + m_z) dA \quad (D.171)$$

Subtracting and adding Equations D.115 and D.116, and simplifying gives

$$(m_n - m_z) \sin \xi = -Q \sin \theta_{\bar{y}} \cot \xi \quad (D.172)$$

$$(m_n + m_c) \cos \xi = -Q \cos \theta_{\bar{y}} \sin \theta_{\bar{x}1} \tan \xi \quad (D.173)$$

Eliminating $m_n - m_c$ and $m_n + m_c$ from Equations D.169 to D.173 gives

$$w_{a1} = -Q \int_A (w_{e,\bar{x}} \sin \theta_{\bar{y}} \cot \xi + w_{e,\bar{y}} \cos \theta_{\bar{y}} \sin \theta_{\bar{x}1} \tan \xi) dA \quad (D.174)$$

$$w_{a2} = Q \cot \xi \int_A \sin \theta_{\bar{y}} dA \quad (D.175)$$

$$w_{a3} = -Q \tan \xi \int_A \cos \theta_{\bar{y}} \sin \theta_{\bar{x}1} dA \quad (D.176)$$

From Figure D.11, the area of the infinitesimal element is

$$dA = 2 dnd\zeta \sin \xi \cos \xi \quad (D.177)$$

Substituting dA from Equation D.177 into Equations D.174, D.175 and D.176, gives

$$w_{a1} = -2Q \int_0^b \int_0^a \left[w_{e,\bar{x}} \phi_2(a_1, a_2, 0) \cos^2 \xi + w_{e,\bar{y}} \phi_3(a_1, a_2, a_3) \sin^2 \xi \right] dnd\zeta \quad (D.178)$$

$$w_{a2} = 2Q \cos^2 \xi \int_0^b \int_0^a \phi_2(a_1, a_2, 0) dnd\zeta \quad (D.179)$$

$$w_{a3} = -2Q \sin^2 \xi \int_0^b \int_0^a \phi_3(a_1, a_2, a_3) dnd\zeta \quad (D.180)$$

$$\text{where } \phi_2(a_1, a_2, 0) = \sin \theta_{\bar{y}} \quad (D.181)$$

$$\phi_3(a_1, a_2, a_3) = \cos \theta_{\bar{y}} \sin \theta_{\bar{x}1} \quad (D.182)$$

The notation reflects the fact that $\theta_{\bar{y}}$ is not a function of a_3 .

Third Order Approximations

Expanding the trigonometric functions in Equations D.181 and D.182 as power series in $\theta_{\bar{y}}$ and $\theta_{\bar{x}1}$, and discarding terms of order higher than the third, gives

$$\phi_2(\alpha_1, \alpha_2, 0) = \theta_{\bar{y}} - \frac{1}{6} \theta_{\bar{y}}^3 \quad (D.183)$$

$$\phi_3(\alpha_1, \alpha_2, \alpha_3) = \theta_{\bar{x}1} \left(1 - \frac{1}{2} \theta_{\bar{y}}^2\right) - \frac{1}{6} \theta_{\bar{x}1}^3 \quad (D.184)$$

These approximations are not quite consistent with the approximations involved in Equations D.159 and D.160 for the rotation angles. Actually,

$$\theta_{\bar{y}} = \tan^{-1} (-w_{\bar{x}}) \quad (D.185)$$

$$\theta_{\bar{x}1} \cong \tan^{-1} w_{\bar{y}} \quad (D.186)$$

Even Equation D.186 is not exactly correct, because $\theta_{\bar{x}1}$, was defined as the rotation about the \bar{x} axis in its rotated position following the rotation $\theta_{\bar{y}}$. Equations D.185 and D.186 can be expanded as

$$\theta_{\bar{y}} = -w_{\bar{x}} + \frac{w_{\bar{x}}^2}{3} - \dots \quad (D.187)$$

$$\theta_{\bar{x}1} = w_{\bar{y}} - \frac{w_{\bar{y}}^3}{3} + \dots \quad (D.188)$$

The use of these expressions does not seem feasible in view of the complexity involved, therefore, the third order terms are discarded.

The following notation is employed in subsequent analysis:

$$\theta_{\bar{y}}(\bar{\alpha}_1, 0, 0) = \eta_{\bar{y}} \quad (D.189)$$

$$\theta_{\bar{x}1}(\bar{\alpha}_1, 0, 0) = \eta_{\bar{x}} \quad (D.190)$$

Therefore, from Equations D.163, D.164, D.189 and D.190,

$$\eta_{\bar{y}} = -w_{e,\bar{x}} \bar{a}_1 \quad (D.191)$$

$$\eta_{\bar{x}} = w_{e,\bar{y}} \bar{a}_1 \quad (D.192)$$

Combining Equations D.163, D.164, D.191 and D.192 gives

$$\theta_{\bar{y}}(\bar{a}_1, a_2, 0) = \eta_{\bar{y}} + a_2 \quad (D.193)$$

$$\theta_{\bar{x}}(\bar{a}_1, 0, a_3) = \eta_{\bar{x}} + a_3 \quad (D.194)$$

Also let

$$\zeta_{\bar{y}} = \eta_{\bar{y}} + \bar{a}_2 \quad (D.195)$$

From Equations D.59, D.165 and D.166,

$$w_{e,\bar{x}} = \frac{b_2}{b_1 \cos \xi} \quad (D.196)$$

$$w_{e,\bar{y}} = \frac{b_3}{b_1 \sin \xi} - \frac{4\bar{y}}{b_1 \sin^2 \xi} \quad (D.197)$$

$$\text{where } b_1 = 4ab \quad (D.198)$$

$$b_2 = b + a \quad (D.199)$$

$$b_3 = b - a \quad (D.200)$$

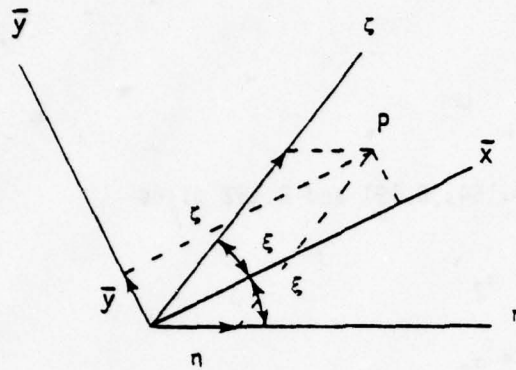


Figure D.12. The \bar{y} coordinate.

Figure D.12 shows the \bar{x}, \bar{y} and n, z coordinates of a point P. From the figure

$$\bar{y} = (z - n) \sin \xi \quad (\text{D.201})$$

Substituting \bar{y} from Equation D.201 into Equation D.197 gives

$$w_{e, \bar{y}} = \frac{b_4(u)}{b_1 \sin \xi} \quad (\text{D.202})$$

$$\text{where } b_4(u) = b_3 + 4u \quad (\text{D.203})$$

$$\text{and } u = n - z \quad (\text{D.204})$$

Eliminating $w_{e, \bar{x}}$ and $w_{e, \bar{y}}$ from Equations D.191, D.192, D.196 and D.202 gives

$$\eta_{\bar{y}} = - \frac{b_2}{b_1 \cos \xi} \bar{a}_1 \quad (\text{D.204.1})$$

$$\eta_x = \frac{b_4(u)}{b_1 \sin \xi} \bar{a}_1 \quad (D.204.2)$$

Let

$\eta_{\bar{y}0}$ and $\zeta_{\bar{y}0}$ = the values of $\eta_{\bar{y}}$ and $\zeta_{\bar{y}}$ corresponding to

$$\bar{a}_1 = \bar{a}_{1,0}, \bar{a}_2 = \bar{a}_3 = \bar{a}_4 = 0$$

Therefore, from Equations D.195 and D.204.1,

$$\eta_{\bar{y}0} = \zeta_{\bar{y}0} = - \frac{b_2}{b_1 \cos \xi} \bar{a}_{1,0} \quad (D.204.3)$$

Evaluation of $\delta W_{a1}(\bar{a}_1, 0, 0)$

This term is needed in Equation D.158.6 for the fictitious force \bar{F}_3 .
From Equation D.178,

$$W_{a1}(\bar{a}_1, 0, 0) = \int_0^b \int_0^a \psi(\bar{a}_1, 0, 0) d\eta d\zeta \quad (D.205)$$

where

$$\psi(\bar{a}_1, 0, 0) = -2Q \left[w_{e,\bar{x}} \phi_2(\bar{a}_1, 0, 0) \cos^2 \xi + w_{e,\bar{y}} \phi_3(\bar{a}_1, 0, 0) \sin^2 \xi \right] \quad (D.206)$$

From Equations D.183, D.184, D.189 and D.190,

$$\phi_2(\bar{a}_1, 0, 0) = \eta_{\bar{y}} \left(1 - \frac{1}{6} \eta_{\bar{y}}^2 \right) \quad (D.207)$$

$$\phi_3(\bar{a}_1, 0, 0) = \eta_{\bar{x}} \left(1 - \frac{1}{2} \eta_{\bar{y}}^2 \right) - \frac{1}{6} \eta_{\bar{x}}^3 \quad (D.208)$$

Substituting $w_{e,\bar{x}}$, $w_{e,\bar{y}}$, ϕ_2 and ϕ_3 from Equations D.196, D.202, D.207 and D.208 gives

$$\begin{aligned} \psi(\bar{a}_1, 0, 0) = & - \frac{2Q}{b_1} \left[b_2 \eta_{\bar{y}} \left(1 - \frac{1}{6} \eta_{\bar{y}}^2 \right) \cos \xi + b_4(u) \eta_{\bar{x}} \left(1 - \frac{1}{2} \eta_{\bar{y}}^2 \right) \sin \xi \right. \\ & \left. - \frac{1}{6} b_4(u) \eta_{\bar{x}}^3 \sin \xi \right] \quad (D.209) \end{aligned}$$

Combining Equations D.204.1, D.204.2 and D.209 gives

$$\psi(\bar{\alpha}_1, 0, 0) = -\frac{2Q}{b_1} \left[-\frac{b_2^2}{b_1} \bar{\alpha}_1 \left(1 - \frac{1}{6} n_{\bar{y}}^2\right) + \frac{\bar{\alpha}_1}{b_1} \left(1 - \frac{1}{2} n_{\bar{y}}^2\right) b_4^2(u) - \frac{1}{6} \frac{\bar{\alpha}_1^3}{b_1^3 \sin^2 \xi} b_4^4(u) \right] \quad (D.210)$$

The only function of the coordinates, n and ζ , in Equation D.210 is $b_4(u)$, where $u = n - \zeta$. Substituting ψ from Equation D.210 into Equation D.205 and integrating gives

$$W_{\alpha 1}(\bar{\alpha}_1, 0, 0) = Q \left[m_1 \bar{\alpha}_1 \left(1 - \frac{1}{6} n_{\bar{y}}^2\right) - m_2 \bar{\alpha}_1 \left(1 - \frac{1}{2} n_{\bar{y}}^2\right) + m_3 \bar{\alpha}_1^3 \right] \quad (D.211)$$

$$\text{where } m_1 = 2 \frac{b_2^2}{b_1^2} J_0 \quad (D.212)$$

$$m_2 = \frac{2}{b_1^2} J_2 \quad (D.213)$$

$$m_3 = \frac{J_4}{3b_1^4 \sin^2 \xi} \quad (D.214)$$

$$\text{and } J_k = \int_0^b \int_0^a b_4^k(u) \, dnd\zeta \quad k = 0, 1, 2, \dots, 4 \quad (D.215)$$

A list of the J_k integrals is given subsequently. Combining terms in Equation D.211 gives

$$W_{\alpha 1}(\bar{\alpha}_1, 0, 0) = Q (m_{12} \bar{\alpha}_1 - m_{13} \bar{\alpha}_1 n_{\bar{y}}^2 + m_3 \bar{\alpha}_1^3) \quad (D.216)$$

$$\text{where } m_{12} = m_1 - m_2 \quad (D.217)$$

$$m_{13} = \frac{1}{6} m_1 - \frac{1}{2} m_2 \quad (D.218)$$

Setting $\bar{\alpha}_1 = \bar{\alpha}_{1,0}$ in Equation D.216, and recalling the definition of $\eta_{\bar{y}0}$ gives

$$W_{\alpha 1}(\bar{\alpha}_{1,0}, 0, 0) = Q (m_{12}\bar{\alpha}_{1,0} - m_{13}\bar{\alpha}_{1,0} \eta_{\bar{y}0}^2 + m_3 \bar{\alpha}_{1,0}^3) \quad (D.219)$$

Combining Equations D.158.10, D.216 and D.219, and employing Equation D.86.1 gives

$$\begin{aligned} \delta W_{\alpha 1}(\bar{\alpha}_1, 0, 0) = Q \left[m_{12} \delta \bar{\alpha}_1 - m_{13} (\bar{\alpha}_1 \eta_{\bar{y}}^2 - \bar{\alpha}_{1,0} \eta_{\bar{y}0}^2) \right. \\ \left. + m_3 (\bar{\alpha}_1^3 - \bar{\alpha}_{1,0}^3) \right] \end{aligned} \quad (D.220)$$

Evaluation of $\Lambda_Q(\bar{\alpha}_1, \bar{\alpha}_2, \bar{\alpha}_3)$

This term is needed in Equation D.158.6, for the fictitious force \bar{F}_3 . From Equation D.151, Λ_Q is seen to depend on $W_{\alpha 2}(\bar{\alpha}_1, \alpha_2, 0)$ and $W_{\alpha 3}(\bar{\alpha}_1, \bar{\alpha}_2, \alpha_3)$.

From Equation D.179,

$$W_{\alpha 2}(\bar{\alpha}_1, \alpha_2, 0) = 2Q \cos^2 \varepsilon \int_0^b \int_0^a \phi_2(\bar{\alpha}_1, \alpha_2, 0) dnd\zeta \quad (D.221)$$

Therefore,

$$\begin{aligned} \int_0^{\bar{\alpha}_2} \frac{\partial}{\partial \bar{\alpha}_1} W_{\alpha 2}(\bar{\alpha}_1, \alpha_2, 0) d\alpha_2 \\ = 2Q \cos^2 \varepsilon \int_0^b \int_0^a \int_0^{\bar{\alpha}_2} \frac{\partial}{\partial \bar{\alpha}_1} \phi_2(\bar{\alpha}_1, \alpha_2, 0) d\alpha_2 dnd\zeta \end{aligned} \quad (D.222)$$

From Equations D.183 and D.193,

$$\phi_2(\bar{\alpha}_1, \alpha_2, 0) = \eta_{\bar{y}} + \alpha_2 - \frac{1}{6} (\eta_{\bar{y}} + \alpha_2)^3 \quad (D.223)$$

Therefore,

$$\frac{\partial}{\partial \bar{\alpha}_1} \phi_2(\bar{\alpha}_1, \alpha_2, 0) = \frac{\partial \eta_{\bar{y}}}{\partial \bar{\alpha}_1} - \frac{1}{2} (\eta_{\bar{y}} + \alpha_2)^2 \frac{\partial \eta_{\bar{y}}}{\partial \bar{\alpha}_1} \quad (D.224)$$

Substituting $\eta_{\bar{y}}$ from Equation D.204.1 into Equation D.224 gives

$$\frac{\partial}{\partial \bar{\alpha}_1} \phi_2(\bar{\alpha}_1, \alpha_2, 0) = - \frac{b_2}{b_1 \cos \xi} \left(1 - \frac{1}{2} \eta_{\bar{y}}^2 - \eta_{\bar{y}} \alpha_2 - \frac{1}{2} \alpha_2^2 \right) \quad (D.225)$$

Integrating Equation D.225 with respect to α_2 , and employing Equation D.195 gives

$$\int_0^{\bar{\alpha}_2} \frac{\partial}{\partial \bar{\alpha}_1} \phi_2(\bar{\alpha}_1, \alpha_2, 0) d\alpha_2 = - \frac{b_2}{b_1 \cos \xi} \bar{\alpha}_2 \left(1 - \frac{1}{2} \eta_{\bar{y}}^2 - \frac{1}{6} \bar{\alpha}_2^2 \right) \quad (D.226)$$

Combining Equations D.222 and D.226, and employing Equation D.215 gives

$$\int_0^{\bar{\alpha}_2} \frac{\partial}{\partial \bar{\alpha}_1} W_{\alpha_2}(\bar{\alpha}_1, \alpha_2, 0) d\alpha_2 = -Q \bar{\alpha}_2 m_{14} \left(1 - \frac{1}{2} \eta_{\bar{y}}^2 - \frac{1}{6} \bar{\alpha}_2^2 \right) \quad (D.227)$$

$$\text{where } m_{14} = 2 \frac{b_2}{b_1} J_0 \cos \xi \quad (D.228)$$

Similarly, from Equation D.180

$$\begin{aligned} \int_0^{\bar{\alpha}_3} \frac{\partial}{\partial \bar{\alpha}_1} W_{\alpha_3}(\bar{\alpha}_1, \bar{\alpha}_2, \alpha_3) d\alpha_3 \\ = - 2Q \sin^2 \xi \int_0^b \int_0^a \int_0^{\bar{\alpha}_3} \frac{\partial}{\partial \bar{\alpha}_1} \phi_3(\bar{\alpha}_1, \bar{\alpha}_2, \alpha_3) d\alpha_3 d\eta d\xi \end{aligned} \quad (D.229)$$

From Equations D.184, D.193 and D.194,

$$\phi_3(\bar{\alpha}_1, \bar{\alpha}_2, \alpha_3) = (\eta_{\bar{x}} + \alpha_3) \left[1 - \frac{1}{2} (\eta_{\bar{y}} + \bar{\alpha}_2)^2 \right] - \frac{1}{6} (\eta_{\bar{x}} + \alpha_3)^3 \quad (D.230)$$

Differentiating Equation D.230 with respect to $\bar{\alpha}_1$, integrating with respect to α_3 , and employing Equation D.195 gives

$$\int_0^{\bar{\alpha}_3} \frac{\partial}{\partial \bar{\alpha}_1} \phi_3(\bar{\alpha}_1, \bar{\alpha}_2, \alpha_3) d\alpha_3 = \frac{\partial \eta_{\bar{x}}}{\partial \bar{\alpha}_1} \left[\left(1 - \frac{1}{2} \zeta_{\bar{y}}^2\right) \bar{\alpha}_3 - \frac{1}{2} \eta_{\bar{x}}^2 \bar{\alpha}_3 \right. \\ \left. - \frac{1}{2} \eta_{\bar{x}} \bar{\alpha}_3^2 - \frac{1}{6} \bar{\alpha}_3^3 \right] - \frac{\partial \eta_{\bar{y}}}{\partial \bar{\alpha}_1} \zeta_{\bar{y}} \left(\eta_{\bar{x}} \bar{\alpha}_3 + \frac{1}{2} \bar{\alpha}_3^2 \right) \quad (D.231)$$

Substituting $\eta_{\bar{x}}$ and $\eta_{\bar{y}}$ from Equations D.204.1 and D.204.2 into Equation D.231, substituting the resulting expression into Equation D.229, and employing Equation D.215 gives

$$\int_0^{\bar{\alpha}_3} \frac{\partial}{\partial \bar{\alpha}_1} W_{\alpha_3}(\bar{\alpha}_1, \bar{\alpha}_2, \alpha_3) d\alpha_3 = -Q\bar{\alpha}_3 \left[m_{15} \left(1 - \frac{1}{2} \zeta_{\bar{y}}^2 - \frac{1}{6} \bar{\alpha}_3^2\right) \right. \\ \left. - \bar{\alpha}_1 \bar{\alpha}_3 m_{16} - \bar{\alpha}_1^2 m_{17} \right] - Q\bar{\alpha}_3 \zeta_{\bar{y}} (m_{18} \bar{\alpha}_1 + m_{19} \bar{\alpha}_3) \quad (D.232)$$

$$\text{where } m_{15} = 2 \frac{J_1}{b_1} \sin \xi \quad (D.233)$$

$$m_{16} = \frac{J_2}{b_1^2} \quad (D.234)$$

$$m_{17} = \frac{J_3}{b_1^3 \sin \xi} \quad (D.235)$$

$$m_{18} = 2 \frac{b_2 J_1 \sin \xi}{b_1^2 \cos \xi} \quad (D.236)$$

$$m_{19} = \frac{b_2 J_0 \sin^2 \xi}{b_1 \cos \xi} \quad (D.237)$$

Combining Equations D.151, D.227 and D.232 gives

$$\begin{aligned}\Lambda_Q = & -Q\alpha_2 m_{14} \left(1 - \frac{1}{2} \eta_{\bar{y}} \zeta_{\bar{y}} - \frac{1}{6} \bar{\alpha}_2^2\right) \\ & - Q\bar{\alpha}_3 \left[m_{15} \left(1 - \frac{1}{2} \zeta_{\bar{y}}^2 - \frac{1}{6} \bar{\alpha}_3^2\right) - \alpha_1 \alpha_3 m_{16} - \alpha_1^2 m_{17}\right] \\ & - Q\bar{\alpha}_3 \zeta_{\bar{y}} (m_{18} \bar{\alpha}_1 + m_{19} \bar{\alpha}_3)\end{aligned}\quad (D.238)$$

Evaluation of $\delta\bar{\Lambda}_4$ and $\delta\bar{\Lambda}_2$

Substituting \bar{y}_D , \bar{x}_D , \bar{A} , $W_{\alpha 2}$ and $W_{\alpha 3}$ from Equations D.69, D.70, D.86, D.179 and D.180 into Equation D.154 gives

$$\bar{\Lambda}_4 = \int_0^b \int_0^a \psi_4(\bar{\alpha}_1, \bar{\alpha}_2, \bar{\alpha}_3) \, dnd\zeta \quad (D.239)$$

where

$$\psi_4 = \frac{Q}{B} [-\phi_2(\bar{\alpha}_1, \bar{\alpha}_2, 0) \cos \xi - \phi_3(\bar{\alpha}_1, \bar{\alpha}_2, \bar{\alpha}_3) \sin \xi] \quad (D.240)$$

Substituting \bar{y}_B , \bar{x}_B , \bar{A} , $W_{\alpha 2}$ and $W_{\alpha 3}$ from Equations D.66, D.67, D.86, D.179 and D.180 into Equation D.157 gives

$$\bar{\Lambda}_2 = \int_0^b \int_0^a \psi_2(\bar{\alpha}_1, \bar{\alpha}_2, \bar{\alpha}_3) \, dnd\zeta \quad (D.241)$$

where

$$\psi_2 = \frac{Q}{A} [-\phi_2(\bar{\alpha}_1, \bar{\alpha}_2, 0) \cos \xi + \phi_3(\bar{\alpha}_1, \bar{\alpha}_2, \bar{\alpha}_3) \sin \xi] \quad (D.242)$$

$\bar{\Lambda}_4$ and $\bar{\Lambda}_2$ can be evaluated simultaneously by adopting the notation

$$\bar{\Lambda}_{4,2} = \int_0^b \int_0^a \psi_{4,2}(\bar{\alpha}_1, \bar{\alpha}_2, \bar{\alpha}_3) \, dnd\zeta \quad (D.243)$$

where

$$\psi_{4,2} = \frac{Q}{c_{4,2}} [-\phi_2(\bar{a}_1, \bar{a}_2, 0) \cos \xi + \phi_3(\bar{a}_1, \bar{a}_2, \bar{a}_3) \sin \xi] \quad (D.244)$$

$$\text{and where } c_4 = b \quad (D.245)$$

$$c_2 = a \quad (D.246)$$

From Equations D.181, D.182, D.193, D.194 and D.195,

$$\phi_2(\bar{a}_1, \bar{a}_2, 0) = \zeta_{\bar{y}} - \frac{1}{6} \zeta_{\bar{y}}^3 \quad (D.247)$$

$$\phi_3(\bar{a}_1, \bar{a}_2, \bar{a}_3) = (\eta_{\bar{x}} + \bar{a}_3) \left(1 - \frac{1}{2} \zeta_{\bar{y}}^2\right) - \frac{1}{6} (\eta_{\bar{x}} + \bar{a}_3)^3 \quad (D.248)$$

Substituting ϕ_2 and ϕ_3 from Equations D.247 and D.248 into Equation D.244, substituting the resulting expression for $\psi_{4,2}$ into Equation D.243, and employing Equation D.215 gives

$$\begin{aligned} \bar{\lambda}_{4,2} = \frac{Q}{c_{4,2}} [-m_4 \zeta_{\bar{y}} \left(1 - \frac{1}{6} \zeta_{\bar{y}}^2\right) + m_5 \bar{a}_3 \left(1 - \frac{1}{2} \zeta_{\bar{y}}^2 - \frac{1}{6} \bar{a}_3^2\right) \\ + m_7 \bar{a}_1 \left(1 - \frac{1}{2} \zeta_{\bar{y}}^2 - \frac{1}{2} \bar{a}_3^2\right) \pm m_8 \bar{a}_1^2 \bar{a}_3 \pm m_9 \bar{a}_1^3] \end{aligned} \quad (D.249)$$

$$\text{where } m_4 = J_0 \cos \xi \quad (D.250)$$

$$m_5 = J_0 \sin \xi \quad (D.251)$$

$$m_7 = \frac{J_1}{b_1} \quad (D.252)$$

$$m_8 = \frac{1}{2} \frac{J_2}{b_1^2 \sin \xi} \quad (D.253)$$

$$m_9 = \frac{1}{6} \frac{J_3}{b_1^3 \sin^2 \xi} \quad (D.254)$$

Expanding the terms inside the brackets in Equation D.249, gives

$$\bar{\Lambda}_{4,2} = \frac{Q}{c_{4,2}} (-m_4 \zeta_{\bar{y}} + m_{10} \zeta_{\bar{y}}^3 + m_5 \bar{\alpha}_3 \pm m_{11} \bar{\alpha}_3 \zeta_{\bar{y}}^2 \pm m_6 \bar{\alpha}_3^3 \\ + m_7 \bar{\alpha}_1 \pm m_{20} \bar{\alpha}_1 \zeta_{\bar{y}}^2 \pm m_{20} \bar{\alpha}_1 \bar{\alpha}_3^2 \pm m_8 \bar{\alpha}_1^2 \bar{\alpha}_3 \pm m_9 \bar{\alpha}_1^3) \quad (D.255)$$

$$\text{where } m_{10} = \frac{1}{6} m_4 \quad (D.256)$$

$$m_{11} = \frac{1}{2} m_5 \quad (D.257)$$

$$m_6 = \frac{1}{6} m_5 \quad (D.258)$$

$$m_{20} = \frac{1}{2} m_7 \quad (D.259)$$

Setting $\bar{\alpha}_1 = \bar{\alpha}_{1,0}$, $\bar{\alpha}_2 = 0$ and $\bar{\alpha}_3 = 0$ in Equation D.255, and recalling the definition of $\zeta_{\bar{y}0}$ gives

$$\bar{\Lambda}_{4,2}(\bar{\alpha}_{1,0}, 0, 0) = \frac{Q}{c_{4,2}} (-m_4 \zeta_{\bar{y}0} + m_{10} \zeta_{\bar{y}0}^3 + m_7 \bar{\alpha}_{1,0} \pm m_{20} \bar{\alpha}_{1,0} \zeta_{\bar{y}0}^2 \\ \pm m_9 \bar{\alpha}_{1,0}^3) \quad (D.260)$$

Equations D.158.11 and D.158.12 can be written

$$\delta \bar{\Lambda}_{4,2}(\bar{\alpha}_1, \bar{\alpha}_2, \bar{\alpha}_3) = \bar{\Lambda}_{4,2}(\bar{\alpha}_1, \bar{\alpha}_2, \bar{\alpha}_3) - \bar{\Lambda}_{4,2}(\bar{\alpha}_{1,0}, 0, 0) \quad (D.261)$$

Combining Equations D.255, D.260 and D.261, and employing Equation D.36.1, gives

$$\delta \bar{\Lambda}_{4,2}(\bar{\alpha}_1, \bar{\alpha}_2, \bar{\alpha}_3) = \frac{Q}{c_{4,2}} [-m_4 (\zeta_{\bar{y}} - \zeta_{\bar{y}0}) + m_{10} (\zeta_{\bar{y}}^3 - \zeta_{\bar{y}0}^3) + m_5 \bar{\alpha}_3 \\ \pm m_{11} \bar{\alpha}_3 \zeta_{\bar{y}}^2 \pm m_6 \bar{\alpha}_3^3 + m_7 \delta \bar{\alpha}_1 \pm m_{20} (\bar{\alpha}_1 \zeta_{\bar{y}}^2 - \bar{\alpha}_{1,0} \zeta_{\bar{y}0}^2) \\ \pm m_{20} \bar{\alpha}_1 \bar{\alpha}_3^2 \pm m_8 \bar{\alpha}_1^2 \bar{\alpha}_3 \pm m_9 (\bar{\alpha}_1^3 - \bar{\alpha}_{1,0}^3)] \quad (D.262)$$

Evaluation of Λ_4 and Λ_2

Substituting \bar{y}_D and \bar{A} from Equations D.70 and D.86 into Equation D.155 gives

$$\Lambda_4 = - \frac{1}{2b \cos \xi} \Lambda_R(\bar{a}_1, \bar{a}_2, \bar{a}_3) \quad (D.263)$$

Substituting \bar{y}_B and \bar{A} from Equations D.67 and D.86 into Equation D.158 gives

$$\Lambda_2 = - \frac{1}{2a \cos \xi} \Lambda_R(\bar{a}_1, \bar{a}_2, \bar{a}_3) \quad (D.264)$$

Equations D.263 and D.264 can be written

$$\Lambda_{4,2} = - \frac{1}{2c_{4,2} \cos \xi} \Lambda_R(\bar{a}_1, \bar{a}_2, \bar{a}_3) \quad (D.265)$$

Substituting W_{a3} from Equation D.179 into Equation D.152 for Λ_R gives

$$\Lambda_R = -2Q \sin^2 \xi \int_0^b \int_0^a \int_0^{\bar{a}_3} \frac{\partial}{\partial \bar{a}_2} \phi_3(\bar{a}_1, \bar{a}_2, a_3) da_3 dnd\tau \quad (D.266)$$

Differentiating Equation D.230 with respect to \bar{a}_2 , and employing Equation D.195 gives

$$\frac{\partial}{\partial \bar{a}_2} \phi_3(\bar{a}_1, \bar{a}_2, a_3) = -\zeta_y(\eta_{\bar{x}} + a_3) \quad (D.267)$$

Therefore,

$$\int_0^{\bar{a}_3} \frac{\partial}{\partial \bar{a}_2} \phi_3(\bar{a}_1, \bar{a}_2, a_3) da_3 = -\zeta_y(\eta_{\bar{x}} \bar{a}_3 + \frac{1}{2} \bar{a}_3^2) \quad (D.268)$$

Substituting $\eta_{\bar{x}}$ from Equation D.204.2 into Equation D.268, substituting the resulting expression into Equation D.266, and employing Equation D.215 gives

$$\Lambda_R = Q\bar{a}_3\zeta_y \left(2 \frac{\bar{a}_1}{b_1} J_1 \sin \xi + \bar{a}_3 J_0 \sin^2 \xi \right) \quad (D.269)$$

Substituting Λ_R from Equation D.269 into Equation D.265 gives

$$\Lambda_{4,2} = - \frac{Q \bar{a}_3 \xi \bar{y}}{c_{4,2}} (2 \bar{m}_7 \bar{a}_1 + \bar{m}_5 \bar{a}_3) \quad (D.270)$$

$$\text{where } \bar{m}_7 = \frac{J_1 \sin \xi}{2b_1 \cos \xi} \quad (D.271)$$

$$\bar{m}_5 = \frac{J_0 \sin^2 \xi}{2 \cos \xi} \quad (D.272)$$

Panel Fictitious Deformations

Equation D.131.1 gives the fictitious deformation of the infinitesimal element corresponding to the shear flow Q . Eliminating e_{fu} from Equations D.131 and D.131.1 gives

$$d\bar{e}_{fQ} = 2 [-\cos^2 \xi (1 - \cos \theta_{\bar{y}}) + \sin^2 \xi \cos \theta_{\bar{y}} (1 - \cos \theta_{\bar{x}1})] d\eta d\zeta \quad (D.273)$$

Replacing $\theta_{\bar{y}}$ and $\theta_{\bar{x}1}$ in Equation D.273 by power series expansions, gives

$$d\bar{e}_{fQ} = \left\{ -2 \cos^2 \xi \left[1 - \left(1 - \frac{\theta_{\bar{y}}^2}{2} + \dots \right) \right] + 2 \sin^2 \xi \left(1 - \frac{\theta_{\bar{y}}^2}{2} + \dots \right) \left[1 - \left(1 - \frac{\theta_{\bar{x}1}^2}{2} + \dots \right) \right] \right\} d\eta d\zeta \quad (D.274)$$

Discarding powers of $\theta_{\bar{y}}$ and $\theta_{\bar{x}1}$ higher than the third gives

$$d\bar{e}_{fQ} = (\theta_{\bar{x}1}^2 \sin^2 \xi - \theta_{\bar{y}}^2 \cos^2 \xi) d\eta d\zeta \quad (D.275)$$

For a skewed element, Equation D.275 yields a fictitious deformation, even when the rotation angles are such that the element does not change shape. Equation D.275 shows that if $\theta_{\bar{x}1} = \theta_{\bar{y}}$, then

$$d\bar{e}_{fQ} = -\theta_{\bar{y}}^2 (\cos 2\xi) d\eta d\zeta \quad (D.276)$$

Thus, the fictitious deformation is not zero, but negative, for $2\xi < 90^\circ$ and $\theta_{\bar{x}1} = \theta_{\bar{y}}$.

Figure D.12.1 shows what happens in this case. The panel has sides of length equal to unity, and the origin of the $\bar{x}\bar{y}$ reference frame is taken at the panel centroid. The rotated position of the panel is shown by dotted lines. The effect of the equal rotations about the \bar{x} and \bar{y} axes is to cause the projection of the panel upon the $\bar{x}\bar{y}$ plane to become smaller, without changing shape. The shear forces, which are equal to the shear flow Q , are seen to move sideways and backwards, consequently, they do negative work. This work is equal to the fictitious deformation, \bar{e}_{fQ} , since \bar{e}_{fQ} corresponds to 0, and is equal to the work done by a unit value of the shear flow. Thus, the fictitious deformation is not zero, even though the panel does not change shape.

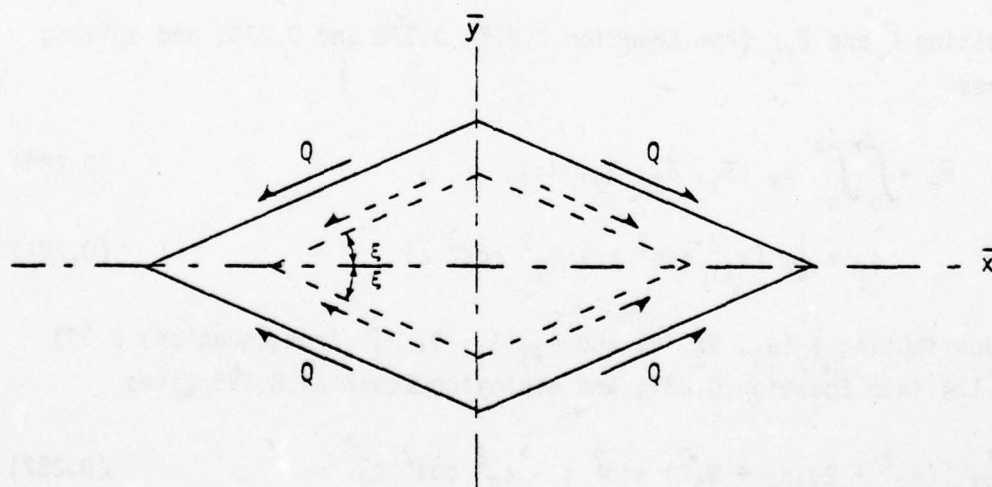


Figure D.12.1 Fictitious deformation for $\theta_{\bar{x}1} = \theta_{\bar{y}}$.

The fictitious deformation of the panel is found by integrating Equation D.275. Therefore,

$$\bar{e}_{fQ} = \int_0^b \int_0^a (\theta_{\bar{x}1}^2 \sin^2 \xi - \theta_{\bar{y}}^2 \cos^2 \xi) dnd\tau \quad (D.277)$$

Equation D.277 gives the fictitious deformation corresponding to the shear flow Q , but the deformation corresponding to the force \bar{F} is desired, where \bar{F} is the force acting on an edge of length "a", when \bar{F} is positive, and of length "b", when \bar{F} is negative, as shown in Figure D.6.1. The work done by \bar{F} should be equal to the work done by Q during a virtual fictitious deformation, therefore

$$\bar{e}_f \bar{F} = \bar{e}_{fQ} Q \quad (D.278)$$

$$\text{But} \quad \bar{F} = Qa' \quad (D.279)$$

$$\text{where} \quad a' = a \quad \text{when } \bar{F} > 0 \quad (D.279.1)$$

$$a' = b \quad \text{when } \bar{F} < 0 \quad (D.279.2)$$

Eliminating \bar{F} and \bar{e}_{fQ} from Equation D.277, D.278 and D.279, and solving \bar{e}_f gives

$$\bar{e}_f = \int_0^b \int_0^a \psi_f (\bar{\alpha}_1, \bar{\alpha}_2, \bar{\alpha}_3) dnd\tau \quad (D.280)$$

$$\text{where} \quad \psi_f = \frac{1}{a'} (\theta_{\bar{x}1}^2 \sin^2 \xi - \theta_{\bar{y}}^2 \cos^2 \xi) \quad (D.281)$$

Substituting $\theta_{\bar{y}}(\bar{\alpha}_1, \bar{\alpha}_2, 0)$ and $\theta_{\bar{x}1}(\bar{\alpha}_1, 0, \bar{\alpha}_3)$ from Equations D.193 and D.194 into Equation D.281, and employing Equation D.195 gives

$$\psi_f = \frac{1}{a'} [(\eta_{\bar{x}}^2 + 2\bar{\alpha}_3 \eta_{\bar{x}} + \bar{\alpha}_3^2) \sin^2 \xi - \zeta_{\bar{y}}^2 \cos^2 \xi] \quad (D.282)$$

Substituting $\eta_{\bar{x}}$ from Equation D.204.2 into Equation D.282, and substituting the resulting expression into Equation D.280 gives

$$\bar{e}_f = \frac{1}{a'} (m_{16} \bar{\alpha}_1^2 + m_{15} \bar{\alpha}_1 \bar{\alpha}_3 + m_{21} \bar{\alpha}_3^2 - m_{22} \zeta_{\bar{y}}^2) \quad (D.283)$$

$$\text{where } m_{21} = J_0 \sin^2 \xi \quad (D.284)$$

$$m_{22} = J_0 \cos^2 \xi \quad (D.285)$$

Setting $\bar{\alpha}_1 = \bar{\alpha}_{1,0}$ and $\bar{\alpha}_3 = 0$ in Equation D.283 gives

$$\bar{e}_{f0} = \frac{1}{a^2} (m_{16} \bar{\alpha}_{1,0}^2 - m_{22} \zeta_{y0}^2) \quad (D.286)$$

The incremental fictitious deformation is

$$\delta \bar{e}_f = \bar{e}_f - \bar{e}_{f0} \quad (D.287)$$

Substituting \bar{e}_f and \bar{e}_{f0} from Equations D.283 and D.286 into Equation D.287 gives

$$\delta \bar{e}_f = \frac{1}{a^2} [m_{16}(\bar{\alpha}_1^2 - \bar{\alpha}_{1,0}^2) + m_{15} \bar{\alpha}_1 \bar{\alpha}_3 + m_{21} \bar{\alpha}_3^2 - m_{22}(\zeta_{\bar{y}}^2 - \zeta_{y0}^2)] \quad (D.288)$$

J - Integrals

Eliminating b_3 , $b_4(u)$ and u from Equations D.200, D.203, D.204 and D.205 gives

$$J_k = \int_0^b \int_0^a [b - a + 4(\eta - \zeta)]^k d\eta d\zeta, \quad k = 0, 1, 2, 3, 4 \quad (D.289)$$

Evaluating J_k for each value of k gives

$$J_0 = a b \quad , \quad (D.290)$$

$$J_1 = a b (a - b) \quad , \quad (D.291)$$

$$J_2 = \frac{ab}{3} (7a^2 - 6ab + 7b^2) \quad , \quad (D.292)$$

$$J_3 = ab (5a^3 - 7a^2b + 7ab^2 - 5b^3) \quad , \quad (D.293)$$

$$J_4 = ab \left(\frac{61}{5} a^4 - 20a^3b + \frac{98}{3} a^2b^2 - 20ab^3 + \frac{61}{5} b^4 \right). \quad (D.294)$$

Final Form of the Shear Panel Equations

The fictitious force and deformation equations are rewritten in a form corresponding to the computer code.

Let

$$\bar{n}_3 = \delta W_{\alpha 1}(\bar{\alpha}_1, 0, 0) \quad (D.295)$$

$$\tilde{n}_3 = \Lambda_Q(\bar{\alpha}_1, \bar{\alpha}_2, \bar{\alpha}_3) \quad (D.296)$$

$$\bar{u}_4 = \delta \bar{\Lambda}_4(\bar{\alpha}_1, \bar{\alpha}_2, \bar{\alpha}_3) \quad (D.297)$$

$$\bar{u}_2 = \delta \bar{\Lambda}_2(\bar{\alpha}_1, \bar{\alpha}_2, \bar{\alpha}_3) \quad (D.298)$$

$$\tilde{u}_4 = \Lambda_4(\bar{\alpha}_1, \bar{\alpha}_2, \bar{\alpha}_3) \quad (D.299)$$

$$\tilde{u}_2 = \Lambda_2(\bar{\alpha}_1, \bar{\alpha}_2, \bar{\alpha}_3) \quad (D.300)$$

Combining Equations D.158.6, D.158.8, D.158.9 and D.295 to D.300 gives

$$\bar{\bar{F}}_3 = \bar{n}_3 + \tilde{n}_3 \quad (D.301)$$

$$\bar{\bar{F}}_4 + \bar{\bar{F}}_3 = \bar{u}_4 + \tilde{u}_4 \quad (D.302)$$

$$\bar{\bar{F}}_2 + \bar{\bar{F}}_3 = \bar{u}_2 + \tilde{u}_2 \quad (D.303)$$

Solving Equations D.158.7, D.301 D.302 and D.303 for the fictitious forces gives

$$\bar{\bar{F}}_Y = n_Y \quad Y = 1, 2, 3, 4 \quad (D.304)$$

$$\text{where } n_3 = \bar{n}_3 + \tilde{n}_3 \quad (D.305)$$

$$n_4 = \bar{u}_4 - n_3 \quad (D.306)$$

$$n_2 = \bar{u}_2 - n_3 \quad (D.307)$$

$$n_1 = -n_2 - n_3 - n_4 \quad (D.308)$$

$$\text{and } u_4 = \bar{u}_4 + \tilde{u}_4 \quad (D.309)$$

$$u_2 = \bar{u}_2 + \tilde{u}_2 \quad (D.310)$$

Let

$$\bar{r} = m_{16}(\bar{\alpha}_1^2 - \bar{\alpha}_{1,0}^2) + m_{15}\bar{\alpha}_1\bar{\alpha}_3 + m_{21}\bar{\alpha}_3^2 - m_{22}(\zeta_{\bar{y}}^2 - \zeta_{\bar{y}0}^2) \quad (D.311)$$

Combining Equations D.288 and D.311 gives

$$\delta \tilde{e}_f = \frac{\bar{r}}{a^T} \quad (D.312)$$

Equations D.304 and D.312 give the fictitious forces and deformations in terms of the panel shear flow Q , the corner displacements $\delta \tilde{e}_1$, $\delta \tilde{e}_2$, $\delta \tilde{e}_3$, $\delta \tilde{e}_4$, the initial corner displacement $\bar{e}_{0,3}$, and the panel dimensions, through Equations D.305, to D.310, D.312, D.295 to D.300, D.220, D.238, D.262 and D.270.

This form of the shear panel equations is considered satisfactory for computer coding. At the time that the Math Model program was being prepared, however, a variation on the method of solving the nonlinear equation of motion was being studied. This variation, later abandoned, called for an expanded form of the shear panel equations, and so the equations were programmed in the expanded form.

To derive the expanded form, let

$$\delta \eta_{\bar{y}} = \eta_{\bar{y}} - \eta_{\bar{y}0} \quad (D.312.1)$$

$$\delta \zeta_{\bar{y}} = \zeta_{\bar{y}} - \zeta_{\bar{y}0} \quad (D.312.2)$$

Combining Equations D.86.1, D.204.1, D.204.3 and D.312.1, gives

$$\delta \eta_{\bar{y}} = - \frac{b_2}{b_1 \cos \xi} \delta \bar{\alpha}_1 \quad (D.312.3)$$

AD-A063 740

DOUGLAS AIRCRAFT CO LONG BEACH CALIF
AIRCRAFT WINDSHIELD BIRD IMPACT MATH MODEL. PART 1. THEORY AND --ETC(U)
DEC 77 P H DENKE

F/G 1/3

F33615-75-C-3105

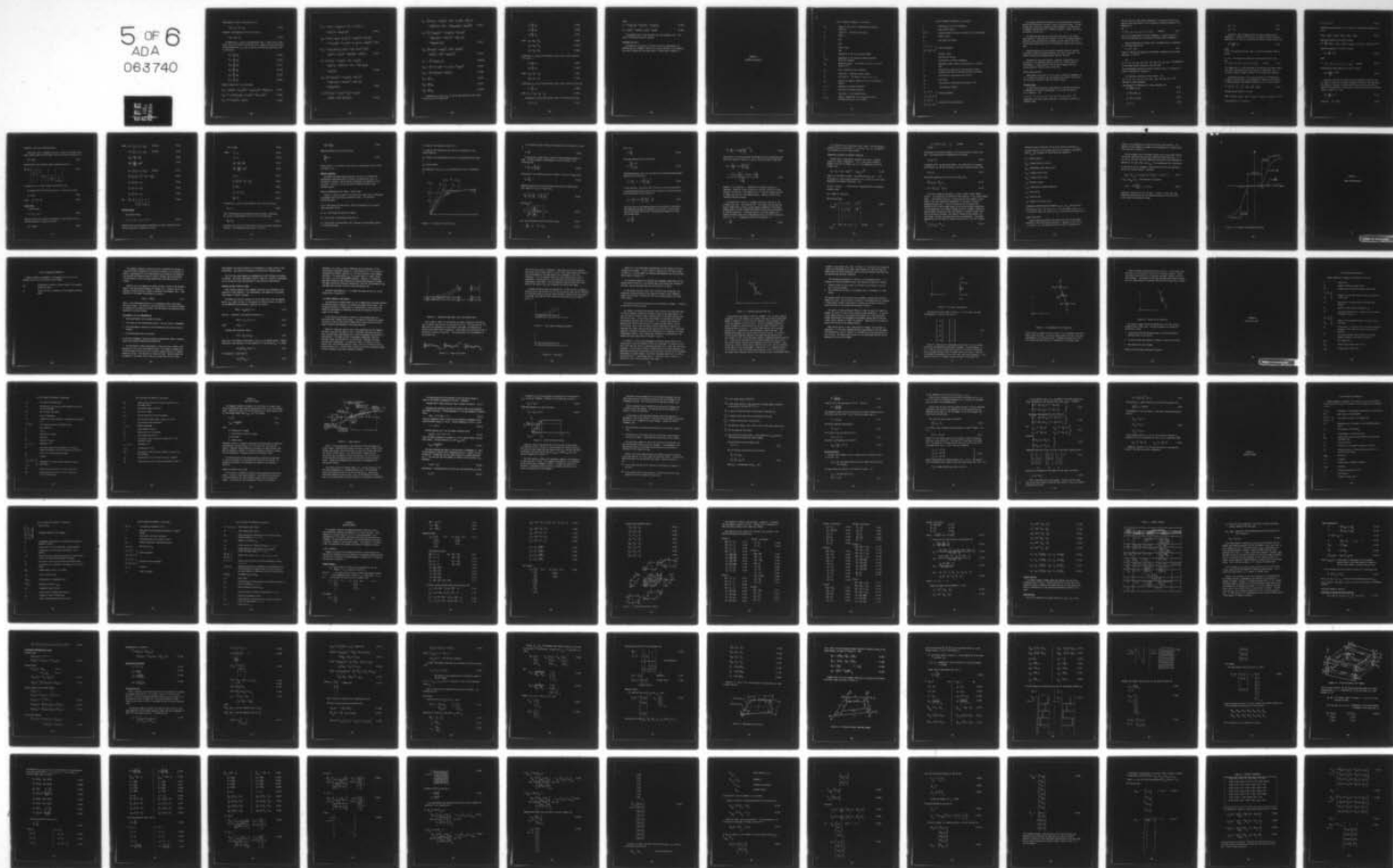
UNCLASSIFIED

MDC-J7174-PT-1

AFFDL-TR-77-99-PT-1

NL

5 OF 6
ADA
083740



From Equations D.195, D.204.3 and D.312.2,

$$\delta \zeta_{\bar{y}} = \eta_{\bar{y}} + \bar{\alpha}_2 - \eta_{\bar{y}0} \quad (D.313)$$

Therefore, from Equations D.312.1 and D.312.4,

$$\delta \zeta_{\bar{y}} = \delta \eta_{\bar{y}} + \bar{\alpha}_2 \quad (D.314)$$

Eliminating $\bar{\alpha}_1$, $\eta_{\bar{y}}$ and $\zeta_{\bar{y}}$ from Equations D.86.1, D.220, D.238, D.262, D.270, D.312.1 and D.312.2, collecting first, second and third order terms in the variables $\delta \bar{\alpha}_1$, $\delta \eta_{\bar{y}}$, $\delta \zeta_{\bar{y}}$, $\bar{\alpha}_2$ and $\bar{\alpha}_3$, and employing Equations D.295 to D.300 gives

$$\bar{n}_3 = \sum_k \bar{n}_{3k} \quad (D.315)$$

$$\tilde{n}_3 = \sum_k \tilde{n}_{3k} \quad (D.316)$$

$$\bar{u}_4 = \sum_k \bar{u}_{4k} \quad (D.317)$$

$$\bar{u}_2 = \sum_k \bar{u}_{2k} \quad (D.318)$$

$$\tilde{u}_4 = \sum_k \tilde{u}_{4k} \quad (D.319)$$

$$\tilde{u}_2 = \sum_k \tilde{u}_{2k} \quad (D.320)$$

where k ranges from 1 to 3, and where

$$\bar{n}_{3,1} = Q [m_{12} \delta \bar{\alpha}_1 - m_{13} (\eta_{\bar{y}0}^2 \delta \bar{\alpha}_1 + 2 \eta_{\bar{y}0} \bar{\alpha}_{1,0} \delta \eta_{\bar{y}}) + 3m_3 \bar{\alpha}_{1,0}^2 \delta \bar{\alpha}_1] \quad (D.321)$$

$$\bar{n}_{3,2} = Q [-m_{13} (2\eta_{\bar{y}0} \delta \eta_{\bar{y}} \delta \bar{\alpha}_1 + \bar{\alpha}_{1,0} \delta \eta_{\bar{y}}^2) + 3m_3 \bar{\alpha}_{1,0} \delta \bar{\alpha}_1^2] \quad (D.322)$$

$$\bar{n}_{3,3} = Q (-m_{13} \delta \eta_{\bar{y}}^2 \delta \bar{\alpha}_1 + m_3 \delta \bar{\alpha}_1^3) \quad (D.324)$$

$$\begin{aligned}\tilde{n}_{3,1} = & Q \left[-m_{14} \left(1 - \frac{1}{2} \eta_{\bar{y}0} \zeta_{\bar{y}0} \right) \bar{\alpha}_2 - m_{15} \left(1 - \frac{1}{2} \zeta_{\bar{y}0}^2 \right) \bar{\alpha}_3 \right. \\ & \left. + m_{17} \bar{\alpha}_{1,0}^2 \bar{\alpha}_3 - m_{18} \zeta_{\bar{y}0} \bar{\alpha}_{1,0} \bar{\alpha}_3 \right] \quad (D.325)\end{aligned}$$

$$\begin{aligned}\tilde{n}_{3,2} = & Q \left[\frac{1}{2} m_{14} (\eta_{\bar{y}0} \delta \zeta_{\bar{y}} + \zeta_{\bar{y}0} \delta \eta_{\bar{y}}) \bar{\alpha}_2 + m_{15} \zeta_{\bar{y}0} \bar{\alpha}_3 \delta \zeta_{\bar{y}} + m_{16} \bar{\alpha}_{1,0} \bar{\alpha}_3^2 \right. \\ & \left. + 2 m_{17} \bar{\alpha}_{1,0} \bar{\alpha}_3 \delta \bar{\alpha}_1 - m_{18} (\zeta_{\bar{y}0} \delta \bar{\alpha}_1 + \bar{\alpha}_{1,0} \delta \zeta_{\bar{y}}) \bar{\alpha}_3 - m_{19} \zeta_{\bar{y}0} \bar{\alpha}_3^2 \right] \quad (D.326)\end{aligned}$$

$$\begin{aligned}\tilde{n}_{3,3} = & Q \left[m_{14} \bar{\alpha}_2 \left(\frac{1}{2} \delta \eta_{\bar{y}} \delta \zeta_{\bar{y}} + \frac{1}{6} \bar{\alpha}_2^2 \right) + m_{15} \bar{\alpha}_3 \left(\frac{1}{2} \delta \zeta_{\bar{y}}^2 + \frac{1}{6} \bar{\alpha}_3^2 \right) \right. \\ & \left. + m_{16} \bar{\alpha}_3^2 \delta \bar{\alpha}_1 + m_{17} \bar{\alpha}_3 \delta \bar{\alpha}_1^2 - m_{18} \bar{\alpha}_3 \delta \zeta_{\bar{y}} \delta \bar{\alpha}_1 - m_{19} \bar{\alpha}_3^2 \delta \zeta_{\bar{y}} \right] \quad (D.327)\end{aligned}$$

$$\begin{aligned}\bar{u}_{4,1} = & \frac{Q}{6} \left(-m_4 \delta \zeta_{\bar{y}} + 3 m_{10} \zeta_{\bar{y}0}^2 \delta \zeta_{\bar{y}} - m_5 \bar{\alpha}_3 + m_{11} \zeta_{\bar{y}0}^2 \bar{\alpha}_3 \right. \\ & \left. + m_8 \bar{\alpha}_{1,0}^2 \bar{\alpha}_3 + 3 m_9 \bar{\alpha}_{1,0} \delta \bar{\alpha}_1 - m_7 \delta \bar{\alpha}_1 + 2 m_{20} \bar{\alpha}_{1,0} \zeta_{\bar{y}0} \delta \zeta_{\bar{y}} \right. \\ & \left. + m_{20} \zeta_{\bar{y}0}^2 \delta \bar{\alpha}_1 \right) \quad (D.328)\end{aligned}$$

$$\begin{aligned}\bar{u}_{4,2} = & \frac{Q}{6} \left(3 m_{10} \zeta_{\bar{y}0} \delta \zeta_{\bar{y}}^2 + 2 m_{11} \zeta_{\bar{y}0} \bar{\alpha}_3 \delta \zeta_{\bar{y}} + m_{20} \bar{\alpha}_{1,0} \bar{\alpha}_3^2 \right. \\ & \left. + 2 m_8 \bar{\alpha}_{1,0} \delta \bar{\alpha}_1 \bar{\alpha}_3 + 3 m_9 \bar{\alpha}_{1,0} \delta \bar{\alpha}_1^2 + m_{20} \bar{\alpha}_{1,0} \delta \zeta_{\bar{y}}^2 \right. \\ & \left. + 2 m_{20} \zeta_{\bar{y}0} \delta \bar{\alpha}_1 \delta \zeta_{\bar{y}} \right) \quad (D.329)\end{aligned}$$

$$\begin{aligned}\bar{u}_{4,3} = & \frac{Q}{6} \left(m_{10} \delta \zeta_{\bar{y}}^3 + m_{11} \bar{\alpha}_3 \delta \zeta_{\bar{y}}^2 + m_6 \bar{\alpha}_3^3 + m_{20} \delta \bar{\alpha}_1 \bar{\alpha}_3^2 \right. \\ & \left. + m_8 \delta \bar{\alpha}_1^2 \bar{\alpha}_3 + m_9 \delta \bar{\alpha}_1^3 + m_{20} \delta \bar{\alpha}_1 \delta \zeta_{\bar{y}}^2 \right) \quad (D.330)\end{aligned}$$

$$\begin{aligned}\bar{u}_{2,1} = & \frac{Q}{a} (-m_4 \delta \zeta_{\bar{y}} + 3 m_{10} \zeta_{\bar{y}}^2 \delta \zeta_{\bar{y}} + m_5 \bar{\alpha}_3 - m_{11} \zeta_{\bar{y}0}^2 \bar{\alpha}_3 - m_8 \bar{\alpha}_1^2 \bar{\alpha}_3 \\ & - 3 m_9 \bar{\alpha}_1^2 \delta \bar{\alpha}_1 + m_7 \delta \bar{\alpha}_1 - 2 m_{20} \bar{\alpha}_1 \zeta_{\bar{y}0} \delta \zeta_{\bar{y}} - m_{20} \zeta_{\bar{y}0}^2 \delta \bar{\alpha}_1) \quad (D.331)\end{aligned}$$

$$\begin{aligned}\bar{u}_{2,2} = & \frac{Q}{a} (3 m_{10} \zeta_{\bar{y}0} \delta \zeta_{\bar{y}}^2 - 2 m_{11} \zeta_{\bar{y}0} \bar{\alpha}_3 \delta \zeta_{\bar{y}} - m_{20} \bar{\alpha}_1 \bar{\alpha}_3^2 \\ & - 2 m_8 \bar{\alpha}_1 \delta \bar{\alpha}_1 \bar{\alpha}_3 - 3 m_9 \bar{\alpha}_1 \delta \bar{\alpha}_1^2 - m_{20} \bar{\alpha}_1 \delta \zeta_{\bar{y}}^2 \\ & - 2 m_{20} \zeta_{\bar{y}0} \delta \bar{\alpha}_1 \delta \zeta_{\bar{y}}) \quad (D.332)\end{aligned}$$

$$\begin{aligned}\bar{u}_{2,3} = & \frac{Q}{a} (m_{10} \delta \zeta_{\bar{y}}^3 - m_{11} \bar{\alpha}_3 \delta \zeta_{\bar{y}}^2 - m_6 \bar{\alpha}_3^3 - m_{20} \delta \bar{\alpha}_1 \bar{\alpha}_3^2 \\ & - m_8 \delta \bar{\alpha}_1^2 \bar{\alpha}_3 - m_9 \delta \bar{\alpha}_1^3 - m_{20} \delta \bar{\alpha}_1 \delta \zeta_{\bar{y}}^2) \quad (D.333)\end{aligned}$$

$$\tilde{u}_{4,1} = -\frac{Q}{b} (2 \bar{m}_7 \zeta_{\bar{y}0} \bar{\alpha}_1 \bar{\alpha}_3) \quad (D.333.1)$$

$$\tilde{u}_{4,2} = -\frac{Q}{b} [2 \bar{m}_7 (\zeta_{\bar{y}0} \delta \bar{\alpha}_1 + \bar{\alpha}_1 \delta \zeta_{\bar{y}}) \bar{\alpha}_3 + \bar{m}_5 \zeta_{\bar{y}0} \bar{\alpha}_3^2] \quad (D.334)$$

$$\tilde{u}_{4,3} = -\frac{Q}{b} [2 \bar{m}_7 \bar{\alpha}_3 \delta \zeta_{\bar{y}} \delta \bar{\alpha}_1 + \bar{m}_5 \bar{\alpha}_3^2 \delta \zeta_{\bar{y}}] \quad (D.335)$$

$$\tilde{u}_{2,1} = \frac{b}{a} \tilde{u}_{4,1} \quad (D.336)$$

$$\tilde{u}_{2,2} = \frac{b}{a} \tilde{u}_{4,2} \quad (D.337)$$

$$\tilde{u}_{2,3} = \frac{b}{a} \tilde{u}_{4,3} \quad (D.338)$$

Eliminating \bar{n}_3 , \bar{n}_3 , \bar{u}_4 , \bar{u}_2 , \tilde{u}_4 and \tilde{u}_2 from Equations D.305, D.309, D.310 and D.315 to D.320 gives

$$n_3 = \sum_k n_{3k} \quad (D.339)$$

$$u_4 = \sum_k u_{4k} \quad (D.340)$$

$$u_2 = \sum_k u_{2k} \quad (D.341)$$

$$\text{where } n_{3k} = \bar{n}_{3k} + \tilde{n}_{3k} \quad (D.342)$$

$$u_{4k} = \bar{u}_{4k} + \tilde{u}_{4k} \quad (D.343)$$

$$u_{2k} = \bar{u}_{2k} + \tilde{u}_{2k} \quad (D.344)$$

Eliminating n_3 , u_2 and u_4 from Equations D.306, D.307, D.339, D.340 and D.341 gives

$$n_4 = \sum_k n_{4k} \quad (D.345)$$

$$n_2 = \sum_k n_{2k} \quad (D.346)$$

$$\text{where } n_{4k} = u_{4k} - n_{3k} \quad (D.347)$$

$$n_{2k} = u_{2k} - n_{3k} \quad (D.348)$$

Eliminating n_2 , n_3 and n_4 from Equations D.308, D.339, D.345 and D.346 gives

$$n_1 = \sum_k n_{1k} \quad (D.349)$$

$$\text{where } n_{1k} = -n_{2k} - n_{3k} - n_{4k} \quad (D.350)$$

Eliminating $\bar{\alpha}_1$ and $\bar{\tau}_y$ from Equations D.86.1, D.311 and D.312.2 gives

$$\bar{r} = \bar{r}_1 + \bar{r}_2 \quad (D.351)$$

where

$$\bar{r}_1 = 2 m_{16} \bar{a}_{1,0} \delta \bar{a}_1 + m_{15} \bar{a}_{1,0} \bar{a}_3 - 2 m_{22} \zeta_{y0} \delta \zeta_{\bar{y}} \quad (D.352)$$

$$\bar{r}_2 = m_{16} \delta \bar{a}_1^2 + m_{15} \delta \bar{a}_1 \bar{a}_3 + m_{21} \bar{a}_3^2 - m_{22} \delta \zeta_{\bar{y}}^2 \quad (D.353)$$

The expanded form is less efficient than the condensed form. This part of the program should be recoded.

MEMBRANES AND CELLS

The method of calculating fictitious forces and deformations for membrane and cell elements, based on the results derived in this appendix for axially loaded bars and shear panels, is described in Appendix H.

APPENDIX E
MATERIAL NONLINEARITY

LIST OF SYMBOLS FOR APPENDIX E (Continued)

n_{TV}	Number of input pairs of temperatures and material properties
P	(Subscript). Indicates plane stress
P_A	$(\bar{E}/E_A) - 1$
R	E_A/\bar{E}
r	$\bar{\sigma}_L/\bar{\sigma}_A$
s	Specific heat
t	Time
T_i	Temperature of the i th structural element
$T_{i\beta-1}$	Temperature of i th structural element applicable during β th increment
T_{Va}	Rectangular matrix. The element in the i th row and j th column is T_i^{j-1}
$t_{\beta-1}$	Time at beginning of β th increment
U	(Subscript). Indicates uniaxial stress
V_p	Column matrix. The element in the i th row is V_{pi}
V_{pi}	Value of the material property P for the i th structural element
x, y, z	Rectangular Cartesian coordinates
α_T	Coefficient of thermal expansion
β	(Subscript). Time increment number
$\delta T_{i\beta-1}$	Change in temperature of i th structural element developed during the $\beta-1$ st increment

LIST OF SYMBOLS FOR APPENDIX E (Continued)

ϵ	Column matrix of strain components
$\bar{\epsilon}$	True uniaxial strain
ϵ^e, ϵ^p	Column matrices of elastic and plastic strain components
$\bar{\epsilon}_p$	Plastic strain
$\bar{\epsilon}_r$	True strain at rupture
$\epsilon_x, \epsilon_y, \epsilon_z$ $\gamma_{xy}, \gamma_{yz}, \gamma_{zx}$ }	Strain components
ν	Poisson's ratio
ρ	Mass per unit volume
σ	Column matrix of stress components
$\bar{\sigma}$	Equivalent stress, equal to true stress in a uniaxial test
σ'	Column matrix consisting of the deviatoric normal stresses, and twice the deviatoric shearing stresses
$\bar{\sigma}_A$	True stress at approximate yield point, A
σ_B	Bar stress
$\bar{\sigma}_L$	True stress at approximate proportional limit
$\bar{\sigma}_r$	True stress at rupture
$\sigma_x, \sigma_y, \sigma_z$ $\tau_{xy}, \tau_{yz}, \tau_{zx}$ }	Stress components
$\sigma_x, \sigma_y, \sigma_z$ $\tau_{xy}, \tau_{yz}, \tau_{zx}$ }	Deviatoric stress components

This appendix describes the method of calculating material compliance matrices for conditions of triaxial, plane, and uniaxial stress. The compliance matrix gives the incremental strains produced in the material of an element, resulting from unit incremental changes of stress, considering the effects of plasticity.

The compliance matrices are calculated on the basis of the Prandtl-Reuss equations. These equations require, as input, the stress components existing at the beginning of the increment, and the slope of the curve of true stress versus true strain for the material, derived from a uniaxial test.

Since the results of uniaxial material property tests are required, the method of employing data derived from such tests is described. The method is based upon the Ramberg-Osgood equation, modified.

The method of calculating material properties corresponding to any temperature, from properties measured in test at a limited number of temperatures, is also presented. The calculation employs the least squares method of fitting a curve to test data.

PRANDTL-REUSS EQUATIONS

These equations are given in Hill's book on plasticity (Reference 13). Hill's notation is modified, and the equations are stated in matrix form, for the cases of triaxial, plane, and uniaxial stress.

Triaxial Stress

In the following discussion, when notation is defined, the notation of Reference 13 is given in parentheses, to facilitate reference to Hill's equations. Let

$\epsilon_x, \epsilon_y, \epsilon_z, \gamma_{xy}, \gamma_{yz}, \gamma_{zx}, (\epsilon_{11}, \epsilon_{22}, \epsilon_{33}, 2\epsilon_{12}, 2\epsilon_{23}, 2\epsilon_{31})$ = the components of the strain tensor referred to a rectangular Cartesian xyz reference frame.

The fact that the shear strain components in the present notation are equal to twice the values in Hill's notation is shown by Equation 10 of Reference 13.

Let

$$\epsilon = \left\{ \epsilon_x \mid \epsilon_y \mid \epsilon_z \mid \gamma_{xy} \mid \gamma_{yz} \mid \gamma_{zx} \right\} \quad (\text{Column}) \quad (\text{E.1})$$

Thus ϵ is a column matrix of strain components. Similarly define ϵ^p and ϵ^e as column matrices of plastic and elastic strain components.

From the definition of plastic strain increments given in Reference 13, following Equation 12,

$$d\epsilon = d\epsilon^p + d\epsilon^e, \quad (\text{E.2})$$

where $d\epsilon$, $d\epsilon^p$ and $d\epsilon^e$ represent infinitesimal increments of the column matrices ϵ , ϵ^p and ϵ^e .

Let

$\sigma_x, \sigma_y, \sigma_z, \tau_{xy}, \tau_{yz}, \tau_{zx}, (\sigma_{11}, \sigma_{22}, \sigma_{33}, \sigma_{12}, \sigma_{23}, \sigma_{31})$ = the components of the stress tensor referred to the xyz frame.

The correspondence between the present notation and Hill's notation is given in Reference 13, Appendix I.

Hill defines a deviatoric stress tensor. Let

$\sigma'_x, \sigma'_y, \sigma'_z, \tau'_{xy}, \tau'_{yz}, \tau'_{zx}, (\sigma'_{11}, \sigma'_{22}, \sigma'_{33}, \sigma'_{12}, \sigma'_{23}, \sigma'_{31})$ = the deviatoric stress components.

From Equation 3 of Reference 13, these components are

$$\sigma'_x = \frac{1}{3}(2\sigma_x - \sigma_y - \sigma_z) \quad (\text{E.3})$$

$$\sigma'_y = \frac{1}{3}(-\sigma_x + 2\sigma_y - \sigma_z) \quad (\text{E.4})$$

$$\sigma'_z = \frac{1}{3}(-\sigma_x - \sigma_y + 2\sigma_z) \quad (\text{E.5})$$

$$\tau'_{xy} = \tau_{xy} \quad (\text{E.6})$$

$$\tau'_{yz} = \tau_{yz} \quad (E.7)$$

$$\tau'_{zx} = \tau_{zx} \quad (E.8)$$

The plastic strain increments, $d\epsilon^P$, are given by Equation 30 of Reference 13. Converting this equation to present notation, employing Equations E.6, E.7 and E.8, and putting the results in matrix form, gives

$$d\epsilon^P = \frac{3/2}{\bar{\sigma}H'} \sigma' d\bar{\sigma} \quad (E.9)$$

where

$\bar{\sigma}$, $(\bar{\sigma})$ = the equivalent stress, equal to twice the octahedral shearing stress,

H' , (H') = the slope of the equivalent stress/plastic strain curve,

and

$$\sigma' = \left\{ \sigma'_x \mid \sigma'_y \mid \sigma'_z \mid 2\tau_{xy} \mid 2\tau_{yz} \mid 2\tau_{zx} \right\} \quad (\text{Column}) \quad (E.10)$$

Hill states that H' is also the slope of the curve of true stress versus true strain, derived from a uniaxial tension or compression test. H' is the only material property required in the Prandtl-Reuss equations.

The equivalent stress, $\bar{\sigma}$, is given by Equation 14 of Reference 13, in terms of the deviatoric stress components. Converting this equation to present notation, and employing Equations E.6, E.7, and E.8, gives

$$\bar{\sigma}^2 = \frac{3}{2} (\sigma_x'^2 + \sigma_y'^2 + \sigma_z'^2 + 2\tau_{xy}^2 + 2\tau_{yz}^2 + 2\tau_{zx}^2) \quad (E.11)$$

Differentiating Equation E.11 gives

$$2\bar{\sigma}d\bar{\sigma} = 3(\sigma_x'd\sigma_x' + \sigma_y'd\sigma_y' + \sigma_z'd\sigma_z' + 2\tau_{xy}d\tau_{xy} + 2\tau_{yz}d\tau_{yz} + 2\tau_{zx}d\tau_{zx}) \quad (E.12)$$

From Equations E.3, E.4 and E.5,

$$\sigma'_x + \sigma'_y + \sigma'_z = 0 \quad (\text{E.13})$$

Differentiating Equations E.3, E.4 and E.5, and employing Equation E.13 gives

$$\sigma'_x d\sigma'_x + \sigma'_y d\sigma'_y + \sigma'_z d\sigma'_z = \sigma'_x d\sigma_x + \sigma'_y d\sigma_y + \sigma'_z d\sigma_z \quad (\text{E.14})$$

Combining Equations E.12 and E.14 gives

$$d\bar{\sigma} = \frac{3/2}{\bar{\sigma}} (\sigma'_x d\sigma_x + \sigma'_y d\sigma_y + \sigma'_z d\sigma_z + 2\tau_{xy} d\tau_{xy} + 2\tau_{yz} d\tau_{yz} + 2\tau_{zx} d\tau_{zx}) \quad (\text{E.15})$$

Combining Equations E.10 and E.15 gives

$$d\bar{\sigma} = \frac{3/2}{\bar{\sigma}} \sigma'^T d\sigma \quad (\text{E.16})$$

where

$$\sigma = \left\{ \sigma_x \mid \sigma_y \mid \sigma_z \mid \tau_{xy} \mid \tau_{yz} \mid \tau_{zx} \right\} \quad (\text{column}) \quad (\text{E.17})$$

Eliminating $d\bar{\sigma}$ from Equations E.9 and E.17 gives

$$d\epsilon^p = \frac{9/4}{\bar{\sigma}^2 H'} \sigma'^T d\sigma \quad (\text{E.18})$$

Equation E.18 gives the plastic strain increments referred to the xyz frame, in terms of the stress increments referred to the same frame, the deviatoric stresses, the equivalent stress, and the slope of the equivalent stress/plastic strain curve, at the point where the equivalent stress is equal to $\bar{\sigma}$. Let

$$C_K^p = \frac{9/4}{\bar{\sigma}^2 H'} \sigma'^T \quad (\text{E.19})$$

$$\text{Therefore} \quad d\epsilon^p = C_K^p d\sigma \quad (\text{E.20})$$

where C_K^p = the plastic compliance matrix.

The elastic strain increments are given in terms of the stress increments, Young's modulus, and Poisson's ratio, for isotropic materials, by

$$d\epsilon^e = C_K^e d\sigma \quad , \quad (E.21)$$

where the well-known isotropic elastic compliance matrix is

$$C_K^e = \frac{1}{E} \begin{bmatrix} 1 & -\nu & -\nu & & & \\ -\nu & 1 & -\nu & & & \\ -\nu & -\nu & 1 & & & \\ & & & 2(1+\nu) & 0 & 0 \\ & & & 0 & 2(1+\nu) & 0 \\ & & & 0 & 0 & 2(1+\nu) \end{bmatrix} \quad , \quad (E.22)$$

and where E and ν = Young's modulus and Poisson's ratio.

Eliminating $d\epsilon^p$ and $d\epsilon^e$ from Equations E.2, E.20 and E.21 gives

$$d\epsilon = C_K d\sigma \quad (E.23)$$

$$\text{where} \quad C_K = C_K^p + C_K^e \quad (E.24)$$

Plane Stress

In plane stress

$$\sigma_z = \tau_{yz} = \tau_{zx} = 0 \quad (E.25)$$

Deleting the rows and columns corresponding to these stresses from the matrices appearing in Equation E.23 gives

$$d\epsilon_p = C_{Kp} d\sigma_p \quad (E.26)$$

$$\text{where } \epsilon_p = \left\{ \epsilon_x \mid \epsilon_y \mid \gamma_{xy} \right\} \quad (\text{Column}), \quad (\text{E.27})$$

$$\sigma_p = \left\{ \sigma_x \mid \sigma_y \mid \tau_{xy} \right\} \quad (\text{Column}), \quad (\text{E.28})$$

$$C_{KP} = C_{KP}^D + C_{KP}^E, \quad (\text{E.29})$$

$$C_{KP}^D = \frac{9/4}{\sigma_p^2 H} \sigma_p \sigma_p^T, \quad (\text{E.30})$$

$$\sigma'_p = \left\{ \sigma'_x \mid \sigma'_y \mid 2\tau_{xy} \right\} \quad (\text{Column}), \quad (\text{E.31})$$

$$\frac{\sigma_p^2}{2} = \frac{3}{2} (\sigma_x'^2 + \sigma_y'^2 + \sigma_z'^2 + 2\tau_{xy}^2), \quad (\text{E.32})$$

$$\sigma'_x = \frac{1}{3} (2\sigma_x - \sigma_y), \quad (\text{E.33})$$

$$\sigma'_y = \frac{1}{3} (-\sigma_x + 2\sigma_y), \quad (\text{E.34})$$

$$\sigma'_z = \frac{1}{3} (-\sigma_x - \sigma_y), \quad (\text{E.35})$$

$$\text{and } C_{KP}^E = \frac{1}{E} \left[\begin{array}{c|c|c} 1 & -\nu & 0 \\ -\nu & 1 & 0 \\ 0 & 0 & 2(1+\nu) \end{array} \right] \quad (\text{E.36})$$

Uniaxial Stress

In uniaxial stress,

$$\sigma_y = \sigma_z = \tau_{xy} = \tau_{yz} = \tau_{zx} = 0 \quad (\text{E.37})$$

Deleting the rows and columns corresponding to these stresses from the matrices appearing in Equation E.23 gives

$$d\epsilon_U = C_{KU} d\alpha_U \quad (E.38)$$

$$\text{where } \epsilon_U = \epsilon_x \quad (E.39)$$

$$\sigma_U = \sigma_x \quad (E.40)$$

$$C_{KU} = C_{KU}^p + C_{KU}^e \quad (E.41)$$

$$C_{KU}^p = \frac{3/4}{\bar{\sigma}_U H'} \sigma_U' \sigma_U'^T \quad (E.42)$$

$$\sigma_U' = \sigma_x' \quad (E.43)$$

$$\bar{\sigma}_U = \frac{3}{2} (\sigma_x'^2 + \sigma_y'^2 + \sigma_z'^2) \quad (E.44)$$

$$\sigma_x' = \frac{2}{3} \sigma_x \quad (E.45)$$

$$\sigma_y' = \sigma_z' = -\frac{1}{3} \sigma_x \quad (E.46)$$

$$C_{KU}^e = \frac{1}{E} \quad (E.47)$$

Eliminating σ_x' , σ_y' and σ_z' from Equations E.44, E.45 and E.46 gives

$$\bar{\sigma}_U = \sigma_x \quad (E.48)$$

Thus, the equivalent stress equals the uniaxial stress. Eliminating $\bar{\sigma}_U$, σ_U' and σ_x' from Equations E.42, E.43, E.45 and E.48 gives

$$C_{KU}^p = \frac{1}{H'} \quad (E.49)$$

Equations E.47 and E.49 give the uniaxial elastic and plastic compliance matrices. The incremental plastic strain is given by

$$d\epsilon_U^P = C_{KU}^P d\sigma_U \quad . \quad (E.50)$$

Combining Equations E.49 and E.50 gives

$$\frac{d\sigma_U}{d\epsilon_U^P} = H' \quad , \quad (E.51)$$

showing that H' is the slope of the uniaxial stress/plastic strain curve, as stated by Hill.

Material Unloading

In coding the Prandtl-Reuss equations, the plan is to employ the elastoplastic compliance matrix as long as the equivalent stress, $\bar{\sigma}$, continues to increase. When $\bar{\sigma}$ starts to decrease, the material is said to unload. The plan is to use the elastic compliance matrix after unloading begins.

ANALYTIC REPRESENTATION OF STRESS - STRAIN CURVE

Figure E.1 shows a uniaxial true stress-true strain curve as developed to represent the Prandtl-Reuss equivalent stress. The following definitions apply:

$\bar{\sigma}$, $\bar{\epsilon}$ = true stress and true strain, where $\bar{\sigma}$ corresponds to the Prandtl-Reuss equivalent stress.

$\bar{\sigma}_r$, $\bar{\epsilon}_r$ = true stress and strain at rupture

$\bar{\sigma}_A$ = true stress at approximate yield point A

$\bar{\sigma}_L$ = true stress at proportional limit, defined by the assigned value of r , as explained later.

\bar{E} = slope of line tangent to curve at $\bar{\sigma} = 0$

E = slope of line intersecting the curve at the proportional limit
(Young's modulus)

E_A = slope of line intersecting the curve at the approximate yield point
A

$\bar{\epsilon}_p$ = plastic strain

The properties E , E_A , $\bar{\sigma}_A$, $\bar{\sigma}_r$, $\bar{\epsilon}_r$ are determine from test, see Reference
14.

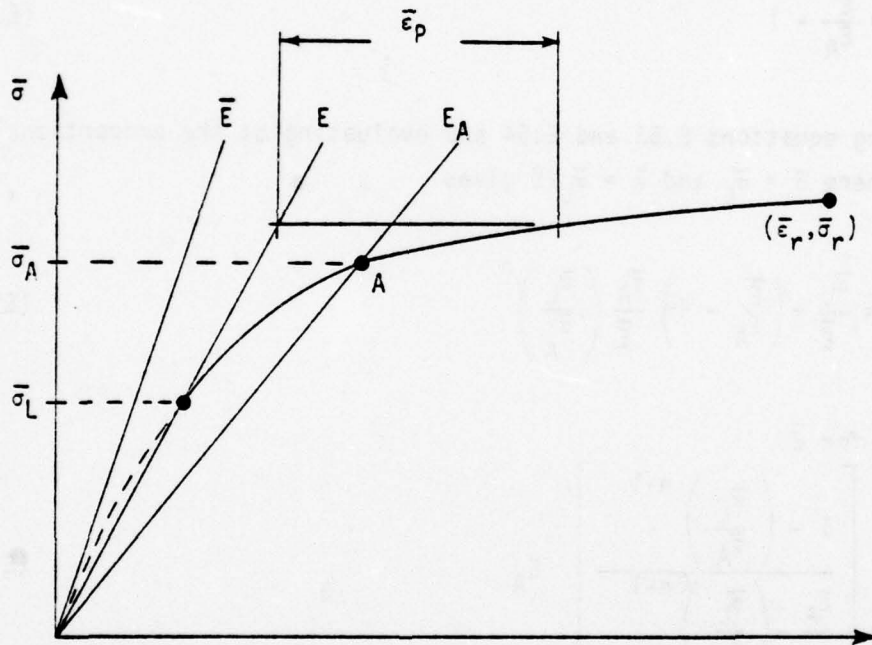


Figure E.1 True Stress, True Strain Curve.

In the elastic region ($0 < \bar{\sigma} \leq \bar{\sigma}_L$) the stress-strain relationship is given by

$$\bar{\epsilon} = \frac{\bar{\sigma}}{E} \quad (E.52)$$

In the plastic region ($\bar{\sigma} \geq \bar{\sigma}_L$) a modified Ramberg-Osgood equation is used. The basic equation from Reference 15 can be written in the following form.

$$\bar{\epsilon} = \frac{\bar{\sigma}}{E} + p_A \frac{\bar{\sigma}_A}{E} \left(\frac{\bar{\sigma}}{\bar{\sigma}_A} \right)^n \quad (E.53)$$

Evaluation of this equation at point A where $\bar{\sigma} = \bar{\sigma}_A$ and $\bar{\epsilon} = \bar{\sigma}_A/E_A$ gives

$$p_A = \frac{\bar{E}}{E_A} - 1 \quad (E.54)$$

Combining equations E.53 and E.54 and evaluating at the proportional limit where $\bar{\sigma} = \bar{\sigma}_L$ and $\bar{\epsilon} = \bar{\sigma}_L/E$ gives

$$\frac{\bar{\sigma}_L}{E} = \frac{\bar{\sigma}_L}{E} + \left(\frac{\bar{E}}{E_A} - 1 \right) \frac{\bar{\sigma}_A}{E} \left(\frac{\bar{\sigma}_L}{\bar{\sigma}_A} \right)^n \quad (E.55)$$

Solving for \bar{E}

$$\bar{E} = \left[\frac{1 - \left(\frac{\bar{\sigma}_L}{\bar{\sigma}_A} \right)^{n-1}}{\frac{E_A}{E} - \left(\frac{\bar{\sigma}_L}{\bar{\sigma}_A} \right)^{n-1}} \right] E_A \quad (E.56)$$

Let r be an assigned value for the ratio $\bar{\sigma}_L/\bar{\sigma}_A$ (E.57)

$$r = \frac{\bar{\sigma}_L}{\bar{\sigma}_A} \quad \text{or} \quad \bar{\sigma}_L = r \bar{\sigma}_A \quad (E.57)$$

Also, let

$$R = \frac{E_A}{E} \quad (E.58)$$

Then from Equations E.56, E.57 and E.58

$$R = \frac{\frac{E_A}{E} - r^{n-1}}{1 - r^{n-1}} \quad (E.59)$$

Combining Equations E.53, E.54 and E.58 gives the modified Ramberg-Osgood equation for the range $\bar{\sigma} > \bar{\sigma}_L$.

$$\bar{\epsilon} = R \frac{\bar{\sigma}}{E_A} + (1 - R) \frac{\bar{\sigma}_A}{E_A} \left(\frac{\bar{\sigma}}{\bar{\sigma}_A} \right)^n \quad (E.60)$$

In the range $\bar{\sigma} > \bar{\sigma}_L$, the plastic part of the strain $\bar{\epsilon}_p$ can be calculated by subtracting the elastic strain given by Equation E.52 from the strain given by Equation E.60, see Figure E.1.

$$\bar{\epsilon}_p = R \frac{\bar{\sigma}}{E_A} + (1 - R) \frac{\bar{\sigma}_A}{E_A} \left(\frac{\bar{\sigma}}{\bar{\sigma}_A} \right)^n - \frac{\bar{\sigma}}{E} \quad (E.61)$$

The plastic part of the compliance matrix as calculated by the Prandtl-Reuss approach requires the reciprocal of the slope H' of the plastic part of the stress strain curve. Differentiating Equation E.61 gives the required value.

$$\frac{1}{H'} = \frac{d\bar{\epsilon}_p}{d\bar{\sigma}}$$

$$\frac{1}{H} = \frac{R}{E_A} + (1-R) \frac{n}{E_A} \left(\frac{\bar{\sigma}}{\bar{\sigma}_A} \right)^{n-1} - \frac{1}{E} \quad (E.62)$$

The value of n can be calculated from Equation E.60 by substituting the strain and stress at rupture, $\bar{\epsilon}_r$ and $\bar{\sigma}_r$, and using natural logarithms.

$$\bar{\epsilon}_r = R \frac{\bar{\sigma}_r}{E_A} + (1-R) \frac{\bar{\sigma}_A}{E_A} \left(\frac{\bar{\sigma}_r}{\bar{\sigma}_A} \right)^n$$

$$n = \frac{\ln \left(\bar{\epsilon}_r - R \frac{\bar{\sigma}_r}{E_A} \right) - \ln(1-R) - \ln \frac{\bar{\sigma}_A}{E_A}}{\ln \frac{\bar{\sigma}_r}{\bar{\sigma}_A}} \quad (E.63)$$

However, R is a function n . Therefore, an iterative solution is indicated. Choose an initial value for n (say 50), solve for R from Equation E.59 and for n from Equation E.63. Using the latest value for n , repeat the loop until convergence occurs. Usually, three or four iterations should be enough.

The proportional limit $\bar{\sigma}_L$ is somewhat arbitrarily defined by the assigned value for r , see Equation E.57. The reason for providing the elastic range $0 < \bar{\sigma} \leq \bar{\sigma}_L$ is that a large number of elements in the finite element model will have insignificant plastic strain and can therefore be treated elastically. Computing time will be saved, because the element stiffness need not be re-generated unless significant plasticity occurs ($\bar{\sigma} > \bar{\sigma}_L$). A suggested value for the parameter r is

$$r = \frac{E_A}{E} \quad (E.64)$$

If a material has no significant plastic range, it can be treated as perfectly elastic by setting $\bar{E} = E = E_A$ and $\bar{\sigma}_L = \bar{\sigma}_A = \bar{\sigma}_r$, and Equation E.52 remains valid until rupture occurs.

TEMPERATURE DEPENDENCE OF MATERIAL PROPERTIES

A Power series is employed to represent the value of a material property in terms of temperature. If V_{pi} is the value of material property P for the i th element, and T_i is the temperature of the i th element, then

$$V_{pi} = a_{p0} + a_{p1}T_i + a_{p2}T_i^2 + \dots + a_{p(n_a-1)}T_i^{n_a-1}, \quad (E.65)$$

where n_a is the number of terms. The coefficients a_{p0}, a_{p1}, \dots are calculated by a least squares procedure to fit a curve to a set of known temperature and property value pairs. Let

$(T_1, V_{p1}), (T_2, V_{p2}), \dots$ = input pairs of temperatures and corresponding property values.

n_{TV} = number of input pairs

Define the matrices

$$T_{Va} = \begin{bmatrix} 1 & T_1 & T_1^2 & \dots & T_1^{n_a-1} \\ 1 & T_2 & T_2^2 & & T_2^{n_a-1} \\ \vdots & \vdots & \vdots & & \vdots \\ \vdots & \vdots & \vdots & & \vdots \end{bmatrix} \quad (E.66)$$

$(n_{TV} \times n_a)$

$$a_p = \{ a_{p0} \mid a_{p1} \mid a_{p2} \mid \dots \} \quad (\text{Column}) \quad (E.67)$$

$(n_a \times 1)$

$$V_p = \left\{ \begin{array}{c|c|c} V_{p1} & V_{p2} & \dots \end{array} \right\} \quad (\text{Column}) \quad (E.68)$$

$(n_{TV} \times 1)$

An equation of the form of Equation E.65 can be written for each input pair. The resulting set of equations can be written

$$T_{Va} a_p = V_p \quad . \quad (E.69)$$

In Equation E.69, T_{Va} and V_p are known. The column matrix of unknown coefficients, a_p , can be calculated by the least squares approach, when

$$n_{TV} \geq n_a \quad . \quad (E.70)$$

Multiplying Equation E.18 on the left by T_{Va}^T gives,

$$T_{Va}^T T_{Va} a_p = T_{Va}^T V_p \quad . \quad (E.71)$$

$$\therefore a_p = (T_{Va}^T T_{Va})^{-1} T_{Va}^T V_p \quad (E.72)$$

The list of material properties is given in PART 2 USER'S MANUAL, Table 2. Ten properties are defined for each material in the finite element model. A set of coefficients a_p is calculated for each property of each material for which temperature dependence is indicated, by means of temperature/value pairs. Material properties are calculated from Equation E.65 for each element based on the current element temperature. If the temperature of an element changes during an increment, because of damping energy converted to heat (see Appendix H, Equation H.338), then for the following increment, the material properties are updated, and the element stiffness and damping matrices are recomputed. The element temperature used for material property calculations in the β th increment is

$$T_{i_{\beta-1}} = T_{i_{\beta-2}} + \delta T_{i_{\beta-1}} \quad (E.73)$$

Therefore, based on Equations E.73 and E.65, material properties $V_{p_{i\beta}}$ are calculated for the i th element and the β th increment as appropriate, where $V_{p_{i\beta}}$ can correspond to the following ten properties:

$E_{i\beta}$ = Young's modulus

$E_{A_{i\beta}}$ = tangent modulus at point A.

$\bar{\sigma}_{A_{i\beta}}$ = approximate yield stress (true)

$\bar{\sigma}_{r_{i\beta}}$ = rupture stress (true)

$\bar{\epsilon}_{r_{i\beta}}$ = rupture strain (true)

$\nu_{i\beta}$ = Poisson's ration

$\alpha_{T_{i\beta}}$ = coefficient of thermal expansion

$\rho_{i\beta}$ = mass density

$s_{i\beta}$ = specific heat

$h_{i\beta}$ = damping to stiffness ratio

Corresponding Ramberg-Osgood parameters $n_{i\beta}$, $R_{i\beta}$, $\bar{\sigma}_{L_{i\beta}}$ are calculated from Equations E.63, E.59, E.64, E.57. If the equivalent stress, $\bar{\sigma}$, is in the plastic range, the value for $1/H_{i\beta}$ is calculated from Equation E.62.

ELEMENT COMPLIANCE

Element compliance matrices are generated for each finite element according to the Prandtl-Reuss formulation. Depending on the value of σ_i relative to σ_{L_i} , the compliance matrix for the i th element may be

elastic, or a combination of elastic and plastic contributions. The material of each element is assumed to be represented by a stress-strain curve similar to Figure E.1.

The bar element has an additional feature which allows axial deformation within specified limits without developing significant load. If e_{C_i} and e_{T_i} are user specified compressive and tensile axial deformations defining a "no load" range, and $e_{B_{i\beta}}$ is the accumulated axial deformation at the end of the β th increment, then equation E.52 will be modified as follows for the bar element. Calculate

$$e_{B_{i\beta}} = e_{B_{i,\beta-1}} + \Delta_{i\beta} C_{KU_i}(t_{\beta-1}) \left[\sigma_{B_i}(t_{\beta}) - \sigma_{B_i}(t_{\beta-1}) \right] \quad (E.74)$$

If $e_{C_i} \leq e_{B_{i\beta}} \leq e_{T_i}$, then Equation E.52 becomes

$$\epsilon_i(t) = 10^6 \frac{\bar{\sigma}_i(t)}{E_{i,\beta+1}} \quad t_{\beta} < t < t_{\beta+1} \quad (E.75)$$

Otherwise, Equations E.52 or E.60 apply. Figure E.2 shows the load-deformation relationship and the compliance equations which are valid within specified deformation ranges.

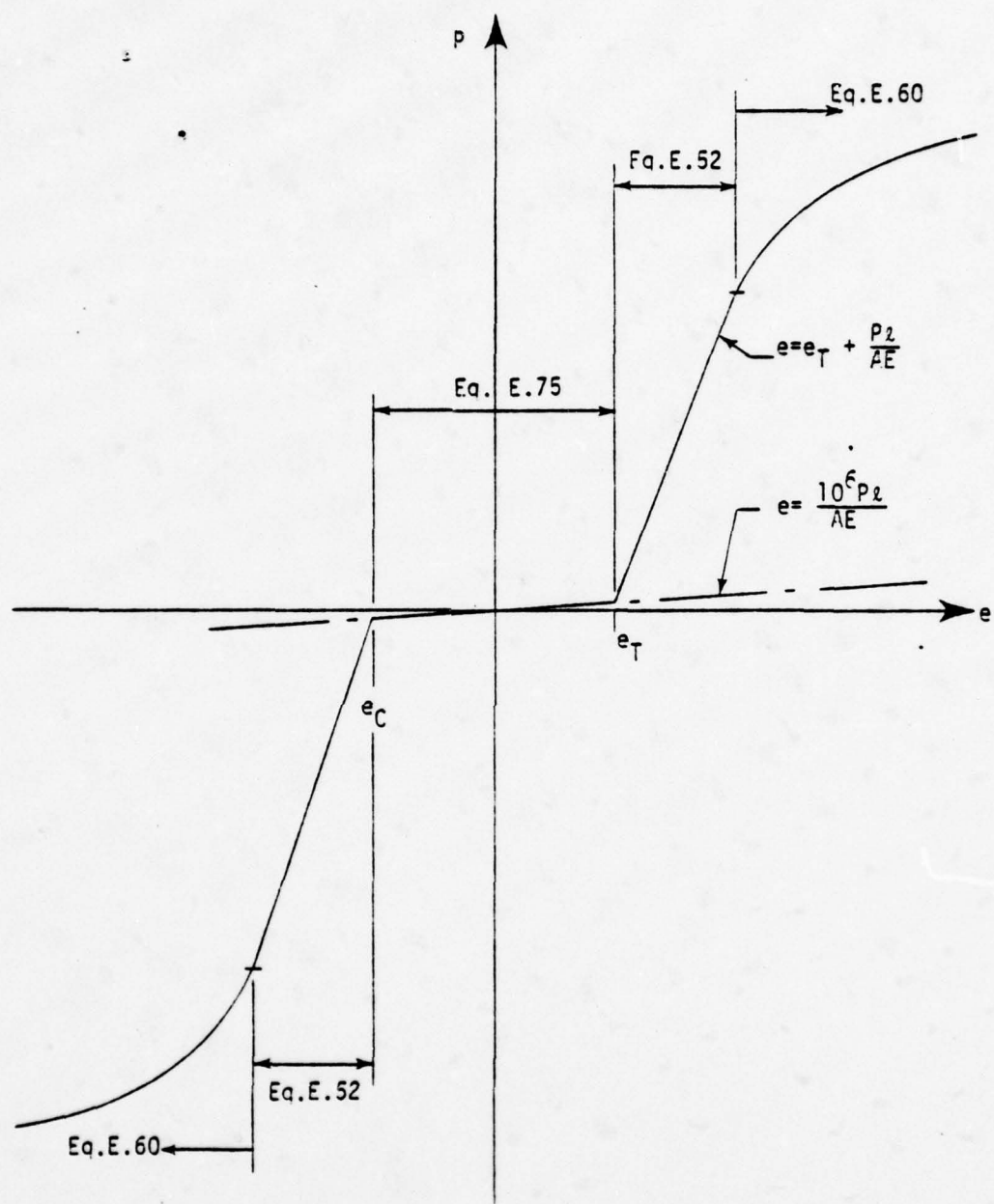


Figure E.2 Bar Element Load-deformation Diagram.

APPENDIX F

MODAL TRANSFORMATIONS

LIST OF SYMBOLS FOR APPENDIX F

Symbols appearing in Appendix F not appearing in this list are defined in the list at the front of this report.

Δ_{m_k}

Column matrix. Natural vibration mode of the undamped structural model

ω_k

Natural vibration frequency of the undamped structural model

This appendix presents a discussion of the transformation employed to reduce the order of magnitude of the matrices appearing in the equation of motion. Requirements for the transformation are considered, the method of calculating free vibration modes is briefly reviewed, and an explanation for the failure of the F-16 canopy geometrically nonlinear analysis is offered.

Equation 102 is the equation of motion written in terms of the displacements in the unconstrained degrees of freedom, $\Delta(t)$. Equation 184 is the equation of motion written in terms of the modal displacements, $\bar{\Delta}(t)$. From Equation 172, the modal transformation is given by

$$\delta\Delta_B(t) = T\delta\bar{\Delta}_B(t) \quad (F.1)$$

where T , the transformation matrix, is a rectangular matrix having more rows than columns. The effect of the transformation is to reduce the number of unknowns in the equation of motion, and the scope of the computing effort required to find the solution.

REQUIREMENTS FOR THE TRANSFORMATION

These requirements can be stated as follows:

1. The columns of the transformation matrix T must be linearly independent.
2. The displacements produced by the transformation must satisfy the constraints.
3. The transformation must be suitable.

In the third statement, the term "suitable transformation" means a transformation that produces acceptable approximations.

The implication of these requirements is that any kinds of modes can be employed, as long as the requirements are met. For example, undamped free vibration modes can be used in the transient response analysis of a damped mechanical system. This approach is frequently taken. Buckling modes can be employed. An analogy can be drawn with closed-form analysis, where

displacements are often expressed as trigonometric or power series in the coordinates. Such series are analogous to arbitrarily selected modes.

The first two requirements are mathematically well defined, and create no problem. The third requirement implies a need for a physical understanding of the motion under consideration in any particular application.

UNDAMPED NATURAL VIBRATION MODES

Free vibration modes of the undamped structure are considered in the remainder of this appendix. For completeness, the method of calculating these modes is briefly reviewed.

The modes are found by setting all of the load terms, and the damping matrix $C_{(\beta)}$, equal to zero, in the equation of motion written in terms of the unconstrained displacements, Equation 102, giving

$$M\ddot{\Delta}(t) + K_{(\beta)}\delta\Delta_{\beta}(t) = 0 . \quad (F.2)$$

Take $\beta=1$. Therefore, from Equations 88 and F.2,

$$M\ddot{\Delta}(t) + K_{(1)}\Delta(t) = 0 , \quad (F.3)$$

$$\text{since} \quad \Delta(t_0) = 0 , \quad (F.4)$$

Consider the sinusoidal motion

$$\Delta(t) = \Delta m_k \sin \omega_k t , \quad (F.5)$$

where Δm_k is an unknown column matrix, and ω_k is an unknown scalar. Substituting $\Delta(t)$ from Equation F.5 into Equation F.3, and taking $K_{(1)} = K$, gives

$$(K - \omega_k^2 M)\Delta m_k \sin \omega_k t = 0 \quad (F.6)$$

This equation is satisfied if

$$(K - \omega_k^2 M)\Delta m_k = 0 \quad (F.7)$$

Therefore, if ω_k and Δ_{mk} are an eigenvalue and an eigenvector of the characteristic equation, Equation F.7, then Equation F.5 is a solution of the equation of motion, Equation F.2, for free vibration of the undamped structure. The column matrix Δ_{mk} is a natural mode, or a modal column. The scalar ω_k is the corresponding frequency. Equation F.7 produces as many modal columns as the structure has unconstrained degrees of freedom. The modes satisfy the structural constraints, since the displacements of the reactions were set equal to zero in deriving Equation 102.

The modal transformation, T , is formed from some, but not all, of the Eigenvectors of Equation F.7.

F-16 CANOPY GEOMETRIC NONLINEARITY

The selection of suitable modes for use in geometrically nonlinear analysis of transient dynamic response is a subject that needs further study. The following discussion is restricted to a consideration of the cause of the difficulty encountered in attempting to analyze the response of the F-16 canopy to bird impact.

To facilitate the discussion, consider a finite element model of a cantilever beam, instead of the canopy. The behavior of the beam is easier to visualize, and the difficulties exemplified by beam behavior are sufficient to explain what happened in the canopy analysis.

Figure F.1 shows two views of such a beam, modelled with cell elements. The solid lines show the model at rest. The dotted lines show the first free vibration mode, approximately as it would be computed from Equation F.7. Now Equation F.7 is based on small displacement assumptions, since all nonlinear terms were discarded in its derivation. Therefore, the mode reflects these assumptions. In particular, point O, at the tip, on the neutral axis, has no motion parallel to the y axis, as it moves to its displaced position at O'. Point A moves slightly to the left, and point B moves an equal distance to the right, because of bending.

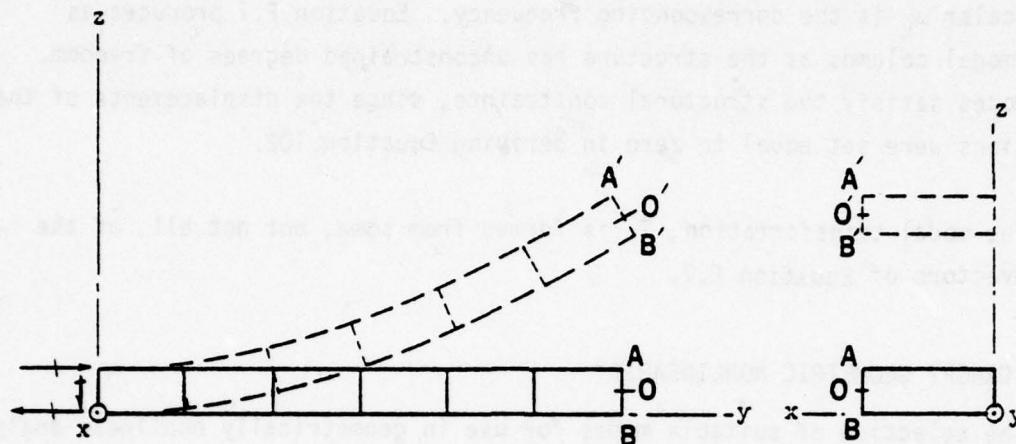


Figure F.1. Cantilever beam model, and first bending mode.

Such a mode is useful in calculating the linear response of the beam to, say, an impact load parallel to z applied at the tip. For good results, the mode should be augmented with some higher order modes, corresponding to several of the next higher frequencies. These modes would have more points of inflection as shown in Figure F.2. The figure shows only displacements of the neutral axis.

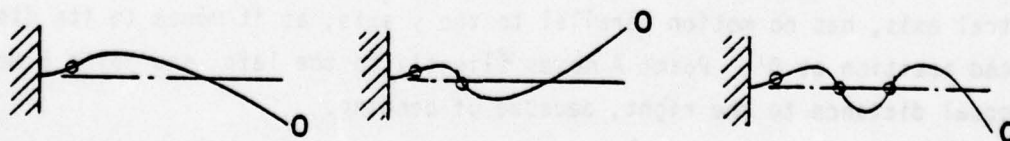


Figure F.2. Higher order modes.

The circles show points of inflection. These modes also have the property that point 0 has no motion parallel to the y axis, because modes that involve axial displacements of the beam neutral axis correspond to very high frequencies. The low frequency modes that involve bending, but no axial deformation of the neutral axis, are subsequently called bending modes, or antisymmetric normal modes. The high frequency modes involving axial deformation of the neutral axis, but no bending, are called axial modes.

Although the bending modes are adequate for a linear analysis of response resulting from a load parallel to the z axis at the tip, they are not sufficient for a nonlinear analysis, because large deflection effects cause axial motion of the beam, even when the load is normal to the neutral axis, as shown in Figure F.3.

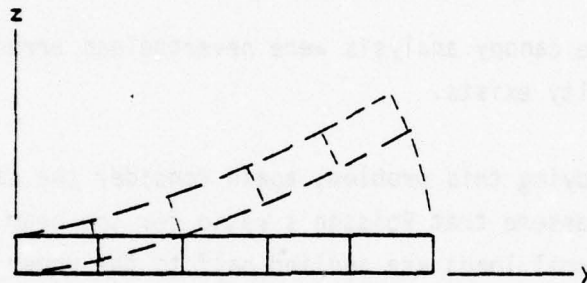


Figure F.3. Axial motion accompanying bending.

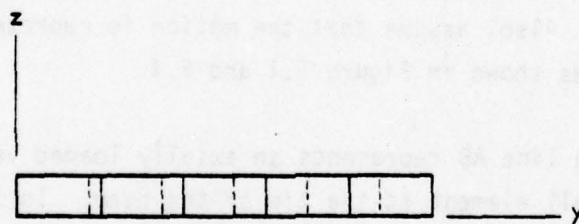


Figure F.4. Axial mode.

Figure F.4 is an approximate representation of the lowest of the high frequency axial modes. If such a mode is combined with the bending mode of Figure F.1, the two modes can represent approximately the true nonlinear motion shown in Figure F.3.

If a nonlinear analysis of the beam were attempted, employing only the bending mode of Figure F.1, the results would show large axial stresses in the beam, because the beam would have to stretch as it bends.

In the canopy nonlinear study, this difficulty was recognized, and consequently modes analogous to the beam axial modes, called tangential modes, were included, in addition to the low frequency modes, which were called "basic".

The results of the canopy analysis were nevertheless erroneous. Evidently an additional difficulty exists.

As a means of studying this problem, again consider the cantilever beam. To simplify matters, assume that Poisson's ratio for the beam material is zero, and that the normal loads are applied half to the upper surface, and half to the lower. In this case, the thickness of the beam should remain approximately constant during the motion. As a further simplification, consider that the nonlinear analysis is being performed without the use of fictitious loads, since the canopy analysis described in Section III indicates that these loads are not the source of the difficulty. Coordinate updating is therefore the means under consideration of accounting for large displacement effects. Also, assume that the motion is represented by the bending and axial modes shown in Figure F.1 and F.4.

In Figure F.1, the line AB represents an axially loaded vertical bar, forming part of the cell element at the tip of the beam. In Figure F.5 the solid line shows bar AB in its displaced position, A'B', after the first time increment. At this point in time, a linear analysis has been performed, to determine the position of the beam, and of bar AB, at the end of the increment. Coordinates have been updated. Bar AB has translated parallel to y, translated parallel to z, and rotated about x. The axial load in the bar is essentially zero, since the analysis was linear.

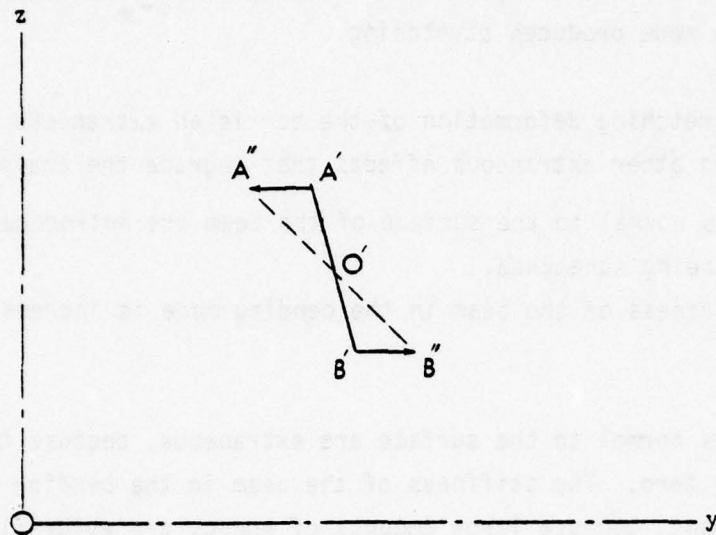


Figure F.5. Displaced position of bar AB.

Now consider what happens in the next increment. At this point, make the assumption, to clarify matters still further, that the bar has no shear node degree of freedom at O , so that the load induced in the bar depends solely on the displacements of joints A and B . The bar displacement during the second increment has contributions from the axial mode of Figure F.4, and the bending mode of Figure F.1. The axial mode produces only translation parallel to y . Therefore this mode introduces no load in the bar. The bending mode produces two kinds of motion of points A and B : (1) A motion in which A and B move equal amounts in the same direction parallel to z . (2) A motion in which A and B move equal amounts in opposite directions parallel to x . These are the same motions that the mode produced when the bar was in its initial vertical position at the beginning of the first increment. When the bar was vertical, neither motion produced axial load in the bar, according to the theory of small displacements. When the bar is in a rotated position, as in Figure F.5, the first motion again produces no axial load in the bar. The second motion stretches the bar, even according to small displacement theory,

as shown by the dotted line, $A'B''$, in Figure F.5. Note that this stretching cannot be counteracted by any other mode, because only one axial and one bending mode are being considered, and only the bar rotation resulting from the bending mode produces stretching.

This stretching deformation of the bar is an extraneous effect. It produces two other extraneous effects that degrade the analytical results:

1. Stresses normal to the surface of the beam are introduced, since the bar is being stretched.
2. The stiffness of the beam in the bending mode is increased by a large amount.

The stresses normal to the surface are extraneous, because they should be essentially zero. The stiffness of the beam in the bending mode is increased a large amount, because large amounts of energy are evidently required to deform the beam in the through-the-thickness direction.

The result of these extraneous effects is that the beam will appear to become very stiff, as soon as bar rotations become appreciable. In the non-linear canopy analysis, the structure did become stiff, when deflections became large enough, and subsequent displacements became smaller than the linear values, instead of larger, as expected. These effects would seem to explain the failure of the canopy analysis.

When the bar AB has a shear node degree of freedom, the situation is aggravated. In this case, suppose that the displacements of the bar nodes are designated as shown in Figure F.6, considering only motions parallel to the yz plane. The Figure shows the bar in its undisplaced position at the beginning of the first increment.

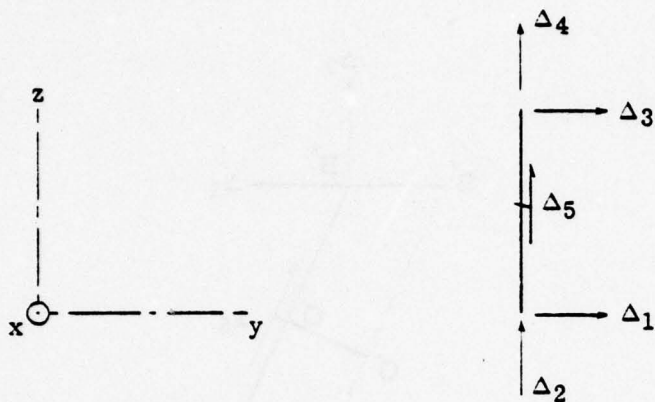


Figure F.6. Bar nodal displacements.

Now consider the axial mode of Figure F.4. In this mode, the nodal displacements of Figure F.6 are given by

$$\begin{Bmatrix} \Delta_1 \\ \Delta_2 \\ \Delta_3 \\ \Delta_4 \\ \Delta_5 \end{Bmatrix} = \begin{Bmatrix} -1 \\ 0 \\ -1 \\ 0 \\ 0 \end{Bmatrix} \quad (\text{F.8})$$

Figure F.7 shows the bar displacements when the bar is in its rotated position at the beginning of the second increment. The displacements Δ_1 , Δ_2 , Δ_3 , and Δ_4 are still specified as parallel to the global coordinates, but Δ_5 becomes inclined, since it remains parallel to the bar. When the displacements corresponding to the axial mode, specified by Equation F.7, are applied to the bar, it assumes the position shown by the dotted line.

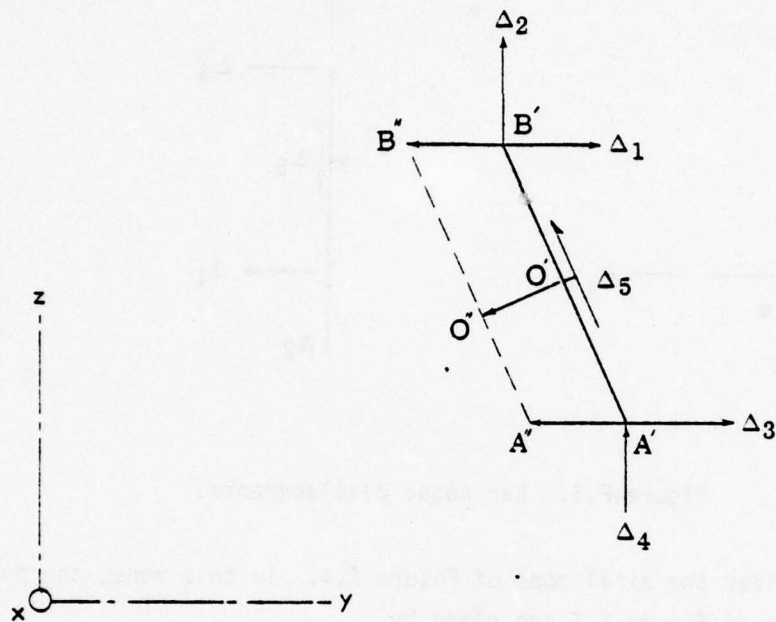


Figure F.7. Displacements of the rotated bar.

Point A moves a distance of one unit parallel to y approaching the origin. Point B moves similarly. But point O moves normal to the bar, since the displacement Δ_5 is specified as zero. Therefore the upper half of the bar stretches and the lower half is compressed, as the figure shows.

Figure F.8 shows the resulting forces on the bar. As the figure shows, the forces on the two ends of the bar are in the same direction. Again, the effect of bar rotation is to introduce extraneous stresses, and stiffness increases. The presence of the shear mode aggravates matters, because the axial mode produces no extraneous effects when the shear node is absent.

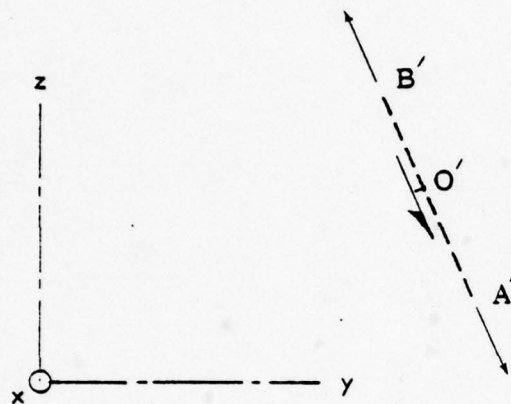


Figure F.8. Forces on the rotated bar.

The choice of modes suitable for geometrically nonlinear analysis evidently needs further study. Possible approaches to overcome the difficulties include:

1. Introducing through-the-thickness modes to eliminate extraneous stresses normal to the surface.
2. Eliminating shear node degrees of freedom to simplify the problem
3. Mode updating for each increment

Further study may suggest additional approaches.

APPENDIX G
BIRD IMPACT LOADS

LIST OF SYMBOLS FOR APPENDIX G

Symbols appearing in Appendix G are defined in this list.

A	Impact point
AB	Normal to surface at impact point
AG	Assumed locus of footprint centroid after impact
$A_{x_j}, A_{y_j}, A_{z_j}$	Moments of a unit load vector at joint j about the x , y and z axes
A_B	Square matrix of coefficients in the joint load equation
\bar{A}_B	Location of the footprint centroid at t_{B-1}
\vec{b}	Unit vector parallel to OA , pointing in the direction of motion of the bird
$B_{x_B}, B_{y_B}, B_{z_B}$	Moments of the centroidal vector at \bar{A}_B about the x , y and z axes
B_B	Column matrix. Multiplied by F_B , this matrix gives the constants on the right hand side of the joint load equation
\vec{d}	Unit vector parallel to AG , pointing in the same general direction as the motion of the bird
D_{B-1}	The distance $A\bar{A}_B$
\vec{D}_{B-1}	Vector joining impact point with A_B
F_{avg}	Average normal impact force

LIST OF SYMBOLS FOR APPENDIX G (Continued)

F_B	8th resultant external load
f_B	Proportion of F_{avg} acting on the structure during the 8th time increment
\vec{F}_B	8th resultant load vector
G	Point of detachment
GH	A normal AG, passing through G, intersecting OA produced at H
$\vec{i}, \vec{j}, \vec{k}$	Unit vectors parallel to the global axes
L	The distance AH
\bar{L}	A line
\bar{L}	Effective bird length
m	Bird mass
\vec{M}	Moment of \vec{P} about \bar{L}
M_x, M_y, M_z	Components of \vec{M}
\vec{n}	Unit vector normal to the surface at A, pointing toward the opposite side of the surface from the bird
OA	Locus of bird centroid before impact
\vec{P}	A vector
$\left. \begin{matrix} P_{xj,8} & P_{yj,8} \\ P_{zj,8} \end{matrix} \right\}$	Components of the load vectors referred to global coordinates
\vec{r}	Vector joining any point on \bar{L} to any point on \vec{P}
\vec{s}_0	Vector joining the origin of global coordinates with the impact point

LIST OF SYMBOLS FOR APPENDIX G (Continued)

\vec{s}_B	Vector joining the origin of global coordinates with the impact point
\vec{t}	Unit vector normal to \vec{b} and \vec{n}
t_d	Duration of impact
t_{B-1}	Time at beginning of the B th increment
v	Bird velocity before impact, relative to target
v'	Bird velocity after detachment
x, y, z	Global coordinates
θ	Angle between OA and AG
$\bar{\theta}$	Impact angle for rigid target
$\vec{\lambda}$	Unit vector parallel to \vec{L}
\vec{u}	Unit vector lying in plane OAB, normal to AG. The centroidal vector
u_x, u_y, u_z	Components of \vec{u}
$\phi_{j,B}$	The magnitude of $\vec{\phi}_{j,B}$
$\vec{\phi}_{j,B}$	Load vector acting on the j th loaded joint during the B th increment
ϕ_B	Column matrix of joint loads for the B th increment
\vec{w}_j	Vector joining origin of global coordinates to joint j

APPENDIX G

BIRD IMPACT LOADS

This appendix presents a procedure for calculating bird impact loads, and for distributing these loads to appropriate joints of the finite element model. Reference 10 gives the following equations for impact duration time t_d , and average impact force, F_{avg} , for rigid targets.

$$t_d = \frac{\tilde{l}}{v} \quad (G.1)$$

$$F_{avg} = \frac{m v \sin \bar{\theta}}{t_d} \quad (G.2)$$

where

\tilde{l} = effective bird length

v = bird velocity relative to target

m = bird mass

$\bar{\theta}$ = impact angle.

Reference 10 shows a triangular force-time distribution based on theoretical considerations, and test results for rigid target and fixed footprint impacts. Compliant target effects are discussed, and some additional test data are presented. However, the complete treatment of compliant targets and bird interactions is beyond the scope of the present effort.

The procedure derived here employs equations equivalent to equations G.1 and G.2, provides for a user specified force-time distribution, not necessarily triangular, and introduces the concept of the traveling footprint.

TRAVELING FOOTPRINT JOINT LOADS

The bird mass is assumed to slide along the transparency surface after impact. Figure G.1 shows impact geometry. Plane OAB contains the locus of the bird centroid, OA, and the surface normal, AB, at the point of impact. The curve CAD is the intersection of OAB with the surface.

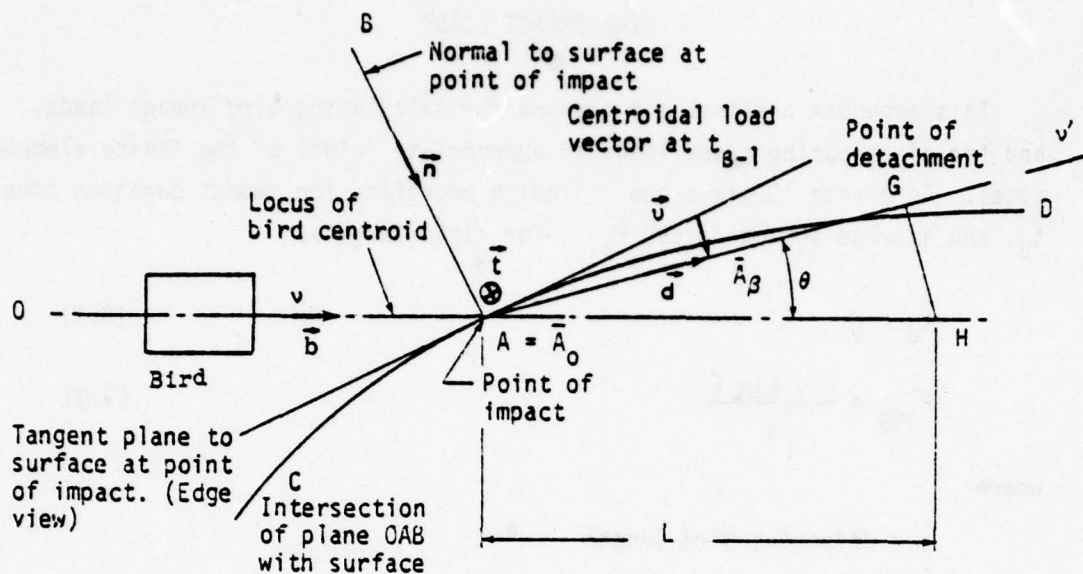


Figure G.1. Impact geometry.

Point A, also designated \bar{A}_0 , is the centroid of the load footprint at initial impact. When the bird strikes the surface, a wave is formed in the surface, that travels with the bird mass, so that the bird does not follow the original surface contour. As a simplification, assume that the centroid of the load footprint follows the straight line, AG, which lies in the plane OAB, and makes an angle θ with the path of the bird before impact. Assume that detachment occurs at point G, not necessarily on the original contour.

The velocity of the bird before impact is v . Let the velocity of the bird after detachment be v' , assumed parallel to AG. Let the average normal force applied by the bird to the surface be F_{avg} . Assume that the average tangential force is zero. Let t_d be the duration of impact, equal to the time required for the bird mass, m , to traverse the distance AG.

The impulse applied by the surface to the bird during impact is equal to the change in momentum of the bird. Therefore,

$$\text{average force} \times \text{impact duration} = \text{mass} \times \text{change in velocity} \quad (\text{G.2.1})$$

Designate the directions parallel and normal to AG as the tangential and normal directions. Writing Equation G.2.1 for the tangential direction gives

$$0 \times t_d = m (v \cos \theta - v') \quad (\text{G.2.2})$$

since the tangential force is zero, and the tangential component of the velocity before impact is $v \cos \theta$. Solving Equation G.2.2 for v' gives

$$v' = v \cos \theta \quad (\text{G.2.3})$$

Writing Equation G.2.1 for the normal direction gives

$$F_{\text{avg}} \times t_d = m (v \sin \theta - 0) \quad (\text{G.2.4})$$

since the normal component of velocity is $v \sin \theta$ before impact, and zero after impact. Solving Equation G.2.4 for F_{avg} gives

$$F_{\text{avg}} = \frac{m v \sin \theta}{t_d} \quad (\text{G.2.5})$$

The user estimates the angle θ , and the point of detachment, G. Draw line GH through G, normal to AG, intersecting OA at H. Define L as the distance AH. Assume that the bird speed along AG is constant and equal to v' . The time that the bird remains in contact with the surface is t_d . Therefore,

$$L \cos \theta = t_d v' \quad (\text{G.2.6})$$

Eliminating v' from Equations G.2.3 and G.2.6, and solving for t_d , gives

$$t_d = \frac{L}{v} \quad (\text{G.2.7})$$

In Figure G.1, \bar{A}_β is the location of the centroid of the footprint at $t_{\beta-1}$, of the β th increment. Therefore, the distance $A\bar{A}_\beta$ is given by

$$D_{\beta-1} = t_{\beta-1} v' \quad (G.2.8)$$

Combining Equations G.2.3 and G.2.8 gives

$$D_{\beta-1} = t_{\beta-1} v \cos \theta \quad (G.2.9)$$

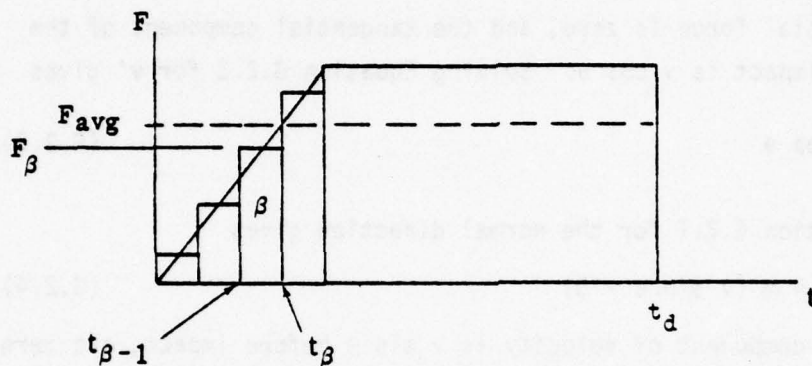


Figure G.2. Impact force-time diagram.

Figure G.2 shows the force applied by the bird mass to the surface, as a function of time. The user is free to select any plausible variation of force with time, except that the duration must be t_d , and the area under the diagram, the total impulse, must be $F_{avg} t_d$, where F_{avg} and t_d are given by Equations G.2.5 and G.2.7.

The total impulse is broken into rectangular segments, not necessarily of equal duration, as shown. Each segment corresponds to a time increment during the nonlinear incremental solution. The resultant load on the structure is considered constant during an increment, and equal to its value at the beginning of the increment.

The area of the β th segment of the total impulse represents the constant load acting on the structure during the β th time increment of the incremental solution. Call this load the β th resultant external load.

The β th resultant load is applied to the structure as pressure over a certain area of the surface. The surface area on which pressure is applied is called the footprint.

In the analysis, the distributed pressure inside the footprint is replaced by a set of load vectors. These vectors are assumed to be parallel, and normal to AG, throughout the impact process. Assume, for the β th increment, that:

1. The load vectors are statically equivalent to the resultant external load.
2. The positions of the vectors relative to each other remain constant during the increment. These positions are defined by joint numbers.

The user inputs numbers of joints that are within the footprint, and that are therefore loaded, during each increment. The components of the load vectors parallel to the global coordinate axes are calculated as functions of joint number and time.

Define a unit vector passing through the footprint centroid, parallel to the load vectors. Call this vector the centroidal vector. The centroidal vector coincides with the resultant load vector. Refer to Figure G.1.
Let

\vec{b} = a unit vector parallel to OA, pointing in the direction of motion of the bird.

\vec{n} = a unit vector normal to the surface at A, pointing toward the inside (opposite side of the surface from the bird).

\vec{t} = a unit vector normal to \vec{b} and \vec{n} .

\vec{d} = a unit vector parallel to AG, pointing in the same general direction as the motion of the bird ($\vec{d} \cdot \vec{b} > 0$).

\vec{s}_0 = a vector joining the origin of coordinates to the point \bar{A}_0 .

\vec{s}_β = a vector joining the origin of coordinates to Point \bar{A}_β

$\vec{D}_{\beta-1}$ = a vector joining Point A with Point \bar{A}_β

\vec{u} = the centroidal vector, a unit vector lying in plane OAB, normal to AG.

\vec{F}_β = the β th resultant load vector.

f_β = force-time distribution factor, or the proportion of F_{avg} acting on the structure during the β th time increment.

The vector \vec{d} must have the property that

$$\vec{d} \cdot \vec{t} = 0 \quad (G.3)$$

Now the following relationships can be written:

$$\vec{s}_\beta = \vec{s}_0 + \vec{D}_{\beta-1}$$

$$\therefore \vec{s}_\beta = \vec{s}_0 + D_{\beta-1} \vec{d}, \quad (G.4)$$

where $D_{\beta-1}$ = the magnitude of $\vec{D}_{\beta-1}$. Also,

$$\vec{t} = \frac{\vec{b} \times \vec{n}}{|\vec{b} \times \vec{n}|} \quad (G.5)$$

where $|\vec{b} \times \vec{n}|$ is the magnitude of $\vec{b} \times \vec{n}$. Similarly

$$\vec{u} = \frac{\vec{t} \times \vec{d}}{|\vec{t} \times \vec{d}|} \quad (G.6)$$

Thus defined, \vec{u} points toward the inside of the surface (opposite side of the surface from the bird). The β th resultant external load is

$$F_{\beta} = f_{\beta} F_{avg} \quad (G.7)$$

and the β th resultant load vector is

$$\vec{F}_{\beta} = F_{\beta} \vec{u} \quad (G.8)$$

From Figure G.2 and the definition of \vec{u}

$$\sin \theta = \vec{b} \cdot \vec{u} \quad (G.9)$$

therefore, from Equations G.2.5 and G.9,

$$F_{avg} = \frac{m v}{t_d} (\vec{b} \cdot \vec{u}) \quad (G.10)$$

Joint Load Vectors

For each time increment, a set of loaded joints is defined as input, by the user. Let

$\vec{\phi}_{j,\beta}$ = the load vector acting on the j th loaded joint during the β th increment.

The load vectors are parallel to the centroidal vector. Let

$$\begin{aligned} \phi_{j,\beta} &= \text{the magnitude of } \vec{\phi}_{j,\beta} \\ \therefore \vec{\phi}_{j,\beta} &= \phi_{j,\beta} \vec{u} \end{aligned} \quad (G.11)$$

Let the components of the units vector \bar{U} be u_x, u_y, u_z .

Select, as the reference plane, whichever coordinate plane (xy, yz, or zx) is normal to the largest component of \bar{U} . Designate, as reference axes, the axes of the reference plane.

Require that the sum of the load vectors be equal to the β th resultant load vector, and that the first moments of the load vectors about the reference axes be equal to the first moment of the β th resultant load vector about the same axes.

Now, since the load vectors are parallel,

$$\sum_j F_{j,\beta} = F_\beta \quad (G.12)$$

It is shown in the literature that the moment of a vector \bar{P} about a line \bar{L} is

$$\bar{M} = \bar{\lambda} \cdot (\bar{r} \times \bar{P}) \quad (G.13)$$

where $\bar{\lambda}$ is a unit vector parallel to \bar{L} , and \bar{r} is a vector joining any point on \bar{L} to any point on \bar{P} . The sense of \bar{M} is the same as the sense of $\bar{\lambda}$. The vector \bar{r} is directed from the point on \bar{L} to the point on \bar{P} . The moments about the x, y, and z axes are, therefore,

$$\left. \begin{aligned} M_x &= \bar{i} \cdot (\bar{r} \times \bar{P}) \\ M_y &= \bar{j} \cdot (\bar{r} \times \bar{P}) \\ M_z &= \bar{k} \cdot (\bar{r} \times \bar{P}) \end{aligned} \right\} \quad (G.14)$$

where \bar{i}, \bar{j} and \bar{k} are unit vectors parallel to x, y and z. The vector \bar{r} can be considered to be a vector joining the origin to any point on \bar{P} . Let

\bar{w}_j = a vector joining the origin to joint j.

If the reference plane is xy, the moments of the load vectors must equal the moments of the resultant load, about x and y. Therefore,

$$\left. \begin{aligned} \sum_j \bar{i} \cdot (\bar{w}_j \times \bar{\phi}_{j,B}) &= \bar{i} \cdot (\bar{s}_B \times \bar{F}_B) \\ \sum_j \bar{j} \cdot (\bar{w}_j \times \bar{\phi}_{j,B}) &= \bar{j} \cdot (\bar{s}_B \times \bar{F}_B) \end{aligned} \right\} \quad (G.15)$$

Therefore, from Equations G.8, G.11 and G.15,

$$\left. \begin{aligned} \sum_j \bar{i} \cdot (\bar{w}_j \times \bar{u}) \phi_{j,B} &= \bar{i} \cdot (\bar{s}_B \times \bar{u}) F_B \\ \sum_j \bar{j} \cdot (\bar{w}_j \times \bar{u}) \phi_{j,B} &= \bar{j} \cdot (\bar{s}_B \times \bar{u}) F_B \end{aligned} \right\} \quad (G.16)$$

Let

$$\left. \begin{aligned} A_{x_j} &= \bar{i} \cdot (\bar{w}_j \times \bar{u}) & B_{x_B} &= \bar{i} \cdot (\bar{s}_B \times \bar{u}) \\ A_{y_j} &= \bar{j} \cdot (\bar{w}_j \times \bar{u}) & B_{y_B} &= \bar{j} \cdot (\bar{s}_B \times \bar{u}) \end{aligned} \right\} \quad (G.17)$$

Therefore,

$$\left. \begin{aligned} \sum_j A_{x_j} \phi_{j,B} &= B_{x_B} F_B \\ \sum_j A_{y_j} \phi_{j,B} &= B_{y_B} F_B \end{aligned} \right\} \quad (G.18)$$

Combining Equations G.12 and G.18 into a single matrix equation gives

$$\underbrace{\begin{bmatrix} 1 & 1 & \dots \\ A_{x_1} & A_{x_2} & \dots \\ A_{y_1} & A_{y_2} & \dots \end{bmatrix}}_{A_B} \underbrace{\begin{bmatrix} \phi_{1,B} \\ \phi_{2,B} \\ \vdots \end{bmatrix}}_{\phi_B} = \underbrace{\begin{bmatrix} 1 \\ B_{x_B} \\ B_{y_B} \end{bmatrix}}_{B_B} F_B \quad (G.19)$$

The matrices are denoted by the symbols written under the equation.

$$\therefore A_B \phi_B = B_B F_B \quad (G.20)$$

The F's are known, the ϕ 's are unknown. The matrix A_B has three rows, and as many columns as there are load vectors. Solve by the method Lagrangian multipliers.

$$\therefore \phi_B = A_B^T (A_B A_B^T)^{-1} B_B F_B \quad (G.21)$$

The resulting ϕ 's satisfy Equation 20, and have the property that

$$\sum_j \phi_{j,B}^2 = \text{a minimum} \quad (G.22)$$

The components of the load vectors in the global coordinate system are given by

$$\begin{aligned} P_{xj,B} &= \phi_{j,B} u_x \\ P_{yj,B} &= \phi_{j,B} u_y \\ P_{zj,B} &= \phi_{j,B} u_z \end{aligned} \quad (G.23)$$

If the reference plane is yz, or zx, write equations analogous to Equation 19 by cyclic permutation of the x, y and z subscripts, where

$$A_{zj} = \vec{k} \cdot (\vec{w}_j \times \vec{u}) \quad B_{zB} = \vec{k} \cdot (\vec{s}_B \times \vec{u}) \quad (G.24)$$

Appendix H contains a list of traveling footprint load equations written in the order required for computation.

APPENDIX H
EQUATION SUMMARY

LIST OF SYMBOLS FOR APPENDIX H

Symbols appearing in Appendix H not defined in this list are defined in the lists at the front of the report or at the beginnings of Appendices C and G.

a', b'	Dimensions of parallelogram approximation to quadrilateral
\bar{a}', \bar{b}'	Edge vectors of parallelogram
$\bar{a}, \bar{b}, \bar{c}$	Unit vectors colinear with element edges
$\bar{d}, \bar{e}, \bar{f}$	
\bar{C}_i	Contribution of ith element to the transformed damping matrix
D_0	Column matrix of offsets \bar{e}_{03}
\bar{e}	Displacements of fictitious forces
\bar{e}_{03}	Offset from a specified parallelogram plane resulting from panel warp
\bar{F}	Fictitious force
\bar{F}_f	Column matrix of symmetric lumped bar forces \bar{F}_S
$\bar{F}_{\bar{F}}$	Rectangular matrix of element forces resulting from unit fictitious forces
$\bar{F}_{\bar{F}}(\bar{\beta})$	Average $\bar{F}_{\bar{F}}$
f, g	Constants
G_f	Column matrix of element dimensions
$G_f(\bar{\beta})$	Average G_f
J	Mechanical equivalent of heat
j	Joint number
k	Element stiffness matrix

LIST OF SYMBOLS FOR APPENDIX H (Continued)

s	Specific heat
$\left. \begin{matrix} \bar{t}_p, \bar{t}_q \\ \bar{t}_r, \bar{t}_s \\ \bar{t}_{pq}, \bar{t}_{rq} \\ \bar{t}_{rs}, \bar{t}_{ps} \end{matrix} \right\}$	Thickness vectors for cell element
T_R	Displacement transformation in reordered unconstrained degrees of freedom
U	Column matrix of joint coordinates, updated geometry
U_0	Column matrix of joint global coordinates, initial geometry
v, \dot{v}	Column matrices of untransformed velocities and accelerations in the unconstrained degrees of freedom
\bar{w}	Unit vector normal to a specified parallelogram plane
$\delta \bar{e}$	Column matrix of incremental displacements of fictitious forces
$\delta \bar{E}_{C_i}$	Element damping energy, i th element
Δ_{m_k}	Natural vibration mode
$\delta^P(\phi)T$	Column matrix of incremental loads
$\delta^P(\phi)T_j$	Partition of matrix $\delta^P(\phi)T$
$\delta \phi_j$	Incremental load on joint j
θ	Column matrix of element edge rotation.
θ_r	Rotation of the r th element edge
u_Δ	Scalar displacement magnification factor

LIST OF SYMBOLS FOR APPENDIX H (Continued)

\bar{u}_1, \bar{u}_2	Unit vectors, orthogonal with \bar{a}
ξ'	Skew angle of parallelogram approximation to quadrilateral
σ	Column matrix of stress components
$\bar{\sigma}$	Equivalent stress, true uniaxial stress
$\sigma_{S\sigma}$	Linear extrapolation transformation matrix
σ_{S1}, σ_{S2}	Partitions of $\sigma_{S\sigma}$
$\left. \begin{array}{l} \sigma_x, \sigma_y, \sigma_z \\ \tau_{xy}, \tau_{yz}, \tau_{zx} \end{array} \right\}$	Stress components
$\left. \begin{array}{l} \sigma'_x, \sigma'_y, \sigma'_z \\ \tau'_{xy}, \tau'_{yz}, \tau'_{zx} \end{array} \right\}$	Deviatoric stress components
σ_1, σ_2	Constants
ω_k	Natural frequency

LIST OF SYMBOLS FOR APPENDIX H (Continued)

l_1, l_2, l_3, l_4	Quadrilateral edge lengths
m_T	Total element mass, scalar
n_{B_k}	Column matrices of contributions to fictitious forces from bar elements, $k = 1, 2, 3$
$n_{j,k}$	elements of matrices n_{S_k}
n_k	Column matrices of fictitious forces, $k = 1, 2, 3$
n_{sk}	Column matrices of contributions to fictitious forces from shear panels, $k = 1, 2, 3$
$\overline{pq}, \overline{rq}$ $\overline{rs}, \overline{ps}$ }	Vectors from joints p to q , r to q , r to s , p to s
$\overline{p}, \overline{q}, \overline{r}, \overline{s}$	Vectors from the origin of global coordinates to joints p, q, r, s .
P_{RUPT}, P_{RUF}	Rectangular matrices of components in the reordered unconstrained degrees of freedom resulting from unit loads in the nodal degrees of freedom and from unit element forces
$\overline{P}_{UPT}, \overline{P}_{UF}$	Transformed P_{RUPT} and P_{RUF}
Q, Q'	Shear flows
r_{B_k}	Column matrices of contributions to fictitious deformations from bar elements, $k = 1, 2$
$\overline{r}_{j,k}$	Scaled elements of matrices r_{S_k}
r_k	Column matrices of fictitious deformations, $k = 1, 2$
r_r	Boolean transformation matrix
r_{S_k}	Column matrices of contributions to fictitious deformations from shear panels, $k = 1, 2$
r_1, r_2	Partitions of r_r

APPENDIX H EQUATION SUMMARY

This appendix contains the equations derived in Section II and in other appendices condensed and summarized in a logical sequence. Where necessary, to provide continuity or to fill gaps encountered in the implementation of the theory, additional definitions and derivations are presented. In some cases duplication of an existing equation is avoided by giving a reference to the equation number. The objective is to provide a basis for generating the computer code needed to implement the theory.

INITIAL GENERATOR

Appendix C contains finite element derivations, and definitions and equations are presented for use in generating the necessary element matrices. The following information on element geometry is prerequisite to evaluating the equations of Appendix C.

Element Geometry

U_{i0} = column matrix of initial joint coordinates for the i th element. It is a partition of matrix U_0 .

Let \bar{p} , \bar{q} , . . . be vectors from the origin of global coordinates to joints p , q , . . . having components equal to their x , y , z coordinates. If p_i , q_i , . . . are the defining joints of the i th element, then

$$U_{i0} = \begin{Bmatrix} \bar{p}_i \\ \bar{q}_i \\ \vdots \\ \vdots \end{Bmatrix} \quad (H.1) \quad \bar{p}_i = \begin{Bmatrix} x_p \\ y_p \\ z_p \end{Bmatrix}_i, \text{ etc.} \quad (H.2)$$

Bar Element

$$U_{i0} = \begin{Bmatrix} \bar{p}_i \\ \bar{q}_i \end{Bmatrix} \quad (H.3)$$

$$\overline{pq}_i = \bar{q}_i - \bar{p}_i \quad (H.4)$$

$$l_i = |\overline{pq}_i| \quad (H.5)$$

$$\bar{a}_i = \overline{pq}_i / l_i \quad (H.6)$$

Membrane Element

$$U_{i0} = \begin{Bmatrix} \bar{p}_i \\ \bar{q}_i \\ \bar{r}_i \\ \bar{s}_i \end{Bmatrix} \quad (H.7) \quad \bar{p}_i = \begin{Bmatrix} x_p \\ y_p \\ z_p \end{Bmatrix}_i, \text{ etc.} \quad (H.8)$$

Calculate the vectors

$$\overline{pq}_i = \bar{q}_i - \bar{p}_i \quad \text{also, } \overline{qp}_i = -\overline{pq}_i \quad (H.9)$$

$$\overline{rq}_i = \bar{q}_i - \bar{r}_i \quad \overline{qr}_i = -\overline{rq}_i \quad (H.10)$$

$$\overline{rs}_i = \bar{s}_i - \bar{r}_i \quad \overline{sr}_i = -\overline{rs}_i \quad (H.11)$$

$$\overline{ps}_i = \bar{s}_i - \bar{p}_i \quad \overline{sp}_i = -\overline{ps}_i \quad (H.12)$$

$$\bar{a}_i = \overline{pq}_i / |\overline{pq}_i| \quad (H.13)$$

$$\bar{b}_i = \overline{rq}_i / |\overline{rq}_i| \quad (H.14)$$

$$\bar{c}_i = \overline{rs}_i / |\overline{rs}_i| \quad (H.15)$$

$$\bar{d}_i = \overline{ps}_i / |\overline{ps}_i| \quad (H.16)$$

$$\bar{e}_i = \overline{ps}_i \times \overline{pq}_i / |\overline{ps}_i \times \overline{pq}_i| \quad (H.17)$$

K- factors, angles and edge lengths are calculated from

$$K_{1i} = -(\bar{a}_i \times \overline{qr}_i) \cdot \bar{c}_i / (\bar{e}_i \times \overline{qr}_i) \cdot \bar{c}_i \quad (H.18)$$

$$K_{2i} = -(\bar{a}_i \times \overline{ps}_i) \cdot \bar{e}_i / (\bar{b}_i \times \overline{rs}_i) \cdot \bar{e}_i \quad (H.19)$$

$$K_{3i} = -K_{2i} (\bar{b}_i \times \overline{qp}_i) \cdot \bar{e}_i / (\bar{c}_i \times \overline{sp}_i) \cdot \bar{e}_i \quad (H.20)$$

$$K_{4i} = -K_{3i} (\bar{c}_i \times \overline{sp}_i) \cdot \bar{a}_i / (\bar{e}_i \times \overline{sp}_i) \cdot \bar{a}_i \quad (H.21)$$

$$K_{5_i} = -(\bar{a}_i \cdot \bar{d}_i) - K_{2_i} (\bar{b}_i \cdot \bar{d}_i) - K_{3_i} (\bar{c}_i \cdot \bar{d}_i) \quad (H.22)$$

$$\theta_{p_i} = \cos^{-1} (-\bar{a}_i \cdot \bar{d}_i) \quad (H.23)$$

$$\theta_{q_i} = \cos^{-1} (\bar{a}_i \cdot \bar{b}_i) \quad (H.24)$$

$$\theta_{r_i} = \cos^{-1} (-\bar{c}_i \cdot \bar{b}_i) \quad (H.25)$$

$$\theta_{s_i} = \cos^{-1} (\bar{c}_i \cdot \bar{d}_i) \quad (H.26)$$

$$a_{p_i} = a_{q_i} = \frac{1}{2} |\overline{pq}_i| \quad (H.27)$$

$$a_{r_i} = a_{s_i} = \frac{1}{2} |\overline{rs}_i| \quad (H.28)$$

$$b_{p_i} = b_{s_i} = \frac{1}{2} |\overline{ps}_i| \quad (H.29)$$

$$b_{r_i} = b_{q_i} = \frac{1}{2} |\overline{rq}_i| \quad (H.30)$$

Cell Element

$$U_{i_0} = \begin{bmatrix} \bar{p}_0 \\ \bar{q}_0 \\ \bar{r}_0 \\ \bar{s}_0 \\ \bar{p}_1 \\ \bar{q}_1 \\ \bar{r}_1 \\ \bar{s}_1 \end{bmatrix}_i \quad (H.31)$$

$$\bar{p}_0 = \begin{bmatrix} x_{po} \\ y_{po} \\ z_{po} \end{bmatrix}_i, \text{ etc.} \quad (H.32)$$

Calculate the thickness vectors

$$\bar{t}_{p_i} = \bar{p}_{1_i} - \bar{p}_{0_i} \quad (\text{H.33})$$

$$\bar{t}_{q_i} = \bar{q}_{1_i} - \bar{q}_{0_i} \quad (\text{H.34})$$

$$\bar{t}_{r_i} = \bar{r}_{1_i} - \bar{r}_{0_i} \quad (\text{H.35})$$

$$\bar{t}_{s_i} = \bar{s}_{1_i} - \bar{s}_{0_i} \quad (\text{H.36})$$

$$\bar{t}_{pq_i} = \bar{t}_{q_i} - \bar{t}_{p_i} \quad (\text{H.37})$$

$$\bar{t}_{rq_i} = \bar{t}_{q_i} - \bar{t}_{r_i} \quad (\text{H.38})$$

$$\bar{t}_{rs_i} = \bar{t}_{s_i} - \bar{t}_{r_i} \quad (\text{H.39})$$

$$\bar{t}_{ps_i} = \bar{t}_{s_i} - \bar{t}_{p_i} \quad (\text{H.40})$$

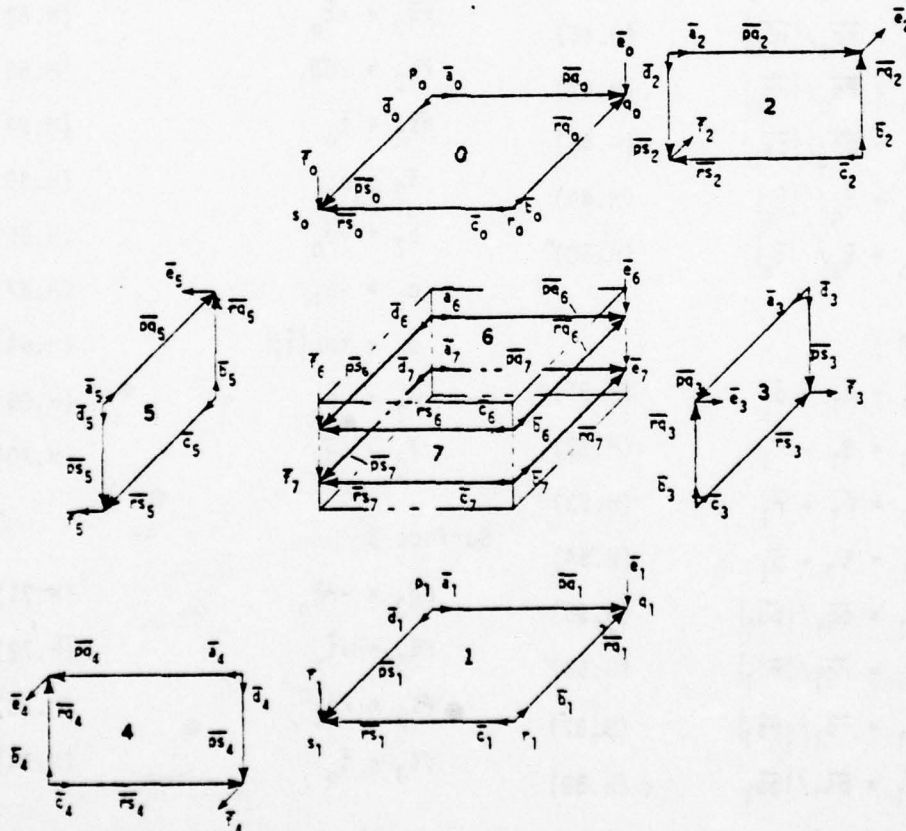


Figure H.1. Surfaces and associated vectors.

The surfaces in Figure H.1 may be warped. Surfaces 0 - 5 represent the true geometric shape of the cell. Surfaces 6 and 7 represent the upper and lower surfaces of the lumped cell element.

Edge vectors and unit vectors for 8 surfaces (with subscript i temporarily omitted) are calculated from

Surface 0

$$\overline{pq}_0 = \bar{q}_0 - \bar{p}_0 \quad (H.41)$$

$$\overline{rq}_0 = \bar{q}_0 - \bar{r}_0 \quad (H.42)$$

$$\overline{rs}_0 = \bar{s}_0 - \bar{r}_0 \quad (H.43)$$

$$\overline{ps}_0 = \bar{s}_0 - \bar{p}_0 \quad (H.44)$$

$$\bar{a}_0 = \overline{pq}_0 / |\overline{pq}_0| \quad (H.45)$$

$$\bar{b}_0 = \overline{rq}_0 / |\overline{rq}_0| \quad (H.46)$$

$$\bar{c}_0 = \overline{rs}_0 / |\overline{rs}_0| \quad (H.47)$$

$$\bar{d}_0 = \overline{ps}_0 / |\overline{ps}_0| \quad (H.48)$$

$$\bar{e}_0 = \bar{t}_q / |\bar{t}_q| \quad (H.49)$$

$$\bar{f}_0 = \bar{t}_s / |\bar{t}_s| \quad (H.50)$$

Surface 1

$$\overline{pq}_1 = \bar{q}_1 - \bar{p}_1 \quad (H.51)$$

$$\overline{rq}_1 = \bar{q}_1 - \bar{r}_1 \quad (H.52)$$

$$\overline{rs}_1 = \bar{s}_1 - \bar{r}_1 \quad (H.53)$$

$$\overline{ps}_1 = \bar{s}_1 - \bar{p}_1 \quad (H.54)$$

$$\bar{a}_1 = \overline{pq}_1 / |\overline{pq}_1| \quad (H.55)$$

$$\bar{b}_1 = \overline{rq}_1 / |\overline{rq}_1| \quad (H.56)$$

$$\bar{c}_1 = \overline{rs}_1 / |\overline{rs}_1| \quad (H.57)$$

$$\bar{d}_1 = \overline{ps}_1 / |\overline{ps}_1| \quad (H.58)$$

Surface 1 (continued)

$$\bar{e}_1 = \bar{e}_0 \quad (H.59)$$

$$\bar{f}_1 = \bar{f}_0 \quad (H.60)$$

Surface 2

$$\overline{pq}_2 = \overline{pq}_0 \quad (H.61)$$

$$\overline{rq}_2 = -\bar{t}_q \quad (H.62)$$

$$\overline{rs}_2 = -\overline{pq}_1 \quad (H.63)$$

$$\overline{ps}_2 = \bar{t}_p \quad (H.64)$$

$$\bar{a}_2 = \bar{a}_0 \quad (H.65)$$

$$\bar{b}_2 = -\bar{e}_0 \quad (H.66)$$

$$\bar{c}_2 = -\bar{a}_1 \quad (H.67)$$

$$\bar{d}_2 = \bar{t}_p / |\bar{t}_p| \quad (H.68)$$

$$\bar{e}_2 = \bar{b}_0 \quad (H.69)$$

$$\bar{f}_2 = -\bar{d}_1 \quad (H.70)$$

Surface 3

$$\overline{pq}_3 = -\overline{rq}_0 \quad (H.71)$$

$$\overline{rq}_3 = -\bar{t}_r \quad (H.72)$$

$$\overline{rs}_3 = \overline{rq}_1 \quad (H.73)$$

$$\overline{ps}_3 = \bar{t}_q \quad (H.74)$$

Surface 3 (continued)

$$\bar{a}_3 = -\bar{b}_0$$

(H.75)

$$\bar{b}_3 = -\bar{t}_r / |\bar{t}_r|$$

(H.76)

$$\bar{c}_3 = \bar{b}_1$$

(H.77)

$$\bar{d}_3 = \bar{e}_0$$

(H.78)

$$\bar{e}_3 = -\bar{c}_0$$

(H.79)

$$\bar{f}_3 = \bar{a}_1$$

(H.80)

Surface 4

$$\bar{p}q_4 = \bar{r}s_0$$

(H.81)

$$\bar{r}q_4 = -\bar{t}_s$$

(H.82)

$$\bar{r}s_4 = -\bar{r}s_1$$

(H.83)

$$\bar{p}s_4 = \bar{t}_r$$

(H.84)

$$\bar{a}_4 = \bar{c}_0$$

(H.85)

$$\bar{b}_4 = -\bar{f}_0$$

(H.86)

$$\bar{c}_4 = -\bar{c}_1$$

(H.87)

$$\bar{d}_4 = -\bar{b}_3$$

(H.88)

$$\bar{e}_4 = \bar{d}_0$$

(H.89)

$$\bar{f}_4 = -\bar{b}_1$$

(H.90)

Surface 5

$$\bar{p}q_5 = -\bar{p}s_0$$

(H.91)

$$\bar{r}q_5 = -\bar{t}_p$$

(H.92)

$$\bar{r}s_5 = \bar{p}s_1$$

(H.93)

$$\bar{p}s_5 = \bar{t}_s$$

(H.94)

$$\bar{a}_5 = -\bar{d}_0$$

(H.95)

Surface 5 (continued)

$$\bar{b}_5 = -\bar{d}_2$$

(H.96)

$$\bar{c}_5 = \bar{d}_1$$

(H.97)

$$\bar{d}_5 = \bar{f}_0$$

(H.98)

$$\bar{e}_5 = -\bar{a}_0$$

(H.99)

$$\bar{f}_5 = \bar{c}_1$$

(H.100)

Surface 6

$$\bar{p}q_6 = \bar{p}q_0 + \beta \bar{t}_{pq}$$

(H.101)

$$\bar{r}q_6 = \bar{r}q_0 + \beta \bar{t}_{rq}$$

(H.102)

$$\bar{r}s_6 = \bar{r}s_0 + \beta \bar{t}_{rs}$$

(H.103)

$$\bar{p}s_6 = \bar{p}s_0 + \beta \bar{t}_{ps}$$

(H.104)

$$\bar{a}_6 = \bar{p}q_6 / |\bar{p}q_6|$$

(H.105)

$$\bar{b}_6 = \bar{r}q_6 / |\bar{r}q_6|$$

(H.106)

$$\bar{c}_6 = \bar{r}s_6 / |\bar{r}s_6|$$

(H.107)

$$\bar{d}_6 = \bar{p}s_6 / |\bar{p}s_6|$$

(H.108)

$$\bar{e}_6 = \bar{e}_0$$

(H.109)

$$\bar{f}_6 = \bar{f}_0$$

(H.110)

Surface 7

$$\bar{p}q_7 = \bar{p}q_0 \times \alpha \bar{t}_{pq}$$

(H.111)

$$\bar{r}q_7 = \bar{r}q_0 \times \alpha \bar{t}_{rq}$$

(H.112)

$$\bar{r}s_7 = \bar{r}s_0 \times \alpha \bar{t}_{rs}$$

(H.113)

$$\bar{p}s_7 = \bar{p}s_0 \times \alpha \bar{t}_{ps}$$

(H.114)

$$\bar{a}_7 = \bar{p}q_7 / |\bar{p}q_7|$$

(H.115)

$$\bar{b}_7 = \bar{r}q_7 / |\bar{r}q_7|$$

(H.116)

$$\bar{c}_7 = \bar{r}s_7 / |\bar{r}s_7|$$

(H.117)

Surface 7 (continued)

$$\bar{d}_7 = \bar{p}s_7 / |\bar{p}s_7| \quad (\text{H.118})$$

$$\bar{e}_7 = \bar{e}_0 \quad (\text{H.119})$$

$$\bar{f}_7 = \bar{f}_0 \quad (\text{H.120})$$

$$\text{where: } \alpha = \frac{3 + \sqrt{3}}{6} \text{ and } \beta = \frac{3 - \sqrt{3}}{6} \quad (\text{H.121})$$

K - Factors for the eight surfaces are calculated from

$$K_{1k} = \frac{-(\bar{a}_k \times \bar{r}q_k) \cdot \bar{c}_k}{(\bar{e}_k \times \bar{r}q_k) \cdot \bar{c}_k} \quad (\text{H.122})$$

$$K_{2k} = \frac{-(\bar{a}_k \times \bar{p}s_k) \cdot \bar{f}_k - K_{1k} [\bar{e}_k \times (\bar{r}s_k - \bar{r}q_k)] \cdot \bar{f}_k}{(\bar{b}_k \times \bar{r}s_k) \cdot \bar{f}_k} \quad (\text{H.123})$$

$$K_{3k} = \frac{-K_{1k} (\bar{e}_k \times \bar{p}q_k) \cdot \bar{f}_k - K_{2k} (\bar{b}_k \times \bar{p}q_k) \cdot \bar{f}_k}{(\bar{c}_k \times \bar{p}s_k) \cdot \bar{f}_k} \quad (\text{H.124})$$

$$K_{4k} = - \frac{K_{3k} (\bar{c}_k \times \bar{p}s_k) \cdot \bar{a}_k}{(\bar{f}_k \times \bar{p}s_k) \cdot \bar{a}_k} \quad (\text{H.125})$$

$$K_{5k} = -(\bar{a}_k \cdot \bar{d}_k) - K_{1k} (\bar{e}_k \cdot \bar{d}_k) - K_{2k} (\bar{b}_k \cdot \bar{d}_k) - K_{3k} (\bar{c}_k \cdot \bar{d}_k) - K_{4k} (\bar{f}_k \cdot \bar{d}_k) \quad (\text{H.126})$$

where $k = 0, 1, 2, \dots, 7$.

Angles and lengths for sub-elements 1 - 8 are

$$\theta_{1i} = \cos^{-1} (-\bar{a}_{6i} \cdot \bar{d}_{6i}) \quad (\text{H.127})$$

$$\theta_{2i} = \cos^{-1} (\bar{a}_{6i} \cdot \bar{b}_{6i}) \quad (\text{H.128})$$

$$\theta_{3_i} = \cos^{-1} (-\bar{c}_{6_i} \cdot \bar{b}_{6_i}) \quad (\text{H.129})$$

$$\theta_{4_i} = \cos^{-1} (\bar{c}_{6_i} \cdot \bar{d}_{6_i}) \quad (\text{H.130})$$

$$\theta_{5_i} = \cos^{-1} (-\bar{a}_{7_i} \cdot \bar{d}_{7_i}) \quad (\text{H.131})$$

$$\theta_{6_i} = \cos^{-1} (\bar{a}_{7_i} \cdot \bar{b}_{7_i}) \quad (\text{H.132})$$

$$\theta_{7_i} = \cos^{-1} (-\bar{c}_{7_i} \cdot \bar{b}_{7_i}) \quad (\text{H.133})$$

$$\theta_{8_i} = \cos^{-1} (\bar{c}_{7_i} \cdot \bar{d}_{7_i}) \quad (\text{H.134})$$

$$a_{1_i} = a_{2_i} = \frac{1}{2} |\overline{pq}_{6_i}|, \quad b_{1_i} = b_{4_i} = \frac{1}{2} |\overline{ps}_{6_i}| \quad (\text{H.135})$$

$$a_{3_i} = a_{4_i} = \frac{1}{2} |\overline{rs}_{6_i}|, \quad b_{2_i} = b_{3_i} = \frac{1}{2} |\overline{rq}_{6_i}| \quad (\text{H.136})$$

$$a_{5_i} = a_{6_i} = \frac{1}{2} |\overline{pq}_{7_i}|, \quad b_{5_i} = b_{8_i} = \frac{1}{2} |\overline{ps}_{7_i}| \quad (\text{H.137})$$

$$a_{7_i} = a_{8_i} = \frac{1}{2} |\overline{rs}_{7_i}|, \quad b_{6_i} = b_{7_i} = \frac{1}{2} |\overline{rq}_{7_i}| \quad (\text{H.138})$$

Element Matrices

The element geometry already summarized together with the source references given in Table H.1 provide the basis for writing the initial generator program to assemble the element matrices for each element type. Where no references exist, the appropriate equations are given in the table.

Model Matrices

The initial generator also creates matrices U_0 , P_{UPT} , P_{UFi} , where:

TABLE H.1. ELEMENT MATRICES

ELEMENT MATRIX	SOURCE REFERENCE			
	BAR	MEMBRANE	CELL	POINT MASS
C_{Ki}	APPENDIX E	APPENDIX E	APPENDIX E	
\bar{K}_i	Eq. C.3	Eq. C.27, C.30, C.61-C.64, C.77	Eqs. C.102-C.109, Tables C.2, C.3, Eqs. C.148, C.151	
\bar{C}_i	Eq. C.12	Eq. C.92	Eq. C.186	
$F_{\bar{F}_i}$	Eq. C.13	Eq. C.93-C.98	Tables C.5, C.6, C.7, Eqs. C.192, C.189.2	
$\sigma_{F_i} = \sigma_{LF_i}$	Eq. C.10	Eq. C.90	Eqs. C.148, C.168, C.169, C.172	
ϵ_{oS_i}	C_{KU_i}	C_{KP_i}	Eq. C.183	
m_i	Eq. C.14	Eq. C.99	Eq. C.193	Eq. C.194
$\delta \bar{e}_{o_{il}}$	Eq. C.7	Eqs. C.83.1, C.83.2	Eqs. C.83.2, C.156	
$\bar{e}'_{T\Delta_i}$	Eq. C.6	Table C.1 $j = 1 - 4$ $= \alpha_{Ti} \sum_j \bar{e}_{aTji}$	Table C.4 $j = 1 - 8$	
k_i		$= F_{\bar{F}_i} \bar{K}_i F_{\bar{F}_i}^T$		
V_i	$= A_{b_i} z_i$	Eq. C.83.6 $= t_{m_i} \sum_j A_{ji}$	Eq. C.128, C.130 $= \sum_j V_{ji}$	
m_{T_i}		$= \rho_i V_i$		

U_0 = matrix of joint coordinates in the global Cartesian coordinate system, assembled from input data.

P_{TF_i} , P_{UPT} = additional force transformation matrices derived at the end of Appendix C.

$$P_{UF_i} = P_{UPT} P_{TF_i} \quad (H.138.1)$$

The column formats of matrices P_{TF_i} and P_{UF_i} are consistent with the element force numbering sequence for the i th element, which may be that of a bar, membrane, or cell. The column format of P_{UPT} is associated with joint and edge degrees of freedom. There are three columns per joint corresponding to the x , y , z global translational degrees of freedom, where the sets of three are adjoined consistent with the joint numbering sequence. After all the joints have been accounted for the remaining columns correspond to edge degrees of freedom numbered in sequence with the associated joints. This is called the total, or "T", degree of freedom format.

The row formats of P_{UPT} and P_{UF_i} are derivatives of the column format of P_{UPT} , where constrained degrees of freedom have been removed. This is called the unconstrained, or "U", degree of freedom format.

However, the efficiency of wave front techniques in the decomposition of stiffness matrices is dependent on the ordering of the equations, or degrees of freedom. Therefore, a reordered unconstrained, or "RU", degree of freedom format is defined in the initial generator program based on the requirements of the decomposition module. The initial generator printout gives a definition of the "RU" format in terms of the "U" format. Matrices P_{RUPT} and P_{RUF_i} are, therefore, generated and used in place of P_{UPT} and P_{UF_i} . The only effect of this substitution is that a more efficient ordering of the degrees of freedom is achieved.

MODAL TRANSFORMATION

$$K = \sum_i P_{RUF_i} k_i P_{RUF_i}^T \quad (H.139)$$

$$M = \sum_i P_{RUF_i} m_i P_{RUF_i}^T \quad (H.140)$$

$$(K - \omega_k^2 M) \Delta_{m_k} = 0 \quad (H.141)$$

$$T_R = [\Delta_{m_1} | \Delta_{m_2} | \dots | \Delta_{m_k} | \dots] \quad (H.142)$$

$$\bar{P}_{UPT} = T_R^T P_{RUPT} \quad (H.143)$$

$$\bar{P}_{UF_i} = T_R^T P_{RUF_i} \quad (H.144)$$

$$\delta \bar{P}_{(\phi)U_\beta}(t_\beta) = \bar{P}_{UPT} \delta P_{(\phi)T_\beta}(t_\beta) \quad (H.145)$$

where $\delta P_{(\phi)T_\beta}(t_\beta)$ = column matrix of components of the incremental external loads in the nodal degrees of freedom for the β th time increment, reference Equation H.387.

The transformed mass matrix remains constant and is calculated from

$$\bar{M} = \sum_i \bar{P}_{UF_i} m_i \bar{P}_{UF_i}^T \quad (H.146)$$

Set \bar{k}_i , \bar{c}_i , $F_{\bar{F}i}$, $\sigma_{L\bar{F}i}$, ϵ_{osi} from the initial generator equal to $\bar{k}_{i(\beta)}$, $\bar{c}_{i(\beta)}$, $F_{\bar{F}i}(t_{\beta-1})$, $\sigma_{L\bar{F}i}(t_{\beta-1})$, $\epsilon_{osi}(t_{\beta-1})$ for use in the nonlinear incremental solution..

NONLINEAR INCREMENTAL SOLUTION

Transformed Stiffness and Damping Matrices

$$\bar{K}_{(\beta)} = \sum_i \bar{P}_{UF_i} F_{\bar{F}i}(t_{\beta-1}) \bar{k}_{i(\beta)} F_{\bar{F}i}^T(t_{\beta-1}) \bar{P}_{UF_i}^T \quad (H.147)$$

$$\bar{C}_{(s)} = \sum_i \bar{P}_{UF_i} F_{\bar{F}_i}(t_{s-1}) \bar{C}_{i(s)} F_{\bar{F}_i}^T(t_{s-1}) \bar{P}_{UF_i}^T \quad (H.148)$$

Transformed Thermomechanical Loads

External Loads

$$\begin{aligned} \bar{P}_{(\phi)U}(t_{s-1}) &= 0 \text{ for } s = 1 \\ \bar{P}_{(\phi)U}(t_s) &= \bar{P}_{(\phi)U}(t_{s-1}) + \delta \bar{P}_{(\phi)U}(t_s) \end{aligned} \quad (H.149)$$

Thermal Effects

$$\begin{aligned} \delta \bar{e}_{o_{i\beta}}(t_s) &= \delta \bar{e}_{o_{i1}} & \text{for } s = 1 \\ &= \delta T_{i\beta-1} \bar{e}_{T\Delta_i}^T & \text{for } s > 1 \\ \delta \bar{F}_{K_{o_{i\beta}}}(t_s) &= -\bar{k}_{i(\beta)} \delta \bar{e}_{o_{i\beta}}(t_s) \end{aligned} \quad (H.150)$$

$$\delta \bar{P}_{K_{o_{i\beta}}}(t_s) = \sum_i \bar{P}_{UF_i} F_{\bar{F}_i}(t_{s-1}) \delta \bar{F}_{K_{o_{i\beta}}}(t_s) \quad (H.151)$$

Inertia, Damping and Stiffness Effects

$$\left. \begin{aligned} \dot{\bar{v}}(t_{s-1}) &= 0 \\ \bar{F}_{C_i}(t_{s-1}) &= \bar{F}_{K_i}(t_{s-1}) = 0 \end{aligned} \right\} \text{for } s = 1$$

$$\bar{P}_{(M)U}(t_{s-1}) = -M \dot{\bar{v}}(t_{s-1}) \quad (H.152)$$

$$\bar{P}_{(C)U}(t_{s-1}) = \sum_i \bar{P}_{UF_i} F_{\bar{F}_i}(t_{s-1}) \bar{F}_{C_i}(t_{s-1}) \quad (H.153)$$

$$\bar{P}_{(K)U}(t_{s-1}) = \sum_i \bar{P}_{UF_i} F_{\bar{F}_i}(t_{s-1}) \bar{F}_{K_i}(t_{s-1}) \quad (H.154)$$

Equilibrium Imbalance

$$\begin{aligned} \delta \bar{P}_{U_{s-1}}(t_{s-1}) &= \bar{P}_{(M)U}(t_{s-1}) + \bar{P}_{(C)U}(t_{s-1}) \\ &\quad + \bar{P}_{(K)U}(t_{s-1}) + \bar{P}_{(\phi)U}(t_{s-1}) \end{aligned} \quad (H.155)$$

Thermomechanical Load Matrix

$$\begin{aligned} \bar{P}_B = & \delta \bar{P}_{K0_B}(t_B) + \delta \bar{P}_{(\phi)U_B}(t_B) \\ & - \bar{P}_{(H)U}(t_{B-1}) - \bar{P}_{(C)U}(t_{B-1}) + \delta \bar{P}_{U_{B-1}}(t_{B-1}) \end{aligned} \quad (H.156)$$

Load Variation Constants

$$\tau_B = t_B - t_{B-1} \quad (H.157)$$

$$\omega_{pB} = \frac{\pi}{50 \tau_B} \quad (H.158)$$

$$c_{pB} = \frac{\omega_{pB} \tau_B}{\sin \omega_{pB} \tau_B} \quad (H.159)$$

$$c_{fB} = \frac{1}{\sin \omega_{pB} \tau_B} \quad (H.160)$$

Iterative Solution

Table 1 describes the iterative loop within an increment which accounts for geometric nonlinearity. As dictated in Step 1 of the table, the matrix of fictitious transformed external loads $\delta \bar{P}_{(f)B}(t_B)$ is made null at the beginning of each increment and is evaluated at the end of each iterative cycle (Step 9) within an increment for use in the next iterative cycle.

The equations needed to generate the input to Step 2 of Table 1 have been summarized, and the output matrices of Step 2 can now be generated by means of the indicated equations. The equations are:

$$A_B = \left[\begin{array}{c|c} 0 & I \\ \hline -\bar{M}^{-1} \bar{K}_{(B)} & -\bar{M}^{-1} \bar{C}_{(B)} \end{array} \right] \quad (H.161)$$

$$(A_B - \lambda_{Bk} I) G_{Bk} = 0 \quad (H.162)$$

$$H_B = [G_{B1} \mid G_{B2} \mid \dots] \quad (H.163)$$

$$= \begin{bmatrix} H_{\Delta B} \\ H_{VB} \end{bmatrix}$$

$$F_B(\tau_B) = \begin{bmatrix} e^{\lambda_{B1} \tau_B} \\ e^{\lambda_{B2} \tau_B} \\ \vdots \\ \cdot \end{bmatrix} \quad (H.164)$$

$$\bar{K}_{C(B)} = \bar{K}_{(B)} - \omega_{pB}^2 \bar{M} + j \omega_{pB} \bar{C}_{(B)} \quad (H.165)$$

$$j = \sqrt{-1} \quad (H.166)$$

$$\delta \bar{\Delta}_{C_B} = \bar{K}_{C(B)}^{-1} \bar{P}_B c_p \quad (H.167)$$

$$\delta \bar{\Delta}_{fB} = \bar{K}_{C(B)}^{-1} \delta \bar{P}_{(f)_B}(t_B) c_{f_B} \quad (H.168)$$

$$y_{C_B} = \begin{bmatrix} \delta \bar{\Delta}_{CR_B} + \delta \bar{\Delta}_{fI_B} \\ \omega_{pB} (\delta \bar{\Delta}_{fR_B} - \delta \bar{\Delta}_{CI_B}) \end{bmatrix} \quad (H.169)$$

where

$\delta \bar{\Delta}_{CR_B}, \delta \bar{\Delta}_{CI_B}$ = real and imaginary parts of $\delta \bar{\Delta}_{C_B}$

$\delta \bar{\Delta}_{fR_B}, \delta \bar{\Delta}_{fI_B}$ = real and imaginary parts of $\delta \bar{\Delta}_{f_B}$

$$y_B(t_{B-1}) = \begin{bmatrix} 0 \\ \bar{v}(t_{B-1}) \end{bmatrix} \quad (H.170)$$

$$C_{aD_B} = H_B^{-1} [y_B(t_{B-1}) - y_{C_B}] \text{ diagonalized} \quad (H.171)$$

$$\begin{aligned} \delta \bar{A}_B(t_B) = & H_{\Delta_B} C_{aD_B} F_B(\tau_B) + (\delta \bar{A}_{CR_B} + \delta \bar{A}_{fI_B}) \cos \omega_{pB} \tau_B \\ & + (\delta \bar{A}_{fR_B} - \delta \bar{A}_{CI_B}) \sin \omega_{pB} \tau_B \end{aligned} \quad (H.172)$$

$$\begin{aligned} \bar{v}(t_B) = & H_{V_B} C_{aD_B} F_B(\tau_B) + \omega_{pB} (\delta \bar{A}_{fR_B} - \delta \bar{A}_{CI_B}) \cos \omega_{pB} \tau_B \\ & - \omega_{pB} (\delta \bar{A}_{CR_B} + \delta \bar{A}_{fI_B}) \sin \omega_{pB} \tau_B \end{aligned} \quad (H.173)$$

$$\begin{aligned} \dot{\bar{v}}(t_B) = & H_{V_B} C_{aD_B} \lambda_{D_B} F_B(\tau_B) - \omega_{pB}^2 (\delta \bar{A}_{CR_B} + \delta \bar{A}_{fI_B}) \cos \omega_{pB} \tau_B \\ & - \omega_{pB}^2 (\delta \bar{A}_{fR_B} - \delta \bar{A}_{CI_B}) \sin \omega_{pB} \tau_B \end{aligned} \quad (H.174)$$

$$\text{where } \lambda_{D_B} = \begin{Bmatrix} \lambda_{B1} \\ \lambda_{B2} \\ \cdot \\ \cdot \\ \cdot \end{Bmatrix} \text{ diagonalized} \quad (H.175)$$

Step 3 need not be performed until postprocessing time.

The Step 4 output matrices are generated from

$$\delta e_{iB}(t_B) = -P_{UF}^T \delta \bar{A}_B(t_B) \quad (H.176)$$

$$\delta \bar{e}_{L_{iB}}(t_B) = F_{F_i}^T(t_{B-1}) \delta e_{iB}(t_B) \quad (H.177)$$

$$\delta F_{K_i}(t_B) = K_{i(B)} [\delta \bar{e}_{L_{iB}}(t_B) - \delta \bar{e}_{f_{iB}}(t_B) - \delta \bar{e}_{o_{iB}}(t_B)] \quad (H.178)$$

$$\bar{F}_{K_i}(t_B) = \bar{F}_{K_i}(t_{B-1}) + \delta \bar{F}_{K_i}(t_B) \quad (H.179)$$

where $\bar{F}_{K_i}(t_{B-1}) = 0$ for $B = 1$

$\delta e_{f_{i_B}}(t_B) = 0$ for the first iteration

In Step 5 the updated coordinates at the element level are calculated from:

$$U_{i_B} = U_{i_{B-1}} + \delta e_{i_B}(t_B) \quad (H.180)$$

= the matrix of joint coordinates for the defining joints of the i th element.

For $B = 1$, $U_{i_{B-1}} = U_{i_0}$, which is a partition of the initial coordinate matrix U_0 .

Step 6 calculations are summarized for each type of element - bar, membrane and cell.

Bar Element

Input matrices are $\bar{F}_{K_i}(t_B)$ and U_{i_B} , where

$$\bar{F}_{K_i}(t_B) = \begin{Bmatrix} \bar{F}_{1i}(t_B) \\ \bar{F}_{2i}(t_B) \end{Bmatrix} \quad U_{i_B} = \begin{Bmatrix} \bar{p} \\ \bar{q} \end{Bmatrix}_{i_B} \quad (H.181)$$

Calculate unit vector \bar{a}_{i_B} and length z_{i_B} from U_{i_B}

$$\overline{pq}_{i_B} = \bar{a}_{i_B} - \bar{p}_{i_B} \quad (H.182)$$

$$z_{i_B} = |\overline{pq}_{i_B}| \quad (H.183)$$

$$\bar{a}_{i_B} = \frac{\overline{pq}_{i_B}}{z_{i_B}} \quad (H.184)$$

Let $\bar{a}_{i\beta}$, $\bar{u}_{1i\beta}$, $\bar{u}_{2i\beta}$ be orthogonal unit vectors where $\bar{a}_{i\beta}$ is colinear with the bar \bar{o} , \bar{a} (as previously defined) and u_{1ip} is in the global X, Y plane.

$$\bar{a}_{i\beta} = \begin{Bmatrix} a_x \\ a_y \\ a_z \end{Bmatrix}_{i\beta}, \quad \bar{u}_{1i\beta} = \begin{Bmatrix} u_{1x} \\ u_{1y} \\ u_{1z} \end{Bmatrix}_{i\beta}, \quad \bar{u}_{2i\beta} = \begin{Bmatrix} u_{2x} \\ u_{2y} \\ u_{2z} \end{Bmatrix}_{i\beta} \quad (\text{H.185})$$

then

$$\bar{u}_{1i\beta} = \frac{1}{\sqrt{a_x^2 + a_y^2}} \begin{Bmatrix} -a_y \\ a_x \\ 0 \end{Bmatrix}_{i\beta} \quad (\text{H.186})$$

$$\bar{u}_{2i\beta} = \frac{1}{\sqrt{a_x^2 + a_y^2}} \begin{Bmatrix} -a_x a_z \\ -a_y a_z \\ a_x^2 + a_y^2 \end{Bmatrix}_{i\beta} \quad (\text{H.187})$$

Except, if $a_x = a_y = 0$ and $a_z = \pm 1.0$, then,

$$\bar{u}_{1i\beta} = \begin{Bmatrix} 1.0 \\ 0 \\ 0 \end{Bmatrix}_{i\beta} \quad (\text{H.188})$$

$$\bar{u}_{2i\beta} = \begin{Bmatrix} 0 \\ a_z \\ 0 \end{Bmatrix}_{i\beta} \quad (\text{H.189})$$

Appropriate matrices for the bar element are:

$$\overline{\overline{F}}_{i_3} = \begin{bmatrix} & & & \\ \overline{u}_1 & \overline{u}_2 & & \\ & & & \\ & & \overline{u}_1 & \overline{u}_2 \\ 0 & 0 & 0 & 0 \end{bmatrix} \quad (7 \times 4) \quad (H.190)$$

(transformation)

$$G_{fi3} = \{l_{i_3}\} \quad (\text{geometry}) \quad (H.191)$$

$$\begin{aligned} \overline{F}_{f_i}(t_B) &= \{\overline{F}_{s_i}(t_B)\} \quad (\text{element force}) \quad (H.192) \\ &= \left[\frac{1}{2} \mid \frac{1}{2} \right] \overline{F}_{K_i}(t_B) \end{aligned}$$

Membrane Element

The input matrices are $\overline{F}_{K_i}(t_B)$ and U_{i_3} , where

$$\overline{F}_{K_i}(t_B) = \begin{bmatrix} \overline{F}_{1_i}(t_B) \\ \overline{F}_{2_i}(t_B) \\ \vdots \\ \overline{F}_{9_i}(t_B) \end{bmatrix} \quad U_{i_3} = \begin{bmatrix} \overline{p} \\ \overline{q} \\ \overline{r} \\ \overline{s} \end{bmatrix} \quad (H.193)$$

Calculate vectors \overline{pq}_{i_3} , \overline{rq}_{i_3} , \overline{rs}_{i_3} , \overline{ps}_{i_3} , \overline{b}_{i_3} , \overline{c}_{i_3} and \overline{d}_{i_3} from U_{i_3} .

$$\bar{p}\bar{q}_{i\beta} = \bar{q}_{i\beta} - \bar{p}_{i\beta} \quad (\text{H.194})$$

$$\bar{r}\bar{q}_{i\beta} = \bar{q}_{i\beta} - \bar{r}_{i\beta} \quad (\text{H.195})$$

$$\bar{r}\bar{s}_{i\beta} = \bar{s}_{i\beta} - \bar{r}_{i\beta} \quad (\text{H.196})$$

$$\bar{p}\bar{s}_{i\beta} = \bar{s}_{i\beta} - \bar{p}_{i\beta} \quad (\text{H.197})$$

$$\bar{b}_{i\beta} = \bar{r}\bar{q}_{i\beta} / |\bar{r}\bar{q}_{i\beta}| \quad (\text{H.198})$$

$$\bar{c}_{i\beta} = \bar{r}\bar{s}_{i\beta} / |\bar{r}\bar{s}_{i\beta}| \quad (\text{H.199})$$

$$\bar{d}_{i\beta} = \bar{p}\bar{s}_{i\beta} / |\bar{p}\bar{s}_{i\beta}| \quad (\text{H.200})$$

Choose a' , b' , and $2\xi'$ for a parallelogram that approximates the quadrilateral membrane.

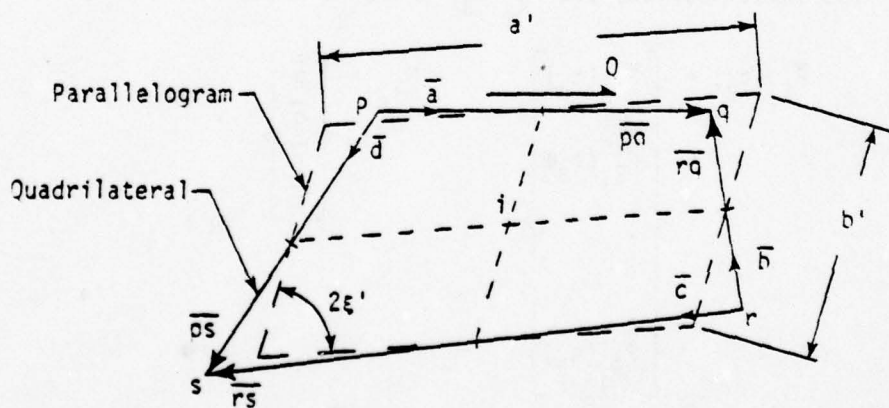


Figure H.2. Replacement parallelogram.

Let a' and b' be the distances between midpoints of opposite sides of the quadrilateral, as shown in Figure H.2. Then

$$\bar{a}'_{i\beta} = -\frac{1}{2} \bar{r}\bar{q}_{i\beta} + \bar{p}\bar{q}_{i\beta} - \frac{1}{2} \bar{p}\bar{s}_{i\beta} \quad (\text{H.201})$$

$$\bar{b}'_{i\beta} = \frac{1}{2} \bar{r}\bar{s}_{i\beta} - \bar{p}\bar{s}_{i\beta} + \frac{1}{2} \bar{p}\bar{q}_{i\beta} \quad (\text{H.202})$$

$$a'_{i\beta} = |\bar{a}'_{i\beta}| \quad b' = |\bar{b}'_{i\beta}| \quad (\text{H.203})$$

$$\xi'_{i\beta} = \frac{1}{2} \left(\cos^{-1} \frac{\bar{a}' \cdot \bar{b}'}{a' b'} \right)_{i\beta} \quad (\text{H.204})$$

Element shear flow Q and element forces \bar{F}_{S1} through \bar{F}_{S4} which produce fictitious forces are shown in Figure H.3.

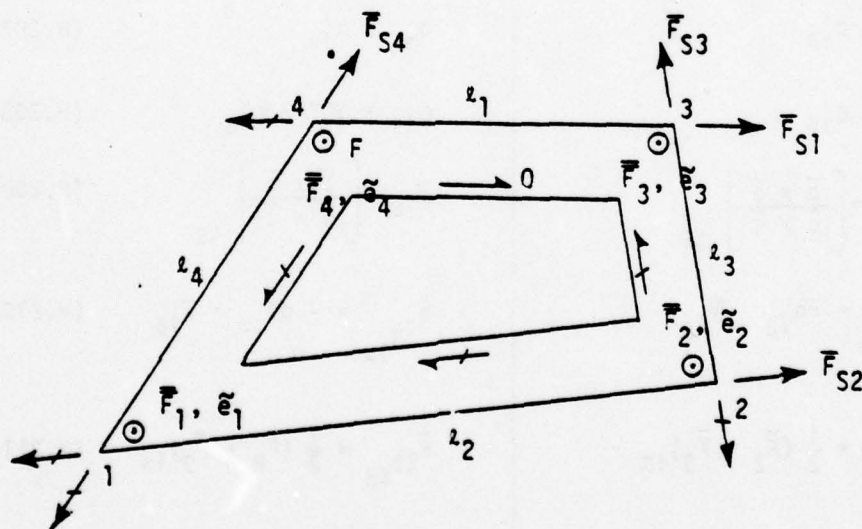


Figure H.3. Fictitious Forces, Membrane Element.

The fictitious forces $\bar{F}_1, \bar{F}_2, \bar{F}_3, \bar{F}_4$ are calculated normal to a plane through corners 2, 1 and 4. See Figure H.3.

\bar{w} = unit vector normal to plane 2, 1, 4 and directed out of the paper in the above view.

w_x, w_y, w_z = components of the unit vector \bar{w} in the global degrees of freedom.

Assume that the approximate shear flow is

$$Q'_{i\beta} = \frac{F_{1i\beta}}{a'_{i\beta}} \quad (H.205)$$

if $Q'_{i\beta} \geq 0$	set	if $Q'_{i\beta} < 0$	set
$a_{i\beta} = a'_{i\beta}$		$a_{i\beta} = b'_{i\beta}$	(H.206)
$b_{i\beta} = b'_{i\beta}$		$b_{i\beta} = a'_{i\beta}$	(H.207)
$\xi_i = \xi'_{i\beta}$		$\xi_{i\beta} = 90^\circ - \xi'_{i\beta}$	(H.208)
$\bar{w}_{i\beta} = \left[\frac{\bar{c} \times \bar{d}}{ \bar{c} \times \bar{d} } \right]_{i\beta}$		$\bar{w}_{i\beta} = \left[\frac{\bar{b} \times \bar{c}}{ \bar{b} \times \bar{c} } \right]_{i\beta}$	(H.209)
$\bar{e}_{03i\beta} = \bar{r}q_{i\beta} \cdot \bar{w}_{i\beta}$		$\bar{e}_{03i\beta} = -\bar{p}q_{i\beta} \cdot \bar{w}_{i\beta}$	(H.210)
$\bar{F}_{S1i\beta} = \frac{1}{2} (\bar{F}_2 + \bar{F}_3)_{i\beta}$		$\bar{F}_{S1i\beta} = \frac{1}{2} (\bar{F}_8 + \bar{F}_9)_{i\beta}$	(H.211)
$\bar{F}_{S2i\beta} = \frac{1}{2} (\bar{F}_4 + \bar{F}_5)_{i\beta}$		$\bar{F}_{S2i\beta} = \frac{1}{2} (\bar{F}_6 + \bar{F}_7)_{i\beta}$	(H.212)

$$\bar{F}_{S3_{iB}} = \frac{1}{2} (\bar{F}_6 + \bar{F}_7)_{iB}$$

$$\bar{F}_{S4_{iB}} = \frac{1}{2} (\bar{F}_8 + \bar{F}_9)_{iB}$$

$$Q_{iB} = Q'_{iB}$$

$$z_{1iB} = |\bar{p}\bar{q}|_{iB}$$

$$z_{2iB} = |\bar{r}\bar{s}|_{iB}$$

$$z_{3iB} = |\bar{r}\bar{q}|_{iB}$$

$$z_{4iB} = |\bar{p}\bar{s}|_{iB}$$

$$\bar{F}_{S3_{iB}} = \frac{1}{2} (\bar{F}_2 + \bar{F}_3)_{iB} \quad (H.213)$$

$$\bar{F}_{S4_{iB}} = \frac{1}{2} (\bar{F}_4 + \bar{F}_5)_{iB} \quad (H.214)$$

$$Q_{iB} = -Q'_{iB} \quad (H.215)$$

$$z_{1iB} = |\bar{p}\bar{s}|_{iB} \quad (H.216)$$

$$z_{2iB} = |\bar{r}\bar{q}|_{iB} \quad (H.217)$$

$$z_{3iB} = |\bar{p}\bar{q}|_{iB} \quad (H.218)$$

$$z_{4iB} = |\bar{r}\bar{s}|_{iB} \quad (H.219)$$

The transformation and reordering matrices for the membrane element are

$$\begin{array}{l} Q'_{iB} \geq 0 \\ F_{iB} = \begin{bmatrix} 1 & 2 & 3 & 4 \\ 1 & & & w_x \\ 2 & & & w_y \\ 3 & & & w_z \\ 4 & w_x & & \\ 5 & & w_y & \\ 6 & & & w_z \\ 7 & w_x & & \\ 8 & & w_y & \\ 9 & & & w_z \\ 10 & w_x & & \\ 11 & & w_y & \\ 12 & & & w_z \\ 13 & & & 0 \\ 14 & & & \\ 15 & & & \\ 16 & & & \end{bmatrix} \quad iB \end{array} \quad \begin{array}{l} Q'_{iB} < 0 \\ F_{iB} = \begin{bmatrix} w_x \\ w_y \\ w_z \\ w_x \\ w_y \\ w_z \\ w_x \\ w_y \\ w_z \\ w_x \\ w_y \\ w_z \\ 0 \\ 0 \end{bmatrix} \quad iB \end{array} \quad (H.220)$$

$$r_{r'is} = \begin{bmatrix} 1 & & & & & & & & \\ & 1 & & & & & & & \\ & & 1 & & & & & & \\ & & & 1 & & & & & \\ & & & & 1 & & & & \\ & & & & & 1 & & & \\ & & & & & & 1 & & \\ & & & & & & & 1 & \\ & & & & & & & & 1 \end{bmatrix}$$

$$r_{r'is} = \begin{matrix} & \begin{matrix} 1 & 2 & 3 & 4 & 5 & 6 & 7 & 8 & 9 \end{matrix} \\ \begin{matrix} 1 \\ 2 \\ 3 \\ 4 \\ 5 \\ 6 \\ 7 \\ 8 \\ 9 \end{matrix} & \begin{bmatrix} 1 & & & & & & & & \\ & & & & & 1 & & & \\ & & & & & & 1 & & \\ & & & & & & & 1 & \\ & & & & & & & & 1 \\ & & & & & & & & \\ & & & & 1 & & & & \\ & & & & & 1 & & & \\ & 1 & & & & & & & \\ & & 1 & & & & & & \end{bmatrix} \end{matrix} \quad (H.221)$$

Geometry and element force matrices for the membrane element are

$$D_{ois} = \left\{ \bar{\epsilon}_{o3} \right\}_{is} \quad (H.222)$$

(1 x 1)

$$G_{fis} = \left\{ \begin{matrix} a' \\ a \\ b \\ \xi \\ z_1 \\ z_2 \\ z_3 \\ z_4 \end{matrix} \right\}_{is} \quad (H.223)$$

(8 x 1)

$$\bar{F}_{fi}(t_s) = \begin{bmatrix} Q_i(t_s) \\ \bar{F}_{S1_i}(t_s) \end{bmatrix} \quad (H.224)$$

(5 x 1)

$$\begin{Bmatrix} \bar{F}_{S2_i}(t_B) \\ \bar{F}_{S3_i}(t_B) \\ \bar{F}_{S4_i}(t_B) \end{Bmatrix}$$

Cell Element

The input matrices are $\bar{F}_{K_i}(t_B)$ and U_{iB} , where

$$\bar{F}_{K_i}(t_B) = \begin{Bmatrix} \bar{F}_{1_i}(t_B) \\ \bar{F}_{2_i}(t_B) \\ \cdot \\ \cdot \\ \cdot \\ \bar{F}_{30_i}(t_B) \end{Bmatrix} \quad U_{iB} = \begin{Bmatrix} \bar{p}_0 \\ \bar{q}_0 \\ \bar{r}_0 \\ \bar{s}_0 \\ \bar{p}_1 \\ \bar{q}_1 \\ \bar{r}_1 \\ \bar{s}_1 \end{Bmatrix}_{iB} \quad (H.225)$$

Using the vector equations for the cell element from ELEMENT GEOMETRY FOR INITIAL GENERATOR, calculate the following vectors:

$$\bar{p}q_{6_{iB}}, \bar{r}q_{6_{iB}}, \bar{r}s_{6_{iB}}, \bar{p}s_{6_{iB}}, \bar{b}_{6_{iB}}, \bar{c}_{6_{iB}}, \bar{d}_{6_{iB}}$$

$$\bar{p}q_{7_{iB}}, \bar{r}q_{7_{iB}}, \bar{r}s_{7_{iB}}, \bar{p}s_{7_{iB}}, \bar{b}_{7_{iB}}, \bar{c}_{7_{iB}}, \bar{d}_{7_{iB}}$$

The iB subscripts will be temporarily omitted.

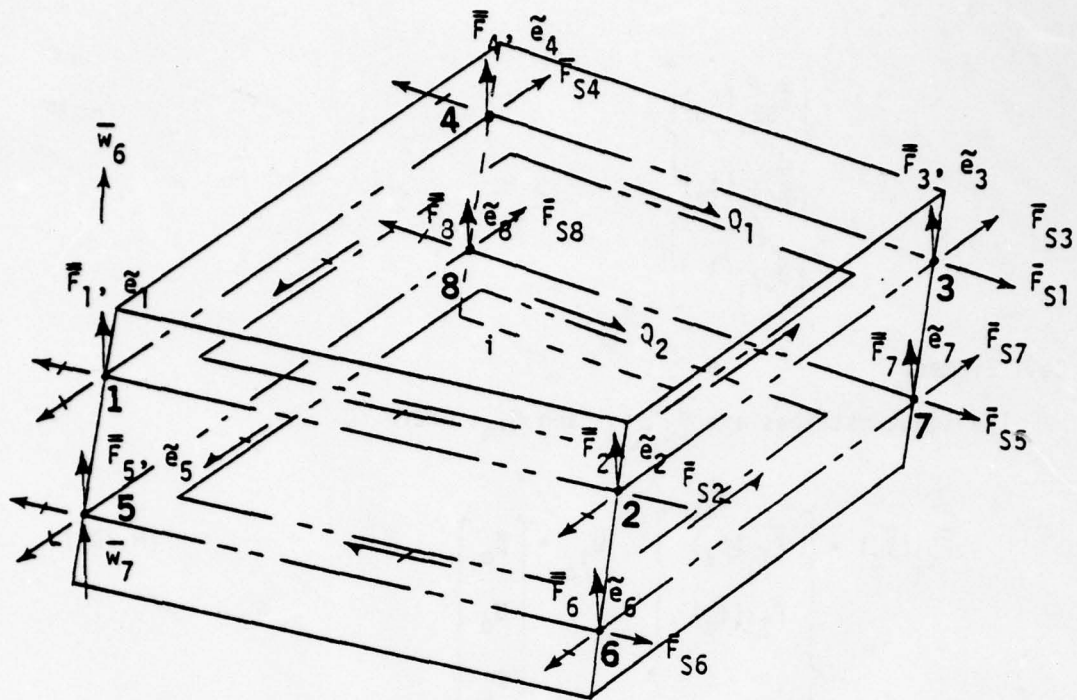


Figure H.4. Fictitious Forces, Cell Element.

The fictitious forces $\bar{F}_1, \bar{F}_2, \bar{F}_3, \bar{F}_4$ are calculated normal to a plane through points 2, 1, 4. Forces $\bar{F}_5, \bar{F}_6, \bar{F}_7, \bar{F}_8$ are normal to a plane through 6, 5, 8.

\bar{w}_6, \bar{w}_7 = unit vectors normal to planes 2, 1, 4 and 6, 5, 8 and directed as shown.

$w_{x6}, w_{y6}, w_{z6}, w_{x7}, w_{y7}, w_{z7}$ = components in the global degrees of freedom of unit vectors \bar{w}_6, \bar{w}_7

$$\bar{w}_6 = \begin{bmatrix} w_{x6} \\ w_{y6} \\ w_{z6} \end{bmatrix} \quad \bar{w}_7 = \begin{bmatrix} w_{x7} \\ w_{y7} \\ w_{z7} \end{bmatrix} \quad (\text{H.225.1})$$

The quantities $\bar{a}'_6, b'_6, \xi'_6, a'_7, b'_7, \xi'_7$ are dimensions of parallelograms which approximate panels 1, 2, 3, 4 and 5, 6, 7, 8 in Figure H.4. Calculate these values as follows.

$$\bar{a}'_6 = \frac{1}{2} \bar{r}\bar{q}_6 - \bar{p}\bar{q}_6 + \frac{1}{2} \bar{p}\bar{s}_6 \quad (\text{H.226})$$

$$\bar{b}'_6 = \frac{1}{2} \bar{r}\bar{s}_6 - \bar{p}\bar{s}_6 + \frac{1}{2} \bar{p}\bar{q}_6 \quad (\text{H.227})$$

$$a'_6 = |\bar{a}'_6|, \quad b'_6 = |\bar{b}'_6| \quad (\text{H.228})$$

$$\xi'_6 = \frac{1}{2} \left(\cos^{-1} \frac{\bar{a}'_6 \cdot \bar{b}'_6}{a'_6 b'_6} \right) \quad (\text{H.229})$$

$$\bar{a}'_7 = \frac{1}{2} \bar{r}\bar{q}_7 - \bar{p}\bar{q}_7 + \frac{1}{2} \bar{p}\bar{s}_7 \quad (\text{H.230})$$

$$\bar{b}'_7 = \frac{1}{2} \bar{r}\bar{s}_7 - \bar{p}\bar{s}_7 + \frac{1}{2} \bar{p}\bar{q}_7 \quad (\text{H.231})$$

$$a'_7 = |\bar{a}'_7|, \quad b'_7 = |\bar{b}'_7| \quad (\text{H.232})$$

$$\xi'_7 = \frac{1}{2} \left(\cos^{-1} \frac{\bar{a}'_7 \cdot \bar{b}'_7}{a'_7 b'_7} \right) \quad (\text{H.233})$$

Calculate approximate shear flow Q'_6

$$Q'_6 = \frac{\bar{F}_1}{a'_6} \quad (\text{H.234})$$

If $Q'_6 \geq 0$

$$a_6 = a'_6$$

$$b_6 = b'_6$$

$$\xi_6 = \xi'_6$$

If $Q'_6 < 0$

$$a_6 = b'_6 \quad (\text{H.235})$$

$$b_6 = a'_6 \quad (\text{H.236})$$

$$\xi_6 = 90^\circ - \xi'_6 \quad (\text{H.237})$$

$$\bar{w}_6 = \frac{\bar{c}_6 \times \bar{d}_6}{|\bar{c}_6 \times \bar{d}_6|}$$

$$\bar{e}_{o_{3,6}} = \bar{r}\bar{q}_6 \cdot \bar{w}_6$$

$$z_1 = |\bar{p}\bar{q}_6|$$

$$z_2 = |\bar{r}\bar{s}_6|$$

$$z_3 = |\bar{r}\bar{q}_6|$$

$$z_4 = |\bar{p}\bar{s}_6|$$

$$Q_6 = Q'_6$$

$$\bar{F}_{S1} = \frac{1}{2} (\bar{F}_2 + \bar{F}_3)$$

$$\bar{F}_{S2} = \frac{1}{2} (\bar{F}_4 + \bar{F}_5)$$

$$\bar{F}_{S3} = \frac{1}{2} (\bar{F}_6 + \bar{F}_7)$$

$$\bar{F}_{S4} = \frac{1}{2} (\bar{F}_8 + \bar{F}_9)$$

$$\bar{w}_6 = \frac{\bar{b}_6 \times \bar{c}_6}{|\bar{b}_6 \times \bar{c}_6|} \quad (H.238)$$

$$\bar{e}_{o_{3,6}} = -\bar{p}\bar{q}_6 \cdot \bar{w}_6 \quad (H.239)$$

$$z_1 = |\bar{p}\bar{s}_6| \quad (H.240)$$

$$z_2 = |\bar{r}\bar{q}_6| \quad (H.241)$$

$$z_3 = |\bar{p}\bar{q}_6| \quad (H.242)$$

$$z_4 = |\bar{r}\bar{s}_6| \quad (H.243)$$

$$Q_6 = -Q'_6 \quad (H.244)$$

$$\bar{F}_{S1} = \frac{1}{2} (\bar{F}_8 + \bar{F}_9) \quad (H.245)$$

$$\bar{F}_{S2} = \frac{1}{2} (\bar{F}_6 + \bar{F}_7) \quad (H.246)$$

$$\bar{F}_{S3} = \frac{1}{2} (\bar{F}_2 + \bar{F}_3) \quad (H.247)$$

$$\bar{F}_{S4} = \frac{1}{2} (\bar{F}_4 + \bar{F}_5) \quad (H.248)$$

Calculate approximate shear flow Q'_7

$$Q'_7 = \frac{\bar{F}_{10}}{a'_7} \quad (H.249)$$

If $Q'_7 \geq 0$

$$a_7 = a'_7$$

$$b_7 = b'_7$$

$$\xi_7 = \xi'_7$$

$$\bar{w}_7 = \frac{\bar{c}_7 \times \bar{d}_7}{|\bar{c}_7 \times \bar{d}_7|}$$

If $Q'_7 < 0$

$$a_7 = b'_7 \quad (H.250)$$

$$b_7 = a'_7 \quad (H.251)$$

$$\xi_7 = 90^\circ - \xi'_7 \quad (H.252)$$

$$\bar{w}_7 = \frac{\bar{b}_7 \times \bar{c}_7}{|\bar{b}_7 \times \bar{c}_7|} \quad (H.253)$$

$$\bar{e}_{03,7} = \bar{r}q_7 \cdot \bar{w}_7$$

$$l_5 = |\bar{p}q_7|$$

$$l_6 = |\bar{r}s_7|$$

$$l_7 = |\bar{r}q_7|$$

$$l_8 = |\bar{p}s_7|$$

$$Q_7 = Q'_7$$

$$\bar{F}_{S5} = \frac{1}{2} (\bar{F}_{11} + \bar{F}_{12})$$

$$\bar{F}_{S6} = \frac{1}{2} (\bar{F}_{13} + \bar{F}_{14})$$

$$\bar{F}_{S7} = \frac{1}{2} (\bar{F}_{15} + \bar{F}_{16})$$

$$\bar{F}_{S8} = \frac{1}{2} (\bar{F}_{17} + \bar{F}_{18})$$

$$\bar{e}_{03,7} = -\bar{p}q_7 \cdot \bar{w}_7 \quad (H.254)$$

$$l_5 = |\bar{p}s_7| \quad (H.255)$$

$$l_6 = |\bar{r}q_7| \quad (H.256)$$

$$l_7 = |\bar{p}q_7| \quad (H.257)$$

$$l_8 = |\bar{r}s_7| \quad (H.258)$$

$$Q_7 = -Q'_7 \quad (H.259)$$

$$\bar{F}_{S5} = \frac{1}{2} (\bar{F}_{17} + \bar{F}_{18}) \quad (H.260)$$

$$\bar{F}_{S6} = \frac{1}{2} (\bar{F}_{15} + \bar{F}_{16}) \quad (H.261)$$

$$\bar{F}_{S7} = \frac{1}{2} (\bar{F}_{11} + \bar{F}_{12}) \quad (H.262)$$

$$\bar{F}_{S8} = \frac{1}{2} (\bar{F}_{13} + \bar{F}_{14}) \quad (H.263)$$

If $Q'_6 \geq 0$

$$\begin{aligned} \bar{F}_{6,1} &= \begin{bmatrix} & & & \bar{w}_6 \\ & & & \\ & & \bar{w}_6 & \\ & \bar{w}_6 & & \\ \bar{w}_6 & & & \end{bmatrix}, & r_{r',1} &= \left\{ \begin{bmatrix} r_1 \\ 0 \end{bmatrix} \right\} \begin{matrix} 9 \\ 21 \end{matrix} \end{aligned} \quad (H.264)$$

(12 x 4) (30 x 9)

If $Q'_6 < 0$

$$\begin{aligned} \bar{F}_{6,2} &= \begin{bmatrix} & & \bar{w}_6 & \\ & \bar{w}_6 & & \\ \bar{w}_6 & & & \\ & & & \bar{w}_6 \end{bmatrix}, & r_{r',2} &= \left\{ \begin{bmatrix} r_2 \\ 0 \end{bmatrix} \right\} \begin{matrix} 9 \\ 21 \end{matrix} \end{aligned} \quad (H.265)$$

(12 x 4) (30 x 9)

If $Q_7^i \geq 0$

$$F_{7,1}^{\bar{w}} = \begin{bmatrix} & & & \bar{w}_7 \\ & & \bar{w}_7 & \\ & \bar{w}_7 & & \\ \bar{w}_7 & & & \end{bmatrix}, \quad r_{r_7,1}^i = \begin{bmatrix} 0 \\ \bar{r}_1 \\ 0 \end{bmatrix} \begin{matrix} 9 \\ 9 \\ 12 \end{matrix} \quad (\text{H.266})$$

(12 x 4) (30 x 9)

If $Q_7^i < 0$

$$F_{7,2}^{\bar{w}} = \begin{bmatrix} & & \bar{w}_7 & \\ & \bar{w}_7 & & \\ \bar{w}_7 & & & \\ & & & \bar{w}_7 \end{bmatrix}, \quad r_{r_7,2}^i = \begin{bmatrix} 0 \\ \bar{r}_2 \\ 0 \end{bmatrix} \begin{matrix} 9 \\ 9 \\ 12 \end{matrix} \quad (\text{H.267})$$

(12 x 4) (30 x 9)

where

$$r_1 = \begin{bmatrix} 1 & & & & & & & & \\ & 1 & & & & & & & \\ & & 1 & & & & & & \\ & & & 1 & & & & & \\ & & & & 1 & & & & \\ & & & & & 1 & & & \\ & & & & & & 1 & & \\ & & & & & & & 1 & \\ & & & & & & & & 1 \end{bmatrix} \quad (\text{H.268})$$

(9 x 9)

$$r_2 = \begin{bmatrix} 1 & & & & & & & & \\ & & & & 1 & & & & \\ & & & & & & 1 & & \\ & & & & & & & & 1 \\ & & & & & & & & & 1 \\ & & & 1 & & & & & & \\ & & & & 1 & & & & & \\ & 1 & & & & & & & & \\ & & 1 & & & & & & & \end{bmatrix} \quad (H.269)$$

(9 x 9)

Constants f and g are defined as

$$f = \frac{3 + \sqrt{3}}{6} \quad (H.270)$$

$$g = \frac{3 - \sqrt{3}}{6}$$

The transformation and reordering matrices for the cell element with subscripts i and β restored are:

If $Q'_{6i\beta} \geq 0$ and $Q'_{7i\beta} \geq 0$

$$F_{F_{i\beta}} = \begin{bmatrix} f F_{F_{6,1}} & g F_{F_{7,1}} \\ g F_{F_{6,1}} & f F_{F_{7,1}} \\ 0 & 0 \end{bmatrix}_{i\beta} \quad (36 \times 8)$$

$$r_{r'_{i\beta}} = \begin{bmatrix} r_{r'_{6,1}} & r_{r'_{7,1}} \end{bmatrix}_{i\beta} \quad (30 \times 18) \quad (H.271)$$

If $Q'_{6i\beta} \geq 0$ and $Q'_{7i\beta} < 0$

$$F_{F_{i\beta}} = \begin{bmatrix} f F_{F_{6,1}} & g F_{F_{7,2}} \\ g F_{F_{6,1}} & f F_{F_{7,2}} \\ 0 & 0 \end{bmatrix}_{i\beta} \quad (36 \times 8)$$

$$r_{r'_{i\beta}} = \begin{bmatrix} r_{r'_{6,1}} & r_{r'_{7,2}} \end{bmatrix}_{i\beta} \quad (30 \times 18) \quad (H.272)$$

If $Q'_{6is} < 0$ and $Q'_{7is} \geq 0$

$$F_{\bar{F}}'_{is} = \begin{bmatrix} f F_{\bar{F}}'_{6,2} & g F_{\bar{F}}'_{7,1} \\ g F_{\bar{F}}'_{6,2} & f F_{\bar{F}}'_{7,1} \\ 0 & 0 \end{bmatrix}_{is} \quad r_{r'}'_{is} = \begin{bmatrix} r_{r'}'_{6,2} & r_{r'}'_{7,1} \end{bmatrix}_{is} \quad (H.273)$$

(36 x 8) (30 x 18)

If $Q'_{6is} < 0$ and $Q'_{7is} < 0$

$$F_{\bar{F}}'_{is} = \begin{bmatrix} f F_{\bar{F}}'_{6,2} & g F_{\bar{F}}'_{7,2} \\ g F_{\bar{F}}'_{6,2} & f F_{\bar{F}}'_{7,2} \\ 0 & 0 \end{bmatrix}_{is} \quad r_{r'}'_{is} = \begin{bmatrix} r_{r'}'_{6,2} & r_{r'}'_{7,2} \end{bmatrix}_{is} \quad (H.274)$$

(36 x 8) (30 x 18)

Geometry and element force matrices for the cell element are:

$$D_{o'}'_{is} = \begin{bmatrix} \bar{e}_{o'}'_{3,6} \\ \bar{e}_{o'}'_{3,7} \end{bmatrix}_{is} \quad (H.275)$$

(2 x 1)

$$G_{f'}'_{is} = \begin{bmatrix} a_6' \\ a_6 \\ b_6 \\ \epsilon_6 \\ z_1 \\ z_2 \\ z_3 \\ z_4 \end{bmatrix} \quad (H.276)$$

(16 x 1)

$$\left\{ \begin{array}{c} a_7' \\ a_7 \\ b_7 \\ \varepsilon_7 \\ z_5 \\ z_6 \\ z_7 \\ z_8 \end{array} \right\}_{i8}$$

$$\begin{array}{l} \bar{F}_{fi8} = \\ (10 \times 1) \end{array} \left[\begin{array}{c} Q_{6i}(t_B) \\ \bar{F}_{S1_i}(t_B) \\ \bar{F}_{S2_i}(t_B) \\ \bar{F}_{S3_i}(t_B) \\ \bar{F}_{S4_i}(t_B) \\ Q_{7i}(t_B) \\ \bar{F}_{S5_i}(t_B) \\ \bar{F}_{S6_i}(t_B) \\ \bar{F}_{S7_i}(t_B) \\ \bar{F}_{S8_i}(t_B) \end{array} \right] \quad (H.277)$$

In Step 6 of Table I the input matrices are $\bar{F}_{Ki}(t_B)$, U_{iB-1} , and U_{iB} , and the output matrices are:

$$\bar{F}_{fiB-1}, \bar{F}_{fi8} \quad (\text{force transformation})$$

$*D_{0_{i_{\beta-1}}}$ (warp offset at $t_{\beta-1}$)

$G_{f_{i_{\beta-1}}}, G_{f_{i_{\beta}}}$ (geometry)

$*r_{r'_{i_{\beta}}}$ (reordering transform)

$\bar{F}_{f_{i_{\beta}}}$ (element forces)

*Do not exist if the i th element is a bar element.

In Step 7 of Table I the average quantities are calculated from

$$\bar{F}_{\bar{f}_{i(\beta)}} = \frac{1}{2} (\bar{F}_{\bar{f}_{i_{\beta-1}}} + \bar{F}_{\bar{f}_{i_{\beta}}}) \quad (H.278)$$

$$G_{f_{i(\beta)}} = \frac{1}{2} (G_{f_{i_{\beta-1}}} + G_{f_{i_{\beta}}}) \quad (H.279)$$

Step 8 of Table I can now be performed. The displacements in the fictitious force degrees of freedom are found from:

$$\delta \tilde{e}_{i_{\beta}}(t_{\beta}) = \bar{F}_{\bar{f}_{i(\beta)}}^T \delta e_{i_{\beta}}(t_{\beta}) \quad (H.280)$$

If the i th element is a bar element, the input matrices are $\delta \tilde{e}_{i_{\beta}}(t_{\beta})$, $G_{f_{i(\beta)}}$, $F_{f_{i_{\beta}}}$.

$$\delta \tilde{e}_{i_{\beta}}(t_{\beta}) = \begin{Bmatrix} \delta \tilde{e}_{1_{i_{\beta}}}(t_{\beta}) \\ \delta \tilde{e}_{2_{i_{\beta}}}(t_{\beta}) \end{Bmatrix} \quad (H.281)$$

$$\begin{Bmatrix} \delta \tilde{e}_{3i_B}(t_B) \\ \delta \tilde{e}_{4i_B}(t_B) \end{Bmatrix}$$

$$G_{fi(\bar{B})} = \left\{ z_{i(\bar{B})} \right\} \quad (H.282)$$

$$\bar{F}_{fi_B} = \left\{ \bar{F}_{Si}(t_B) \right\} \quad (H.283)$$

Calculate:

$$\theta_{1i_B}(t_B) = \frac{1}{z_{i(\bar{B})}} \left[\delta \tilde{e}_{3i_B}(t_B) - \delta \tilde{e}_{1i_B}(t_B) \right] \quad (H.284)$$

$$\theta_{2i_B}(t_B) = \frac{1}{z_{i(\bar{B})}} \left[\delta \tilde{e}_{4i_B}(t_B) - \delta \tilde{e}_{2i_B}(t_B) \right] \quad (H.285)$$

Let $n_{ki_B} = \begin{Bmatrix} n_{1,k} \\ n_{2,k} \\ -n_{1,k} \\ -n_{2,k} \end{Bmatrix}_{i_B}$ where $k = 1, 2, 3$ (H.286)

$$\theta_{i_B} = \begin{Bmatrix} \theta_{1i_B}(t_B) \\ \theta_{2i_B}(t_B) \\ -\theta_{1i_B}(t_B) \\ -\theta_{2i_B}(t_B) \end{Bmatrix} \quad (H.287)$$

Then fictitious force matrices for the bar are

$$n_{1i_3} = -\theta_{i_3} \bar{F}_{fi_3} \quad (H.288)$$

$$n_{2i_3} = 0 \quad (H.289)$$

$$n_{3i_3} = \frac{1}{6} \theta_{i_3}^3 \bar{F}_{fi_3} \quad (H.290)$$

(where each element of θ_{i_3} is cubed)

Fictitious deformation matrices are

$$r_{1i_3} = 0 \quad (H.291)$$

$$r_{2i_3} = -\frac{1}{4} z_{i_3} \left[\theta_{1i_3}^2(t_3) + \theta_{2i_3}^2(t_3) \right] \begin{Bmatrix} 1.0 \\ 1.0 \end{Bmatrix} \quad (H.292)$$

If the i th element is a membrane element, the input matrices are

$$\delta \bar{e}_{i_3}(t_3) = \begin{Bmatrix} \delta \bar{e}_{1i_3}(t_3) \\ \delta \bar{e}_{2i_3}(t_3) \\ \delta \bar{e}_{3i_3}(t_3) \\ \delta \bar{e}_{4i_3}(t_3) \end{Bmatrix} \quad (H.293)$$

$$D_{0i_3-1} = \begin{Bmatrix} \bar{e}_{0i_3-1} \end{Bmatrix} \quad (H.294)$$

$$G_{fi(\bar{3})} = \begin{Bmatrix} a'_{i(\bar{8})} \\ a_{i(\bar{8})} \\ b_{i(\bar{3})} \\ \epsilon_{i(\bar{8})} \\ \lambda_{1i(\bar{8})} \\ \lambda_{2i(\bar{8})} \\ \lambda_{3i(\bar{8})} \\ \lambda_{4i(\bar{8})} \end{Bmatrix} \quad (H.295)$$

$$\bar{F}_{fi_3} = \begin{Bmatrix} Q_i(t_3) \\ \bar{F}_{S1_i}(t_3) \\ \bar{F}_{S2_i}(t_3) \\ \bar{F}_{S3_i}(t_3) \\ \bar{F}_{S4_i}(t_3) \end{Bmatrix} \quad (H.296)$$

In the membrane element, contributions to the fictitious forces and deformations come from both the shear panel and the bar elements. Appendix D equations for the shear panel contributions are not duplicated but are instead referenced by equation numbers listed in Table H.2 in logical sequence.

Evaluation of the equations in the order listed in Table H.2 results in shear panel fictitious forces $n_{1,k\beta}$, $n_{2,k\beta}$, $n_{3,k\beta}$, $n_{4,k\beta}$ (where $k = 1,2,3$) and fictitious deformations $\bar{r}_{k\beta}$ (where $k = 1,2$).

Form the matrices

$$n_{Sk_{i\beta}} = \begin{bmatrix} n_{1,k_{i\beta}} \\ n_{2,k_{i\beta}} \\ n_{3,k_{i\beta}} \\ n_{4,k_{i\beta}} \end{bmatrix}, \quad k = 1,2,3 \quad (\text{H.296.1})$$

$$r_{Sk_{i\beta}} = \begin{bmatrix} \frac{1}{a'_{i(\beta)}} \bar{r}_{k_{i\beta}} \\ 0 \\ 0 \\ 0 \\ 0 \\ 0 \\ 0 \\ 0 \\ 0 \end{bmatrix}, \quad k = 1,2 \quad (\text{H.296.2})$$

TABLE H.2. APPENDIX D EQUATIONS

D.66, D.67, D.69, D.70, D.88, D.89, D.90, D.92,
 D.198, D.199, D.204.3, D.312.3, D.314, D.290 through
 D.294, D.212, D.213, D.214, D.250, D.251, D.272,
 D.258, D.252, D.271, D.253, D.254, D.256, D.257,
 D.217, D.218, D.228, D.233, D.234 through D.237,
 D.259, D.284, D.285, D.321, D.322, D.324 through
 D.333, D.333.1, D.334 through D.338, D.342,
 D.343, D.344, D.347, D.348, D.350, D.352, D.353

By inspection of Figure H.3, define edge rotation angles as follows:

$$\theta_{1_{i\beta}}(t_\beta) = \frac{1}{z_{1_{i(\beta)}}} \left[\delta \bar{e}_{3_{i\beta}}(t_\beta) - \delta \bar{e}_{4_{i\beta}}(t_\beta) \right] \quad (H.297)$$

$$\theta_{2_{i\beta}}(t_\beta) = \frac{1}{z_{2_{i(\beta)}}} \left[\delta \bar{e}_{2_{i\beta}}(t_\beta) - \delta \bar{e}_{1_{i\beta}}(t_\beta) \right] \quad (H.298)$$

$$\theta_{3_{i\beta}}(t_\beta) = \frac{1}{z_{3_{i(\beta)}}} \left[\delta \bar{e}_{3_{i\beta}}(t_\beta) - \delta \bar{e}_{2_{i\beta}}(t_\beta) \right] \quad (H.299)$$

$$\theta_{4_{i\beta}}(t_\beta) = \frac{1}{z_{4_{i(\beta)}}} \left[\delta \bar{e}_{4_{i\beta}}(t_\beta) - \delta \bar{e}_{1_{i\beta}}(t_\beta) \right] \quad (H.300)$$

In-plane rotations are ignored. Therefore, bar contributions to the fictitious forces and deformations are based on out-of-plane rotations only. The bar contributions are

$$\begin{matrix} n_{B1_{iB}} \\ (4 \times 1) \end{matrix} = \begin{bmatrix} -\bar{F}_{S2_i}(t_B) \theta_{2_{iB}}(t_B) - \bar{F}_{S4_i}(t_B) \theta_{4_{iB}}(t_B) \\ \bar{F}_{S2_i}(t_B) \theta_{2_{iB}}(t_B) - \bar{F}_{S3_i}(t_B) \theta_{3_{iB}}(t_B) \\ \bar{F}_{S1_i}(t_B) \theta_{1_{iB}}(t_B) + \bar{F}_{S3_i}(t_B) \theta_{3_{iB}}(t_B) \\ -\bar{F}_{S1_i}(t_B) \theta_{1_{iB}}(t_B) + \bar{F}_{S4_i}(t_B) \theta_{4_{iB}}(t_B) \end{bmatrix} \quad (H.301)$$

$$n_{B2_{iB}} = 0 \quad (H.302)$$

$$\begin{matrix} n_{B3_{iB}} \\ (4 \times 1) \end{matrix} = \frac{1}{6} \begin{bmatrix} \bar{F}_{S2_i}(t_B) \theta_{2_{iB}}^3(t_B) + \bar{F}_{S4_i}(t_B) \theta_{4_{iB}}^3(t_B) \\ -\bar{F}_{S2_i}(t_B) \theta_{2_{iB}}^3(t_B) + \bar{F}_{S3_i}(t_B) \theta_{3_{iB}}^3(t_B) \\ -\bar{F}_{S1_i}(t_B) \theta_{1_{iB}}^3(t_B) - \bar{F}_{S3_i}(t_B) \theta_{3_{iB}}^3(t_B) \\ \bar{F}_{S1_i}(t_B) \theta_{1_{iB}}^3(t_B) - \bar{F}_{S4_i}(t_B) \theta_{4_{iB}}^3(t_B) \end{bmatrix} \quad (H.303)$$

$$r_{B1_{iB}} = 0 \quad (H.304)$$

$$\begin{matrix} r_{B2_{iB}} \\ (9 \times 1) \end{matrix} = -\frac{1}{4} r_{r'_{iB}} \begin{bmatrix} 0 \\ l_{1i(\bar{\theta})} \theta_{1_{iB}}^2(t_B) \\ l_{1i(\bar{\theta})} \theta_{1_{iB}}^2(t_B) \\ l_{2i(\bar{\theta})} \theta_{2_{iB}}^2(t_B) \\ l_{2i(\bar{\theta})} \theta_{2_{iB}}^2(t_B) \end{bmatrix} \quad (H.305)$$

AD-A063 740

DOUGLAS AIRCRAFT CO LONG BEACH CALIF
AIRCRAFT WINDSHIELD BIRD IMPACT MATH MODEL. PART 1. THEORY AND --ETC(U)
DEC 77 P H DENKE

F/G 1/3

F33615-75-C-3105

UNCLASSIFIED

MDC-J7174-PT-1

AFFDL-TR-77-99-PT-1

NL

6 OF 6
ADA
063740

U.S. AIR FORCE



END

DATE
FILMED

3 -79
DDC

$$\left\{ \begin{array}{l} z_{3i}(\bar{g}) \quad \theta_{3i\beta}^2(t_\beta) \\ z_{3i}(\bar{g}) \quad \theta_{3i\beta}^2(t_\beta) \\ z_{4i}(\bar{g}) \quad \theta_{4i\beta}^2(t_\beta) \\ z_{4i}(\bar{g}) \quad \theta_{4i\beta}^2(t_\beta) \end{array} \right\}$$

If the i th element is a cell element, the input matrices are

$$\delta \bar{e}_{i\beta}(t_\beta) = \left\{ \begin{array}{l} \delta \bar{e}_{1i\beta}(t_\beta) \\ \delta \bar{e}_{2i\beta}(t_\beta) \\ \cdot \\ \cdot \\ \delta \bar{e}_{8i\beta}(t_\beta) \end{array} \right\} \quad (\text{H.306})$$

$$D_{0i\beta-1} = \left\{ \begin{array}{l} \bar{e}_{03,6i\beta-1} \\ \bar{e}_{03,7i\beta-1} \end{array} \right\} \quad (\text{H.307})$$

$$G_{fi}(\bar{g}) = \left\{ \begin{array}{l} a'_{6i}(\bar{g}) \\ a_{6i}(\bar{g}) \\ b_{6i}(\bar{g}) \\ \xi_{6i}(\bar{g}) \\ z_{1i}(\bar{g}) \end{array} \right\} \quad (\text{H.308})$$

$$\begin{bmatrix} l_{2i}(\bar{\theta}) \\ l_{3i}(\bar{\theta}) \\ l_{4i}(\bar{\theta}) \\ a'_{7i}(\bar{\theta}) \\ a_{7i}(\bar{\theta}) \\ b_{7i}(\bar{\theta}) \\ \epsilon_{7i}(\bar{\theta}) \\ l_{5i}(\bar{\theta}) \\ l_{6i}(\bar{\theta}) \\ l_{7i}(\bar{\theta}) \\ l_{8i}(\bar{\theta}) \end{bmatrix}$$

$$\bar{F}_{fiB} =$$

$$\left\{ \begin{bmatrix} Q_{6i}(t_B) \\ \bar{F}_{S1i}(t_B) \\ \bar{F}_{S2i}(t_B) \\ \bar{F}_{S3i}(t_B) \\ \bar{F}_{S4i}(t_B) \\ Q_{7i}(t_B) \\ \bar{F}_{S5i}(t_B) \\ \bar{F}_{S6i}(t_B) \\ \bar{F}_{S7i}(t_B) \\ \bar{F}_{S8i}(t_B) \end{bmatrix} \right\}$$

(H.309)

Evaluate the equations in Table H.2 for shear panel contributions to fictitious forces and deformations two times, see Tables H.3 and H.4.

TABLE H.3. FIRST EVALUATION

INPUT	FOR k VALUES OF:	CALCULATE	RENAME
$a = a_6 i(\bar{\beta})$	1, 2, 3	$n_{1,k} i\beta$	
$b = b_6 i(\bar{\beta})$	1, 2, 3	$n_{2,k} i\beta$	
$\xi = \xi_6 i(\bar{\beta})$	1, 2, 3	$n_{3,k} i\beta$	
$\bar{e}_{03} = \bar{e}_{03,6i\beta-1}$	1, 2, 3	$n_{4,k} i\beta$	
$Q = Q_6 i\beta$	1, 2	$\bar{r}_k i\beta$	
$\delta\bar{e}_{1,2,3,4} = \delta\bar{e}_{1,2,3,4} i\beta(t_\beta)$			$\bar{r}_{1,k} i\beta$

TABLE H.4. SECOND EVALUATION

INPUT	FOR k VALUES OF:	CALCULATE	RENAME'
$a = a_7 i(\bar{\beta})$	1, 2, 3	$n_{1,k} i\beta$	$n_{5,k} i\beta$
$b = b_7 i(\bar{\beta})$	1, 2, 3	$n_{2,k} i\beta$	$n_{6,k} i\beta$
$\xi = \xi_7 i(\bar{\beta})$	1, 2, 3	$n_{3,k} i\beta$	$n_{7,k} i\beta$
$\bar{e}_{03} = \bar{e}_{03,7i\beta-1}$	1, 2, 3	$n_{4,k} i\beta$	$n_{8,k} i\beta$
$Q = Q_7 i\beta$	1, 2	$\bar{r}_k i\beta$	$\bar{r}_{10,k} i\beta$
$\delta\bar{e}_{1,2,3,4} = \delta\bar{e}_{5,6,7,8} i\beta(t_\beta)$			

Then the shear panel contributions to the fictitious forces and deformation for the cell are:

$$\begin{matrix} n_{S_{k\beta}} \\ (3 \times 1) \end{matrix} = \begin{bmatrix} n_{1,k\beta} \\ n_{2,k\beta} \\ n_{3,k\beta} \\ n_{4,k\beta} \\ n_{5,k\beta} \\ n_{6,k\beta} \\ n_{7,k\beta} \\ n_{8,k\beta} \end{bmatrix} \quad k = 1, 2, 3 \quad (H.310)$$

$$\begin{matrix} r_{S_{k\beta}} \\ (30 \times 1) \end{matrix} = \begin{bmatrix} \frac{1}{a_{6i}(\bar{\beta})} & \bar{r}_{1,k\beta} \\ 0 \\ 0 \\ 0 \\ 0 \\ 0 \\ 0 \\ 0 \\ 0 \\ \frac{1}{a_{7i}(\bar{\beta})} & \bar{r}_{10,k\beta} \\ 0 \\ 0 \\ \cdot \\ \cdot \\ \cdot \\ 0 \end{bmatrix} \quad k = 1, 2 \quad (H.311)$$

By inspection of Figure H.4, define edge rotation angles as follows:

$$\theta_{1iB}(t_B) = \frac{1}{L_{1i}(\bar{B})} [\delta \tilde{e}_{3iB}(t_B) - \delta \tilde{e}_{4iB}(t_B)] \quad (H.312)$$

$$\theta_{2iB}(t_B) = \frac{1}{L_{2i}(\bar{B})} [\delta \tilde{e}_{2iB}(t_B) - \delta \tilde{e}_{1iB}(t_B)] \quad (H.313)$$

$$\theta_{3iB}(t_B) = \frac{1}{L_{3i}(\bar{B})} [\delta \tilde{e}_{3iB}(t_B) - \delta \tilde{e}_{2iB}(t_B)] \quad (H.314)$$

$$\theta_{4iB}(t_B) = \frac{1}{L_{4i}(\bar{B})} [\delta \tilde{e}_{4iB}(t_B) - \delta \tilde{e}_{1iB}(t_B)] \quad (H.315)$$

$$\theta_{5iB}(t_B) = \frac{1}{L_{5i}(\bar{B})} [\delta \tilde{e}_{7iB}(t_B) - \delta \tilde{e}_{8iB}(t_B)] \quad (H.316)$$

$$\theta_{6iB}(t_B) = \frac{1}{L_{6i}(\bar{B})} [\delta \tilde{e}_{6iB}(t_B) - \delta \tilde{e}_{5iB}(t_B)] \quad (H.317)$$

$$\theta_{7iB}(t_B) = \frac{1}{L_{7i}(\bar{B})} [\delta \tilde{e}_{7iB}(t_B) - \delta \tilde{e}_{6iB}(t_B)] \quad (H.318)$$

$$\theta_{8iB}(t_B) = \frac{1}{L_{8i}(\bar{B})} [\delta \tilde{e}_{8iB}(t_B) - \delta \tilde{e}_{5iB}(t_B)] \quad (H.319)$$

The bar contributions to the fictitious forces and deformations for the cell element are given with simplified notation where the subscripts i and B and the symbol (t_B) are moved outside the column matrix brackets.

$$\begin{matrix} n_{B1}{}_{iB} = & \begin{bmatrix} -\bar{F}_{S2}{}^{\theta_2} - \bar{F}_{S4}{}^{\theta_4} \\ \bar{F}_{S2}{}^{\theta_2} - \bar{F}_{S3}{}^{\theta_3} \\ \bar{F}_{S1}{}^{\theta_1} + \bar{F}_{S3}{}^{\theta_3} \\ -\bar{F}_{S1}{}^{\theta_1} + \bar{F}_{S4}{}^{\theta_4} \\ -\bar{F}_{S6}{}^{\theta_6} - \bar{F}_{S8}{}^{\theta_8} \end{bmatrix} \\ (8 \times 1) \end{matrix} \quad (H.320)$$

$$\begin{bmatrix} \bar{F}_{S6}^{\theta_6} - \bar{F}_{S7}^{\theta_7} \\ \bar{F}_{S5}^{\theta_5} - \bar{F}_{S7}^{\theta_7} \\ -\bar{F}_{S5}^{\theta_5} + \bar{F}_{S8}^{\theta_8} \end{bmatrix}_{iB}(t_B)$$

$$\begin{aligned} n_{B2}_{iB} &= 0 \\ (3 \times 1) \end{aligned} \quad (H.321)$$

$$\begin{aligned} n_{B3}_{iB} &= \frac{1}{6} \begin{bmatrix} \bar{F}_{S2}^{\theta_2^3} + \bar{F}_{S4}^{\theta_4^3} \\ -\bar{F}_{S2}^{\theta_2^3} + \bar{F}_{S3}^{\theta_3^3} \\ -\bar{F}_{S1}^{\theta_1^3} - \bar{F}_{S3}^{\theta_3^3} \\ \bar{F}_{S1}^{\theta_1^3} - \bar{F}_{S4}^{\theta_4^3} \\ \bar{F}_{S6}^{\theta_6^3} + \bar{F}_{S8}^{\theta_8^3} \\ -\bar{F}_{S6}^{\theta_6^3} + \bar{F}_{S7}^{\theta_7^3} \\ -\bar{F}_{S5}^{\theta_5^3} - \bar{F}_{S7}^{\theta_7^3} \\ \bar{F}_{S5}^{\theta_5^3} - \bar{F}_{S8}^{\theta_8^3} \end{bmatrix}_{iB}(t_B) \\ (8 \times 1) \end{aligned} \quad (H.322)$$

$$r_{B1}_{iB} = 0 \quad (H.323)$$

$$\begin{aligned} r_{B2}_{iB} &= -\frac{1}{4} r_{r'_{iB}} \begin{bmatrix} 0 \\ x_{1i}(\bar{\theta}) \theta_{1iB}^2(t_B) \\ x_{1i}(\bar{\theta}) \theta_{1iB}^2(t_B) \\ x_{2i}(\bar{\theta}) \theta_{2iB}^2(t_B) \\ x_{2i}(\bar{\theta}) \theta_{2iB}^2(t_B) \end{bmatrix} \\ (30 \times 1) \end{aligned} \quad (H.324)$$

$$\left\{ \begin{array}{c} l_{3i}(\bar{B}) \theta_{3i\beta}^2(t_\beta) \\ l_{3i}(\bar{B}) \theta_{3i\beta}^2(t_\beta) \\ l_{4i}(\bar{B}) \theta_{4i\beta}^2(t_\beta) \\ l_{4i}(\bar{B}) \theta_{4i\beta}^2(t_\beta) \\ 0 \\ l_{5i}(\bar{B}) \theta_{5i\beta}^2(t_\beta) \\ l_{5i}(\bar{B}) \theta_{5i\beta}^2(t_\beta) \\ l_{6i}(\bar{B}) \theta_{6i\beta}^2(t_\beta) \\ l_{6i}(\bar{B}) \theta_{6i\beta}^2(t_\beta) \\ l_{7i}(\bar{B}) \theta_{7i\beta}^2(t_\beta) \\ l_{7i}(\bar{B}) \theta_{7i\beta}^2(t_\beta) \\ l_{8i}(\bar{B}) \theta_{8i\beta}^2(t_\beta) \\ l_{8i}(\bar{B}) \theta_{8i\beta}^2(t_\beta) \end{array} \right\}$$

Then fictitious force and deformation matrices for the membrane and cell elements are:

$$n_{1i\beta} = n_{S1i\beta} + n_{B1i\beta} \quad (H.325)$$

$$n_{2i\beta} = n_{S2i\beta} \quad (H.326)$$

$$n_{3i\beta} = n_{S3i\beta} + n_{B3i\beta} \quad (H.327)$$

$$r_{1i\beta} = r_{S1i\beta} \quad (H.329)$$

$$r_{2_{i\beta}} = r_{S_{2_{i\beta}}} + r_{B_{2_{i\beta}}} \quad (H.329)$$

For bar, membrane and cell elements

$$\bar{F}_{K_{i\beta}}(t_3) = n_{1_{i\beta}} + n_{2_{i\beta}} + n_{3_{i\beta}} \quad (H.330)$$

$$\delta \bar{e}_{f_{i\beta}}(t_3) = r_{1_{i\beta}} + r_{2_{i\beta}} \quad (H.331)$$

Step 9 of Table 1 is now performed as follows:

$$\delta \bar{P}_{(\bar{F})_B}(t_3) = \sum_i \bar{P}_{UF_i} F_{\bar{F}_i(\bar{B})} \bar{F}_{K_{i\beta}}(t_3) \quad (H.332)$$

$$\delta \bar{P}_{Kf_B}(t_3) = \sum_i \bar{P}_{UF_i} F_{\bar{F}_i}(t_{3-1}) \bar{k}_{i(\beta)} \delta \bar{e}_{f_{i\beta}}(t_3) \quad (H.333)$$

$$\delta \bar{P}_{(f)_B}(t_3) = \delta \bar{P}_{(\bar{F})_B}(t_3) + \delta \bar{P}_{Kf_B}(t_3) \quad (H.334)$$

Step 10 requires that Steps 2 through 9 be repeated for a specified number of iterations.

Step 11 lumped element damping forces are computed from:

$$\bar{F}_{c_i}(t_3) = - \bar{c}_{i(\beta)} F_{\bar{F}_i}^T(t_{3-1}) \bar{P}_{UF_i}^T \bar{v}(t_3) \quad (H.335)$$

Also, the incremental element damping energy (if element temperature changes are required) is calculated from:

$$\delta \bar{E}_{c_{i\beta}}(t_3) = \frac{\tau_B}{2} \left[\bar{v}^T(t_{3-1}) \bar{c}_{i(\beta)} \bar{v}(t_{3-1}) + \bar{v}^T(t_3) \bar{c}_{i(\beta)} \bar{v}(t_3) \right] \quad (H.336)$$

$$\text{where } \bar{c}_{i(\beta)} = \bar{P}_{UF_i} F_{\bar{F}_i}(t_{3-1}) \bar{c}_{i(\beta)} F_{\bar{F}_i}^T(t_{3-1}) \bar{P}_{UF_i}^T \quad (H.337)$$

Element temperature change due to damping energy dissipated as heat (if required) is calculated from

$$\delta T_{iB} = \frac{\delta \bar{E}_{C_{iB}}(t_B)}{J s_i m_{Ti}} \quad (H.338)$$

where J is the mechanical equivalent of heat, s_i is the specific heat for the material of the i th element and m_{Ti} is the total mass of the i th element.

Step 12 updated transformation matrices $F_{\bar{F}_i}(t_B)$ and $\sigma_{L\bar{F}_i}(t_B)$ are generated by re-evaluating appropriate equations from Table H.1 using joint coordinates from the updated matrices U_{iB} .

Steps 13, 14 and 15 are accomplished at the beginning of the next increment.

In addition to the steps outlined in Table 1, the element stresses and strains are calculated at the end of the increment from the following generalized equations.

$$\sigma_i(t_B) = \sigma_{s\sigma} \sigma_{L\bar{F}_i}(t_B) \bar{F}_{K_i}(t_B) \quad (H.339)$$

$$\epsilon_i(t_B) = \epsilon_i(t_{B-1}) + \epsilon_{\sigma s_i}(t_{B-1}) \sigma_{L\bar{F}_i}(t_B) \delta \bar{F}_{K_i}(t_B) \quad (H.340)$$

If the i th element is a bar or membrane, the matrix $\sigma_{s\sigma}$ is an identity, and the matrix $\sigma_{L\bar{F}}$ is equal to $\sigma_{\bar{F}B}$ (bar element) or $\sigma_{\bar{F},LPM}$ (membrane element). If the i th element is a cell, then $\sigma_{s\sigma}$ is a transformation matrix to linearly extrapolate quantities at the lumped element level to the mid-points of the upper and lower surfaces of the cell.

$$\sigma_{s\sigma}(\text{cell}) = \begin{bmatrix} \sigma_{S1} & \sigma_{S2} \\ \sigma_{S2} & \sigma_{S1} \end{bmatrix} \quad (H.341)$$

(12 x 12)

where

$$\sigma_{S1} = \begin{bmatrix} \sigma_1 & & & \\ & \sigma_1 & & \\ & & 1 & \\ & & & \sigma_1 & \\ & & & & 1 & \\ & & & & & 1 & \end{bmatrix}, \quad \sigma_{S2} = \begin{bmatrix} \sigma_2 & & & & & \\ & \sigma_2 & & & & \\ & & 0 & & & \\ & & & \sigma_2 & & \\ & & & & \sigma_2 & \\ & & & & & 0 & \\ & & & & & & 0 \end{bmatrix} \quad (H.342)$$

$$\sigma_1 = \frac{1 + \sqrt{3}}{2}, \quad \sigma_2 = \frac{1 - \sqrt{3}}{2} \quad (\text{H.343})$$

The Prandtl-Reuss equivalent stresses $\bar{\sigma}_i(t_B)$ are calculated as follows:

Bar Element

$$\bar{\sigma}_i(t_B) = |\sigma_i(t_B)| \quad (\text{H.344})$$

Membrane Element

$$\sigma_i(t_B) = \left\{ \sigma_x \mid \sigma_y \mid \tau_{xy} \right\}_i(t_B) \quad (\text{column}) \quad (\text{H.345})$$

$$\sigma'_{xi}(t_B) = \frac{1}{3} (2 \sigma_x - \sigma_y)_i(t_B) \quad (\text{H.346})$$

$$\sigma'_{yi}(t_B) = \frac{1}{3} (-\sigma_x + 2 \sigma_y)_i(t_B) \quad (\text{H.347})$$

$$\sigma'_{zi}(t_B) = \frac{1}{3} (-\sigma_x - \sigma_y)_i(t_B) \quad (\text{H.348})$$

$$\bar{\sigma}_i(t_B) = \left[\frac{3}{2} (\sigma_x'^2 + \sigma_y'^2 + \sigma_z'^2 + 2 \tau_{xy}^2) \right]_i^{1/2}(t_B) \quad (\text{H.349})$$

Cell Element

$$\sigma_i(t_B) = \left\{ \sigma_{xc} \mid \sigma_{yc} \mid \sigma_{zc} \mid \tau_{xyc} \mid \tau_{yzc} \mid \tau_{zxc} \mid \sigma_{xd} \mid \sigma_{yd} \mid \sigma_{zd} \mid \tau_{xyd} \mid \tau_{yzd} \mid \tau_{zxd} \right\}_i(t_B) \quad (\text{H.350})$$

$$\sigma'_{xc}_i(t_B) = \frac{1}{3} (2 \sigma_{xc} - \sigma_{yc} - \sigma_{zc})_i(t_B) \quad (\text{H.351})$$

$$\sigma'_{yc}_i(t_B) = \frac{1}{3} (-\sigma_{xc} + 2 \sigma_{yc} - \sigma_{zc})_i(t_B) \quad (\text{H.352})$$

$$\sigma'_{zc}_i(t_B) = \frac{1}{3} (-\sigma_{xc} - \sigma_{yc} + 2 \sigma_{zc})_i(t_B) \quad (\text{H.353})$$

$$\bar{\sigma}_{ci}(t_B) = \left[\frac{3}{2} (\sigma_{xc}'^2 + \sigma_{yc}'^2 + \sigma_{zc}'^2 + 2 \tau_{xyc}^2 + 2 \tau_{yzc}^2 + 2 \tau_{zxc}^2) \right]_i^{1/2}(t_B) \quad (\text{H.354})$$

$$\sigma'_{xdi}(t_3) = \frac{1}{3} (2 \sigma_{xd} - \sigma_{yd} - \sigma_{zd})_i(t_3) \quad (H.355)$$

$$\sigma'_{ydi}(t_3) = \frac{1}{3} (-\sigma_{xd} + 2 \sigma_{yd} - \sigma_{zd})_i(t_3) \quad (H.356)$$

$$\sigma'_{zdi}(t_3) = \frac{1}{3} (-\sigma_{xd} - \sigma_{yd} + 2 \sigma_{zd})_i(t_3) \quad (H.357)$$

$$\bar{\sigma}_{di}(t_3) = \left[\frac{3}{2} (\sigma_{xd}^2 + \sigma_{yd}^2 + \sigma_{zd}^2 + 2 \tau_{xyd}^2 + 2 \tau_{yzd}^2 + 2 \tau_{zxd}^2) \right]_i^{1/2}(t_3) \quad (H.358)$$

If the material nonlinearity is accounted for, then element matrices $\bar{k}_i(t_3)$, $\bar{c}_i(t_3)$, and $\bar{e}_{\sigma s_i}(t_3)$ are generated as necessary by re-evaluating appropriate equations from Table H.1 using updated material properties, see Appendix E. Then, in preparation for beginning the solution for the next increment set:

$$3 = 3 + 1 \quad (H.359)$$

$$\bar{k}_i(3) = \bar{k}_i(t_{3-1}) \quad (H.360)$$

$$\bar{c}_i(3) = \bar{c}_i(t_{3-1}) \quad (H.361)$$

Now go back to "NONLINEAR INCREMENTAL SOLUTION" and repeat the calculations.

LINEAR INCREMENTAL SOLUTION

The equations previously summarized for the nonlinear incremental solution are valid for the linear incremental solution when the following modifications are introduced.

1. Matrices \bar{k}_i , \bar{c}_i , $F\bar{F}_i$ are constant. Therefore, \bar{k} and \bar{c} are calculated once and are valid for all increments.
2. The matrix δT_i is null for all β .

3. The thermomechanical load matrix can be calculated from

$$\bar{P} = \delta \bar{P}_{K08}(t_s) + \delta \bar{P}_{(\phi)U8}(t_s) + \bar{M} \dot{\bar{V}}(t_{s-1}) + \bar{C} \bar{V}(t_{s-1}) \quad (H.362)$$

where

$$\delta \bar{P}_{K08}(t_s) = 0 \text{ for } s > 1 \quad (H.363)$$

4. The matrices $\delta \bar{P}_{U8}(t_s)$ and $\delta \bar{P}_{(f)8}(t_s)$ are null for all s .
5. The eigensolution λ and H need be calculated only once and is valid for all s .
6. The exponential matrix $F_s(\tau_s)$ and the mechanical impedance matrix $\bar{K}_{C(s)}$ need not be re-computed if $\tau_s = \tau_{s-1}$.
7. Updated coordinates and fictitious forces and deformation are not computed.
8. Damping forces and damping energy are not computed.

POSTPROCESSING

Accumulated transformed displacements and untransformed nodal displacements are:

$$\bar{\Delta}(t_s) = \bar{\Delta}(t_{s-1}) + \delta \bar{\Delta}_s(t_s) \quad (H.364)$$

$$\Delta(t_s) = \bar{P}_{UPT}^T \bar{\Delta}(t_s) \quad (H.365)$$

Coordinates of the deformed structure, with optional magnification of displacements are

$$U(t_s) = U_0 + u_{\Delta} \Delta(t_s) \quad (H.366)$$

where u_{Δ} is a scalar magnification factor.

Untransformed nodal velocities and accelerations are calculated from the transformed velocities and accelerations $\bar{v}(t_\beta)$ and $\bar{\dot{v}}(t_\beta)$.

$$v(t_\beta) = \bar{P}_{UPT}^T \bar{v}(t_\beta) \quad (H.367)$$

$$\dot{v}(t_\beta) = \bar{P}_{UPT}^T \dot{\bar{v}}(t_\beta) \quad (H.368)$$

The volume of printout may be limited by providing options to selectively print displacements, velocities, accelerations, coordinates and element forces, stresses and strains.

EXTERNAL LOADS GENERATION

The equations for calculating external loads are derived in Appendix G.

$$\bar{t} = \frac{\bar{b} \times \bar{n}}{|\bar{b} \times \bar{n}|} \quad (H.369)$$

$$\bar{u} = \frac{\bar{t} \times \bar{d}}{|\bar{t} \times \bar{d}|} \quad (H.370)$$

$$t_d = \frac{L}{U} \quad (H.371)$$

$$F_{avg} = \frac{m \cdot U}{t_d} (\bar{b} \cdot \bar{u}) \quad (H.372)$$

$$F_\beta = f_\beta F_{avg} \quad (H.373)$$

$$D_{\beta-1} = t_{\beta-1} v \cos \theta \quad (H.373.1)$$

$$\bar{s}_\beta = \bar{s}_0 + D_{\beta-1} \bar{d} \quad (H.374)$$

$$B_{x\beta} = \bar{i} \cdot (\bar{s}_\beta \times \bar{u}) \quad (H.375)$$

$$B_{y\beta} = \bar{j} \cdot (\bar{s}_\beta \times \bar{u}) \quad (H.376)$$

$$B_{z\beta} = \bar{k} \cdot (\bar{s}_\beta \times \bar{u}) \quad (H.377)$$

j = joint number

For all potentially loaded joints j , calculate

$$A_{xj} = \bar{i} \cdot (\bar{w}_j \times \bar{u}) \quad (H.378)$$

$$A_{yj} = \bar{j} \cdot (\bar{w}_j \times \bar{u}) \quad (H.379)$$

$$A_{zj} = \bar{k} \cdot (\bar{w}_j \times \bar{u}) \quad (H.380)$$

For those joints j_1, j_2, \dots loaded during during the s th increment, assemble A_s and B_s as follows:

If $u_x > u_y$ and $u_x > u_z$

$$A_s = \left[\begin{array}{c|c|c} 1 & 1 & \dots \\ A_{yj1} & A_{yj2} & \dots \\ A_{zj1} & A_{zj2} & \dots \end{array} \right], \quad B_s = \left\{ \begin{array}{c} 1 \\ B_{ys} \\ B_{zs} \end{array} \right\} \quad (H.381)$$

If $u_y > u_x$ and $u_y > u_z$

$$A_s = \left[\begin{array}{c|c|c} 1 & 1 & \dots \\ A_{xj1} & A_{xj2} & \dots \\ A_{zj1} & A_{zj2} & \dots \end{array} \right], \quad B_s = \left\{ \begin{array}{c} 1 \\ B_{xs} \\ B_{zs} \end{array} \right\} \quad (H.382)$$

If $u_z > u_x$ and $u_z > u_y$

$$A_s = \left[\begin{array}{c|c|c} 1 & 1 & \dots \\ A_{xj1} & A_{xj2} & \dots \\ A_{yj2} & A_{yj2} & \dots \end{array} \right], \quad B_s = \left\{ \begin{array}{c} 1 \\ B_{xs} \\ B_{ys} \end{array} \right\} \quad (H.383)$$

Calculate joint loads from

$$\begin{aligned}\phi_B &= A_B^T (A_B A_B^T)^{-1} B_B F_B \\ &= \left\{ \phi_{jB} \right\}\end{aligned}\quad (H.384)$$

Calculate incremental joint loads from

$$\delta\phi_{jB} = \phi_{jB} - \phi_{jB-1} \quad (H.385)$$

Calculate incremental nodal degree of freedom loads at each loaded joint from

$$\begin{aligned}\delta P_{(\phi)T_{jB}} &= \delta\phi_{jB} \begin{bmatrix} \cdot \\ \cdot \\ u_x \\ u_y \\ u_z \\ \cdot \\ \cdot \\ \cdot \end{bmatrix} \\ (3n_j \times 1) &\end{bmatrix}\end{aligned}\quad (H.386)$$

where the row locations for u_x , u_y , u_z are equal to $3j-2$, $3j-1$, $3j$; and n_j is the total number of joints. Then the incremental external load matrix for the B th increment is

$$\delta P_{(\phi)T_B}(t_B) = \sum_j \delta P_{(\phi)T_{jB}} \quad (H.387)$$

REFERENCES

1. Przemieniecki, J. S., Theory of Matrix Structural Analysis, McGraw-Hill Book Company, New York, 1968.
2. Timoshenko, S. P., and Gere, J. M., Theory of Elastic Stability, McGraw-Hill Book Company, New York, 1961.
3. Timoshenko, S., and Woinowsky-Krieger, S., Theory of Plates and Shells, McGraw-Hill Book Company, New York, 1959.
4. Lindberg, G. M., Olson, M. D., and Cowper, G. R., "New Developments in the Finite Element Analysis of Shells", DME/NAE Quarterly Bulletin, No. 1969 (4).
5. Pickard, J., FORMAT - Fortran Matrix Abstraction Technique, Volume V, Engineering User and Technical Report, AFFDL-TR-66-207, Volume V, October 1963.
6. IBM Application Program, System/360 Continuous System Modeling Program User's Manual, Program Number 360 A-CX-16X.
7. Rhodes, G. F., Damping Static Dynamic, and Impact Characteristics of Laminated Beams Typical of Windshield Construction, AFFDL-TR-76-156, September 1977.
8. Lawrence, J. H., Jr., et. al., Windshield Technology Demonstrator Program - Detail Design Options Study, AFFDL-TR-77-1, December 1976.
9. Coker, M. J., Hoffman, J. B., Lawrence, J. H., Jr., Windshield Technology Demonstrator Program - Canopy Detail Design Options Study, Douglas Aircraft Company Report MDC J7176, April 1978.
10. Barber, J. P., Wilbeck, J. S., and Taylor, H. R., Bird Impact Forces and Pressures on Rigid and Compliant Targets, UDRI-TR-77-17, March 1977.
11. Morley, L.S.D., Skew Plates and Structures, Macmillan, 1963.
12. Denke, P. H., A General Digital Computer Analysis of Statically Indeterminate Structures, NASA TN D-1666, December 1962.
13. Hill, R., The Mathematical Theory of Plasticity, Oxford at the Clarendon Press, 1960.
14. Greene, F. E., Testing for Mechanical Properties of Monolithic and Laminated Polycarbonate Materials, Volume I, Technical Report AFFDL-TR-77-96, October 1977.
15. Ramberg, W. and Osgood, W. R., Description of Stress-Strain Curves by Three Parameters, National Advisory Committee for Aeronautics, Technical Note No. 902, July 1943.